BLOODSTAIN PATTERN ANALYSIS: SCRATCHING THE SURFACE

B A J LARKIN

PhD   2015

BLOODSTAIN PATTERN ANALYSIS: SCRATCHING THE SURFACE

BETHANY ALEXANDRIA JANE LARKIN

A thesis submitted in partial fulfilment of the requirements of Manchester Metropolitan University for the degree of Doctor of Philosophy

School of Science and the Environment, Manchester Metropolitan University

2015

ABSTRACT

Bloodstain Pattern Analysis (BPA) is a forensic application of the interpretation of distinct patterns which blood exhibits during a bloodletting incident, providing key evidence with its ability to potentially map the sequence of events. The nature of BPA has given the illusion that its evidentiary significance is less than that of fingerprints or DNA, relying solely on the interpretation of the analyst and focusing very little on any scientific evaluation. Recent preliminary literature studies have involved a more quantitative approach, developing directly crime scene applicable equations and methodology, which have established new ways of predicting the angle of impact, impact velocity, point of origin of blood and blood pattern type. Using these new equations and further improving on them to include a variation of impact surfaces, surface properties (i.e. porosity, roughness, manufacturing process etc.) and changes in blood properties is the principal focus of this work.

The primary objective of this research is to expand the knowledge of blood and surface interactions and generate general equation/s or quantitative approaches that encompasses some of the possible conditions, in relation to Bloodstain Pattern Analysis (BPA), which may be encountered at a crime scene. Overall validating BPA and supporting a more reputable / respected scientific field giving credence to its usage within criminal trials.

This thesis is presented in three parts:

The first part explores blood, its characteristics and how manipulating the components of blood (i.e. packed cell volume, PCV), can alter the way a bloodstain forms and dries. Since packed cell volume is instrumental in the overall viscosity of blood, which ultimately determines the final bloodstain diameter via the natural fluctuation exhibited throughout the body and by the individual human characteristics, it was deemed necessary to investigate its effect on the interpretation of bloodstains. Packed cell volume was found to alter the size of bloodstains significantly, where increments in their diameter were experienced when PCV% was decreased; angled impacts were unaffected.

The mechanism of drying blood was also analysed, the current understanding being that blood dries primarily by the Marangoni Effect. However this is found to be

altered when PCV% is considered; low PCV% exhibits a strong Coffee Ring Effect where higher PCV% levels dry by the Marangoni Effect.

Other drying characteristics considered were volume analysis, skeletonisation and the halo effect where PCV% was manipulated. Volume analysis methods were significantly affected by PCV%, where new drying constants were established and several established scientific methods were shown to be unreliable at determining the volume.

The second part of this thesis investigates surface interaction, exploring the fundamentals of various common surface types, and how individual features (i.e. surface roughness) affect the interpretation of bloodstains; four common surfaces were considered (wood, metal, stone/tile and fabric). Blood drop tests were performed at different heights and angles where recently formulated equations were applied to the results to create new constants, which could be used to distinguish between surface types. Wood and fabric were found to alter the spread of blood most significantly, constants increased or decreased substantially, compared to the original value.

The last part of this thesis expands the groundwork set forth in part two. Surfaces were manipulated, either by heat or cleaning. Since it is possible that blood may interact with a surface which may have been cleaned (to remove blood, or simply to clean surface prior to any blood impaction) or heated (i.e. radiators), it is important to fully explore surface alterations which commonly occur in an everyday environment and therefore are highly probable to be encountered at a crime scene. Surface manipulation is investigated in the form of a heated surface, where a blood boiling curve reminiscent of the water boiling curve was created establishing four visibly recognizable boiling regimes. Heat was found to decrease the resultant bloodstain diameter, separate blood into its components and create reduction rings as the temperature increased. An equation accounting for these changes was deduced, further showing how simple alterations to the surface, which have previously been overlooked, can interfere with the results. Further surface manipulation was implemented in the form of cleaning, since cleaning can be performed before blood impacts, therefore causing a surfactant layer, of after blood has impacted the surface, indicating crime evasion.

Secondary analysis of blood on a heated surface in conjunction with cleaning was implemented, establishing the effectiveness of presumptive testing and the ability

to extract valuable DNA. Initial presumptive testing and DNA extraction was found to be successful for all temperatures, however when various cleaning methods were applied (a common occurrence at crime scenes) DNA testing produced negative results at temperatures of 50°C onwards.

Fabric washing, using various household detergents and methods of washing/drying were also evaluated. Detergents significantly increased the resultant diameters of bloodstains, secondary rings were experienced on all polyester and silk fabrics, establishing constants relating to the secondary ring produced. Repeated cycles of washing were found to produce a stable fabric after 6 cycles, for most fabric types.

No other type of investigation of blood will yield so much useful information as an analysis of the blood distribution patterns – **Dr Paul Leland Kirk** (BPA expert)

CONTENTS

LIST OF TABLES

LIST OF FIGURES

1. INTRODUCTION

In the philosophical words of Edmond Locard 'every contact leaves a trace,' [1 - 3] which is the basic principle behind forensic science, a science that utilises evidence left at crime scenes to establish a connection between the crime and its perpetrator. [1 - 3] Forensic science can be defined simply as the application of science pertaining to the law. [1 - 3] It is through these words that the world of forensics has expanded, creating a network of scientists which have made it extremely difficult for a criminal not to be linked to their committed crime. Since every crime scene tells a story, it takes only the correct interpretation of evidence to unveil the story, creating a true representation of the preceding events. Forensic investigators are contingent on this fact, depending on vital forms of evidence to help solve complex crimes and bring justice to victims. [4 - 6] Bloodstain Pattern Analysis (BPA) epitomises this objective, using the formation of blood as it impacts a surface to determine the sequence of events and general movement of the perpetrator and / or victim throughout the scene. [7, 8] BPA has become an increasingly employed forensic discipline due to bloods presence at crime scenes and the weight it holds as a form of evidence within the legal system. [4 - 6]

BPA has been a much overlooked field, although it is evident that people generally acknowledged the presence of blood as being directly connected with death / a violent act, demonstrated even in early cave drawings and ancient paintings, [9] investigators overlooked the potential of blood patterns until the 1960s. Although the 'father' of BPA is widely accredited to Dr Herbert L. MacDonell [9, 10, 11] it was in fact the successful affidavit presented in 1966 by Dr Paul Kirk in the renowned case of Samuel Sheppard (accused of murdering his wife) [7] which first catapulted BPA into the realm of an acceptable / prominent form of evidence in legal proceedings. [4 - 6]

Presently BPA has been utilised in many high profile cases *e.g.* The Road Rage killer.[12] Unfortunately due to the relatively late application of blood as an evidence form, the field still remains somewhat subjective, where analysis can differ depending on the analyst's interpretation. A recent example of this discrepancy is attested in the case of David Camm,[13] an Indiana State trooper sentenced to life imprisonment in 2002 for the murder of his wife and two children, who were found,

shot to death in their car in the family's garage.[13] The case was centred around the interpretation of blood specks found on Camm's t-shirt.[13] Experts stated that the blood spatter was created by impact spatter as a result of Camm shooting his wife; however other experts argue that the blood is simply caused by a transfer when Camm pulled his child from the car.[13] It is now firmly believed that there was a miscarriage of justice, on the 24th October 2013 after the third trial David Camm was acquitted. Unfortunately this is not the only case in which problems with bloodstain analysis has arisen (*i.e.* Billie–Joe Jenkins; expiration *vs* impact spatter). [14] It is through cases like these [13 - 16] and the prevalence of violent crime that has subsequently enhanced public scrutiny upon the police and forensic scientists to produce more efficient, repeatable and accurate methods of interpretation. The main aim of this research is to expand on the limited research currently available regarding the interaction of bloodstains and impact surfaces. Quantitative analysis (using the below equations) will be performed in the hopes of generating an easily applicable method which can be utilised at crime scenes and ultimately support the scientific validation of this 'subjective' discipline.

Steps towards a more scientific quantitative evaluation method have already begun. Wonder introduced the SAADD system, which provided objective criteria in which to identify blood patterns. Focusing on the size of the stains, distribution and the appearance of the overall pattern. [9] Other methods have introduced the effects of important physical properties of blood (viscosity, surface tension and density) on the bloodstains final appearance. [17 - 19] Previous studies have overlooked the accountability of these ever fluctuating parameters within the production of a bloodstain, providing only constants for a typical blood drop (*i.e.* such as a fixed droplet diameter of 4.6 mm). [20]

Hulse – Smith *et al* [18] led the way in this novel research utilising the Reynolds and Weber numbers and applying them to the interpretation of bloodstain patterns. The Reynolds and Weber numbers accumulate all of the aforementioned physical parameters of blood, allowing for a full exploration of the physical variations a blood drop may display. The Reynolds number (*Re*) is a dimensionless ratio relating the ratio of fluid inertia to viscous forces, essentially quantifying these two forces for known flow conditions. [18] The Reynolds number (*Re*) is expressed in equation (1) where D_o is the drop diameter, V_o is the impact velocity, μ is the (blood) viscosity and ρ is the (blood) density. Equally the Weber number (*We*) detailed in equation (2) expresses the ratio of inertia to surface tension forces, where σ is surface tension: [18]

$$Re = \frac{\rho D_o V_o}{\mu} \tag{1}$$

$$We = \frac{\rho D_o V_o^2}{\sigma} \tag{2}$$

Further exploration revealed that the Reynolds number can be further applied to find the maximum drop spread diameter to drop diameter ratio, where D_{max} corresponds to the maximum drop spread diameter (the greatest expansion when the blood droplet initially impacts the surface). [18] The development of this equation (3) suggests that when inertia from the drop impact is high enough surface tension can be neglected, Weber and Reynolds numbers equating to $We \gg Re^{0.5}$ are required to satisfy the above statement. [18]

$$\frac{D_{max}}{D_o} = \frac{Re^{0.25}}{2} \tag{3}$$

Due to the difference between the final stain diameter, D_s (diameter of dried bloodstain, see Figure 1), and D_{max} as the drop rebounds being very subtle it can be stated that D_s is equivalent to D_{max}. [18]

Figure 1: A bloodstain expressing the final bloodstain diameter (mm), D_s.

A correction value (C_d) was added to the above equation (3) to rectify for experimental inconsistencies encountered between measured and calculated values, [18] where C_d equates to 1.11 producing equation (4):

$$\frac{D_s}{D_0} = C_d \frac{Re^{0.25}}{2} \tag{4}$$

The Weber number can be used in a similar manner in the calculation of number of spines N. As a blood drop impacts a surface the drop expands outwards and creates irregularities on the periphery of the stain, these observations are universally referred to as spines (Figure 2).

Figure 2: A bloodstain displaying visible spines on the periphery.

Spines are defined as an edge characteristic on the periphery of the stain, [21] observed as any rise and fall beyond an otherwise smooth rim. [18] This includes waves, triangles, lines or other protrusions. [18] The number of spines, N is defined by equation (5). Again a correction factor C_n is employed (see equation 6) to account for the discrepancies when spines are counted as this is a somewhat subjective process, where C_n corresponds to a value of 0.838;

$$N = 1.14\sqrt{We} \tag{5}$$

$$N = 1.14C_n\sqrt{We} \tag{6}$$

Hulse-Smiths' work provides an excellent basis for the current research, where these equations can be utilised and altered accordingly to the impacted surface. Other work by Hulse - Smith do provide more insight into surface interaction using the above equations for surfaces such as drywall, wood and paper [22] however their work is limited in terms of crime scene applicability, where many variations of wood / paper are found. The location of a crime scene is an unforeseeable aspect of forensic investigation and therefore all possible circumstances cannot be accounted for; crimes can occur in warehouses, outdoors, the home and a great number of other places, where there may be a variety of conditions and prospective surfaces which can influence the morphology of resultant bloodstains.
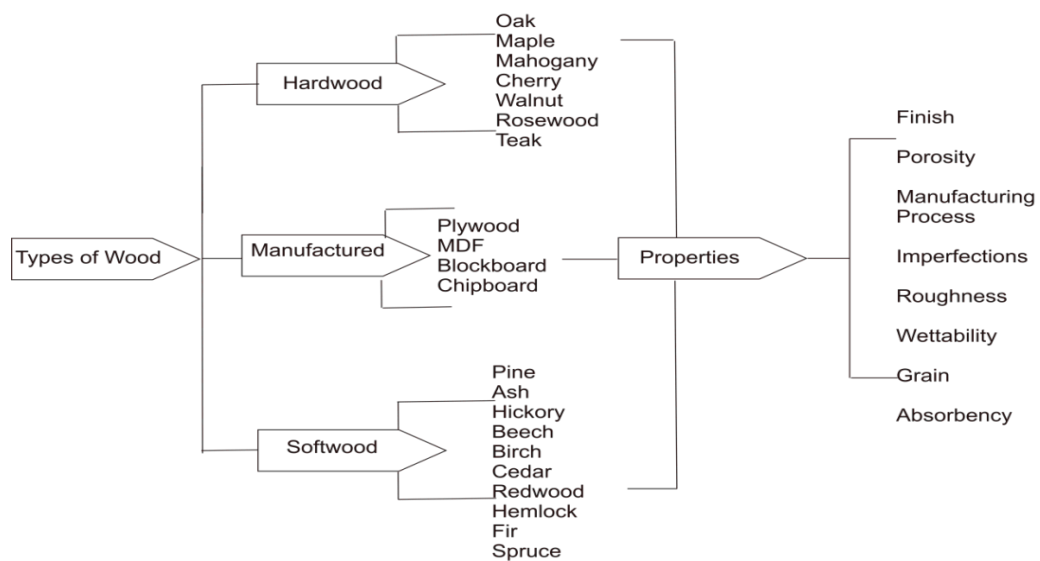
Figure 3: An overview of different wooden surfaces and physical properties. Adapted from Ref [23].

It is these variations that will be investigated within this research; surfaces will be stripped to its fundamentals and investigated. For example, if we consider the variants of wood, [23] as expressed in Figure 3, each wood surface type will interact differently with blood as a consequence of the physical properties and manufacturing process, consequently producing a variety of different resultant bloodstains.

Due to the limited research into blood and surface interactions there are a number of factors that must be explored not least the physical properties of both the surface (*i.e.* roughness, topography) and the blood itself (*i.e.* PCV %) but also the conditions of the surface, for instance if it is heated in the case of a radiator. During this study many of these aforementioned bases will be approached culminating in a final equation or several equations. To accomplish this a combination of blood drop tests, DNA analysis and presumptive testing will be utilised in conjunction with the above - mentioned pre-determined equations proposed by Hulse- Smith *et al.* [18] The mission to find a purely quantitative reliable method of pattern analysis has been the aim of many Bloodstain Pattern Analysts and therefore results obtained from this study could be of significance for both use in the field and presentation in criminal trials.

1.1 AIMS AND OBJECTIVES

Academic Aim: To improve the scientific understanding of bloodstain pattern analysis and generate directly applicable quantitative approaches which will in turn establish a standard way of analysis within a Crime Scene.

 Objectives:

2.1 - To examine aspects of blood that will heavily influence the blood patterns produced such as, PCV % and its possible effect upon viscosity.

2.2 - To assess and evaluate how appropriate current quantitative methods of analysis within BPA are when real life conditions such as the varying surfaces are encountered.

2.3 - To develop new equations and easier methods of analysis when blood patterns are encountered, pertaining to the aforementioned varying surfaces.

2.4 - To establish a valid and appropriate standard protocol pertaining to the collection and preservation of BPA evidence, this can be used as a direct reference at crime scenes.

1.2   BACKGROUND

1.2.1 What is Bloodstain Pattern Analysis?

Bloodstain Pattern Analysis (BPA) is the forensic study of blood formations created at crime scenes during a bloodletting incident. [8, 9, 11 24] Analysts study the shapes, sizes and locations of bloodstains in order to determine the physical events which created them. These blood patterns are utilised to ascertain certain factors such as: [20]

- Sequence of events
- Movement through the scene
- Positions (*i.e.* sitting, standing etc.) of victim, assailant or objects.
- Area of origin of bloodletting incident
- Has the body been moved
- Minimum number of blows executed
- Possible weapon type

The analysis of bloodstains is achieved a number of ways. Direct scene evaluation is preferable however when this option is not available, analysis of scene photographs (scaled) is an alternative. [8, 24] In order to accomplish a thorough evaluation bloodstain analysis is done in conjunction with clothing analysis, weapons analysis *etc*. and require access to hospital records, post-mortem examination, post-mortem photographs, lab reports, crime scene reports and statements. [8, 24]

1.2.2   History of BPA

The customary belief is that Bloodstain Pattern Analysis is a recent forensic discipline, and it is true that up until the 1950s the field was neglected, however we can date the recognition of BPA as a "crime solving" technique back to the 1890s when the Polish scientist Dr Eduard Piotrowski recognised their importance. [8, 9, 11 24]

Prior to the development of BPA as a forensic speciality, artists and authors recognised the importance of blood and its patterns. References to 'gouts and

splashes which lay all around' and 'there were murderers, steeped in the colours of their trade' were made by Sir Arthur Conan Doyle (A Study in Scarlet; 1887) and William Shakespeare (MacBeth; 1606) respectively, where they used the presence of blood to indicate death, perpetrator identification and to highlight a violent criminal act had taken place. [4, 9, 24] There are even earlier allusions to the significance of blood, the 17,000 year old cave painting 'How to Kill a Horse' [9] is believed to depict arterial breaching. [9]

1.2.2.1 BPA Historical Figures

BPA has made substantial advancements in recent times however it is the initial groundwork put down by the following researchers which has made BPA a significant discipline within the field of forensic science. [4, 8, 9, 11, 24]

1.2.2.1.1 Dr Eduard Piotrowski

Dr Eduard Piotrowski conducted the first major research (controversial for its use of live rabbits) in 1895 regarding the analysis of bloodstains for the purpose of criminal investigation. [4, 8, 9, 11, 24] Piotrowski wrote a paper entitled 'Concerning the Origin, Shape, and Direction of Bloodstains following Head Wounds caused by Blows' where he highlighted the importance of a bloodstain tail in origin directionality. [4, 8, 9, 11, 24]

1.2.2.1.2 Dr Victor Balthazard

Dr Victor Balthazard was a French criminalist who performed original research in 1939 concerning bloodstain pattern trajectories. [4, 8, 9, 11, 24] Balthazard later worked alongside the now infamous Herbert MacDonell outlining the significances of elliptical stains and the use of the width to length ratio; used to determine the angle of impact. [4, 8, 9, 11, 24]

1.2.2.1.3 Dr Francis Camps

A French pathologist who worked on the Setty case in 1949. Stanley Setty had been missing for 2 weeks, when his body was discovered in a marsh, it was then a question of finding the primary crime scene. Dr Camps uncovered stab wounds to the victim which would he said "have bled profusely", he concluded that the original crime

scene would hold a significant bloodstain. [4, 8, 9, 11, 24] This proved to be the case, highlighting the distinct link between blood and crime, even alluding to possible sequencing capabilities. [4, 8, 9, 11, 24]

1.2.2.1.4   Hans Gross

Mr Gross wrote the book Criminal Investigations in 1892 where the German discussed observations he made of bloodstain patterns while evaluating crime scenes. Gross wrote about the directionality of stains, pointing to the shape as an indicator of direction of travel. [4, 8, 9, 11, 24]

1.2.2.1.5   Dr Josef Radziki

Dr Josef Radziki introduced 3 categories of bloodstain patterns in his work 'Bloodstain Prints in the Practice of Technology'; 1- bloodstains resulting from an extravasation/fluid leakage, 2- bloodstains caused by some form of instrument and 3-bloodstain which have been altered *i.e.* wiping. These 3 categories are now commonly referred to as *passive, projected and transfer*. [4, 8, 9, 11, 24]

1.2.2.1.6   Dr Paul Leland Kirk

Dr Paul Kirk, a biochemist professor at UC Berkley, was one of the most influential people in the field of forensic science, especially Bloodstain Pattern Analysis. [4, 8, 9, 11, 24] He has been involved in very high profile cases; The Burton Abbott case and his most famous case Dr Sam Sheppard. Dr Sam Sheppard was arrested for the murder of his wife Marilyn in 1955, through numerous retrials Dr Sheppard maintained his innocence. During the last retrial Dr Paul Kirk presented an affidavit on the blood patterns present at the scene, his interpretation showed the relative position of the attacker and the victim and he concluded that the perpetrator was left handed, which Dr Sheppard was not. Dr Kirk's evidence exonerated Dr Sheppard. Sheppard's story was immortalised in the film, 'The Fugitive' which is believed to be heavily based on this case. [4, 8, 9, 11, 24]

1.2.2.1.7   Dr Herbert Leon MacDonell

MacDonell, considered to be the 'Father of BPA', together with the Law Enforcement Assistance Administration (LEAA), conducted experimental research

into the recreation and duplication of bloodstains found at crime scenes for the purpose of reconstruction. [4, 8, 9, 11, 24] From this research he published 'Flight Characteristics and Stain Patterns of Human Blood' in 1971; later he revised this (1982) under a new title 'Bloodstain Pattern Interpretation' and in 1993 he wrote 'Blood Patterns,' all highly influential books. [4, 8, 9, 11, 24]

MacDonell, with many other experts, formed the International Association of Bloodstain Pattern Analysts (IABPA) in 1983, the society now consists of over 800 members whose purpose is to publicise the discipline, create standards of training and interpretation, and to promote BPA research. [4, 8, 9, 11, 24]

1.3   Bloodstain Pattern Terminology

Bloodstains can be created a number of ways, studying these patterns can assist in ascertaining the mechanism behind the creation of the bloodstains. Determining how the patterns were created is vital if an accurate reconstruction is to be established. [24]

There are six basic reproducible pattern types, these include:

- Blood ejected from a point source
- Blood ejected over time from an object in motion
- Blood ejected in a streaming ejection
- Blood dispersed through air as a function of gravity
- Blood that accumulates or flows on a surface
- Blood deposited through transfer

1.3.1   Blood Patterns

Wonder, [9] and Gardner and Bevel [24] split bloodstain patterns into two groups (Figure 4), spatter and non-spatter. These categories where used to create a flow diagram in which recognisable blood patterns were classified. More information regarding stain description is provided within Appendix 1.

```
                          Blood
            ┌───────────────────┴───────────────────┐
         Spatter                                 Non-Spatter
      ┌──────┴──────┐                          ┌──────┴──────┐
   Linear        Non-Linear               Irregular        Regular

  - Spurt        - Expiration             - Smear          - Pattern
                                                             Transfer
  - Cast-off     - Impact                 - Blood into
                                            Blood          - Saturation
  - Drip Trail   - Mist
                                          - Gush/Splash     - Flow
                 - Drip
                                          - Swipe
```
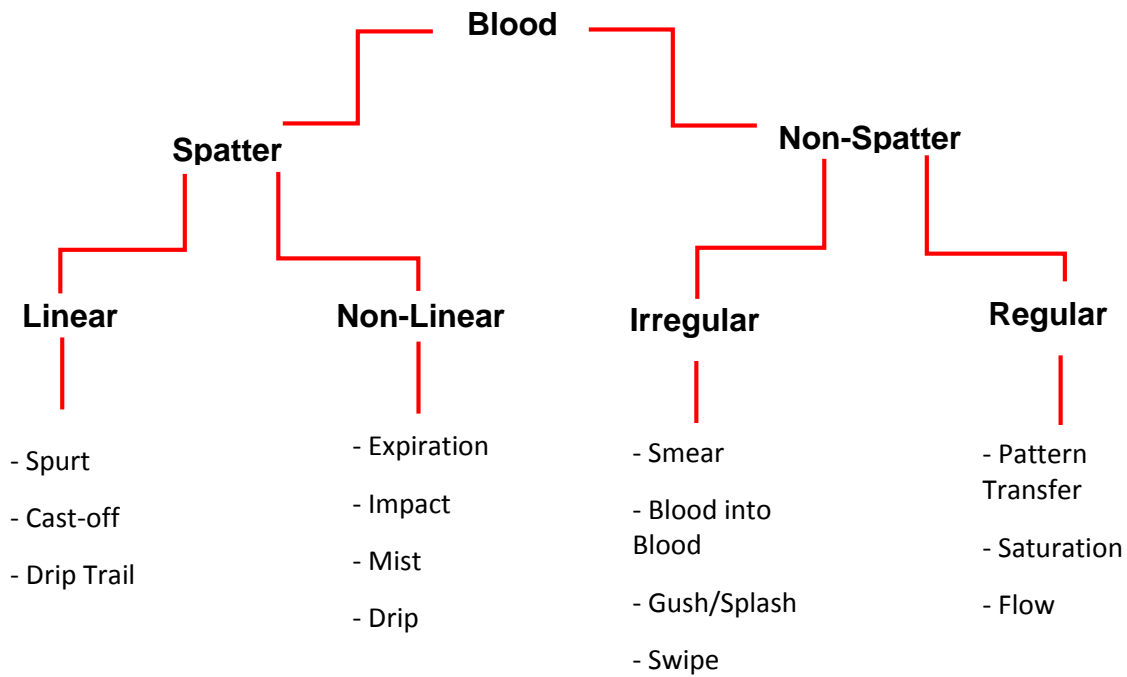
Figure 4: Flow chart expressing blood stains in to two categories; spatter and non-spatter.

The Terminology used by Gardner, Bevel and Wonder has been formalised by the Scientific Working Group for Bloodstain Pattern Analysis and now forms the standard of BPA terminology.

1.3.2 Directionality

The directionality of a blood drop can be determined using the shape of the resultant bloodstain. When the drop hits the surface it will keep travelling in the same path that it was travelling prior to hitting the surface. [4, 8, 9, 11, 24]

Figure 5: Arrows indicate direction which bloodstain was travelling using tail and scallops of a bloodstain.

The tail/spines/scallops point to the direction of travel (Figure 5), therefore the opposing direction points to where the drop originated. Directionality can be used to

determine the movement within the crime scene at the time of the bloodletting event (*i.e.* running, walking). [4, 8, 9, 11, 24]

1.3.3 Area of Convergence

The area of convergence is a shared area where individual bloodstains can be traced, it represents a 2-D size and shape of the Area of Origin. [9] Strings or a pen and ruler can been used to draw a line through the centre of well-formed bloodstains which are extended back into the direction from which they came. [4, 8, 9, 11, 24] The strings or lines will cross if they are the result of a single impact, an area of convergence will be formed rather than a point, since no two drops will originate from the same point. [4, 8, 9, 11, 24]
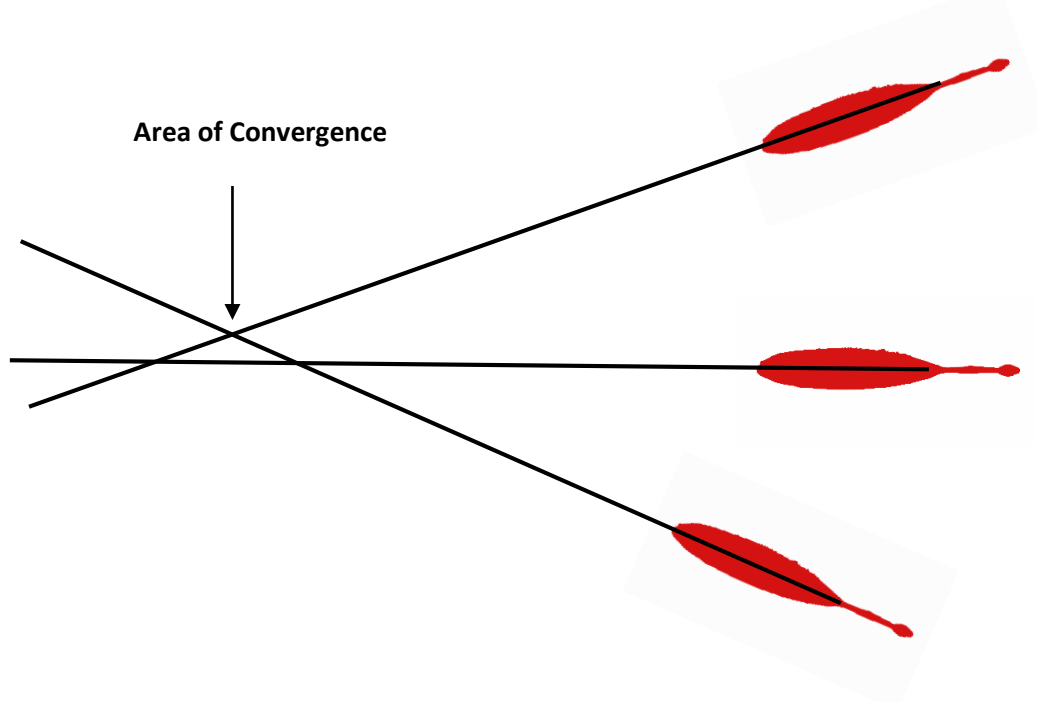
Figure 6: Area of convergence, a common area where bloodstains intercept.

1.3.4 Angle of Impact

The angle of impact measures the acute angle created between the blood drop and the surface it lands on. It is particularly useful as it is used to calculate the area of origin. [4, 8, 9, 11, 24]
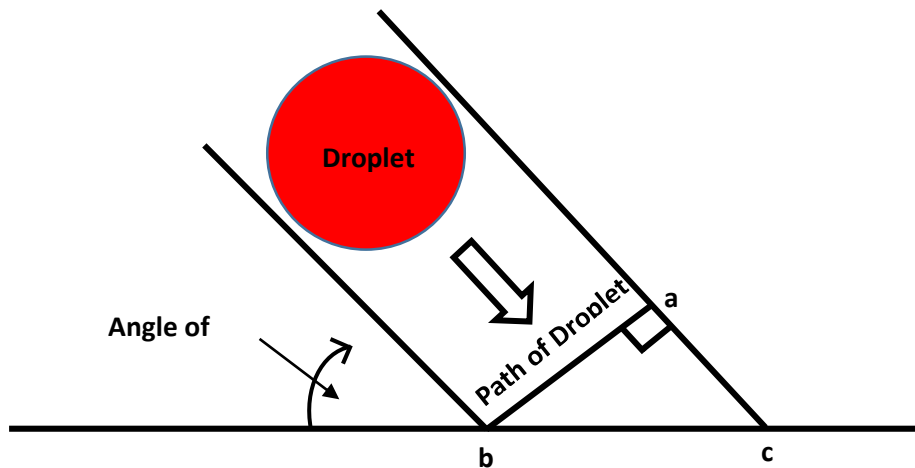
Figure 7: Diagram representing the theory of the occurrence of angled impacts

The angle of impact is currently measured using the width (w) and elliptical length (l) of the bloodstain.

Figure 8: An elliptical directional bloodstain indicating where measurements should take place for angle of impact calculation.

Note: measurements do not include the tail, spines, scallops or satellite spatter; only the main body of the stain is measured. [4, 8, 9, 11, 24]

The angle of impact (θ) is calculated using the following equation 7;

$$Sin\theta = (W/L) \tag{7}$$

Results are an indication of angle of impact and generally give a 5 – 7° margin of error, depending on the operator. [4, 8, 9, 11, 24]

1.3.5 Area of Origin

The determination of the area of origin is significant; it identifies where the blood source was located at the time the distribution of blood was generated. It gives a 3D indication of the area where the bloodletting incident occurred. [4, 8, 9, 11, 24] This can prove or disprove a person's statement pertaining to the sequence of events, *i.e.* a person stating they were on the floor defending themselves however stains indicate that the person was standing. [4, 8, 9, 11, 24]

There are currently three methods for calculating the Area of Origin:

1.2.5.1 Method 1: Graphing

The Area of Origin can be established by graphing the convergence distance for each stain (x), measured in cm. Axis (y) is the height above the floor, or distance from the ceiling / wall to the bloodstain. [4, 8, 9, 11, 24]
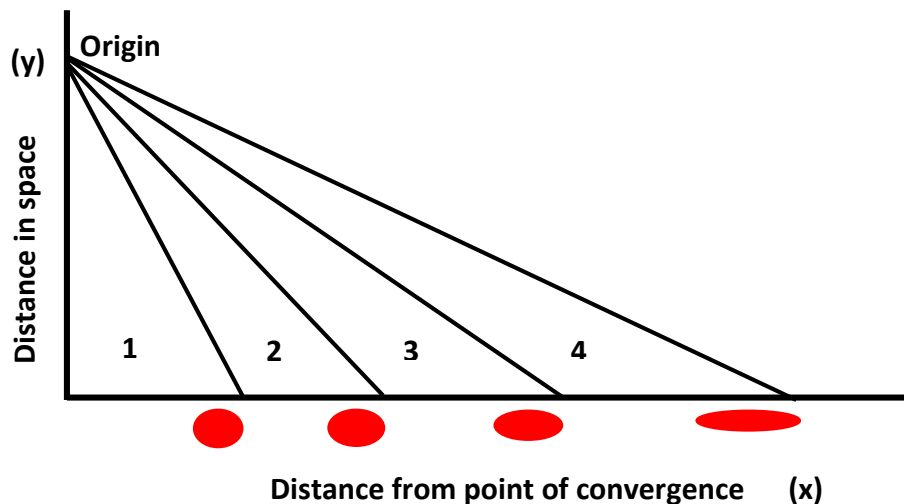
Figure 9: Graphical representation of the area of origin determination for bloodstains

1.2.5.2 Method 2 – Tangent Function

The second technique is the tangent method. [4, 8, 9, 11, 24] This is the method currently employed by bloodstain analysts. It involves the rearrangement of the following equation:

$$Tan\theta = H/D \tag{8}$$

Where θ is the angle of impact, D is the distance from the bloodstain to the area of convergence and H equates to the unknown distance above the target. [4, 8, 9, 11, 24]

1.2.5.3 Method 3 – Stringing

The final method is the stringing method. This involves the placing of strings in the centre of appropriate bloodstains, the string is then stretched to determine an area of origin, lines are drawn and individual angle of impacts are determined for each bloodstain. [4, 8, 9, 11, 24] This method ultimately provides a 3-D representation of impact spatter.

There are other methods of analysis which are constantly developing, these involve of computer programs (*i.e.* Backtrack, Hemospat) to generate a 3-dimensional perspective. Currently the tangent method is still the analytical method of choice. [4, 8, 9, 11, 24]

1.3.6   Edge Characteristics

During the impacting of blood on a surface protrusions may occur on the periphery of the bloodstain, caused by irregularities in the surface or height/force from which the blood has fallen. [4, 8, 9, 11, 24]

Spines or fingers can be present around the periphery of the stain, they are affected by the surface roughness.

Figure 10: Bloodstain spines

Scallops, ordinarily, only occur on an angled impact, they are similar to spines but are longer and irregular in shape.

Figure 11: Bloodstain scallops

Tails are found on angled impacts where the bloodstain has trailed. They can be used to determine the direction of travel.

Figure 12: Bloodstain tail

1.4   Blood Properties and Characteristics

Blood, is loosely defined as a Non - Newtonian fluid, where viscosity is dependent on shear rate, [25] its complex structure and temperamental qualities make it one of the most difficult substances to extract concordant information from, particularly when applied to the analysis of blood drops and flight characteristics. Blood consists of plasma, red blood cells, white blood cells and platelets. [25] The varying levels in which the combinations of these components are found and the fluid dynamics involved are fundamental in the difficulties faced in final analysis. Packed cell volume (PCV %) is essentially the ratio of red blood cells to whole blood content; its effect on viscosity and density is well documented where an increase is associated with cell percentage increase. [9, 26] Viscosity is a fundamental parameter in the study of Bloodstain Pattern Analysis (BPA) affecting the spread of blood due to the

resistance to flow. [27] Resulting viscosity values are heavily reliant on; temperature, time, shear rate and as previously stated, packed cell volume. A multitude of studies have been executed exploring how the viscosity can ultimately determine the size of the bloodstain diameter [4, 5, 9, 20], with the general consensus being that the higher the viscosity the smaller the resultant bloodstain. Other studies involving the manipulation of viscosity with drugs [27 - 28] and alcohol [20] have also been investigated, finding they significantly decrease the dynamic viscosity, showing how easily manipulated viscosity can be. There has yet to be however any exploration into the importance of PCV % and its possible effect on the viscosity within the field of Bloodstain Pattern Analysis; experts tend to focus on viscosity effects rather than the fundamental parameters which give rise to the observed effect. [4, 5, 9, 20] The variance in the PCV % levels is not only dependent upon location within the body [9] where values can deviate from 30 – 52 % [9] but is influenced by the lifestyle of the person. Packed cell volume levels as low as 15 % have been documented for persons who are drug abusers, chronic alcoholics, malnourished and / or elderly. [9] Similarly new-borns, people suffering from shock, extreme exercisers and heart attack victims have very high PCV % reaching 75 %; [9] with values deviating from the normal to such an extent research concerning PCV% could offer some interesting insights especially when considering bloodstain size and appearance.

1.4.1 Blood Drying

Another highly influential biological parameter displayed within blood is drying. [9, 29 - 32] This process is manipulated by surface type (*e.g.* wettability), environmental conditions and climate, acting like a catalyst when conditions are particularly warm. [33]

The drying process of liquids in general is a fascinating topic, with recent investigations unearthing some interesting conclusions. The 'coffee-ring effect' has been identified where liquids display a 'ring' similar to that seen when a drop of coffee dries, where suspended particles are pushed and collected on the periphery of the drop. [34, 35] Yunker *et al* [36] have revealed that it is the shape of the suspended particle that is the driving force behind the coffee-ring effect and by simply changing the shape of the particles from spherical to elongated / ellipsoidal and uniformly dispersing these within the colloidal substance causes an attraction between particles. [36] Due to the nature of the ellipsoidal foreign particles being anisotropic (directionally dependent),

this prevents the particles from reaching the drop periphery and therefore dispersing evenly throughout the drop. [36]

In recent studies by Brutin *et al* [37] it has been identified that the Marangoni Effect is the mechanism by which blood dries, where surface tension forces drive the drying effect. [38] A surface tension gradient is observed and is the driving force for blood drying where the difference in surface tension, for instance, occurs between red blood cells and plasma. [38] Brutin *et al* [37] performed these experiments using a digital camera at a high optical zoom which does limit the overall visual analysis capable, preventing true insights into particle travel, which may allow for further interpretation in to drying. Although this research [37] offers insight into blood drying effects it does not allow the effect of PCV % to be addressed, as previously specified packed cell volume is a changeable parameter within blood and could alter drying significantly.

It is not merely the mechanism in which blood dries that is of importance but what dried blood can reveal about the committed crime. Original volume estimation can provide vital information as to the condition of the victim if the body is absent, it can also be of medical significance giving an indication of expected survival time. There are several methods of volume analysis [39 - 42], the oldest and currently the most reliable is the dry weight method formulated by Lee *et al*. [39] Lee *et al* [39] conducted several experiments where the dried blood is scraped off the surface and weighed. This weight is then multiplied by the 3.25, a corrected constant derived again by Lee *et al*, [39] to find the original volume. This method however is limited since it is only suitable for non-absorbent surfaces and can be time consuming as the bloodstain must be fully dried and scraped completely from the surface.

Lee *et al* developed many more methods of volume analysis, [39] indirect approaches which can be used when direct methods are deemed unsuitable, where a unit of the bloodstain is weighed, and an acetate overlay incorporated with a grid of 1cm squares can be placed over the top of the blood pool. [39] More recent direct methods involve the utilisation of spectrophotometry, where the absorption of haemoglobin is measured [40] and photography, where digital image software calculates the surface area; this was found to closely correlate to the volume. [41] Other observations that can be made pertaining to the drying of blood are; skeletonisation, [4] where the outline of the blood is still present when the stain is wiped, and the halo effect, [42] where a ring is apparent on the periphery of the stain; these techniques may be used to sequence an event. For example the ring will appear red when a drop is

first deposited onto a surface and then is followed by a swipe after a small amount of time. When this sequence is switched the ring will appear the same colour as the surface in which it has impacted. [42]

However, as previously detailed (see section 1.3), blood can differ greatly person to person; [9] it is unknown what the significances of such changes in the components of blood will have on the drying bloodstains. Consequently the following research explores the fundamental parameters of the drying effects of both human and equine blood, the influence of PCV % when applied to drying time, volume estimation, drying effects and resultant bloodstain size, and ultimately what consequences this pertains to the field of BPA; as such this work is of both fundamental and applied importance.

1.5   Blood Drop Formation

The study of drop formation has been researched for the last 100 years, providing insight into key processes such as inkjet printing. Gaining knowledge of this subject is of high importance if we are to understand the mechanics behind blood stain patterns.

Water has similar properties to blood therefore much of the work exploring drop formation is based on the previous studies of water droplets.

Rein [43] described the phenomena of water drops impacting solid and liquid surfaces, which included bouncing, spreading and splashing. In this work Rein [43] used and developed analytical models to predict maximum final stain diameter following impact. Consideration was given to the liquid properties; surface tension and viscosity which play a vital role in droplet spreading, proportionately increasing the resistance to spreading. The Reynolds (equation 1) and Weber (equation 2) numbers describe these liquid properties. Further exploration into droplet spreading was carried out by Pasandideh-Fard *et al* [44] where water was photographed dropping onto a stainless steel surface, these computer generated photographs were used to develop a model to predict the maximum drop spread diameter (D_{max}) following impact. Spines, the protrusions exhibited around the edge of a drop / bloodstain, were investigated by Mehdizadeh *et al* [45] continuing the innovative work of Balthazard *et al*, [46] who originally introduced and correlated the number of spines found on the periphery of a

bloodstain with the release height of the drop, they however used water drops to create an analytical solution for the calculation and prediction of number of spines. [45]

The evolutionary development of a bloodstain is a more complex process; the forces acting upon a blood drop, the impacted surface and the composition of the blood itself dictate the size, shape and overall appearance of the resultant bloodstain. [7 - 9] Early works by the pioneers of BPA, Dr Paul Kirk [47] and Dr Herbert L. MacDonell, [20] have involved the formation of circular bloodstains. This comprised dropping blood onto surfaces at a 90º angle with results revealing an increase of bloodstain diameter with increasing impact velocity up to terminal velocity (approximately above 200cm), where forces reach an equilibrium and diameters cease to increase. [20, 47]

More recent developments within BPA have established equations that can be readily applied at Crime Scenes; [17, 18] these equations can deduce the angle and direction of the impacting blood drop with the use of the size and shape of the final bloodstain; [17, 18] within these equations important physical properties of blood were considered, namely the viscosity, surface tension and density. [7 - 9]

Collaborating all of the above data Hulse-Smith et al [18] generated equations applicable to the formation and impacting of blood drops. These equations (4 and 6) allowed the impact velocity of a blood droplet impacting a horizontal surface to be determined from the number of spines around the bloodstain and the stains size. Developing on this work Knock et al [17] investigated into the effect of the angle of impact, offering a new way of predicting the origin of a bloodstain. [24] The conventional way of determining the origin of impact is an archaic method known most commonly as the stringing method. [24] The stringing method is a simple procedure to determine the area of convergence, a shared area in which all stains in a distribution originate. [24] An alternate more relevant method is that of the tangent method, where the procedure is similar to that of the stringing method however lines instead of strings are drawn and origins are established using the tangent of the angle of impact and multiplying by the distance to the convergence. [24] However, again this is a very laborious exercise and requires expertise/experience when choosing the convergence site. Knock et al developed a new equation which considers all the physical properties, impact velocity and angle of the impacting blood: [17]

$$ab = 111.74 \ (\ Re^{0.5} We^{0.25})^{0.75} D_o D_o + 0.00084 \qquad (9)$$

where *a* and *b* are the width and elliptical length of the bloodstain respectively. [17] Knock *et al* found that the impact angle could be neglected as it is independent of the bloodstain size and therefore angles are excluded from the final equation to determine bloodstain size. [17] It is noted however that there is a discrepancy within the research where the first value changes from 111.74 to 11.74 and that this may alter the results by a factor of 10. Investigations into the effects of angles upon the number of spines, *N*, were also undertaken, again unveiling a new equation where an angle of impact was included to the power of three: [17]

$$N = 0.76 We^{0.5} \sin^3\theta \qquad\qquad (10)$$

This is an excellent step in the making BPA, a discipline noted for its subjective nature, [17, 18, 24, 47] more quantitative and scientifically minded, this will be a point of discussion later.

1.6 Surface Interactions

The impact surface is of great importance, it is what dictates the final overall appearance and size of the bloodstain. [14, 20, 47] The substantial number of possible surfaces that blood may contact during a bloodletting incident makes Bloodstain Pattern Analysis particularly difficult. General observations regarding surface type have been made; Kirk [47] observed the difference between absorbent and non-absorbent surfaces, absorbent surfaces allow the blood drop to spread due to a capillary action whereas non-absorbent surfaces will repel from the surface creating a thinner initial stain. [47] MacDonell dispensed drops on various surface types (glass, paper, wood, corrugated cardboard etc.) commenting on the surface roughness as creating distorted asymmetrical stains and increased splash. [20]

Some single surface detailed analysis research has been performed on fabrics and blood drops, due to the preponderance of blood found on the clothing of both the victim and the assailant. [48 - 54] Similar findings to the general observations first summarized by Kirk [47] were obtained; the bloodstain size depends on the characteristics of the surface, decreasing the bloodstain size as the absorbance increases. [48 - 54] These however are observations and again demonstrate the lack of quantitative analysis within this field. However, some important insights are made in these studies, for instance early works by White [51] focused on blood impacts, finding that the angle of impact measured became unreliable due to the degree of distortion

a bloodstain experiences when it impacts upon a fabric. [51] Other investigations [48 – 50, 52 - 54] have primarily focused on the difference between projected stains and transfer stains, these studies do not help with the current issue, verifying the science in the interpretation of bloodstains.

Currently there are few statistically viable work conducted on the interaction of blood on fabrics. [48, 49] De Castro *et al* [48] investigated individual passive, transferred and absorbed blood drops on 2 types of cotton apparel. De Castro *et al* found that the stain size was not dramatically different however the number of satellite spatter changed significantly depending on height. [48] It is noted that the authors standardised the fabrics using the protocol outlined in section 8A of BS EN ISO 6330/A1:2009, a procedure procured for the domestic washing and drying of garments which produces a standardised fabric. [55] Fabrics are laundered 6 times (washing cycles) and dried flat following section 10C of the same method. [55] Although this standardisation method is good practice as it should provide consistent, replicable results, it is not indicative of real-life where fabrics/clothes are washed using various methods, detergents and are dried using different techniques. The second quantitative study involved the distinguishability of one fabric surface from another with the use of satellite spatter. [49] Two fabrics of similar composition were evaluated. They discovered there to be a statistical difference relating to the roughness of the surface and the number of satellite spatter produced. [49] Concluding that as surface roughness increases so does the number of satellite spatter and that this is directly related to the composition of the fabric (synthetic vs. natural fibres). [49]

New recent works have focused on surface related quantitative analysis, Hulse - Smith *et al* [18] introduced separate equations which were developed for three different surface types, following on from his earlier work where a general equation was established. [18] Although this is an excellent basis for future surface related research it is an unrealistic approach, as previously discussed there are many varieties of a particular surface (*i.e.* porosity, surface finish) and testing one version cannot possibly be emblematic of the overall surface type. Studies need to address the properties of a surface before any real equations can be formulated.

It is not purely the type of surface which effects the formation of a bloodstain; the condition of the surface will also influence the final stain. For instance if the surface is heated; blood could impinge common heated surfaces such as a radiator, heated flooring, oven or stove potentially heating any impinging blood up to temperatures of

900° C. [56] Previous investigations into acts of arson and homicides that have involved fire give an indication as to the potential effects of heat on blood. [57 – 58] These cases however only show the effects of extreme heat, where the heat is applied after blood spillage often leaving the bloodstain covered in soot; instead of a pre-heated surface where the bloodstain may be cooked. There has yet to be any published research on the effects of blood on a heated surface with respect to BPA, however there is an extensive library of research exploring water droplets and various other liquids impinging heated surfaces. [24, 40 – 43] Much of this research has been performed with the use of high speed photography, analysing the rebound of the drop and the way in which the drop behaves when heated. [59 – 63] Four major heating regimes of liquid media have been identified by Nukijama: [62] 1) Natural Convection; 2) Nucleate Boiling; 3) Transition Boiling; and 4) Film Boiling. These regimes where first established for pool boiling, where the heated surface is submerged in a static liquid, [63] with subsequent work revealing their applications within liquid sprays and in liquid drops. [63] A boiling curve demonstrating the occurrence of these regimes was diligently created by Farber and Scorah *et al*, [63] where heat flux is plotted against ΔT (T_w – T_{sat}, the difference in surface temperature (ΔT) and temperature of the liquid's saturation point respectively). Natural convection is the natural heat flow and occurs when T_w (surface temperature) is equal to room temperature or slightly above; increasing T_w towards the maximum boiling point (100°C) creates nucleation zones where bubbles start to form in the centre of the liquid. [62] The third regime, transition, occurs directly after the nucleation regime and ends at the Leidenfrost point. [59] The Leidenfrost point takes place during the Leidenfrost effect where the temperature of the surface is substantially hotter than the liquid's boiling point usually at $\Delta T \geq 120^oC$ and above. During the Leidenfrost effect initial rapid evaporation occurs instantaneously creating a stable layer of vapour between the liquid and the surface, exemplified in the dropping of cooking oil into a hot pan where this effect is put into action, oil skids around the metal pan never making contact with the surface. In this regime, the liquid does not fully contact the surface and therefore overall takes a longer time to evaporate. The last regime is the film boiling regime where the Leidenfrost effect is realised. [62] Since water constitutes 83% of whole blood it is thought that it may behave it a similar way and therefore these regimes should fit the analysis of heated blood.

Similarly there has been only one published investigation into the effect of a cold surface and impacting blood, where Leak *et al* [64] described bloodstains found during an outdoor crime scene search, where bloodstains were located on snow. The freezing temperatures (2°F/16°C) caused a discolouration of the blood and created an overall puffiness to the stain; this led to the initial mis–interpretation of the stains as being brain matter. [64] Again some water droplet studies can offer more insights, where drops formed ice pellets at the impact sight, [65] the solidified drops were noted for the protrusions present on the top of the drop and the deformation of the final shape. [44] However these protrusions were found to be surface dependent, and only appeared on hydrophilic surfaces and not on hydrophobic surfaces. [57]

Despite all the above research there have been few developments (*i.e.* objective criteria) [9] which can realistically be used during a crime scene situation. Many factors are missing from the current equations meaning BPA is still being analysed using the old subjective methods.

1.7 Further uses of Blood evidence

It is not only for the patterns it leaves to why blood is an important form of evidence; blood is an excellent source of DNA (deoxyribonucleic acid) which is essentially a genetic fingerprint of an individual. [66] DNA (deoxyribonucleic acid) is a long molecule consisting of two polynucleotide strands wound around each other connected via hydrogen bonds forming the distinct double – strand helix.

Each strand consists of a sugar-phosphate backbone and organic bases attached in pairs. [66] There are four types of nucleotides within DNA, which are able to connect pairs in any order and at various lengths; these four nucleotides differ in that they contain a different base (adenine, thymine, guanine, and cytosine), it is the sequence of these bases which is unique to the individual. [66] Although only 0.1% of a person's genetic code differs from any other there has yet to be two individuals (with the exception of identical twins) with the same DNA profile. [66] The presence of DNA in such samples as; blood, semen, human tissue, is the pretext behind their prevalence as an extremely useful forensic technique, with DNA databases cataloguing the profiles of individuals reaching 7.8 million profiles in the USA [67]and over 6 million in the UK. [68]

Since 1984 when Alec Jeffreys first introduced the potential of DNA analysis as a forensic technique, [66] its evidentiary significance has been apparent, providing the basis for scientific testimony and evaluation which can be utilised within criminal trials. This has led to perpetrators resorting to innovative ways of 'covering up' their crime; *i.e.* cleaning away bloodstains. There have been significant reports upon the possible effects of cleaning of crime scenes; [67 - 69] criminals are now attempting to eliminate any trace of DNA via various methods of cleaning. Previous investigations have been undertaken into commonly used methods of cleaning such as water, 10% bleach and detergents. [66] A study conducted by Harris *et al* [66] on the cleaning of different substrates and the ability to extract a DNA profile discovered that although bleach had deleterious qualities, it did not eliminate the entire profile, in fact the efficiency in which DNA was extracted was dependent upon the substrate from which DNA was collected.[66] Bright *et al* [70] further supported these findings with research on cleaning reagents using multiplex kits (Identifiler™ and PowerPlex® Y) where again cleaning reagents proved ineffective at removing the DNA. This research however only confirms conventional methods of cleaning, crime evasion / committing the 'perfect' crime is heavily publicised within the media and popular television shows and it therefore seems inevitable that new more innovative ways of cleaning the scene will be attempted, using stronger solvents that due to the world wide web may be easier to access.

As stated by Harris *et al* [66] it is in fact the substrate which determines how effective the DNA extraction will be. Extractions performed on certain dyed fabrics are particularly problematic where dyes can inhibit the PCR (Polymerase Chain Reaction) causing heterozygote imbalance, allelic dropout, stutter and non-specific artefacts (*i.e.* primer dimer). [71] Generally DNA extraction has proven possible on most other surfaces, Stein *et al* [72] investigated the typing of biological stains on typically encountered crime scene surfaces; glass, metal, paper, adhesive tape and plastic, finding that all samples could be profiled regardless of the surface type. [72] The robust nature of DNA offers a stability that most other evidence forms lack, its survival through difficult environment conditions such as humidity, [73] direct UV exposure [73] and fire [58] has been well documented. Currently it is unknown if DNA will survive if applied to a pre-treated surface, for instance the effect of DNA left on a heated surface, where the DNA could be affectively "cooked," which could subsequently destroy the DNA. As explained above it is a realistic possibility that blood, could spatter onto a heated

surface *i.e.* a radiator. Like BPA, DNA is still a relatively new field in relation to other forensic disciplines; incredible advances have been made in the last 40 years making it one of the most (alongside fingerprints) important evidence forms. [2, 3]

1.8   Real Science?

Even with BPA being readily used as an evidence form in both UK and US courts, there are still sceptics who do not believe it to have any scientific merit. [75 - 77] BPA is considered to be a subjective discipline, with the basis of its analysis being on the recognition of patterns identified by experienced analysts. The main issue this presents is the variation in professional opinion when analysing blood patterns, this issue has been raised multiple times over the years and is still a very present problem.

Discrepancies can occur in several levels of analysis with disputes ranging from the correct way to measure a bloodstain to the taxonomy and categorisation of stains. Taxonomy is important in any discipline but is crucial in forensic disciplines as it will be referred to in court. Having a structured and easily explainable taxonomy makes court presentations simpler, providing the 'expert' with strong support which they can state their conclusions on. BPA does have a formalised standard international taxonomy which is available from the SWGSTAIN website, however it appears that other well established experts still follow their own taxonomy leading to confusion when collaborating with other experts and presenting findings in court. MacDonell referred to them as dynamics where size of stains distinguishes the action; Low velocity Spatter (LVIS≥4mm), Medium Velocity Spatter (1mm≤MVIS≥4mm) and High Velocity Spatter (HVIS≤1mm). [11] In 2002 another taxonomic system was developed by Bevel and Gardner, [24] here patterns were classified into three categories: Passive, Transfer and Dynamic, in 2005 James *et al* [4] altered this to Passive, Transfer and Projected. Recently Wonder [9] documented the stains as spatter and non-spatter (Appendix 1), creating a flow chart which categorised the patterns into each classification. This method was modified by Bevel and Gardner [24] who developed a flow chart with a comprehensive methodology and stain description, an excellent and portable equipment piece which can be carried to the crime scene by analysts. A complete description of each stain is essential as it provides support for the analyst should they be questioned about their conclusions in a courtroom scenario.

The lack of a unified taxonomy amongst BPA professionals gives the impression that the basis of BPA analysis is loose and subjective, less rigorous than other forensic fields such as fingerprints which has a universal taxonomy used by all fingerprint experts (*e.g.* whorl, loop *etc.*). It is up to the BPA community as a whole to adopt the SWGSTAIN terminology, cementing the groundwork for which all interpretations are based.

A further bone of contention within the field of BPA is the error associated with the majority of the calculations performed. For example the angle of impact. It seems simple to measure the elliptical length and width of a stain, however, every analyst does it differently. Since stains are not always perfectly round or smooth, sometimes protrusions are present on the periphery, it is difficult to gauge where the stain actually begins and ends. Computer programs such as Backtrack which are supposed to enhance the way interpretation can be performed carry this error, where analysts have to stencil round the stain. Leading analysts to over or under estimate the angle of impact. Steps towards solving this problem have been crafted, standard stencils have been developed which can be placed on the stain, giving a guideline of the parts of the stain to include. Other methods such as halving the stain then doubling the length measurement has become the practiced method. Amendments to computer programs have been established to improve the accuracy at which the angle of impact can be calculated. Despite these amendments the manual method of measuring is still considered the most accurate therefore it is a case of standardising training. The IABPA offer many courses, basic and advanced which should be attended by all BPA analysts. The courses are presented by experts who will be equipped to divulge a standard way of measuring which would decrease analyst errors. It is important for all those thinking of a career to attend these courses, therefore maintaining the integrity of BPA as a forensic discipline.

Recent years have been a testing time for the field of Bloodstain Pattern Analysis, doubts being raised publicly over its overall accuracy and applicability to complex crime scenes. [76, 77] The case of David Camm is most likely the main cause of people's recent intense scrutiny of the field. [76, 77] In 2002 David Camm was convicted of a triple murder (his wife; Kim, son; Brad, and daughter; Jill), his conviction was largely based on the interpretation of bloodstain pattern evidence. [77] Since the first trial, five renowned BPA experts [77] have assisted on the case, each interpreting the stains differently, disagreeing on the nature of 8 bloodstains found on Camm's T-

shirt. Were they impact stains (*i.e.* backspatter from shooting) or were the stains caused by transfer (*i.e.* Camm moving his son and performing CPR)? [77] On the 24th October 2013 after the third trial David Camm was acquitted. There are other underlying issues this case has brought to light. One of the experts claimed a new form of bloodstain, 'the painted fibre' supposedly only visible when blood is transferred to a fabric and is not evident when blood impacts the surface by force. Since there is no literature available on this discovery it was particularly damaging to the BPA field, leading people to believe BPA experts will fabricate evidence to fit their theories. Therefore it is important that experts publish their findings, avoiding this confusion in the future.

The other weakness this case exposed was the lack of surface interaction understanding. As demonstrated (see Section 1.6) surface analysis has been neglected so far in the field, researchers giving broad interpretations (*i.e.* non-absorbent vs absorbent) rather than focusing on surface properties (*i.e.* porosity, composition).

Although experts try to mimic the surface as closely, to the crime scene surface during a reconstruction, as possible, the exact surface is not always available. Therefore it is important to understand how fundamental changes to surfaces such as the porosity, surface finish etc. effect the formation and spreading of bloodstains.

It is clear from the above observations why BPA is sometimes considered unscientific, however positive strives have been taken towards changing this misconception.

The research presented in this thesis aims to expand the knowledge of blood and surface interaction, by applying quantitative techniques, with the hope of improving understanding and helping towards the verification of BPA as an essential scientific forensic discipline.

2. METHODS AND MATERIALS

2.1 Blood

Human and Equine blood were utilised throughout this work. Equine blood was obtained from TCS-Biosciences Limited. Human blood (ethically approved as governed by the Ethics Committee at Manchester Metropolitan University; see Appendix 2) was freshly drawn on the day of the experiment using a venepuncture; blood was drawn into purple blood tubes containing the anticoagulant EDTA. Blood was refrigerated at 4°C in 20 mL aliquots sealed with Para film for storage between experiments.

2.2 Blood Drop Tests

Blood drop experiments were performed using different sized pipettes, from varying heights (30.5cm, 60.9cm, 91.4cm and 121.9cm or 50cm, 100cm, 150cm and 200cm) and onto different surfaces, which were secured and flat at time of blood deposition. A diverse range of heights were used to create varying impact velocities V_o. Velocities were calculated using the equation: [18]

$$V_o = \sqrt{2gh} \qquad\qquad (11)$$

where g is the acceleration of gravity and h is the release height of the blood which is measured from the tip of the pipette to the impact surface. The heights were chosen as they were comparable with previous research and were high enough to negate the effect of oscillations, since the drops would dampen before impact. [5] However these heights were not high enough to reach terminal velocity, therefore all drops were still deemed to be in acceleration.

Temperature is an important factor requiring careful consideration and control since it affects the viscosity of the blood, which can lead to stain distortion. [27] Therefore all blood was maintained at room temperature during all experimentation, although it is noted that body temperature is approaching 37°C and could potentially give differing real life results. It was found that mimicking body temperature would be problematic to establish and keep at a constant, especially when air exposure and temperature of the equipment were considered. Drops were executed by the same

analyst throughout the experiment with minimal pressure and were measured with a magnifying loupe.

The room in which the experiments were conducted was temperature controlled (at 22°C). The temperature was monitored using a steel ibutton temperature data logger. All surfaces and equipment were left in the room to condition for 24 hours before experiments began.

2.2.1   Pipettes

Two different sized pipettes were utilised, 1 mm and 1.77 mm (inner tip diameter), two sizes were used to ensure results are consistent and to give differing drop diameter values. The inner diameters of the pipettes were measured using an inside micrometer. Blood drop volumes were also calculated, where blood was dropped into a measuring cylinder, the drops were then counted until a volume of 1 mL was reached. Using this data the drop volumes were calculated as; 48 µL (1 mm pipette) and 67 µL (1.77 mm pipette). Pipettes were changed every 5 drops to avoid any dry blood disrupting the drop formation.

2.2.2   Rugometer

The surface roughness of each experimental surface (*i.e.* Table 1) was deduced using a TESA-rugosurf 10 at 5 different points since this parameter is known to affect the observed number of spines [18] and gives greater applicability to real life scenarios when surfaces are not all the same. The rugometer (TESA-rugosurf 10) works by running a probe along the surface and taking an average measurement of the roughness.

Surfaces	Roughness (µm) (N=5)
Paper	2.62 ± 0.20
Plastic	0.72 ± 0.15
Tile	0.07 ± 0.01
Cold Rolled Steel	0.54 ± 0.20

Table 1: Average surface roughness of each experimental surface.

All surfaces were cleaned with 1% ethanol and paper towel and rinsed with deionised water, where surfaces were then left to dry and stabilise in temperature before any blood drops were performed.

2.2.3   Slow Motion Filming

Blood drops were filmed in slow motion at 1200 fps (frames per second) using the Casio Ex-F1 Digital Camera, enabling the capture of scaled still images of the blood drops as they departed the pipette tip to allow the drop diameters, D_o, to be deduced as depicted in Figure 13.

A.)   **B.)**
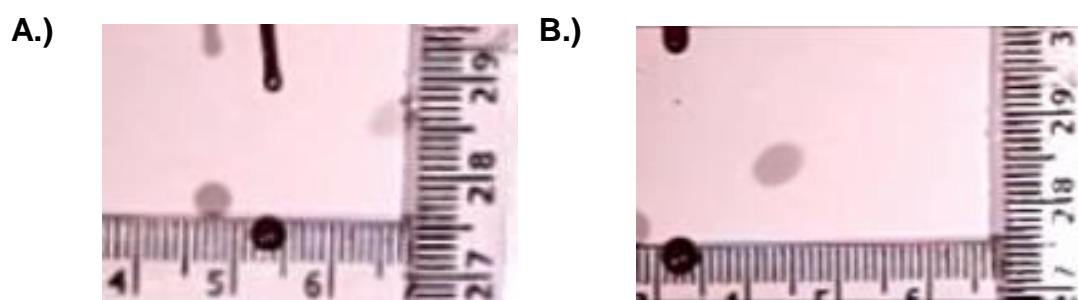
Figure 13: Scaled stills of blood drops. Image A shows a still of defibrinated equine blood drop using a 1mL pipette (1 mm inner tip diameter); Image B is of defibrinated equine blood drop using a 1mL pipette (1.77 mm inner tip diameter).

Drops were discharged as close to the ruler as possible to avoid any size distortion.

2.2.4   Bloodstain Measuring

As aforementioned (section 1.7) it is important to establish a standard method of stain measurement, therefore avoiding discrepancies in results attributed to analyst error.

The following method was adhered to for circular stain measuring:
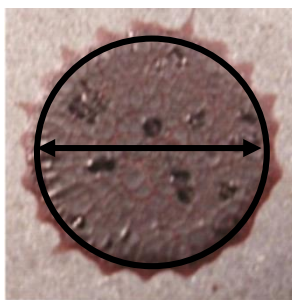
A circular stain is measured using the diameter/width, this excludes any spines or fingers on the periphery of the bloodstain (see Figure 14).

A magnifying loupe was utilised.

Figure 14: Circular bloodstain depicting the actual diameter to be measured.

Similarly, angled impact stains were measured using the below approach.
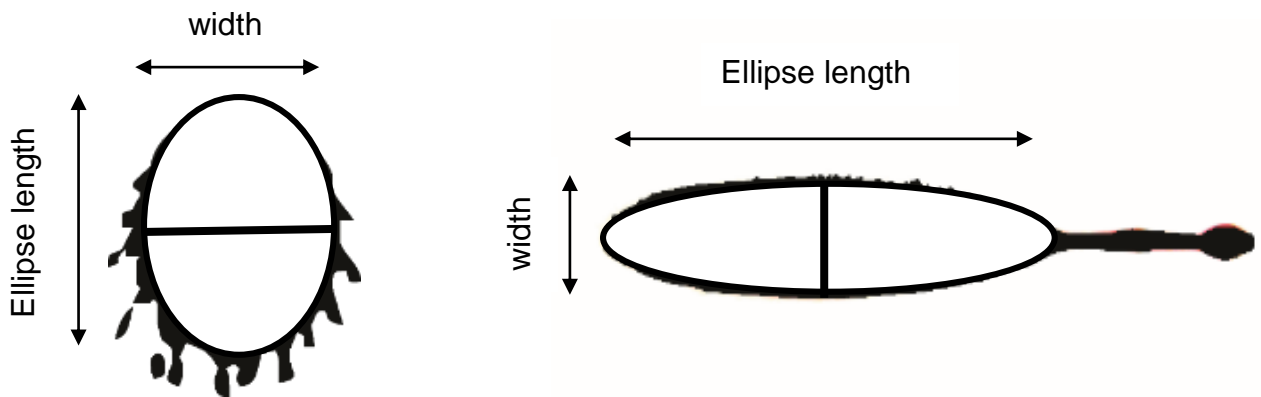
Figure 15: Angled impacts showing the diameter and ellipse length measured

Again the diameter/width of the stain was measured excluding any scallops/spines. The ellipse length was consistently calculated, through all trials, by measuring half the length of the stain up to the diameter (half length), this number was then doubled to give the total ellipse length (Figure 15). This method is used as it excludes the tail and scallops and gives a full ellipse length which is vital in order to calculate an accurate angle of impact.

2.3   Part I Experimentation Equipment

2.3.1   Rheometer

A cone and plate rheometer (Kinexus Pro Rheometer) was utilised throughout this study to measure the viscosity of blood. It is used to determine the viscosity in fluids whose value does not remain constant, due to the shear forces present within the liquid. [78, 79]

A cone and plate type rheometer consists of a horizontal plate and a shallow cone. Liquid is placed onto the plate and the cone is lowered into the liquid. [78, 79] The plate is then rotated and the force of the cone is measured. The viscosity is expressed as the ratio of shear stress to shear rate, where the stress equates to the torque and the shear rate relates to the angular velocity. [78, 79]

Blood viscosity was measured at shear rates of $100s^{-1}$ as this is when the viscosity becomes constant and a single value can be determined. [18] Shear rates do not go above $100s^{-1}$ within this research; therefore this is a valid approach. [18]

2.3.2   Tensiometer

A tensiometer is used to measure the surface tension of a liquid or a surface.
The type of tensiometer utilised in this research was the Du Noüy Ring Tensiometer (CSC Du Nouy Precision Tensiometer), where a platinum ring is submerged in a liquid, the ring is then slowly extracted. [80, 81] Once the ring is resting on top of the liquid a measurement can be taken. The ring must be clean and free of scratches to attain an accurate reading. [80, 81]

2.3.3   Goniometer

A goniometer is used to measure the contact angle of liquids on a surface. [81, 82]

A drop of liquid is deposited onto the surface whilst being filmed using a CCD (charged-coupled device) camera. The drop profile of the captured image is then extracted and computer software is used to fit the Young-Laplace equation: [81, 82]

$$\Delta P = \gamma \left(\frac{1}{R_1} \middle| \frac{1}{R_2} \right) \tag{12}$$

where γ is the interfacial tension, P equates to the pressure and radius is defined as

R. [81, 82] The contact angle is important as it describes the degree of wetting which ultimately determines the spreading of the liquid.

2.3.4 Microscope

An optical microscope (bright-field microscopy) uses reflection and absorption to investigate the properties of substances. [83, 84]

The sample is placed on the stage of the microscope where an incandescent light, situated beneath the sample, is shone through the sample where it is collected by an objective lens, positioned above the stage. [83, 84] An aperture, contained within the lens condenser, controls the amount of light and focus on the sample. [83, 84] The objective lens magnifies the light and transmits an image to the eyepiece.

The microscope utilised in this study is attached to digital imaging equipment (Leica DFC365FX), this allows the image to capture both still and filmed images.

2.3.5 Spectrophotometer

A spectrophotometer is an analytical instrument which quantitatively measures the reflectance/ transmittance of a material. [85, 86]

It uses a photometer which measures a light beam's intensity as a function of its colour. The spectrophotometer used in this research was a UV spectrophotometer (Spectrophotometer Model 6305 UV-VIS and Spectruino Arduino Spectrometer) this focuses on the UV and visible regions of the spectrum. [85, 86] Samples are usually prepared in cuvettes (plastic, glass and quartz) and light is shone through the sample. An absorbance spectrum is formed which plots the absorbance vs wavelength. The wavelength λ_{max} is the most important wavelength, where the absorbance is at its greatest. [85] It is characteristic of each compound and provides details on structure which can be used to obtain high sensitivity when further testing is performed.

2.3.6 Hematocrit Centrifuge

Similar to a normal centrifuge, it spins a solution at a high frequency for a selected time frame. [87, 88] The PCV% of blood was determined using a hematocrit centrifuge. Blood is placed in a capillary tube (microhematocrit tube), the tube is positioned in a hematocrit centrifuge which spins the blood at 10,000 RPM for 5 minutes. The blood is separated into plasma, red blood cells and a buffy coat (white blood cells and

platelets). The lengths of the blood and red cells are measured to obtain a percentage.
[82, 83]

2.4   Part II Experimentation Equipment

2.4.1   Smoothness & Air Permeance (Bendtsen Type)

The roughness or smoothness of the sample is measured by establishing the volume or air that passes through the material at a given pressure. The test is performed accordingly. [89, 90]

The sample is placed on the glass plate, a measuring head is placed on the sample. Air is then passed through the flat metal ring and sample at a given pressure. The pressure difference is read. [89, 90]

2.4.2   Scanning electron microscope (SEM)

A Scanning Electron Microscope (SEM) is utilised throughout this study to capture images of the surfaces. [91, 92]

An SEM is a type of electron microscope which produces highly magnified images of a sample by scanning it with a focused beam of electrons. [91, 92]

The electrons interact with the atoms in the sample, producing signals which can detect and hold information regarding the surface's topography and composition. [86, 87]

2.5   Part III Experimentation Equipment

2.5.1   Furnace and Hot Plate

A furnace was used to heat surfaces to temperatures of up to 250°C, the temperature was maintained with the use of a hot plate, which was placed underneath the surfaces as testing proceeded. The temperatures were tested with an infra-red temperature gun.

2.5.2   Infra-Red Spectrometer

The infra-red (IR) spectrometer focuses on the infrared region of the electromagnetic spectrum, where light has longer wavelengths and occur at a lower frequency than those in the visible light. [93, 94] Molecules absorb at specific frequencies which are characteristic of their structure, IR uses this fact as an identifier. Spectroscopy is performed by passing a beam of infrared light through the sample, when the IR frequency matches that of the vibrational frequency an IR spectrum is formed. [93, 94] The IR spectrum created plots the wavelength/frequency against the absorbance/transmittance. A Fourier Transform Infrared Spectroscopy (FTIR) is the type of IR utilised within this work, [94] which works in a similar way to IR however the FTIR runs several scans, uses an interferometer and uses Fourier Transforms to convert the interferogram into an IR spectrum. [94]

PART I:
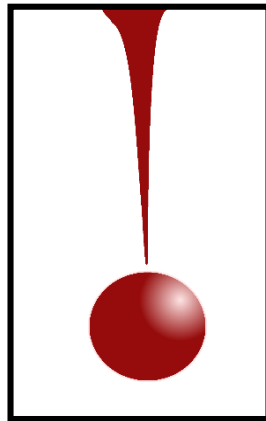
BLOOD

3. BLOOD CHARACTERISTICS

The following chapter discusses blood and its components, where three studies were undertaken to gain a better understanding of how blood components/blood substitutes may alter the current analysis of bloodstains.

3.1 Blood

Blood, is a Non – Newtonian pseudoplastic fluid, where viscosity is dependent on shear rate. [95 - 99] It has a complex structure which is temperamental in nature, where changes in behaviour can occur in accordance with the composition, health and environmental conditions of the blood. It is a suspension of solid materials in an aqueous solution consisting of plasma, red blood cells (RBCs), white blood cells (WBCs) and platelets. [95 - 99] Blood is a life-sustaining fluid circulated around the body through blood vessels by the pumping action of the heart, it contributes to around 7% of a human's body weight (approx. 5 litres), accounting for its regular occurrence at violent scenes of crime.

3.1.1 Red Blood Cells

.
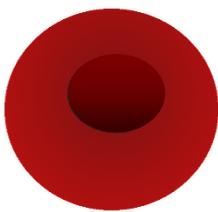
Figure 16: A red blood cell

Red blood cells (erythrocytes) make up the majority of the suspended material (4 – 6 million per mm^3), they are formed in the bone marrow and are responsible for the transportation of oxygen to the cells and carbon dioxide away from them. [95 - 99] RBCs are normally biconcave shaped and measure 7 to 8 μm in diameter with a thickness of 2 μm. [95 - 99] Haemoglobin is present within the erythrocytes, it is a metalloprotein in which the oxygen is transported. [95 - 99]

Since oxygen has low solubility in water, which is a major constituent of blood, there needs to be an oxygen transport protein which permits oxygen to become soluble, this is provided by haemoglobin. Two αβ dimers combine to form the complete haemoglobin molecule. [95 - 99] The haemoglobin structure consists of four heme groups, a ring-shaped molecule. In the centre of each heme is an iron atom (giving blood its red colour), which is available to bind to an oxygen molecule, allowing for transportation. [95 - 99]

3.1.2 White Blood Cells
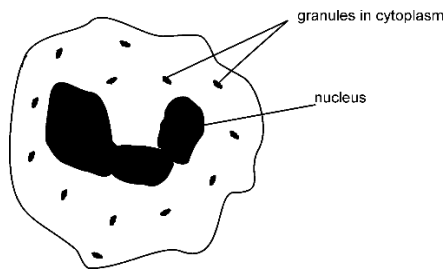
Figure 17: A white blood cell

White blood cells (leukocytes) are found in the lymph nodes and unlike the RBCs have a nucleus and therefore harbour DNA. [95 - 99] There are fewer WBCs in blood (5000-11000 per mm^3) than RBCs and their primary function is to fight infection. Leukocytes come in several subtypes *e.g.* lymphocytes, monocytes etc., based on the morphological and tinctorial (colouring/staining) characteristics when stained. [95 - 99]

3.1.3   Platelets

Platelets (thrombocytes) are instrumental in the clotting process, forming the initial plug on a wound and sending out chemicals which trigger other parts of the clotting process. [95 - 99] A normal platelet count is between 150,000 and 450,000 platelets per microliter of blood. They are 2 – 4 μm in size and are released from the megakaryocyte (a bone marrow precursor). [95 - 99] The megakaryocyte is a large cell which breaks into fragments, these fragments are known as platelets. [95 - 99]

3.1.4   Plasma

Plasma is the aqueous portion of blood, in this, proteins, carbohydrates, fats, minerals, antibodies and clotting materials are dissolved in water (up to 95% of the total volume). [95 - 99] It is pale yellow in colour and contributes to around 55% of the total volume of whole blood. Plasma is vital for the preservation of the human body, keeping electrolytes balanced and protecting the body from infection. [95 - 99]

Blood serum is blood plasma minus the clotting factors, this is often the case when performing blood pattern experiments where coagulation would cause difficulties.

3.15   Coagulation

Coagulation is the complex process of blood clotting initiating when a wound is formed; there are several stages: [98]

Primary hemostasis - This is the first stage where blood vessel constriction (vasoconstriction) and platelet aggregation at the site of vessel injury takes place. [93]

During this stage the blood vessel wall muscle constricts reducing blood flow and platelets form a "plug" at the wound site. [99]

Intrinsic pathway

Vascular surface changes

XII ——→ XIIa

XI ——→ XIa

IX ——→ IXa

VIII

Extrinsic pathway

Tissue thromboplastin

VII ————————→ VIIa

Common pathway

Prothrombin (II)

X

Xa + V

Thrombin

XIIIa ←—— XIII

Fibrinogen (I) ——→ Fibrin monomer ——→ Fibrin polymer ——→ Stable fibrin
Clot formation
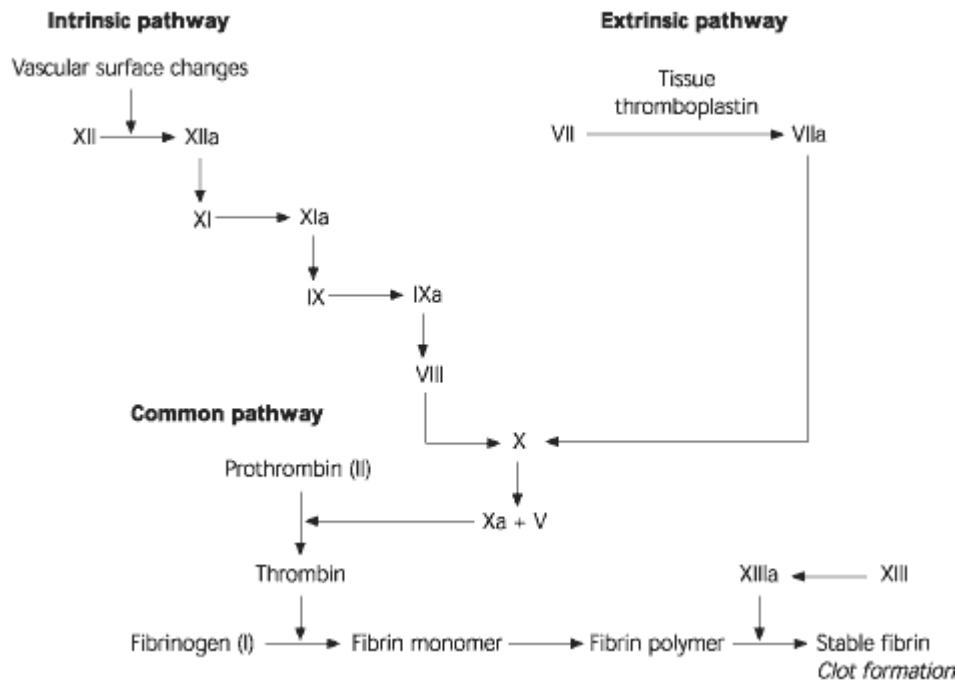
Figure 18: Coagulation process, showing both intrinsic and extrinsic pathways. [99]

Secondary hemostasis – This stage is when the clot is formed. The clotting process involves a sequence of interactions between several blood components called coagulation factors; there are 13 principal coagulation factors. [99] There are two separate pathways in which coagulation can be initiated; intrinsic and extrinsic (Figure 18). Intrinsic means inside the blood vessel, extrinsic means outside the blood vessel, each process results in the production of fibrin. Fibrin (a sticky protein) creates a mesh which traps platelets, blood cells, and plasma. [99]

Clot retraction – clot retraction is the process by which the fibrin meshwork contracts, squeezing out its fluid contents. The result is an insoluble clot that can withstand the friction of blood flow. [99]

3.1.6   Viscosity

Viscosity is a fundamental parameter in the study of Bloodstain Pattern Analysis (BPA) affecting the spread of blood due to the resistance to flow. [28] Generally the value of whole blood viscosity is 4.5 mPa.s. [18] Resulting viscosity values are heavily reliant on temperature, time, shear rate and packed cell volume. Shear rate is the change in velocity when one layer of fluid passes over another. A number of studies

have been executed exploring how the viscosity can ultimately determine the size of the bloodstain diameter [4, 5, 9, 20], with the general consensus being that the higher the viscosity the smaller the bloodstain. Other studies involving the manipulation of viscosity with drugs [27 - 28] and alcohol [20] have also been investigated, finding they significantly decrease the dynamic viscosity, showing how readily viscosity can be manipulated.

3.1.7   Blood Grouping

A blood group or blood type is the classification of blood based on the presence or absence of inherited antigenic substances on the surface of red blood cells (RBCs). [95 - 99] The blood type is inherited and represents a contribution from both parents. There are 33 recognised human blood type systems, two of the most medically significant being the ABO and RH systems. The ABO system is mostly associated with blood transfusion, persons may have type A, type B, type O, or type AB blood. O is the most common type of blood throughout the world, however this can deviate depending on the country/continent; *i.e.* Type B is predominant in Asia. [95 - 99] The Rhesus system (Rh) is used in conjunction with the ABO system. This system was developed on the basis of the presence or absence of the D antigen on the red blood cell surface. [95 - 99] This information is combined with the ABO blood type where a person with A type blood could be classified as A negative or positive. The majority of the population are positive for the D antigen, again this is dependent on other factors, such as ethnicity. [95 - 99]

3.1.8   Surface Tension

Surface tension is the force (resistance), caused by the molecular friction within the fluid, which prevents the penetration or break up of blood. Blood surface tension measures $5.1 - 5.7 \times 10^{-2}$ N/m. [18]

3.1.9   Adhesion and Cohesion

Adhesion is the attraction between unlike molecules, for instance blood on a weapon. Cohesion is the attraction between like molecules, this attraction is what maintains the spherical shape exhibited when blood falls. [9, 10, 11]

3.1.10 Packed Cell Volume

Packed cell volume (PCV %) is the ratio of red blood cells to plasma content in total whole blood volume; its effect on viscosity is well documented where an increase is associated with cell percentage increase. [9, 26, 27]

The variance in the PCV % levels is not only dependent upon location within the body [9] where values can deviate from 30 – 52 % [9] but is influenced by the lifestyle of the person. Packed cell volume levels as low as 15 % have been documented for persons who are drug abusers, chronic alcoholics, pregnant, malnourished and / or elderly. [9] Similarly new-borns, people suffering from shock, extreme exercisers and heart attack victims have very high PCV % reaching 75 %. [9]

3.2 _EXPLORING THE APPLICATIONS OF EQUINE BLOOD IN BPA

Initial investigation of surface interactions with blood were conducted with a human blood substitute, which was thought to have been the most resourceful and economical way of conducting preliminary experiments. Animal blood has been concluded as the closest and therefore the most suitable alternate, however it seems that currently only porcine blood is most prominently utilised. [5, 17 - 18] This poses difficulties as porcine blood is extremely difficult to obtain, often requiring the use of a slaughter house which again raises several issues; ethical, moral and safety (blood is unscreened). Safety aspects are paramount when dealing with any biological fluid; the use of animal blood has been acknowledged as a safe substitute to human blood, decreasing but not eliminating the risks of coming into contact with pathogens and diseases, *i.e.* HIV, Hepatitis etc. [5] Despite the dependable reputation of porcine blood, other animal bloods are still employed. A study by Christman *et al* [74] compared various animal bloods (swine, bovine, equine and porcine) to determine suitability as a human blood substitute, where impacts and general appearance of the blood were compared. [100] Although their study gives an insight into the functionality of animal blood as a human blood substitute it uses now out-dated terminology (low impact velocity etc.) and suffers from any real statistical analysis which is considered obligatory within the forensic field. Due to the foundations of this project being primarily blood related it is thought essential to fully establish the suitability of equine blood as a more commercially available, animal friendly [101, 102], human blood substitute in the interpretation of bloodstain patterns. In order to accomplish this aim, visual observations the point of origin and equations developed by Hulse-Smith *et al* [18] (see introduction) which allowed direct comparisons with previous results where porcine blood was utilised, were used.

Using the general experimental method, stipulated in section 3, two samples of equine blood were tested, each with different anti-clotting methods employed; the first was defibrinated, where the fibrin (an essential component in clotting) is removed. Second an anticoagulant was utilised, Alsever's, which is considered to be the most stable and commonly used anticoagulant. [102] Last, attention was turned to the

consideration of the age of blood and its potential effect upon BPA experimentation. It is well documented that age of porcine blood alters bloodstains; decreasing the diameter of the resultant bloodstain as the blood ages [5] and therefore considerations pertaining to shelf life (time viable after opening the container or first exposing the blood to air) have to be made when conducting experiments or crime scene reconstruction to account for these changes. Presently it is unknown if this is the case for equine blood as there is no definitive published shelf-life, this was duly explored since any such changes would need to be accounted for in future BPA activities to avoid possible misinterpretations of patterns.

3.2.1 Experimental

3.2.1.1 Resources

All equine blood (defibrinated and Alsever's) was obtained from TCS-Biosciences Limited at a PCV % (Packed Cell Volume) of 45%. Human blood was freshly drawn on the day of the experiment using a venepuncture; blood was drawn into purple blood tubes containing the anticoagulant EDTA.

3.2.1.2 Method

Blood drop tests for all bloods were dispensed according to the instructions stipulated in the Materials and Methods section. Four different surfaces were utilised: paper, plastic, tile and steel. Surfaces were new; paper (80mgs; standard A4,) plastic sheet (Medium Density Polyethylene), tile (ceramic gloss) and cold rolled steel. The surface roughness of each experimental surface (Table 1) was deduced using a TESA-rugosurf 10 at 5 different points.

Blood drops D_o were established using the slow motion filming described in the Method and Materials section. [4]

Release Heights (cm)	Impact Velocity (m/s)
30.5	2.45
60.9	3.46
91.4	4.24
121.9	4.89

Table 2: Release heights of blood drops calculated from the tip of pipette to the impacting surface and converted into impact velocity via the use of Equation (11).

A diverse range of heights were used to create varying impact velocities V_o as expressed in Table 2, velocities were calculated using the equation described in the experimental section. Here it was assumed that the path of the blood drop can be defined by the equations for the movement of a rigid object, therefore disregarding parameters such as drag. [17] These particular heights were chosen as they can be directly compared to the results obtained by Hulse-Smith *et al* [18] who also used animal blood (porcine) as a human blood substitute. It is noted that there is a possibility of oscillation during the initial phase of the falling drop, however studies have shown that this oscillation is less dramatic than that produced in a raindrop and is therefore likely not to have a marked effect. [24] It has also been demonstrated that the drop oscillation will not be a significant factor as oscillation does not occur after 40cm release height, which is below most of the heights used in this experiment. [5]

3.2.1.3   Age Experiment

The same experimental procedure was adhered to for the aged equine blood, though D_o was not deemed necessary to calculate as diameter and number of spines were the focal interests of the aged blood. Drops were again manually dispensed from heights of 30.5, 60.9, 91.4 and 121.9 cm onto a paper surface (80mgs, A4 standard). Drops were repeated 5 times and stain diameters were measured using a magnifying loupe. Viscosity measurements were performed using a Kinexus Pro Rheometer.

3.2.2. Results and Discussion

3.2.2.1   Blood Type properties

	Equine Blood [24, 102]	Porcine Blood [18]	Human Blood [104]
Density (kg/m^3)	1050	1062	1052 - 1063
Viscosity (mPa.s)	3.3 – 5.6	3.4 – 6.1	3.8 – 5.1
Surface Tension (x 10 $^{-2}$ N/m)	5.1	5.3 – 5.8	5.1 – 5.7
PCV (%)	32 - 46	38.9 – 46.3	40.0 – 45.0

Table 3: A comparison of published values obtained for the physical properties of equine, porcine and human blood (all unadulterated).

The physical properties of blood are of high importance since they determine the resultant pattern of blood and are utilised in many of the aforementioned equations (see introduction). Taking this into consideration, the physical properties of equine, [24, 102] porcine [18] and human blood [104] are compared in Table 3 which show there to be no difference between physical properties of equine blood [103, 104] with that of porcine and human blood, [4] suggesting its potential use in BPA.

3.2.2.2   Drop Diameters

Slow motion filming, as detailed in the experimental section was performed enabling the capture of scaled still images of the blood drops as they are dispensed from the pipette tip to allow the drop diameters, D_o to be determined.

Drops were discharged as close to the scale as possible (1cm) to avoid any size distortion. Such drop diameters result in an average drop diameter value of 4 mm and 5 mm when defibrinated blood was utilised, 3.5 mm and 4 mm when Alsever's blood was dropped and lastly 4 mm and 4.5 mm when human blood was (utilising the 1 mm and 1.77 mm inner tip diameter pipettes respectively). These results are in agreement with previous blood drop diameters reported by Hulse-Smith *et al* [18] and Willis *et al* [104] where human [104] and porcine blood were utilised [18], showing no difference in size (between 3.0 mm and 4.3 mm) or general shape of the droplet exhibited.

3.2.2.3 Animal Blood vs Human Blood

Firstly, the size of blood stains (D_s) produced when all blood types are released from heights of 30.5, 60.9, 91.4 and 121.9 cm were considered; these particular heights were chosen so direct comparisons could be made later with those values obtained for porcine blood. [18] Blood was dropped onto paper with a 1 mL pipette (1.77 mm inner tip diameter), stains were left to dry completely and then measured using a magnifying loupe. Inspection of Figure 19 explores the magnitude of the bloodstain diameter (D_s) as a function of release height revealing that the anti-coagulated (Alsever's) equine blood has a marked effect upon the size of the blood stain produced.
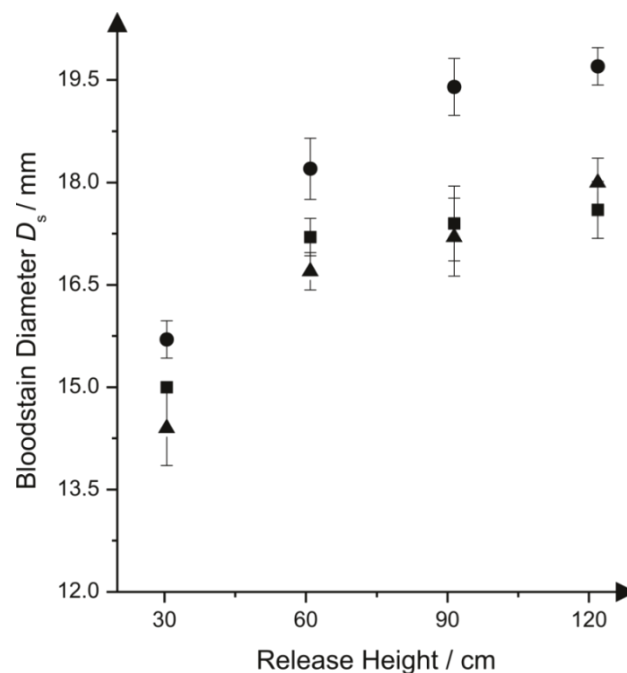
Figure 19: Comparisons of blood stain diameters (D_s) for defibrinated equine blood (squares, ■), human blood (triangles, ▲) and anti-coagulated equine blood (circles, ●) dropped upon a paper surface, identifying that defibrinated equine blood gives the greatest comparability to human blood; *N* = 5.

Blood stains are evidently larger in diameter with the use of Alsever's equine blood; this is an unexpected outcome as we have previously discussed, this form of anticoagulant is the most stable and commonly used. [101] When investigations into the physical properties of the blood types were conducted we found that the Alsever's equine blood has a much lower viscosity of 2.5 mPa.s compared to that of defibrinated equine blood and human blood, which gave viscosity values of 4.7 mPa.s and 3.7 mPa.s respectively. Dynamic viscosity measurements were carried out on the blood using a Kinexus Pro Rheometer where viscosity measurements were obtained at room

temperature (25°C). Viscosity verses shear rate peaks were formulated since viscosity is affected by shear rate, however, at shear rates of 100s^{-1} (which should be experienced throughout this study) the peak peters out to a constant; this constant was therefore taken as the viscosity of the blood. The diverse range of viscosity values are likely to be the explanation behind the much larger bloodstain diameters exhibited for the Alsever's equine blood, as viscosity decreases, fluid, in this case blood, flows more freely and therefore travels further; resulting in a larger bloodstain diameter. Unpaired t-tests were performed in order to establish the statistical significance of the results. Each equine blood was statistically compared to human blood, taking the largest stain sizes exhibited, where the largest difference was observed. It was found that Alsever's equine blood is statistically significantly different to human blood with a *p* value of 0.0001, signifying that the use of Alsever's does have a significant effect on the bloodstain diameter displayed and therefore is not an appropriate human blood substitute. Conversely when defibrinated equine blood was statistically compared to human blood the results were not found to be statistically different from human blood with a *p* value of 0.1411. This implies that defibrinated equine blood is the more viable human blood alternative, as it exhibits bloodstains that are of a similar size and importantly the behaviour is not statistically significantly different from that of human blood.

3.2.2.4 Effects of surface roughness

Blood impacting upon different experimental surfaces was evaluated next, as a variety of surfaces will provide various surface roughnesses (texture of a surface). Figure 20A and Figure 20B demonstrate the observed average bloodstain diameters (D_s) obtained when defibrinated equine blood was dropped onto paper, plastic, tile and cold rolled steel.
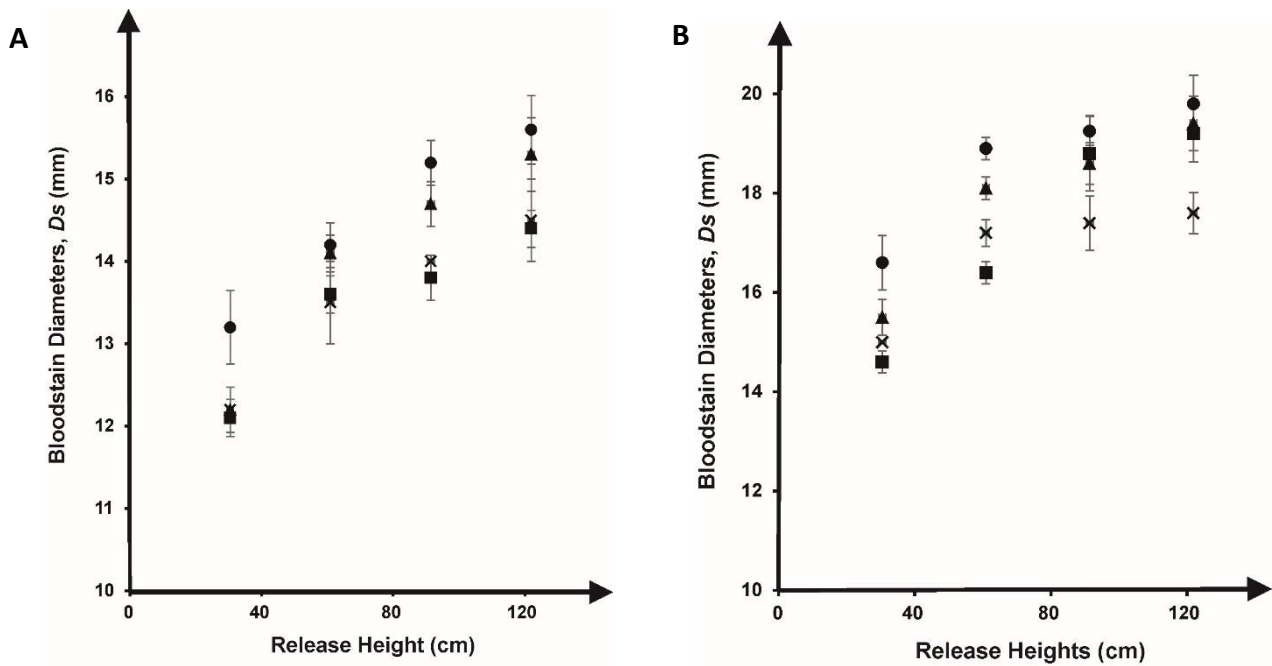
Figure 20 : Blood stain diameters for defibrinated equine blood released upon different surfaces from a range of release heights; paper (crosses, **X**), plastic (triangles, ▲), tile (circles, ●) and cold rolled steel (squares, ■); **A**: using a 1 mL pipette (inner tip diameter 1 mm) and **B**: using a 1 mL pipette (inner tip diameter 1.77 mm); $N = 5$.

When comparing surface roughness, in accordance with the final stain diameters (D_s) ascertained during the drop tests, it is apparent that there is an effect; however due to the inconsistency of the tested surfaces, that is the surface roughness is heterogeneous in nature, there are anomalies within the results. This is demonstrated in Figure 20A where it appears that the smaller stains were produced on the cold rolled steel in place of paper where the surface was much rougher. It is nevertheless evident from the observed blood stains that there is a decrease in stain diameter in accordance with surface roughness, such that the lowest roughness value gives larger bloodstain diameters (D_s). This could further be related to the original drop diameter, where the 5 mm droplets (D_o) produced significantly larger bloodstains than those of the 4 mm droplet. Similar results were exhibited for both Alsever's equine blood (Figure 21A and 21B) and human blood (Figure 22A and 22B), where bloodstains decreased when the surface roughness increased.
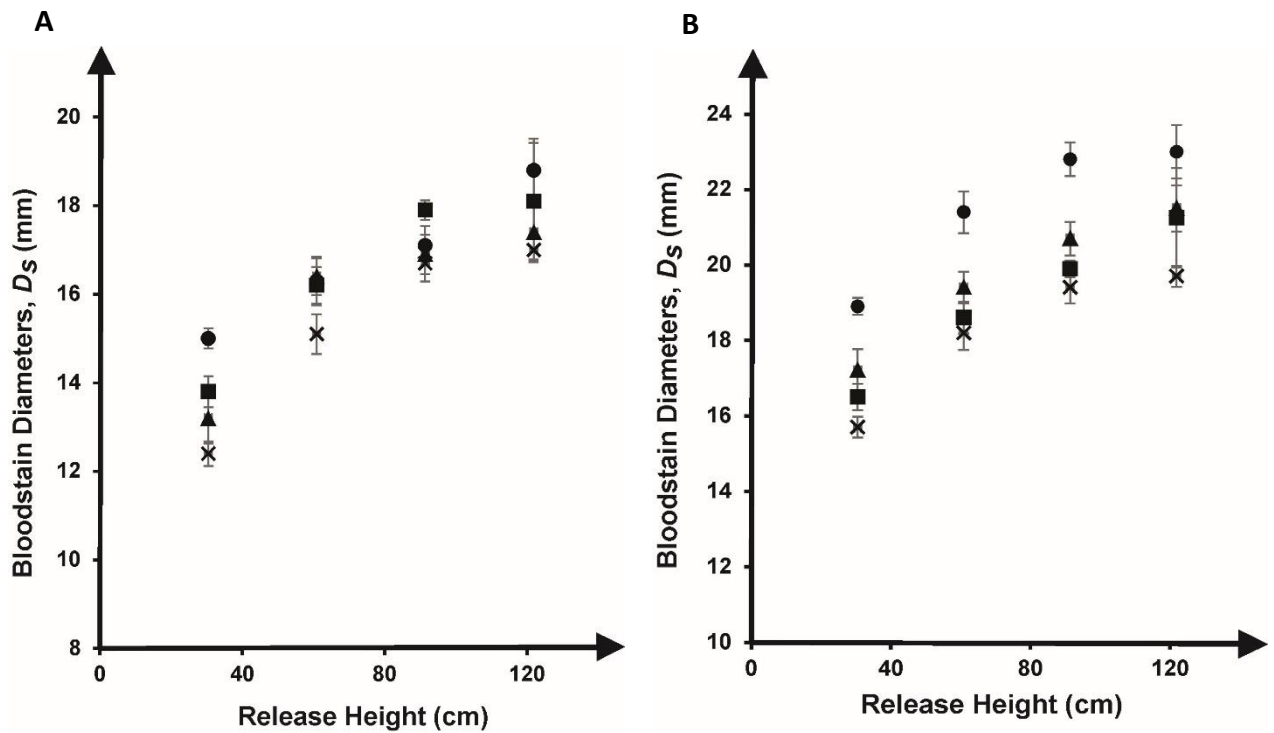
Figure 21: Blood stain diameters (D_s) for Alsever's blood released upon different surfaces from a range of release heights; paper (crosses, **X**), plastic (triangles, ▲), tile (circles, ●) and cold rolled steel (squares, ■); **A**: using a 1 mL pipette (inner tip diameter 1 mm) and **B**: using a 1 mL pipette (inner tip diameter 1.77 mm); $N = 5$.
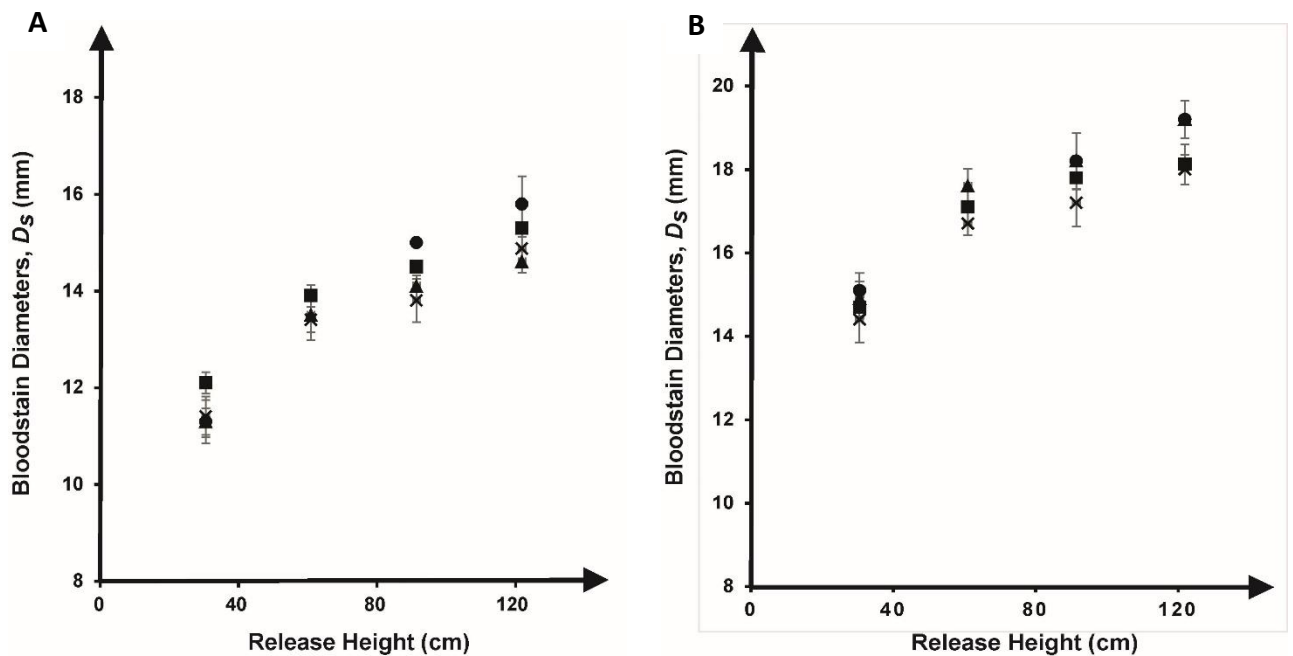
Figure 22: Blood stain diameters (D_s) for human blood released upon different surfaces from a range of release heights; paper (crosses, **X**), plastic (triangles, ▲), tile (circles, ●) and cold rolled steel (squares, ■); **A**: using a 1 mL pipette (inner tip diameter 1 mm) and **B**: using a 1 mL pipette (inner tip diameter 1.77 mm); $N = 5$.

This is further demonstrated by performing t-tests where all p values for the three bloods were found to be statistically significant, $p < 0.0015$. When we compare all three bloods it is evident that Alsever's equine blood on the whole generates much larger stains than that of human and defibrinated equine blood, this is consistent with the results reported earlier (see blood type section).

Further investigations were performed with the use of equations (3) - (6). Figure 23 A-C depicts the ratio of drop spread (D_s / D_o) in relation to the Reynolds number where lines of 'best fit' where undertaken.
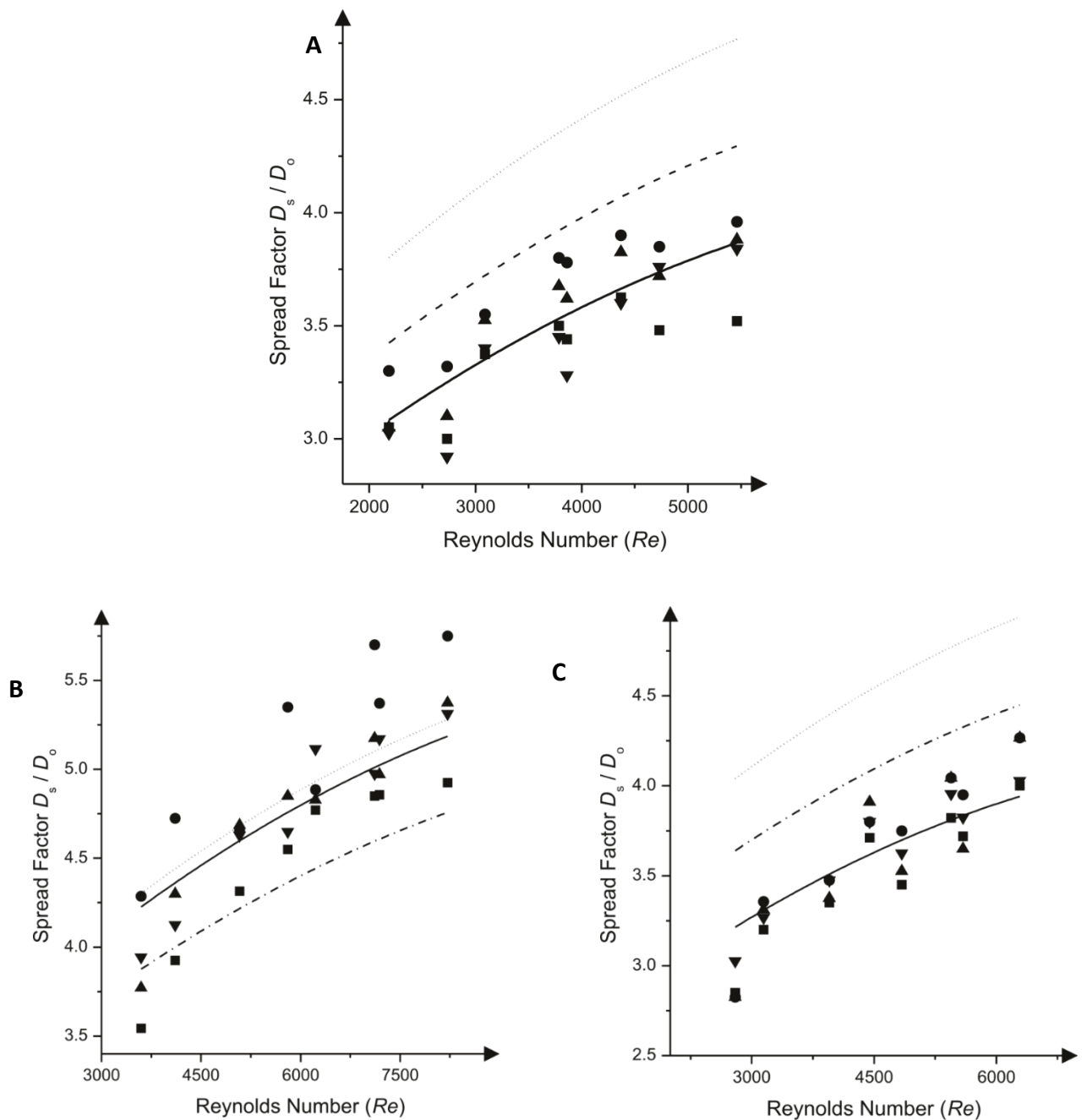
Figure 23: A new line of 'best fit' (solid line) was established when considering the spread factor versus the Reynolds number on different surfaces; paper, plastic, tile and cold rolled steel. Comparing this to the original line of 'best fit' (dotted line) using equation (3) [18] and the line of 'best fit' (dashed line) developed by Hulse-Smith *et al* [18] using equation (4) using three type of blood; A: Defibrinated Equine Blood B: Alserver's treated equine blood, and C: Human Blood; $N = 5$.

Equations (3) and (4) are pre-existing equations and were found not to completely satisfy the data obtained with any of the 3 bloods tested, therefore new constants were established that gave a 'best fit' to the scatter data presented. New constants (C_d) were found to equal 0.9, 1.09 and 0.88 for defibrinated equine blood, Alserver's equine blood and human blood respectively. Comparing the three constants, it is clearer that Alserver's equine blood is inconsistent with human blood and it would

therefore be advised that defibrinated blood is used when conducting BPA reconstructions or general experimentation. Similarly when the number of spines was considered, for each blood, in relation to the Weber number, new constants were again developed which 'best fit' the given data more effectively than the original equations (5) and (6).
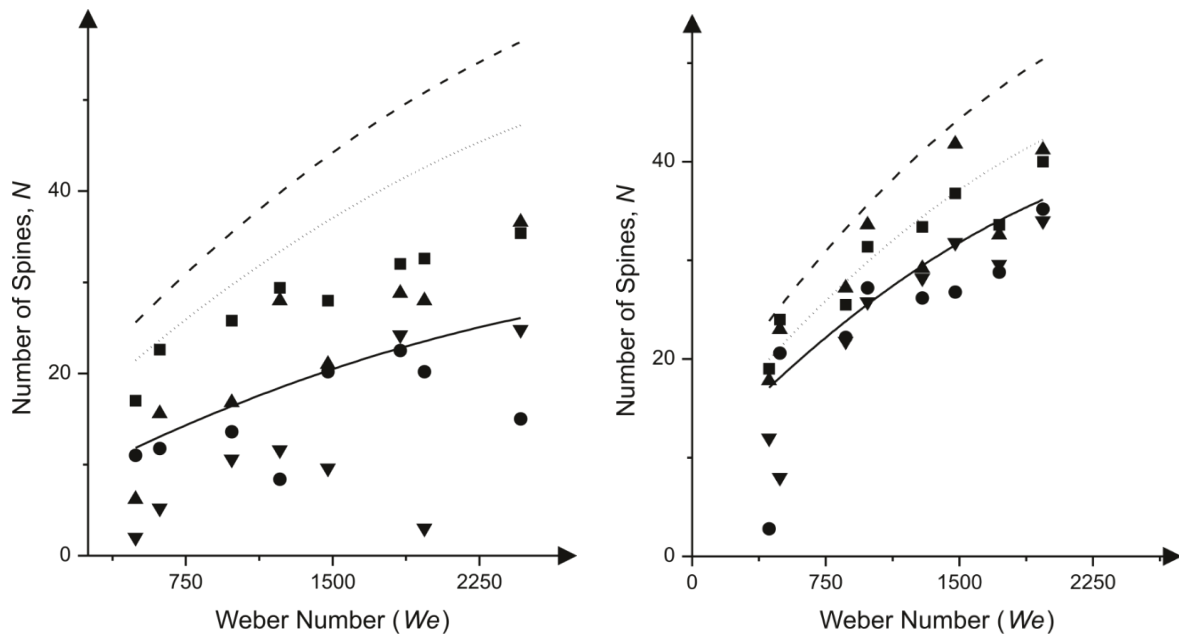
Figure 24: The number of spines, N as a function of the Weber number exhibited on different surfaces; paper, plastic, tile and cold rolled steel versus the Weber number. The number of spines is highly influenced by the surface roughness consequently leading to a new constant being developed, with the use of a line of 'best fit.' The new line of 'best fit' (solid line) fitted the scatter spread more accurately compared to the original line of 'best fit' (dotted line) using equation (5) [18] and the line of 'best fit' (dashed line) incorporated by Hulse Smith *et al* [18] using equation (6), three types of blood were tested; **A**: Defibrinated Equine Blood **B**: Alsever's treated equine blood, and **C**: Human Blood; $N = 5$.

This found the new constants (C_n) to be; 0.46, 0.72 and 0.45 for defibrinated equine blood, Alsever's equine blood and human blood, shown in Figure 24A - C. All calculations were determined using the physical properties expressed in Table 4 and the viscosity values determined earlier for each blood type. Clearly the range of scatter observed gives a large error on C_n, due to the number of spines being greatly affected by the impacting surface and the tile surface finish which is clearly pulling down the C_n value. Note the deviation from that predicted previously by Hulse-Smith [18] suggesting that counting the number of spines is subjective.

It can therefore be concluded that a decrease in drop diameter and an increase in surface roughness ultimately produce smaller blood stains. This is concurrent with previous research in which porcine blood was tested. [18] It can also be concluded that defibrinated equine blood is overall more suitable as a human blood substitute, giving

consistently comparable results throughout experimentation and on any surface type. Results obtained for number of spines observed when using all bloods are also in excellent agreement with previous research, [18] showing that the rougher the surface, the greater preponderance of spines. It is noted that there is a lower overall number of spines acquired within this study compared to that of Hulse-Smith [18] however, this may be attributed to the physical property deviations of the tested bloods or the subjective technique of counting spines. All data is provided in Appendix 3.

3.2.2.5   Area of Origin

The area of origin provides the analyst with a 3D perspective, helping them to 'picture' the incident and therefore giving greater insight into the series of events. [4] The application of the area of origin is a vital piece of information, which highlights the area in which a blood spatter was generated.

A

B

Figure 25: Blood impacts used to calculate the area of origin for both A: human blood and B: defibrinated equine blood.

Here the tangent method was utilised to calculate the Area of Origin, where bloodstains and the area of convergence were measured manually. Only human blood and defibrinated equine blood were compared for this section of analysis as the Alsever's equine blood proved to be providing less comparable results to that of human blood throughout the previous experiments and further experimentation was deemed frivolous. To create the area of origin, a series of impacts were generated

using a Proctor Little Nipper Rat Trap [®], where 1 – 1.5 mLs of blood was loaded onto the edge of the trap. The rat trap catch was covered in tape to prevent blood soaking into the wood. The trap was set onto a large sheet of paper at ground level and at 12 cm height to create differing area of origins. When the rat trap device snapped the impact spatter collected onto the paper (lining) where it could be measured and visually compared. Traps were cleaned thoroughly between snaps and different traps (same make) were used for each height. Figures 25A and 25B show the impacts of human and defibrinated equine blood, respectively. Although visually both blood impacts may look very similar and are hard to distinguish from one another, when the criteria set forth by Wonder [9] is adhered to it is apparent that they are very different. The left side of the spatter depicts the origin of the spatter, when these are compared it is clear than human blood has visibly smaller stains than those produced when horse blood was used, this is due to the viscosity of horse blood being higher than human blood. However, when the area of origin were calculated for all impacts it was found that both could accurately calculate the area of origin and that only a small variance between the two existed of around ± 2 cm, which is relatively insignificant in terms of determining an area of origin.

3.2.2.6   New vs Aged Blood

Finally the effects of age on equine blood was evaluated. New equine blood and aged equine blood (over the time period 12 days, 14 days and 57 days) were all compared, defining the differences by alteration in diameter size and number of spines.
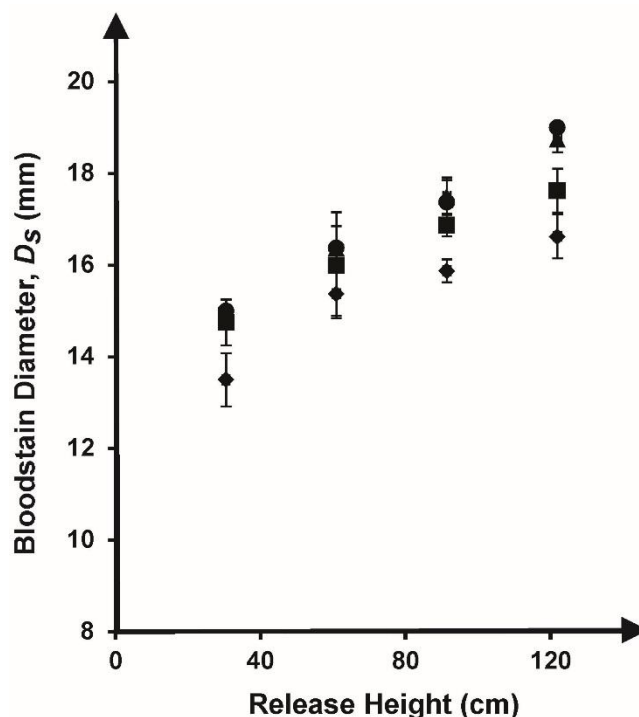
Figure 26: Aging defibrinated equine blood released (using a 1mL pipette; 1.77 inner tip diameter) from a range of heights (30.5, 60.9, 91.4 and 121.9 cm). It is clear that a decrease in the blood stain diameter is observed as the blood gets older. The age of the equine blood ranged from 57 days old (diamonds), 14 days old (squares), 12 days old (circles) to new blood (triangles); $N = 5$.

Figure 26 illustrates the differences experienced; diameters were found to significantly decrease after 14 days by up to 6.38 % and decrease further after 57 days up to 12.78 %. A student t-test was performed to determine the significance of these results, a p value of 0.0003 was calculated using the values for 57 days and fresh blood at a height of 120 cm and a p value of 0.0020 when 14 days was compared to fresh blood at the same height. These results are considered to be statistically significant and therefore it can be stated that age of blood has a significant effect on the bloodstain diameter. The aging process of blood increased the viscosity to 5mPA.s and 5.3 mPa.s for 14 and 57 days respectively, ultimately resulting in smaller stains. [5] However it was found that the PCV% was unaffected. [105] It is unknown why this affect occurred but is thought to be accounted for by the effects of aging in RBCs (Red Blood Cells). [105] Plasma viscosity can be a discounted factor since previous studies [105] have found that plasma viscosity increases due to fibrinogen production and this has been removed in our blood. Age was not found to have any effect on the number of spines observed, where spines were counted for bloodstains at various ages. Results concur with previous reports, where aged porcine blood was investigated and resulted in a decrease in diameter size. [5] Consideration should be made when undertaking future

experiments to the time period in which equine blood can be utilised as it is clear that age has a significant effect on the bloodstains produced.

3.2.3 Summary

It has been established that defibrinated equine blood can be used as a BPA human blood substitute. Equine blood follows the same trend as both the human and porcine blood [5] in that when drop height increases so does the resultant stain diameter. When utilising the pre-existing equations it was recognised the need for new constants to 'best fit' the given data. New values for the Reynolds numbers are smaller than one obtained previously for porcine blood but do not deviate that greatly from the original equation as to be questionable. When the human blood constant and defibrinated equine blood constant were compared they deviated little with one another, conversely Alsever's equine blood was found to be inconsistent to human blood and therefore not a viable substitute. Constant values for the Weber number suggest a much lower progression of number of spines than values found for porcine blood; this is accounted for by the subjective nature of spine counting.

Aged defibrinated equine blood presented large changes in diameter size as the blood got older, deviations amounting to 12.78 % when blood was 57 days old, this is thought to be related to the change in the viscosity of the blood over time and the effect of the aging process upon the RBCs. Similar deviations are experienced when porcine blood is utilised [5].

Overall it can be concluded that defibrinated equine blood is a reliable substitute for human blood, any deviations experienced from the previously reported results obtained from the utilisation of porcine blood are due to inconsistent physical properties used for the comparisons. Further analysis using a greater variation in physical properties and impacted surfaces needs to be undertaken; this will provide a greater understanding of the true usefulness of these more quantitative approaches.

3.3 PACKED CELL VOLUME AND ITS EFFECTS ON BPA

As demonstrated in the work by Hulse-Smith *et al* [18] viscosity is a fundamental parameter in the study of Bloodstain Pattern Analysis, affecting the spread of blood due to the resistance to flow. [7] Resulting viscosity values are heavily reliant on temperature (higher temperatures equating to lower viscosity readings and vice versa for lower temperatures), shear rate (rate of change of velocity when one layer of fluid passes over an adjacent layer) and packed cell volume. [80, 106, 107] The importance of PCV % and its clear effect on viscosity have been overlooked within the field of BPA. [7, 108 - 109]

The variance of these PCV levels has been documented, where levels can fluctuate from 15- 75% depending on lifestyle, gender and position in the human body. Taking these facts into account and the known effects PCV % has on viscosity [7] PCV % is applied as a parameter of blood, observing its effect on the size of bloodstain diameters and its overall impact on BPA.

3.3.1 Experimental

Human blood was utilised throughout this research, ethical approval was obtained prior to any experiments and granted by Manchester Metropolitan University. Only one donor was utilised throughout this study to maintain consistency and control over parameters. In order to study the effect of PCV, blood was centrifuged twice at 3000 rpm for 10 minutes. Different volumes of red blood cells to plasma were added to create varying packed cell volumes, generating percentages between 15 and 75 %. Packed cell volumes were then checked, filling three - quarters of a capillary tube with the sample and centrifuging at 12, 000 rpm for 5 minutes; the blood separates into its components and the percentage of blood cells can be determined using a micro-hematocrit chart.

Blood was dropped (according to the methods and materials section) using different sized pipettes, from varying heights (50, 100, 150 and 200 cm), angles (20 º, 40 º, 60 º, 80 º and 90 º) created utilising a spatter board and on different surfaces (paper, tile, plastic and steel), each of the different packed cell volume percentages

were tested. The surface roughness (R_a) of the surfaces was calibrated at 5 different points using TESA-rugosurf 10 acquiring average values expressed in Table 1. Drop diameters were measured using slow motion imaging, as described in the section 3.1.2.

All bloodstain diameters were analysed for alterations in size and overall appearance using a magnifying loupe.

3.3.2   Results and Discussion

3.3.2.1   Viscosity, Surface Tension and Drop Diameter

Dynamic viscosity measurements were carried out on human blood for all of the PCV levels, a Kinexus Pro rheometer was utilised where viscosity measurements were obtained at room temperature (25°C) and body temperature (37°C). Viscosity verses shear rate peaks were formulated since viscosity is affected by shear rate, however, at shear rates of $100s^{-1}$ (which is experienced throughout this study) the peak peters out to a constant; this constant was therefore taken as the viscosity of the blood. [4] The viscosity measurements were taken three times to obtain an average.
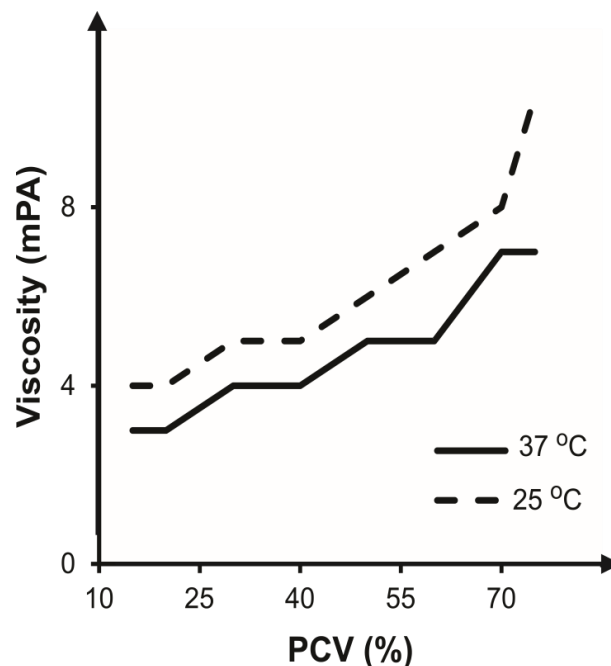
Figure 27: Viscosity measurements at different PCVs (15 – 75 %) determined at two temperatures; room temperature (25°C) and body temperature (37°C).

Figure 27 depicts the changes in viscosity in accordance with PCV%, finding that as PCV% decreases the viscosity decreases, this result is in agreement with

previous studies. [11, 12] A correlation evaluation was performed however the coefficient (R^2 = 0.69) was determined to be too low to be useful.

The surface tension of blood at all PCVs was determined using a CSC Du Nouy Precision Tensiometer. Interestingly, it was found that there were no differences in surface tensions when all PCV levels were compared.

Last, drop diameters were quantified for each PCV levels and pipette types (1mm, 1.7 mm inner tip diameter). Slow motion filming, as detailed in the experimental section was performed enabling the capture of scaled still images of the blood drops as they depart the pipette tip allowing drop diameters, D_o, to be deduced. Average drop diameters were found to be 3.57 ± 0.05 mm (drop volume 48 μL) and 4.2 ± 0.05 mm (drop volume 67 μL) (utilising the 1 mm and 1.77 mm inner tip diameter pipettes respectively) and did not deviate when the PCV% was altered. This is in agreement with the above findings regarding surface tension; the surface tension of the blood in flight gives rise to its spherical shape therefore if this remains unaffected, it stands to reason that the drop will also remain unchanged.

3.3.2.2   PCV% vs. Bloodstain Diameter

Firstly the effects that PCV% had upon bloodstain diameters were explored, D_s by performing a series of blood drop experiments for each PCV %.

Figure 28 illustrates the linear decrease of diameter size as PCV % increases, this is due, as previously stated, to the effects PCV % has on viscosity. The viscosity decreases as PCV % decreases creating a less viscous fluid and a greater ease of movement and spread.
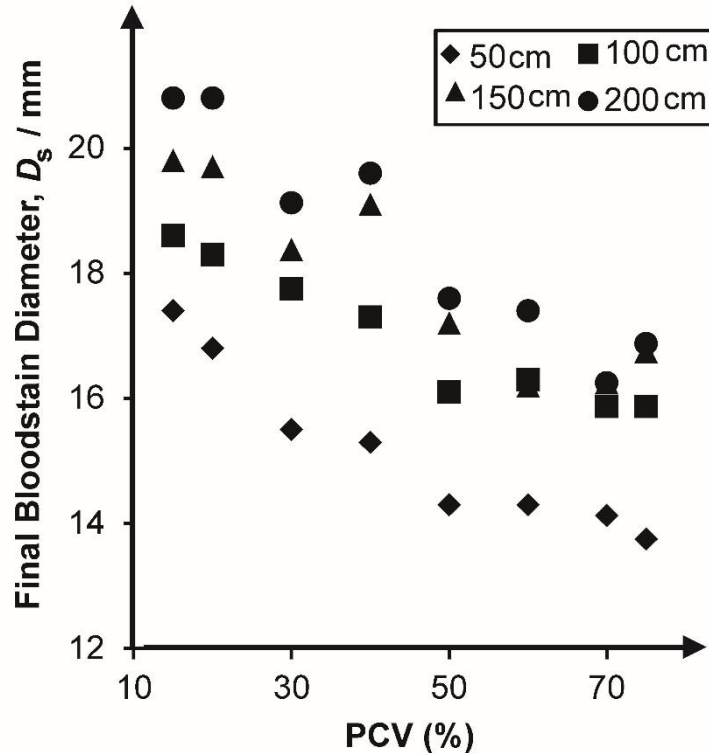
Figure 28: Final bloodstain diameters for human blood, containing different PCV levels, released from varying heights onto a paper surface using a 1 mL pipette (inner tip diameter 1.77 mm).

There was a maximum decrease of bloodstain diameter equating to 3.93, 4.10, 4.83 and 6.00 mm, when considering the different surfaces; paper, plastic, steel and tile respectively and the use of the larger pipette (1.7 mm inner diameter) from all heights. These values are equivalent to between a 26.50 - 35.07 % maximum decrease when the highest and lowest PCV % values (15 % and 75 %) were considered. However, when the difference of normal human levels of PCV % (around 40 %), to the higher (75 %) and then the lower (15 %) PCV % levels are considered, this change is less prominent, becoming 16.15 - 23.91 % and 6.00 − 12.07 % respectively. By performing t-tests the true significance of these bloodstain alterations can be established, if the highest (75%) and lowest PCV (15%) levels are compared a p value of less than 0.0001 is obtained, for all surface types, which acknowledges that this data is extremely significant. However, aforementioned there is unlikely to be such extremes (15 – 75%), therefore it is proposed to adopt a middle (normal) PCV level of 40 % and compare this with the highest and lowest PCV% levels. When considering the lowest level (15%) with a normal level (40%) for all surfaces, p values of 0.0001 - 0.0322 are deduced, which are still considered to be very statistically

significant, similarly if the highest level (75%) is compared with the normal level (75%) extremely statistically significant *p* values of 0.0001 - 0.0002 are obtained. Overall this provides the very real insight that PCV % does have a very significant effect on bloodstain diameter decreasing / increasing the final stain diameter by up to 35.07 %.

Noting that angle of impacts and the sequencing of events are centred on the size of a bloodstain, experts should be aware of the implementations of PCV % and its implications on how future BPA activities should be approached, perhaps determining the extremes and using statistical analysis to establish if the result is changed significantly when PCVs are considered.

3.3.2.3 PCV% vs. Spread Factor

Using the equations established by Hulse – Smith *et al* [18] the spread factors of all the PCVs samples were compared. First, calculations for the Reynolds numbers were conducted using a standard viscosity value (0.0048 kg/ms) quoted by Hulse – Smith *et al*, [18] this value is consistent with a 40 % PCV level (at room temp) and therefore can be used to evaluate the extent of spread factor change. Equations 2 and 3 were utilized, where the original constant (C_d) of 1.11 was implemented; new constants for PCV were subsequently created using Excel® to generate lines of 'best fit' and quantify the difference in spread factors.
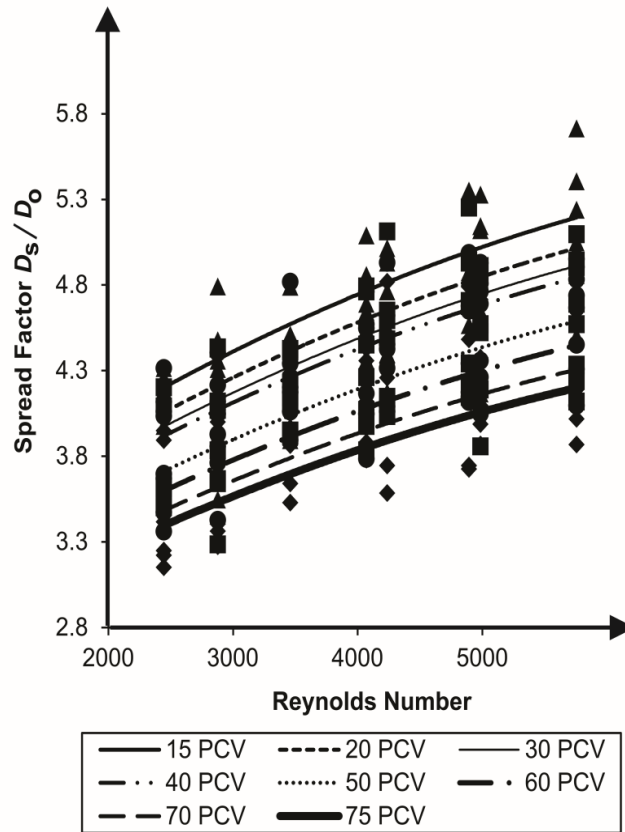
Figure 29: A depiction of the spread factor versus the Reynolds number when utilising human blood (containing varying PCV levels) on different surfaces; paper, plastic, tile and cold rolled steel. Lines of 'best fit' were calculated for each PCV %, where new constants were established (see Table 4 for a clearer view of the constants).

Figure 29 illustrates the new constants established for each PCV %. It is evident that the PCV % has a marked effect on the spread of the blood drop, altering the constant by (+) 6.96 % and (−) 15.35 % when comparing the average PCV (40 %) with the lowest PCV (15 %) and highest PCV (75 %), respectively. Statistics assessing the average PCV against the lowest and the highest PCV were carried out to verify the significance of these results, a p value of less than 0.0001 was obtained, clearly showing that PCV % significantly affects the spread factor of the blood drop. Since only the standard value for viscosity [15] was used further calculations were necessary where all viscosity values (at room temp) were incorporated for each corresponding PCV %.

PCV	C_d ($\mu = 0.0048$ kg/ms)	C_d (μ measured at PCV %)
15	1.19	1.14
20	1.15	1.10
30	1.12	1.14
40	1.11	1.12
50	1.05	1.11
60	1.02	1.12
70	0.99	1.12
75	0.96	1.17

Table 4: New constant values established for varying PCVs using equation (3) when different viscosity values were implemented.

Table 4 expresses the new constant values, where the results appear much closer to the original constant (C_d = 1.11) proposed by Hulse – Smith *et al.* [18] However in exploring the statistical significance between the values, using 40% as the standard, *p* values of a very high significance are still achieved, and therefore it may not merely be the viscosity that is effecting the spread factor. It is unclear at present what the underlying cause for the differing constants is. It is conceivable that as shear rate affects viscosity it is not effectively possible to determine a constant value and therefore the measured viscosity values may not be 100% accurate if the correct shear rate ($100s^{-1}$) was not reached. Other possible causes could be the way in which the blood interacts with the surface (wetting), drying effects and measuring discrepancies (analyst error).

After exploring the effects of PCV % on bloods spreading capabilities it can asserted that there is a significant effect when comparing the highest PCV % values with the lowest PCV % values (15 % and 75 %). In terms of the real life applications, PCV % can vary within people due to lifestyle or psychological state. [2] For example if a person is in a panicked state packed cell volume would be expected to increase [2] and therefore would decrease the size of the resultant bloodstain diameter (D_s) in the

case of bloodshed, and is therefore extremely relevant in terms of its application within BPA. Future investigation where blood is a source of evidence need to consider the factor of PCV % and time should be taken to ascertain if the lifestyle or psychological state especially as bloodstain size is used in other areas of BPA pertaining to impact and pattern type and maybe misleading.

3.3.2.4 PCV% vs. Angle of Impact

The Angles of Impact (AOI) are a vital piece of information, providing the preliminary step to attaining the Area of Origin. [1, 2, 14, 18] To find the angle of impact of a bloodstain, we used equation (7).

Five angles were tested on three surface types (paper, plastic and steel), where AOIs were subsequently determined. It was found that calculated AOIs did not alter despite the varying PCV level. It was noted that stains in general were larger when lower PCVs were utilised and vice versa when higher PCVs were considered, however the elliptical length and width adjusted accordingly and therefore did not affect the final angle.

These results to can be applied to the current knowledge of the creation of an impact spatter, where the applied force has to overcome the surface tension. Since the surface tension remained unchanged throughout experimentation and the new knowledge that viscosity doesn't affect the angle of impact (see above) it is expected that there would be no effect on the impact spatter created and therefore equally the calculation of area of origin would remain unaffected. However the overall stain is either larger or smaller than it would be at an average PCV%, this could lead to misinterpretation of pattern types which are reliant on size (*i.e.* spurt vs gush), in accordance with the criteria set forth by Wonder. [9]

3.3.3 Summary

For the first time the effect of varying PCVs on the evaluation of resultant bloodstains has been explored. Using PCV % of 15 - 75 % it was determined that diameters (D_s) significantly decreased as packed cell volume increased; this is explained by the viscosity increase which would have ensued. New constants for each PCV% were found when spread factor was investigated, where equations implemented by Hulse – Smith et al [18] were applied. Although generally acknowledged as passive stains (due to them usually being produced as a result of

gravity), though they can also be a result of a projection, [13, 14, 18 - 19] *circular bloodstains can used to establish impact velocity and sequence of events, i.e. if a person is stood still and blood is dripping from a weapon this can indicate positioning.* [13, 14, 18 - 19] *With the knowledge that PCV% can alter the size of a bloodstain this should be integrated into any calculations regarding bloodstain size where differences from the average value (45%) with regards to the lowest and highest extremes of PCV% should be calculated, therefore establishing an error range. Investigators should try to establish potential PCV% altering conditions such as pregnancy, anaemia and drug use (i.e. doctor's patient history). There may also be opportunities at crime scenes where fresh blood pooling is present (thus easier to obtain an adequate amount of sample) and therefore every opportunity should be seized to obtain a sample for haematological testing.* [13, 14, 18 – 19]

Last it was discovered that PCV% does not alter the calculated angle of impact, this is an important result since angles of impact are used to find the area of origin, the area of origin is vital when establishing an impact site. Further investigations could be carried out using more surface types, drying and blood warmed to body temperature. Also further exploration into different blood patterns should be investigated (i.e. spatters, spurts, pools) to establish the overall effect of PCV% and potential blood collecting methods should also be explored so an accurate PCV% measurement can be obtained from the scene.

3.4 THE MECHANISM OF DRYING BLOOD AND VOLUME ANALYSIS

As previously detailed (see section 4.1.10), blood can differ greatly from person to person; [4] it is unknown what the significances of such changes in the components of blood will have on the drying of bloodstains. Consequently this study explores the fundamental parameters of the drying effects of both human and equine blood, the influence of PCV % when applied to drying time, volume estimation and drying effects, and ultimately what consequences this pertains to the field of BPA; as such this work is of both fundamental and applied importance.

3.4.1 Experimental

3.4.1.1 Blood and PCV% Preparation

Two types of blood were utilised throughout this study; defibrinated equine blood provided by TCS-Biosciences Limited (PCV 50 %) and screened EDTA (Ethylenediaminetetraacetic acid) treated human blood type O+ supplied by a local blood bank. Fresh blood could not be utilised due to the size of the equipment used, as the blood would have clotted before analysis could proceed.

Blood samples were heated to 37° C before dropping in order to align to real life applications where blood would evacuate the body at body temperature in a violent assault. Blood samples were stored at 4° C when not required for experimentation.

In order to study the effect of PCV, human blood was centrifuged twice using the same parameters as previously stipulated. Different volumes of red blood cells to serum were added to create varying packed cell volumes, generating percentages between 15 and 75 %. Packed cell volumes were then checked using the procedure described in section 3.2.6. Equine blood was used for volume estimation, due to its availability in abundance; the same method above for the preparation of PCV concentrations was followed.

3.4.1.2 Microscope analysis

Defibrinated equine blood and human blood were individually dropped onto a microscope slide using a syringe and subsequently filmed using a Leica AF6000

microscope and Leica DFC340FX camera until completely dry at room temperature (24° C). Temperature was controlled in an incubator in which the microscope was encased, this avoided any turbulent air that may have disrupted or altered drying and prevented heat from the lamp disrupting drying. Blood serum for both human and equine blood were analysed by centrifuging the blood at 2988 rpm for 15 minutes at 4° C, separating it into serum and red blood cells and carefully extracting the serum using a pipette, the aforementioned method was then used to examine the drying effect.

Blood drops were performed for each of the different packed cell volume percentages and the drying process was recorded again using the Leica microscope.

3.4.1.3 Volume and Drying analysis

Three types of volume analysis were conducted;

Scaled Photograph – Three PCVs (15, 40 and 75%) were analysed on two different surface types (vinyl and laminate wood). Blood (5 – 50mL) was poured onto the surface where it was left to naturally flow to a stop. Scaled photographs were taken of each of the bloodstains using a Casio Ex-F1 Digital Camera and surface areas were determined using the image software Image J. [41]

Dry Weight – This method is only suitable for non-absorbent surfaces therefore only vinyl and laminate wood were included for experimentation. [42] Three PCVs were tested (15, 40 and 75%), blood volumes (5mL, 10mL and 20mL) were deposited onto the surfaces as stipulated above and left to dry overnight. Stains were scraped off the surface using a sterilised razor blade, scrapings were placed into closed containers and weighed. Wet and dry weights for 1mL of blood were determined for each of the PCVs to obtain a constant. [42]

Spectrophotometry – Again three PCVs were evaluated (15, 40 and 75%); calibration graphs were generated, volumes of 10 μL - 100 μL diluted with distilled water up to 100mL were made for each PCV, a series of sonification and vortex-mixing were incorporated in order to fully mix the blood. [40] Absorbance measurements were performed at 412 nm, which has been found to be λ_{max} when an absorption spectra measurement was performed between wavelengths of 300 – 700 nm. [40]

Blood volumes of 5mL, 10mL and 20mL were tested on different surfaces (carpet, vinyl and laminate wood), where blood was decanted onto the different

surfaces and left to dry for two days. [40] Dependent on the surface type, the stains were either scraped or the stain was cut away from the surface and deposited into 500mL beakers filled to the mark with distilled water. [40] These were then left overnight to soak and dissolve. When all blood had been fully mixed (no floating particles) a 1:50 dilution was made, again with distilled water. Absorbance measures were carried out. [40]

Drying times were established by skeletonisation rate, where blood drops for each PCV% were deposited on a plastic surface, drops were wiped at various time increments; 1 minute, 5 minutes, 10 minutes, 20 minutes, 40 minutes, an hour and final dried spot (5 drops for each time interval).

The Halo effect was also investigated; drops (at heights of 10 cm and 40 cm) and swipe patterns were performed for each PCV% and left to air dry. [115] Once dry, drops were deposited on top of the swipes and similarly swipes were positioned on top of the dried drops. [115]

3.4.2   Results and Discussion

3.4.2.1   Defibrinated Equine v Human Blood

During forensic investigation it is not always suitable to utilise human blood, given that the potential risks of biological infection are often too severe. [20] Equine blood has been identified as a viable human blood substitute when reconstructing violent crimes, offering a safer alternative. [21] In comparing the physical properties of human and equine blood (see Table 2) it is readily observed that both have similar characteristics and should potentially therefore yield similar results.
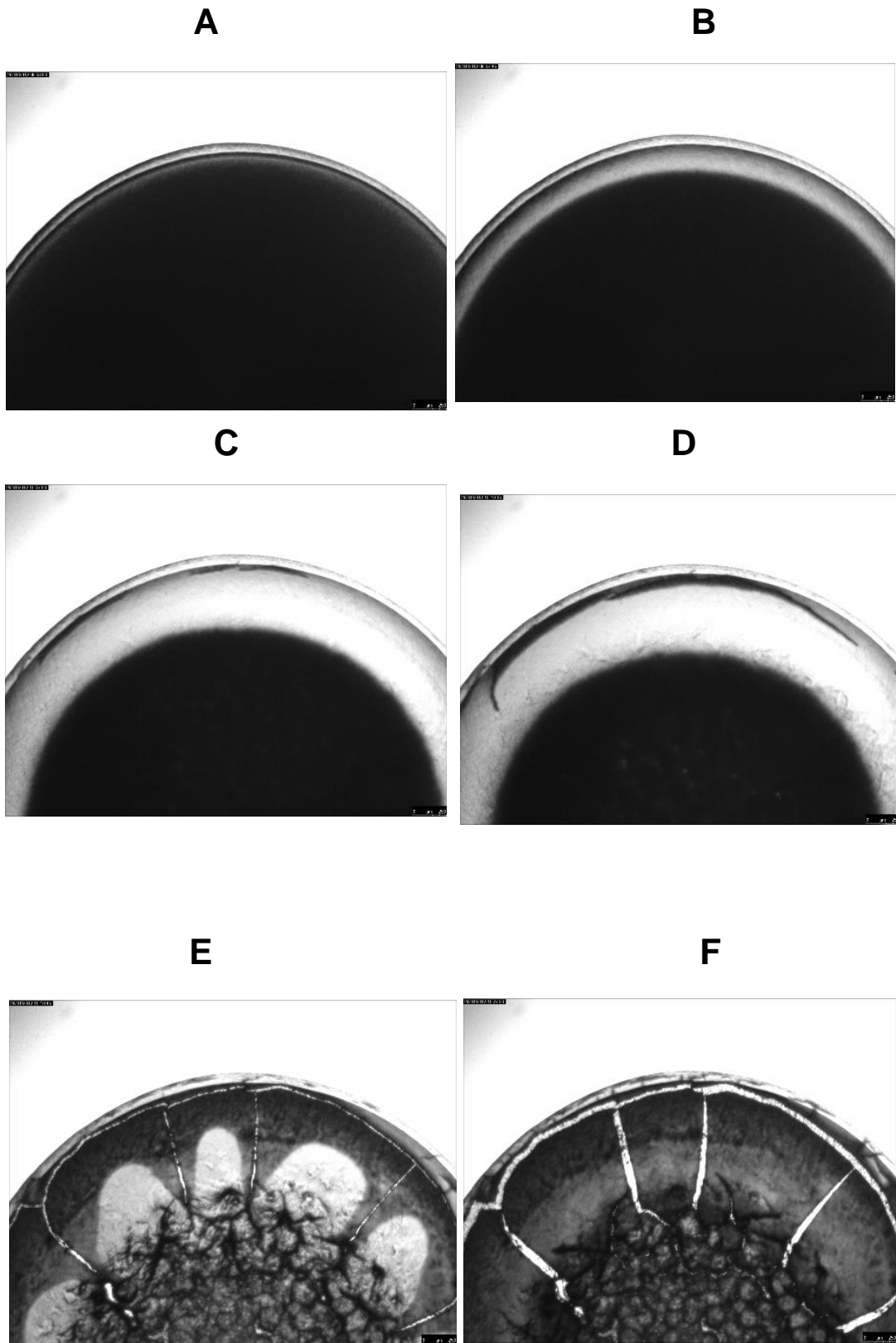
Figure 30: A series of images depicting the drying of defibrinated equine blood at room temperature, acquired using a 2.5 x 0.07 magnification Leica microscope. (*t* = 42 minutes)

Figure 30 depicts a series of images of defibrinated equine blood captured under a Leica microscope at 2.5 x 0.07 magnification, where the images show the drying of a blood drop.
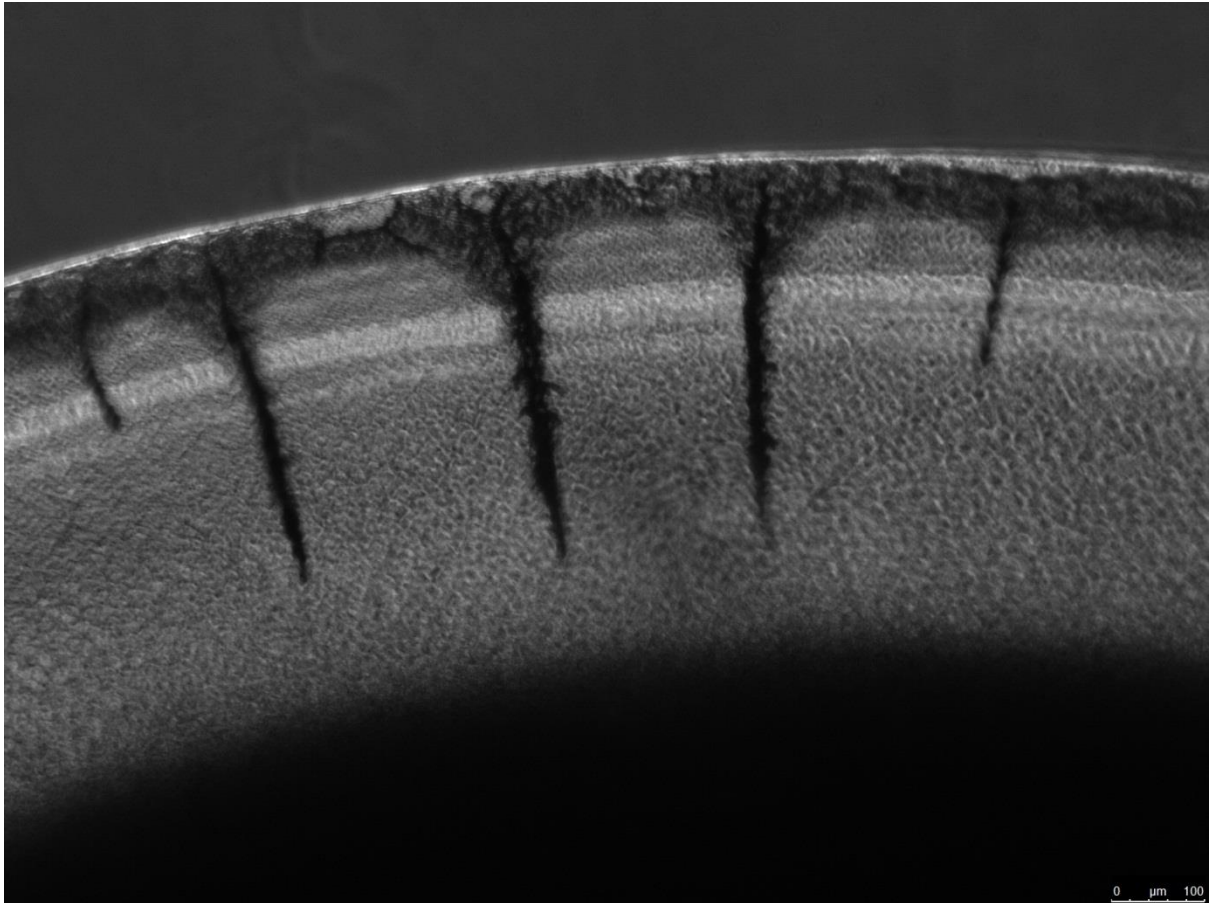
Figure 31: A close up of equine blood magnified by 2.5 x 0.07 using a Leica microscope, showing particle build upon the edge of the blood drop.

If this is magnified further, as shown in Figure 31, we can perceive the build-up of suspended particles on the periphery of the blood drop similar to that observed during the 'coffee-ring effect' (Figure 32).
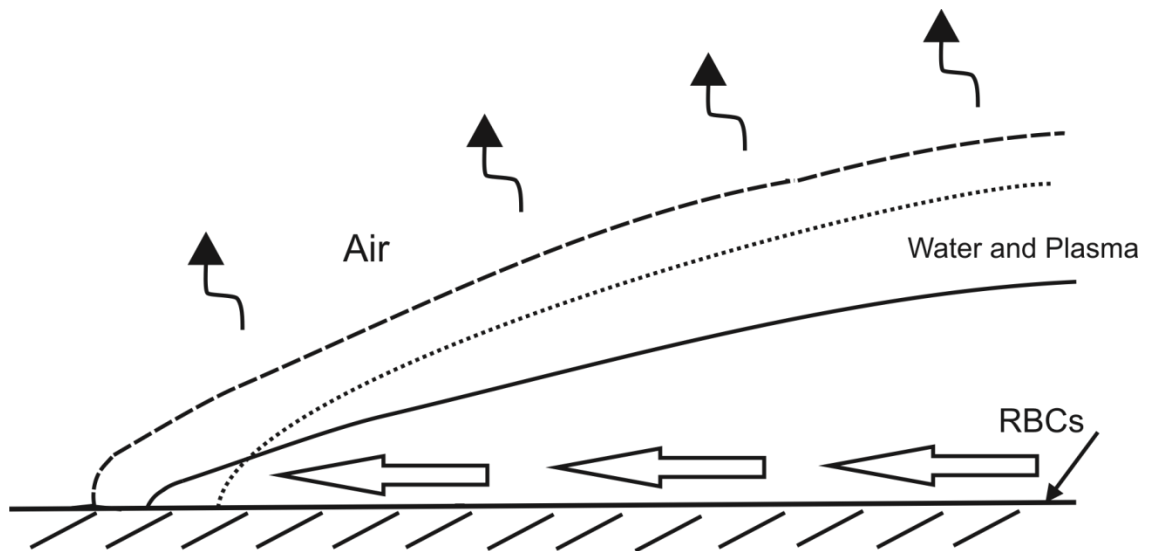
Figure 32: Schematic diagram depicting bloods 'coffee - ring effect,' evaporation ensuing over the entirety of the drop surface. Red blood cells (RBCs) flow towards the edge of the drop, where edges are pinned to the surface. Surface tension increases attracting more blood particles to the edge, creating a capillary flow.

In comparison of images acquired for equine blood to that of human blood (see Figure 33) it is apparent that there are no distinct differences in appearance except clearer images, which can be attributed to the defibrination process undertaken on the equine blood by the manufacturer. Both blood samples display the same general drying mechanism where the red blood cells builds on the periphery of the drop; however this is only clear under high magnification and is not overtly obvious through a 2.5 x 0.07 magnification. There is also evidence that the overall driving force behind the blood drop drying is a weak Marangoni flow, where blood clearly dries inwards towards the centre of the drop where surface tension is greatest and where the majority of red blood cells lie. This observation is verified by previous studies performed by Brutin *et al.* [37]
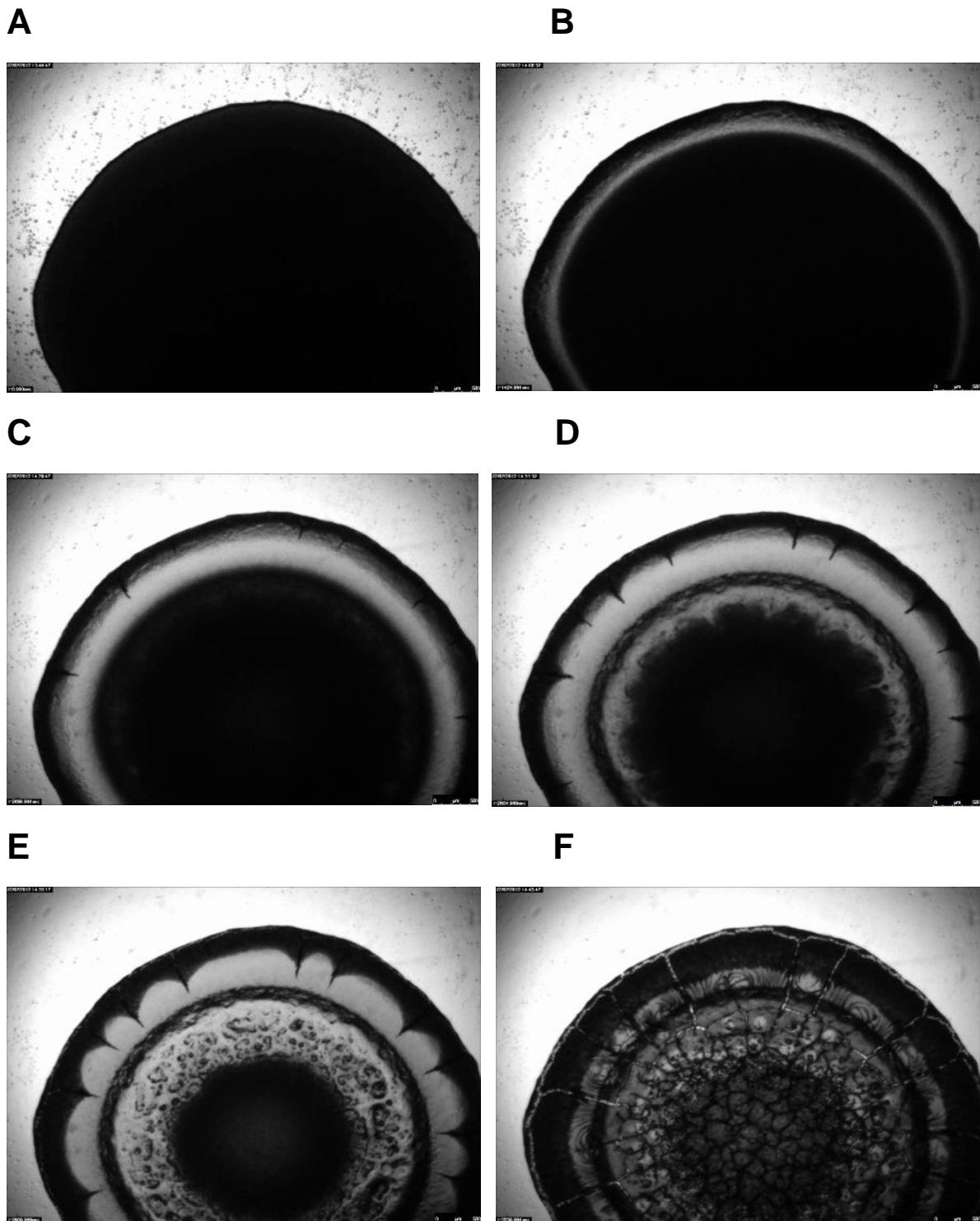
Figure 33: A series of images depicting the drying of human blood at room temperature, acquired using a 2.5 x 0.07 magnification Leica microscope. (t = 42 minutes)

Blood, however, does not dry uniformly and there is still a ring clearly present on the periphery, therefore Marangoni flow cannot be the only driving force operating for the drying of the blood drop as previously stipulated in the work by Brutin *et al*. [37]

Although Brutin *et al* [37] could identify the Marangoni flow the use of a digital camera to record the drying of the blood drops displayed less detail than that of a microscope used in this study, therefore some details such as the build-up of red blood cells on the stain periphery were overlooked. Similar remarks can be made for human and equine blood serum which was extracted after centrifuging for 15 minutes.
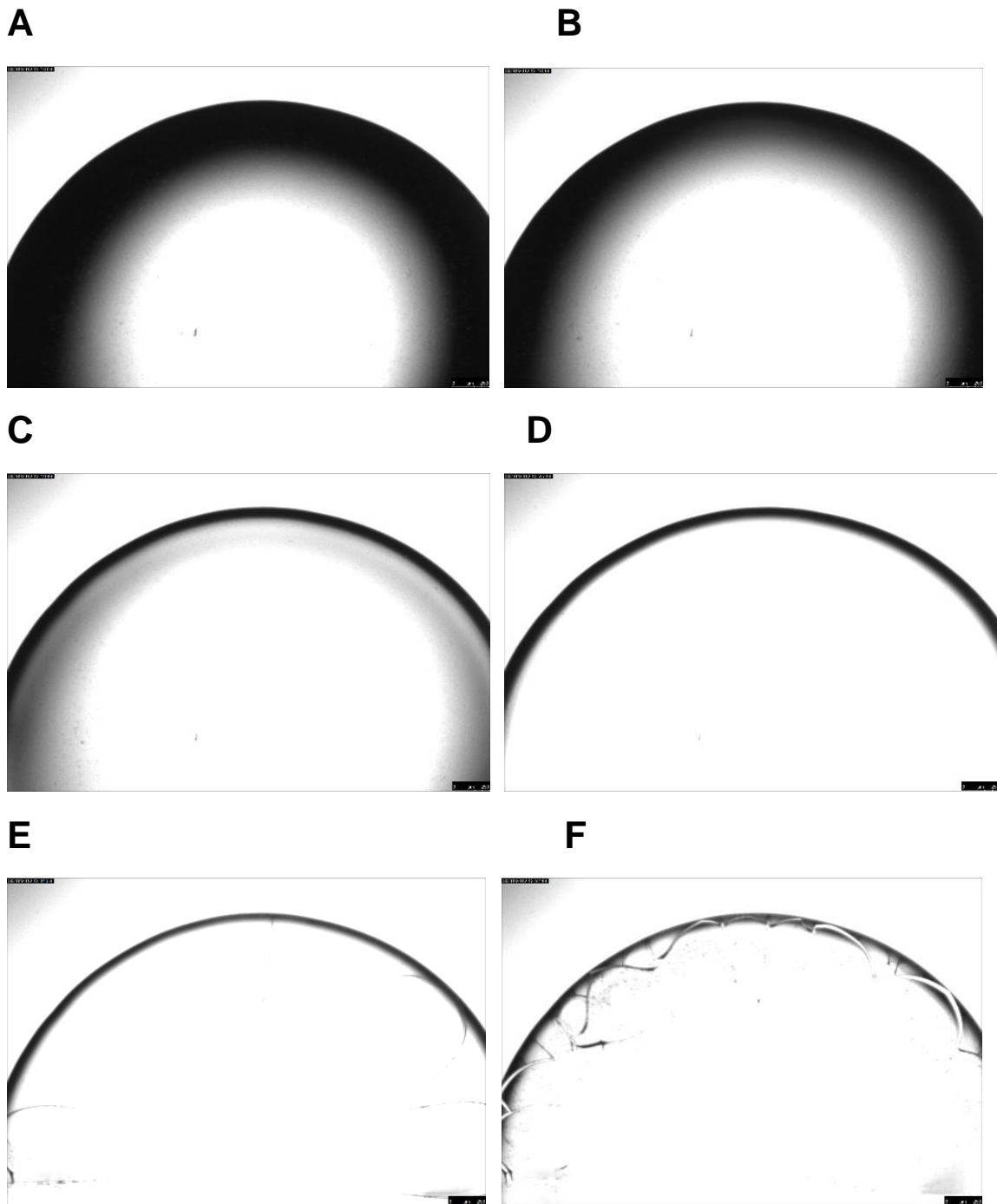
Figure 34: Blood serum from the defibrinated equine blood was extracted after centrifuging, due to the defibrinating process blood seems to have haemolysed and therefore the serum is not as completely clear as anticipated, demonstrated by the darker regions on the depicted on the series of images below. (t = 39 mins)
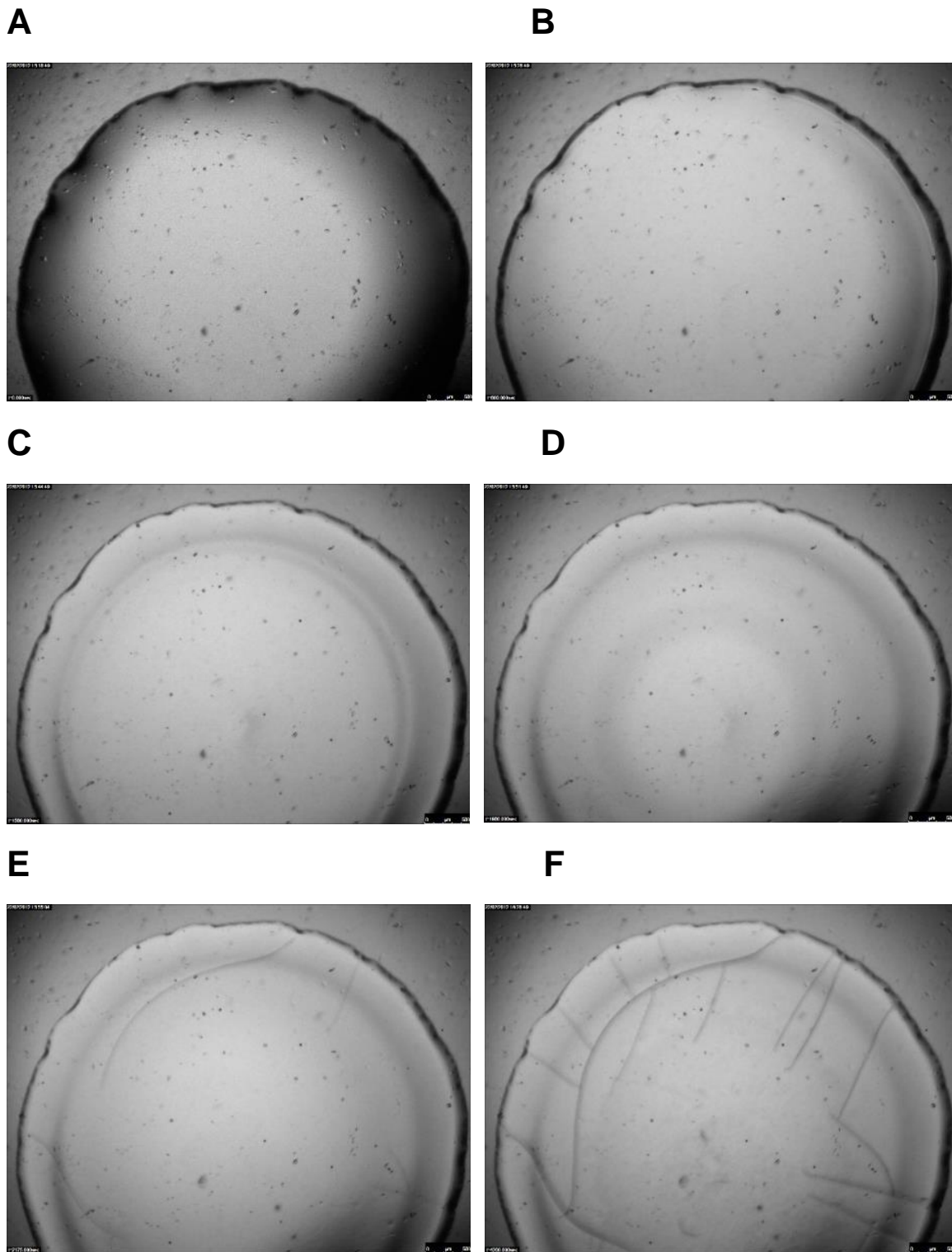
Figure 35: Human blood serum is depicted in a series of images below showing the drying process. (*t* = 38 mins)

Both blood serums (Figure 34 and 35) exhibit similar drying mechanisms, *viz.* the coffee ring effect, where there is clear flow towards the periphery of the drop where particles start to accumulate. The mechanism is best represented in Figure 34, the equine serum, the blood had clearly haemolysed which is most likely a result of the

defibrination process, leaving deposits of haemoglobin within the serum and therefore provides a visible contrast against the clear serum. Drying times of human and equine blood drops were also compared and it was found that there were no significant differences in times.

3.4.2.2   Effects of PCV % upon the drying mechanism

A range of PCV % were tested from 15 to 75 % as this relates to the lowest and highest values experienced in potential victims / injured parties. [4] Figures 36 through to 38 depict the drying processes exhibited by changing the PCV %.

A

B
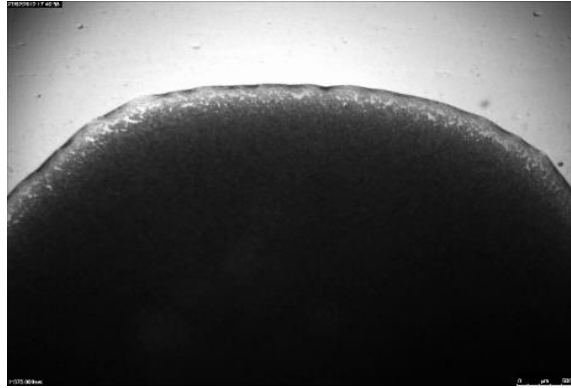
C
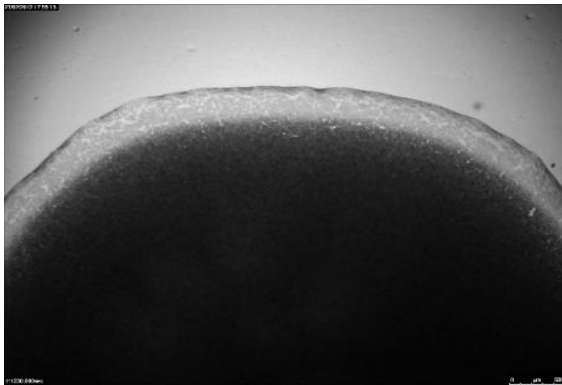
D
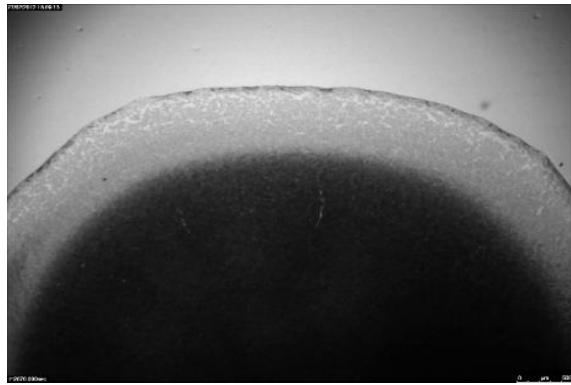
E
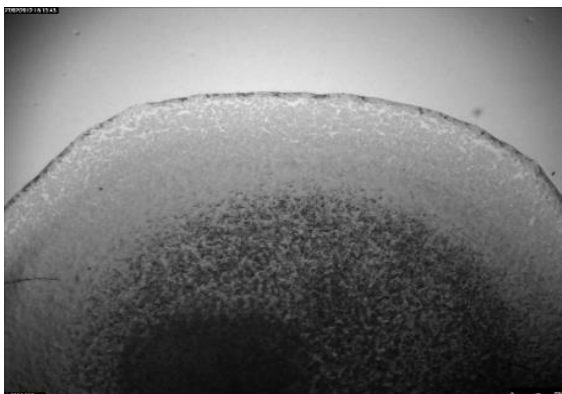
F
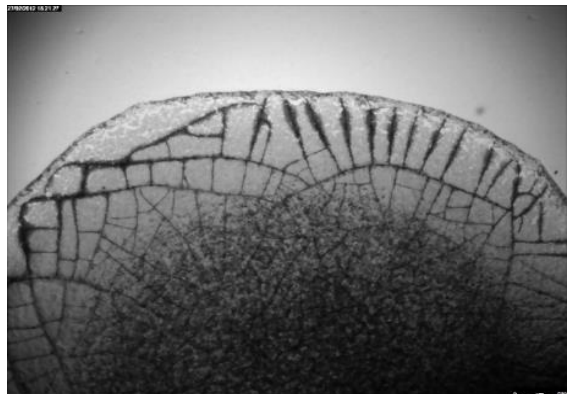
Figure 39: A sequence of images demonstrating the drying effect of human blood at a PCV % of 15 % were gathered using a 2.5 x 0.07 magnification microscope objective. (t = 40 mins)

A

B

C
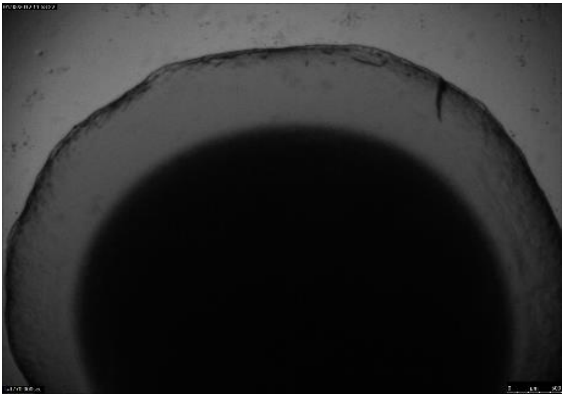
D
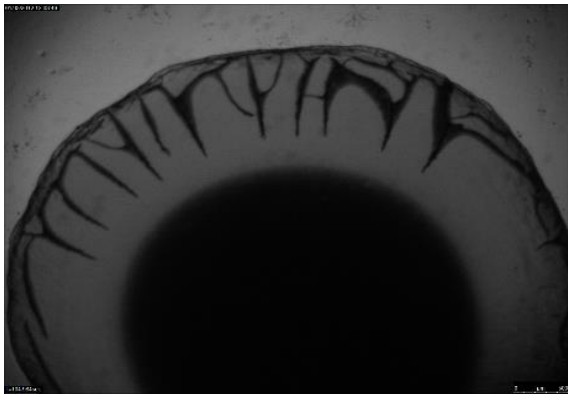
E
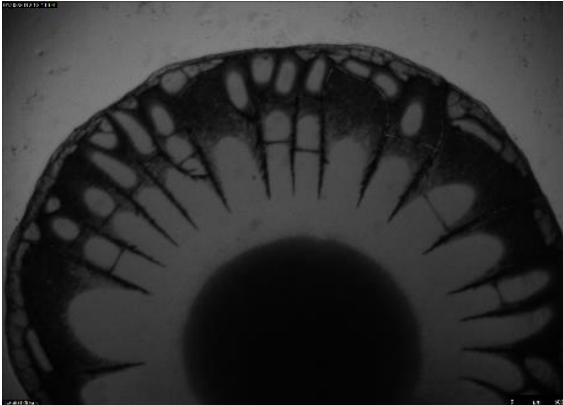
F
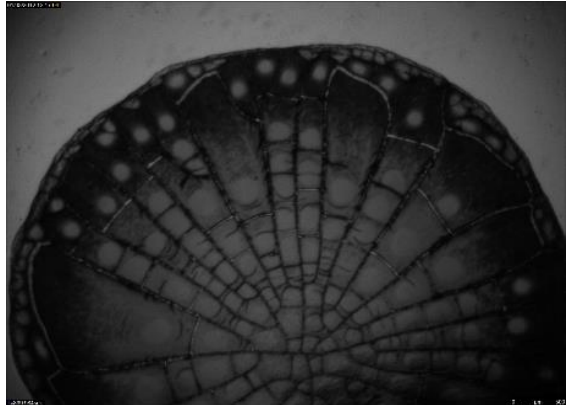
Figure 37: Images collected with the use of a Leica microscope at magnification 2.5 x 0.07 demonstrating the drying effect of human blood at a PCV % of 40 %. ($t = 42$ mins)

The lower percentages (Figure 36) show the drop to be more transparent in appearance when microscopically viewed; this is due to the overwhelming proportions of plasma present in the lower packed cell volumes.
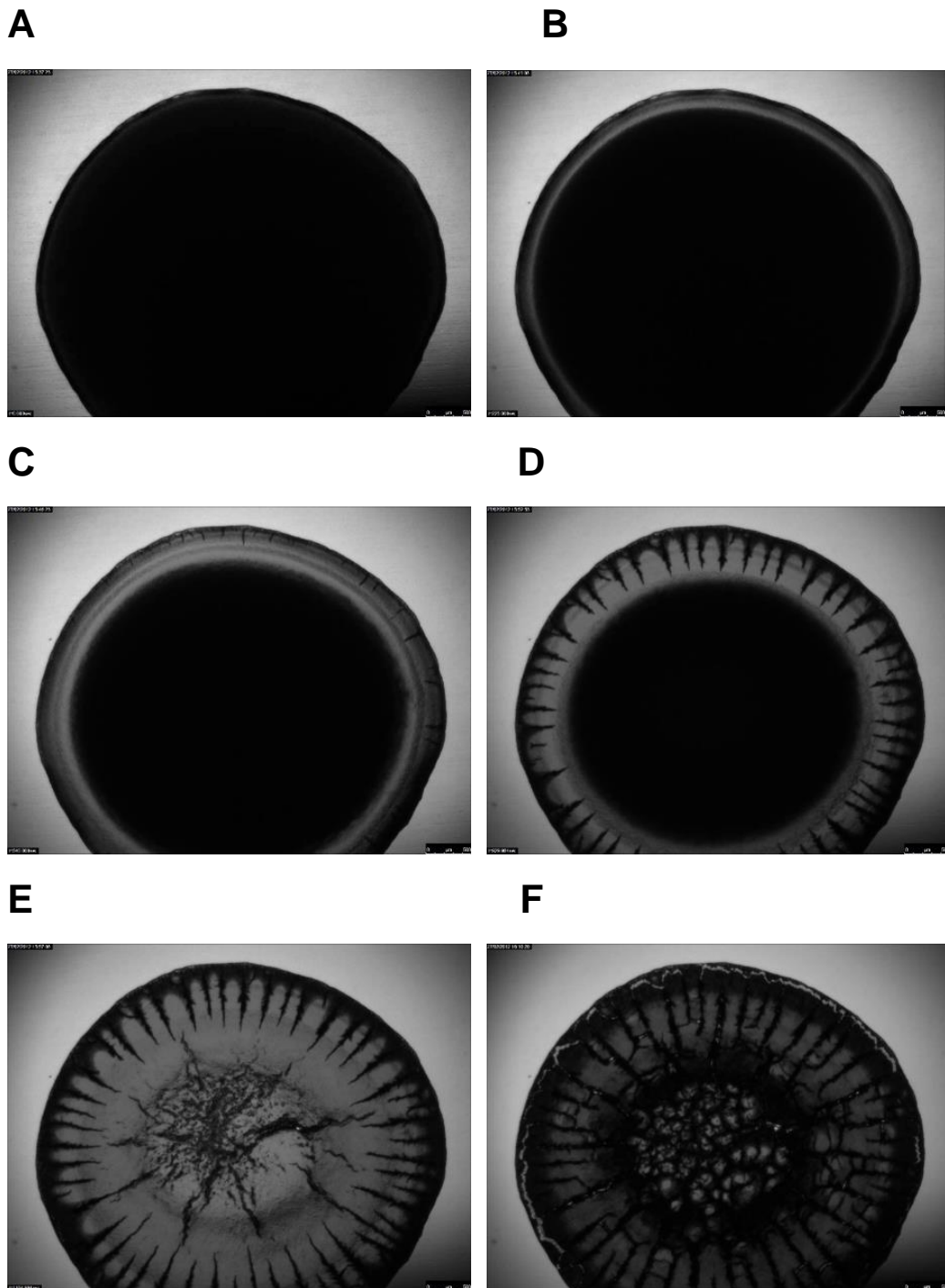
Figure 38: A sequence of images collected using a microscope at magnification of 2.5 x 0.07, demonstrating the drying effect of human blood at a PCV % of 75 %. (t = 42 mins)

Comparing the lower values of PCVs with the higher values (Figure 38) an apparent absence of a ring in lower concentrations is observed, where all red blood cells are observed in the centre of the drop, this is strange considering the previous results for serum, where the coffee ring effect (see section 1.3.1) seemed to be the driving drying force. Since individual RBCs in a bloodstain are difficult to visualise

under a microscope, due to compactness, it is possible that there is a ring present, however it is observably smaller when we compare PCV% images (Figure 36 and 38). The opposite can be said for higher cell concentrations where the ring is at its densest and a raised inner ring is visible which can be explained as the overpopulation of red blood cells in the centre. The Marangoni flow appears to be at its strongest at lower levels of PCV % where the difference in surface tension will be at its greatest, when the Marangoni flow is at its strongest this reverses the 'coffee-ring effect,' or blood ring effect, explaining the appeared lack of the peripheral ring on the lower packed cell volume percentages.

3.4.2.3   PCV % - Drying Time, Blood Skeletonisation Rate and the Halo Effect

The Halo Effect is an extremely important tool in ascertaining the sequence of events, [116] where the colour of the outer most ring or 'halo' (Figure 39A) can indicate the order in which the bloodstains were produced. All PCVs were tested (15 – 75 %) to establish any significant changes to either the size of the halo or its appearance. In this limited study it was found that bloodstains only displayed red halos, which is typically exhibited when the drop was deposited first, followed by a swipe, [116] when the PCV% was at 50% or higher. When the pattern sequence was reversed it was observed that no halos (surface coloured) were presented. It was also observed that as the PCV% increased the halos were hard to recognise as the blood was a lot darker and therefore produced a darker swipe. Although there were no halos exhibited in these instances other circumstances (*i.e.* different surfaces, temperature) which may have an impact on this observation cannot be excluded.
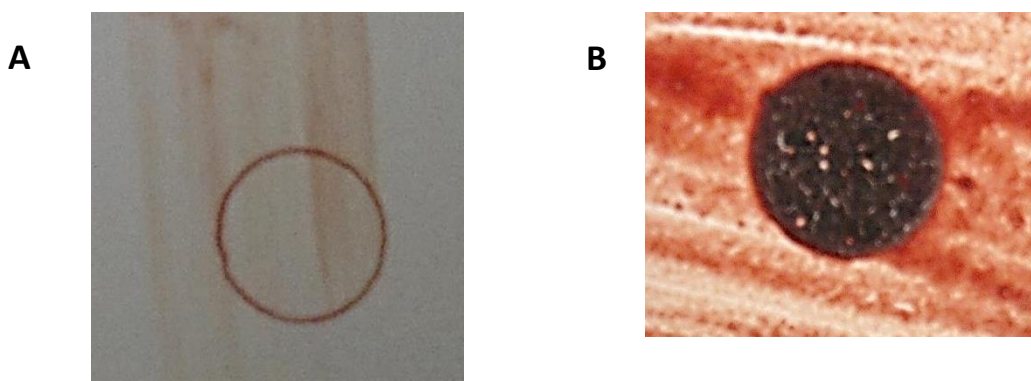
Figure 39: A- The skeletonisation of blood, where a clear ring is left behind when the bloodstain has been wiped. B- The Halo Effect, a visible red outer ring / 'halo' can be seen on the periphery of the bloodstain. A red ring is observed when a drop followed by a swipe action has occurred.

Skeletonisation is useful when testing the drying time of blood, [5] where blood is wiped away and visible ring is left (Figure 39B). There was found to be no significant

effect on the end time in which the blood drops dried when PCV% was incorporated. However it was noted that higher PCVs initially seemed to start drying more quickly, where skeletonisation rings appeared thicker after the first few wipes were performed.

3.4.2.4 PCV% - Pool Blood Volume estimation

3.4.2.4.1 Photograph

Since not all bloodstains are able to be transported, either by removal of the bloodstain by scraping or the removal of the surface in which the blood has impacted, photographing is the next practical solution. Scaled photographs were taken of bloodstains at various volumes (5 - 50 mL), PCVs (15%, 40% and 75%) and on different surfaces (vinyl and laminate wood).
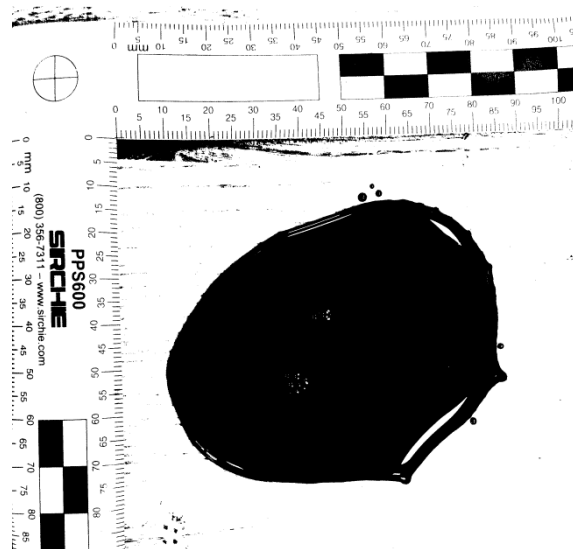
Figure 40: A scaled bloodstain photograph, here, image software, Image J has been used to alter the threshold of the photograph allowing for the surface area to be measured.

Surface areas were found using the image software Image J (Figure 40), comparing these values with the original volumes the following calibration graphs could be formulated (Figure 41), where constants were found for the calculation of the original volume.
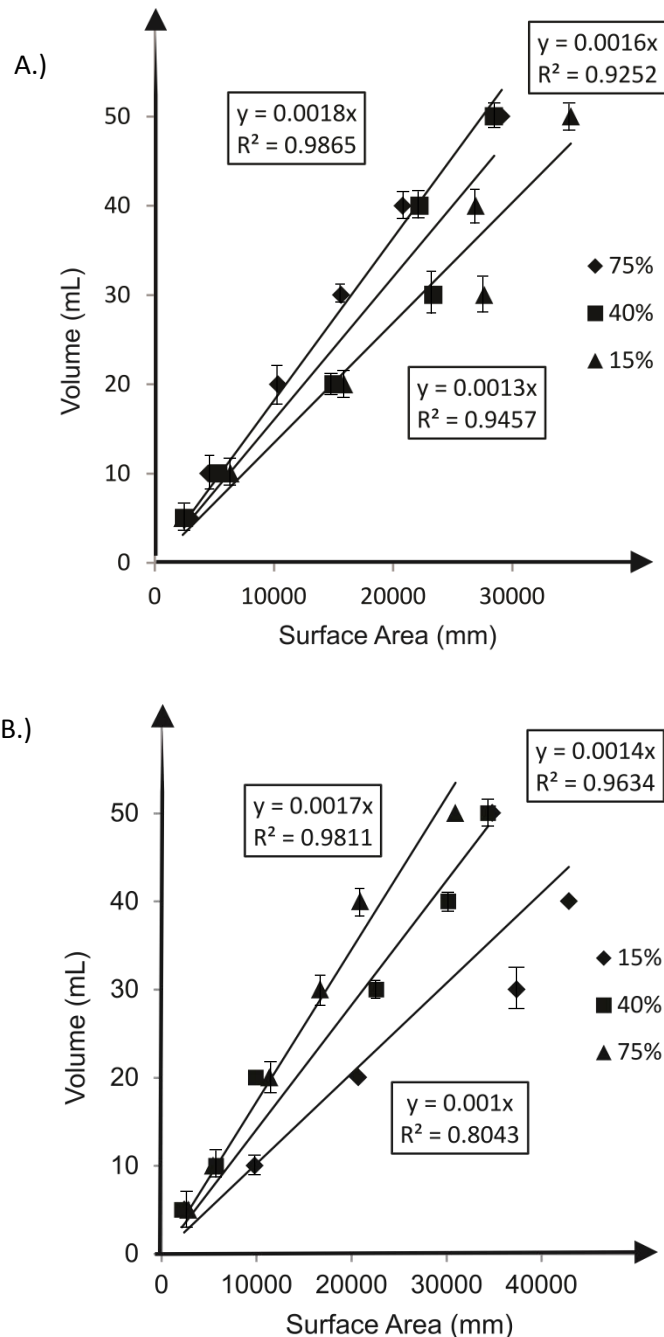
Figure 41: Calibration graphs expressing surface areas of bloodstains versus original volume on two different surface types: A- vinyl and B- laminate wood.

Figure 41A displays the lines of 'best fit' (y = mx) for volumes on a vinyl surface, it is observed that the constant (m) changes with PCV%, the corresponding constants (*i.e.* 15% PCV, 0.0013) are multiplied by the surface area (found using Image J) to give the original volume. A constant (0.0015) was obtained for all PCVs collectively (average), again using a line of 'best fit', the constant, however, was found not to be suitable leading to errors of ±6.78 - 49.47% in final volume estimation. Similarly this was found to be true for laminate wood (Figure 41B) where the constant (m) for all PCVs equated to (0.0013) and gave errors of ±1.87 - 43.95%. It is clear from the high error

percentages that are present when trying to collate all PCV data that PCVs need to be analysed individually, indicating the importance of this information at a crime scene when investigating volume analysis. Unfortunately PCV% cannot be identified in dried blood and therefore cannot be ascertained at a crime scene, since this method without the knowledge of PCV% has excessive error rates it is not advised to use this technique. It is noted that the type of surface had no substantial effect, however both surfaces are non-porous and therefore this may differ when a porous surface is used. It was also observed that as the PCV% decreased the surface area increased due to the viscous forces being reduced, allowing the liquid to spread further. This is an important observation as other volume estimations which have not been included in this study also require the measurement of the area of the bloodstain, or the reconstruction of the bloodstain and this may prove difficult when considering PCV% and potential spread.

3.4.2.4.2 Dry Weight

The dry weight method is currently considered to be the most accurate method of volume estimation at a crime scene for non-porous media. Lee *et al* [39] developed this method by generating a constant, which could be used to determine the original volume (*V*). This involves taking the dry weight of liquid blood from the wet weight of blood, where the wet weight of 1 mL of blood was found to correspond to 10.2 mg and the dry weight of 1mL of blood was found to be 2.4 mg. However it seems that the calculation is incorrect, Lee *et al* [39] uses the weight loss (10.2 – 2.4 = 7.8) and divides by the dry weight (2.4) to find the drying constant, which is calculated to give the (corrected) value of 3.25, as described by equation (13).[1] Unfortunately this does not give the original volume unless the dry weight is again added; see equation 14.

$$V = Dry\ Weight \times 3.25 \tag{13}$$

$$V = (Dry\ Weight \times 3.25) + Dry\ Weight \tag{14}$$

---

[1] Following the publication of Lee's approach, an erratum was published in which the original error in the calculation of the drying constant was corrected from the (incorrect) published value of 4.167 to 3.25. In fact, the drying constant was shown in the erratum to derive from a plot of dry weight of blood against the original volume which resulted in the mathematical relationship: original volume = weight x 4.167 mL/0.1 mg. In fact, 4.167 should be replaced with the more accurate 4.1364 which is found from plotting the same data as Lee but using the line of best fit produced via Microsoft TM Excel.

If however we divide the wet weight (10.2) by the dry weight (2.4) this will then give the correct constant and subsequently the final and correct equation (15):

$$V = Dry\ Weight \times 4.25 \qquad (15)$$

All PCVs were tested for the drying rate of 1 mL; Table 5 expresses the results, where drying constants were generated.

PCV %	Wet Weight (mg) (W_w)	Dry Weight (mg) (W_d)	W_w / W_d ($W_c{}^{PCV}$)
15	1027.00	126.10	8.14
20	1028.00	131.60	7.81
30	1026.30	157.70	6.51
40	1026.50	190.03	5.40
50	1010.80	230.87	4.38
60	1005.30	265.70	3.78
70	993.40	297.33	3.34
75	980.90	298.00	3.29

Table 5: Reference table depicting dry weight constants $W_c{}^{PCV}$ derived for a range of PCVs.

There is a significant decrease in the drying constant as the PCV increases; this can be attributed to the drying process. Normal blood is generally composed of around 45% PCV, red blood cells have a typical water content of 72% - 73%, [102, 104] plasma has an average water content value of 93% - 94% and whole blood has a water content of 83%. Taking this into consideration, when PCVs are fluctuated, water content can deviate from 77.5% – 90.5% for 15 % - 75% PCV, respectively. Since water will be evaporated as the blood dries, it is understandable that dried blood of a PCV% of 15 will weigh less than that of 75% PCV. Unpaired student *t*-tests were conducted to verify the significance of the data, constants for 15% *vs.* 75%, 15% *vs.* 40% and 40% *vs.* 75% were all compared. Every comparison undertaken resulted in a *p*-value of less than 0.0001; this is considered to be extremely statistically significant. It can therefore be concluded that PCV% has a significant effect on the dry weight of blood. Consequently the constant originally devised by Lee *et al* [39] is quantitatively altered:

$$V = W_d W_c^{PCV} \qquad (16)$$

where W_d is dry weight, V is the original volume and W_c^{PCV} is the dry weight constant with the inclusion of PCV%. Consequently a reference table is added (Table 5) to allow for PCV% fluctuations in calculations.

Surface Type and PCV%		Constant (W_c^{PCV})
Wood	15% PCV	8.178
	40% PCV	5.210
	75% PCV	3.321
Vinyl	15% PCV	8.137
	40% PCV	5.242
	75% PCV	3.461

Table 6: A comparison of surface type and dry weight constants *(W_c^{PCV})* when PCV% has been incorporated, showing there to be no significant difference between surface type.

Further experiments were performed for three PCVs (15, 40, and 75 %) where three different volumes (5 mL, 10 mL and 20 mL) were poured onto vinyl and laminate wood and left to dry overnight. Again calibration graphs were constructed to verify the above constants for greater volumes, the constant (W_c^{PCV}) (Table 6) was found to be in excellent agreement with the previous data and are found to be independent of the type of surface. As previously stated PCV% cannot yet be verified in dry blood, consequently the dry weight method is not considered a viable method of analysis and therefore is not recommended as a form of crime scene volume estimation. A possible solution could be to measure the extremes either side of the average value and include them in the final estimation, giving a range in error.

3.4.2.4.3   Spectrophotometry

The basis of this methodology is the absorbency (*molar absorption coefficient)* of haemoglobin at a wavelength of 412 nm. Varying volumes (10µL – 100µL) of blood were used to create calibration graphs for 15, 40 and 75 PCV%.
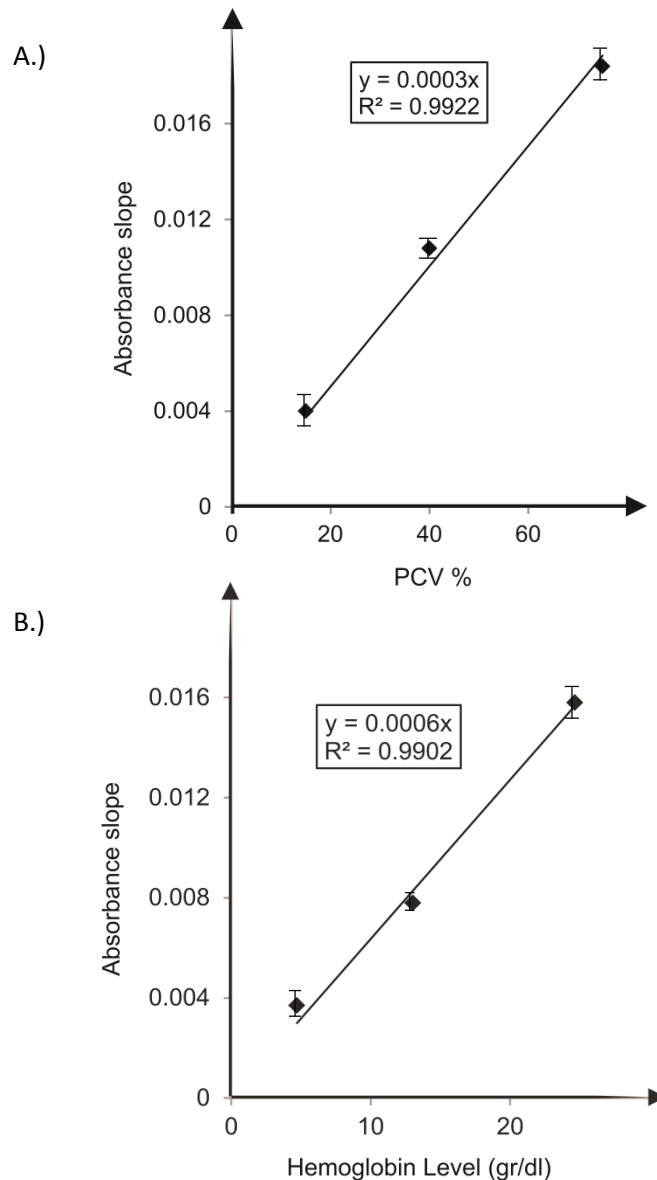
Figure 42: Representations of: A- PCV% and B- haemoglobin levels, against constants (*m*).

The corresponding calibration plots were found to be linear in nature, where the lines of 'best fit' were determined to correspond to: y = 0.0158x, R^2 = 0.8622 (75% PCV), y = 0.0078x, R^2 = 0.9522 (40% PCV) and y = 0.0037x, R^2 = 0.9665 (15% PCV), where x is PCV% and y is absorbance. Using these lines of 'best fit' (slope) a further calibration graph for PCV% was constructed, again a line of 'best fit' was formulated; y = 0.0002x, R^2 = 0.9915 (Figure 42 A), where *x* is PCV% and *y* is the absorbance slope. As the basis of this research is PCV% and previous research was focused around haemoglobin levels the calibration results are slightly different, giving a lower value for the absorbance. However through the introduction of equation (17) we can convert PCV% to haemoglobin values:

$$PCV\% = \left[0.0485(ctHb) + 0.0083\right]x100 \qquad (17)$$

where $ctHb$ (blood concentration of haemoglobin) has the units mmolL^{-1}. Therefore the calibration now becomes: y = 0.0006x; R^2 = 0.9902 (see Figure 42 B). The obtained results are now in a much better agreement with the previously reported value for the line of best fit, although they are still slightly lower, which could be attributed to the expansion of the haemoglobin range under investigation, *i.e.* 4.71 - 24.6 gr/dl (R^2 = 0.99) as opposed to 13.3 – 14.5 gr/dl (R^2 = 0.87). [40]

Three types of surfaces were utilised (carpet, vinyl and laminate wood), where three different volumes were analysed (5mL, 10mL and 20mL). Table 7 expresses the absorbance results.

PCV%	Material	5mL (Average Absorption)	10mL (Average Absorption)	20mL (Average Absorption)
15%	Wood	0.060	0.128	0.161
	Vinyl	0.065	0.093	0.277
	Carpet	0.047	0.124	0.322
40%	Wood	0.016	0.364	0.576
	Vinyl	0.081	0.233	0.425
	Carpet	0.174	0.399	0.825
75%	Wood	0.243	0.551	1.252
	Vinyl	0.433	0.669	1.295
	Carpet	0.359	0.780	1.341

Table 7: Haemoglobin absorbance measured at 412 nm for different volumes, various PCVs and different surface types.

It is apparent that PCV% affects the absorbance levels, generally increasing the absorption peak as the PCV% increases; this is to be expected, since red blood cells increase as PCV increase, and corroborates previous investigations using haemoglobin levels. Ordinarily the calibration graph (Figure 42A) for PCV% versus constants could be used to rectify these differences, providing new constants for each PCV, however it is clear that the surface in which the blood has impacted/ dried on has a considerable effect on the absorbance level. Percentage error rates for each surface were calculated to be: carpet ± 6.08 - 36.59, vinyl ± 2.42 - 47.83 and laminate wood ± 0.92 - 45.77. It is therefore evident that calibrations need to be undertaken for each surface type, this is still possible if a sample of the surface is taken from the crime scene. Ultimately this method, although it accounts for haemoglobin and PCV%

fluctuation, is still not functional as a volume estimation method, again due to there being no way of measuring the haemoglobin level or PCV% from dried blood, however this method is much more promising that the previous two since it at least acknowledges the significance of PCV%.

3.4.3   Summary

It has been determined that blood does in fact dry in a similar way to the 'coffee-ring effect,' it's mechanism depicted in Figure 30, where the edges of the drop are pinned to the impact surface creating a contact angle which when decreased produces a capillary flow and in turn increases surface tension. This causes the collection of particles (i.e. red blood cells) on the drop periphery; such an effect is now termed the blood ring effect. [38, 39] Further research exploring the deformation of red blood cells (in diseases such as Thrombotic Microangiopathy) and how this effects drying should be examined. Particle shape (i.e. sphere to elongate) has been previously demonstrated to play a vital role in the drying mechanism when considering the coffee-ring effect [38] and could therefore potentially change the drying process. It is important to recognise the processes which drive the drying effects and how physical differences between individuals alter these processes as this may ultimately effect drying times.

Finally the application of PCV % has been investigated. It has been widely reported that packed cell volume physically alters viscosity values and would therefore be expected to modify blood drops. Observations under magnification revealed that the drying mechanism changes as PCV decreases, seemingly displaying a much lower coffee-ring effect but maintaining a strong Marangoni flow; this is due to the red blood cells being mainly located within the centre of the drop where surface tension is at its strongest pulling particles inwards. Drying observations which can be used to determine sequencing and volume of blood patterns were also investigated. It was discovered that the halo effect does not appear on bloodstains with less than 50% PCV, limiting its value as an events sequencer. However this study is limited and warrants further investigation using varying conditions. The overall drying time was not affected by PCV%, this was tested using skeletonisation where a ring remains when the stain is wiped. Three volume estimations were carried out; dry weight, scaled photographs and spectrophotometry. Although all three in theory work after some alterations to account for PCV% and surface type, none are viable options as PCV% cannot yet be identified in dried blood. This research was conducted merely to

highlight the importance of considering PCV% in blood experiments and calculations. It is important in future investigations to consider PCV %, with the causes behind such high and low PCV % being centred on health and lifestyle it would be detrimental to an investigation to ignore it. Investigators should try to establish potential PCV% altering conditions wherever possible, such as; pregnancy, anaemia and drug use (i.e. doctor's patient history). There may also be opportunities at crime scenes where blood pooling is present and therefore every opportunity should be seized to obtain a sample for haematological testing.

3.5 CONCLUSIONS

This section has investigated the influence components and substitute blood types have on bloodstains.

Firstly a substitute blood for human blood was explored. Since human blood may contain diseases such as HIV, which is potentially deathly, blood substitutes are often employed as a safe alternative. Current alternatives include porcine and sugar based substitutes, however they are difficult to obtain or are unrealistic and therefore lack the reliability to produce a viable substitute.

Equine blood is a more readily available animal blood and is ethically gathered from the horses, however only limited research had previously been performed on equine bloods applicability to real human blood. In the first study this was investigated. Horse blood was found to be a viable substitute, mimicking the stain size and spread of human blood (similar C_d values). This result is only valid, however, with certain anticoagulants. Alsever's anticoagulant created a less viscous blood, increasing the stain size significantly. Defibrinated equine blood exhibited bloodstains which closely resembled human blood and therefore is concluded to be a reliant human blood substitute.

Secondly, packed cell volume was explored, since PCV% directly effects the viscosity and subsequently the spread of liquid. Varying PCV% levels were tested, ranging from 15%-75% which relate to certain physiological occurrences within a human (*i.e.* anaemia). Results found that PCV% significantly affected the size of bloodstain diameters, where diameters decreased as PCV% increased. This result was anticipated since PCV% directly relates to the viscosity of blood, thus effectively altering the spread of blood due to the change in resistance to flow. Angled impacts remained unchanged, suggesting that spread was evenly distorted throughout the stain; length and width are the same, therefore cancelling changes out. However since the bloodstain increases in size it still possible that misinterpretations of patterns may arise (*i.e.* a mist pattern *vs.* impact pattern, or a spurt *vs.* a gush).

Finally the drying mechanism of blood has been evaluated. Marangoni flow/ effect was recently attributed to be the sole driving force of blood drying. [33] Studies within this research found similar conclusions, however also discovered that

Marangoni was not the lone drying force; the coffee ring effect was also present, creating small, thick ring around the periphery of the stain. This was further altered when PCV% was considered, where lower PCV% exhibited a predominantly coffee ring driven drying compared to higher PCV% where a Marangoni flow acted alone.

Further drying studies evaluated volume analysis, skeletonisation and the halo effect. The PCV% was found not to change the skeletonisation or halo effect, however volume analysis was altered substantially. There are several methods of establishing the volume of bloodstains; each of these was evaluated to determine the effect PCV% had on the reliability/validity of the methods. All volume estimation methods were found to be unreliable once PCV% is considered. As blood is predominantly water (83%), when drying occurs most of this water evaporates leaving a smaller, less heavy stain. When PCV% is changed this can increase / decrease the water content significantly, due to water content in plasma and red blood cells. Most methods of volume determination do not account for either the change in the weight nor the decrease in flow due to viscosity changes, since most volume estimation is reliant on size/ spread/ weight of the blood it is unsurprising that these methods are unreliable when blood components are changed. Therefore extremes should be calculated, therefore establishing an error which can be applied to the final estimation.

In conclusion, this section has highlighted how the simple manipulation of RBC ratio, which occurs naturally, can alter the way bloodstains spread, mechanism of blood drying and ultimately result in unreliable methods of volume estimation.

It is important to establish how PCV% affected bloodstains not only for the benefits it holds when evaluating stains at crime scenes but for accuracy when conducting experiments, where PCV% can and should be controlled, setting provisions where this is not possible.

PART II:
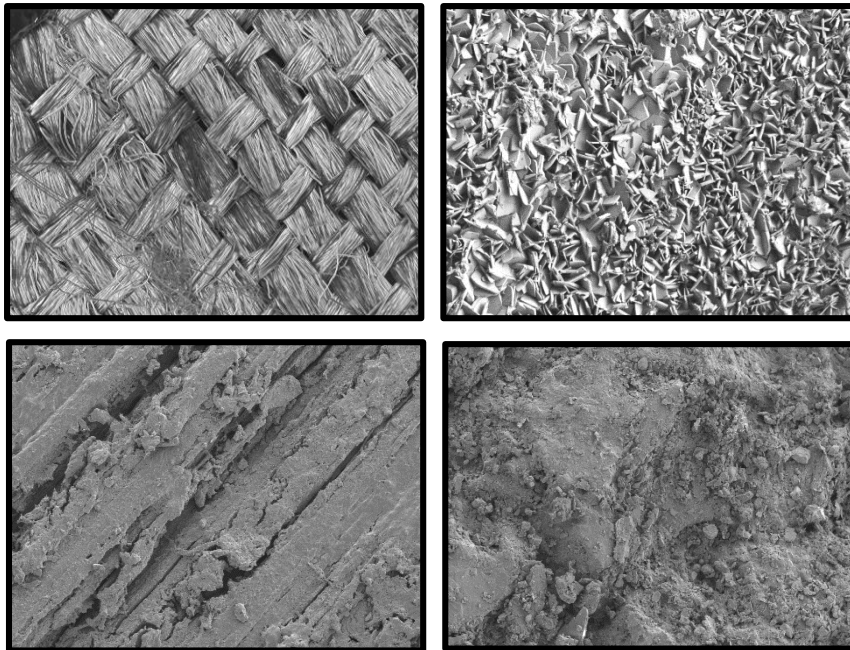
IMPACT SURFACES

4. SURFACES

Look around the room you are in, no doubt it will have a floor, a ceiling and walls, what are they made from? How are they decorated? Typically a room will house a variety of different surfaces, for example floors can be made from wood, be carpeted or tiled. One of the main factors that must be considered when interpreting bloodstain patterns is the impact surface. The topography and composition of the surface is important as it can affect the size, shape and spreading of blood.

It is an impossible feat to test every single surface possible, not only are there too many but the conditions which they can be found in are variable (finishes, weathering, temperature and wear and tear). Therefore the following analysis only scratches the surfaces of this topic, however it should offer valuable insights into surface interaction which has, so far, not been researched in this depth before.

4.1 Surface Finish

Surface Finish (surface topography) is the deliberate manufacturing /modification of a surface to create a certain product, *e.g.* a polished finish. [119 − 122] Finishing processes can be exercised to: improve appearance, change wettability, weathering resistance, wear resistance, modify electrical conductivity, remove flaws or wettability, and control the surface friction.

There are a multitude of manufacturing processes *e.g.* polishing, abrasive blasting, honing, chemical milling *etc.* Each manufacturing process produces a different surface texture. [119 − 122]

Surface finish is defined using three characteristics:

4.1.1 Surface Roughness - Surface roughness is effectively the small irregularities found on the surface, which are inherent in the material or production process. Roughness plays a vital role in determining how the surface will react with a given environment, where rougher surfaces tend to wear more quickly. [119 − 122]

The surface roughness will also affect the way liquids impinge and spread on a surface, a factor which is significant when topic at hand is considered. [119 − 122]

4.1.2　Lay

Lay - Lay or directionality is the direction of the surface pattern (Figure 43), which is determined by the production process. [119 – 122]

Radial	**Vertical**	**Horizontal**
Circular	**Isotropic**	**Cross-Hatched**
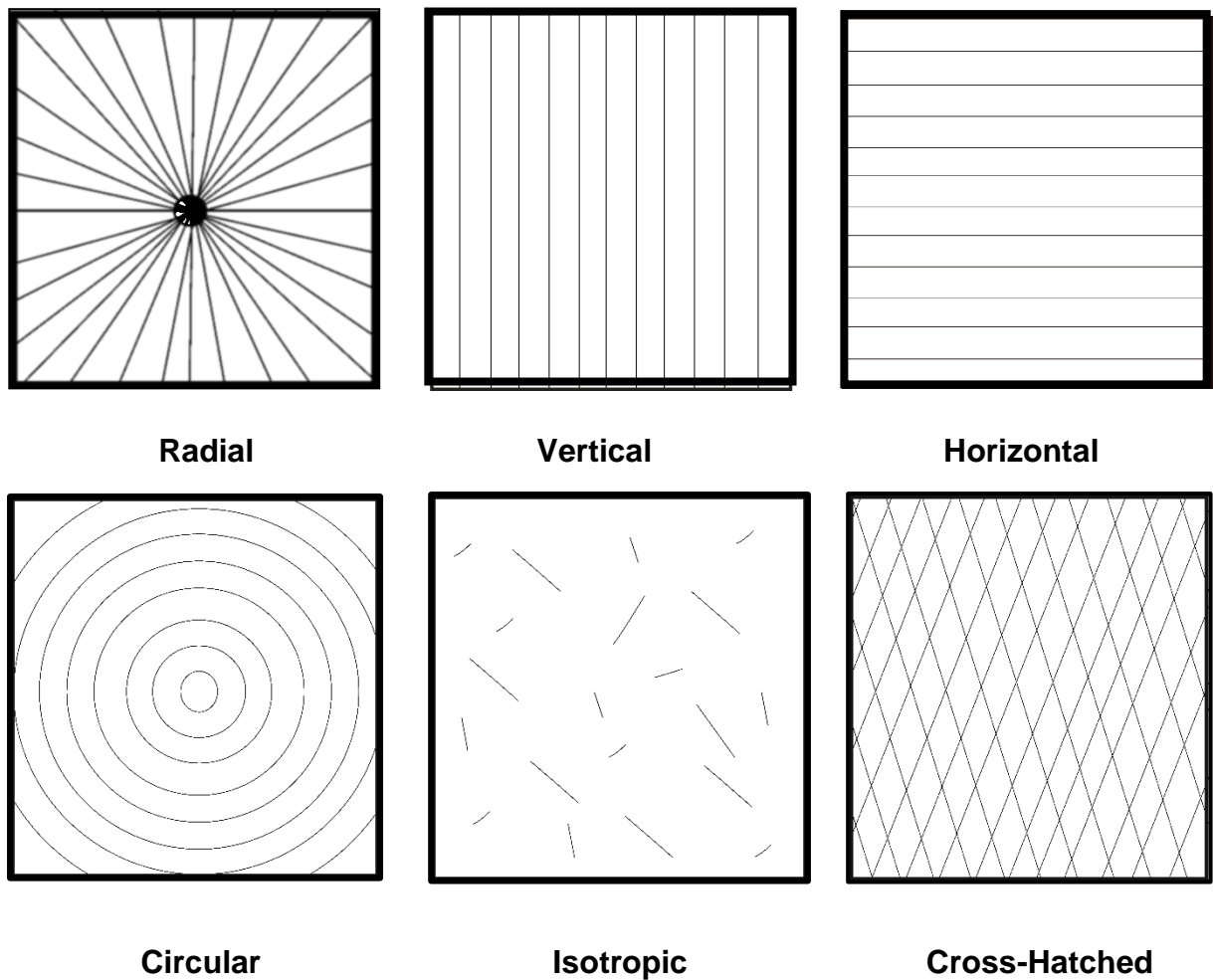
Figure 43: Six main types of surface lay, created through the production process. [119 – 122]

4.1.3　Waviness

Waviness - Waviness is a broader measure than surface roughness which measures surface irregularities caused by instabilities (warping, vibrations, or deflection) experienced during the machining process. [119 – 122]

4.2 PRELIMINARY SURFACE ANALYSIS

Since there has been little quantitative research performed presently with regards to blood drops and the known direct correlation there is between roughness and fluid flow, [14, 20, 47] surface roughness was the first surface property to be investigated.

4.2.1 Initial Observations

As some previous experimentation (section 3.2) on different surfaces had already been carried out during the validation of defibrinated equine blood as a viable human blood substitute, initial observations and calculations were undertaken using the data collected.

When comparing surface roughness, in accordance with the final stain diameters (D_s) ascertained during the drop tests, it was apparent that there is an effect; however due to the inconsistency of the tested surfaces, that is the surface roughness is heterogeneous in nature, there are anomalies within the results. This is demonstrated in Figure 20 where it appears that the smaller stains were produced on the cold rolled steel when compared to the paper, where the surface was much rougher. It is nevertheless evident from the observed blood stains that there is a decrease in stain diameter in accordance with surface roughness, such that the lowest roughness value gives larger bloodstain diameters (D_s). Similar results were exhibited for both Alsever's equine blood (Figure 21) and human blood (Figure 22), where bloodstains decreased when the surface roughness increased. Further verified by performing t-tests where all p values for the three bloods were found to be extremely statistically significant, $p < 0.0015$.

Initial conclusions could therefore be formed stating that a decrease in drop diameter and an increase in surface roughness ultimately produce smaller blood stains. This is concurrent with previous research in which porcine blood was tested. [18] Spines were also evaluated, counting them on the periphery of the bloodstain. Results obtained for the number of spines observed when using all bloods were also in excellent agreement with previous research, [18] showing that the rougher the surface, the greater preponderance of spines.

4.3   ANGLED SURFACE STUDY

4.3.1   Experimental

Impact angles (22.7°, 43.5°, 56.3°, 61.6°, 78.8° and 90°) were created by moving surfaces vertically to create a multitude of angles ranging from 22.7º to 90º. Heights of 50 – 200 cm were chosen as blood drop release heights as these could be easily correlated with previous values when angled impacts were considered. [17]

4.3.2   Results and Discussion

4.3.2.1   Considering the surface type - Paper

The first surface to be considered was paper which has been previously utilised in research by both Knock *et al* [17] and Hulse-Smith *et al* [18] and is therefore an appropriate approach to allow a direct method comparison to be made and ensure the validity of the equine blood which is utilised throughout the investigation. When considering angled impacts both the width (*a*) and elliptical length (*b*) of the stain are noted, as a bloodstain elongates as the angle increases. In order to use the correlations of the Reynolds and Weber numbers it is necessary to use dimensionless constant, α for angled impacts:

$$\alpha = \frac{ab}{D_o^2} \qquad (18)$$

Measurements of the width and length of the bloodstain were undertaken. Equation (19) was utilised to identify the stain size *S*, which is a generic equation used to find the area of an ellipse:

$$S = \frac{\pi ab}{4} \qquad (19)$$

Knock *et al* [17] created further theoretical parameters Re_I and Re_{IM} which were found to be proportional to the Weber and Reynolds numbers, where Re_I is the original equation [17] (equation 20) and Re_{IM} is the (mis)printed equation (equation 21) developed after countless experiments undertaken on a variety of liquids: [17]

$$Re_I \propto Re^{1/2} We^{1/4} \qquad (20)$$

$$Re_I \propto (Re^{1/2}We^{1/4})^{0.75} \qquad (21)$$

Table 8 shows the relationships of various parameters (Equations 18 – 21) to determine the best correlation; these parameters have previously been demonstrated to give excellent correlations. [17]

Equation	Vertical 90° y = mx + c	Vertical 90° y = mx	All data y = mx + c	All data y = mx
S *vs. Re*	$R^2 = 0.61$	$R^2 = 0.54$	R^2 ² = 0.53	$R^2 = 0.45$
S *vs. We*	$R^2 = 0.47$	$R^2 = -0.71$	$R^2 = 0.40$	$R^2 = -0.69$
S *vs. ReD_oD_o*	y = 0.002x + 59.751 $R^2 = 0.93$	y = 0.003x $R^2 = 0.74$	y = 0.002x + 68.891 $R^2 = 0.82$	y = 0.003x $R^2 = 0.64$
S *vs. $Re_ID_oD_o$*	$R^2 = 0.92$	$R^2 = 0.76$	$R^2 = 0.8$	$R^2 = 0.66$
S *vs. $Re_{IM}D_oD_o$*	$R^2 = 0.83$	$R^2 = 0.65$	y = 0.1247x + 32.937 $R^2 = 0.84$	y = 0.1463x $R^2 = 0.81$
α *vs. Re*	$R^2 = 0.93$	$R^2 = 0.28$	$R^2 = 0.67$	$R^2 = 0.16$
α *vs. $Re^{0.5}$*	$R^2 = 0.93$	$R^2 = 0.92$	$R^2 = 0.67$	$R^2 = 0.67$
α *vs. We*	$R^2 = 0.92$	$R^2 = -3.18$	$R^2 = 0.65$	$R^2 = -2.53$
α *vs. Re_I*	$R^2 = 0.93$	$R^2 = 0.35$	$R^2 = 0.67$	$R^2 = 0.21$
α *vs. Re_{IM}*	$R^2 = 0.93$	$R^2 = 0.80$	$R^2 = 0.67$	$R^2 = 0.56$

Table 8: Various parameters correlated against stain size found paper to establish the most significant R^2 values and therefore the best coefficient.

It was found that stain size exhibits poor correlations when plotted against the original Weber and Reynolds number expressing a coefficient of just $R^2 = 0.4$ and $R^2 = 0.53$ respectively. However when the theoretical parameters were used, (Re_I, Re_{IM}, $Re^{0.5}$, $We^{0.5}$) as introduced by Knock *et al* [17] much more effective coefficients were observed ranging from $R^2 = 0.67$ to $R^2 = 0.84$ (see Figure 44) when all data points were considered (angled and vertical impacts).
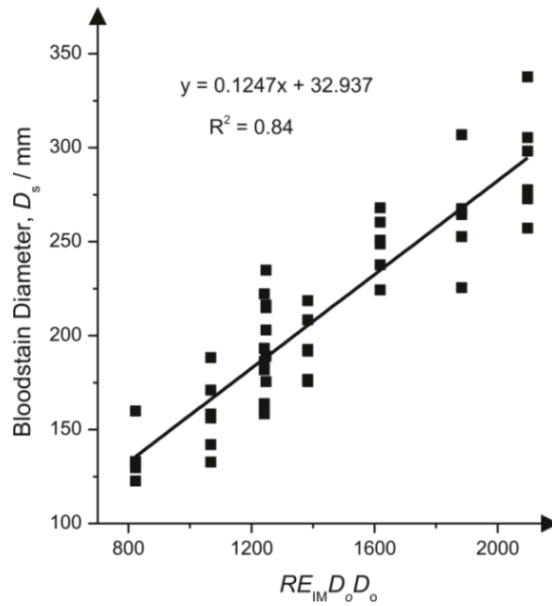
Figure 44: Resultant stain size exhibited on paper at various impact angles plotted against $RE_{IM}D_oD_o$

Using the most significant correlation these parameters can be applied to the mathematical equation introduced by Knock *et al*: [17]

$$ab = m_1 MD^2_o + c_1 \qquad (22)$$

where m_1 and c_1 are constants and M is an non-dimensional number *i.e.* ReD_oD_o.

Similarly to previous work [17] the number of spines exhibits significant correlations, which is shown in Table 9, were found when the square root of the Weber number and Re_{IM} were employed.

Equation	Vertical 90° y = mx+ c	Vertical 90° y = mx	All data y = mx+ c	All data y = mx
N vs. Re	$R^2 = 0.96$	$R^2 = 0.66$	$R^2 = 0.20$	$R^2 = 0.20$
N vs. We	$R^2 = 0.93$	$R^2 = -1.64$	$R^2 = 0.19$	$R^2 = 0.03$
N vs. We$^{0.5}$	$R^2 = 0.96$	$R^2 = 0.91$	$R^2 = 0.20$	$R^2 = 0.16$
N vs. Re$_l$	$R^2 = 0.96$	$R^2 = 0.71$	$R^2 = 0.20$	$R^2 = 0.20$
N vs. Re$_{IM}$	$R^2 = 0.97$	$R^2 = 0.94$	$R^2 = 0.20$	$R^2 = 0.19$

Table 9: Number of spines correlated against various parameters to establish the best correlation coefficient, R^2 value.

Next to be considered was the effect of the angle of impact upon the correlations which have shown to be significant when considering the vertical impact. When stain size is analysed the most significant correlation occurs when θ is zero, this

is due to the same quantity of blood existing regardless of the angle of impact. [17] Reflecting upon this stain size can now be expressed as the following equation:

$$ab = 0.1247 \, (Re^{0.5}We^{0.25})^{0.75}D_o D_o + 32.937 \qquad (23)$$

In comparison with the previous study [17] a difference in final equation is found, whereby the constant m_1 was significantly larger equating to 111.74 and constant c is much smaller at a value of 0.00084. [17] After exploration into these values it is found that they are incorrect or misquoted in the Knock *et al* and give an erroneous answer as a result.

					N			
Equation	-2	-1	0	0.5	1	2	3	4
$N = mResin^n\theta + c$	—	—	—	—	y = 0.0086x - 6.6605 0.88	y = 0.0075x + 0.6681 0.92	0.87	0.80
$N = mResin^n\theta$	—	—	—	—	y = 0.0068x 0.84	y = 0.0077x 0.92	0.82	0.65
$N = mWe^{0.5}sin^n\theta + c$	—	—	—	—	0.89	y = 0.7364x + 0.3884 0.92	0.87	0.80
$N = mWe^{0.5}sin^n\theta$	—	—	—	—	0.84	y = 0.747x 0.92	0.82	0.66
$N = mRE_l D_o D_o sin^n\theta + c$	—	—	—	—	0.73	y = 0.0042x + 3.5178 0.82	y = 0.0039x + 6.5979 0.80	0.75
$N = mRE_l D_o D_o sin^n\theta$	—	—	—	—	0.73	y = 0.0048x 0.80	y = 0.0051x 0.70	0.53
$N = mRE_{IM} D_o D_o sin^n\theta + c$	—	—	—	—	0.76	y = 0.0204x + 2.2475 0.83	0.80	0.74
$N = mRE_{IM} D_o D_o sin^n\theta$	—	—	—	—	0.80	y = 0.0222x 0.82	0.72	0.55

Table 10: The most significant R^2 values when considering angled impacts on paper correlated against the number of spines.

Lastly the data expressed for the number of spines considering impact angle was analysed, as depicted in Table 10, very high correlation coefficients with a value of $R^2 = 0.92$ were observed when using the square root of the Weber number. Using a previously derived equation (24) where n is a constant and θ is the impact angle, an equation (25) which considers the angle of impact with the number of spines can now be denoted ;

$$y = m \, x \, \sin n \, \theta + c \qquad (24)$$

$$N = 0.75 W e^{0.5} \sin^2 \theta \qquad (25)$$

The constant n has now changed from the previous value [17] of 3 to 2; however constant m has remained unchanged. Due to the uncertain nature of spines and their calculation, it is difficult to establish the correct equation constants as both produce realistic spine values. It would therefore be advised not to use spines in analysis at all; they offer no concrete results and add an unnecessary and time consuming aspect to an already complex analytical field.

4.3.2.2   Considering the surface type - Steel and Plastic

The effects of angles on different surfaces, namely plastic and steel were investigated. It has already been widely recognised that surface roughness is highly influential in the final appearance of the bloodstain and is therefore an anticipated exploration which was not previously undertaken by Knock *et al* whose work centred around paper. [17] Similarly to that of the paper surface, blood was dropped from a range of heights at varying impact angles onto both surface types (steel and plastic) where widths and elliptical lengths were subsequently measured.

	Vertical 90°	Vertical 90°	All data	All data
Equation	y = mx+ c	y = mx	y = mx+ c	y = mx
S *vs. Re*	$R^2 = 0.60$	$R^2 = 0.56$	$R^2 = 0.49$	$R^2 = 0.45$
S *vs. We*	$R^2 = 0.44$	$R^2 = -0.46$	$R^2 = 0.36$	$R^2 = -0.51$
S *vs. Re*$D_o D_o$	y = 0.002x + 54.995 $R^2 = 0.93$	y = 0.003x $R^2 = 0.83$	y = 0.003x + 61.693 $R^2 = 0.80$	y = 0.003x $R^2 = 0.70$
S *vs. Re$_I$*$D_o D_o$	$R^2 = 0.91$	$R^2 = 0.38$	$R^2 = 0.78$	$R^2 = 0.7$
S *vs. Re$_{IM}$*$D_o D_o$	y = 0.1407x + 14.095 $R^2 = 0.96$	y = 0.1499x $R^2 = 0.95$	y = 0.1448x + 19.574 $R^2 = 0.83$	y = 0.1576x $R^2 = 0.82$
α vs. Re	$R^2 = 0.95$	$R^2 = 0.60$	$R^2 = 0.67$	$R^2 = 0.31$
α vs. Re$^{0.5}$	$R^2 = 0.97$	$R^2 = 0.94$	$R^2 = 0.67$	$R^2 = 0.67$
α vs. We	$R^2 = 0.88$	$R^2 = -2.07$	$R^2 = 0.61$	$R^2 = -2.00$
α vs. Re$_I$	$R^2 = 0.94$	$R^2 = 0.61$	$R^2 = 0.65$	$R^2 = 0.32$
α vs. Re$_{IM}$	$R^2 = 0.94$	$R^2 = 0.90$	$R^2 = 0.65$	$R^2 = 0.59$

Table 11: R^2 values established when considering the correlation of various parameters against stain size exhibited upon a steel surface.

	Vertical 90°	Vertical 90°	All data	All data
Equation	y = mx+ c	y = mx	y = mx+ c	y = mx
S *vs. Re*	$R^2 = 0.69$	$R^2 = 0.60$	$R^2 = 0.58$	$R^2 = 0.55$
S *vs. We*	$R^2 = 0.54$	$R^2 = -0.90$	$R^2 = 0.44$	$R^2 = -0.44$
S *vs. Re*$D_o D_o$	y = 0.002x + 76.053 $R^2 = 0.95$	y = 0.003x $R^2 = 0.65$	y = 0.002x + 58.239 $R^2 = 0.88$	y = 0.003x $R^2 = 0.77$
S *vs. Re$_I$*$D_o D_o$	$R^2 = 0.94$	$R^2 = 0.69$	$R^2 = 0.87$	$R^2 = 0.78$
S *vs. Re$_{IM}$*$D_o D_o$	y = 0.1119x + 44.648 $R^2 = 0.96$	y = 0.1411x $R^2 = 0.89$	y = 0.1405x + 17.771 $R^2 = 0.91$	y = 0.1521x $R^2 = 0.8985$
α vs. Re	$R^2 = 0.85$	$R^2 = 0.12$	$R^2 = 0.82$	$R^2 = 0.49$
α vs. Re$_I$$^{0.5}$	$R^2 = 0.87$	$R^2 = 0.87$	$R^2 = 0.84$	$R^2 = 0.82$
α vs. We	$R^2 = 0.86$	$R^2 = -3.44$	$R^2 = 0.77$	$R^2 = -1.89$
α vs. Re$_I$	$R^2 = 0.89$	$R^2 = 0.25$	$R^2 = 0.82$	$R^2 = 0.52$
α vs. Re$_{IM}$	$R^2 = 0.90$	$R^2 = 0.75$	$R^2 = 0.82$	$R^2 = 0.78$

Table 12: Resultant stain sizes on a plastic surface correlated against numerous parameters to determine the best coefficient R^2 value.

Stain sizes were correlated against numerous parameters, as shown in Tables 11 and 12 and exhibited profound correlations when ReD_oD_o, $RE_{IM}D_oD_o$ and $RE_ID_oD_o$ were used. When the most significant parameters were applied and a further consideration of impact angle (θ) is added it was again observed that the best correlation was exhibited when θ is zero, cementing the evaluation that stain size is not directly influenced by angle of impact. [17] Final stain size equations for both steel (equation 26) and plastic (equation 27) were therefore generated using equation (22) and the parameter $RE_{IM}D_oD_o$ which exhibited coefficient values of 0.83 and 0.91:

$$ab = 0.1448\ (Re^{0.5}We^{0.25})^{0.75}D_oD_o + 19.574 \qquad (26)$$

$$ab = 0.1405\ (Re^{0.5}We^{0.25})^{0.75}D_oD_o + 17.771 \qquad (27)$$

Tables 13 and 14 evaluate the correlation of the number of spines for steel and plastic respectively, where low correlations were realised in both the vertical impact and in considering all the data (angles 22.7^o to 90°). The number of spines (N) is affected by the surface (steel) it impacts and could explain the low correlations due to the lack of surface roughness to produce a significant amount of stain disruption and subsequently the production of spines.

Equation	Vertical 90° $y = mx+ c$	Vertical 90° $y = mx$	All data $y = mx+ c$	All data $y = mx$
N vs. Re	$R^2 = 0.75$	$R^2 = 0.53$	$R^2 = 0.35$	$R^2 = 0.24$
N vs. We	$R^2 = 0.73$	$R^2 = 0.70$	$R^2 = 0.32$	$R^2 = 0.31$
N vs. $We^{0.5}$	$R^2 = 0.71$	$R^2 = 0.50$	$R^2 = 0.32$	$R^2 = 0.22$
N vs. Re_I	$R^2 = 0.74$	$R^2 = 0.52$	$R^2 = 0.34$	$R^2 = 0.23$
N vs. Re_{IM}	$R^2 = 0.73$	$R^2 = 0.42$	$R^2 = 0.34$	$R^2 = 0.19$

Table 13: The number of spines on a steel surface correlated against various theoretical parameters to determine significant R^2 value.

	Vertical 90°	Vertical 90°	All data	All data
Equation	y = mx+ c	y = mx	y = mx+ c	y = mx
N vs. Re	$R^2 = 0.31$	$R^2 = 0.25$	$R^2 = 0.29$	$R^2 = 0.25$
N vs. We	$R^2 = 0.19$	$R^2 = 0.18$	$R^2 = 0.26$	$R^2 = 0.26$
N vs. We$^{0.5}$	$R^2 = 0.18$	$R^2 = 0.16$	$R^2 = 0.25$	$R^2 = 0.22$
N vs. Re$_I$	$R^2 = 0.24$	$R^2 = 0.21$	$R^2 = 0.27$	$R^2 = 0.24$
N vs. Re$_{IM}$	$R^2 = 0.24$	$R^2 = 0.17$	$R^2 = 0.27$	$R^2 = 0.20$

Table 14: R^2 values established when correlating number of spines exhibited on a plastic surface with several theoretical parameters.

Although there were no distinctive correlations, spines were still investigated at different impacting angles (viz. Table 15 and 16) to verify their usefulness, however again no significant correlations were realised. The use of different surfaces has exposed the variability of spines as a BPA concept and their ultimate unsuitability within this scientific discipline.

	N							
Equation	-2	-1	0	0.5	1	2	3	4
$N = mRe\,sin^n\theta + c$	—	—	—	—	y = 0.0066x - 8.5947 0.65	y = 0.0054x - 1.8795 0.59	0.52	0.46
$N = mRe\,sin^n\theta$	—	—	—	—	y = 0.0043x 0.56	y = 0.0048x 0.58	0.51	0.41
$N = mWe^{0.5}sin^n\theta + c$	—	—	—	—	y = 0.6263x - 8.1468 0.59	y = 0.507x - 1.4733 0.55	0.50	0.42
$N = mWe^{0.5}sin^n\theta$	—	—	—	—	y = 0.416x 0.52	y = 0.4667x 0.54	0.49	0.37
$N = mRE_I D_o D_o sin^n\theta + c$	—	—	—	—	y = 0.0038x - 6.414 0.70	y = 0.0034x - 1.5335 0.67	0.61	0.54
$N = mRE_I D_o D_o sin^n\theta$	—	—	—	—	y = 0.0028x 0.64	y = 0.0031x 0.67	0.60	0.50
$N = mRE_{IM} D_o D_o sin^n\theta + c$	—	—	—	—	0.59	0.54	0.49	0.43
$N = mRE_{IM} D_o D_o sin^n\theta$	—	—	—	—	0.46	0.50	0.48	0.43

Table 15: R^2 values obtained when correlations using various theoretical parameters against the number of spines when considering an angled steel surface.

Equation	N							
	-2	-1	0	0.5	1	2	3	4
$N = mRe\sin^n\theta + c$	—	—	—	—	y = 0.0052x - 9.3138 0.63	y = 0.0041x - 3.8227 0.56	0.49	0.43
$N = mRe\sin^n\theta$	—	—	—	—	y = 0.0027x 0.47	y = 0.0031x 0.51	0.48	0.42
$N = mWe^{0.5}\sin^n\theta + c$	—	—	—	—	y = 0.5015x - 9.2637 0.61	y = 0.3967x - 3.6509 0.53	0.46	0.40
$N = mWe^{0.5}\sin^n\theta$	—	—	—	—	y = 0.2624x 0.45	y = 0.2969x 0.49	0.46	0.40
$N = mRE_I D_o D_o \sin^n\theta + c$	—	—	—	—	y = 0.0029x - 6.8545 0.62	y = 0.0025x - 3.1577 0.59	0.54	0.48
$N = mRE_I D_o D_o \sin^n\theta$	—	—	—	—	y = 0.0017x 0.51	y = 0.002x 0.56	0.53	0.48
$N = mRE_{IM} D_o D_o \sin^n\theta + c$	—	—	—	—	y = 0.0192x - 8.4438 0.70	0.65	0.58	0.51
$N = mRE_{IM} D_o D_o \sin^n\theta$	—	—	—	—	y = 0.0127x 0.60	0.64	0.57	0.48

Table 16: The most significant correlations of number of spines against parameters when varying angled impacts upon a plastic surface are performed.

4.3.2.3   Considering the surface type – All Surface Data

Lastly all data (steel, paper and plastic) was collated to see if a general equation could be identified that relates to all surfaces studied in this work. (see Appendix 4) Table 17 demonstrates the correlations of stain size against various parameters.

	Vertical 90°	Vertical 90°	All data	All data
Equation	y = mx+ c	y = mx	y = mx+ c	y = mx
S vs. Re	$R^2 = 0.58$	$R^2 = 0.53$	$R^2 = 0.52$	$R^2 = 0.48$
S vs. We	$R^2 = 0.45$	$R^2 = -0.62$	$R^2 = 0.39$	$R^2 = -0.53$
S vs. ReD_oD_o	y = 0.002x + 63.6 $R^2 = 0.87$	y = 0.003x $R^2 = 0.70$	y = 0.002x + 62.941 $R^2 = 0.82$	y = 0.003x $R^2 = 0.70$
S vs. $Re_ID_oD_o$	$R^2 = 0.85$	$R^2 = 0.72$	$R^2 = 0.8$	$R^2 = 0.71$
S vs. $Re_{IM}D_oD_o$	y = 0.1208x + 29.029 $R^2 = 0.89$	y = 0.1397x $R^2 = 0.87$	y = 0.1367x + 23.427 $R^2 = 0.85$	y = 0.152x $R^2 = 0.8337$
α vs. Re	$R^2 = 0.78$	$R^2 = 0.31$	$R^2 = 0.70$	$R^2 = 0.32$
α vs. $Re^{0.5}$	$R^2 = 0.79$	$R^2 = 0.78$	$R^2 = 0.71$	$R^2 = 0.70$
α vs. We	$R^2 = 0.75$	$R^2 = -2.40$	$R^2 = 0.65$	$R^2 = -2.06$
α vs. Re_I	$R^2 = 0.78$	$R^2 = 0.37$	$R^2 = 0.69$	$R^2 = 0.34$
α vs. Re_{IM}	$R^2 = 0.79$	$R^2 = 0.70$	$R^2 = 0.69$	$R^2 = 0.62$

Table 17: Significant R^2 value correlation coefficients were exhibited when plotting various parameters against the stain size presented on all surfaces (paper, steel and plastic).

Again it was observed that the highest data correlation when stain size was plotted against $RE_{IM}D_oD_o$, displaying an R^2 value of 0.85 when all data points were considered (not just vertical impacts), with the knowledge from the previous two experiments that angle of impact bears no effect on the stain size, as the velocity tends to zero (equal zero). Equation (22) was used and constants were applied to create a new equation which combines all surface data;

$$ab = 0.1367 (Re^{0.5}We^{0.25})^{0.75}D_oD_o + 23.427 \qquad (28)$$

It is interesting to note that when all equations were compared (23 and 26 – 28) that there was no significant difference between them offering excellent prospects for applications at a Crime Scene where numerous surfaces are encountered. Note that this is the first time that an extensive quantitative surface study has been performed. Equation (28) merely offers a basis for future surface analysis where a greater range of surface roughness maybe explored.

	Vertical 90	Vertical 90	All data	All data
Equation	y = mx+ c	y = mx	y = mx+ c	y = mx
N vs. Re	$R^2 = 0.21$	$R^2 = 0.20$	$R^2 = 0.20$	$R^2 = 0.18$
N vs. We	$R^2 = 0.17$	$R^2 = 0.12$	$R^2 = 0.18$	$R^2 = 0.17$
N vs. We$^{0.5}$	$R^2 = 0.17$	$R^2 = 0.16$	$R^2 = 0.18$	$R^2 = 0.17$
N vs. Re$_l$	$R^2 = 0.19$	$R^2 = 0.18$	$R^2 = 0.19$	$R^2 = 0.18$
N vs. Re$_{IM}$	$R^2 = 0.19$	$R^2 = 0.16$	$R^2 = 0.19$	$R^2 = 0.15$

Table 18: Number of spines presented upon all surfaces (paper, plastic and steel) correlated against various parameters to determine significant R^2 value.

Lastly, spines were proven to be insignificant when all surface data were analysed collectively, Table 18 demonstrates this, showing the insignificance of spines when both vertical impacts all data are considered mirroring previous results. When angled impacts were incorporated (Table 19) a maximum correlation of just $R^2 = 0.54$ was experienced, this is extremely low and therefore could be taken no further in terms of equation formulation.

	N							
Equation	-2	-1	0	0.5	1	2	3	4
$N = mResin^n\theta + c$	—	—	—	—	y = 0.0068x - 8.1897 0.54	y = 0.0057x - 1.6781 0.52	0.47	0.42
$N = mResin^n\theta$	—	—	—	—	y = 0.0046x 0.47	y = 0.0052x 0.51	0.46	0.38
$N = mWe^{0.5}sin^n\theta + c$	—	—	—	—	y = (0.7853x + 22.928) 0.52	0.50	0.45	0.40
$N = mWe^{0.5}sin^n\theta$	—	—	—	—	0.46	0.49	0.44	0.36
$N = mRE_lD_oD_osin^n\theta + c$	—	—	—	—	0.51	y = 0.0033x - 0.3911 0.52	0.49	0.44
$N = mRE_lD_oD_osin^n\theta$	—	—	—	—	0.48	y = 0.0033x 0.52	0.47	0.39
$N = mRE_{IM}D_oD_osin^n\theta + c$	—	—	—	—	y = 0.0185x - 6.6343 0.50	y = 0.0161x - 1.105 0.51	0.46	0.42
$N = mRE_{IM}D_oD_osin^n\theta$	—	—	—	—	0.46	0.50	0.46	0.38

Table 19: Correlation coefficients (R^2) established after plotting the number of spines against a series of parameters when angled impacts upon all surface types (steel, paper and plastic) are enforced.

4.3.3   Summary

After investigation into the effects of various surfaces on the angle of impact, a useful equation has been formulated for the first time which includes all surfaces to enable a stain size to be established where $ab = 0.1367 (Re^{0.5}We^{0.25})^{0.75}D_oD_o + 23.427$. However this formula has a correlation coefficient of just 0.85 so merely forms a basis to provide insights and start to allow the subject to become semi-quantitative. Note though, this would not be sufficient enough to use in a crime scene scenario, since it is only 85% reliable and due to BPAs use in legal proceedings where 'proof beyond reasonable doubt' is vital to sustaining a conviction or an acquittal.

It is recognised throughout this investigation that there was a need for a more proficient and structured procedure of analysis as there appears to be substantial differences when experimental research is compared, for instance the significance of spines within BPA analysis has been brought into question within this paper and yet seems to be noteworthy in other studies. [17 - 18]

It is found that although spines did follow the general pattern of increasing with release height, spines are insignificant and hold no real purpose this context. Spines do not tell us anything unique about a bloodstain that we do not already know from interpreting the size of the bloodstain. However spines can be utilised to determine directionality and evaluate surface finish, so are useful in real crime scene scenarios when interpreting bloodstain patterns. Size and diameter interpretation of a bloodstain seems to be the more viable option in this study, giving more consistent and applicable results.

4.4 SINGLE SURFACE ANALYSIS

It is not only the surface type alone which can alter bloodstains (*i.e.* stone, metal, wood etc.), [14, 18, 20, 47] the individual properties which are divided into sub-types within one surface can also potentially alter the way a liquid (blood) impinges on the target surface.

This chapter is divided into individual surfaces where characteristics such as the finish, grade, roughness and density *etc.* are taken into consideration. Detailed analysis of individual surface types has not currently been investigated prior to this work and therefore should provide some novel insights into surface impacts.

4.5 WOOD

Wood is over 400 billion years old and is one of the most important renewable resources in the world providing fuel, construction material, furniture, paper etc. [123 – 126] The use of wood to this extent makes it one of the most common surfaces expected to be encountered at a crime scene, and subsequently its likely interaction with blood should a blood shedding incident occur. The complex nature of wood however means that blood interactions may vary significantly. The way wood naturally develops creates variations in wood grain, porosity, colour, surface finish and imperfections (*i.e.* knots), this does not include how we ourselves manufacture (*i.e.* engineered, solid) and treat wood (*i.e.*varnish). [123 – 126]

The following study investigates some of these variations, considering surface finish, wood type, wood grade and engineered *vs.* solid wood.

4.5.1 Formation of Wood

Wood is a hard fibrous material manufactured from trees and woody plants, it is found in the roots and stems, growing in concentric layers (Figure 45). [123 – 126] These layers are visible when they are sliced through the trunk or any other part of the woody plant (revealing cross-section). [123 – 126]
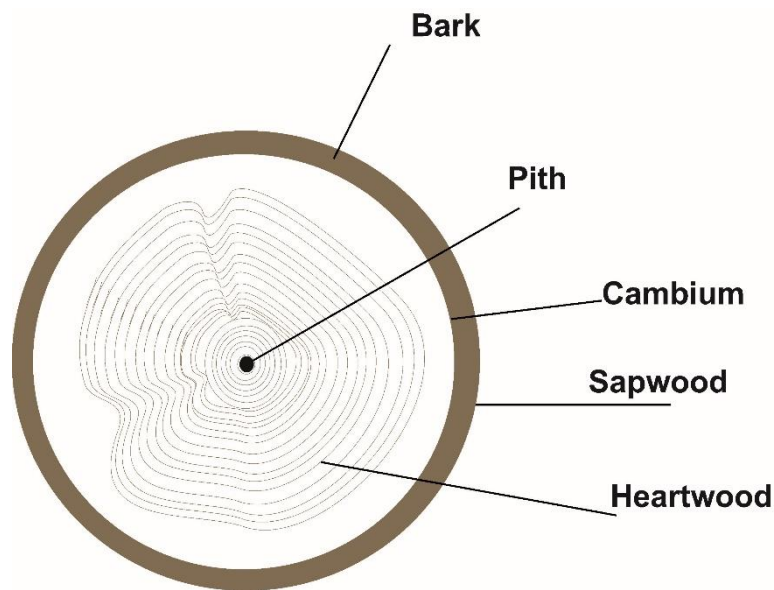
Figure 45: Cross-section of a tree trunk, showing the development of wood.

Figure 45 shows the formation of wood. At the centre is the pith a vascular tissue made up of spongy parenchyma cells. Surrounding the pith is the heartwood consisting of dead cells which offer support to the plant/tree. [123 – 126] Sapwood forms the following layer carrying the nutrients (water, minerals and sugars) from the roots to the leaves. Next is a layer of cambium (a thin layer of living cells) covered by a protective layer of bark, it is responsible for the manufacture of wood. [123 – 126] At the beginning of each growing season the cambium grows rapidly producing a springwood which is light in colour. [123 – 126] As the season progresses and the climate warms growth declines creating a much darker summerwood which is harder and denser than springwood. During the winter months when the weather is cold the cambium stops growing awaiting the arrival of spring. This cycle produces distinctive growth rings. [123 – 126]

4.5.2 Hardwood vs Softwood

Woods are categorised into two classifications: hardwood and softwood. Although generally the physical characteristics and makeup of the wood help classify them into either a hardwood or a softwood this is not always the case. For example Balsa wood (hardwood) is much softer than any softwoods and yew wood (softwood) is harder than most hardwoods. [123 – 126]

Hardwood - Hardwood grows from deciduous and broad-leaf evergreen trees. All hardwoods are angiosperms (flowering plants) which are the most assorted and largest group of land plants. [123 – 126] Flowering plants are categorised as those who shed their leaves in autumn and winter (*i.e.* maple, oak etc.). The structure of a hardwood is more complex than that of softwood, where xylem vessels (hollow tubes) transport water to and throughout the tree (Figure 46). [123 – 126] The structure is denser as the cell walls are lined with lignin a hard material which supports the plant above the surface. The quantity of lignin is the main factor creating the namesake hardness associated with hardwood. [123 – 126]
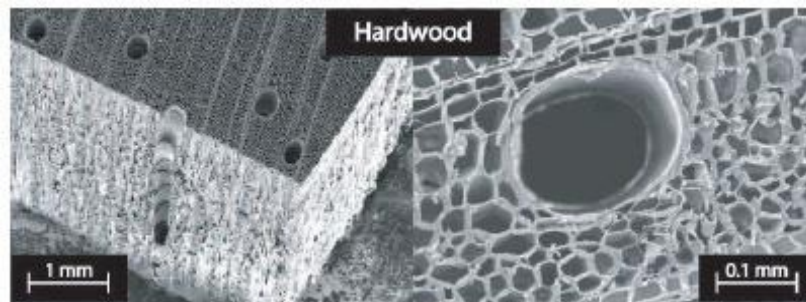
Figure 46: Structure of hardwood, with observable vessels which transport water throughput the tree. [127]

Types: There are around 100 times more species of hardwood than softwood. Examples of the most common hardwoods are: balsa, beech, mahogany, maple, oak, teak, and walnut. [123 – 126]

Uses: Due to the hardness/density of hardwoods they are used to make numerous items such as: furniture, flooring, construction materials, utensils, instruments and paper/tissue. [123 – 126]

Softwood – Softwoods come from coniferous (gymnosperm) trees which have needles instead of leaves, these needles last all year round (Evergreen). [123 – 126] Unlike hardwood softwoods rely on medullary rays and tracheids to transport water and produce sap (Figure 47). [123 – 126] The structure is vascular accounting for the lower density and 'softness'. Softwoods also contain lignin though in lower quantities than in hardwoods and of a slightly different composition. [123 – 126]
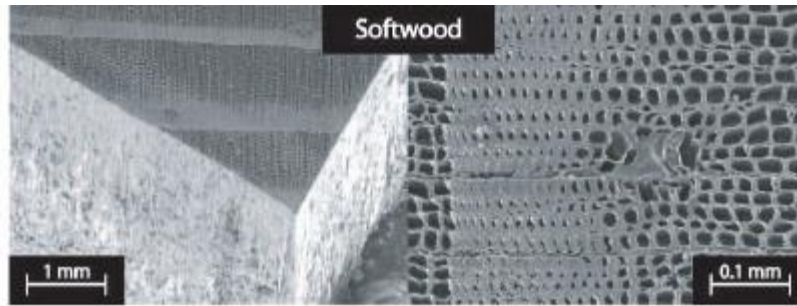
Figure 47: Structure of softwood, a vascular structure with medullary rays and tracheids which transports water and produce. [127]

Types: Some examples of softwood: cedar, fir, pine, redwood, spruce, and yew. [123 – 126]

Uses: As softwoods grow faster than hardwoods they are cheaper and can therefore provide a less expensive option. Some uses of softwoods are: building components (*i.e.* doors), timber, furniture, medium-density fibreboard (MDF), Christmas trees and paper (softwoods have longer fibres and are more suited for paper products such as paper bags, cardboard and shipping containers). [123 – 126]

4.5.3   Characteristics of Wood

4.5.3.1   Grain

Two types of wood cells are created during the cambium growth. [128 – 130] Long and narrow longitudinal cells that align themselves with the axis of the trunk, limb, or root. The longitudinal cells are responsible for the wood's grain. The second type of cells are ray cells which extend out from the pith, perpendicular to the axis. [128 – 130] There are two classifications of grain; open and closed. When vessels are sliced open they create pores, these are visible to the naked eye and are defined as open grain. [128 – 130] For those which cannot be detected these are characterised as closed grain. Softwoods do not contain vessels and therefore have neither. [128 – 130]

There are four longitudinal cell grain patterns: [129]

Straight grain: the longitudinal cells grow straight and parallel to the axis of the trunk.
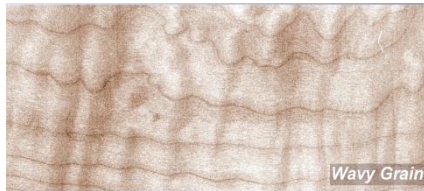
Wavy grain: the cells ripple in short, even waves. Sometimes producing a curly figure.

Interlocked grain: the cells spiral around the trunk, reversing direction every few growth rings. Producing a ribbon figure.

Irregular grain: the cells deviate around knots in no recognisable pattern.

Fig_____ grain pat__

Grain type can change depending on h_____s re-categorised into a further grain type:

End Grain - When the board is sawn across the grain (perpendicular to the grain direction and the growth rings), revealing end grain.

Plain Grain – Wood is cut parallel to the grain direction and tangent to the growth rings.

Quarter Grain – Board is cut parallel to the grain direction but through the radius of the growth rings.

4.5.3.2   Growth Rings

Wood forms by the increase of diameter where existing wood and inner bark are encased by more wood layers; a process known as secondary growth. Growths occurs annually or seasonally, leading to the development of growth rings, visible at the end of logs or in a cross-section of a tree trunk. [128 – 130] Rings tend to be lighter and darker shades, where the lighter colour is produced in the early stages of wood development

(springwood) and darker wood is produced in the latter stages (summerwood). The size and colour of the rings can vary dramatically depending on the type of wood. [128 – 130]

4.5.3.3   Knots

A knot is a type of imperfection in a piece of wood which will affect the properties of the wood, for instance render it weaker more easily broken. [128 – 130] A knot is created when lower branches die but remain attached, layers continue to grow around it therefore producing a knot. Knots can also provide a visual effect providing decorative aspects and visual interest. [128 – 130]

4.5.3.4   Grade

Wood is available in many grade types, categorised for the defects, colour variation, stiffness, strength and sap presence they contain. [130]

The four main grades for wood flooring are: [130]

Prime – The highest grade, where boards will have a minimal amount of knots and imperfections (sapwood and filler defects). [130]

Select – A mixture of prime boards and other planks, wood boards display an infrequent number of knots, heartwood and colour variation and mineral streaking.

Classic / Character – More knots are apparent and checks are visible (cracks across the growth ring). Colour variation between boards is high. It is sometimes referred to as natural.

Rustic – The most popular grade for its character and low price. There are a large amount of knots present, checks and end shake (cracks between the rings). Also contains heavy grain markings and high colour variation. [130]

This grading system is similar through all wooden surfaces (*i.e.* worktops), however the names of the categories change. For instance A, B and C teak grades, where A is the highest and C is the lowest. [130]

4.5.4   Finishes

Wood finishes provide protection and refinement to the wood surface. [131, 132] The first step of wood finishing is sanding, scraping or planning the surface. Corrections are made to the wood such as nail holes filled with putty. The wood is finally stained, coloured and/ or protected *etc.* using numerous techniques. [131, 132]

4.5.4.1   Green Wood Finishes

There are a variety of eco-friendly finishes: beeswax, linseed oil, safflower oil and carnauba wax. These are all naturally occurring and therefore are more eco-friendly than the chemically based finishes, though synthetic versions are available. [131, 132]

4.5.4.2   Varnish

Varnish is used as both a preservative and for decorative purposes, providing a high end finish for furniture. [131, 132] There are many types of varnish which will fit the specifications and use that is desired, they can be bought as water or oil based, matte or high-gloss and either transparent or coloured. For interior or exterior use as specified on the label. [131, 132]

4.5.4.3   Stain

Provides both a decorative and preservative finish. Stain soaks into the wood, darkening or colouring it. It is available in matte, gloss, water-based and oil-based. [131, 132] Can be used both on the interior and the exterior; using a varnish to protect the stained surface.

4.5.4.4   Dye

Like the stain dyes can be used to change or enhance the colour of the wood. Provide a matt finish and are available as a water-based and oil-based finish. [131, 132] Similar to the stain finish, dye can be used both on the interior and exterior (if protected by varnish).

4.5.4.5   Wax

Provides a transparent or translucent decorative finish and can be buffed to a high gloss. [131, 132] Similar to the oil finish wax nourishes and protects the wood, however wax is a high maintenance finish needing several coats and constant upkeep. Both

water-based and oil-based types are available and is only suitable for interior use. [131, 132]

4.5.4.6   Oil

Oil provides a transparent finish which both nourishes and protects the wood. Can be used both internally and externally but must be applied to unsealed wood as it will not penetrate a sealed surface. [131, 132]

4.5.4.7   Wood Preserver

This is supplied as a transparent or coloured with a matter or semi-gloss finish and are available as water or oil-based. Wood preserver is for exterior use only preventing rot and insect damage. [131, 132]

4.6   BLOOD IMPACTING WOOD

Since wood is one of the most versatile natural resources in the world it is used readily in the households, at places of work and other public places. This increases the chances of blood interacting with a wooden surface such as a flooring, furniture or buildings constructed of wood.

The difficulty BPA experts face is the wide varieties of wood types, wood grades, finishes and manufacturing processes (solid or engineered) that are available. The following research looks at three popular wood types (maple, oak and walnut), altering the finish, grade and manufacturing process to evaluate how the individual properties effect the interpretation of bloodstains.

4.6.1   Experimental

Human blood (PCV: 37 %) was utilised, collected from the Manchester Royal Infirmary blood bank. Blood drop experiments were performed using the method described in section 2.2. Three types of wood were utilized:

Oak: is the most popular hardwood, with over 60 species split into either white or red types. It is a strong, heavy wood with large pores which give oak a noticeable grain and rough texture.

species of maple only 5 of these are imported commercially into the UK. Maple is very hard and resistant to wear, the pores are small creating a fine, smooth texture.

Walnut: known for its versatility it is a popular high end wood (used for making cabinets, flooring etc.). Walnut is a strong, durable wood with a variety of grains making it particularly desirable as a design wood.

The woods were of different grades (rustic, natural and prime), finishes (matt lacquer, stain lacquer, oil and untreated) and manufacturing processes (engineered and solid).

The following woods were used:
European Maple Oak, Clear Oil Oak, Oak Natural Siera Matt Lacquered, Maple Silk Matt Lacquered, Natura American Black Walnut Rosshill, Natura Walnut Ironbank Mississippi, Quickstep Villa Walnut Satin Lacquer, Kahrs Maple Toronto Satin Lacquer, Kahrs Walnut Rustic Nature Oil, Maple Ultra Matt Lacquered, Oak Silk Matt, Kahrs Maple Bevelled Edge Rustic, Kahrs Maple Natural Satin Lacquer, Kahrs Linnea Walnut Bloom Prime Satin Lacquer, Kahrs Linnea Walnut Microbevelled Edge Prime Matt Lacquer, Natura Walnut Lacquered Satin Lacquer, Kahrs Oak Sienna Natural, Natura Oak Prime Parquet, Kahrs Oak Siena Engineered Natural, Oak Solid Plank Untreated.
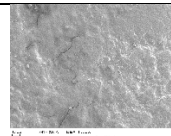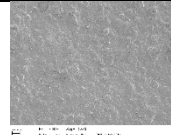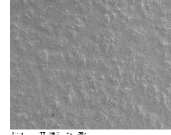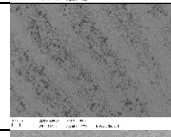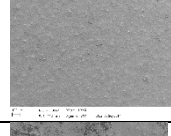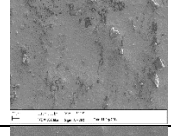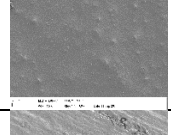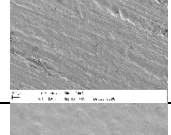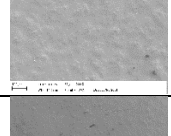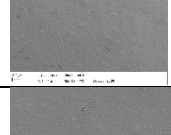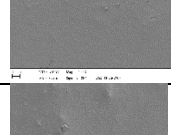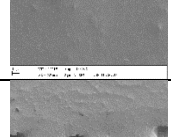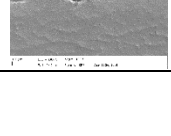
Blood was released from heights of 50, 100, 150 and 200 cm and at various angles (20°, 40°, 60°, 80°, 90°). Bloodstains were measured and analysed using equations (1, 3 and 4).

4.6.2   Results and Discussion

4.6.2.1   Blood Drops on Wood Surfaces

Twenty common wood surfaces were tested to establish the effect each had on bloodstains. SEMs of the surfaces were performed and roughnesses were evaluated for each surface (Table 20). Blood was released from 4 different heights, using two pipette types and bloodstains were measured and compared (see Appendix 5).

Wood and Characterisation	SEM	Finish	Manufacturing Process	Grade	Roughness
European Maple Oak (Pitted)		Satin Lacquer	Solid	Prime	2.01
Clear Oil Oak (Pitted)		Oil	Solid	Rustic	1.07
Oak Natural Siera Matt Lacquered (Bumped)		Matt Lacquer	Engineered	Natural	1.55
Maple Silk Matt Lacquered (Smooth)		Satin Lacquer	Engineered	Prime	0.64
Natura American Black Walnut Rosshill (Smooth)		Satin Lacquer	Engineered	Rustic	1.14
Natura Walnut Ironbank Mississippi (Bumped)		Matt Lacquer	Engineered	Rustic	1.26
Quickstep Villa Walnut Satin Lacquer (Bumped)		Satin Lacquer	Engineered	Natural	1.02
Kahrs Walnut Rustic Nature Oil (Striated)		Oil	Engineered	Rustic	1.19
Maple Ultra Matt Lacquered (Pitted)		Matt Lacquer	Solid	Rustic	1.99
Oak Silk Matt (Smooth)		Matt Lacquer	Solid	Rustic	0.64
Kahrs Maple Bevelled Edge Rustic (Smooth)		Satin Lacquer	Engineered	Rustic	1.03
Kahrs Maple Natural Satin Lacquer (Bumped)		Satin Lacquer	Engineered	Natural	0.90
Kahrs Linnea Walnut Bloom Prime Satin Lacquer (Pitted)		Satin Lacquer	Engineered	Prime	1.70
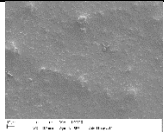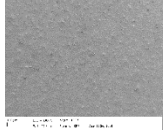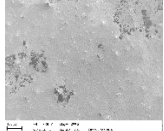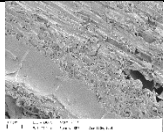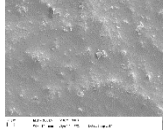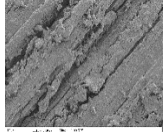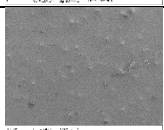
Kahrs Linnea Walnut Microbevelled Edge Prime Matt Lacquer (Bumped)		Matt Lacquer	Engineered	Prime	3.77
Natura Walnut Lacquered Satin Lacquer (Smooth)		Satin Lacquer	Solid	Natural	1.45
Kahrs Oak Sienna Natural (Bumped)		Matt Lacquer	Engineered	Natural	2.61
Natura Oak Prime Parquet (Striated)		Untreated	Solid	Prime	5.55
Kahrs Oak Siena Engineered Natural (Bumped)		Satin Lacquer	Engineered	Natural	1.97
Oak Solid Plank Untreated (Striated)		Untreated	Solid	Rustic	5.89
Kahrs Maple Toronto Satin Lacquer (Bumped)		Satin Lacquer	Engineered	Prime	1.60

Table 20: Physical characteristics of the 20 wood types used in this study.

Figures (49 and 50) illustrate the size of bloodstain diameters when blood impacted on each wood surface for both pipette sizes.

Bloodstains on all wood surfaces were found to follow the same trends, as height increased so did the diameter of the bloodstains. Where sharp increases were observed for the drop at lower heights then reaching 200cm most bloodstains reached terminal velocity, therefore bloodstains desisted increasing or the increase was less pronounced.
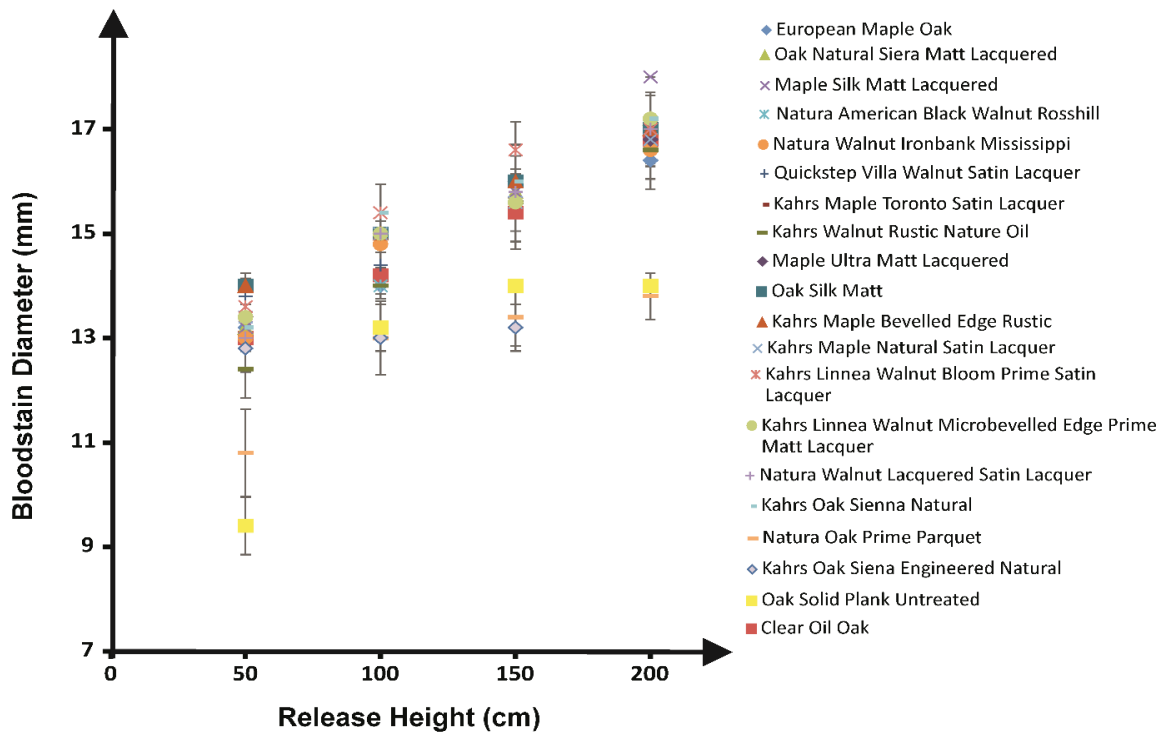
Figure 49: Bloodstain Diameters on all 20 wood types from various heights; 50cm, 100 cm, 150cm and 200cm, using the 1mm pipette.
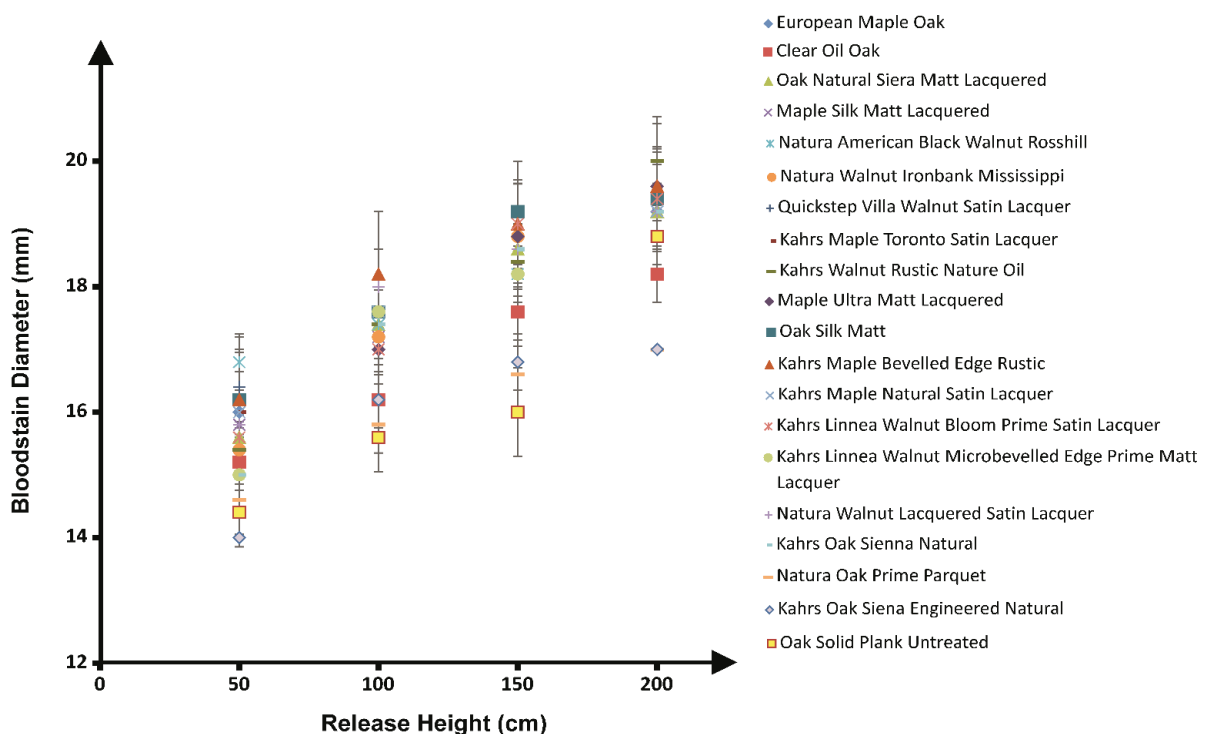
Figure 50: Bloodstain Diameters on all 20 wood types from various heights; 50cm, 100 cm, 150cm and 200cm, using the 1.77 mm pipette.

This effect is well documented and was an expected result. Comparing these results to the roughness's we find that the rougher surfaces give the smaller bloodstains. This

is due to the resistance the rougher surfaces forces on the spreading of the drop. It can also be attributed to the increased splash experienced on rougher surfaces, where satellite spatter are formed around the periphery of the stain, therefore decreasing the volume of the bloodstain and subsequently the eventual diameter.

Next, Reynolds (equation 1) numbers using the physical properties of blood (viscosity is 5mPa.s) were calculated.
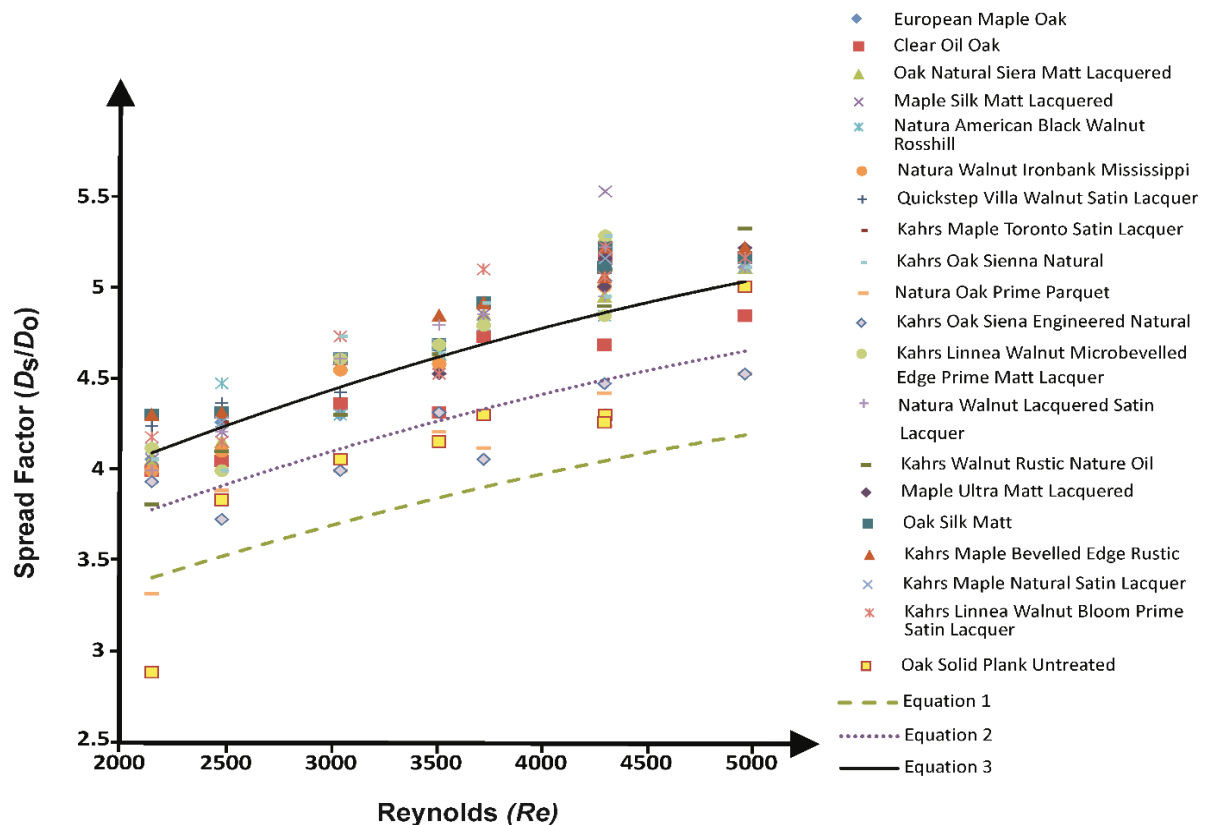
Figure 51: A new line of 'best fit (solid line) was established when considering the spread factor versus the Reynolds number utilising human blood on various wood types. Comparing this to the original line of 'best fit' (dashed line) using equation (3) and the line of best fit (dotted line) developed by Hulse-Smith *et al* [18] using equation (4); *N*=5

These were graphed against the spread factor of bloodstains to determine a constant (Figure 51). A new constant equalling 1.20 was developed for C_d, deviating from the original value (1.11) devised by Hulse-Smith *et al.* Viscosity measurements are similar in both studies, 5 mPa.s in the current study compared to 4.8 mPa.s, therefore thechange can be attributed to the surface. Wood surfaces produce larger bloodstains in general when analysed separately to other surface types.

4.6.2.2 Wood Characteristics

Since each wood was finished, manufactured and graded differently, woods were split onto categories to determine if changes in bloodstain size could be pinpointed to a particular factor/s. Firstly, wood type was evaluated. Three types of wood were utilised in this study; maple, oak and walnut. Figures 52 A and B show that maple and walnut are similar in the size of stains they produce, almost mapping each other exactly. Oak, however, seemed to consistently produce smaller bloodstains.
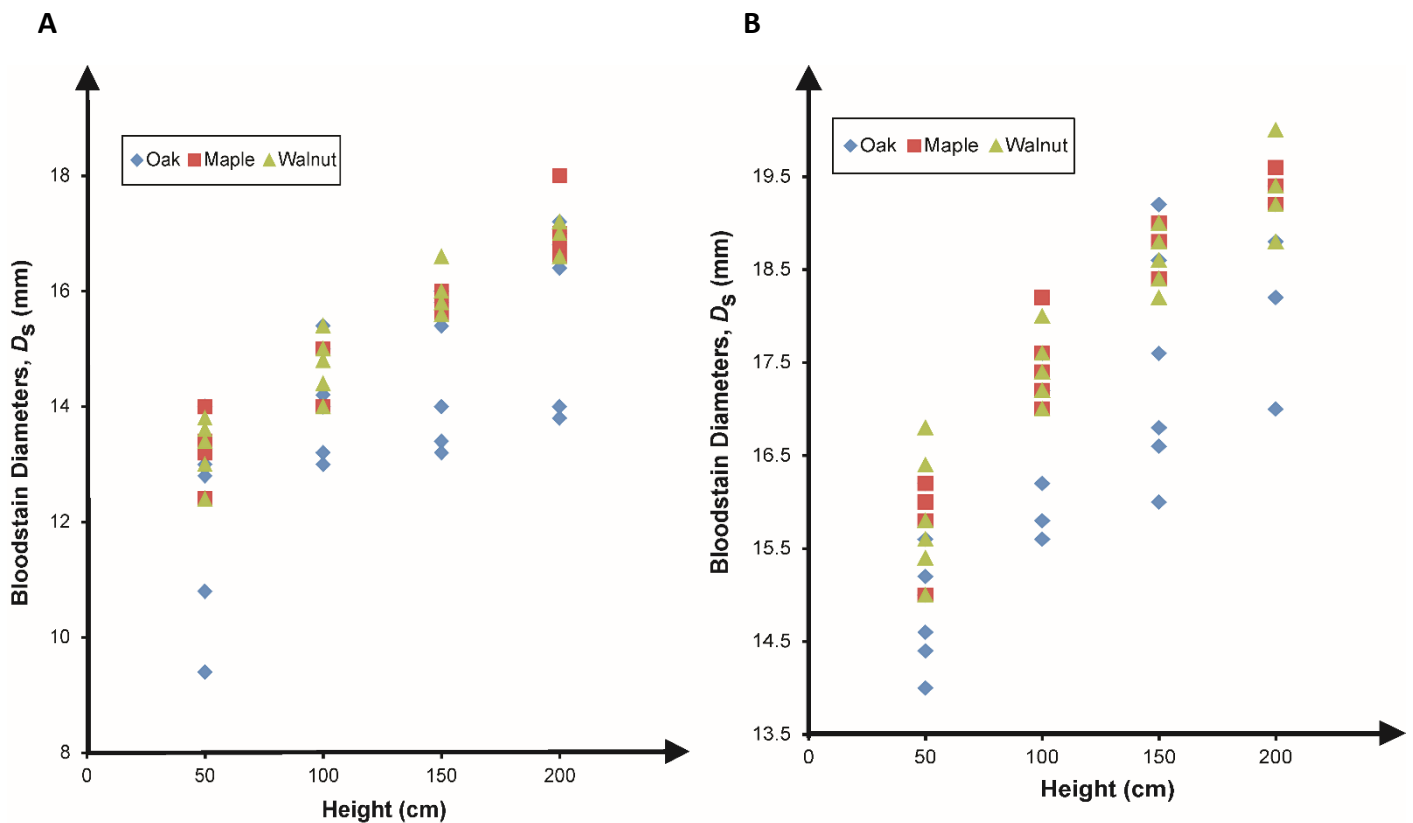
Figure 52: Bloodstain Diameters depicted the effect of wood type, where blood was deposited using A- 1mm pipette and B- 1.77mm pipette.

Since oak has large pores, porosity is high, therefore leading to smaller bloodstains. The wood characteristics table (Table 20) show that on average oak has a rougher surface, again accounting for the smaller bloodstains produced.

Constant values were calculated for each wood type to fully evaluate the changes between them. Again Reynolds and Spread Factors were graphed and lines of 'best fit' were drawn, constants (*Cd*) 1.16, 1.23 and 1.22 were found for oak, maple and walnut, respectively. These constant support the previous evaluation that maple and walnut produce similar results and oak yield significantly smaller results.

The grade of the wood and manufacturing process were analysed next (Figures 53 and 54).
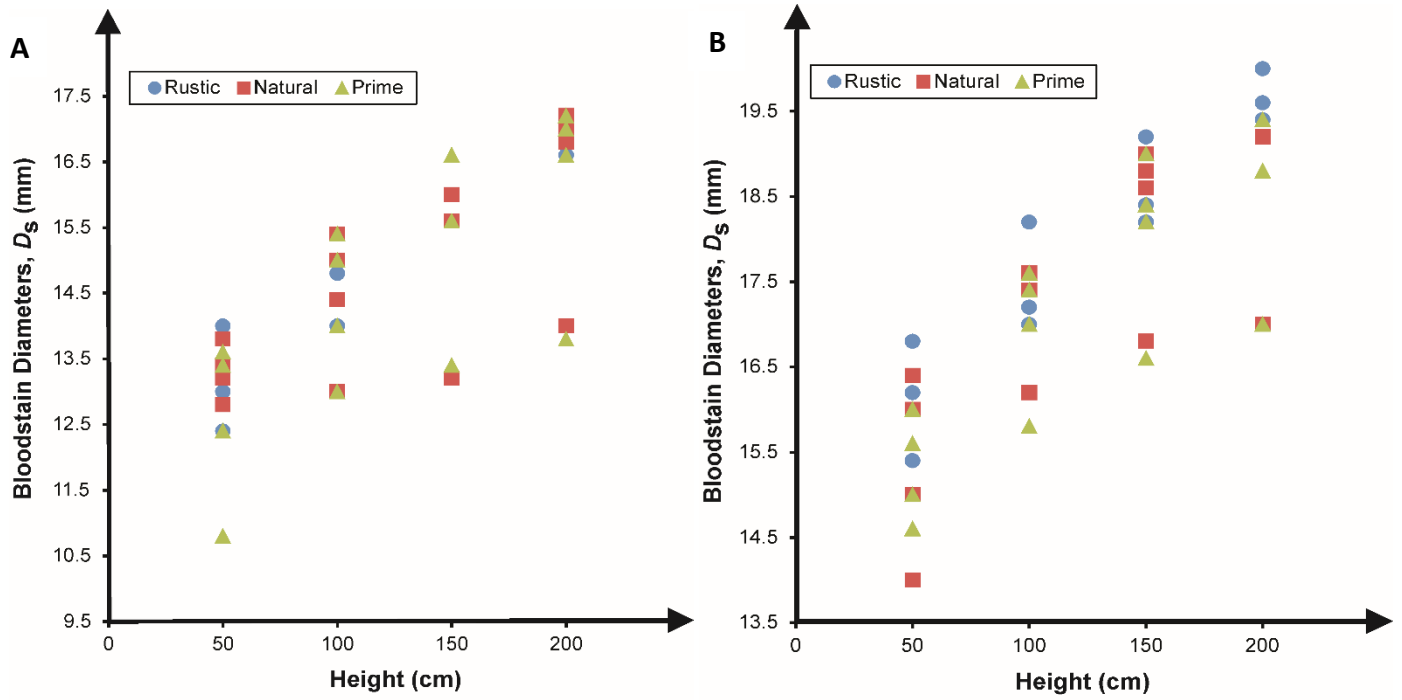
Figure 53: Bloodstain Diameters depicted the effect of wood grain, where blood was deposited using A- 1mm pipette and B- 1.77mm pipette.
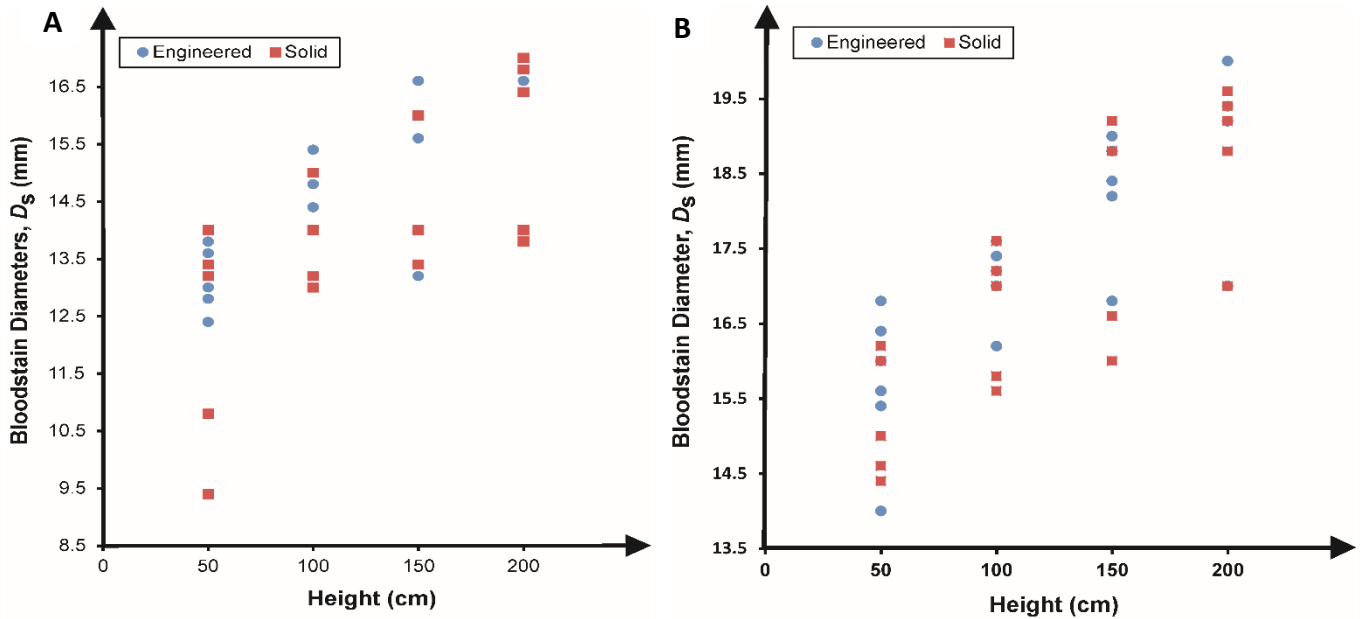
Figure 54: Bloodstain Diameters depicted the effect of the manufacturing process of wood, where blood was deposited using A- 1mm pipette and B- 1.77mm pipette.

Both were found to show no distinctive pattern, where bloodstains from each process / grade mingled amongst each other. This suggests that neither wood grade nor manufacturing process are determinant factors as to the size of bloodstains.

Lastly the treatment was investigated (Figure 55A and B).
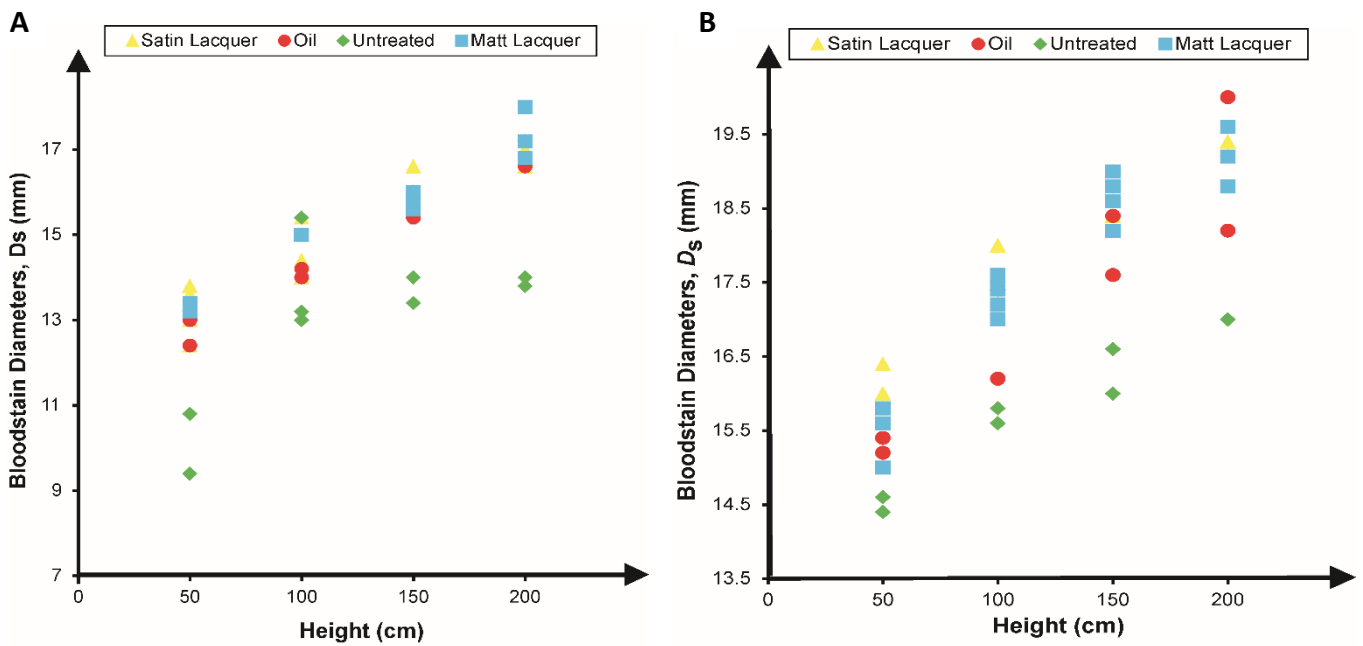
Figure 55: Bloodstain Diameters depicted the effect of surface finish, where blood was deposited using A- 1mm pipette and B- 1.77mm pipette.

A distinct pattern was discovered; the smallest bloodstains were created when the wood was unfinished (not treated), most likely the result of the porous properties of the wood when left untreated. Larger stains were generated when lacquer finishes were utilised. Lacquers produce a smoother surface and inhibit the natural porosity of the wood.

The Reynolds and Spread Factors of each treatment type were plotted, where new constants Cd were determined; 1.22, 1.23, 1.07, 1.13 for satin lacquer, matt lacquer, untreated and oil finishes, respectively. Again this further supports the conclusion that the lowest blood spreading occurs when the wood is unfinished and that lacquers either satin or matt produce very similar results to one another.
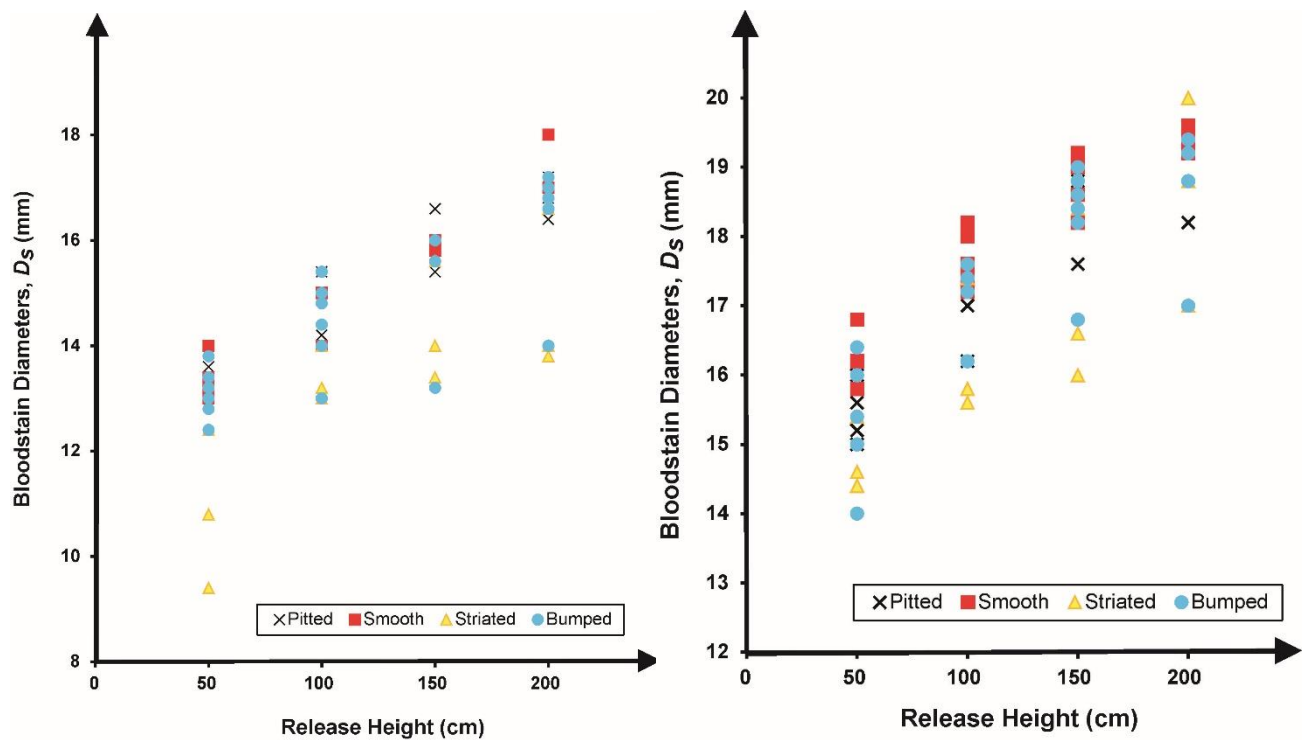
Figure 56: Bloodstain Diameters depicted the effect of surface characteristics, where blood was deposited using A- 1mm pipette and B- 1.77mm pipette.

All woods were characterised into four groups (pitted, smooth, striated and bumped) according to their physical appearance (see Table 20 for characterisation). Figures 56 A and B show that smooth surfaces produced bigger resultant bloodstains, however all bloodstains did not differ substantially from one another regardless of the surface characteristics. A reason for this could be attributed to the surface finish, since this dictates the overall texture of surface, thus covering any defects or distinct features of the surface to a typical surface finish.

Angled impacts were also investigated, errors up to 29.02% were observed when acute impacts were tested (20ºC). Angles were found to consistently decrease for every wood type tested. Surface finish did not affect the degree of error exhibited with angled impacts.

4.6.3 Summary

Three wood types were evaluated during this study. The woods were finished, graded and manufactured differently to fully understand the effects certain characteristics had on a bloodstain.

Walnut and maple were discovered to behave very similarly, producing nearly carbon copy diameter results and very close spread factor constants. Oak was found to produce much smaller bloodstains, since oak is generally rougher and bears bigger grains and therefore a larger porosity.

Manufacturing processes and grades of wood where found to have no discernible effect on blood stain size.

Lacquered finishes, both satin and matt, gave much larger stains than oil and untreated wood finishes. Again this can be attributed to the natural porosity of wood and roughness, which ultimately effect the spread of liquids.

New constants were found for several factors, the largest deviations were calculated for the finishes, where lacquers produced constant of 1.23 or 1.22, and untreated wood had a constant of 1.07. This indicates that although wood type does heavily influence the size of a bloodstain, the finish is the overriding factor.

4.7 FABRICS

Textiles or fabrics are woven materials composed of a network of fibres (thread / yarn). The thread is created by spinning raw fibres (*i.e.* wool, cotton etc.), the thread is then woven, knitted, crocheted, knotted or pressed together to form the fabric.

Fabrics have a variety of uses: clothing, carpets, upholstered furnishings, beds, art, quilts, backpacks etc. The presence of fabrics in everyday life make the probability of interaction with blood during a blood-letting incident high.

4.7.1 Fabric Composition

There are several methods of fabric composition: [133 - 134]

Weaving – this involves the interlacing of long threads (warp) with a set of crossing thread (weft). Although some weaving can be done by hand it is generally completed using a frame or a loom. [133]

There are three main types of weaves (see below), most other types are deviations on the main three.

Plain Weave
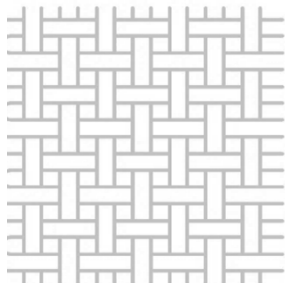
Figure 57: Plain weave [135]

Plain weaves are the most common type of weave, they are simplistic but are the most stable. The pattern created in the plain weave is symmetrical, where the warp fibre passes under and over each weft alternatively. [133] Due to its high stability it is one of the most difficult weaves to drape, it has high levels of fibre crimp (waviness) which gives low mechanical properties, therefore this type of weave is not often used for larger fibres (heavy fabrics).

Satin

Figure 58: Satin weave [135]

The satin weave appears differently on each side of the fabric. The front of the fabric consists of mainly warps running over three or more weft threads, the reverse has fibres predominately running in the weft direction. [133] The number of warp or weft fibres crossed and passed under, before the pattern repeats is known as the harness number, typically this is 4, 5 and 8 in a satin weave. Unlike plain weaves satin weaves have a high level of drape and low crimp and therefore impart good mechanical properties. Although the satin weave allow fibres to be tightly woven the weave has very low stability. [133]

Twill
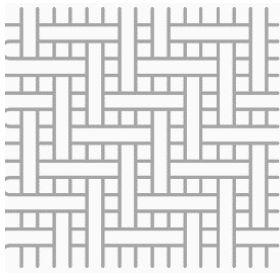
Figure 59: Twill weave [135]

Similarly to the satin weave the twill weave crosses several warps or wefts consecutively and is asymmetric, therefore appears different on each side. [133] Unlike the satin weave fibres cross a maximum of two warps/wefts, where one or more warp fibres alternatively weave over and under two weft fibres in a repetitive pattern, creating a much more stable fabric. This repetitive pattern creates a straight or diagonal rib to the fabric. The twill weave has a high drape, reduced crimp and high mechanical properties. [133]

Knitting and Crocheting – Knitting and crocheting comprise of the interlacing of loops of thread using a knitting needle or crochet hook. [136] Both processes are different, knitting uses several active loops at once before the interlocking loop is passed through, crocheting only uses one active loop at any one time. Knitting may be done by hand or machine. In contrast to weaving knitting creates a very stretchy fabric which in some cases can stretch as much as 500%, knitting was originally created for garments (*i.e.* tights) explaining the need for its extensive elasticity. [136]

There are two main types of knitting: weft and warp. [136] The most common type is weft knitting where the loops run perpendicular to the course of the thread. Weft knitting can produce an entire fabric from one piece of thread. Conversely in warp knitting the loops and courses are parallel and a new piece of thread is needed for every loop. [136]

Knitting can also comprise of different stitches:

| Knit and Purl [137] | Cable and Twist [138] | Plaited Stitch [138] |

| Eyelet and Lace [139] | Slipped Stitch Patterns [140] | Rib Stitch [141] |
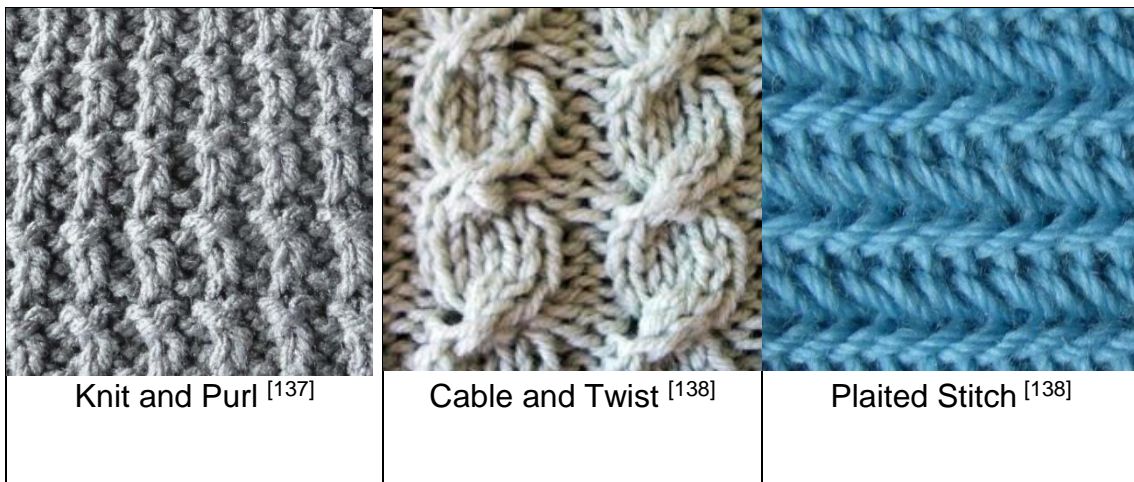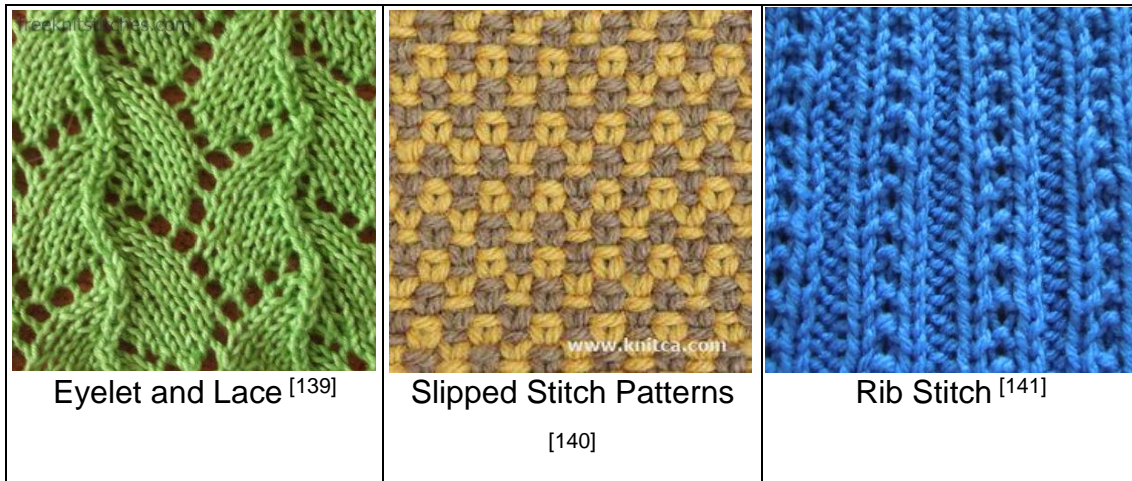
Table 21: Various important knit types
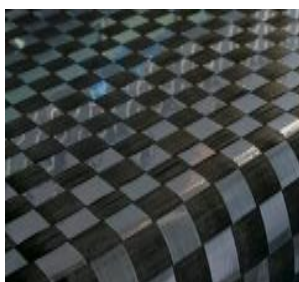
Figure 60: STF [143]

Spread Tow Fabric (STF) – Spread Tow Fabric is an ultra-lightweight fabric produced by the spreading of carbon fibre threads (tow) into thin tapes, this tapes are then woven as a warp and weft. [142] This method of fabrication has many advantages, avoids crimps in the fabric, reduces the weight by stopping the accumulation of matrix at interlacing points and increases mechanical properties (thinness, drape *etc*). [142]

Figure 61: A braid [143]

Braiding / Plaiting – Braids / Plaits are usually created with three strands of fabric (hair or wires) interlaced and crossed over one another (zigzagging). [144] Other plait types add-in odd strands to create a wider structure. This technique is used to fashion dog leads, belts, whips and rope. [144]

Figure 62: lace fabric. [145]

Lace – uses a backing and the interlocking, looping, twisting or braiding of yarns together independently to create a fine openwork fabric which comprises of patterned holes. [146] The holes are generated by the removal of threads or can be achieved during the construction process. Lace can be made by either hand or machine and cotton is usually the fabric of choice, though linen, silk, copper, synthetic, silver and gold threads have be known to be utilised. [146] There are numerous types of lace, categorised by how they are made. These include: Needle lace,

Cutwork, Bobbin lace, Tape lace, Knotted lace, Crocheted lace, Knitted lace, Machine-made and Chemical lace.

Nonwoven – non-woven fabric is manufactured by the bonding of 100% polypropylene fibres (*i.e.* felt), this may be achieved using thermal, mechanical or adhesive bonding. [148] Non-woven fabrics are generally manufactured for single use and are made for specific functions such as cushioning, absorbency, insulation, liquid repellence *etc.* [148] Combined with other materials non-woven fabrics can be used for a multitude of purposes *i.e.* clothing, engineering, home furnishings, health care and many more.
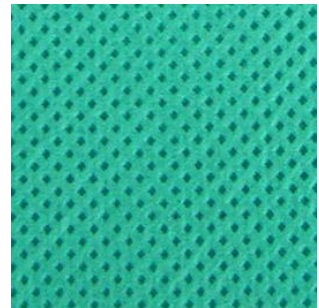
Figure 63: nonwoven fabric. [147]

4.7.2   Fabric Finishes

Figure 64: tie-dye fabric [150]

Dye – changing the colour of a fabric can be achieved by dyeing, this requires the use of water (a gallon of water for every pound of clothing) and the dye. [149] Patterns in the fabric can be created using resist dyeing processes such as tie-dyeing, where areas of the fabric at tied off (see Figure 63). Fabrics may also be drawn on using wax, another form of resist dyeing where the dye will not adhere to the areas covered in wax (known as batik). [149]

Bleaching – used to turn a fabric white or make the fabric paler, chemicals in bleach inhibit the chromophores present in most dyes and pigments. [151]
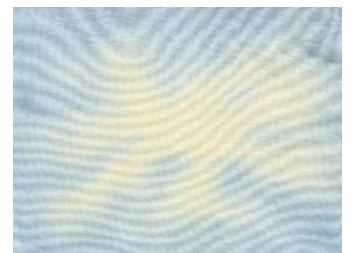
Figure 65: bleached fabric [151]

Figure 66: Chinese embroidery [153]

Embroidery – the technique of weaving textiles or coloured stitches into the fabric to create patterns or colour contrasts. [152]

Figure 67: wood block printing [155]

Printing – is the application of colour and definite design to fabric. Printing can achieved via several methods, these include: Woodblock printing (see Figure 67) Hand block printing, Perrotine printing, Engraved copperplate printing, Roller printing, cylinder printing, or machine printing, Stencil printing, Screen-printing and Digital textile printing. [154]

Finishing Agents – Chemicals are added to the fabrics to improve certain physical properties. For example formaldehyde and starching, improve the resistance to creasing and staining.

4.7.3   Types of Fabric

There are over 295 types of fabrics categorised by where they are sourced: animal, plant, mineral, and synthetic. [156] The following descriptions are of fabrics which will be used in the study where only the most popular fabrics were investigated.

4.7.3.1   Wool

Wool is a natural fibre obtained from sheep (Figure 68), goats, alpacas, yaks and rabbits. [156] In the case of wool obtained from sheep (the most common type) the sheep is shorn and the wool is divided into four categories: fleece, broken, bellies, and locks.

Figure 68: A Swaledale sheep, a breed of domestic sheep named after the Yorkshire valley in England. [157]

Quality of the fleece is established by wool classing, a technique which considers the fibre diameter, crimp, yield, colour and staple strength. Diameter is the most important

parameter, where the wool is measured in microns, the smaller the diameter the finer the fabric and subsequently the better the quality (used for garments < 25 microns).

Wool is both hydrophobic and hygrophobic where the exterior of the wool fibres repel liquid and the interior attracts the liquid, respectively. [156]

Global wool production is about 1.3 million tonnes per year, of which 60% goes into clothing. Other products produced using wool are, rugs, blankets, insulation, upholstery, nappies, body armour *etc.*

4.7.3.2 Silk

Figure 69: A silkworm moth [159]

Silk is a natural protein fibre (fibroin) produced by insect larvae to create cocoons, which can then be woven into a fabric. [158] Silks are produced by many insects (*i.e.* spiders) the most recognised is that produced by the silkworm caterpillar (*Bombyx mori*) (Figure 69). The silkworm is now bred in captivity, regulating the amount of silk produced. The eggs of the silkworm take around 14 days to hatch into larvae, it is during the pupal stage (third instar) when the larvae spin their cocoon, made of raw silk produced by their salivary gland. [158] In captivity this stage is when the silk cocoon would be boiled, killing the silkworm and making the silk easier to unravel. This occurs as the moth releases proteolytic enzymes to make a hole in the cocoon in which the moth can exit. The enzymes are destructive to the silk, causing breakages and reducing the silk's value. The process of killing the silkworm larvae has been heavily criticised, specifically by Mahatma Gandhi going against the Ahimsa philosophy of "not to hurt any living thing," he promoted the use of cotton spinning machine, wild silk and Ahimsa silk (aka peace silk). [159] Silk is one of the strongest natural fibres, it has a smooth, soft, non-slip finish. However it has low elasticity, loses nearly a quarter of its strength when wet and in most cases (as a garment) requires special cleaning (*i.e.* dry cleaning) as the fabric may shrink when washed. [158]

Silk has many uses, these include: garments (shirts, ties, blouses *etc.*)*,* furnishings, upholstery, parachutes and artillery gunpowder bags *etc.*

4.7.3.3   Cotton

Cotton fibres are grown from the cotton plant Gossypium indigenous to the Americas, Africa, Australia and India, the cotton grows in a boll and is mainly made of pure cellulose. [160]

Cotton is picked from the bolls and is spun into thread which in turn is woven to create cotton fabric. [160] Currently the world production of cotton reaches around 25 million tonnes.

Figure 70: Gossypium, the cotton plant, located in America, Africa, Australia and India [161]

Its uses are vast, providing textile for garments (socks, t-shirts *etc.*), towels, bed sheets, tents, explosive manufacture (nitrocellulose), cotton paper, bookbinding, coffee filters *etc.* [160]

There are several other varieties of cotton;

- Shiny cotton: here the fibre is processed creating a shiny appearance (mimicking the appearance of satin) and hydrophobic reaction to liquids.

- Egyptian cotton: regarded as the best cotton fibre worldwide, the Egyptian rich soil and humid conditions allow the growth of long cotton fibres which are spun into fine threads. [160]

 - Pima cotton: comparable to Egyptian cotton due to the fine cotton threads which are spun. It is grown in Peru, Australia and Southwest United States, and produces long fibres which are longer than ordinary cotton but shorter than that produced in Egyptian cotton. [160]

4.7.3.4 Nylon

Nylon is one of the most commonly used polymers. [165] It is synthesised by reacting two large molecules (Adipic acid and Hexamethylenediamine) together using high heat (around 285°C) and pressure in an autoclave. [165] The combination of these two chemical causes a reaction known as condensation polymerisation, where a large molecule commonly known as nylon-6,6 is produced. Other nylons can be manufactured by varying the starting molecule (Adipic acid). [165]
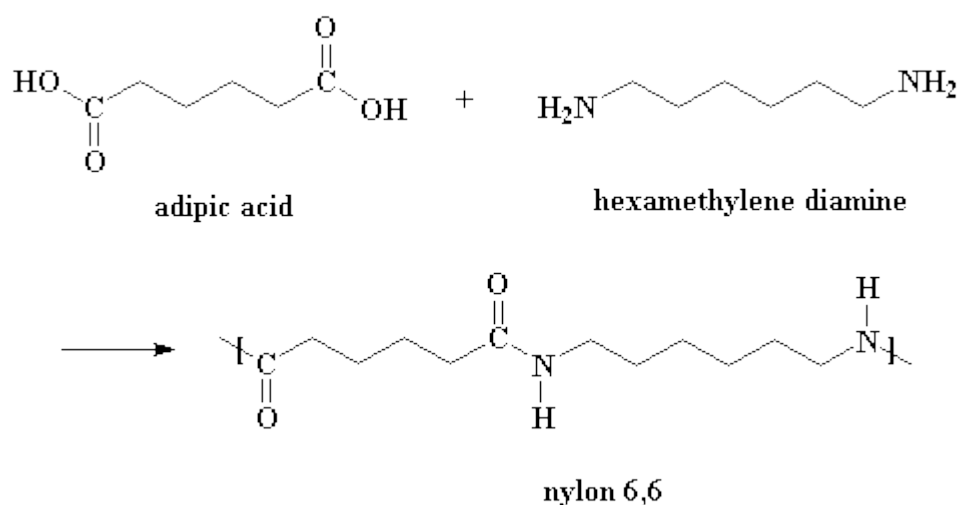
Figure 71: The chemical reaction responsible for the production of Nylon [166]

Nylon is one of the most versatile synthetic fibres, responsible for garments such as stocking/tights, fishing nets, ropes, parachutes and machine components. [160]

Like polyester, nylon, can be combined with other materials to create a composite. In conjunction with materials such as glass or carbon fibre (thermoplastic composites) higher density materials are formulated which can be employed in car component making (*i.e.* engines). [165]

Since nylon is essentially a synthetic plastic it has certain physical property advantages which most natural fabric do not possess without modification. Nylon is highly resistant to water, tough, resilient and impenetrable to insects, mold and fungi. [165]

4.7.3.5   Polyester

Polyester is a polymer, formed by the chemical reaction between an acid and alcohol, where two or more molecules react to create a much larger molecule. [165] There are many polyesters, however the two types were are most commonly associated with fabrics; PCDT (poly-1, 4-cyclohexylene-dimethylene terephthalate) and polyethylene terephthalate (PET). Although PCDT has a greater elasticity and resilience to wearing, PET is the more popular of the two. [165]

$$HO - CH_2 - CH_2 - OH + HO - \overset{\overset{\textstyle O}{\|}}{C} \hspace{-0.5em} \left\langle\!\!\!\bigcirc\!\!\!\right\rangle \hspace{-0.5em} \overset{\overset{\textstyle O}{\|}}{C} - OH$$

Ethylene Glycol   **Terephthalic Acid**

$$\longrightarrow \left[O - \overset{\overset{\textstyle O}{\|}}{C} \hspace{-0.5em} \left\langle\!\!\!\bigcirc\!\!\!\right\rangle \hspace{-0.5em} \overset{\overset{\textstyle O}{\|}}{C} . CH_2 - CH_2 - O \right]$$

Polyethylene Terephthalate
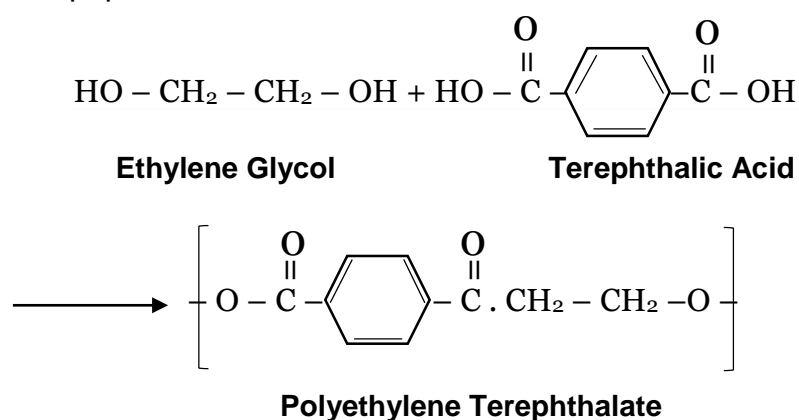
Figure 72: The chemical reaction responsible for the production of Polyester (PET). [166]

Polyester is used extensively in the fabrics industry for products such as: shirts, pants, bed sheets, upholstered furniture *etc.* [165] It also has industrial uses, bottles, films, wire, capacitors, plastic reinforcements *etc.* Recent research has work on the development of a new form of polymer, as strong as Kevlar (used for bulletproof vests) with the hope that it can be utilized in the manufacture of cars and airplanes. [165]

Polyester is mainly used in conjunction with other fibres, improving the physical properties of the fabric (*i.e.* water resistance, stain resistant) had it been made with completely natural fibres. [165]

Of all the synthetics available in the market (nylon, rayon, acrylics) polyester leads the way, averaging around 18 million tons per year. They can be produced easily and affordably, with a range of physical properties.

4.7.3.6　Linen

Figure 73: *Linum usitatissimum,* flax plant used for the production of linen [167]

Linen is a fabric consisting of fibres of the flax plant (*Linum usitatissimum*). [168] Flax fibres are very high in cellulose and are located in the stem of the plant between the woody central tissue and the outer epidermis. [168] The flax fibre is extracted first by rotting using water or dew (retting) and then by scutching the stalks, whereby the pith is mechanically broken down. The natural colour of linen varies (ivory, tan, grey and ecru), white linen is created through bleaching. [168]

Linen is used for a variety of product such as: towels, aprons, bed linens, tablecloths, upholstery, clothing (t-shirts, trousers etc.) and bags. It is an absorbent fabric which is low in elasticity, strong and highly wear resistant. [168]

4.7.3.7　Denim

Figure 74: Denim Fabric [169]

Denim is a cotton fabric assembled using a twill weave with blue (indigo) and white thread; where the warp threads are dyed (*i.e.* blue) and the weft threads are white. [170] Traditionally the denim is woven with 100% cotton however presently it is a mixed fabric adding other threads such as polyester and lycra to prevent shrinkage and enhance elasticity. [170]

Denim is mainly used for the manufacture of clothing such as jeans, dungarees etc.

4.8 BLOOD IMPACTING FABRIC

Fabrics are a particularly difficult surface for the interpretation of bloodstain patterns, evident in the case of David Camm (see introduction) where the misinterpretation led to a miscarriage of justice and doubts cast of the reality of BPA as a forensic discipline.

This study investigates fabric types and the effect these have on the impact of blood from various heights and angles.

4.8.1 Experimental

4.8.1.1 Resources

All equine blood (defibrinated) was obtained from TCS-Biosciences Limited at a PCV % (Packed Cell Volume) of 43%.

In order to be representative of real-life the most common types of fabrics, [160] for clothing, were tested: Cotton Duck, Cotton Jersey Ecru, Cotton Poplin, Denim, Fuji Silk, Heavyweight Cotton, Jupiter Linen, Light Grey Polyester Twill, M&S T-shirt Jersey, Medium Habotai Silk, Peasant Cotton, Poly Satin Heavy, Poly/linen/rayon Pandora Devore, Raised Natural Cotton, Resida Bump Cotton, Silk Chiffon, Silk Dupion, Wool Delaine (bleached) and Wool mix suiting. These fabrics were purchased new and used without alteration.

4.8.1.2 Methods

Fabrics were characterised using several tests (see Table 24 for results). The surface roughness of each fabric was determined using the Smoothness & Porosity Tester (Bendtsen Type). Porosity was established by following the fluid re-saturation method according to Ref 171. Fourier Transform Infra-red spectrometry (FTIR) was also utilized to verify the composition of the fabrics and lastly Scanning Electron Microscope images (SEMs) were taken of each fabric to ascertain the structure of the fabric (*i.e.* weave).

Blood drops were dispensed manually using two different sized pipettes, 1 mm and 1.77 mm (inner tip diameter), from varying heights (50 cm, 100 cm, 150 cm and

200 cm) (Table 22), at various impact angles (20º, 40 º, 60 º, 80 º, 90 º) and onto different fabric types.

Release Heights (cm)	Impact Velocity (m/s)
50	3.13
100	4.43
150	5.42
200	6.26

Table 22: Release heights of blood drops calculated from the tip of pipette to the impacting surface and converted into impact velocity with the use of Equation (11).

A minimum amount of pressure was applied to the pipette each time and the drops were performed by the same analyst to maintain continuity. Drops were repeated 5 times and stain diameters were measured using a magnifying loupe.

4.8.2 Results and Discussion

4.8.2.1 Blood Drops on Fabrics

Twenty common fabric types were tested to establish the effect each had on bloodstains. Blood was released from 4 different heights and bloodstains were measured and compared. (see Appendix 6)
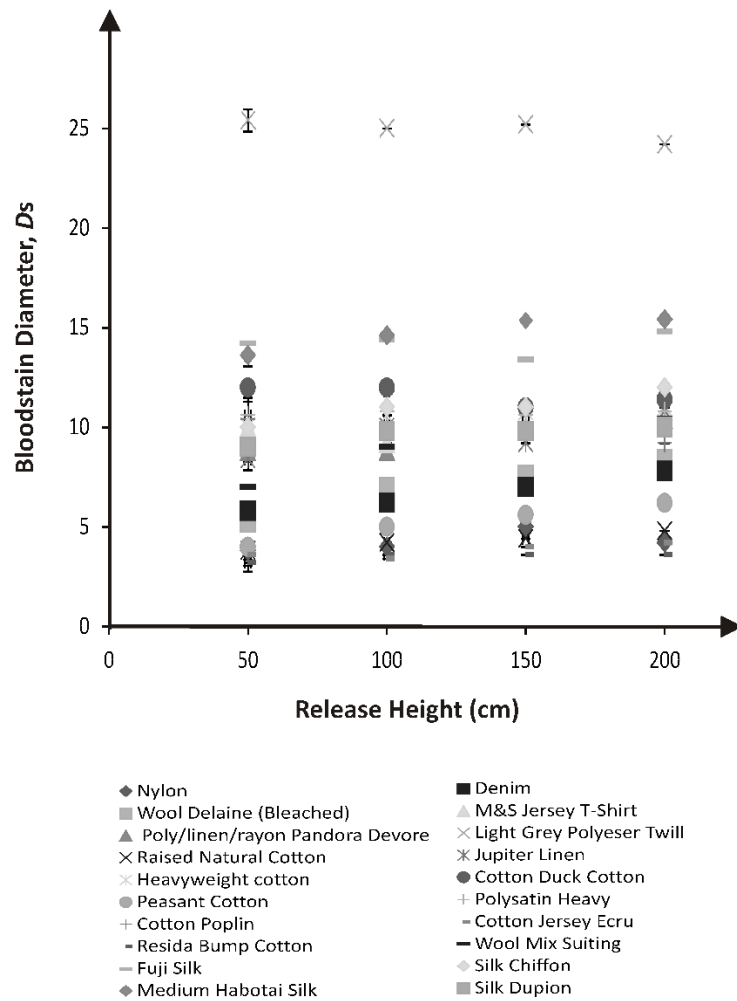
Figure 75: Bloodstain diameters on all 20 fabric types from various heights; 50 cm, 100 cm, 150 cm and 200 cm, using the 1 mm pipette (inner tip diameter). $N = 5$.

Figures 75 and 76 depict the size of the bloodstain diameters for the 1mm pipette and the 1.77mm pipette, respectively, at the aforementioned heights. These figures show that blood impacts do not follow the same trend when faced with each fabric type; increasing in size as the height increases.
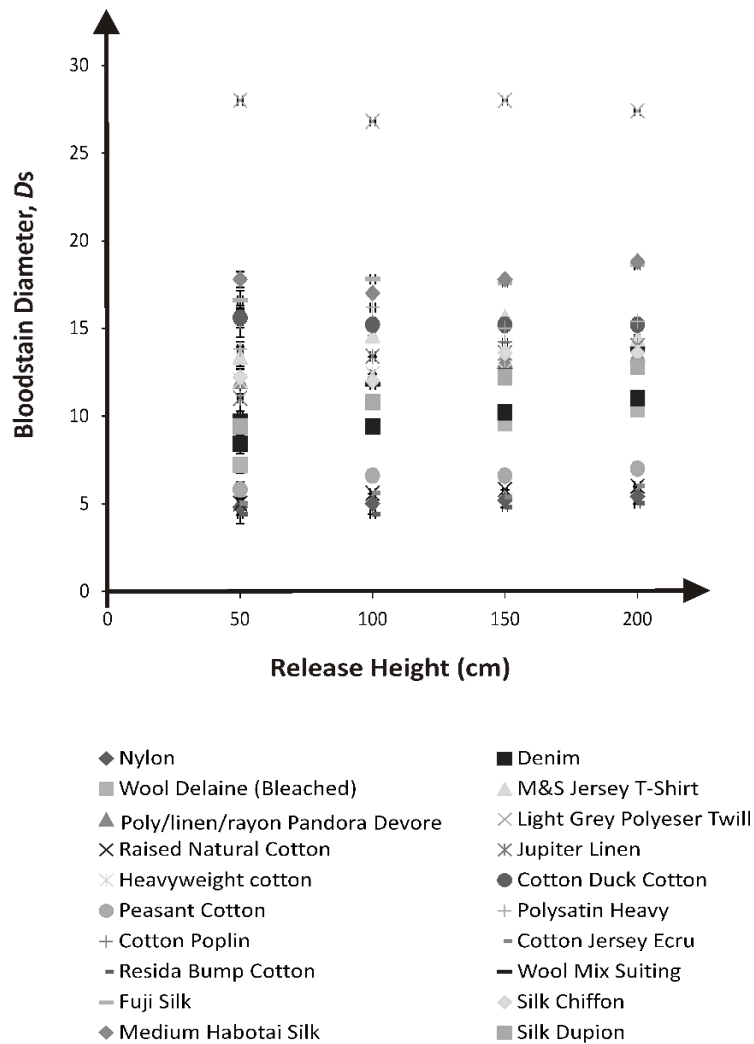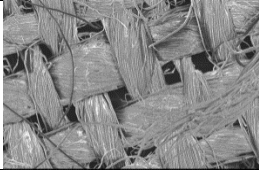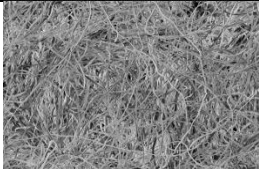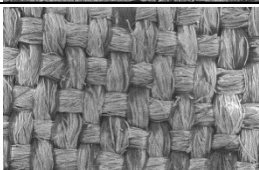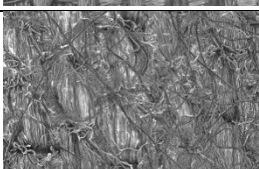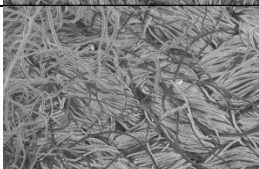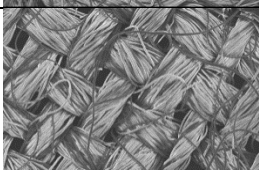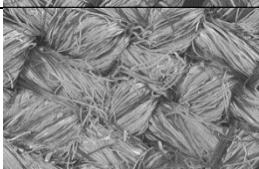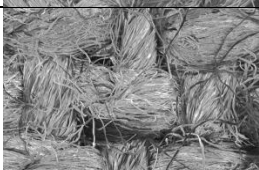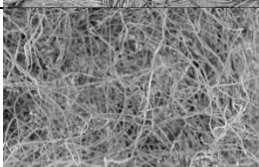
Figure 76: Bloodstain diameters on all 20 fabric types from various heights; 50 cm, 100 cm, 150 cm and 200 cm, using the 1.77 mm pipette (inner tip diameter). *N = 5*

In some cases (M&S T-shirt Jersey, Light Polyester Grey Twill, Cotton Duck, Polysatin Heavy, Cotton Poplin, Resida Bump Cotton, Fuji Silk, Nylon and Jupiter Linen) the bloodstain actually increases, then decreases, or stays relatively similar in size in spite of the height increase. When we compare this data with the characteristics of the fabrics (Table 23) it seems that the surface roughness and porosity does not affect the size of the bloodstain, however the thickness of the fabric appears to have a profound effect on bloodstain size *i.e.* Jupiter Linen and Polysatin/ Silk Dupion.

Type of Fabric	SEM	Composition And Characterisation	Roughness (mL/min)	Thickness (mm)	Weight (g)	Porosity (%)
Jupiter Linen		Light weight even plain weave	4600	0.23	3.05	91.62
Raised Natural Cotton		Plain weave Cotton with soft raised finish	4200	0.62	6.4	86.98
Fuji Silk		plain even weave Silk, Medium-weight fabric, woven from spun silk fibres	2300	0.16	1.82	90.49
Heavyweight Cotton		Twill weave heavy Cotton	4200	0.39	5.05	96.84
Cotton Jersey Ecru		Knit Interlock pattern; knit one, purl one	4500	0.47	4.3	83.04
Wool Mix Suiting		Plain Weave	3200	0.34	4.42	83.87
Wool Delaine (bleached)		Plain Weave	5000	0.26	2.52	85.60
Poly/linen/rayon Pandora Devore		Plain weave	4600	0.39	5.74	94.86
Peasant Cotton		Plain weave	4800	0.63	7.63	93.91
Resida Bump Cotton		Thick coarse loose Plain weave	4500	1.38	9.04	95.05
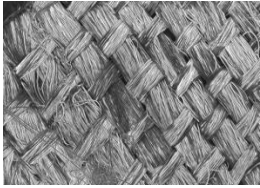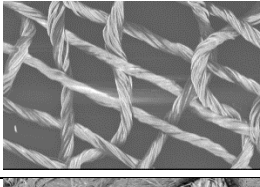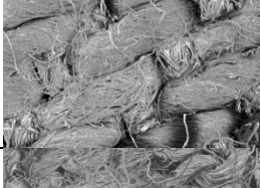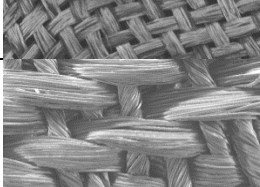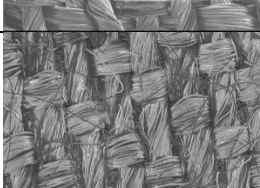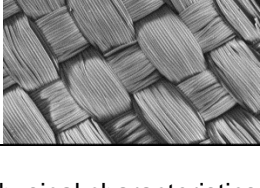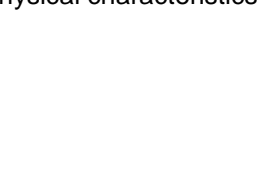
Silk Dupion		Tight plain weave	4200	0.21	2.09	87.50
Silk Chiffon		loose, plain weave and tightly twisted single crêpe yarns in both warp and weft	4000	0.09	0.34	88.02
Denim		Tight twill weave	5000	0.72	7.19	93.52
M&S T-Shirt Jersey		tight knit pattern (moss stitch), 1 knit, 1 purl	5600	0.35	2.85	95.22
Cotton Duck		Plain weave	4200	0.60	8.48	97.03
Medium Habotai Silk		Plain close weave	1400	0.07	0.67	82.05
Light Grey Polyester Twill		Twill weave	4000	0.23	2.18	98.21
Polysatin Heavy		Twill weave	2500	0.22	3.06	89.52
Cotton Poplin		Plain tight weave	3600	0.36	4.37	86.65
Nylon		Plain tight weave	4400	0.30	7.18	N/A Water-proof

Table 23: Physical characteristics of the 20 fabrics used in this study.
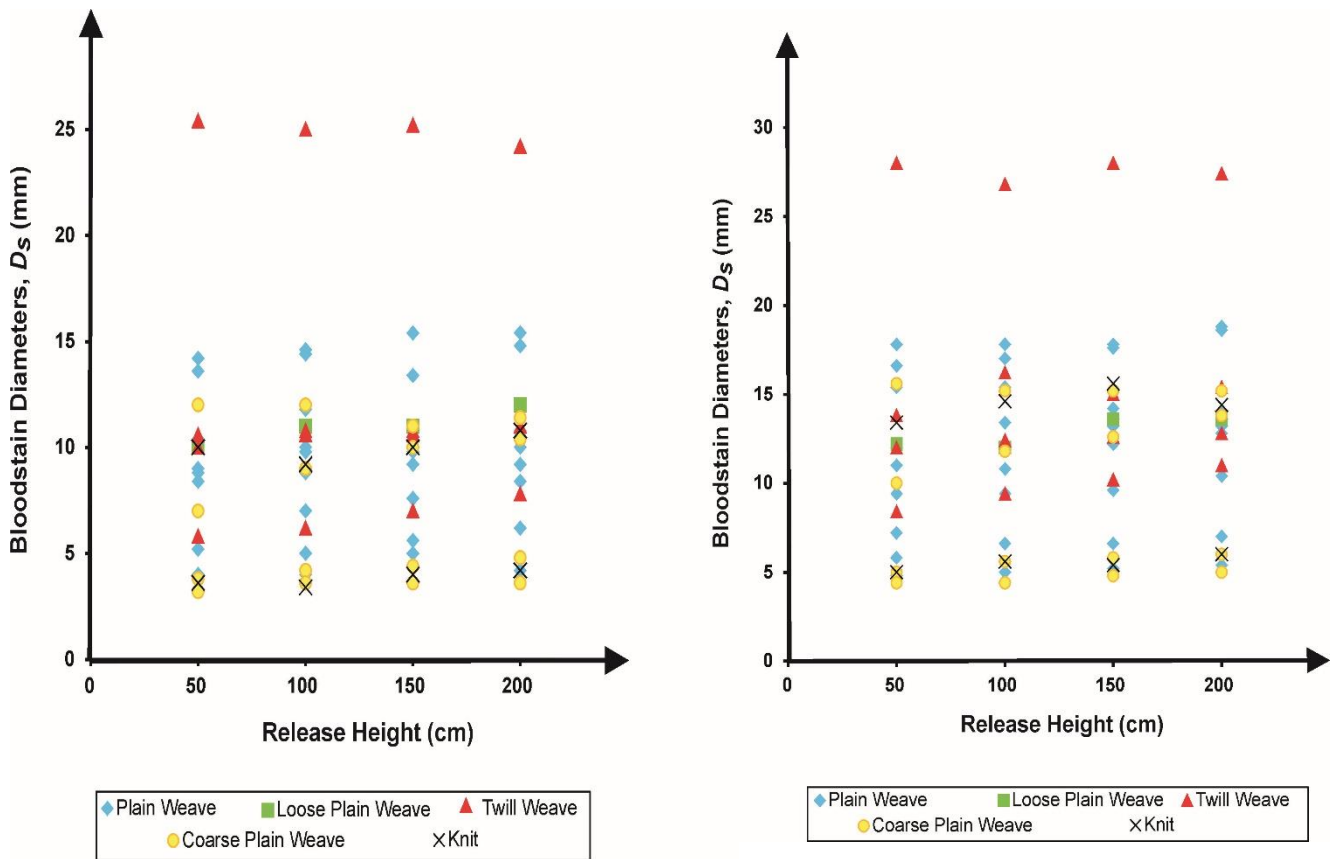
Figure 77: Bloodstain Diameters depicted the effect of fabric composition, where blood was deposited using A- 1mm pipette and B- 1.77mm pipette.

The composition of the fabrics were explored next. Fabrics were categorised into 5 groups; plain weave, loose plain weave, coarse plain weave, twill weave and knit. Figures 77 A and B display the effects the fabric composition has on the spreading of blood and final bloodstain. There was found to be no distinct difference between the diameter of bloodstains and the fabric composition, there was a range of sizes experienced independent of how the fabric was made (i.e. plain weave vs. twill weave).

There was an unusual phenomenon observed when polyester and silk fabrics were tested, a secondary ring was produced. This is similar to the ones observed by Slemko [50] who documented this occurrence on silk alone. A further 3 polyester fabrics were examined, where a secondary ring was observed on every polyester fabric (Figure 78A) at some stage.
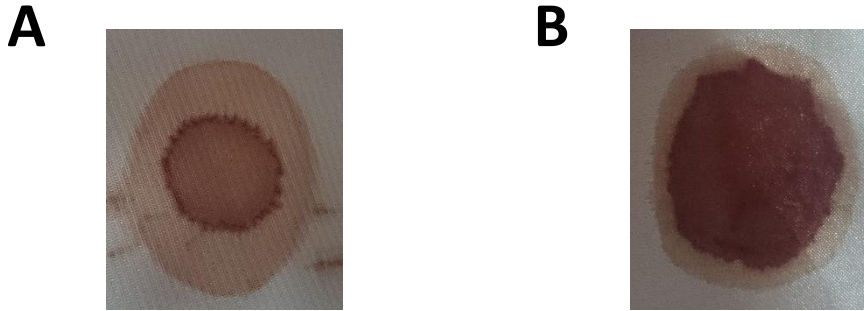
Figure 78: Secondary rings (a diffused outer ring) depicted on two fabric types; A – Polyester (Grey Polyester Twill) and B – Silk (Fuji)

This secondary ring on polyester was found not to be constant, as the degree of diffusion depended on the height from which the blood drop was released and the type of polyester. Four types of silk were examined, again this phenomenon was apparent on all of the silks (Figure 78B). However only two of the silk fabrics produced symmetrical rings at which were calculated to be at reduction constants of 1.24 and 1.25 for Fuji and Habotai silk, respectively.
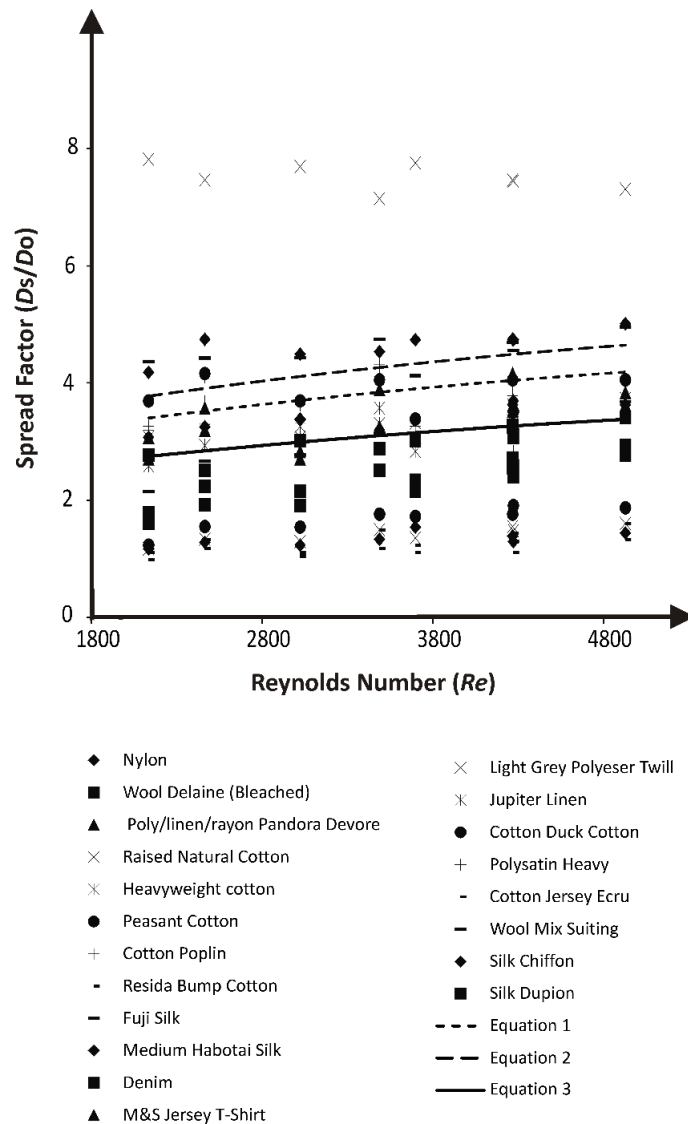
Figure 79: A new line of 'best fit' (solid line) was established when considering the spread factor versus the Reynolds number utilising defibrinated equine blood on different fabric types. Comparing this to the original line of 'best fit' (dotted line) using equation (2) [18] and the line of 'best fit' (dashed line) developed by Hulse-Smith *et al* [18] using equation (3); *N = 5*

Further analysis on the flat drops was undertaken, using the Reynolds number and spread factor to determine a constant (Figure 79). A previous constant for an array of surfaces was produced by Hulse-Smith *et al* [18], this was found to be 1.11; however when we consider fabrics this is decreased to 0.81. This decrease is most likely a result of the production of smaller stains due to the absorption and surface qualities of fabric (see Table 23). Since the surfaces used in the Hulse-Smith *et al* study [18] were mostly limited and non-porous (*i.e.* glass, tile) in nature they created larger stains and subsequently a bigger constant value; clearly the equation derived by Hulse-Smith is not applicable to fabrics.

Angled impacts were also considered (*data not included*), where angles of 20º, 40 º, 60º and 80 º (experimental) were investigated. It was found that all angled stains differed from the experimental angle, in most cases they were smaller (with only a few exceptions which were larger) than the experimental impact angle. It is thought that the blood absorbs more quickly on this surface type and therefore the stain produced is significantly smaller (up to 75.18 %), this conclusion is concurrent with the results obtained in White's study. [51] Therefore it is deemed not appropriate to use angled impacts when discussing bloodstains on clothing unless further detailed research is conducted into individual fabrics and reduction constants can be determined, or extensive testing is performed on the questioned fabric in the case of a reconstruction.

4.8.3 Summary

Fabric bloodstain interpretation is a fundamental element within the practice of BPA. Blood often interacting clothing and upholsteries in a blood shedding incident. Recent cases (Camm case) have highlighted the problematic nature of fabrics, where stains can alter dramatically due to the surface.

This study has investigated blood interactions with 20 common fabric types, applying equation and statistical analysis to fully comprehend the nature of the alteration, Current research has only explored observational approaches, without any quantitative analysis.

Results showed that fabrics do not follow the usual trend of increasing in stain diameter as height increases. Analysis of this trend revealed that a possible reason for this was the thickness of the fabric and not a result of the porosity or roughness of the fabric.

A new constant for the spread factor was developed, where C_d equalled 0.81, compared to the original constant devised by Hulse-Smith et al [18] of 1.11. The decrease in constant is attributed to the consistent production of smaller stains, due to the absorption qualities of the fabric. Since most of the surfaces analysed by Hulse-Smith et al [18] where non-porous and therefore produced larger stains.

Secondary rings were found to be exhibited on all silk and polyester fabrics, where reduction constants were calculated for two silk types (1.24; Fuji silk and 1.25; Habotai silk).

Angled impacts were found to be immeasurable due to the distortion created when blood impacted the fabric, developing large errors (75.1%) in the calculated angle where stains where significantly smaller.

Overall fabrics were found to significantly alter final bloodstains in a multitude of ways. The changes do not act in a predictable way and therefore it is advised that direct fabric matches be used when evaluating bloodstains for a reconstruction.

4.9   METAL

Metals are naturally occurring elements, which are extracted from the Earth, ores containing the metals are mined and metals are recovered by chemical or electrolytic reduction. [172]

Metals are available in abundance and variety of forms offering a wide range of properties that are invaluable in applications such as construction, thermal conduction, electrical conduction etc. [172] Their use in these countless applications has secured their place in homes, offices and public domains. This makes the likelihood of blood interacting with a metal surface during a crime scene scenario all the more probable.

4.9.1   Metal composition

Metals are closely packed atoms which are formed in one of the following three crystalline structures: [172-173]

1) body-centred cubic (BCC)
2) face-centred cubic (FCC)
3) hexagonal close-packed (HCP)

Atoms of metals readily lose their outer shell of electrons, resulting in free flowing electrons. This provides metal with its ability to transmit heat and electricity. [172 - 173]

4.9.2   Categories of Metals

4.9.2.1   Base metal

A base metal is defined as a metal that oxidizes and/or corrodes easily and reacts with dilute Hydrochloric Acid to form hydrogen, *i.e.* iron, nickel. [172 - 173]

4.9.2.2   Ferrous metal

Ferrous metals refer to metals containing iron, *i.e.* steel. [172 - 173]

4.9.2.3   Noble metal

Are often rare metals such as gold, platinum *etc.* They are resistant to corrosion and oxidation. [172 - 173]

4.9.2.4   Precious metal

A rare metal of high economic value. They are generally highly conductive, and do not react with chemicals. [172 - 173]

4.9.3   Metal types

4.9.3.1   Aluminium

Aluminium is the second most widely used metal in the world, due to its affinity to oxygen it is almost never found in its elemental state. [174 -175] Aluminium is most commonly extracted from the bauxite ore, found near the Earths' crust. There are two steps in the production of aluminium; 1- extraction of alumina (aluminium oxide) from bauxite using the Bayer Process, 2- smelting of aluminium metal from alumina. [174 - 175]

Aluminium is lightweight, highly conductive, reflective and easily manufactured, therefore it has many applications, including the construction of aircrafts, trains, cars, packaging, furniture, street lights and baseball bats etc. [174 -175]

4.9.3.2   Steel

There are over 3,500 grades of steel, each displaying different physical, chemical and environmental properties. [176] Steel is composed of iron and carbon, it is the level of carbon which determines steel's properties (0.1-1.5%). Other elements are present, such as manganese, sulphur etc. [176]

The production of steel is a laborious process which can be divided into six: [176]

1- Ironmaking: raw materials (iron ore, coke, lime) are melted in a blast furnace.
2- Primary Steelmaking: Basic Oxygen Steelmaking (BOS) or Electric Arc Furnace (EAF) methods are utilised. [176]
   BOS- oxygen is blown through the metal, reducing the carbon.
   EAF- recycled steel scrap is fed through a high power electric arc (1650°C), where steel is melted and can be shaped. [176]

3- Secondary Steelmaking: molten steel is treated, elements are added or removed in order to alter the composition. [176]

4- Continuous Casting: casted into a cool mould to solidify.

5- Primary Forming: steel is formed into various shapes, i.e. hot rolling. During this stage defects are eliminated. [176]

6- Manufacturing, fabrication, finishing: final shaping is completed i.e. shaping (cold rolling), coating, heat treatment, surface treatment etc. [176]

There are four main types of steel; [176]

Carbon steels – split into low (mild steel), medium and high

Alloy steels – alloys are added *i.e.* manganese, silicon etc.

Stainless steels – noted for its corrosion resistance, this steel type has a minimum of 10.5 % chromium present, which forms the protective film across the surface.

Tool steels – steel combined with high temperature alloys i.e. tungsten.

Application

Steel, due to its numerous grades, has many applications, these include: [176]

Packaging, transport, construction (*i.e.* stadiums, high-rise buildings), washing machines, microwaves, radiators etc.

4.9.3.3 Copper

Copper can be found in its native state though it is most commonly located in sulphide ores, oxide ores and carbonate ores. [177] The copper is extracted by smelting, leaching and electrolysis. Copper is also present in minerals; malachite, cuprite and chalcopyrite (most common). [177]

Second to only silver, copper is an extremely effective conductor of both heat and electricity. [177] It is also malleable and ductile, explaining its application in plumbing pipes. Other applications include cookware and coins *etc.* [177]

4.9.3.4 Zinc

Zinc (HCP structure) is extracted from ore containing zinc sulphide, zinc blende or sphalente. It is inherent in the environment, present in rocks, minerals, water, air, animals, humans and plants. [178]

Zinc is extracted from the earth's crust, present in four deposit types: [178]

1. Volcanic hosted massive sulphides (VMS)
2. Carbonate hosted
3. Sediment hosted
4. Intrusion related

Zinc is the fourth most popular metal in the world, with its strong noncorrosive properties it namely for its uses as a coating/ galvanizing other metals (*i.e.* steel). [178]

It is also used for: construction, transport, electrical appliances and general engineering. [178]

4.9.3.5   Brass

Brass is an alloy metal composed of copper and zinc, varying the rate of these components yields different properties, ordinarily brass consists of 67% copper and 33% zinc. [179] Lead is sometimes added to the brass to improve machinability. [179]

Brass is malleable, has acoustic properties, soft and has a shiny smooth texture. These properties make brass perfect for producing musical instruments, fireplace trim, bells and padlocks. [179]

4.9.4   Finishes

There are several types of finish, which are applied to the surface of the metal to protect, change the colour, strength, wettability and texture of the surface. [180]

Below are the finishes investigated in the study: [180]

Galvanizing – applies a protective zinc coating using the submersion of steel or iron in a bath of molten zinc, to prevent rusting. [180]

Anodising – electrolytic passivation process to increase the thickness of natural oxide on the surface of the metal. [180]

Sandblasting – applying a stream of abrasive material under high pressure to a smooth surface.

Polishing – abrasives are glued to a work wheel or leather strap and the surface is worked to a high-end finish. [180]

Brushed – polishing metal with a grit belt.

4.10 BLOOD IMPACTING METAL

The application of metal into household items, and its structural benefits means it is readily available for the incidental collision of blood on a metal surface during a bloodletting incident.

The following research investigates the interaction of blood and metal.

Twenty common metals, consisting of several types and finishing, were tested. Blood drops were performed from different heights and angles, where equations and quantitative analysis could be completed on the result obtained.

4.10.1 Experimental

All human blood (PCV% 43%) used in this study was obtained from Manchester Royal Infirmary and stored at 4°C whilst awaiting experimentation.

Several different metals were analysed, where 5 common metal types were analysed; aluminium, brass, steel, zinc and copper. Multiple versions of each surface were used, each with a different surface finish (polished, brushed, anodised, galvanized, unfinished and sand-blasted).

The following lists the metals tested:

Aluminium Satin Anodised, Brushed Satin Aluminium, Stucco Aluminium, Natural Semi Bright Aluminium, Bright Polished Aluminium, Copper Mirror Polish, Mild Steel, Galvanized Mild Steel, Zintec Sheet, Stainless Steel Brushed, 316 Stainless Steel, 430 Bright Steel, 430 Brush Stainless Steel, 430 Circles Stainless Steel, Stainless Sheet Super Mirror, Zinc Sheet Metal, Quartz Zinc Sheet Metal, Brass Mirror Polish, Copper Sheet Metal, Natural Semi Bright Aluminium-Sandblasted, Mild Steel-Sandblasted, 316 Stainless Sheet- Sandblasted and 430 Bright Stainless Steel-Sandblasted.

Numbers such as 430 refer to the grade of the steel, the most common being 430, 316 and 330.

Roughness measures, using the rugometer (section 2.2.2) and SEM images (section 2.4.2) were performed for each surface type.

Blood drop test were conducted according to the description in section 2.2.Two types of pipettes were utilised, and drops were deposited from heights (50, 100, 150 and 200 cm) and at angles of (20°, 40°, 60°, 80° and 90°).

Bloodstains were measured using a magnifying loupe and results were analysed using equations set forth by Hulse-Smith *et al.* [15]

4.10.2 Results and Discussion

4.10.2.1 Bloodstain Diameter vs. Metals

Blood drop experiments were performed for each surface type, where drops were repeated 5 times to obtain concordant results.

Figures 80 and 81 depict the results observed when both the 1mm and 1.77mm (inner tip diameter) pipettes were utilised for drops deposited at various heights. (see Appendix 7)
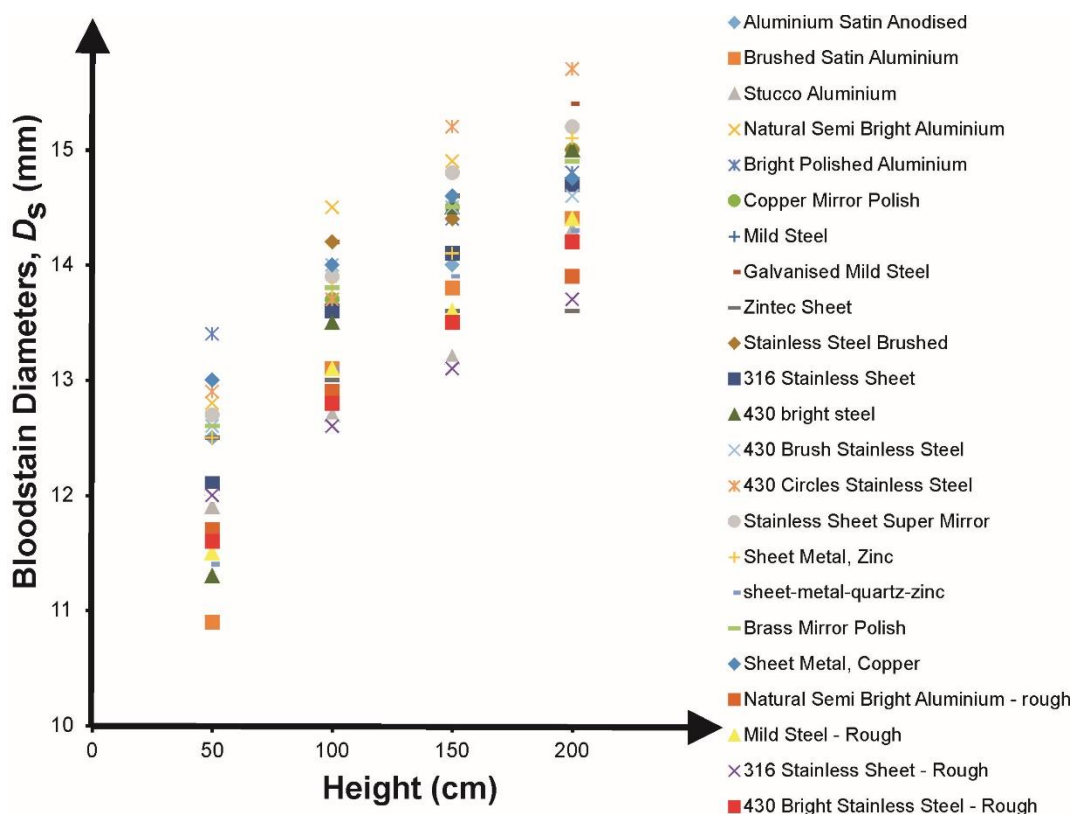
Figure 80: Bloodstain diameters on all 20 metal types from various heights; 50 cm, 100 cm, 150 cm and 200 cm, using the 1 mm pipette (inner tip diameter). *N = 5*.
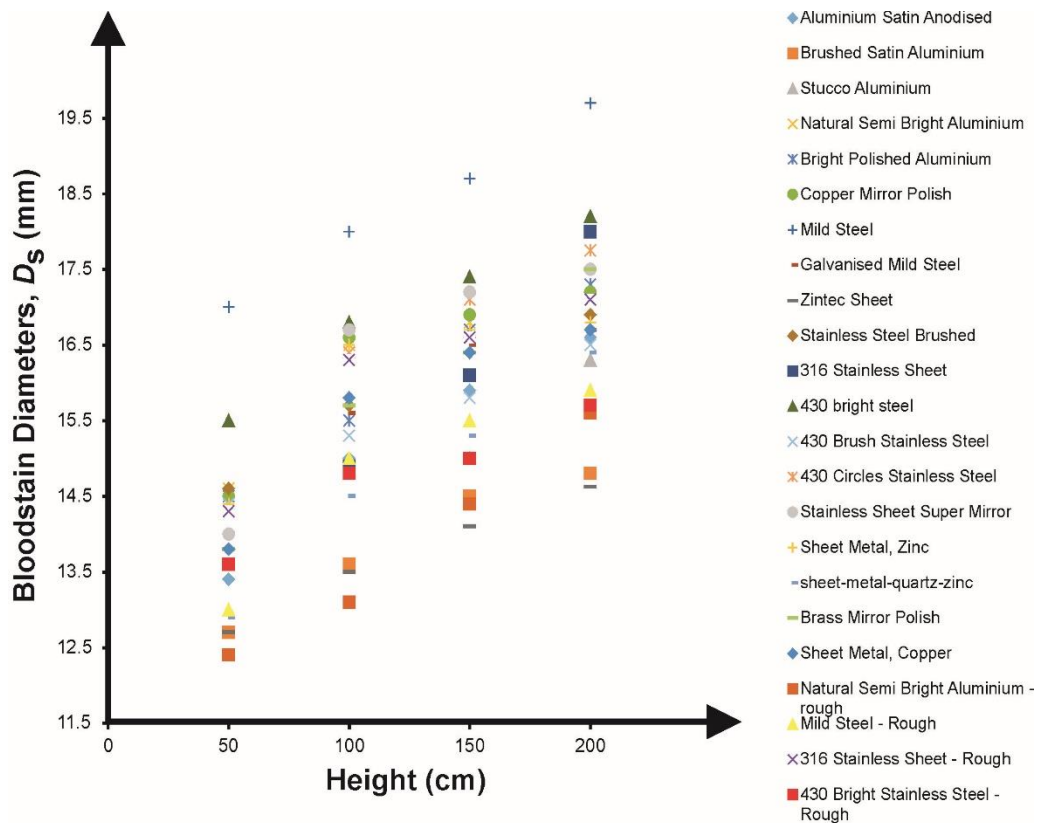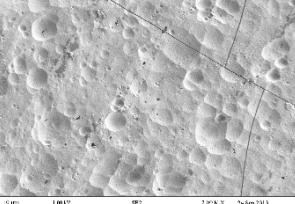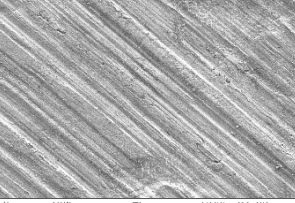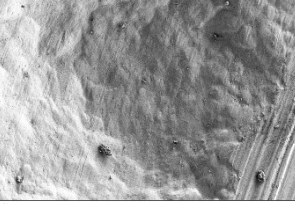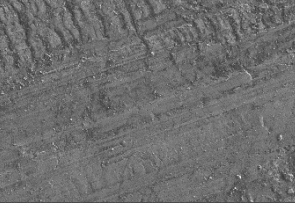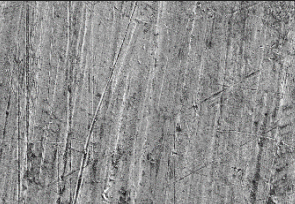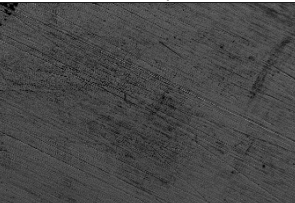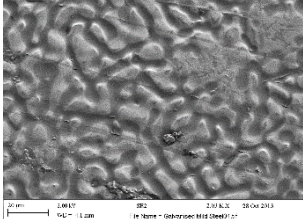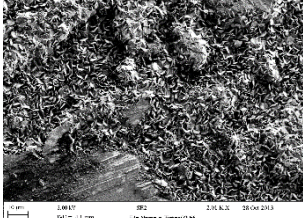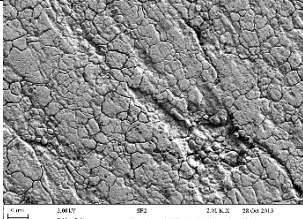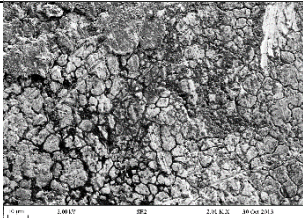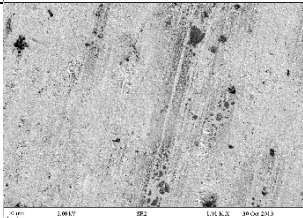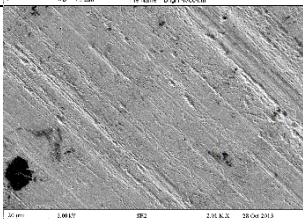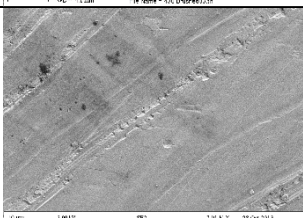
Figure 81: Bloodstain diameters on all 20 metal types from various heights; 50 cm, 100 cm, 150 cm and 200 cm, using the 1.77 mm pipette (inner tip diameter). *N = 5*.

Results show that bloodstain diameter increases in size as height increases; this is in excellent agreement with experiments performed previously and fits the general assumption made by analysts for the impaction of blood *vs*. height. Using Table 24, which lists the metals and describes their characteristics it is found that the diameter is indicative of the surface roughness. Bloodstain diameters generally decreased in size as the surface roughness increased, for instance brushed satin aluminium (R_a = 2.513) produced consistently smaller stains than 430 Bright Steel (R_a = 0.072). Though this was not always the case, where copper sheet (R_a = 0.05, the lowest surface roughness tested) exhibited bloodstains with mid-range values. Metals were further categorised into metal type (*i.e.* steel) and surface finish to establish if a pattern could be attributed to the change in bloodstain diameters (*i.e* polished surfaces produced smaller stains). Note angle tests were performed where no distinct difference was found for the experimental angle compared to the calculated angle.

Metal Names and Characterisation	SEM	Types	Finish	Roughness
Aluminium Satin Anodised (Pitted)		Aluminium	Anodised	0.328
Brushed Satin Aluminium (Striated)		Aluminium	Brushed	2.513
Stucco Aluminium (Pitted)		Aluminium	Unfinished	1.373
Natural Semi Bright Aluminium (Striated)		Aluminium	Polished	0.518
Bright Polished Aluminium (Striated)		Aluminium	Polished	0.075
Copper Mirror Polish (Striated)		Copper	Polished	0.05
Mild Steel (Textured)		Steel	Unfinished	0.952

Galvanised Mild Steel (Textured)		Steel	Galvanised	0.308
Zintec Sheet (Textured)		Steel	Unfinished	1.018
Stainless Steel Brushed (Cracked)		Steel	Brushed	0.65
316 Stainless Sheet (Cracked)		Steel	Unfinished	0.115
430 bright steel (Striated)		Steel	Polished	0.072
430 Brush Stainless Steel (Striated)		Steel	Brushed	0.478
430 Circles Stainless Steel (Striated)		Steel	Brushed	0.095
Stainless Sheet Super Mirror (Scratched)		Steel	Polished	0.0675
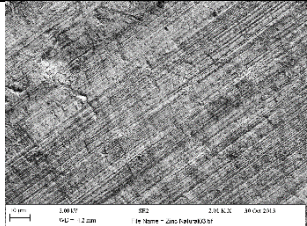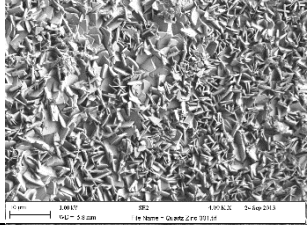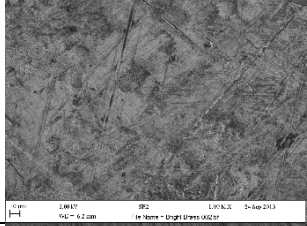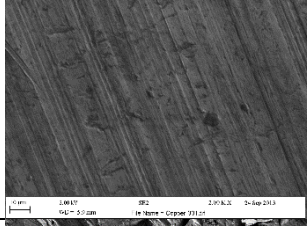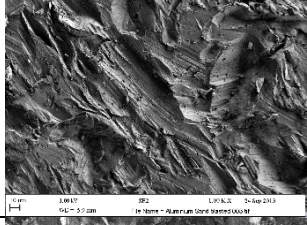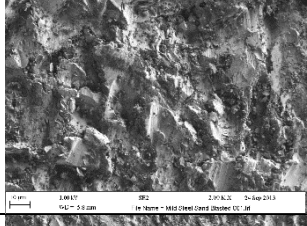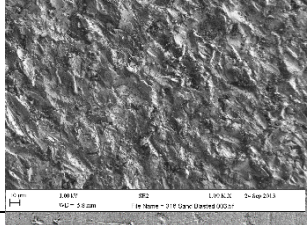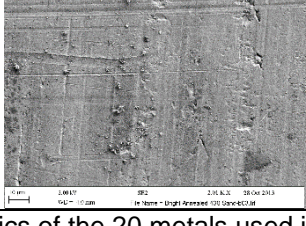
Sheet Metal, Zinc (Striated)		Zinc	Unfinished	0.168
sheet-metal-quartz-zinc (Striated)		Zinc	Unfinished	0.457
Brass Mirror Polish (Scratched)		Brass	Polished	0.065
Sheet Metal, Copper (Striated)		Copper	Unfinished	0.07
Natural Semi Bright Aluminium - rough (Textured)		Aluminium	Sand-Blasted	2.13
Mild Steel - Rough (Textured)		Steel	Sand-Blasted	2.26
316 Stainless Sheet - Rough (Textured)		Steel	Sand-Blasted	2.17
430 Bright Stainless Steel - Rough (Striated)		Steel	Sand-Blasted	1.59

Table 24: Physical characteristics of the 20 metals used in this study.

Firstly, metal types were analysed. Figures 82 A and B show the size of bloodstains when compared to the type of metal surface used, where both pipette types were used.

Zinc and aluminium produced smaller stains than other metal types; however, the results did not deviate enough from other metal values for the type of metal to be considered as a causative factor in the final bloodstain size.
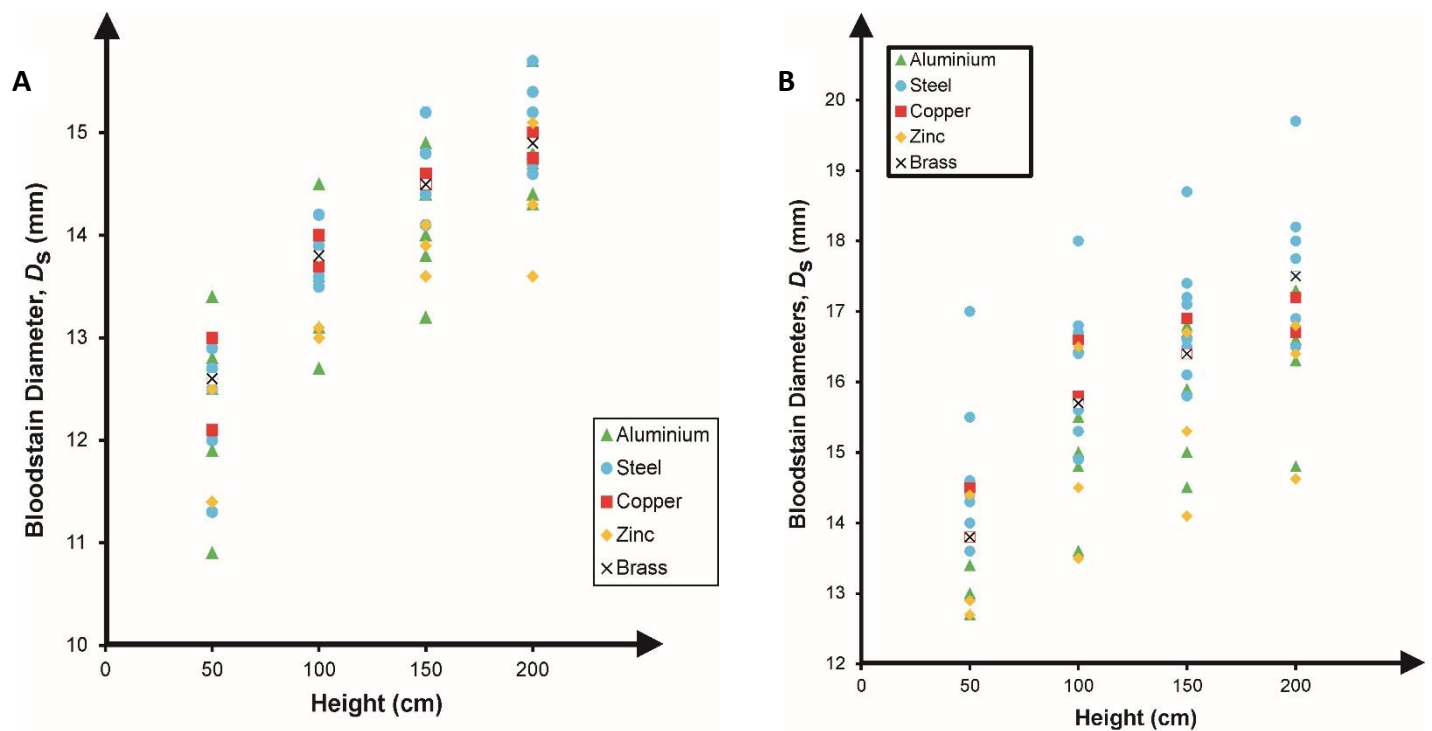
Figure 82: Categorised bloodstain diameters on 5 main metal types from various heights; 50 cm, 100 cm, 150 cm and 200 cm, using the A - mm pipette (inner tip diameter), B - 1.77 mm pipette (inner tip diameter), $N = 5$.

Next the surface finish was investigated (Figures 83A and B). No discernible pattern was exhibited when surface finish was considered, however sand-blasted surface did generally produce smaller bloodstains. Again, these were not found to be small enough to be distinguishable between other surface finishes. Therefore surface finish is not a deciding factor on the size of the resultant bloodstain produced.
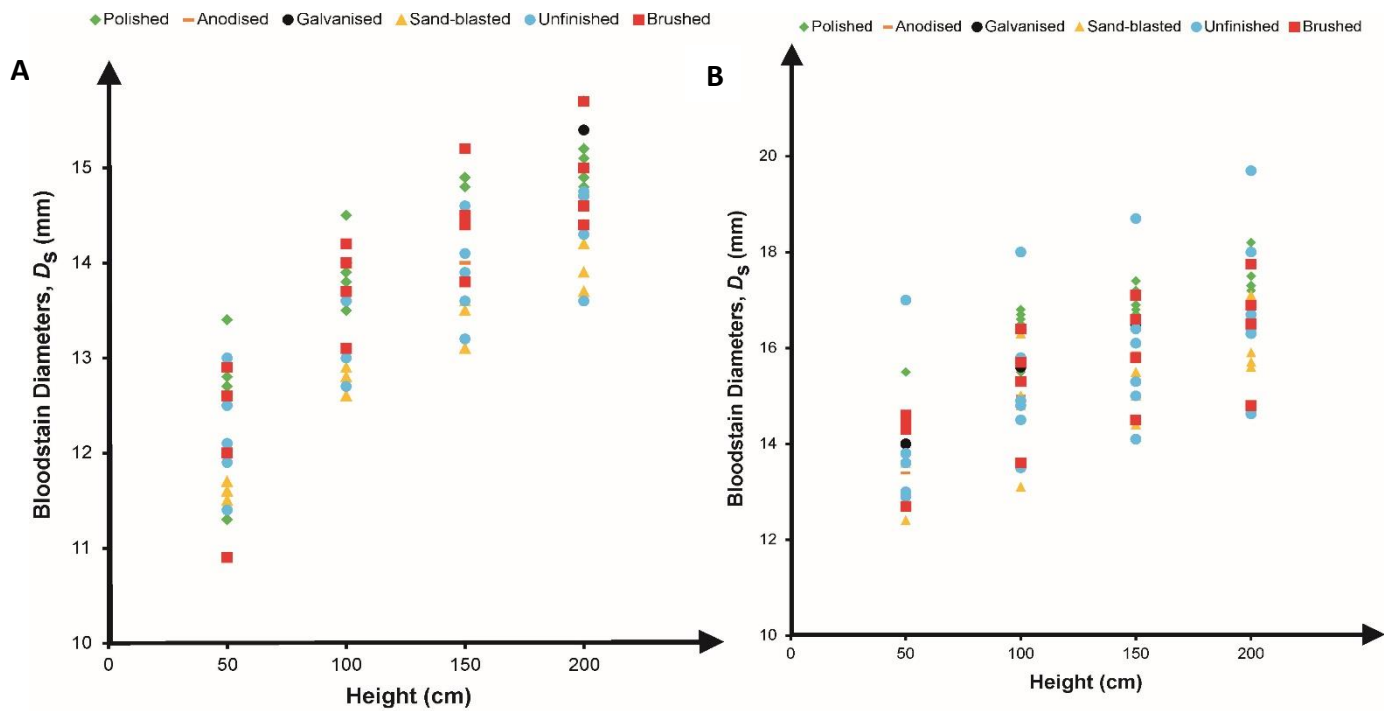
Figure 83: Bloodstain diameters on all 20 metal types, categorised by their surface finish, from various heights; 50 cm, 100 cm, 150 cm and 200 cm, using the A - mm pipette (inner tip diameter), B - 1.77 mm pipette (inner tip diameter), $N = 5$.
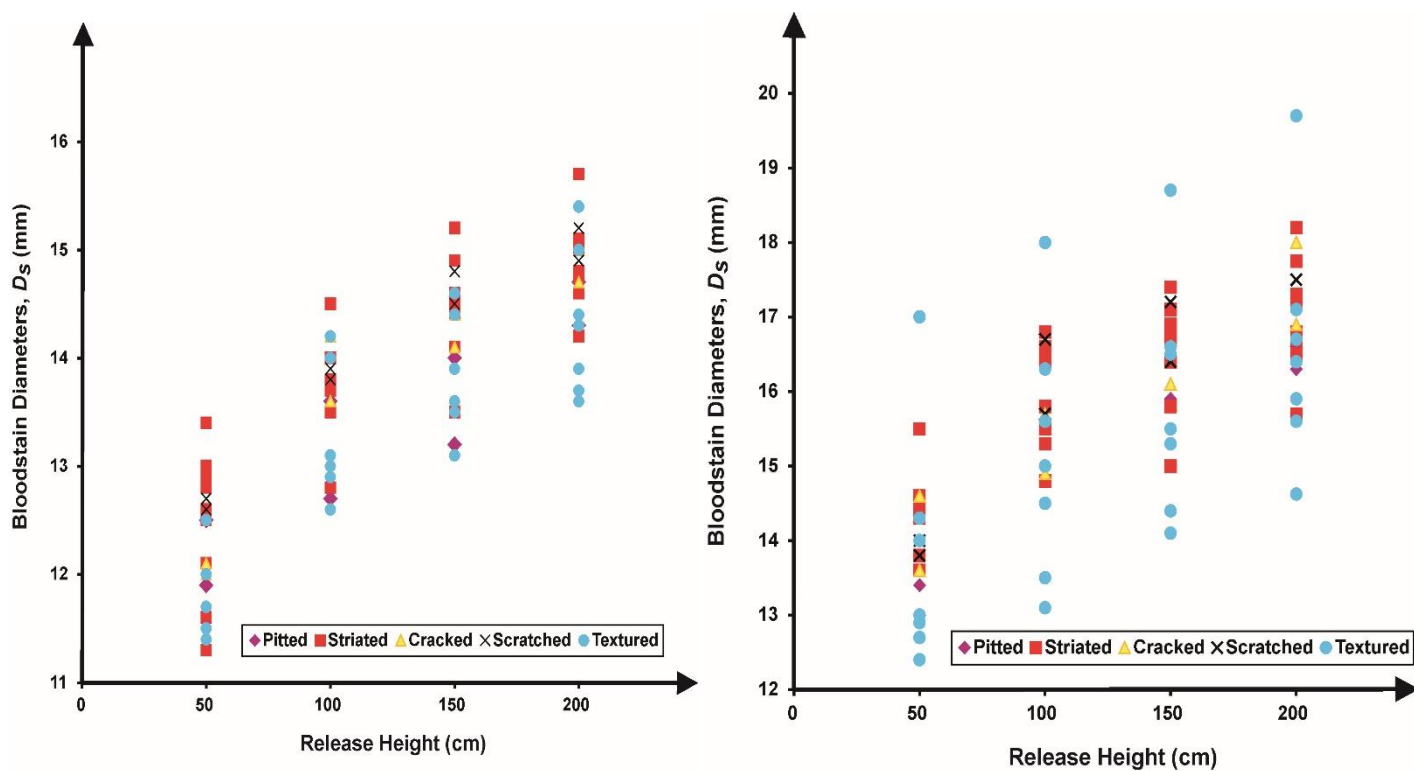
Figure 84: Bloodstain Diameters depicted the effect of surface characteristics, where blood was deposited using A- 1mm pipette and B- 1.77mm pipette.

Referring to Table 24, metals were further categorised depending on their physical appearance, characterising the metals into 5 groups; pitted, striated, cracked, scratched and textured. Surfaces were expected to alter the size of the bloodstains due to certain surface characteristics, *i.e.* pitted surfaces may cause smaller bloodstains due to blood falling into the pits rather than spreading as it would on a completely flat, smooth surface. However this does not appear to be the case, a variety of bloodstain sizes were apparent independent of the surface characteristic (Figures 84 A and B). A possible reason for this may be attributed to the surface finish, since the finish is on the top layer of the surface this could render some surface characteristics redundant, as the blood would not actually interact with them.
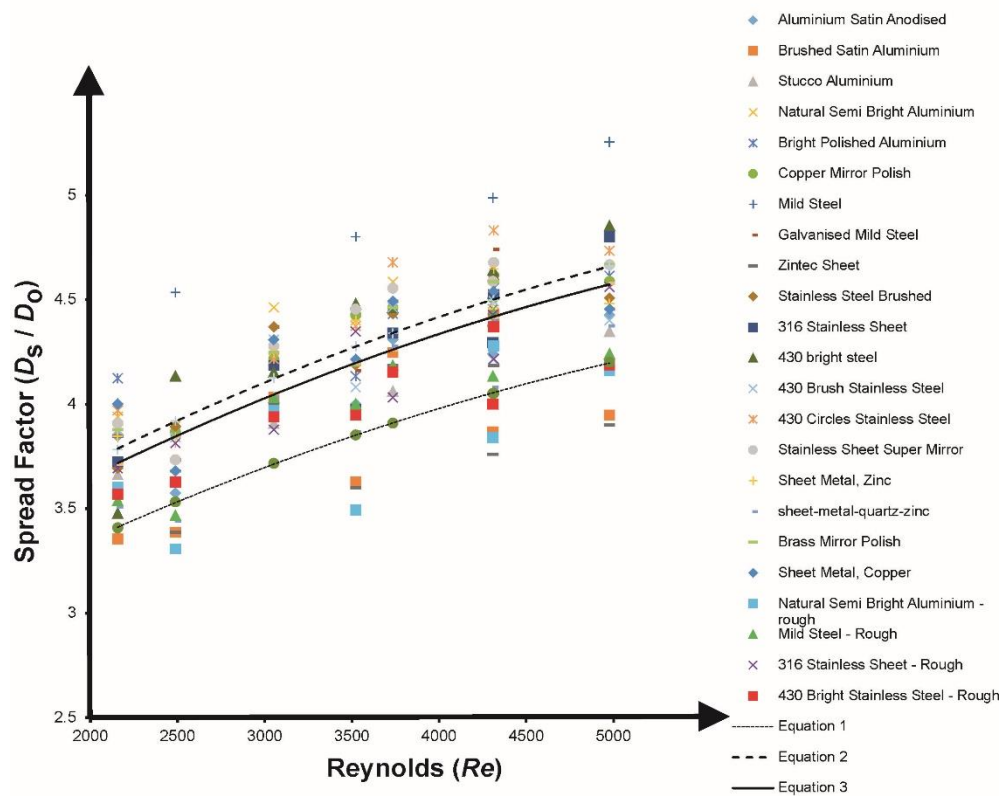
Figure 85: A new line of 'best fit' (solid line) was established considering the spread factor versus the Reynolds number on different metal surfaces. Comparing this to the original line of 'best fit' (dotted line) using equation (3) [18] and the line of 'best fit' (dashed line) developed by Hulse-Smith *et al* [18] using equation (4).

Lastly Reynolds numbers and spread factors were calculated using equations (1, 3 and 4) where lines of 'best fit' were graphed (Figure 85) and a new constant was established. The new constant equated to 1.09, which slightly deviates from the original value determined by Hulse-Smith *et al*, where C_d equals 1.11. Since these

constant are not significantly different it can be concluded that metal surfaces do not significantly alter the way a bloodstain forms, in spite of the type of metal and surface finish utilised.

4.10.3 Summary

Since metal is a readily used resource in most environments, it is very accessible to interaction with blood which may be expelled during a crime scene scenario. This study has evaluated the impinging of blood on metal surfaces, where 5 common metal types and 5 surface finishes were analysed. Blood drop tests were performed from different heights and using two pipette tip types.

Results found that the higher the release height the larger the bloodstain, this was consistent for each metal type. This result is expected and is one of the fundamental principals in BPA, first established in the 1950s. Roughness of the surface was a determinant factor in the size of the final bloodstain diameter produced, where bloodstains were smaller when the surface was rougher. However, this was not always the case. Further analysis splitting the metals into types and finishes was completed. Aluminium, zinc and sand-blasting the surface were found to produce smaller bloodstains, however these stains were not significantly smaller than those produced by other metal types and finishing techniques. It is therefore concluded that neither metal type nor finishing technique dictates the end bloodstain diameter, however the general roughness does.

Spread factors were also considered, where a new constant ($C_d = 1.09$) was developed using the equations (3 and 4) set forth by Hulse-Smith et al [18] the new constant is close to the original close; 1.11. Therefore, it was concluded that metal surfaces do not deviate significantly from any other surface type, hence it does not warrant any special consideration when analysing blood impacting metal surfaces in a crime scene scenario.

4.11 STONE AND TILE

Rocks have been used for tools since the Stone Age, they are made up of naturally occurring mineraloids or minerals. [181 - 183]

Presently rocks have multiple applications such as stairs, driveways, stepping stones, paving, walls, columns, sculptures, floors, sinks and many more. [181 - 183]

Similarly to wood, stone would be expected to be present in a number of crime scene scenarios and therefore in this section will investigated as a potential blood impact surface. [181 - 183]

4.11.1 Stone Types

Stone can be categorised into three types of rocks:

4.11.1.1 Sedimentary

Sedimentary rocks are produced by the erosion of rocks. Eroded fragments accumulate on the sea/river bed or on land where they are then buried (by more layers of rock fragments) and compressed to form sedimentary rocks. [181 - 183]

There are two classifications of sedimentary rocks: clastic and non-clastic. Clastic sedimentary rocks comprise of clasts, defined as fragments of pre-existing rocks or minerals. Further categorisation is possible according to the size of clasts: Boulder>200µm, Gravel 2 - 200 µm, Sand 0.06 - 2 µm and Mud < 0.002 – 0.06. [181 - 183]

Non-clastic sedimentary rocks are defined as rocks in which fragments have not been transported but precipitated directly from water, therefore no clasts are present.

The sedimentary rocks using in this study are:

4.11.1.1.1 Sandstone

Sandstone is composed of small grains of minerals, rocks or organic matter and a cement like material (*e.g.* calcite clays and silica) to bind the grains together. [184] The name sandstone does not refer to the material from which the stone is composed but rather the size of the grains. [184]

Figure 86: Sandstone

Sandstone is a very hard stone with a homogeneous grain structure, it has low porosity and is resistant to weathering and wear. [184]

Uses: construction, paving, statues and glass making.

4.11.1.1.2   Limestone

Figure 87: Limestone

Limestone is composed of skeletal fragments from marine organisms (*i.e* coral) where minerals such as calcite and aragonite bind together to form the rock. [185]

Limestone is a hard rock with low porosity with high resistant to wear and weather. [185]

Uses: glass making, road construction, steel making, paving, statues, monuments, construction and neutralising soil. [185]

4.11.1.1.3   Travertine

Figure 88: Travertine

Travertine is a form of limestone constructed by the precipitation of calcium carbonate minerals from the mouth of hot springs or limestone caves. [185]

It is a soft stone with holes and troughs this makes them extremely porous and difficult to finish. [185]

Uses: building construction, monuments, amphitheatres *(i.e.* the Coliseum) and paving [185]

4.11.1.2 Metamorphic

Metamorphic rocks are formed from the 'change in form' (metamorphism) of existing rocks. Where the original rock (igneous or sedimentary) is subjected to pressure and high heat > 200°C. This causes changes to the mineralogy, chemistry and texture of the rock. [186]

There are two types of metamorphic rocks:

1) Foliated: due to uneven pressure and heat bands are formed in the rock, where minerals have aligned. [186]

2) Non-foliated: Non- layered rocks, a result of even pressure being applied throughout the rock. [186]

4.11.1.2.1 Marble

Figure 89: Marble

Marble is the result of the metamorphism of sedimentary rocks, namely limestone. The metamorphism causes recrystallization of the carbonate grains, marble is therefore made of interlocking carbonate crystals. [186]

Marble is extremely strong, has very low porosity and is resistant to most things (*i.e.* erosion, fire) [186]

Uses: construction, tile, flooring, statues, monuments.

4.11.1.2.2 Slate

Figure 90: Slate

Slate can be composed of shale, clay or volcanic ash. It is a type of metamorphic foliated rock, which is very finely grained. [186] The foliation (repetitive layering) is apparent when the rock is cut parallel. [186]

Slate is hard and brittle, has a very porosity and is resistant to erosion. [186]

Uses: roofs, paving, chalkboards and snooker/billiards/pool beds.

4.11.1.3 Igneous

Igneous rocks are rocks formed by the cooling and crystallization of magma. There are two types of igneous rocks: 1- volcanic and 2- plutonic. [187]

Volcanic – formed when a volcanic eruption occurs and the magma rises to the surface as lava, the rapid cooling cause's small crystals to form. The rocks have characteristics which indicate its journey; flow banding; formed by the shearing of lava flow, open cavities where gases have escaped. [187]

Plutonic – are formed within the Earth's crust as the magma cools. Conversely to volcanic rocks plutonic rocks cool slowly creating large crystals and a coarse grain structure. [187]

4.11.1.3.1 Granite

Granite is a plutonic igneous rock it consists of quartz and feldspar, which has formed in the earth's crust. [187]

It is an extremely hard rock (only diamond is harder) with a low porosity and high resistance to wear and erosion. [187]

Uses: building, statues, kitchens, flooring, roofing etc.

Figure 91: Granite

4.11.2 Finishes

A variety of finishes are available for stones, offering protection, colour change, practicalities (non-slip floors) and high end finish. [188 - 191]

The following finishes are those to be explored in the research: [188 - 191]

Polished: uses fine abrasives which rubbed against the surface to give a high gloss finish.

Honed: gives a smooth matt finish, recommended as a floor finish. This is produced when the polishing process is stopped before it reaches the high gloss finish is achieved. Abrasives are used which are less fine than those use for a polished finish. [188 - 191]

Tumbled: produces a worn look, where stones are placed in a barrel along with grit (i.e. silicon carbide) and liquid (water). [188 - 191]The barrel is rotated so the rocks collide with the grit and are slowly polished. [188 - 191]

 Flamed: stone is exposed to high temperature flames whilst wet, this triggering thermal shock which causes grains to rise to the surface, creating a rough textured surface.

Riven: where stone is split along the natural cleavage plane. Seen mostly in slate. [188 - 191]

Sand-blasted: creates a textured surface by applying high pressured jet of small grains across the surface. [188 - 191]

5.11 BLOOD IMPACTING STONE AND TILE

Since the use of stone for important applications such as building, flooring etc has been around for thousands of years the high probability of stone occurring in some form at a crime scene is highly likely. [191]
The following research investigates the interaction of blood and stone.

Twenty-one common stone and tile types, consisting of several types and finishing, were tested. Blood drops were performed from different heights and angles, where equations and quantitative analysis could be completed on the results obtained.

5.11.1 Experimental

All human blood (PCV% 43%) used in this study was obtained from Manchester Royal Infirmary and stored at 4°C whilst awaiting experimentation.

Several different stone and tile types were analysed, where 8 common stone types were analysed; granite, marble, ceramic, porcelain, sandstone, limestone, travertine and slate. Multiple versions of each surface were used, each with a different surface finish (polished, unfinished, flamed, honed, riven and tumbled).

The following lists the stones and tiles tested:

Travertine (Classic Tumbled Unfilled Travertine, Classic Honed Travertine Paving, Silver Latte Tumbled Travertine Paving Opus Pattern, Classic Travertine Filled and Honed, Classic Chipped Edge Filled and Honed Travertine Opus Pattern), Limestone (Yellow Limestone Paving), Sandstone (Indian Sandstone Paving Raj Blend Tumbled, Indian Sandstone Paving Raj Blend Economy, Indian Sandstone Paving Sahara Yellow Calibrated, Indian Sandstone Paving Rippon Buff, Indian Sandstone Paving Modak Calibrated), Slate (Brazilian Black Slate Paving and Rusty Slate Paving), Porcelain (Sandstone Rivon Porcelain and Super White Matt Porcelain), Ceramic (Ceramic Matt and Ceramic Polished) and Beige Marble Polished.

Roughness measures, using the rugometer (section 2.2.2) and SEM images (section 2.4.2) were performed for each surface type.

Blood drop test were conducted according to the description in section .Two types of pipettes were utilised, and drops were deposited from heights (50, 100, 150 and 200 cm) and at angles of (20°, 40 °, 60 °, 80 ° and 90 °).

Bloodstains were measured using a magnifying loupe and results were analysed using equations set forth by Hulse-Smith *et al* [18]

5.11.2   Results and Discussion

5.11.2.1   Bloodstain *vs.* Stone Surfaces

Blood drop tests were performed on all stone surfaces where the blood was deposited from 4 different height (see Appendix 8) and at a range of angles. Figures 92 and 93 depict the effect stone surfaces had on the bloodstain diameter produced when blood is released using both the 1mm pipette (inner tip diameter) and the 1.7mm pipette (inner tip diameter). Diameters were found to increase as height increased until terminal velocity (ordinarily around 200 cm) was reached, where diameter increases become less pronounced.
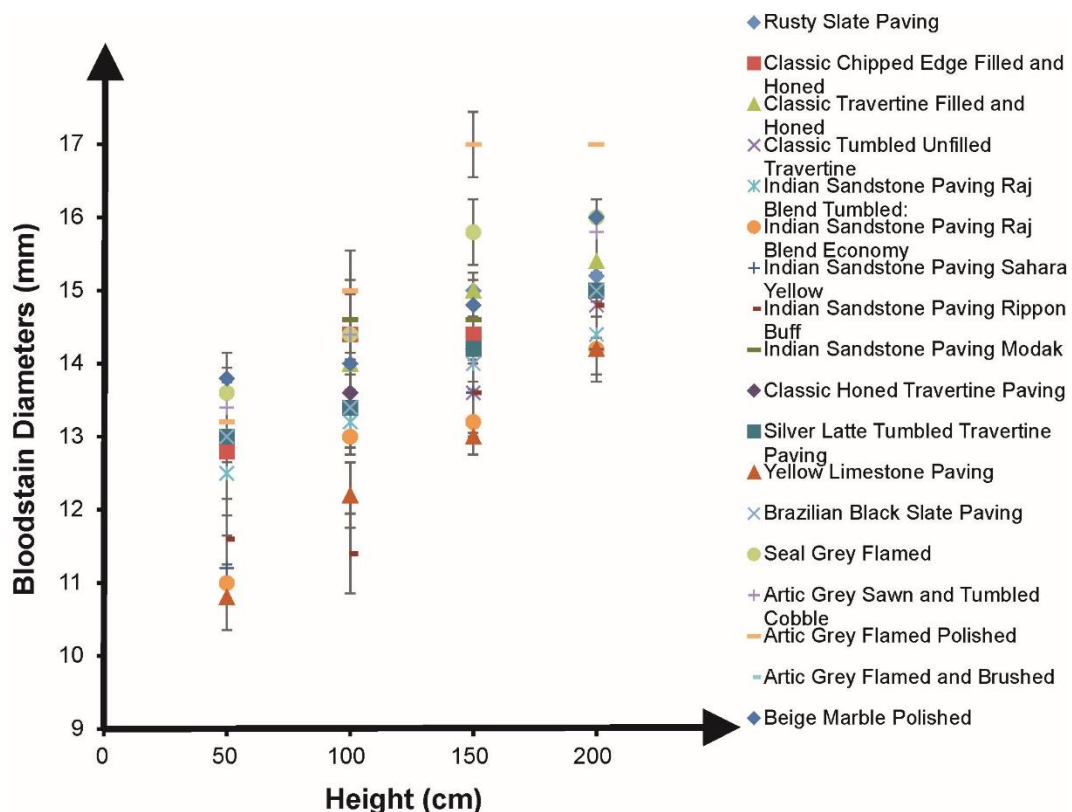
Figure 92: Bloodstain diameters on all stone surfaces from various heights; 50 cm, 100 cm, 150 cm and 200 cm, using the 1 mm pipette (inner tip diameter). *N = 5.*
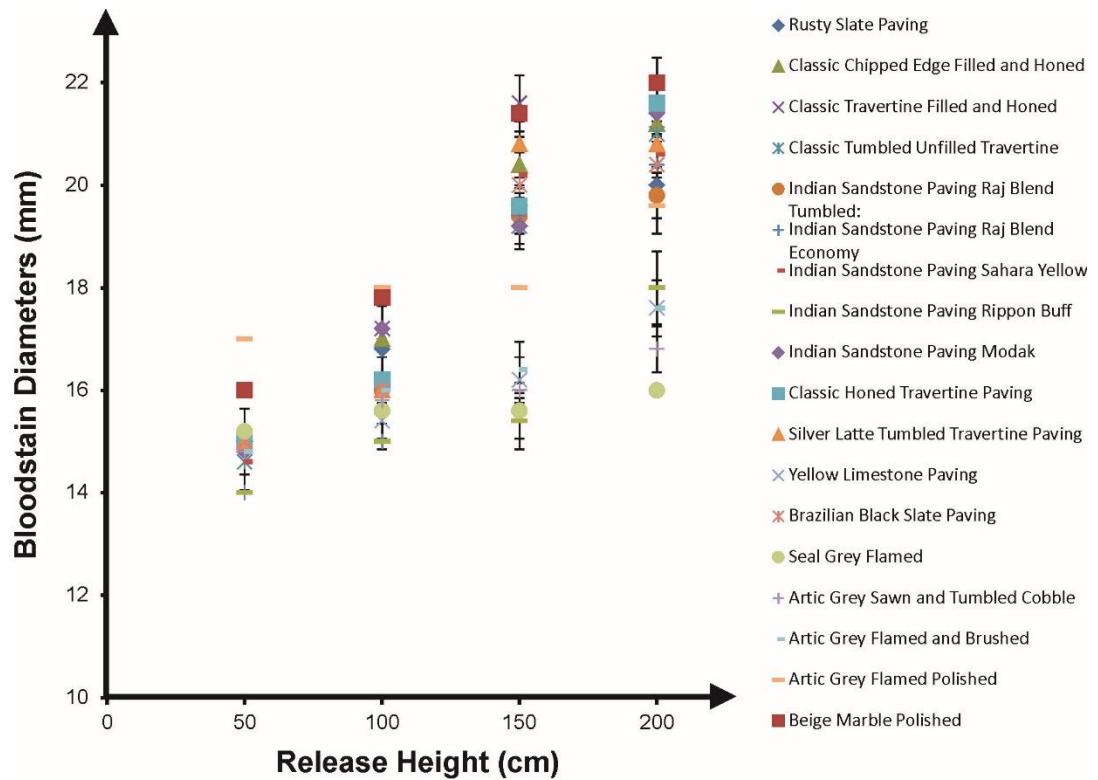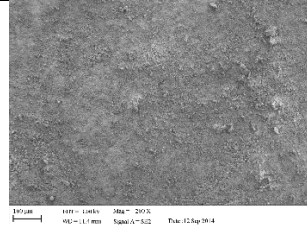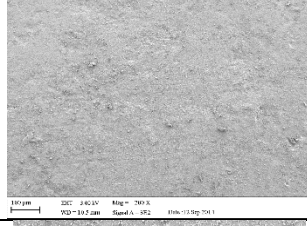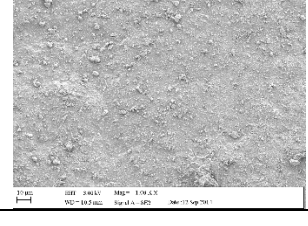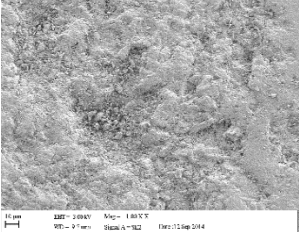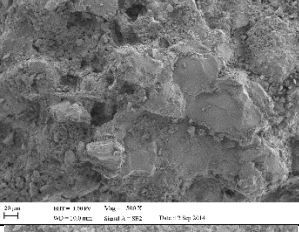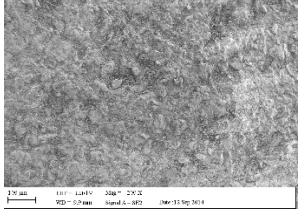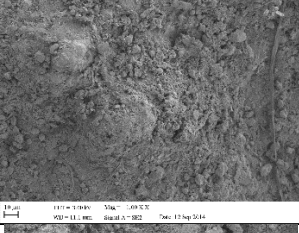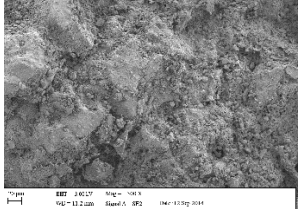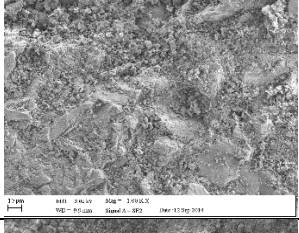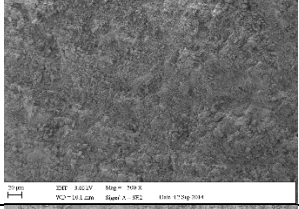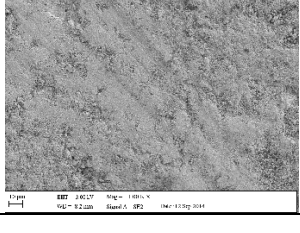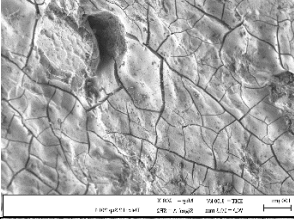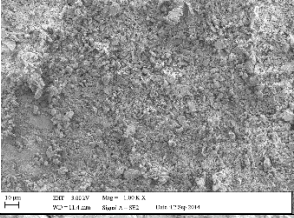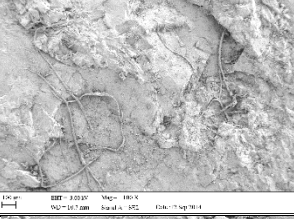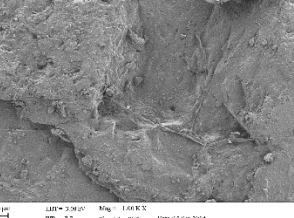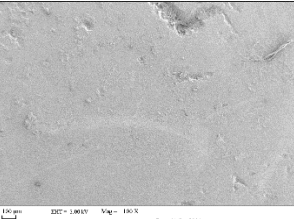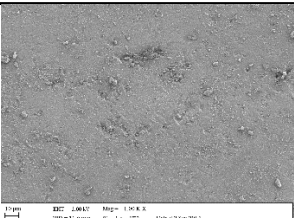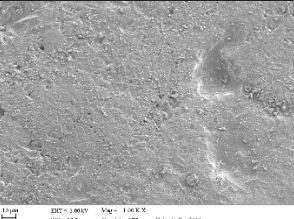
Figure 93: Bloodstain diameters on all stone surfaces from various heights; 50 cm, 100 cm, 150 cm and 200 cm, using the 1 mm pipette (inner tip diameter). $N = 5$.

Using Table 25, which lists the characteristics of each surface, it was determined that roughness is a dominant factor in the deciding upon the final bloodstain size.

Stone and Tile names and Characterisation	SEM	Type	Finish	Roughness. Ra (µm)
Rusty Slate Paving (Smooth)		Slate	Riven	3.46
Classic Chipped Edge Filled and Honed (Smooth)		Travertine	Honed	0.30
Classic Travertine Filled and Honed (Smooth)		Travertine	Honed	0.65

379

Classic Tumbled Unfilled Travertine (Textured)		Travertine	Honed, Tumbled	5.39
Indian Sandstone Paving Raj Blend Tumbled (Textured)		Sandstone	Tumbled	9.40
Indian Sandstone Paving Raj Blend Economy (Textured)		Sandstone	Riven	8.58
Indian Sandstone Paving Sahara Yellow (Textured)		Sandstone	Riven	9.61
Indian Sandstone Paving Rippon Buff (Textured)		Sandstone	Buff	8.64
Indian Sandstone Paving Modak (Textured)		Sandstone	Riven	9.41
Classic Honed Travertine Paving (Textured)		Travertine	Honed	2.72
Silver Latte Tumbled Travertine Paving (Textured)		Travertine	Honed, Tumbled	0.73

Yellow Limestone Paving (Cracked)		Limestone	Riven	10.91
Brazilian Black Slate Paving (Textured)		Slate	Riven	3.31
Seal Grey Flamed (Pitted)		Granite	Flamed	6.10
Artic Grey Sawn and Tumbled Cobble (Pitted)		Granite	Tumbled	5.67
Artic Grey Flamed and Brushed (Pitted)		Granite	Flamed	7.20
Artic Grey Flamed Polished (Smooth)		Granite	Polished	0.03
Beige Marble Polished (Smooth)		Marble	Polished	1.36
Ceramic Matt (Pitted)		Ceramic	Matt	1.15
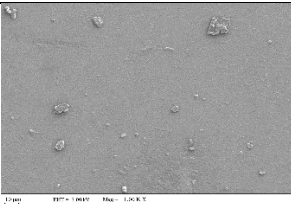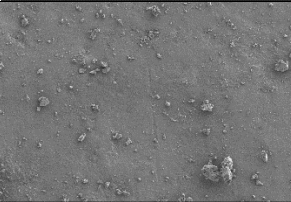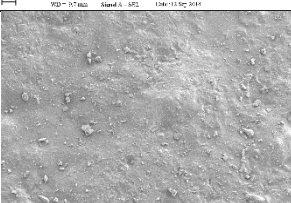
Ceramic Polished (Smooth)		Ceramic	Polished	1.90
Porcelain matt (Smooth)		Porcelain	Matt	0.30
Sandstone Rivon (Smooth)		Porcelain	Matt	5.35

Table 25: Physical characteristics of the stone and tile surfaces used in this study.

Rougher surfaces such as yellow limestone paving produced smaller stains compared to smoother surfaces *i.e.* Classic Travertine Filled and Honed, which exhibited much larger stains. There are many factors which can produce roughness, the main factor which would cause roughness in the case of stone are grains/ pores. Pores are open cavities within and on top of the surface, this causes irregularities and increases the porosity of the surface. Therefore blood cannot spread as far, since blood is soaked into the stone rather than on top of it and the increase in friction due to the irregularities on the surface.

This is not the case for both pipette types. For instance seal grey flamed granite produced one of the largest bloodstain diameters of all stone types when the 1mm pipette is used, however when the 1.77mm pipette is used it exhibits one of the smallest diameters. This suggests that volume may be a serious factor when considering surface interaction, especially when the surfaces are porous. It is suspected that the increase in volume when considering very rough surfaces is caused by the volume overcoming the roughness, therefore producing larger bloodstains and absorbing onto the surface rather than into it. Angled impacts were also evaluated, where the largest distortion was found at the acuter angles, sometimes leading to a 46% error rate.

Further observations were employed, where stones were categorised into type of stone (travertine, limestone etc.) and finishing process (honed, polishes etc.), to establish a direct link between stain size and a dominant characteristic.

Figures 94A and B express the type of stone used and the bloodstain produced for pipette types 1mm and 1.77mm, respectively. Figure 94A shows that overall granite produces the larger stains and limestone/ sandstone generate smaller stains, though the differences are not pronounced enough to be able to distinguish between stone types since some of the sandstone bloodstains (*i.e.* Indian Sandstone Paving Rippon Buff) generate similar bloodstain diameters to granite, likely due to the type of finish employed. Figure 94B does not follow the same trend as the first figure (94A), all stone types appear to be mingled regardless of their stone type. Again this indicates that volume is a considerable factor when evaluating blood impacting stones.
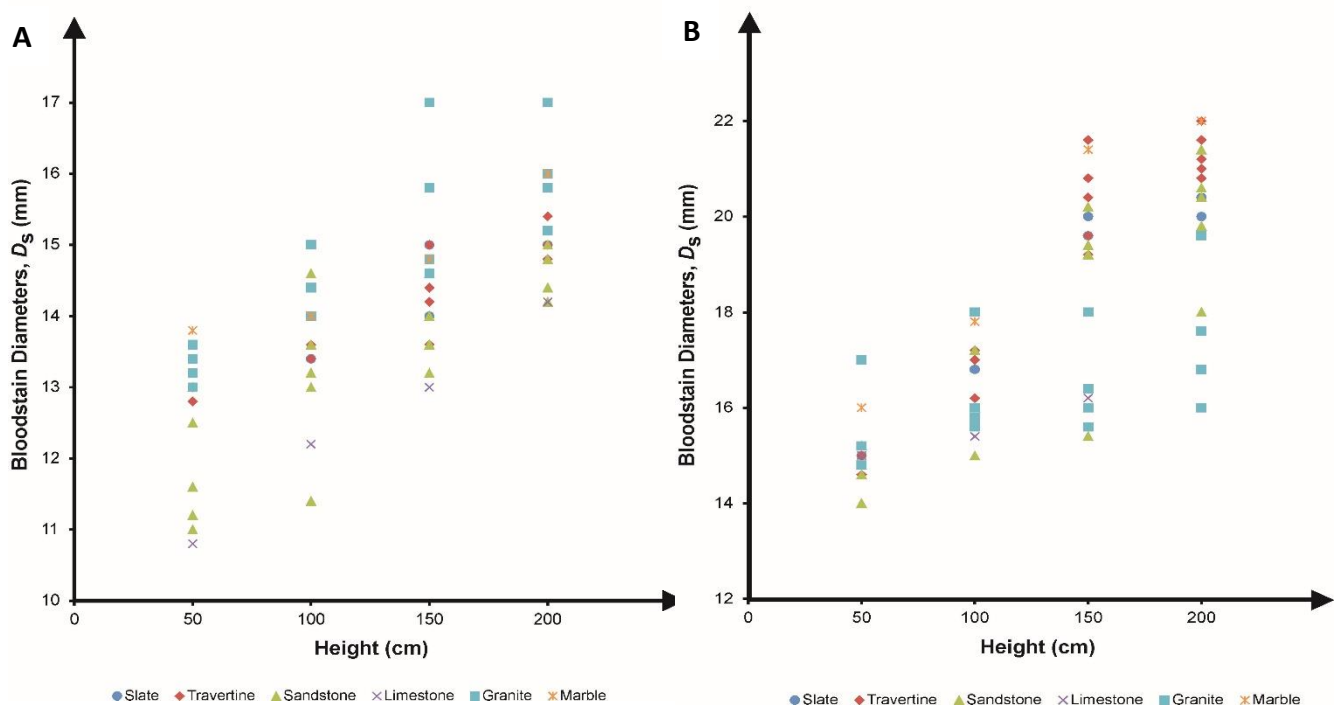
Figure 94: Categorised bloodstain diameters on 5 main stone types from various heights; 50 cm, 100 cm, 150 cm and 200 cm, using the A - mm pipette (inner tip diameter), B - 1.77 mm pipette (inner tip diameter), $N = 5$
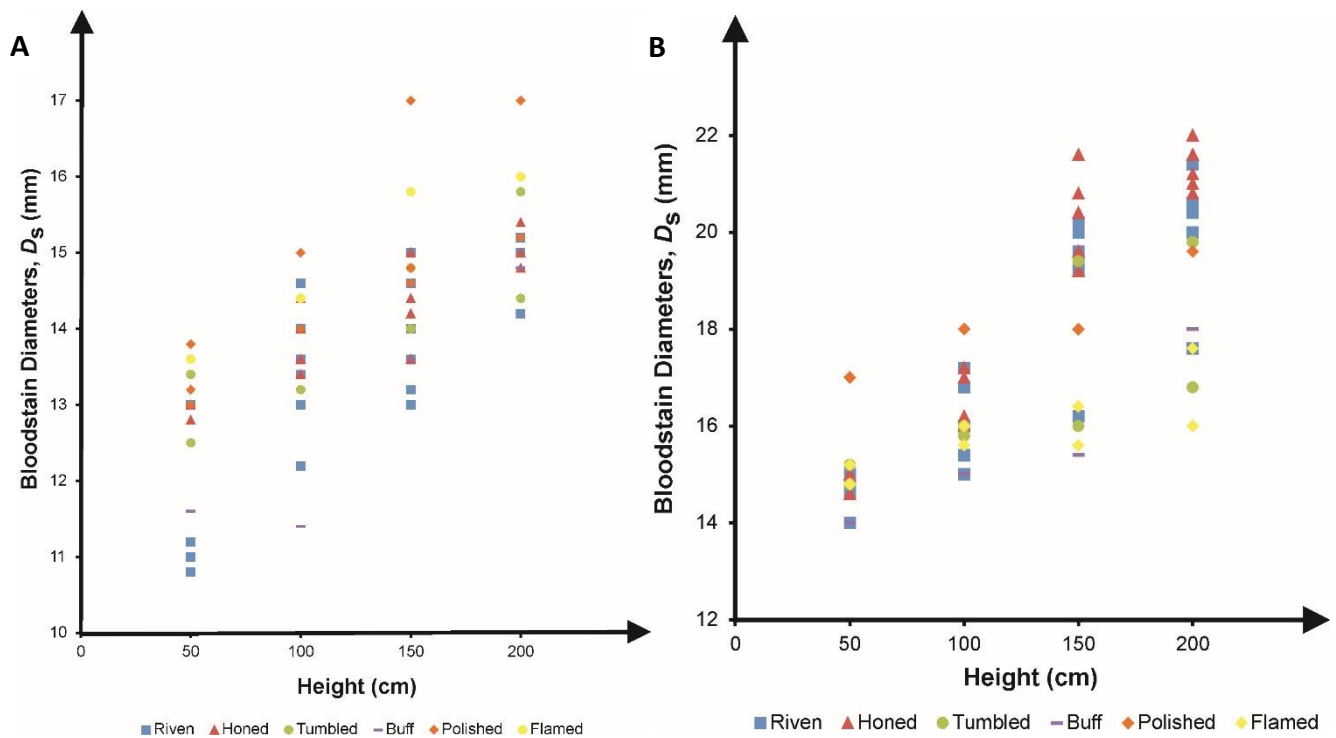
Figure 95: Bloodstain diameters on all stone types, categorised by surface finish, from various heights; 50 cm, 100 cm, 150 cm and 200 cm, using the A - mm pipette (inner tip diameter), B - 1.77 mm pipette (inner tip diameter), $N = 5$

Next surface finishes were analysed, expressed as Figure 95A and B, for a 1mm pipette and 1.77 mm pipette, respectively. Figure 95A shows riven finish produced the smaller bloodstains and polished/flamed exhibited larger bloodstains, since riven gives the rougher finish this result is expected. Again the 1.77mm pipette result did not mimic those found using the smaller pipette tip, where bloodstains are inter-mingled independent of their surface finish. Further supporting the conclusion that volume of blood has a marked effect on how blood interacts with a stone surface.
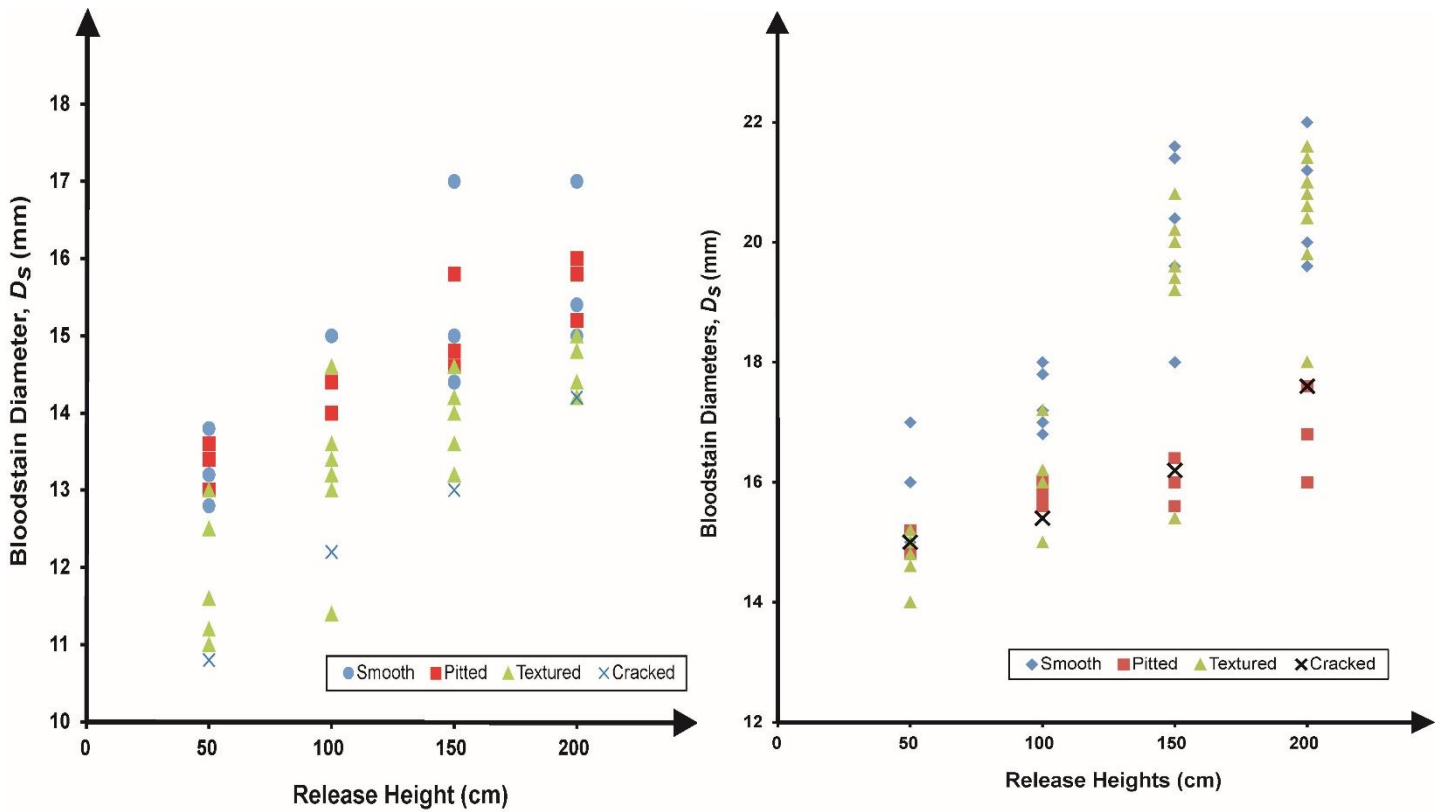
Figure 96: Bloodstain diameters on all stone types, categorised by surface characteristics, from various heights; 50 cm, 100 cm, 150 cm and 200 cm, using the A - mm pipette (inner tip diameter), B - 1.77 mm pipette (inner tip diameter), $N = 5$

Further analysis was performed, this time, comparing the surface characteristics of the stones against the bloodstain size. Surface were categorised into 4 characteristic types; smooth, pitted, textured and cracked (see Table 25), based on their physical appearance using SEM images. Results showed (Figures 96 A and B) that smooth surfaces produced larger bloodstains; this can be linked to the surface roughness. The other surface characteristics (pitted, cracked and textured) did not differ substantially from one another in the sizes of bloodstains they created.

Lastly, spread factors were considered (Figure 97). Reynolds numbers and spread factors were calculated using equations 1, 3 and 4 and plotted against one another. A line of 'best fit' was drawn onto the plot, were a new constant was derived for equation 4, where C_d equates to 1.16 which is substantially higher than that proposed by Hulse-Smith *et al*, where C_d equals 1.11.
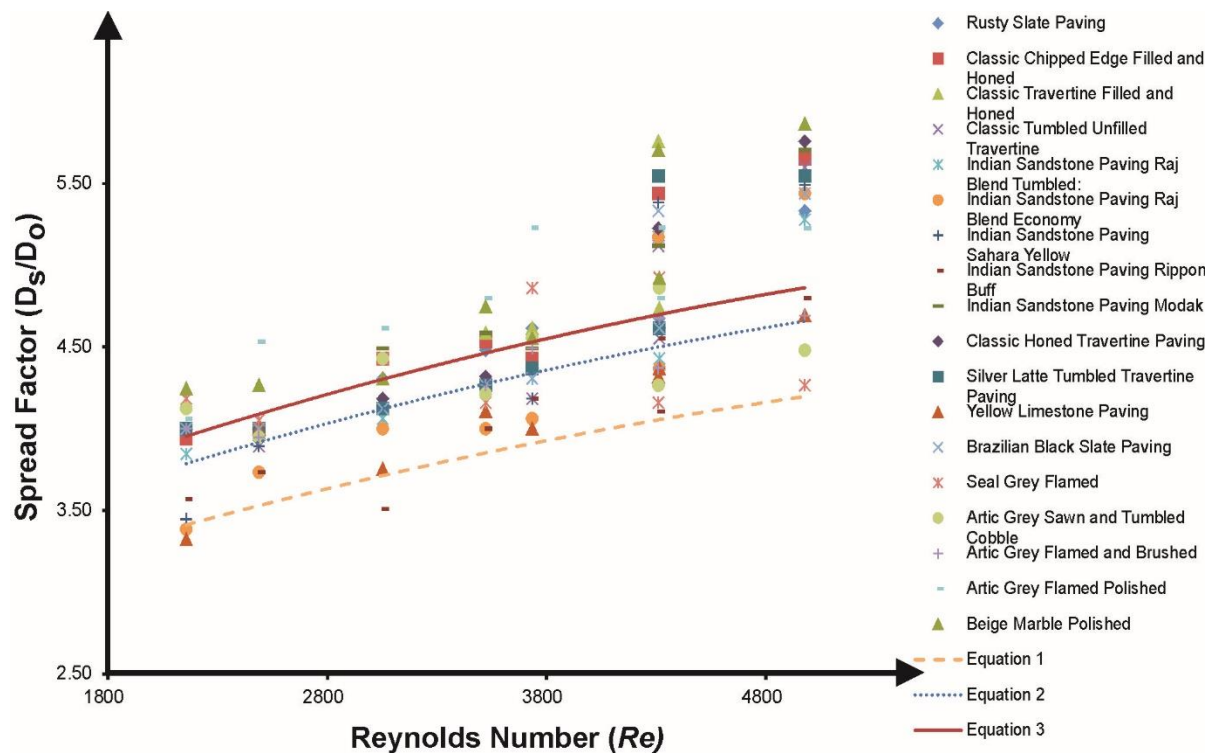
Figure 97: A new line of 'best fit' (solid line) was established considering the spread factor versus the Reynolds number on different stone surfaces. Comparing this to the original line of 'best fit' (dotted line) using equation (3) [18] and the line of 'best fit' (dashed line) developed by Hulse-Smith *et al* [18] using equation (4).

This new constant suggests that blood spreads further when stone surfaces are impacted, this can be attributed to the surface finish. Some surface finishes will cause the blood to spread due to the absorption qualities, where liquid is effectively carried along the surface rapidly spreading, similar to that exhibited on a fabric surface. Polished surfaces, where friction is minimal, will also have assisted in the spreading of the blood, since there is nothing present to stop it reaching until the first dry ring (coffee ring) is formed.

5.11.2.2 Bloodstain Diameter vs. Tile Surfaces

The second part of this experiment explored the use of tile as an impact surface. The same procedure was adhered to as above (stones).

Figures 98 and 99 express the results for blood impacting tile using a 1mm pipette and 1.77mm pipette, respectively.
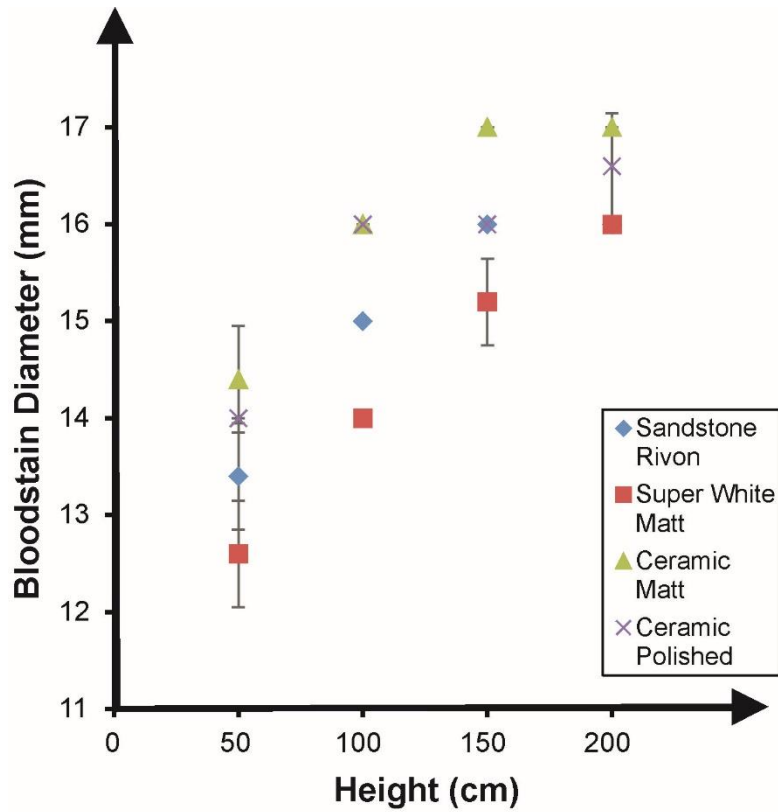
Figure 98: Bloodstain diameters on all tile surfaces from various heights; 50 cm, 100 cm, 150 cm and 200 cm, using the 1 mm pipette (inner tip diameter). $N = 5$
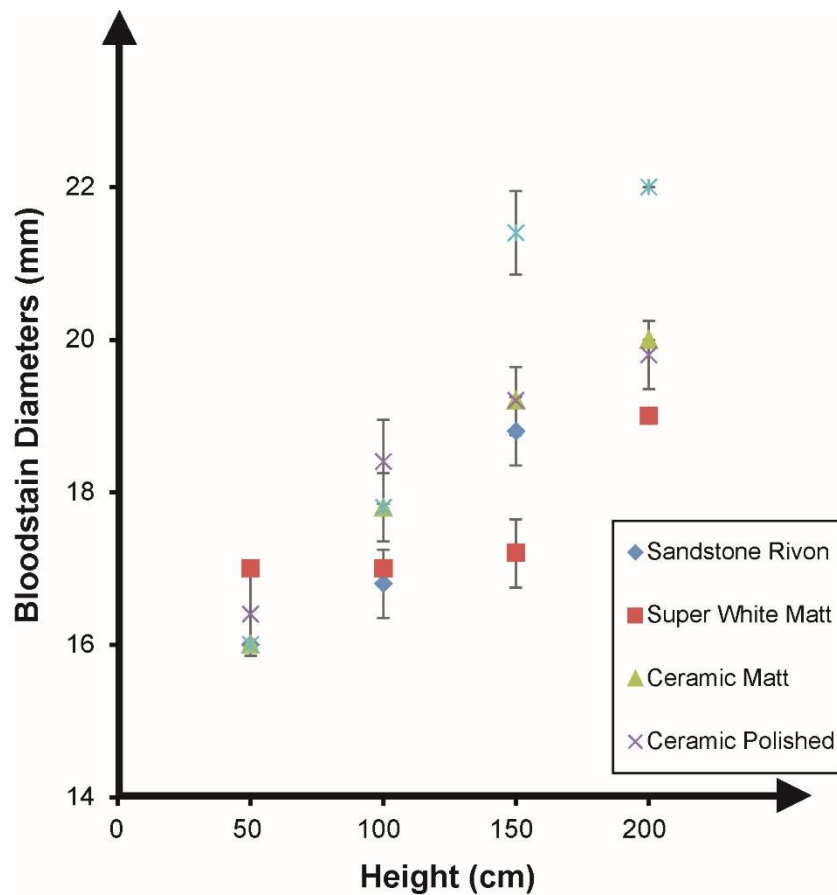
Figure 99: Bloodstain diameters on all tile surfaces from various heights; 50 cm, 100 cm, 150 cm and 200 cm, using the 1.77 mm pipette (inner tip diameter). $N = 5$

Figure 98 and 99 show that there is no distinct pattern emerging between the type of tile used and the bloodstain observed. Both figures express white matt tile (porcelain) as consistently producing the smallest bloodstains, comparing this to the table of characteristics (Table 25) it is evident that this tile is the roughest and therefore would be expected to produce smaller bloodstains than the others, due to the increased friction. Other bloodstain results appear to be random and do not follow a trend, either by finish or by type.
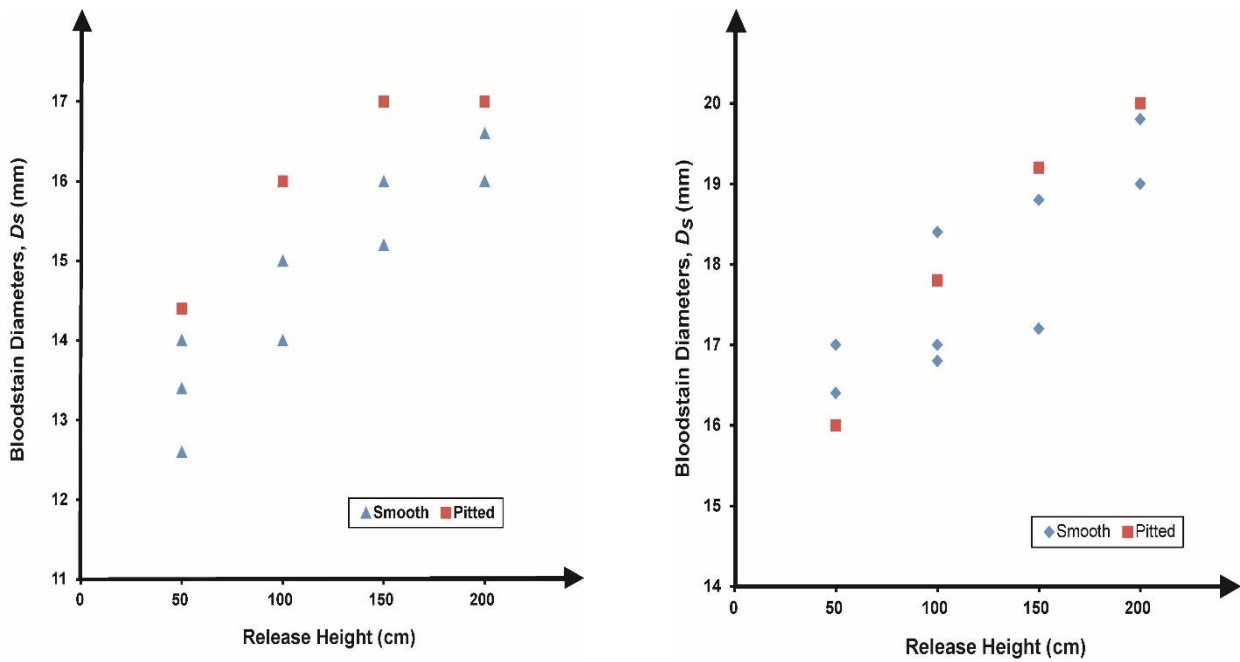
Figure 100: Bloodstain diameters on all tile types, categorised by surface characteristics, from various heights; 50 cm, 100 cm, 150 cm and 200 cm, using the A - mm pipette (inner tip diameter), B - 1.77 mm pipette (inner tip diameter), $N = 5$.

Again, surfaces were categorised into surface characteristics, pitted and smooth, depending on the SEM images produced. Figure 100 A depicts bloodstains produced on tile surfaces using a 1mL (1mm inner tip diameter), where pitted surfaces produced larger bloodstains. This is unexpected, since smoother surfaces would typically produce larger bloodstains, ordinarily attributed to the surface roughness. When this figure is compared to Figure 100 B it is clear that the volume of blood impacting the surface affects the size of the bloodstain and the way it interacts with the surface.
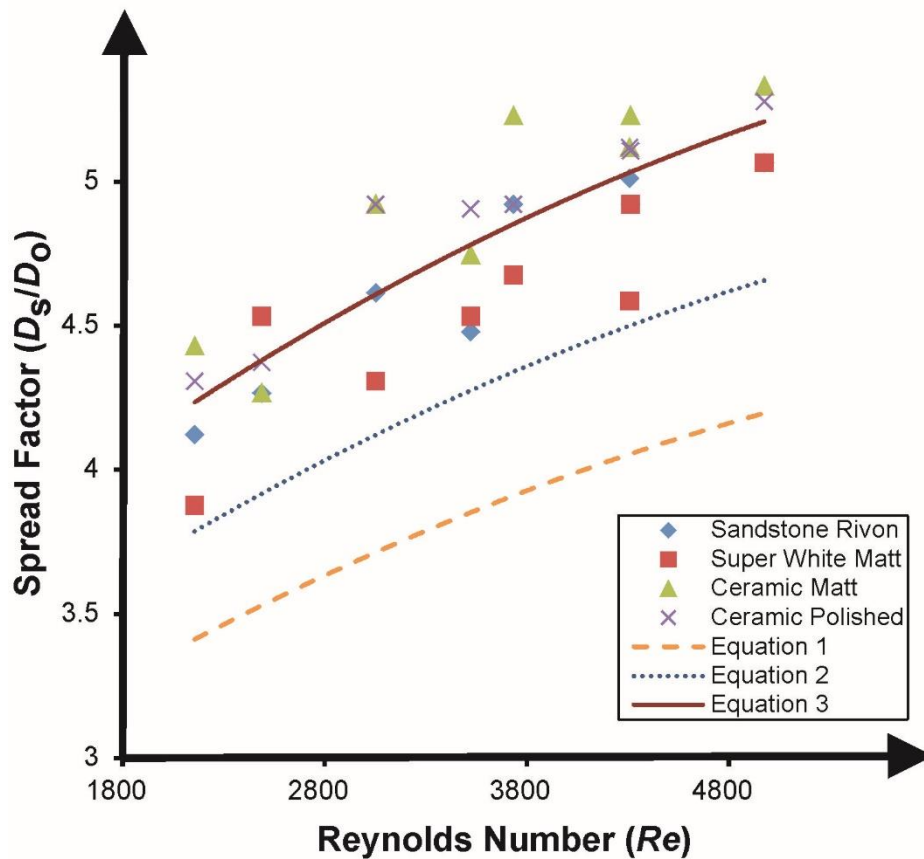
Figure 101: A new line of 'best fit' (solid line) was established considering the spread factor versus the Reynolds number on different tile surfaces. Comparing this to the original line of 'best fit' (dotted line) using equation (3) [18] and the line of 'best fit' (dashed line) developed by Hulse-Smith *et al* [18] using equation (4).

Lastly the spread factor constant (Figure 101) was calculated using the above method. A new constant equating to 1.24 was derived; again, this is considerably higher than that calculated by Hulse-Smith *et al.* [18] If this is compared to the Table 26, which lists the characteristics it is clear that roughness is the causative factor. Since the majority of the tile surfaces are much lower in roughness than the stones or surfaces used in the work by Hulse-Smith *et al* [18] the liquid is allowed to spread much further without any real resistance, therefore creating larger bloodstains.

5.11.3 Summary

Stone is an ancient material used for thousands of years to build and create art masterpieces, during this study, stone and tile have been investigated for their effects on the impact and spread of blood.

Blood was released onto various types of tile and stone surfaces from different heights and using two types of pipette. Results showed that roughness is a dominant factor in the determination of bloodstain size. This result can be altered however when volume of a blood drop is considered, where surface roughness in some instances was overcome allowing the bloodstain to spread farther. This observation is unique to this surface type, previous surfaces have followed the same trend regarding roughness dictating the stain size regardless of volume utilised.

Spread factors were considered, where the Reynolds number and spread factor were calculated using equations 3 and 4. A graph was plotted, where a new line of best fit was created, leading to the formulation of a new constant value for both stone and tile surfaces separately. Constant values of 1.16 and 1.24 were found for the stone and tile surfaces, respectively. Compared to the original value noted by Hulse - Smith et al [18] both of these values are substantially higher. This is again attributed to the surface roughness where absorptive and finish properties (i.e. polished – low friction) allowed blood to spread further than those surfaces used in the Hulse-Smith et al [18] study.

Since volume and surface porosity appear to be related further studies should be conducted to establish maximum levels of absorption in certain surfaces, like stone, so corrections can be made if deemed necessary.

5.12   CONCLUSION

The objective of this section was to explore the importance of surface interaction, focusing on surface characteristics and common surface types which are likely to be encountered at a crime scene.

Firstly general surfaces were investigated together, where blood drops were dispensed at different heights and angles on three surface types; paper, steel and plastic.

New equations were established, developing on the work conducted by Knock *et al* [17], where one surface type is used. Several equations had to be formulated since each surface was significantly different from the other; therefore, further work researching each surface alone was then conducted.

Four surface types were analysed (wood, stone and tile, metal and fabric), each with a diverse range of attributes and very different surface composition.

All surfaces were subject to analysis using SEMs and roughness measures to determine the topography of the surface. Blood drops tests were performed on each surface from 4 different heights and a range of angles, using two volume types of pipette to thoroughly investigate the effect on bloodstain patterns.

Equations were utilised to determine the degree of disruption caused when these surface types were employed. Reynolds numbers and spread factors were calculated to ascertain a constant, which could be compared to the constant derived by Hulse-Smith *et al,* equating to C_d 1.11.

Wood, stone, tile and fabric were found to deviate significantly from the original value (1.11), where constants were calculated to be 1.20, 1.16, 1.24 and 0.81 respectively, These results are largely attributed to the roughness and absorptive properties of the surfaces. Wood, stone and tile surfaces were finished using a range of methods, altering the natural porosity associated with these types of surfaces.

Volume, in some circumstances, altered the way blood spread across rough surfaces. Stone surfaces exhibited different results when different pipettes were used, where the volume seemed to overcome the surface roughness producing a larger bloodstain.

Overall all surfaces reacted differently to the impaction of blood, the overwhelming factor which dictated the size of stains in most surfaces was the surface roughness, though a standard surface roughness constant could not be found which encompassed all surfaces.

PART III:
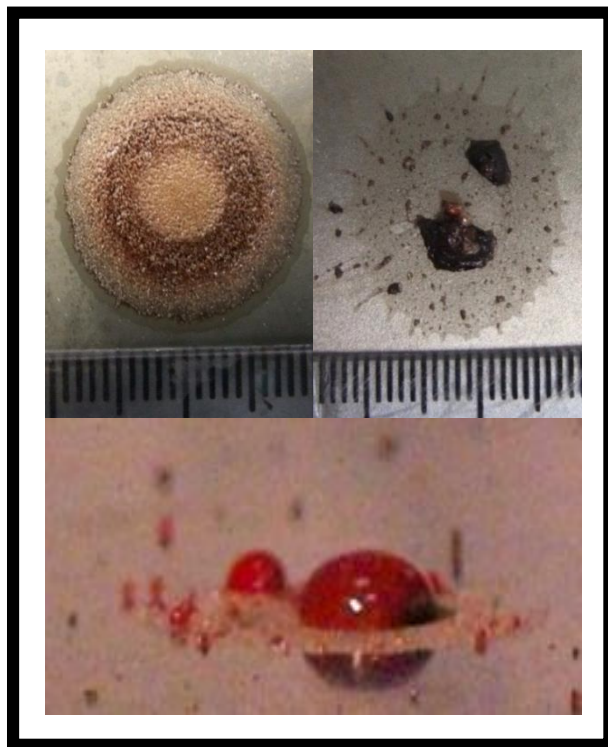
SURFACE MANIPULATION

5 MANIPULATING SURFACES

As aforementioned in section 1.6, surfaces can come in various conditions, either by natural forces (*i.e.* rust) or manipulation by people (*i.e.* polished). This chapter will investigate how we ourselves change the surface, since this has had little research conducted on it compared to environmental changes, which we cannot control.

5.1 HEATED SURFACES

Heated surfaces in the context of BPA have never been studied before (Section 1.6), since heated surfaces such as oven stoves, radiators or underfloor heating are present in crime scenes it seems any significant results could have a substantial effect on the way blood patterns are analysed. The following studies will investigate how various heated surfaces alter the spreading of impacting blood drops.

5.1.1 UNDERFLOOR HEATING

Although underfloor heating is thought to be a fairly recent home luxury the technique of heating the floor dates back thousands of years (5,000 BC), where people would draft smoke from fires through the stone covered trenches which were excavated in the floors of underground dwellings. [192 - 193] The smoke would heat the floor and subsequently the heat would radiate the room, warming the entire dwelling. Nowadays modern underfloor heating is provided by either fluid filled pipes or electrical cables. [192 - 193]

Electric underfloor heating - made up of a network of wires under the floor which can cover large areas. [194 - 196] The wires lie on top of a layer of insulation and are connected to the thermostat and mains power supply. Heating mats are also available, again comprising of a network of wires, this is often the cheaper option. [192 - 193]

Water underfloor heating – are comprised of a network of pipes which are connected to the boiler and pump hot water around the room. Since this system needs water to

be at a lower temperature than a radiator it is much more efficient and cost effective in the long term. [194 - 196]

Generally underfloor heating reaches temperatures of around 32ºC and has become a firm favourite in households due to its efficiency and the benefit of it being hidden so as to frees up wall space (unlike radiators) and leave clean lines of a room unspoiled therefore being the more aesthetically pleasing option. [194 - 196]

Underfloor heating can be used on a variety of surface types including: carpet, ceramic, vinyl, timber, laminate and marble.

5.2   UNDERFLOOR HEATING STUDY

The following study explores the effects of underfloor heating on the size and appearance of bloodstains. For this, a number of surfaces (stone paving, tiles and wood flooring) were investigated at various temperatures and bloodstain size and appearance were analysed.

5.2.1   Experimental

The blood utilised was human blood obtained from Manchester Royal Infirmary blood bank. Blood was measured at a PCV% of 37%, where viscosity equalled   5 mPa.s.

Blood drop tests were performed according to the method described in section (2.2). Drops were deposited on three different surface types: stone paving, tile and wood flooring, however a multitude of each surface type was utilised to provide a thorough representation of flooring.

Stone Paving – Travertine (Classic Tumbled Unfilled Travertine, Classic Honed Travertine Paving, Silver Latte Tumbled Travertine Paving Opus Pattern, Classic Travertine Filled and Honed, Classic Chipped Edge Filled and Honed Travertine Opus Pattern), Limestone (Yellow Limestone Paving), Sandstone (Indian Sandstone Paving Raj Blend Tumbled, Indian Sandstone Paving Raj Blend Economy, Indian Sandstone Paving Sahara Yellow Calibrated, Indian Sandstone Paving Rippon Buff, Indian Sandstone Paving Modak Calibrated), Slate (Brazilian Black Slate Paving and Rusty Slate Paving).

Tile - Porcelain (Sandstone Rivon Porcelain and Super White Matt Porcelain), Ceramic (Ceramic Matt and Ceramic Polished) and Beige Marble Polished

Wood Flooring – Oak (European Maple Oak, Clear Oil Oak, Oak Natural Siera Matt Lacquered, Oak Silk Matt, Kahrs Oak Sienna Natural, Natura Oak Prime Parquet, Kahrs Oak Siena Engineered Natural and Oak Solid Plank Untreated), Maple (Maple Silk Matt Lacquered, Kahrs Maple Toronto Satin Lacquer, Maple Ultra Matt Lacquered, Kahrs Maple Bevelled Edge Rustic and Kahrs Maple Natural Satin Lacquer) and Walnut (Natura American Black Walnut Rosshill, Natura Walnut Ironbank Mississippi, Quickstep Villa Walnut Satin Lacquer, Kahrs Walnut Rustic Nature Oil, Kahrs Linnea Walnut Bloom Prime Satin Lacquer, Kahrs Linnea Walnut Microbevelled Edge Prime Matt Lacquer and Natura Walnut Lacquered Satin Lacquer).

Drops were released from 30cm using the 1mm (inner tip) pipette. Surfaces were heated, to 25ºC, 30ºC and 40ºC; just above the maximum temperature of underfloor heating, using a hot plate and the temperature was monitored using an infra-red temperature gun. Surfaces were also monitored for the time taken to cool from maximum temperature to evaluate how long surfaces retain heat.

5.2.2   Results and Discussion

5.2.2.1   Heated Stone Surface

Figure 102 depicts the results when blood was dropped on heated stone surfaces, showing that for most surfaces the bloodstains decreased or increased in size but did not deviate much from the original value, when the surface was at room temperature. (see Appendix 9 for full data)
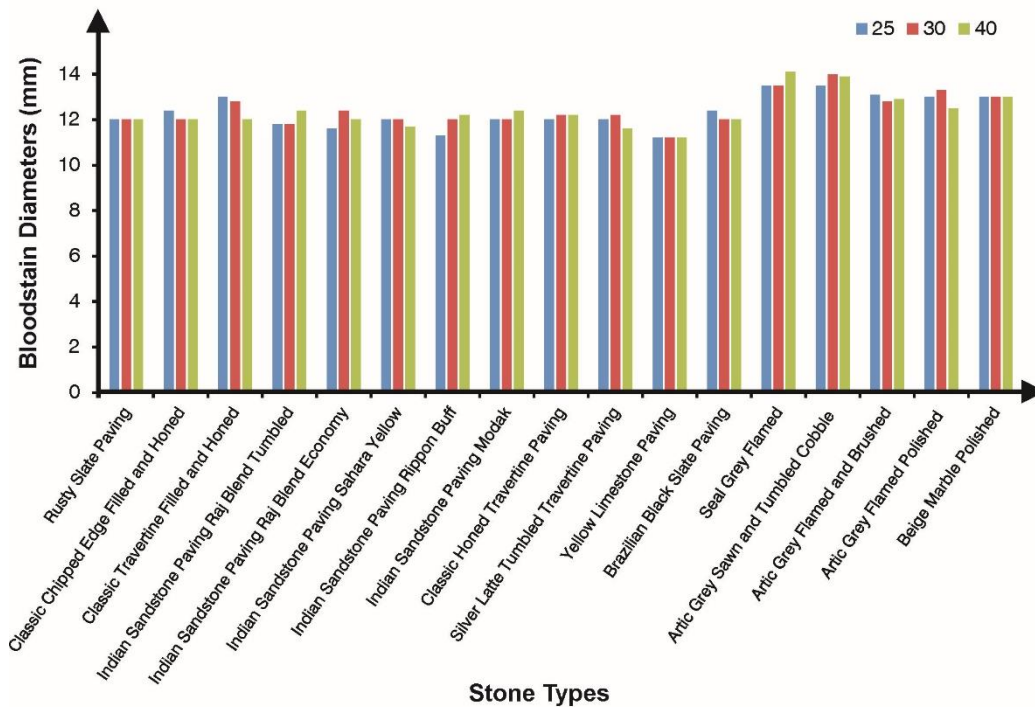
Figure 102: Representation of the effect of heated stone surfaces on the size of bloodstains

Stone Type	p value (25 vs 30)	Sign. Yes or no	p value (25 vs 40)	Sign. Yes or no
Rusty Slate Paving	1.000	x	1	x
Classic Chipped Edge Filled and Honed	0.141	x	0.1411	x
Classic Travertine Filled and Honed	0.347	x	0.0001	✓
Indian Sandstone Paving Raj Blend Tumbled	1.000	x	0.0598	x
Indian Sandstone Paving Raj Blend Economy	0.050	x	0.1411	x
Indian Sandstone Paving Sahara Yellow	1.000	x	0.172	x
Indian Sandstone Paving Rippon Buff	0.000	✓	0.005	✓
Indian Sandstone Paving Modak	1.000	x	0.1411	x
Classic Honed Travertine Paving	0.347	x	0.3466	x
Silver Latte Tumbled Travertine Paving	0.141	x	0.1411	x
Yellow Limestone Paving	1.000	x	1	x
Brazilian Black Slate Paving	0.141	x	0.1411	x
Seal Grey Flamed Granite	1.000	x	0.0431	✓
Artic Grey Sawn and Tumbled Cobble Granite	0.056	x	0.1411	x
Artic Grey Flamed and Brushed Granite	0.094	x	0.195	x
Artic Grey Flamed Polished Granite	0.040	✓	0.0001	✓

Table 26: Student t-tests were performed to attain the significance of the results obtained when the surface temperatures on stone surfaces are compared; 25°C vs. 30°C and 25°C vs. 40°C; $N = 5$.

Statistical analysis was performed to ascertain if the differences in diameter were significant. Unpaired student t-tests were calculated for each surface change (Table 26).

Results showed that temperature effected the Artic Grey Flamed Polished Granite and Indian Sandstone Paving Ripon Buff, significantly changing the bloodstain diameter during both temperature steps. A possible explanation for temperatures effect on only these two surfaces is the finish; both were finished with a type of polish. Though there was found to be no effect when marble type surfaces were analysed, which exhibited a similar finish. Since Artic Grey Flamed Polished Granite and Indian Sandstone Paving Ripon Buff were finished on one side, it is possible that the temperature on the surface did not reflect the actual temperature of the stone at the bottom and within the structure, therefore there could be a delay or enhancement of heat transfer, explaining the erroneous results.

5.2.2.2 Heated Tile Surface

Tiles were analysed next (Figure 103); statistical analysis was employed to establish the significance of the results.
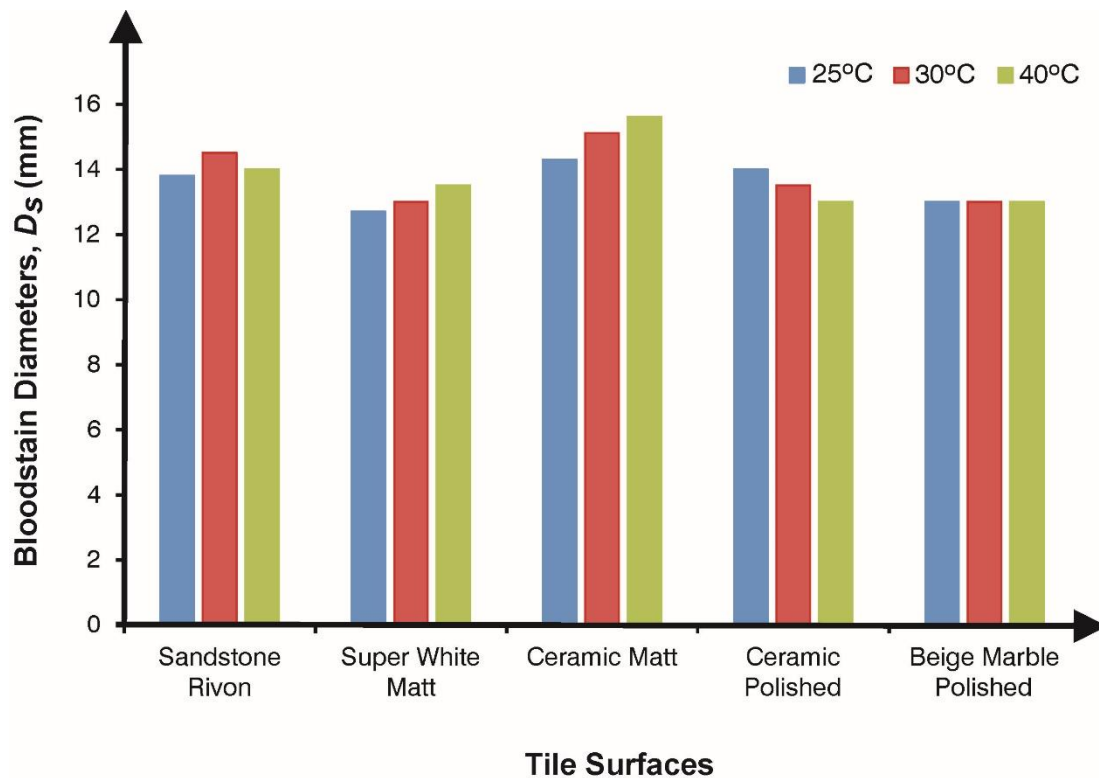
Figure 103: Bloodstain diameters results when blood drops have impacted heated tile surfaces.

Ceramics (matt and polished) were found to change significantly at both temperature intervals (25 vs 30 and 25 vs 40) (Table 27), though both reacted differently. Ceramic polish tile bloodstain diameters decreased as temperature increased, this could be a result of the difference in roughness at the top and bottom of the tile, the bottom being rougher, thus creating a lesser heat transfer leading to smaller stains. Larger stains would be expected as heat decreases the viscosity and therefore liquid would flow more freely, resulting in the production of large stains.

Tile Type	p value (25 vs 30)	Sign. Yes or no	p value (25 vs 40)	Sign. Yes or no
Sandstone Rivon	0.000	✓	0.347	X
Super White Matt	0.172	X	0.004	✓
Ceramic Matt	0.007	✓	0.002	✓
Ceramic Polished	0.000	✓	0.000	✓
Beige Marble Polished	1.000	X	1.000	X

Table 27: Student t-tests were performed to attain the significance of the results obtained when the surface temperatures on tile surfaces are compared; 25°C vs. 30°C and 25°C vs. 40°C; $N = 5$.

Conversely ceramic matt tile bloodstain diameters increased as temperature increased, due in part to the increase in viscosity but could also be attributed to the surface finish. The super white matt tile behaved in a similar way to the ceramic matt tile (increasing), surface finish is the most probable cause of the bloodstain diameter change, since the SEMS characterised (Table 25) the two tile as different (smooth vs. divots). Rougher surfaces hold and transfer heat more efficiently than smoother polished surfaces which reflect heat. The surface finish and decrease in viscosity of blood would then work in tandem to produce larger stains.

5.2.2.3   Heated Wood Surface

Lastly heated wood surfaces were investigated.
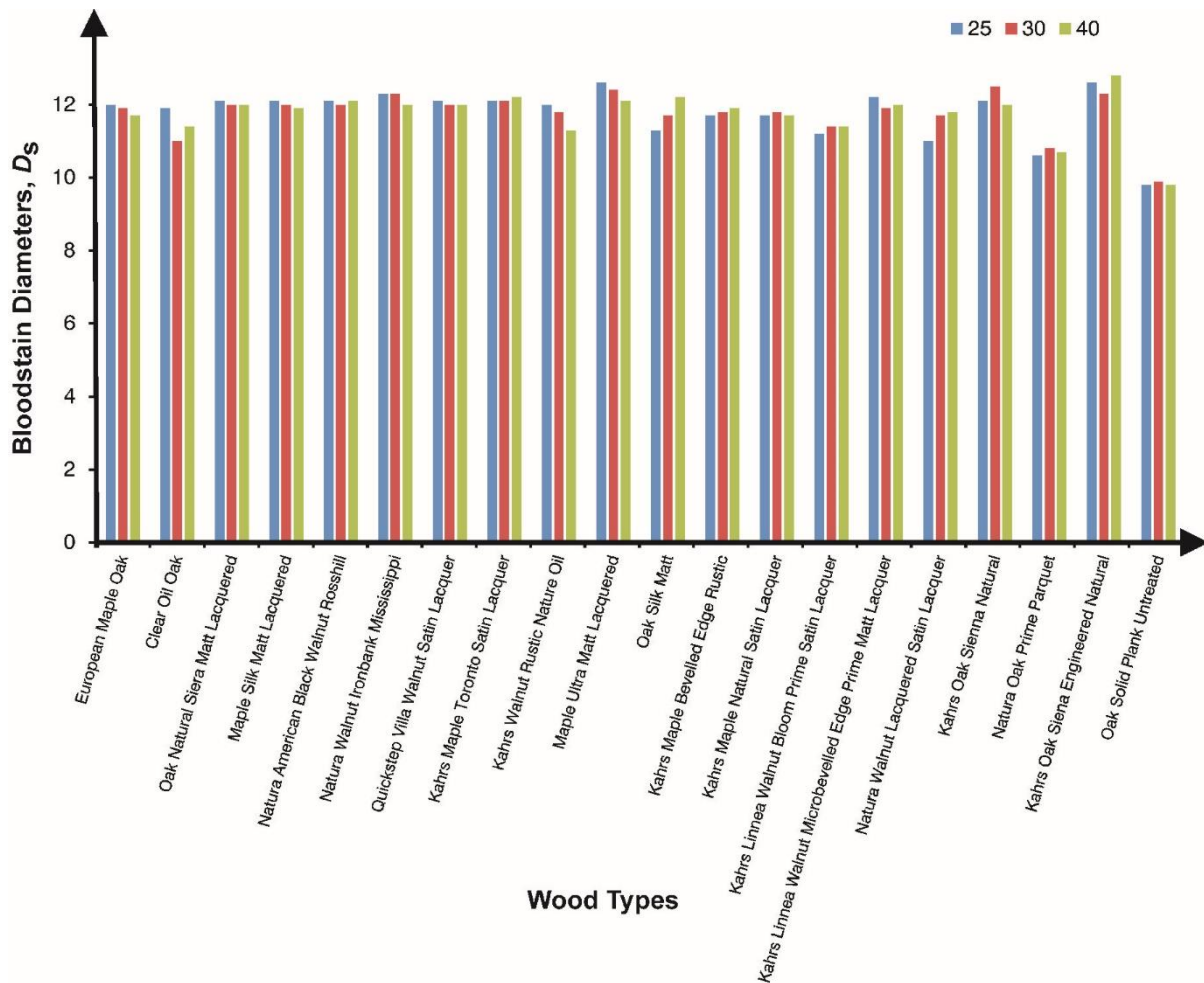
Figure 104: A depiction of bloodstain diameter results which have impacted 20 different heated wood surfaces.

Only 3 surfaces altered the bloodstain size significantly (Table 28) when the temperature was increased to 30°C; Clear Oil Oak, Natura Walnut Lacquered Satin Lacquer and Kahrs Oak Sienna Natural. (Figure 104) At 40°C surface temperature wood displayed further significant changes in diameter, though the surface does not ordinarily reach such a high temperature when underfloor heating is utilised. The 40°C temperature was used to give an indication when possible changes may occur as a frame of reference. These results have no discernible pattern and cannot be explained, none of the surfaces effected at 30°C are finished, graded, typed, manufactured or characterised (via SEM) the same.

Wood Type	p value (25 vs 30)	Sign. Yes or no	p value (25 vs 40)	Sign. Yes or no
European Maple Oak	0.347	X	0.040	✓
Clear Oil Oak	0	✓	0.008	✓
Oak Natural Siera Matt Lacquered	0.347	X	0.347	X
Maple Silk Matt Lacquered	0.347	X	0.195	X
Natura American Black Walnut Rosshill	0.347	X	1.000	X
Natura Walnut Ironbank Mississippi	1.000	X	0.040	✓
Quickstep Villa Walnut Satin Lacquer	0.347	X	0.347	X
Kahrs Maple Toronto Satin Lacquer	1.000	X	0.545	X
Kahrs Walnut Rustic Nature Oil	0.141	X	0.000	✓
Maple Ultra Matt Lacquered	0.195	X	0.008	✓
Oak Silk Matt	0.050	X	0.001	✓
Kahrs Maple Bevelled Edge Rustic	0.580	X	0.242	X
Kahrs Maple Natural Satin Lacquer	0.580	X	1.000	X
Kahrs Linnea Walnut Bloom Prime Satin Lacquer	0.242	X	0.242	X
Kahrs Linnea Walnut Microbevelled Edge Prime Matt Lacquer	0.094	X	0.141	X
Natura Walnut Lacquered Satin Lacquer	0.008	✓	0.004	✓
Kahrs Oak Sienna Natural	0.004	✓	0.347	X
Natura Oak Prime Parquet	0.397	X	0.724	X
Kahrs Oak Siena Engineered Natural	0.371	X	0.486	X
Oak Solid Plank Untreated	0.545	X	1.000	X

Table 28: Student t-tests were performed to attain the significance of the results obtained when surface temperatures on wood surfaces are compared; 25°C vs. 30°C and 25°C vs. 40°C; $N = 5$.

Overall underfloor heating in most instances does not significantly affect the size of the bloodstains produced. However this can depend heavily on the type of floor used *i.e.* ceramic, and the finish (polished) incorporated.

5.2.2.4   Bloodstain Observations

Although the diameter of bloodstains was found not to significantly alter general observations proved more insightful. Bloodstains appeared darker as temperature increased (Figure 105), since recent developments in determining the age of bloodstains are reliant on the colorimetry the heating of a bloodstain could effectively artificially age the bloodstain giving an inaccurate time frame. [197 – 199] Some preliminary age analysis was performed on the bloodstains to determine if the above statement was true / false.
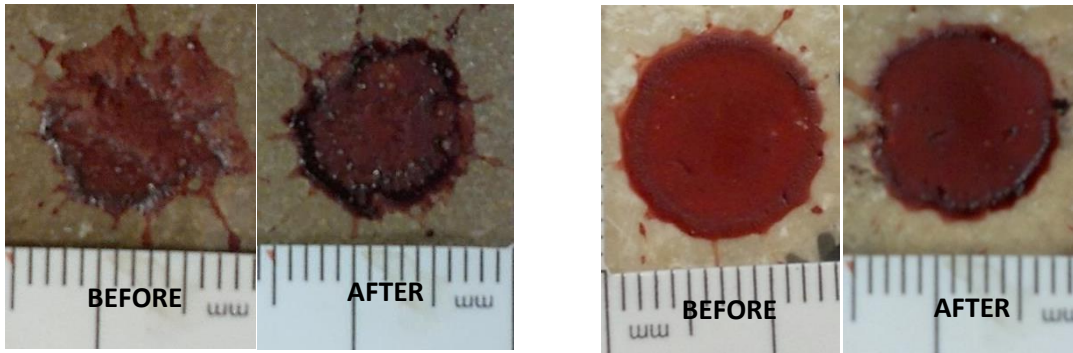
Figure 105: Bloodstains showing the effect of heated surfaces on the appearance of the bloodstain, where before depicts blood on a surface at room temperature and after shows bloodstains which have impacted a heated surface (40°C).

Three surfaces were examined: granite, porcelain tile and ceramic tile. Blood was deposited onto each surface heated to various temperatures (room, 30°C and 40°C) and change in light intensity was monitored using a portable spectrophotometer Spectruino.

Figures 106 - 108 show that there is an increase in light intensity when bloodstains, formed on higher surface temperatures, were analysed. This is identical to what is believed to happen as blood ages, the blood changes colour, darkening as the blood is deoxygenated when exposed to air; the addition of heat mimics this behaviour.
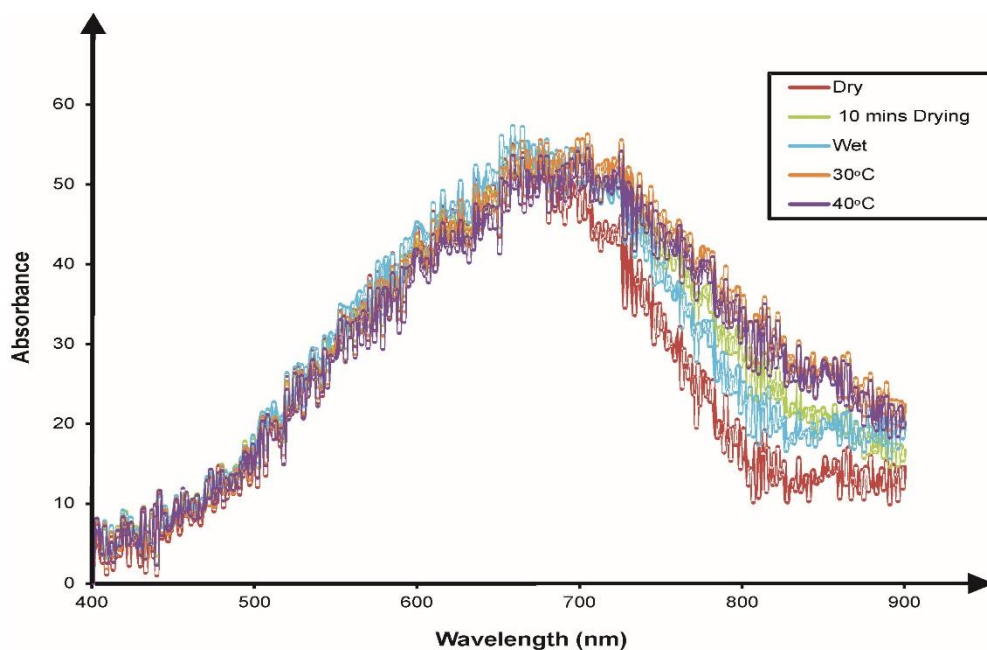
Figure 106: Spectrum depicting the increase in absorbance as the bloodstain is heated on a porcelain surface
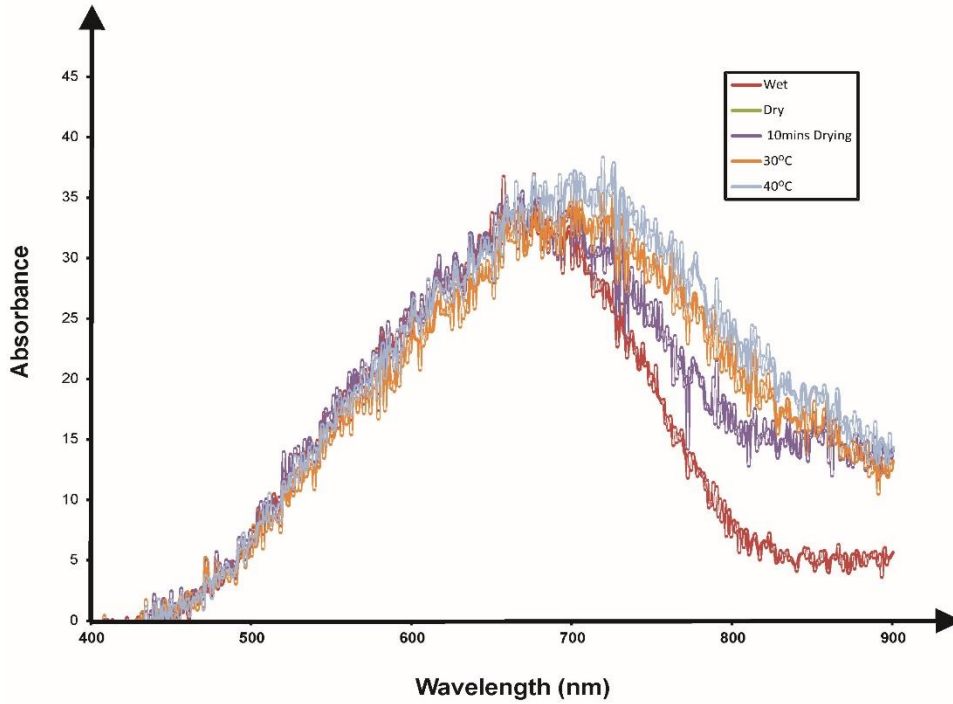
Figure   107:
Spectrum depicting the increase in absorbance as the bloodstain is heated on a granite surface
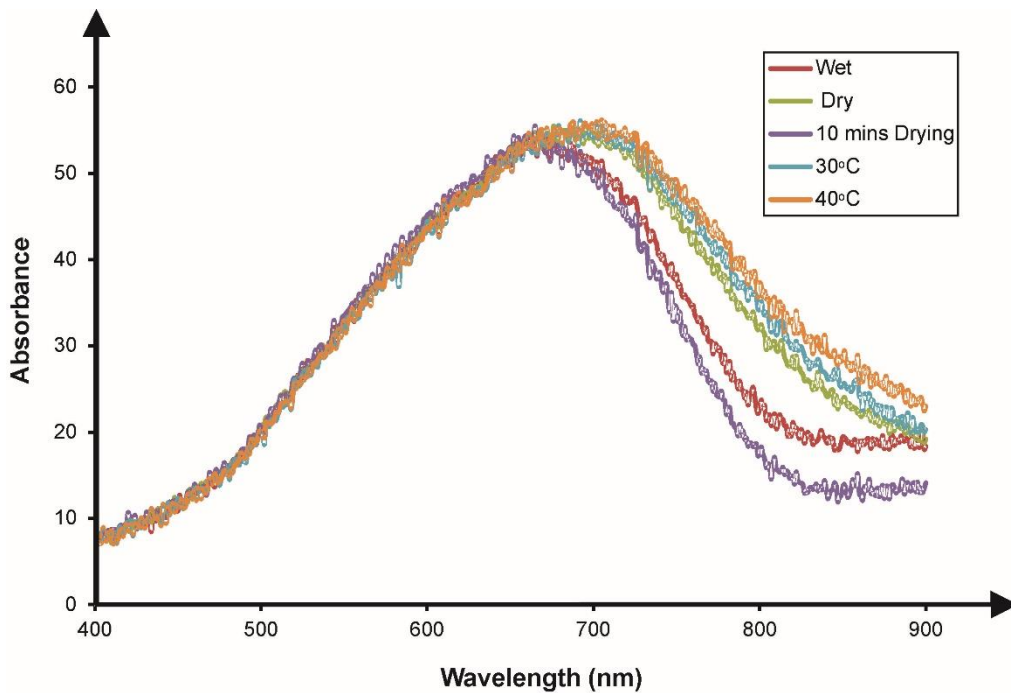
Figure 108: Spectrum depicting the increase in absorbance as the bloodstain is heated on a tile surface

Unpaired student t-tests were performed, where entire data sets were compared against one another to determine significance. Tables (29 - 31) express the results obtained from the statistical analysis. Fresh refers to blood when it was deposited onto

the surface (not heated), fresh drying is blood after initial drying has begun (monitored by drying on the edge of the stain), around 10 minutes and dried is when blood has fully dried, this is the most important comparison as it is the one analysts will be expected to encounter at scenes of crime.

State of Blood (surface not heated)	30°C	40°C
Fresh Drying	0.622	0.161
Fresh	0.002	0.000
Dried	0.002	0.000

Table 29: Results for student t-tests of spectrophotometry results for bloodstains on a ceramic tile surface.

State of Blood (surface not heated)	30°C	40°C
Fresh Drying	0.109	0.000
Fresh	0.086	0.459
Dried	0.109	0.541

Table 30: Results for student t-tests of spectrophotometry results for bloodstains on a porcelain surface.

Table 31: Results for student t-tests of

State of Blood (surface not heated)	30°C	40°C
Fresh Drying	0.627	0.008
Fresh	0.000	0.00
Dried	0.001	0.00

spectrophotometry results for bloodstains on a granite surface.

Statistical analysis reveals that the changes in light intensity are significant when comparing the most important factor, fully dried blood, for two of the three surfaces. As the porcelain is a darker and less reflective surface (matt finish) than the ceramic and granite surface, which exhibit polished finishes and are white and light grey in colour, respectively. This outcome is not unexpected as currently research into the aging of blood using shifts in light intensity has only successfully tested bright highly reflective surfaces. [197 – 199]

The preliminary analysis performed here indicates that temperature does have a significant effect on bloodstains, aging them prematurely. This insight is important and should be analysed further to determine the extent to which heated bloodstains mimic aged blood.

5.2.3 Summary

The effect of underfloor heating on three floor types has been examined; tile, wood and stone. Bloodstain diameters were demonstrated to increase in size as surface temperature increased. This is due to the known effect temperature has on viscosity, where viscosity increases as temperature increases, therefore allowing the blood to spread and flow further on the surface. Though the results did not show a conclusive pattern, it is believed that surface finish is the overriding factor, since rougher surfaces retain heat.

Observations revealed that the bloodstain darkens as temperature increases. Further analysis was performed using a spectrophotometer to evaluate light intensity and results were compared to recent research used to determine age of bloodstains. The data was found to correlate, leading to the conclusion that temperature prematurely ages the blood, therefore mimicking an old bloodstain. [197 – 199] *This conclusion is important as the technique for evaluating the age of a bloodstain is in its early stages and therefore needs to consider such circumstances whilst developing the method.*

5.3   COMMON HEATED SURFACES

There are a multitude of hot surfaces which could be present at crime scenes, *i.e.* stoves, radiators etc. [200 - 203] These surfaces can reach temperatures much higher than that of underfloor heating and would therefore be expected to exhibit different results. Presently it is unknown how higher temperatures will effect impacting blood (section 1.6), as currently only the data is available referring to the effects of fire.

Common heated surfaces found in the home: [200 - 203]

Radiators – are a modern appliance used to radiate heat throughout a room. There are six types of radiators: steam, cast iron, hot water, heat convectors, electric convectors, and baseboard heaters. Heat is produced either by steam or heated water connected to the boiler. [200]

Oven Stove – oven stoves (hobs), used for cooking, are often made from metal, ceramic etc. The hobs themselves can reach temperatures above 200ºC. [201]

Kitchen Splashbacks – installed around the oven stove, it protects the underlying wall from oil, grease and heat. [202]

Fireplace – the fireplace trim and mantel can be constructed from brass, copper *etc.* [203]

5.4   HEATED METAL STUDY

This study investigates the effects of heated surfaces on Bloodstain Pattern Analysis, where temperatures reaching 250ºC were employed. The boiling curve for water was investigated and modified accordingly to fit impacting blood.

5.4.1   Experimental

Only steel (0.54 µm R_a) was used for this investigation. The steel was heated to temperatures of 40 - 250° C using a furnace; temperatures were maintained during the drop process by the use of a hot plate placed underneath the metal plate and monitored using a infra-red temperature gun. The steel was also sand blasted to

create a different surface roughness which was calculated to give an average R_a value of 0.89 μm.

Results and Discussion

Effect of temperature upon the bloodstain diameter, D_s

Depicted in Figure 109 is a typical boiling curve for water at 1 atm (atmosphere) which shows the effect of surface heat flux as a function of excess temperature, expressed by $\Delta T = T_w - T_{sat}$ (^{o} C) where T_w is the surface temperature and T_{sat} is the saturation temperature as defined by the Clausius - Clapeyron equation, [62] in the case of water T_{sat} is equal to 100°C.
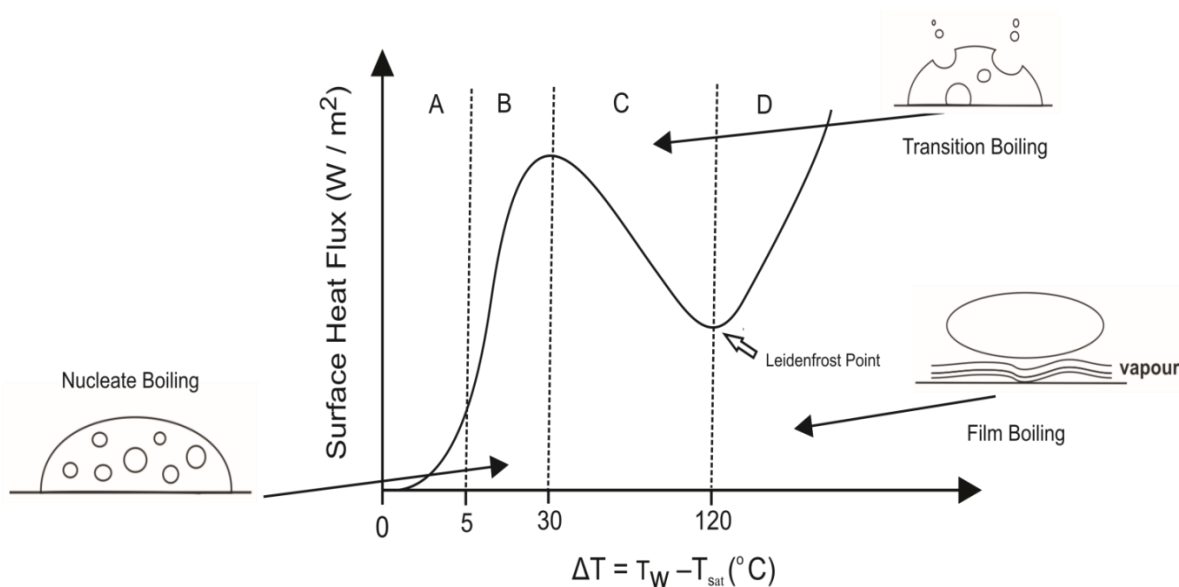
Figure 109: A typical boiling curve highlighting the boiling regimes for water; A: natural convection (around room temperature), B: nucleation boiling regime, C: transition boiling regime and D: film boiling regime.

The boiling curve for water (Figure 109) shows the four well-known regimes which correspond to A) natural convection, B) nucleation boiling, C) transition boiling and D) film boiling regime. [62] Note the Leidenfrost point and beyond this region the Leidenfrost Effect occurs (see section 1.5). This boiling curve was used to interpret the different temperatures that blood is exposed to when impacting and encountering heated surfaces.

Firstly the size of bloodstains (D_s) was considered, blood was released from heights onto cold rolled steel which has been heated to temperatures between 24 - 250° C, pertaining to previously identified boiling regimes; [62] (see Figure 109).
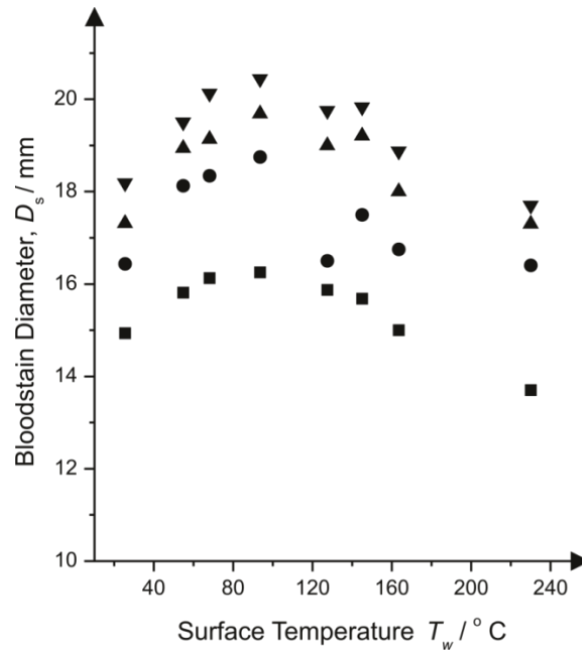
Figure 110: Effect of bloodstain diameters (D$_s$) for equine blood released onto cold rolled steel held at a range of temperatures and released from a range of heights; 30.5 cm (squares ■), 60.9 cm (circles ●), 91.4 cm (triangles ▲), 121.9 cm (upside-down triangles ▼) using a 1 mL pipette (inner tip diameter 1.77 mm). Note that at each surface temperature, each data point is an average of 20 blood drops (N= 20).

Figure 110 depicts the analysis of the observed bloodstain diameter (D$_s$) upon impacting surface temperatures released from a range of heights where a noticeable pattern is evident, where the bloodstain diameter (D$_s$) was observed to initially increase, which then starts to decrease when the boiling point of blood is approached, assumed to occur at 100°C. Beyond this point the bloodstain diameter was observed to reduce as the surface temperature was increased up to 230°C. The observations in Figure 110 were interpreted in terms of the blood drop expanding due to the addition of heat, which likely arises due to the dependence of viscosity versus temperature, such that up to the boiling point of blood, an increase in D$_s$ is observed (Figure 110). Beyond this point, D$_s$ decreases with temperature, likely due to evaporation being the overriding parameter evaporating the water component of blood. Since blood is comprised of approximately 83% water, [204] the maximum boiling point should theoretically be similar to that of water or very close.

Blood Impacts in the Natural Convection Regime
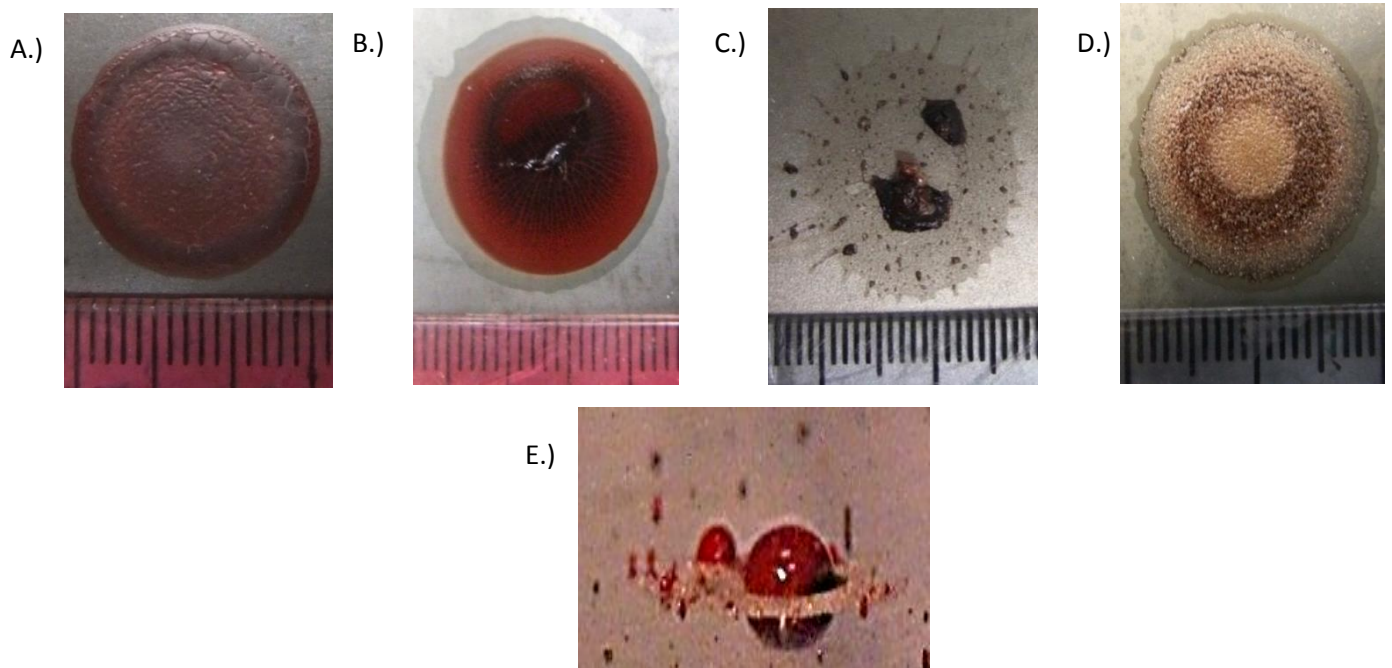
Figure 111: Images of 4.2 mm (D_o) blood droplets impacting upon a horizontal steel surface held over a range of temperature parameters; A: Room temperature (24°C), B: 60°C, C: 100°C, D: 140°C and E: 230°C.

This regime, shown as section (A) on Figure 111, involves natural heat flow and temperatures of around 24°C (room temperature) and just below the boiling point of blood. [59] As shown in Figure 110, the effect of the overall diameters were at their most substantial when in the natural convection regime (see section 1.6) before any form of significant evaporation transpires. It was acknowledged that there appears to be a clear reduction in bloodstain diameter D_s from the initial impact of the droplet to when it is dry, leaving a "doughnut" type shape bloodstain, as depicted in Figure 111B, this effect occurs when temperatures are of 50°C $\leq T_w$ and at room temperature (see Figure 110A). Further investigation into this reduction was performed, by centrifuging the blood separating it into serum and red blood cells, and individually dropping them onto the cold rolled steel (Figure 112A and B). As shown in Figure 112, it is evident that a separation of the blood into serum and red blood cells creates this perceived reduction; the red blood cells collect in the centre of the bloodstain thus creating a hardened bubble when completely dry, with the serum generating the visible outer ring.
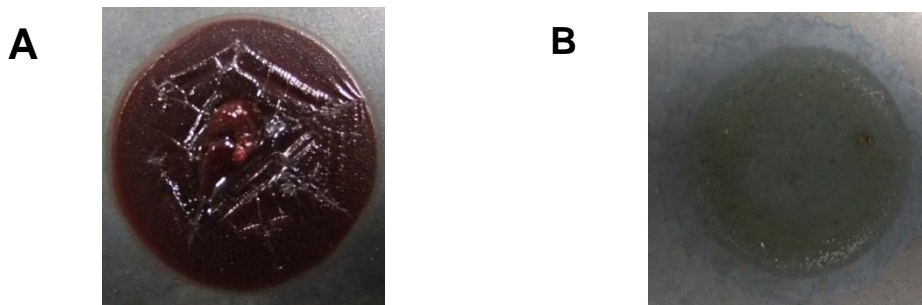
Figure 112: Image of blood impacting a cold rolled steel surface which has been heated to 60° (T_w = 60° C) following the centrifuging of the blood and individually dropping both resultant components. Parameters: 30.5 cm release drop height; A: red blood cells and B: serum.

The observed reduction of the bloodstain D_s is uniform in its shape and is typically from 2.14 to 3.625 mm in size (width of the secondary ring) with temperatures over the range of 50 to 85° C respectively. This observation is termed the "secondary ring."

Hence, when T_w (surface temperature) is above 50° C and below the blood boiling point (100°C) the equation can now be written as:

$$\left(\frac{D_s}{D_o}\right)_{T_w} = C_d^{heated} \frac{Re^{0.25}}{2}$$

(28)

A new constant representing all of the data for surface temperatures of 50 to 85° C, when this secondary ring is observed was developed where C_d [heated] the inner bloodstain equals 0.97. Such a value is similar to 1.11 reported previously. [18]

Further analysis requiring capturing camera footage of the blood drop impacting and subsequently evaporating on the heated steel was employed, allowing calculations of the evaporation rate, K, formulated using the equation below: [59]

$$-\frac{dD_s^2}{dt} = K$$

(29)

where D_s is the diameter of the bloodstain, t is the time and K is the evaporation coefficient, which remains approximately constant when considering larger drops (300 μm and above). [205] The average evaporation rate, K, acquired at temperatures of 80° C, when the reduction of the first ring is most prominent, was found to correspond to 0.3 mm^{2}s^{-1}.

Blood Impacts in the Nucleation Boiling Regime

Figure 111C depicts a typical bloodstain diameter (D_s) that is in the nucleation boiling regime (see Fig 109), occurring at temperatures of 90 – 120° C. In this regime the overall diameters were decreased as evaporation ensued due to the realisation of the maximum boiling point at 100°C. Similarly to the natural convection regime, there was a clear reduction followed by a series of uniform rings. Initial velocity, V_o predetermines the number of rings the bloodstain encompasses, the greater the initial velocity, V_o and therefore the higher the release height is, the greater number of rings are observed this is due to the increase in bloodstain diameter size; heights of 121.9 cm and 91.4 cm produce 5 distinct rings compared to only 4 and 3 rings observed at heights of 60.9 cm and 30.5 cm respectively. The production of the rings can be explained when the falling and successive splashing of the blood drop is observed as it contacts the solid horizontal surface, there is a development of uniform capillary waves / rings as the drop strikes and settles on the surface. It is evident that the inner and outer ring impact the surface first and the middle ring follows later; the inner and outer ring vaporize instantaneously as they touch the surface pushing the majority of the red blood cells to the middle layer, explaining the darker appearance of the central ring and increased vaporisation time. When drops at lower temperatures were compared the drop impacts the surface similarly, however due to the lower temperature instant vaporisation does not ensue and therefore the drop dries and evaporates uniformly. This regime is one of the most important when considering blood pattern recognition. During the nucleation regime bubbles form in the liquid, this is reminiscent of the vacuoles present when blood is expirated. This is an important insight since heated blood could be mistaken as expirated blood, which is vital when determining useful patterns at a crime scene.

Blood Impacts in the Transition Boiling Regime

Further decline in bloodstain diameter (D_s) was observed due to the rapid evaporation experienced at the higher temperatures (120°C - 230°C). A significant alteration in the appearance of the final bloodstain (D_s) was observed, depicted in Figure 111D where sporadically hardened red blood cells within the serum stain are all that remain. The blood drop vaporizes the instant it contacts the surface, driving the red blood cells to the centre of the bloodstain; evaporation starts on the periphery of the bloodstain and

gravitates to the centre, withdrawing the entirety of water within the bloodstain. This type of bloodstain in particular would be difficult to unearth at a crime scene, the hardened red blood cells on top of the stain are fragile and can be removed by a gentle breeze/flow of air, the serum stain may prove difficult to detect depending on the surface colour it impinges.

Blood Impacts in the Film Boiling Regime

During the film boiling regime the Leidenfrost effect occurs, the Leidenfrost effect is when the surface temperature is significantly hotter than the liquid's boiling point, in this case the blood's boiling point (120° C ≤ ΔT). When the blood drop strikes the surface a layer of vapour between the blood and the contact surface developed preventing instantaneous evaporation therefore the blood skated across the surface, depicted in Figure 111E. The appearance of the bloodstains in the film boiling regime is not significantly different from that displayed in the transition regime where a hard inner circle of red blood cells and a surrounding ring of vaporised serum are formed. However there was a loss in bloodstain shape; the stain became distorted due to the explosion and initial vaporisation when the droplet impacted the extremely hot surface.
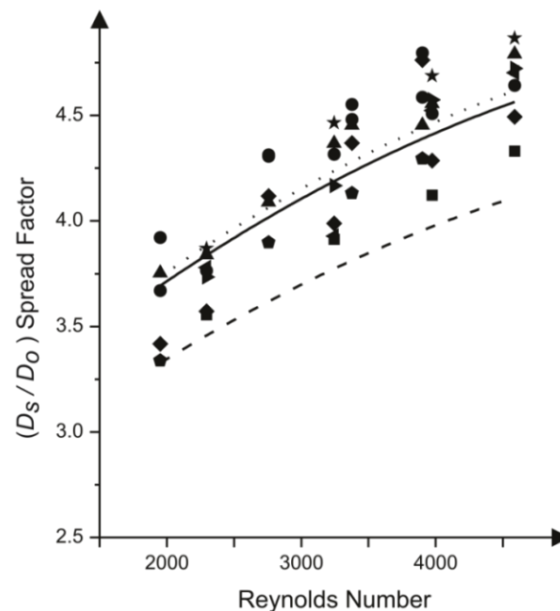
Figure 113: The effect of various surface (cold rolled steel) temperatures over the range of 24 - 250° C (25.5 (diamond), 54.75 (pentagon), 68 (triangle), 93.5 (star) 127.5 (upside down triangle), 145 (sideways triangle), 163.5 (circle), 230 (square)) upon equine blood released from different heights, in terms of the spread factor (D_s / D_o) as a function of the Reynolds Number. Three best fit lines were used: Dashed line produced using equation (3); Dotted line developed by Hulse - Smith et al [18] using equation (4); a solid line, new line of best fit created purposefully for this data spread. Note that in each case each data point is an average of 20 blood drops (N= 20).

Although there was a significant difference between bloodstains D_s, when all the data (*i.e.* all initial bloodstain diameters for each temperature) is transfigured into the spread factor (D_s / D_o), it was evident that there is actually little difference and the temperature has no significant effect on the general scatter spread. Figure 113 highlights this using lines of 'best fit' created by utilising previously defined equations and therefore establishing a new constant of for C_d ^{heated} corresponding to 1.12, which is not dissimilar to the original value of 1.11 observed by Hulse- Smith *et al* .[18]

Effect of temperature upon Number of Spines, *N.*
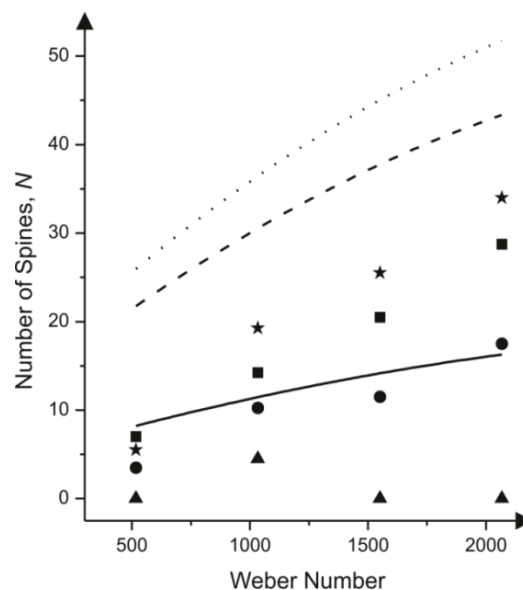
Figure 114: Analysis of the number of spines exhibited from equine blood impacting on cold rolled steel at temperatures of; 24.6° C (squares), 52.5° C (circles), 92.5° C (triangles) and 150° C (stars) verses the Weber number. The number of spines is highly influenced by the surface roughness consequently leading to a new constant being developed, with the use of a line of 'best fit.' The new line of 'best fit' (solid line) fitted the scatter spread more accurately compared to the original line of 'best fit' (dotted line) using equation (5) and the line of best fit (dashed line) incorporated by Hulse Smith et al [18] using equation (6). Note each data point is an average of 20 blood drops (N= 20).

Figure 114 depicts the general scatter of data relating the number of spines to the Weber number, there is a considerable deviation from the expected data when applying equation (5) requiring the development of a new constant, C_n= 0.315 considerably different to the original value of 0.838, obtained by Hulse - Smith et al. [18] The increase in temperature had a clear effect on the number of spines exhibited however the effect did not follow a noticeable pattern, the subsequent expansion in diameter, D_s, would have anticipated an increase in the amount of spines exhibited, and this was not the case. As previously stated the bloodstain diameter, D_s, expands in the natural convection regime, around 50°C yet when a temperature of 52.5°C was

applied the number of spines decreases. Spines could not be calculated at the highest temperatures due to the distorted shape of the bloodstain. These results imply that the use of spines as an evaluation tool is not viable when heat is applied. However it is noted that there is a significant increase in satellite spatter when temperatures reach the film boiling regime which could warrant future further investigation to establish a pattern.

Effect of surface roughness

Only the 1.77 mm pipette was utilised in this experiment for the comparison of surfaces due to unforeseen difficulties when heating the rougher steel.

The cold rolled steel was sand blasted to create a rougher surface; a rougher surface affects the bloodstain diameter, D_s, expecting a smaller bloodstain to be the resultant. Problems arose when heating the rougher surface; the coarser surface made it difficult to heat the steel to the correct surface temperature, for example the new maximum boiling point was equated to be at 60°C; 60°C was the highest temperature the rougher surface was able to reach when 100°C was attempted in the furnace, this problem continued through all of the boiling regimes. Only one side of the steel was sand blasted, meaning the heat from the untouched surface which would have been at the correct temperature could have been radiating through the steel affecting the blood stains in the normal boiling regimes but not altering the surface temperature. Due to this factor it was not thought necessary to develop a new boiling curve as the resulting curve may not be an accurate representation of the actual temperatures achieved and the highest temperature was not achievable resulting in the absence of the film boiling regime from the final results of the sand blasted steel.
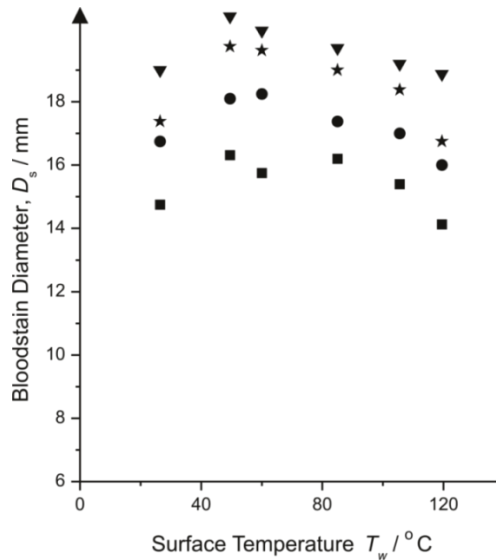
Figure 115: The effect of bloodstain diameter as a function of surface temperature, equine blood released using a 1.77 mm (inner tip diameter) pipette from heights of; 30.5 cm (squares) 60.9 cm (circles), 91.4 cm (stars) and 121.9 cm (triangles) upon sand blasted steel., Each data point is an average of 20 blood drops (N= 20).

Similarly to the cold rolled steel, the diameter D_s slowly increased when heat was initially applied; when the maximum boiling point was achieved a subsequent decline in bloodstain diameter D_s size was experienced as demonstrated in Figure 115. However rise and fall of bloodstain diameters was observed earlier at lower temperatures.
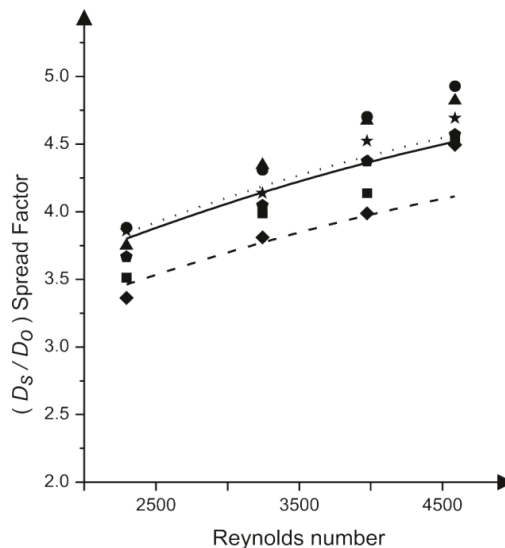
Figure 116: A plot of spread factor as a function of the Reynolds Number, equine blood dropped upon sand blasted steel at temperatures of 24 – 160° C. Line of 'best fit' (solid line), leading to a better fit for the given scatter data compared with the original line of 'best fit' (dashed line) found using equation (3) and the line of 'best fit' (dotted line) using equation (4). Each data point is an average of 20 blood drops (N= 20).

Again there was little effect upon the spread factor verses the Reynolds number (Figure 116), using equations (3 and 4) a scatter constant of C_d^{heated} = 1.1 was

416

established which is similar to the original constant $C_d = 1.11$ and the constant acquired for cold rolled steel, 1.12. Despite the difficulty in accomplishing the necessary temperatures no significant changes in bloodstain diameter size were observable between surfaces, however this can only be loosely surmised since a direct comparison cannot be made due to the aforementioned difficulties.

Lastly the boiling curve for water (Figure 109) was revisited and adapted to illustrate impacting blood.
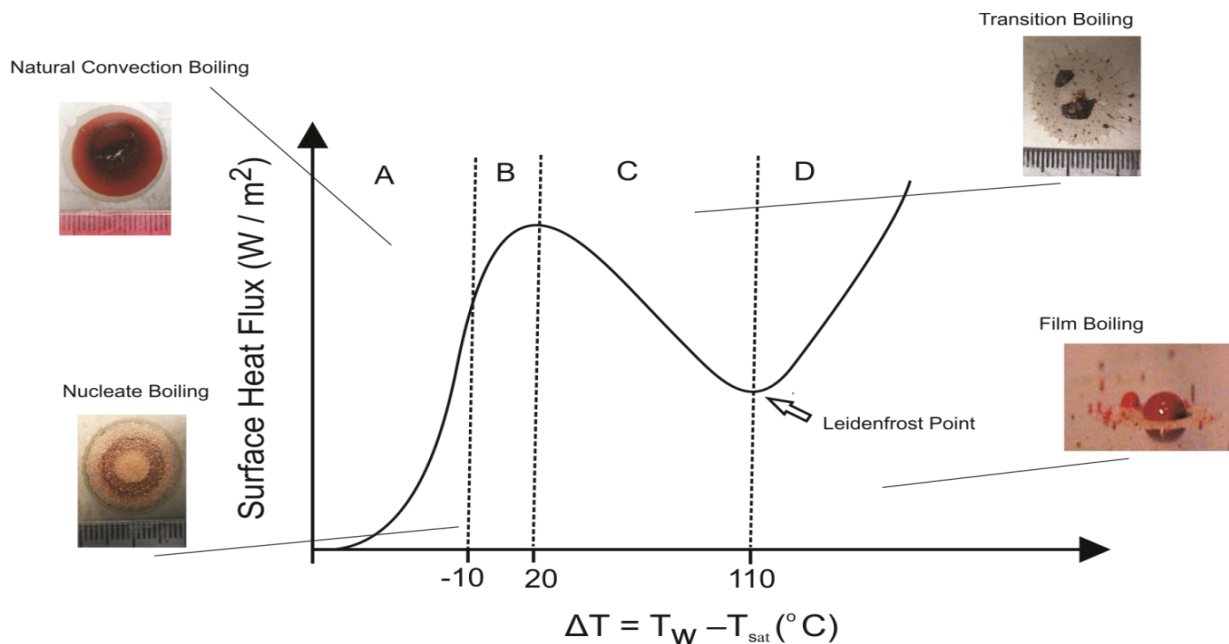
Figure 117: A typical boiling curve highlighting the boiling regimes for blood; A: natural convection (around room temperature), B: nucleation boiling regime, C: transition boiling regime and D: film boiling regime.

Figure 117 depicts a typical boiling curve for blood at 1 atm which clearly shows the typical blood impacts one will observe when blood impacts upon a heated surface. Note that there are slightly differing values when comparing the blood boiling curve to that of water, primarily it is recognised that regimes tend to occur approximately 10 - 20° C earlier for that of blood. An explanation for this could be the impurity of blood, unlike water it contains, salts, proteins and other impurities that will ultimately alter its boiling value. Regimes were recognised by the distinct change in bloodstain appearance (Figure 111A - E) as temperature increased, the Leidenfrost point was used as a reference marker.

5.4.3   Summary

It has been demonstrated for the first time that there is a distinct pattern in bloodstain diameters when they impinge a heated surface, where bloodstain diameters experienced an increase up to temperatures of 90° C and then subsequently decrease at a parallel rate as temperature increases. This suggests a steady evaporation once the boiling point is achieved. Four boiling regimes previously identified for water pooling and droplets[62] can be equally applied to blood at slightly higher temperatures, an anticipated outcome due to blood composing of 83 % water. [204] During these regimes changes to the appearance of the final bloodstains D_s were observed; rings were formed where separation of blood into its components takes place. A new constant when considering this separation was developed, C_d ^{heated}. Further rings developed when the temperature was increased; 5 rings were found on bloodstains released onto a 90^oC surface at heights of 121.9 and 91.4 cm. A correlation between height, thus the initial velocity V_o of the blood drop and the number of rings was ascertained, where lower heights produced fewer rings due to the size of the bloodstain.

Lastly, the appearance of spines was counted and deemed to be insignificant when blood is dropped on to a heated surface; their appearance becomes sporadic and does not follow any general pattern. There was however an increase in the amount of satellite spatter experienced especially in the higher temperatures, this could perhaps substitute spines in cases of heat exposure and should be analysed further to attain their true significance.

Overall it can be concluded that heated surfaces do have a significant effect on bloodstains (D_s) changing their appearance and size dramatically. Ultimately possibly leading to a misinterpretation of patterns (expired stain vs heated stain).

5.5   SURFACE CLEANING

Another method of surface manipulation is cleaning. There are two ways cleaning may affect bloodstains: 1- pre-treatment and 2- post-treatment.

5.5.1   Pre-treatment Cleaning

Pre-treatment cleaning is cleaning carried out before blood has impacted the surface. Potentially altering the surface texture creating a surfactant layer of the cleaning solution and possibly changing the absorbance properties of the surface, effecting the spread of the liquid.

5.5.2   Post-treatment Cleaning

Post–treatment is where cleaning was performed to remove the blood from the surface, in essence "covering up" the blood spill. This method destroys the bloodstain patterns and could affect presumptive testing and DNA analysis (see section 1.7).

The following research looks at both these methods, using appropriate cleaning methods and household detergents/cleaning solutions.

5.6   HEATED SURFACE CLEANING

Following the research of blood on a heated surface it was deemed appropriate to evaluate other possible effects that the heat may have upon blood and its detection. With the knowledge that blood evidence is a valuable source of DNA and the ever increasing ways criminals are attempting to cover-up their crimes (see section 1.7), several cleaning methods in conjunction with heat were tested. The results reflect the effectiveness of three established presumptive tests and the ability of successfully extracting DNA from blood that has been both cleaned and dropped onto a heated surface.

In this study, two different routes of analysis was employed; the first was a high salt extraction, conventional PCR and gel electrophoresis, utilising REDTaq® ReadyMix™ PCR Reaction Mix and Variable Number Tandem Repeats (VNTRs). The second method involved a silica based extraction, real-time PCR based DNA quantitation, end

point PCR and capillary electrophoresis, using the AmpFISTR®NGM SElect™ PCR Amplification Kit. This comparison was made to evaluate the effectiveness of the newer technique over the older technique when considering an extreme case of DNA degradation. The advances in DNA analysis mean that new methods are continually replacing older methods; however these newer methods are very high in price and may not be economically feasible for poorer countries. Therefore if it is found that the cheaper method is a viable option, especially under the most extreme circumstances that can be faced at a crime scene (cleaning and heat exposure) it can offer a cheaper yet still accurate alternative method of analysis.

5.6.1 Experimental

All blood utilised was collected fresh on the day of analysis, where a venepuncture was performed on the donor and extracted blood was collected in a BD Vacutainer® whole blood tube, containing the anticoagulant EDTA. Blood was refrigerated at 4°C for storage until required for experimentation. All chemicals were supplied by Sigma-Aldrich and were of the highest analytical grade available.

5.6.1.1 Sample Preparation

A series of 50 µL blood drops were deposited onto a steel surface, using a Gilson® pipette, which had previously been cleaned to remove any possible contaminants, firstly using acetone and finally with triple deionised water where it was left to naturally dry/evaporate at room temperature. After a minimum of 1 hour drying time to enable the complete drying of the blood drops, a total of six cleaning procedures (plus a control sample) were performed. These are as follows: 10 % bleach solution (sodium hypochlorite solution), soap and water (1:1 dilution), cold water (20°C), warm water (45°C), 1M NaCl + 1M NaOH solution (reported as a DNA degrading agent) [206 - 207] and soda water. Bloodstains were cleaned off the surface until no visible trace (to the naked eye) of them remained. This procedure was performed at various temperatures, where the steel surface was heated, using an oven furnace, to temperatures of 50°C, 150°C and 250°C prior to blood being dropped. An infrared temperature gun was utilized to ensure correct temperatures were reached and maintained throughout the experiment.

5.6.1.2 Presumptive Test Preparation

Three presumptive tests for blood were performed on all bloodstains after temperature and cleaning treatments. Each presumptive test solutions were made in accordance with Refs [204 - 206]. For clarity the exact composition of each is as follows:

Luminol: consisted of a luminol stock solution (1g luminol and 7.5g potassium in 125 mL of distilled water) and a 3% hydrogen peroxide solution. [204] When performing the test a mixture of 10 mL luminol stock solution and 10 mL of the hydrogen peroxide solution was used. [204] The analysis was performed in a darkened room where the mixture was simply sprayed (with a spray bottle) over the area under investigation. When the surface luminesced; this was recorded as a positive result for the presence of blood as suggested by a previous report. [204]

TMB (Tetramethylbenzidine): 0.2g TMB dissolved in 10 mL, which was refrigerated for storage until required, and a 3% hydrogen peroxide solution. [206] The test was performed by swabbing the area of interest, where a series of 2 drops of TMB (stock solution) were applied followed by 2 drops of the hydrogen peroxide solution. [206] A positive indication for blood was expressed when the swab turned a blue/green colour; no colour change denoted a negative result as described in a previous study. [206]

Kastle Meyer (KM): 0.1g phenolphthalein, 25% w/v sodium hydroxide solution, 0.1g zinc powder, 70% ethanol and distilled water, 3% hydrogen peroxide solution, distilled water and 70% ethanol. [205] Similarly to the TMB test, the area under examination was swabbed, where again a series of drops are added; 2 drops of the 70 % ethanol solution, followed by 2 drops of the KM stock solution and lastly 2 drops of the 3% hydrogen peroxide solution. [205] Again, a positive result for the presence of blood is indicated by a colour change, in this case an intense pink colour is observed.

All presumptive tests were made fresh on the day of experimentation and were performed three times to ensure consistency. Negative and positive controls were employed to ensure that the presumptive tests were functioning properly. A bloodstain was used as the positive control and a blank surface was used as the negative control.

5.6.1.3 Sample Collection

Two sampling techniques were employed, swabbing and scraping. [4] Swabbing was performed with a class IIA Eurotubo wooden and cotton sterile swab; the swab was slightly moistened with triple distilled water and the swab was rubbed over the area under investigation. Scraping was performed using single edge razor blades, the

blades were sterilised before use. Each bloodstain was scraped using a new razor blade to avoid any cross contamination. All temperature ranges were tested for both techniques 3 times to attain uniform results, a total of 24 samples were prepared and compared. It is noted that other collection techniques such as mini- tapes could have been utilised; however these tend to be used for fabric materials whereas scraping and swabbing are recognised collection techniques for blood / dried blood on a number of surfaces. [4]

5.6.1.4   First Analytical Technique

A high salt extraction was performed as follows; [212] the bloodstain / cleaned area was swabbed using a sterile swab moistened in triple deionised water, the swab was then cut into a 1.5 mL eppendorf tube where a 150 µL of triple deionised water was added. After 1 hour 150 µL of TNES (10mM Tris, 400mM NaCl, 100mM EDTA, 0.6% SDS) buffer (warmed to 56°C) and 10 µL of Proteinase K were added, the solutions were left to incubate overnight at 56°C in a water bath. [212] The following day 41.5 µL of 6M NaCl (pre-warmed to 37°C) was included into the sample mixture, which was subsequently vortexed for 15 seconds and then microfuged (13000 x g) for 10 mins. The next step involved the careful removal of 300 µL of supernatant to a new tube where an equal volume of 100% EtOH (300 µL) was added. [212] Again the solution was microfuged (13000 x g) for 10 mins, however this time the supernatant was disposed of and the pellet remained in the tube where 200 µL of 70% EtOH was added and the solution was microfuged again, this time for 5 mins. Removal of supernatant followed, where care was taken not to lose the pellet. This last step was repeated once more as some blood samples can be very unclean. The pellet was then left to air dry for 10 mins. Lastly 25 µL of TE (10 mM Tris-Cl, 1 mM EDTA) buffer was added to the dry pellet which was then vortexed and left for 1 hour at room temperature ready for ethidium bromide gel preparation. [212] Samples were run at 120 V on a 0.8 % Agarose gel for 45 minutes, where the gel was subsequently exposed to UV light to visualize any DNA bands.Samples were run at 120 V on a 0.8 % Agarose gel for 45 minutes, where the gel was subsequently exposed to UV light to visualize any DNA bands. Subsequent measurements were conducted using the Nanodrop, a device used to quantify the amount of DNA present in a sample.

Further analysis utilising a conventional PCR amplification [213 - 214] was carried out, where a REDTaq® ReadyMix™ PCR Reaction Mix was utilized. The primers used

(below) amplified the locus D1S80, [215 - 216] a common VNTR used in forensic identification. [215 - 216] The locus is found on chromosome 1, the largest human chromosome, 29 different alleles of the locus are presently known ranging in sizes of 200 bp to 700 bp. [215 - 216] The amplified DNA was successively run on an ethidium bromide gel.

5.6.1.5 Second Analytical Technique

A silica based extraction was performed as per Ref. [217] Real-time PCR using a Human Quantiplex Kit (Qiagen, UK) upon a RotorGene real-time PCR machine (Qiagen, UK) was carried out on the extracts, quantifying the amount of DNA present in each sample. These results were used to determine which samples were the most suitable candidates to be analysed by capillary electrophoresis (CE) where full profiles may be ascertained as well as providing data to optimal the template amount for subsequent PCR analysis. These samples were amplified using AmpFLSTR® NGM SElect™ PCR Amplification Kit (STR loci; D3S1358, vWA, D16S539, D2S1338, D8S1179, D21S11, D18S51, D19S433, TH01, FGA, Amelogenin, D10S1248, D22S1045, D2S441, D1S1656, D12S391) using the Veriti Thermal Cycler (Life Technologies, UK) as per manufacturer's instructions. The amplicons then fragment analysis using an ABI3130 Genetic Analyser equipped with Genemapper V3.2 Software.

5.6.2 Results and Discussion

5.6.2.1 Presumptive Testing

First, three types of presumptive testing (luminol, TMB and Kastle–Meyer) were performed on all bloodstains at varying temperatures after the cleaning methods (10 % bleach solution (sodium hypochlorite solution), soap and water (1:1 dilution), cold water (20ºC), warm water (45ºC), 1M NaCl + 1M NaOH solution) had been completed. Observations made prior to cleaning revealed flaking of the bloodstains at surface temperatures of 50 – 150ºC, making the overall cleaning much easier due to the easy removal of the brittle flakes without much physical exertion. Higher temperatures however were found to burn the blood into the steel surface and therefore were much harder to remove without leaving a trace outline of where the blood had been deposited. Presumptive testing was performed an hour after cleaning, giving the surface enough time to dry and cool; all tests were performed three times. Initial

analysis revealed that temperature alone, contrary to previous reports, has no effect upon the ability to detect the blood using any of the presumptive techniques. However when we explored the use of these techniques when various cleaning methods had been employed it was found that heat has an effect.

	Temperatures of Impacted Surface (°C)			
Cleaning Methods	Room Temp	50°C	150°C	250°C
Luminol				
None	✓	✓	✓	✓
Cold water	✓	✓	✓	x
Soap and water	✓	✓	✓	✓
10% Bleach	✓	x	x	x
1M NaCl + NaOH	✓	✓	x	x
Club soda	✓	✓	✓	✓
Warm water	✓	✓	✓	x
TMB				
None	✓	✓	✓	✓
Cold water	✓	✓	✓	✓
Soap and water	✓	✓	✓	✓
10% Bleach	✓	✓	✓	✓
1M NaCl + NaOH	✓	✓	✓	✓
Club soda	✓	✓	✓	✓
Warm water	✓	✓	✓	✓
Kastle-Meyer				
None	✓	✓	✓	✓
Cold water	✓	✓	✓	✓
Soap and water	✓	✓	x	x
10% Bleach	✓	x	x	x
1M NaCl + NaOH	✓	x	x	x
Club soda	✓	✓	x	x
Warm water	✓	✓	✓	x

Table 32: Comparisons of the effects of various cleaning methods and temperatures on three presumptive tests (luminol, TMB and Kastle – Meyer) used for the establishing the presence of blood. Tests were run three times to ensure consistency, a total of 252 samples were compared overall for this section of experimentation. ✓ - positive for presence of blood and x - negative for presence of blood.

Table 32 demonstrates the effect of both cleaning, and the effect of a heated surface upon the efficiency of the blood visualising techniques; a tick signifies a positive result for the presence of blood, which was indicated via a colour change/luminescence (20 seconds). Similarly a cross indicates a negative result for the presence of blood where

no colour change or luminescence was experienced after a period of 20 seconds. Tests were performed three times where the rule of 2 out of 3 results (*i.e.* 2 positives and 1 negative) were considered a majority and therefore taken as the final result. There was however no deviations between the three runs performed; all results were either positive or negative for all three attempts. All cleaning presented no effects when applied at room temperature, as the heat is increased, negative results start to emerge, for example at 50°C when the stain was cleaned with the bleach solution both luminol and KM tests returned a negative result. At 250°C this pattern persists, returning more negative results for 4 out of 7 of the cleaning methods when luminol is used and 5 out of 7 when KM was utilized. It is unclear why these negative results start to emerge as temperature increases, as temperature alone appears to have no effect. A possible explanation could be that the heat weakens the haemoglobin structure and therefore when cleaning is performed it is easier to remove any trace of blood, using the more aggressive cleaning methods (*i.e.* bleach). TMB appeared to be the most robust method of presumptive testing, yielding positive results for all cleaning methods tested. It is suggested that future presumptive testing where crime scene cleaning is suspected is performed using the TMB test, as although it is a time consuming test, gives rise to more consistent results when the bloodstain has been removed by cleaning.

There are countless other blood presumptive tests (leuchomalachite green, fluorescein etc.), [24] however many of these are out-dated since they are thought to use highly carcinogenic substances (an obvious Health and Safety issue) or are less reliable than the aforementioned three.

5.6.2.2 First Analytical Technique

5.6.2.2.1 Ethidium Bromide Gels

The first ethidium bromide gel implemented was to compare the sample collecting method of swabbing versus scraping both of which are readily employed collection techniques at crime scenes. [24] Initial analysis of Figure 118 illustrates that both swabbing and scraping produce viable DNA samples and are therefore equally as suitable as collection techniques. This is further supported by the Nanodrop results that show concentrations for swabbing and scraping to be very similar, except in the

case of the highest temperature (250°C) where scraping did not yield any results due to the difficulty in removing the sample.
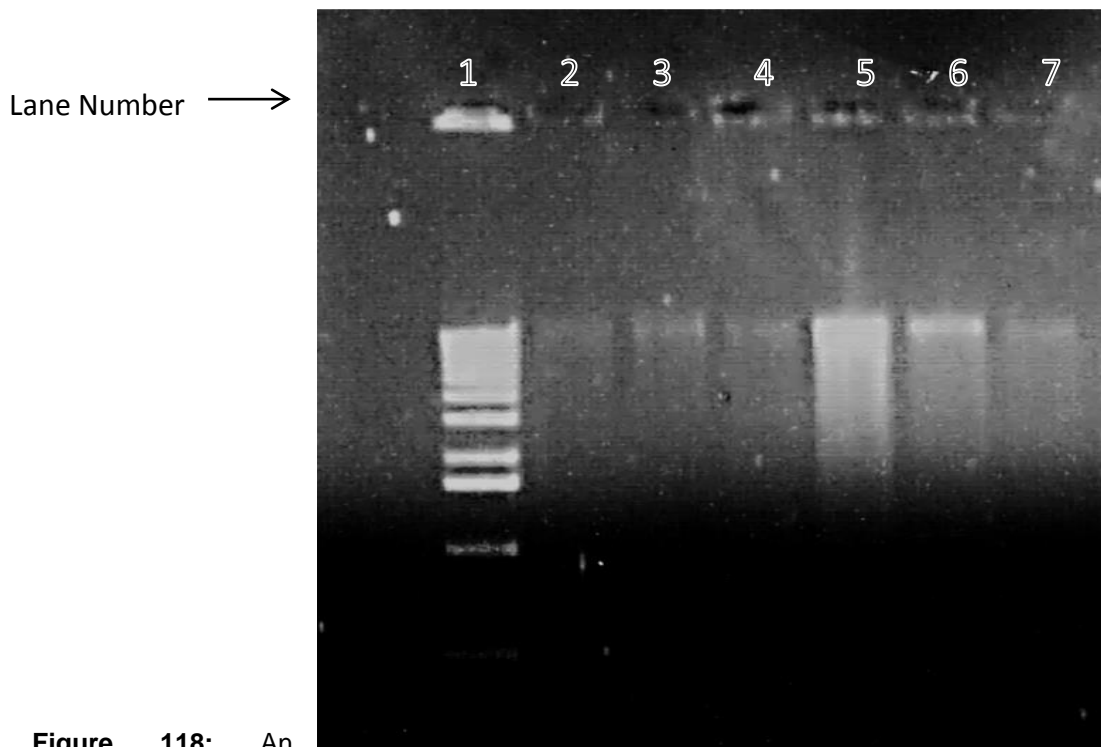
Figure 118: An ethidium bromide gel comparing the DNA exhibited when two different sample collecting techniques were employed where the steel plate had been heated to 250°C; Lane 1: 1KB ladder, Lanes 2-4: scraping and Lanes 5-7: swabbing.

The Nanodrop, a device used to quantify the amount of DNA present in a sample, it is a type of spectrophotometer basing its analysis on wavelengths; therefore if the sample is unclean erroneous results are to be expected. Unpaired t-tests to establish the statistical significance of the difference in DNA concentrations when employing the two collection methods were performed. Results found p values of between 0.1917 - 0.4246 when comparing each temperature step with the collection method, these values are not considered to be statistically significant and therefore confirm the claim that either method of DNA collection is viable.

Lane Number →
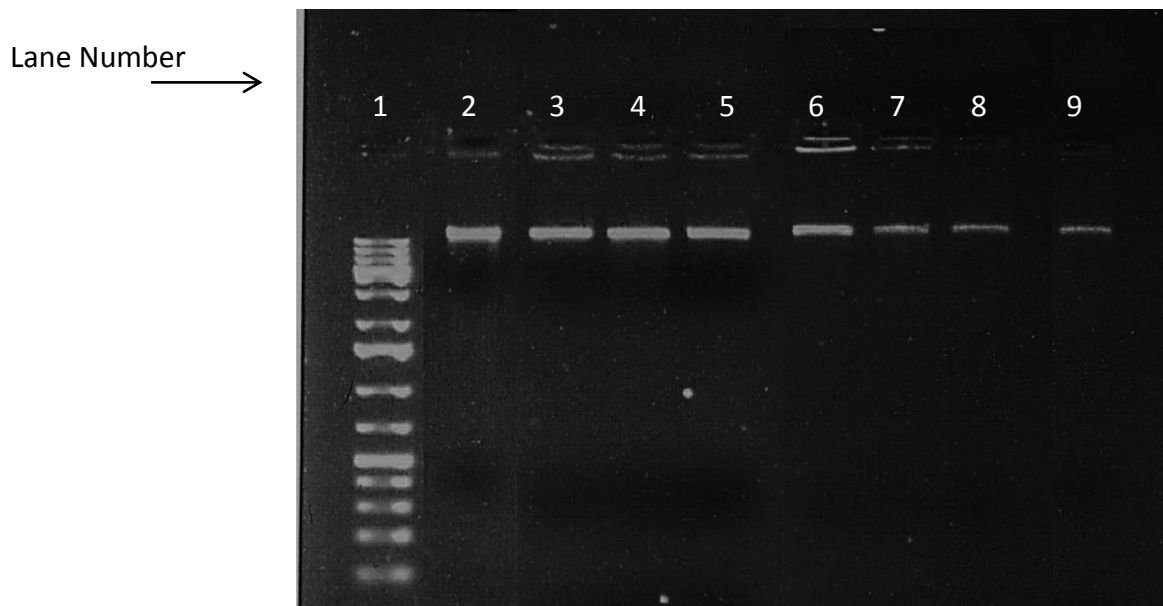
Figure 119: The effects of temperature on DNA represented in an ethidium bromide gel; Lane 1: 1 KB ladder, Lanes 2 – 3: blood dropped on to a steel plate pre-heated to room temperature, Lanes 4 – 5: blood dropped on a steel plate pre-heated to 50°C, Lanes 6 – 7: blood dropped on a steel plate pre-heated to 150°C, Lanes 8 – 9: blood dropped on to a steel plate pre-heated to 250°C.

Further analysis utilising the Nanodrop reveals that the concentration of DNA significantly decreases with temperature, this is not apparent when Figure 119 is observed, which depicts the effect of temperature on DNA analysis using an ethidium bromide gel. Table 33 demonstrates the Nanodrop results showing that the concentration of DNA nearly halves with every temperature step.

Temperature (°C)	Scrape DNA concentration(ng/µL)	Swab DNA concentration (ng/µL)
Room	46.40	38.08
50	19.75	14.58
150	4.50	5.90
250	-	2.75

Table 33: Effect of temperature of the impacting surface (steel) on the concentration of DNA measured with a Nanodrop.

Again unpaired t-tests were performed to ascertain the statistical significance of the results; DNA concentration results for the highest and lowest temperatures were compared for both collection techniques. Results found p values of 0.0042 and 0.0182 when scraping and swabbing were employed, respectively, both values are considered to be extremely statistically significant. This suggests that temperature influences the concentration of DNA significantly, decreasing the concentration as

temperature increases, but does not eliminate or denature the DNA at theses exposures.

Figure 120: An imag[...]g and temperature (room) on the ability to extract DNA. Lane 1: 1KB ladder, Lane 2 –4: no cleaning performed, Lane 5– 6: cleaned with cold water, Lane 7- 8: cleaned with warm water, Lane 9 –10: cleaned with carbonated water, Lane 11– 12: cleaned with soap and water, Lane 13–14: cleaned with 10% bleach, Lane 15 – 16: cleaned with 1M NaCl + 1M NaOH.

Further DNA extractions (Figure 120) were performed after the employment of the cleaning methods, all results were negative for the presence of DNA leading us to a possible two conclusions; either the cleaning processes destroyed all of the DNA or the chosen method of analysis (ethidium bromide gel) could not detect the extremely small amounts of DNA that may have been present.

Ethidium bromide gels have a limit of detection of just 0.5 – 5 ng/band [217] where after the cleaning process picograms of DNA are most likely to be present.

5.6.2.2.2 PCR testing

Due to the limit of detection for ethidium bromide gels being at nanogram levels, further exploration was deemed necessary using PCR, which can detect DNA levels at picogram level. [218] As temperature was judged to have no effect on the ability to extract DNA (see earlier) only one temperature step was felt necessary to PCR, the highest temperature condition (250°C) was consequently chosen, where the six different cleaning methods plus a negative control were employed (again repeated 3 times totalling 21 samples), positive controls are denoted as no cleaning performed. Figure 121 demonstrates the amplification of the locus D1S80; observing the only

presence of DNA in lane 8, where the bloodstain was not treated with a cleaning process.
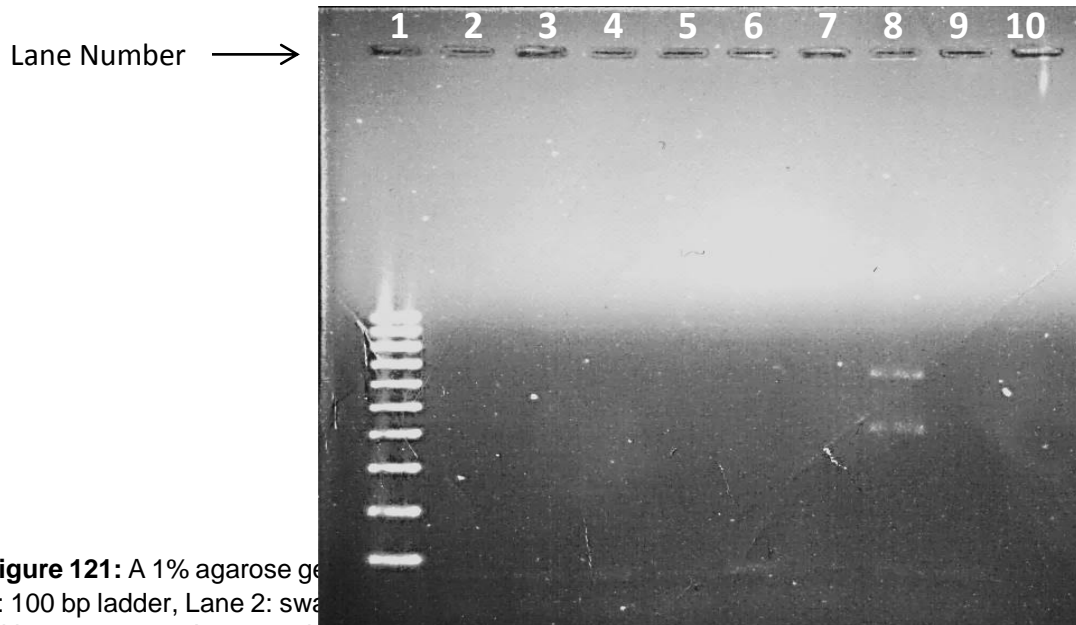
Figure 121: A 1% agarose g[...]80;Lane 1: 100 bp ladder, Lane 2: sw[...]:cleaned with warm water, Lane 5: cleaned with carbonated water, Lane 6:cleaned with soap and water, Lane 7:cleaned with 10% household bleach, Lane 8: no cleaning performed, Lane 9: cleaned with 1M NaCl + 1M NaOH, Lane 10: negative control (distilled water).

With the previous knowledge that the treatment of heat causes a decrease in DNA concentration but does not eliminate it, it can be concluded that the absence of any DNA is a result of cleaning; this is further supported by the appearance of a DNA band (Figure 121, lane 8) where heat but no cleaning was employed. Water acts as a lysing agent; [219] therefore it is a plausible result that even the use of plain water can eliminate DNA. It is noted however that these results are highly dependent on the 'cleaner,' where effectiveness of DNA elimination depends on how hard and for how long you scrub, in this study bloodstains were scrubbed until they could no longer be visualised via the naked eye.

5.6.2.3 Second Analytical Technique

Real-time PCR (using the AmpFLSTR® NGM SElect™ PCR Amplification Kit) was use to quantify the amount of DNA present within each sample, 28 samples were tested (4 different temperatures with 6 cleaning methods and blanks). It was found that only four samples, those which were exposed only to different surface temperatures where no form of cleaning had been attempted, showed presence of DNA. Table 34 expresses the DNA concentrations, it is noted that as temperature

increases the amount of DNA decreases. Student t-tests were performed to explore the significance of the results, a value for *p* was found to be 0.0001, and is therefore considered to be extremely significant. Hence, it can now be stated that heated surfaces do have a significant effect on DNA analysis, decreasing but not eliminating it as the surface temperature rises.

Temperature (°C)	DNA concentration (ng/µL)
Room (25)	1.302
50	1.221
150	0.719
250	0.145

Table 34 - Quantiplex results quantifying the effect of temperature of the impacting surface (steel) on the concentration of DNA.

Based on the results using the Quantiplex kit it was determined that only the four surface temperature affected samples were worthwhile advancing to the next stage of analysis, being the most viable samples in which to obtain a full profile. However, as a precaution, the room temperature samples for each cleaning method were also analysed (7 samples). Samples were amplified (see experimental section) and analysed using Capillary Electrophoresis. It was found that full DNA profiles could be obtained from all samples which were exposed solely to different surface temperatures without any subsequent cleaning. Figures 122 and 123 demonstrate the apparent effects of degradation by surface temperature, where both the Relative Fluorescence Units (RFU) and ratios (between the low molecular weight markers and the high molecular weight markers) decrease as temperature rises, this is characteristic of a degraded DNA profile.
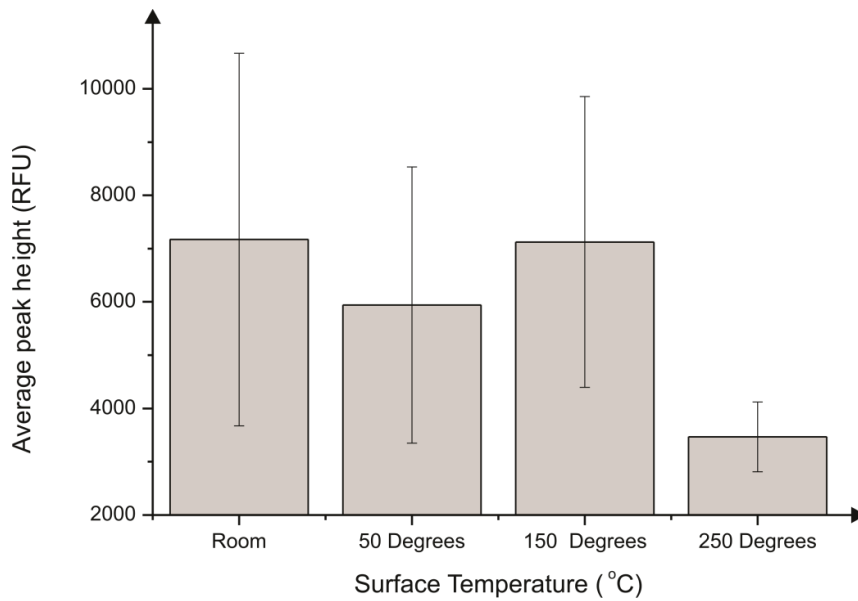
Figure 122: A graphical representation of the average RFU value for peak height across the EPG when incorporating different surface temperatures alone without cleaning.
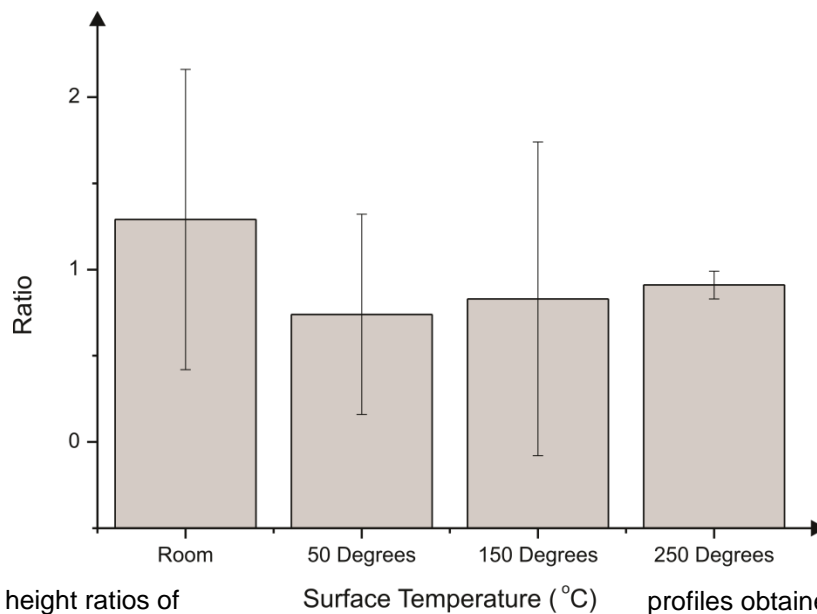
Figure 123: Peak height ratios of profiles obtained when DNA was deposited on to a heated surface.

Again statistical analysis was performed to evaluate the significance of the results, when the RFU values (for room temp and 250°C) were considered the data was found to be extremely statistically significant giving a *p* value of 0.0002, however when the ratios (for room temp and 250°C) were analysed a *p* value of 0.4178 was found which is deemed as not statistically significant. Given that the full profile could be recovered successfully for all temperatures it is reasonable to assume that temperature does not have a significant effect on the quality of DNA recovered.

Next the capillary electrophoresis results were analysed for the 7 samples where cleaning had been performed (room temp; 25°C); it was discovered that only partial profiles could be recovered. Match probabilities were calculated from these partial profiles, expressed in Table 35, to evaluate the strength of the profiles as potential evidence in a forensic case.

Cleaning Method (At Room Temp)	Match Probability Odds (1 in)
1M NaCl + NaOH	3
Bleach	3
Cold Water	1150
Soda Water	-
Warm Water	12
Soap and Water	260

Table 35 - Probabilities partial profiles were exposed to different cleaning techniques. Match obtained from after samples

Given that the match probability of the full profile was measured to be 4.262E+26 and the low probabilities displayed in Table 35, the profiles obtained after cleaning were deemed unusable and would not be used as forensic evidence. (Appendix 10) Therefore it can be stated that cleaning completely removes any viable trace of DNA in this study, again this may dependent on the 'cleaner' and surface type. It was also noticed that the effect of cleaning appeared to contribute additional DNA to the result. The STR analysis was carried out in DNA clean condition and the negative controls showed no amplification at all; however, extraneous DNA was detected in the results following cleaning (Appendix 10). Further investigation shows there to be several alleles present, expressing multiple contamination. This may be attributed to people involved in the manufacturing process (*i.e.* soap manufacturing, paper towel manufacturing), where several people could have come into contact with the materials utilised in this study, before they are packaged.

5.6.2.4 Old v New Techniques

The two methods (salt extraction with PCR *vs* silica extraction with real-time PCR) of analysis used in this paper are compared. The first method, by DNA standards, is an old outdated technique and the second method uses up-to-date technology and is standard in most forensic laboratories. Both methods differ significantly in price here it is investigated why this might be.

Findings indicate that both methods work and draw the same conclusions, temperature decreases the amount of available DNA and, in this study, cleaning eliminates any trace of viable DNA. There are limitations to the former method however; the agarose gel analysis can be highly inaccurate when trying to quantify the DNA, often errors occurring due to band distortion. The gels in this study were used purely to show that DNA was present, instead the Nanodrop was used for quantification. Gel electrophoresis also lacks any real qualitative capabilities, merely showing the presence of DNA, although some bands appeared to fade, indicating less DNA, as temperature increased.

Surprisingly the VNTR worked well despite its reputation as being unsuitable for degraded samples, due to the fragment sizes. Both extraction techniques were successful in spite of there being no purification step in the high salt extraction method. Overall it can be concluded that although the first method is old and out-dated the technique remains robust, where even in the most extreme circumstances (i.e. heat/cleaning or both) viable DNA can be extracted using the cheapest methods available. This leaves economical options open to poorer countries which may not be able to afford the more expensive methods of analysis, where at least preliminary analysis of the DNA, *i.e.* is a profile feasible, can be carried out.

5.6.3   Summary

In this study a combination of surface heat and cleaning on the ability to extract DNA was explored. Both a high salt extraction and silica based extraction procedure were utilised, attempting to extract DNA after treatment of 4 varying temperatures and six different cleaning methods. After exposure to three presumptive tests for blood (luminol, TMB and Kastle – Meyer) it was discovered that the 10% bleach is the most effective cleaning agent and temperature alone does not have an effect on the ability to detect blood. TMB was found to be the most effective method of testing for the

presence of blood after cleaning; it is therefore advised that this be the presumptive method of choice when cleaning has been employed at crime scenes.

After exploring the effects of surface temperature on the ability to extract viable DNA it was found that the surface's temperature decreases but does not eliminate the amount of DNA available for extraction and that even at 250ºC (for a small exposure period) a full profile can be obtained. Cleaning (using cleaning solutions) conversely was found to eliminate DNA completely in all cases, with all cleaning techniques. This outcome is unexpected due to the known recovery of DNA from washed clothing which was exposed to higher temperatures of around 50ºC, [220] therefore results can be attributed to two factors; firstly, the vigorous cleaning routine employed by the analyst and it is impossible to cover all possible cleaning techniques of the cleaner due to the individuality of the person and their situation at the time of the crime (i.e. are they in a hurry), in this experiment surfaces were only cleaned until blood appeared to have gone, therefore different results could be obtained if the time for cleaning increased/ reduced or of the person used less/more exertion. Secondly results can be assigned to the type of surface utilised, the steel used in this experiment was non-porous and therefore will not retain the blood / DNA as well as the clothing used in ref [220], further exploration into different types of surfaces which can be heated (i.e. different types of metal) should be investigated to fully understand the implications of surface type and DNA recovery.

Finally two different routes of analysis (salt extraction with PCR vs silica extraction with real-time PCR) were compared in order to explore whether greater expenditure actually gives the better results which could otherwise not be reached with a cheaper method. It was found that both methods reach the same end conclusion; this is surprising as VNTRs are especially prone to degradation due to their size and yet, sufficient amounts of DNA could still be extracted and analysed. There are limitations to the older method ((salt extraction with PCR) that quality of DNA cannot be assessed accurately, however the method is robust enough to still be used comfortably for preliminary analysis of DNA, offering a cheaper alternative.

5.7 FABRIC LAUNDERING

The wear and tear of fabrics is a key concern when bloodstains are analysed on clothing. The difference between a new piece of fabric and one which has been repeatedly washed, dried, ironed etc. could have major implications on how the blood impacts and absorbs into fabric, *i.e.* build-up of detergent creating a surfactant layer.

It is noted that fabrics can be standardised following the protocol outlined in 8A BS ENISO 6330/A1:2009. This will be explored to establish if this concept is applicable to all fabric types and to the impaction of blood.

The following study will investigate bloodstains on various fabrics and the effects laundering, drying and repeated cycles have upon fabrics and subsequently the blood that impacts them.

5.7.1 Experiment

Six commercially available washing detergents were investigated: Ariel (Actilift), Daz (Regular), Persil (Colour Powder), Surf (with Essential Oils), Fairy (Non-Bio) and Bold 2 in 1 (Lavender and Camomile), these were chosen as they were found to be the most popular brands used amongst the general population. [221]

The washing machine used throughout this investigation was the Hoover DYN 8144 D and the tumble dryer was a Hotpoint Aquarius Ultima Reversomatic Dryer Super De Luxe TL31. A rinse cycle was performed on the washing machine before beginning any testing.

Hand washing was performed where water was heated to 30°C, monitored using a thermometer. The recommended amount of washing detergent (guided by manufacturer of the packaging) was dissolved in the warm water. The fabrics were allowed to soak for 10 minutes, scrubbed clean, soaked for a further 10 minutes, then rinsed using cold water.

Blood drop experiments were performed as described in section 2.2. Stains were measured once they were fully dried, therefore there was a degree of wicking present.

5.7.2 Results and Discussion

5.7.2.1   Detergent Form and Type

There are many varieties of washing detergent, for this study 6 were considered (Ariel, Daz, Persil, Surf, Fairy and Bold 2 in 1). These detergents were chosen as they were found to be the most popular and widely used in the home. [221 - 222] Fourier Transform Infra-Red was performed on each detergent, the spectrums produced were fundamentally similar as Fairy, Bold and Daz are produced by the same company (Procter and Gamble). Before any analysis was conducted on the effect of different detergents it was important to establish the influence the form in which the detergent was in had when applied to the fabric. Detergent comes in many forms, [217] the forms tested in this paper were: capsule, liquid and powder. Only 8 of the 20 fabrics (Cotton Poplin, Medium Habotai Silk, Denim, M&S T- Shirt Jersey, Light Grey Polyester Twill, Jupiter Linen, Wool Delaine and Nylon) were tested during this preliminary experiment, each chosen for their characteristic differences and fabric type. Fabrics were both hand-washed and machine washed and dried 3 different ways (air dry, radiator dry and tumble dry). The manufacturer's recommendations were followed regarding the amount of detergent used and a rinse cycle was run between washes (30°C) to ensure all detergent had gone from the washing machine. Blood drop tests were performed using the larger pipette (1.77mm inner diameter) from a height of 50 cm. Results showed that in general the form of detergent did not have a significant effect on the size of the bloodstain produced. In fact the results highlighted the possibility of an effect when different methods of drying and washing are considered (this will be discussed later). Since there was deemed to be no significant difference when the form of detergent was considered, powder was used for the remaining experiments.

Powder is used in most homes and is more cost effective than any other forms of detergent.
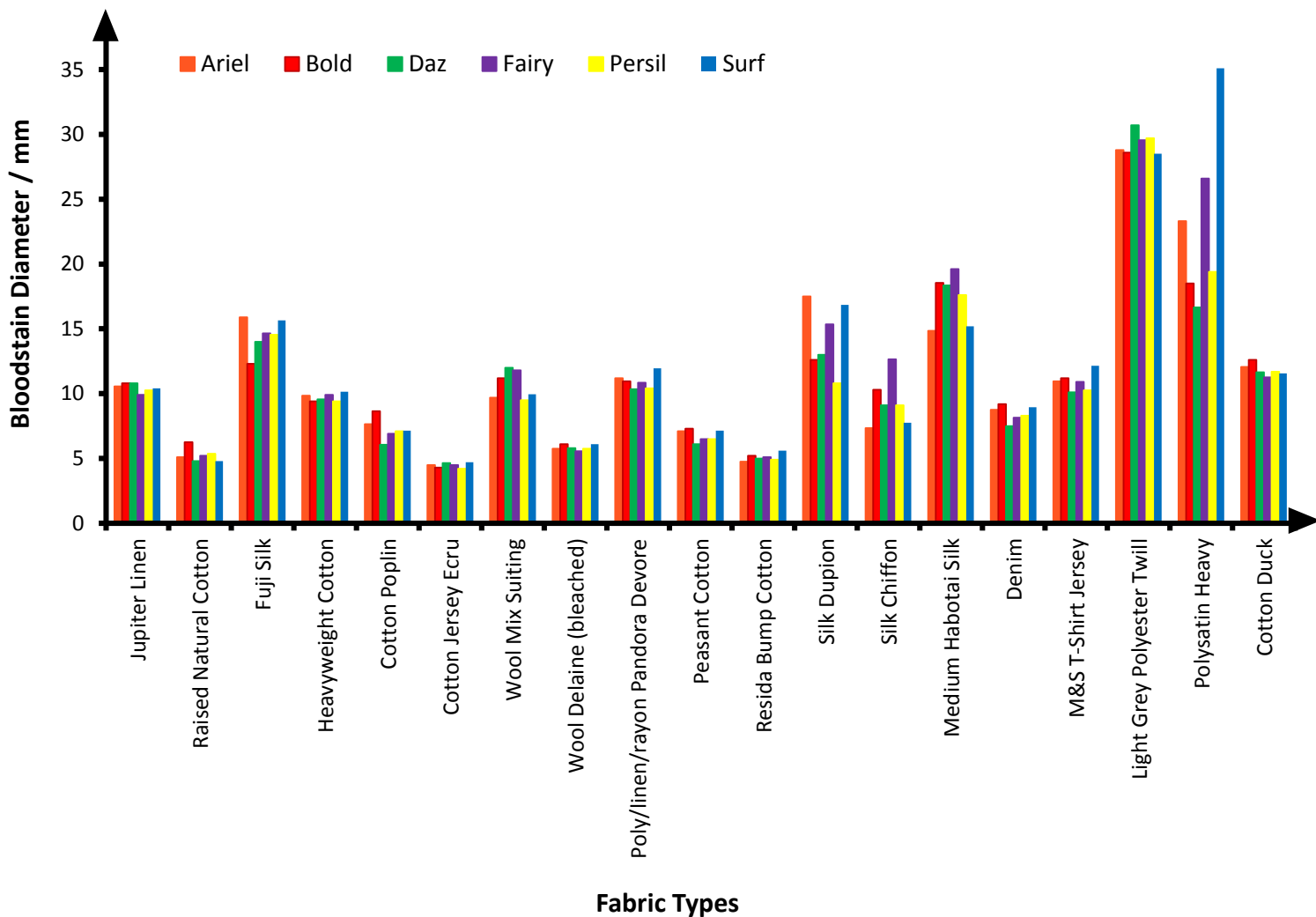
Figure 124: Average bloodstain diameters when blood impacted fabric after it had been machine washed with 6 different detergent types. *N = 5*

Next the six common brands of detergent were assessed. Two washing techniques were employed (machine and hand) and fabrics were radiator dried (dial number 3; 20° C) Figure 124 shows the results amassed after the use of these 6 detergents; finding bloodstain diameters significantly increased in size independent of the detergent type. Results varied when a different washing technique (Figure 125) was

incorporated, where fabrics which were hand washed displayed little significant difference (Table 36) when detergents were considered.
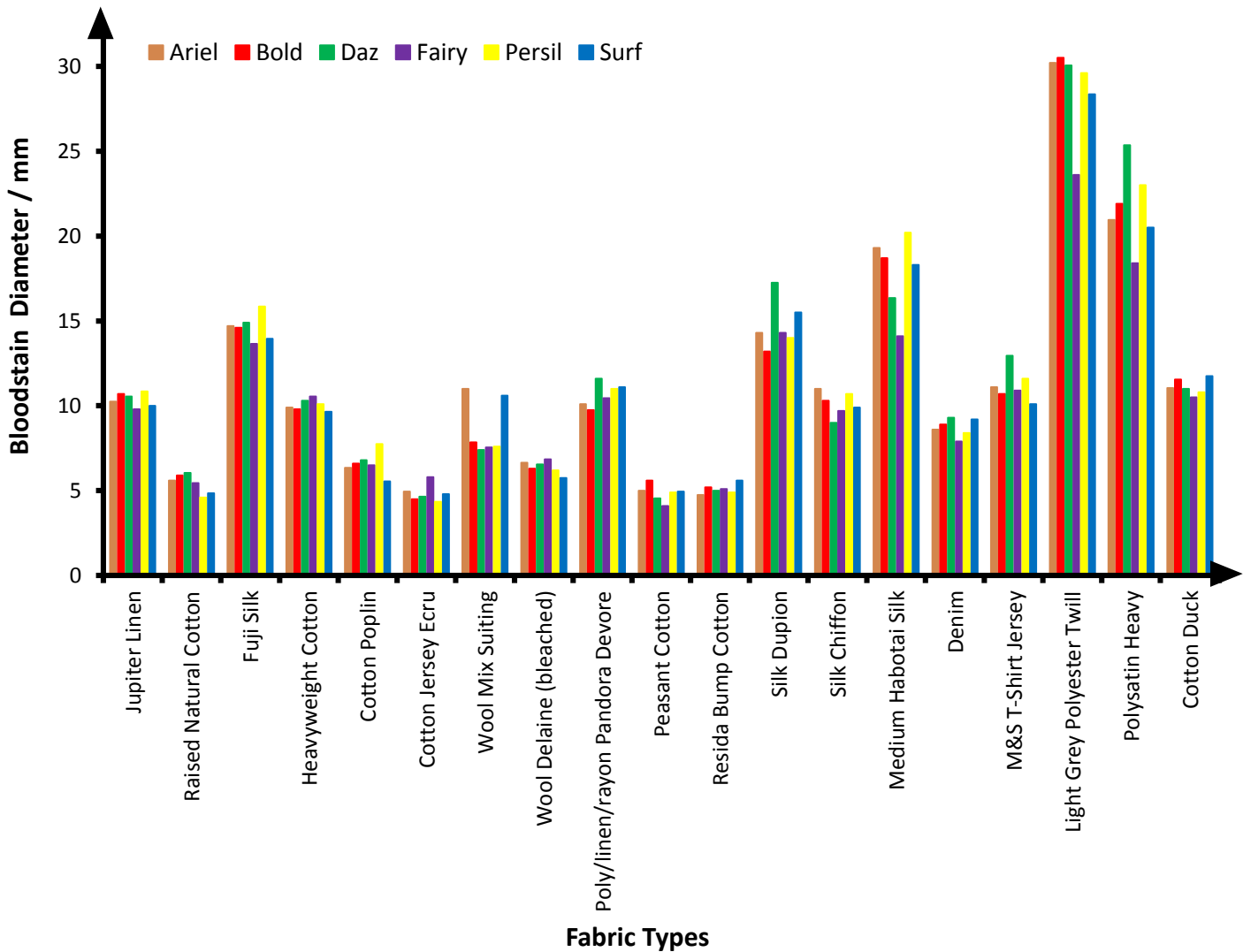
Figure 125: Average bloodstain diameters when blood impacted fabric after it had been hand washed with 6 different detergent types. $N = 5$

Fabrics which were machine washed offered more significant changes to the diameter size, this is perhaps the cause of the degree of agitation the fabric goes through when it is being mechanically cleaned. Table 36 compares the two washing techniques using the p values obtained after employing the unpaired student t-test. It is clear that washing technique is a determinant factor in the size of the final bloodstain, showing significant differences for almost all of the fabric independent of the detergent used.

Type of Fabric	p value Aerial	Sig. Yes (✓) or No (x)	p value Bold	Sig. Yes (✓) or No (x)	p value Daz	Sig. Yes (✓) or No (x)	p value Fairy	Sig. Yes (✓) or No (x)	p value Persil	Sig. Yes (✓ or No (x)	p value Surf	Sig. Yes (✓) or No (x)
Jupiter Linen	0.31	X	0.63	X	0.38	X	0.68	X	0.06	X	0.25	X
Raised Natural Cotton	0.09	X	0.16	X	0.00	✓	0.21	X	0.00	✓	0.71	X
Fuji Silk	0.00	✓	0.00	✓	0.02	✓	0.00	✓	0.00	✓	0.00	✓
Heavyweight Cotton	0.74	X	0.07	X	0.00	✓	0.00	✓	0.00	✓	0.06	X
Cotton Poplin	0.00	✓	0.00	✓	0.02	✓	0.10	X	0.23	X	0.00	✓
Cotton Jersey Ecru	0.00	✓	0.36	X	1.00	X	0.00	✓	0.43	X	0.48	X
Wool Mix Suiting	0.00	✓	0.00	✓	0.00	✓	0.00	✓	0.00	✓	0.20	X
Wool Delaine (bleached)	0.00	✓	0.38	X	0.00	✓	0.00	✓	0.10	X	0.17	X
P/L/R Pandora Devore	0.00	✓	0.00	✓	0.00	✓	0.08	X	0.07	X	0.00	✓
Peasant Cotton	0.00	✓	0.00	✓	0.00	✓	0.00	✓	0.00	✓	0.00	✓
Resida Bump Cotton	0.00	✓	0.00	✓	0.00	✓	0.00	✓	0.00	✓	0.00	✓
Silk Dupion	0.00	✓	0.20	X	0.00	✓	0.04	✓	0.00	✓	0.02	✓
Silk Chiffon	0.00	✓	1.00	X	0.81	X	0.00	✓	0.00	✓	0.00	✓
Medium Habotai Silk	0.00	✓	0.82	X	0.00	✓	0.00	✓	0.00	✓	0.00	✓
Denim	0.46	X	0.39	X	0.00	✓	0.42	X	0.75	X	0.27	X
M&S T-Shirt Jersey	0.62	X	0.15	X	0.00	✓	1.00	X	0.00	✓	0.00	✓
Light Grey Polyester Twill	0.05	✓	0.00	✓	0.56	X	0.00	✓	0.84	X	0.83	X
Polysatin Heavy	0.00	✓	0.00	✓	0.00	✓	0.00	✓	0.00	✓	0.00	✓
Cotton Duck	0.00	✓	0.00	✓	0.00	✓	0.00	✓	0.01	✓	0.44	X

Table 36: Student t-tests were performed to attain the significance of the results obtained when we compare both washing techniques; hand and machine. N = 5**.**

Overall it is observed that washing detergents increase the size of the bloodstains in any form, however this effect seems to be more apparent when incorporating a certain washing technique (*i.e.* machine wash).

5.7.2.2 Dry Cleaning

Since some of the fabrics would ordinarily require dry cleaning as they are too delicate to wash in the machine or by hand, dry cleaning was employed for selected fabrics to investigate the effects. Fuji Silk, Chiffon Silk, Wool Mix Suiting, Silk Dupion, Medium Habotai Silk and Wool Delaine were examined, each was dry cleaned at the shop Tumble Dwyers in Bolton using a standard method. [223]
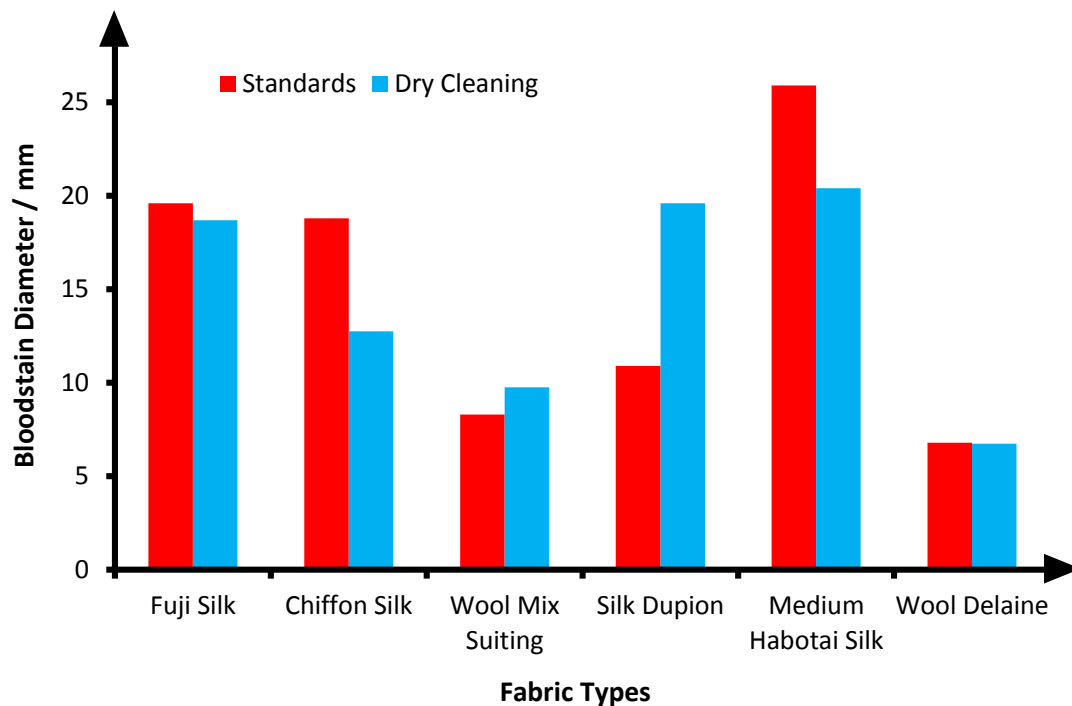
Figure 126: Comparison of diameter of bloodstains on non-laundered (standard) fabrics and fabrics after dry cleaning. N = 5

Figure 126 depicts the difference in bloodstain diameter after dry cleaning compared to the standard with plain fabric. It is evident that dry cleaning has a profound effect on the fabric, leading to both smaller and larger bloodstain diameters dependent on the fabric type. If these results are compared to those obtained when either machine or hand washing was employed we find that they follow exactly the same trend. However, it would be expected that these results would eventually alter if repeated cycles or use of the harsher washing techniques (machine) were constantly utilised.

5.7.2.3 Drying Techniques

Three different types of drying methods were examined; air dry (line), radiator dry (dial 3) and tumble dry (40°C for 1 hour). Fabrics were hand washed with no detergent so any changes to the diameter would be directly related to the drying method. Drop tests were performed at 50cm (see section 2.2). The most significant results were obtained when radiator dry was compared with tumble drying (Table 37), showing that it is not necessarily the heat that changes the fabric significantly. Higgins *et al* [224] validates this finding stating that, 'it is the tumbling action in the tumble dryer which has the greatest influence on the dimensional stability and distortion.' [224] Tumble drying generally produced smaller stains for most of the fabric types, indicating that the tumble action causes a shrinkage in the fabric therefore producing smaller bloodstains. It is also possible that the tumbling action disrupts the wetting capabilities of the fabric, therefore changing the absorbency and overall spread of the blood drop. Air drying produced results most similar to the original unwashed fabric, this was an expected result as unlike radiator drying; which dries the fabric with rapid heat and tumble drying; which uses a combination of heat and tumble action, air drying relies on the fabric drying naturally and therefore interferes with the fabric less.

Type of Fabric	p value Air vs. Rad	Significant Yes (✓) or No (x)	p value Air vs. Tumble	Significant Yes (✓) or No (x)	p value Rad vs. Tumble	Significant Yes (✓) or No (x)
Jupiter Linen	0.00	✓	0.00	✓	0.01	✓
Raised Natural Cotton	0.01	✓	0.00	✓	0.02	✓
Fuji Silk	0.00	✓	0.69	x	0.04	✓
Heavyweight Cotton	0.81	x	0.23	x	0.21	x
Cotton Jersey Ecru	0.03	✓	0.00	✓	0.23	x
Wool Mix Suiting	0.00	✓	0.02	✓	0.10	x
Wool Delaine (bleached)	0.02	✓	0.00	✓	0.05	✓
Poly/linen/rayon Pandora Devore	0.03	✓	0.08	✓	0.01	✓
Peasant Cotton	0.02	✓	0.00	✓	0.00	✓
Resida Bump Cotton	0.00	✓	0.00	✓	0.05	x
Silk Dupion	0.01	✓	0.00	✓	0.01	✓
Silk Chiffon	0.40	x	0.00	✓	0.00	✓
Denim	0.06	x	0.00	✓	0.00	✓
M&S T-Shirt Jersey	0.00	✓	0.00	✓	0.01	✓
Cotton Duck	0.04	✓	0.00	✓	0.32	x
Medium Habotai Silk	0.00	✓	0.00	✓	0.84	x
Light Grey Polyester Twill	0.00	✓	0.00	✓	0.00	✓
Polysatin Heavy	0.60	x	0.12	x	0.01	✓
Cotton Poplin	0.21	x	0.00	✓	0.00	✓

Table 37: A comparison of the results produced when different drying techniques were employed; a student t-test was used to determine significance. N = 5

This result is supported by the method (section 8A of BS EN ISO 6330/A1:2009) [55] used by many researchers to stabilise fabrics, where the drying process stipulates 'air dried flat.'[55]

It is noted that heavyweight cotton exhibits no change regardless of the drying procedure, this is most likely due to the composition. A twill weave (heavyweight cotton structure) is a looser weave than a plain weave, therefore ay manipulation of the fabric my result in a significant change in the way the fabric behaves (*i.e.* absorbency).

5.7.2.4   Machine Washing Temperatures

The temperature at which we wash our clothes will depend very much on the type of fabric being washed and the degree of soiling. Most clothing is washed between 30°C and 40°C and for the most soiled clothes the temperature is increased up to 60°C as recommended by the fabric manufacturers. All fabrics (excluding nylon) were washed at 30°C, 40°C and 60°C without detergent so the effects of temperature could be solely explored.
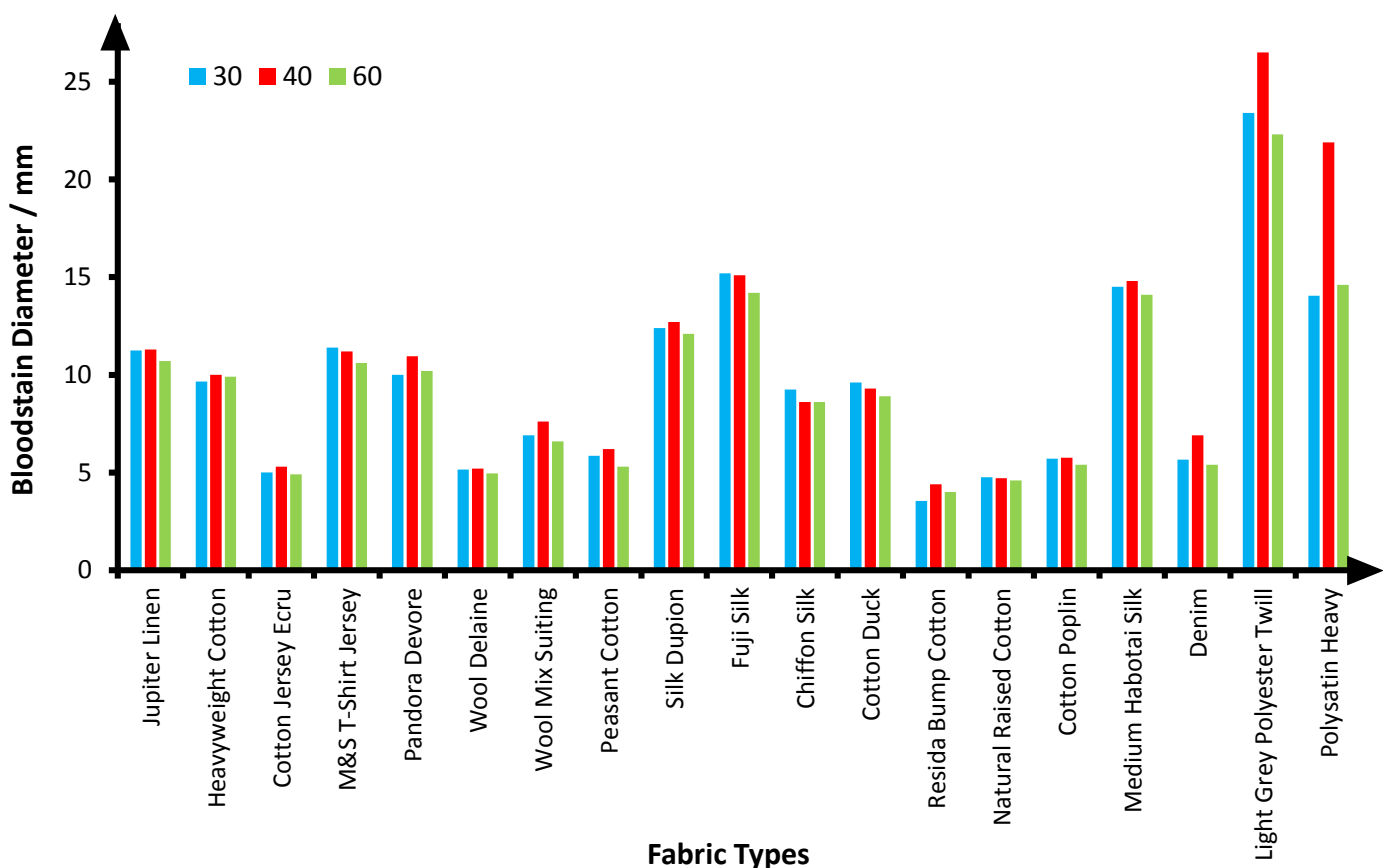
Figure 127: A representation of the average bloodstain diameters created when blood impacted fabrics washed at 3 different temperatures; 30°C, 40°C and 60°C. *N = 5.*

Figure 127 depicts the outcomes of the various temperatures on each fabric type. The majority of the fabrics exhibited a distinct pattern, where the bloodstain diameter increased at 40°C and then decreased when the fabric was washed at 60°C. A possible explanation for this is the impact of the heat on the fabric, causing the fabric to expand and then shrink at higher temperatures.

Type of Fabric	p value 30 °C V 40 °C	Significant Yes (✓) or No (x)	p value 30 °C V 60 °C	Significant Yes (✓) or No (x)	p value 40 °C V 60 °C	Significant Yes (✓) or No (x)
Jupiter Linen	0.84	X	0.07	X	0.03	✓
Heavyweight Cotton	0.00	✓	0.13	X	0.58	X
Cotton Jersey Ecru	0.09	X	0.43	X	0.04	✓
M&S T-Shirt Jersey	0.36	X	0.00	✓	0.01	✓
Pandora Devore	0.00	✓	0.43	X	0.00	✓
Wool Delaine	0.71	X	0.22	X	0.10	X
Wool Mix Suiting	0.01	✓	0.23	X	0.00	✓
Peasant Cotton	0.27	X	0.06	X	0.00	✓
Silk Dupion	0.54	X	0.55	X	0.18	X
Fuji Silk	0.82	X	0.03	✓	0.03	✓
Chiffon Silk	0.01	✓	0.02	✓	1.00	X
Cotton Duck	0.26	X	0.02	✓	0.1	X
Resida Bump Cotton	0.00	✓	0.01	✓	0.01	✓
Natural Raised Cotton	0.81	X	0.46	X	0.64	X
Cotton Poplin	0.79	X	0.15	X	0.09	X
Medium Habotai Silk	0.48	X	0.30	X	0.12	X
Denim	0.00	✓	0.27	X	0.00	✓
Light Grey Polyester Twill	0.00	✓	0.07	X	0.00	✓
Polysatin Heavy	0.00	✓	0.30	X	0.00	✓

Table 38: Statistical analysis (student t-test) comparing *p* values for three temperatures. N = 5

Statistical analysis was performed (see Table 38) using an unpaired student t-test, it is evident that most fabrics experienced a significant change around 40º C and stabilised at 60ºC.

Since temperature clearly has an effect on the fabric it is important to consider this in reconstructions, especially as the effect is not predictable; sometimes increasing the crime scene bloodstain diameters and other times decreasing depending on fabric type.

5.7.2.5   Repeated Cycles

The International Organisation for Standardisation [55] states that the fabric becomes standardised after 6 continuous cycle washes, therefore this has been incorporated as the "norm" when other analysts have conducted work on fabrics. [44-48] Here this theory is tested, extending the number of cycles to 10 and testing with and without detergent.

Table 39 shows the progression of cycles without detergent, Table 40 expresses these changes as p values after unpaired student tests were performed.

No. of cycles	Average diameter of bloodstains (mm)									
	Peasant Cotton	Poly/ Linen/ Rayon Pandora Devore	Poly Satin Heavy – Primary ring	Poly Satin Heavy – Secondary ring	Raised Natural Cotton	Resida Bump Cotton	Silk Chiffon	Silk Dupion	Wool Delaine	Wool Mix Suiting
0	5	11.9	8.6	15.6	4	4.9	11.6	11.8	0.64	8
1	5.8	11.2	10.2	16.8	4.7	5	10	12.2	5.8	8.2
2	5.7	11	10.4	16.8	4.8	4.5	9.8	11.8	5.7	7.7
4	5.2	11	9.8	15.6	5.1	4	9.7	11.4	5.5	7.7
6	5.2	11	8.4	12.7	5	4	9.6	11	5.1	7.2
8	5.2	10.8	7.4	10.3	5	4	8.9	10.8	5.1	7.1
10	5	10.6	7.8	11.5	4.9	4	8.3	10.5	4.9	6.9

No. of cycles	Average diameter of bloodstains (mm)									
	Cotton Duck	Cotton Jersey Ecru	Cotton Poplin	Denim	Fuji Silk	Heavy-weight Cotton	Jupiter Linen	Polyester Twill – Primary ring	Polyester Twill – Secondary ring	M&S T-Shirt Jersey	Medium Habotai Silk
0	10.4	4.5	5	6.6	19.9	11.6	11	13.7	22.2	10.6	20.6
1	9.5	5	5.9	7.2	15.9	11.9	12.4	13.4	22.2	8.7	16.8
2	9.5	4	5.8	6.6	15	10.9	11.6	12.2	22	9	16.4
4	9.4	4	5.7	6.7	14.4	10	11.6	12.2	21.8	8	16
6	9.4	4	5.6	6.7	14.4	10	11.2	13.2	22.4	7.2	14.9
8	9.3	4	5.6	6.4	14.2	10	11	12	22.4	7	15.4
10	9.1	4	5.6	6.3	14.3	10	10.6	12.2	22.2	6.8	15.4

Table 39: Average bloodstain diameters on 19 fabrics for up to 10 cycles without the use of detergent.

Type of Fabric	p value standard vs. 1 cycle	Sig. Yes (✓) or No (x)	p value standard vs. 2 cycles	Sig. Yes (✓) or No (x)	p value standard vs. 4 cycles	Sig. Yes (✓) or No (x)	p value standard vs. 6 cycles	Sig. Yes (✓) or No (x)	p value standard vs. 8 cycles	Sig. Yes (✓) or No (x)	p value standard vs. 10 cycles	Sig. Yes (✓) or No (x)
Jupiter Linen	0.00	✓	0.04	✓	0.04	✓	0.61	X	1.00	X	0.14	X
Chiffon Silk	0.00	✓	0.00	✓	0.00	✓	0.00	✓	0.00	✓	0.00	✓
Fuji Silk	0.00	✓	0.00	✓	0.00	✓	0.00	✓	0.00	✓	0.00	✓
Medium Habotai Silk	0.00	✓	0.00	✓	0.00	✓	0.00	✓	0.00	✓	0.00	✓
Peasant Cotton	0.00	✓	0.01	✓	0.35	X	0.35	X	0.35	X	1.00	X
Heavyweight Cotton	0.29	X	0.08	X	0.00	✓	0.00	✓	0.00	✓	0.00	✓
Cotton Poplin	0.01	✓	0.00	✓	0.01	✓	0.04	✓	0.04	✓	0.04	✓
Resida Bump Cotton	0.35	X	0.14	X	0.00	✓	0.00	✓	0.00	✓	0.00	✓
Raised Natural Cotton	0.01	✓	0.00	✓	0.00	✓	0.01	✓	1.00	X	0.00	✓
Denim	0.06	X	1.00	X	0.72	X	0.74	X	0.53	X	0.42	X
Pandora Devore	0.01	✓	0.00	✓	0.03	✓	0.00	✓	0.00	✓	0.00	✓
Cotton Jersey Ecru	0.01	✓	0.01	✓	0.06	X	0.01	✓	0.01	✓	0.01	✓
M&S T-Shirt Jersey	0.01	✓	0.03	✓	0.00	✓	0.00	✓	0.00	✓	0.00	✓
Silk Dupion	0.47	X	1.00	X	0.49	X	0.07	X	0.06	X	0.04	✓
Wool Delaine	0.06	X	0.03	✓	0.01	✓	0.00	✓	0.00	✓	0.00	✓
Wool Mix Suiting	0.35	X	0.04	✓	0.35	X	0.00	✓	0.01	✓	0.00	✓
Cotton Duck	0.03	✓	0.03	✓	0.02	✓	0.02	✓	0.01	✓	0.01	✓
Polysatin Heavy	0.05	X	0.02	✓	1.00	X	0.00	✓	0.00	✓	0.00	✓
Light Grey Polyester Twill	0.45	X	0.17	X	0.13	X	0.33	X	0.35	X	0.23	X

Table 40: Student t-tests (standards vs. cycle number) performed to attain significance of results for repeated cycles without detergent. $N = 5$

Using both (detergent and repeated cycles) a change is observed in all the fabrics but the Light Grey Polyester and the Denim, where persistent washing had no effect on the size of the bloodstain. A pattern was apparent when the bloodstain sizes were analysed, as the cycle number increases the bloodstain diameter decreases. It is noted that most but not all fabrics stabilise after 6 continuous cycles, where polysatin and chiffon silk exhibit significant changes between the sixth and tenth cycle when statistical analysis was performed. However we acknowledge that chiffon silk would be dry cleaned ordinarily so would not be expected to stabilise at all when machine washed. Using the characteristics table (Table 23) these changes in bloodstain diameter can be affiliated with the composition of the fabric. For example the fabrics with tight plain weaves (*i.e.* Peasant Cotton etc.) or tight twill weaves (*i.e.* Light Grey Polyester Twill, Denim etc.) tended to either not change at all or stabilise much quicker after continuous cycles. This is important when scene reconstructions are attempted since history of the fabric (wash history) will most likely be unknown. Finding the stable point for a fabric provides a maximum change which the fabric will experience, thus providing limits and a standard error in which to base final conclusions on.

No. of cycles	Average diameter of bloodstains (mm)										
	Cotton Duck	Cotton Jersey Ecru	Cotton Poplin	Denim	Fuji Silk	Heavy-weight Cotton	Jupiter Linen	Polyester Twill - Primary	Polyester Twill – Secondary	M&S T-Shirt Jersey	Medium Habotai Silk
0	10.4	4.5	5	6.6	19.9	11.6	11	13.7	22.2	10.6	20.6
1	9.5	4	6.4	7.4	15.8	10.9	12.3	13.5	23.6	10.8	17.2
2	10.2	4.2	6.6	8.2	15.8	11	12.4	13.6	22.4	10.8	18.3
4	10.4	4.5	7.1	8.4	15.8	11	12.8	13.4	22	10.8	18.8
6	10.4	5.3	8.4	8.4	16.2	11	12.6	14.4	23	10.8	19
8	10.4	5.5	8.9	8.6	16.5	11.2	12.8	14.6	23.4	10.8	18.8
10	10.5	6.1	9.6	8.8	16.6	11.3	13.4	15	23.6	11	19

No. of cycles	Peasant Cotton	Poly/ Linen/ Rayon Pandora Devore	Poly Satin Heavy - Primary	Poly Satin Heavy - Secondary	Raised Natural Cotton	Resida Bump Cotton	Silk Chiffon	Silk Dupion	Wool Delaine	Wool Mix Suiting
0	5	11.9	8.6	15.6	4	4.9	11.6	11.8	6.4	8
1	7.1	11.2	10.4	16.5	4.4	4.7	10	14.8	6.1	10
2	7.9	12	12.2	18	5	4.9	10.6	8.2	6.2	10.2
4	8.6	12.2	12.2	18.8	6.1	5	11	8.4	6.3	10.4
6	8.6	12.4	11.2	19	6.2	5	11	12.8	6.4	10.6
8	10.2	12.5	12	18.2	6.3	5.1	11.2	14.6	6.3	10.7
10	10.2	12.4	12.4	17.8	7	5.2	11.2	15.8	6.2	11

Table 41: Average bloodstain diameters on 19 fabrics for up to 10 cycles with the use of detergent. N = 5

Next the effect continuous cycles had when detergent was added was investigated; surf powder detergent was added after every cycle as it would be in real life. Table 41 shows the changing in bloodstain diameters as the number of cycles with detergent increases. Conversely to the results found without detergent when detergent is added, in most cases, bloodstains appear to increase in size. It is not known why this occurs, a possible explanation is the build-up of an enzymatic or surfactant layer on the surface from the detergent which maybe altering the degree of wetting and wicking. This steady increase in bloodstain diameter is expected, considering the results exhibited for the initial tests in the detergent form and type section. Again statistical analysis was performed in the form of unpaired student t-tests expressed in Table 42, showing that the increasing of cycles (with detergent) significantly increases the bloodstain diameter. It is noted that in some instances (*i.e.* Fuji Silk, Wool Mix Suiting etc.) the diameters decreased then steadily increased and four fabrics (Light Grey Polyester Twill, M&S T-shirt Jersey, Resida Bump Cotton and Wool Delaine) were found not to change significantly at all (although diameters did increase). Further statistical analysis was implemented to establish fabric stability after 6 cycles, where the sixth cycle results were compared to the tenth cycle. It was determined that most fabrics were stable after 6 cycles, where no significant diameter changes were experienced, however 6 fabrics continued to significantly increase in diameter.

Type of Fabric	p value standard vs. 1 cycle	Sig. Yes (✓) or No (x)	p value standard vs. 2 cycles	Sig. Yes (✓) or No (x)	p value standard vs. 4 cycles	Sig. Yes (✓) or No (x)	p value standard vs. 6 cycles	Sig. Yes (✓) or No (x)	p value standard vs. 8 cycles	Sig. Yes (✓) or No (x)	p value standard vs. 10 cycles	Sig. Yes (✓) or No (x)
Jupiter Silk	0.00	✓	0.00	✓	0.00	✓	0.00	✓	0.00	✓	0.00	✓
Chiffon Silk	0.00	✓	0.07	X	0.27	X	0.27	X	0.24	X	0.24	X
Fuji Silk	0.00	✓	0.00	✓	0.00	✓	0.00	✓	0.00	✓	0.00	✓
Medium Habotai Silk	0.00	✓	0.00	✓	0.05	✓	0.01	✓	0.00	✓	0.01	✓
Peasant Cotton	0.00	✓	0.00	✓	0.00	✓	0.00	✓	0.00	✓	0.00	✓
Heavyweight Cotton	0.03	✓	0.04	✓	0.04	✓	0.04	✓	0.18	X	0.37	X
Cotton Poplin	0.00	✓	0.00	✓	0.00	✓	0.00	✓	0.00	✓	0.00	✓
Resida Bump Cotton	0.40	X	1.00	X	0.61	X	0.35	X	0.37	X	0.09	X
Raised Natural Cotton	0.07	X	1.00	X	0.00	✓	0.00	✓	0.00	✓	1.00	X
Denim	0.03	✓	0.00	✓	0.00	✓	0.00	✓	0.00	✓	0.00	✓
Pandora Devore	0.01	✓	0.35	X	0.46	X	0.10	X	0.01	✓	0.10	X
Cotton Jersey Ecru	0.01	✓	0.27	X	1.00	X	0.01	✓	0.02	✓	0.00	✓
M&S T-Shirt Jersey	0.72	X	0.72	X	0.76	X	0.72	X	0.72	X	0.52	X
Silk Dupion	0.00	✓	0.00	✓	0.00	✓	0.05	✓	0.00	✓	0.00	✓
Wool Delaine	0.20	X	0.49	X	0.72	X	1.00	X	0.67	X	0.49	X
Wool Mix Suiting	0.00	✓	0.00	✓	0.00	✓	0.00	✓	0.00	✓	0.00	✓
Cotton Duck	0.03	✓	0.54	X	1.00	X	1.00	X	1.00	X	0.77	X
Polysatin Heavy	0.09	X	0.00	✓	0.00	✓	0.00	✓	0.00	✓	0.00	✓
Light Grey Polyester Twill	0.67	X	0.33	X	0.14	X	0.82	X	0.80	X	0.62	X

Table 42: Student t-tests (standards vs. cycle number) performed to attain significance of results for repeated cycles with detergent. $N = 5$.

Fabric characteristics were investigated as possible cause for these changes, there was found to be no relation between fabric characteristics (weave/knit, porosity, thickness and roughness) and stability of continuously washed fabric.

5.7.3 Summary

During this study the effects various fabrics types, washing and drying techniques, detergent type, temperature and number of cycles has on bloodstains, namely their size.

This study has revealed some important findings, which are pertinent to the interpretation of bloodstain on fabrics. It was found that although neither the detergent type nor form has a significant effect on the bloodstains produced the techniques used to wash and dry the fabrics are highly influential in the stains final appearance. Both machine washing and tumble drying offered the most significant differences to the original (untouched fabric) values, this may be attributed to the degree of agitation experienced in both these techniques which lead to fabric distortion, i.e. shrinking.

Other factors which were found to have a determinant effect on the final bloodstain was the number of cycles. For both with and without detergent were tested and found converse results. When detergent was not used the size of the bloodstain decreased and when detergent was added for each cycle the size increased accordingly. These changes can be attributed to the degree of wettability which is likely effected by the surfactants/enzymes found in washing detergents.

Temperature was also discovered to have a marked effect on the size of the bloodstains produced. As higher temperatures tend to cause a shrinkage in the fabric smaller stains resulted, though this was not apparent in all fabrics, where exhibited larger stains.

The overwhelming factor which attributed to most of the bloodstain changes was the fabric type. Since all fabrics are different; in composition, thickness, porosity, wettability etc. it is impossible to predict or obtain a recognisable pattern of change which encompasses all fabrics. This is why it is important for analysts to try to match the evidence fabric as close as possible when running tests. The problem that this work now highlights is the fabric history, which will usually be unknown. For instance if the fabric has a history of being machine washed at high temperatures then tumble dried, how will this affect the ability to interpret the patterns exhibited effectively? Clearly such important issues need to be considered in the field of bloodstain pattern fabric analysis where misinterpretation can lead to errors that can be costly, and bring the field of BPA into disrepute.

5.8 CONCLUSIONS

The final section has investigated the effects of surface manipulation on the final bloodstain.

Much research has focused on environmental effects such as rain, UV etc. [73] on the final bloodstain, where researchers have neglected the more apparent bloodstain manipulation potential, which is present in our homes. Blood can impinge on many surfaces, which are not only different in type of material but can possess changes imparted by humans such as the heating or cleaning of a surface.

The first part of this section focuses on the effects of heat, both high and low temperatures.

Firstly, underfloor heating was evaluated. Three surface types were investigated; stone, tile and wood. Since all three can become very cold, especially in the winter, the practice of underfloor heating has become ever more present in the household, providing a cost-effective and efficient way of heating room. Surfaces were heated to a maximum temperature of 40°C as underfloor does not reach more than 32°C ordinarily. All surface types showed no significant changes when surfaces were heated, though some of the rougher surfaces (*i.e.* matt ceramic tile) presented an affinity to blood, producing larger stains. This is thought to be associated with the ability of rougher surfaces to absorb heat more efficiently compared to polished surfaces. In turn, this is thought to decrease the viscosity and ultimately alter the size of the bloodstain produced.

Secondary analysis was performed on the underfloor heating studies as observations found stains to appear much darker after impacting a heated surface. Since previous aging studies have focused on the colorimetry of bloodstains it was important to investigate the potential for heat to prematurely age bloodstains. A spectruino (portable UV spectrophotometer) was utilised for this preliminary analysis. Results showed that there was an increase in absorbance as surface temperature increased and the stains got darker. This result mimicked that which occurs when a bloodstains age. Although this is only preliminary analysis it was thought important to perform these secondary experiments to ensure that factors such as heat are accounted for as the application of bloodstain age analysis develops.

The next heated study focused on high surface temperatures that would be experienced if blood impinged on a radiator or hot stove. The temperatures used were associated with the boiling curve and its regimes (nucleation, natural convection, transition and film boiling). The boiling curve was found to fit the heating of blood with a slight temperature change, where regimes appear earlier. Bloodstains increased in diameter, due to heats effect on viscosity, then decreased after 90° C where evaporation commenced. There were several observable influences heat had on the final bloodstain, the main being the production of a secondary ring, where blood separated into its components and yielded a reduction constant (C_d ^{heated}). Heat was concluded to affect the size and appearance of bloodstains, where bloodstains had a distinct appearance dependent on surface temperature, this could be used in crime scene scenarios to predict surface temperature at the time of impact.

A further study investigated the effect surface temperature had on the efficiency of DNA extraction, this was further expanded to include surface cleaning. Due to popular TV shows and the public's growing knowledge of evidence forms, cleaning has become a popular crime evasion technique, where evidence is simply wiped away. Results showed that temperature had some effect on the ability to amplify and extract DNA, decreasing the amount of viable DNA available for extraction as temperature increased. Bleach was the most efficient method of DNA removal when presumptive testing was examined, where TMB was evaluated to be the best presumptive test method when cleaning is suspected. All types of cleaning, even plain water, removed DNA when evaluated using salt extraction with PCR and silica extraction with real-time PCR. Evaluating the effectiveness of cleaning is difficult since in a real crime scene environment it is expected that people will clean a surface differently, *i.e.* more thorough, in a rush *etc.* therefore less controlled than the experiment.

Last a final study demonstrating the different technique of fabric cleaning and drying was performed. Here detergent type and form, washing technique (machine, hand), drying technique (air, radiator, tumble dryer), repeated cycles and temperature were all investigated for their effects on blood impaction. Blood drop tests were performed on 20 fabric types. Detergents significantly increased the size of the bloodstain produced, possibly a result of the build-up of surfactant effecting the surface tension of the surface. Secondary rings occurred on polyester and silk fabrics resulting in constants for the diffused secondary ring. Tumble drying and machine washing yielded significant changes to the bloodstain size, though these changes did not follow

a discernible pattern. Repeated cycles were evaluated both with and without detergent; fabric stability was found for most fabrics at 6 cycles. Higher temperatures (washing machine) were found to result in a reduction in the bloodstain diameter. The results found during these experiments show that many factors should be considered when evaluating bloodstains on a fabric. Pre-treatment is an important factor, although it is unlikely this information will be available to the analyst, it is imperative that analysts consider certain possibilities and make adjustments accordingly (*i.e.* determine limits of change/ test fabric stability).

Overall this section has proven that we ourselves can manipulate surfaces, whether intending to or not. Although it is not possible to account for and test all viable scenarios, the observations made in this work highlight how everyday tasks such as cleaning or cooking could inadvertently alter the way blood behaves when it impacts a surface. These factors have not previously been considered and should draw analyst's attention to surface importance, not only what it is made from but its condition and history of use.

6. OVERALL CONCLUSIONS

 This thesis was presented in three main parts; blood (composition), impact surfaces and surface manipulation. The purpose of this research was to broaden the field of study concerning the interaction of blood with surface and introduce quantitative techniques of analysing bloodstains.

To accomplish this, blood alone was considered first. One of the main issues with blood is its complexity. This is especially important when trying to reconstruct events using experimentation. Blood generally follows the laws of physics in flight, the way it spreads and interacts with a surface can depend on its components.

During this thesis, research was conducted on packed cell volume which represents the ratio of red blood cells to plasma content in whole blood. The importance of this characteristic is its significant effect on viscosity, effectively increasing viscosity as PCV% increases and vice versa when decreased. Since PCV% is altered in the body, during physical activity, pregnancy, illnesses and drug use it would stand to reason that there is ample probability a range of PCV% may be encountered during a blood shedding incident. Two studies considering the effects of PCV% were performed, firstly PCV% was investigated relating to angle of impact and single stain analysis; secondly, drying mechanisms were studied where PCV% was manipulated to observe drying behaviour and estimation of drying volume. Overall PCV% was found to significantly affect bloodstain interpretation in both studies. The increasing of PCV (to around 75%) produced smaller bloodstains, due to the increase in viscosity and subsequent resistance to flow and spread. This effect did not carry through to the angled impacts, since the spread would be even in both dimensions, length and width, therefore any alteration is cancelled out. Drying studies showed a change in drying mechanism depending on PCV%, where smaller PCVs exhibited a purely coffee ring driven drying process compared to higher PCV% which dried by a Marangoni effect. Volume analysis was also performed where the introduction of PCV% to the current methods of analysis resulted in unreliability. Most volume analysis relies on weight or spread, since PCV% causes an increase/decrease in viscosity this effects spread and therefore this becomes an unreliable method of volume analysis. The alteration in PCV% will also increase/decrease the water content, according to the amount of

plasma present, this in turn effects evaporation, which subsequently alters the weight of the remaining bloodstain.

In conclusion it has been shown that PCV% is a vital component in BPA, not only altering patterns and stain size but disrupting the drying mechanism and refuting current volume analysis methodology.

The second part of this thesis focused on surface interactions, since blood can interact with a number of surfaces during a crime scene scenario it is important to evaluate these surfaces to a greater extent. The first study evaluated angled impacts on a multitude of surfaces where recently derived equations were adjusted for three surface types. This study highlighted the need for further exploration into surface properties, since three separate equations were needed for each surface type. For the preceding studies, surfaces were explored for their individual properties, namely surface roughness, porosity and composition. Four surface types were assessed; fabric, wood, metal and stone/tile. Surfaces were characterised using SEMs, roughness testers and absorption testers. All surfaces reacted differently to the impacting of blood. Wood, stone/tile and fabric significantly altered the spread factor of blood, in most cases (apart from some fabric) increasing the spread. Surface roughness was the leading cause of this alteration, the friction disrupted the blood flow in cases of high surface roughness which produced smaller bloodstains. Volume of blood was a major factor when stone surfaces were considered, due to the absorptive properties of stones. When larger volumes of blood were deposited onto the surface, surface roughness was, in some instances, overcome, therefore producing larger stains.

Thickness of the surface in fabric analysis was found to be the overriding factor on the final stain size produced. This is likely attributed to the porosity of fabrics, where fabrics act like filter paper. This leads blood to seep through thinner surfaces and spread when porosity is high; compared to thicker fabrics, which produce a smaller more stable stain which does not spread.

Though surface roughness in most instances was found to be the main factor effecting stain size, standard equations could not be created. Roughness was not comparable between surfaces *i.e.* a stone surface with the same roughness as a metal surface did not produce the same size resultant bloodstain. Therefore pointing to multiple factors contributing to the final stain size.

The evaluation of surfaces has taught that it is surface roughness which is the important characteristic of a surface and that it is important when considering crime scene reconstruction, to specifically use the surface encountered at the scene of crime. If this option is not available the first provision should be to test the same surface type (*i.e* wood) with the exact or near as possible surface roughness exhibited on the scene sample.

The last part of this thesis evaluated the effect of surface manipulation on BPA. Two types of surface manipulation were analysed; heat and cleaning. Heated surfaces are available in abundance around our houses, work places and public domains (*i.e.* radiators, underfloor heating). Heated surfaces had not been approached in terms of effects on BPA, where research focused on effects on DNA or fire damage. Two heat focused studies were conducted, firstly underfloor heating was evaluated on common surface types where surfaces were heated to a maximum of 40°C. The second study analysed much higher temperatures (up to 250°C) where results were fitted to boiling curve, established for the analysis of water pool boiling.

The first study found no significant changes in bloodstain diameter when surface temperature was increased, however there was an apparent change in bloodstain appearance. Bloodstains became darker as surface temperature increased, further analysis was undertaken using a spectrophotometer to evaluate the changes. Current developing methods of age analysis use spectrophotometry to estimate the age of a bloodstain, relying on the colour of the bloodstain. It was put forward that increasing surface temperature gives the impression of prematurely aging the bloodstain, this was supported by the preliminary analysis conducted in this study. There was an increase in absorbance as the stain darkened (surface temperature increased), this was similar to the effect exhibited when stains age. This observation is significant since aging techniques are in the early stages of development it is important to highlight potential flaws which may affect the overall reliability of the method.

The second study focused on the boiling regimes of liquid. Surfaces were heated up to temperatures of 250°C and blood drop tests were performed to establish any effects on stain size and appearance. Stains were found to increase in size when temperature increased up to 60°C, this is due to the increase in viscosity when heated. Stains then decreased after 60°C where evaporation would ensue, effectively decreasing water content significantly and subsequently decreasing stain size. Bloodstains fit into the boiling curve but at slightly lower temperatures, since 83% of blood is water this result

was expected. The appearance of the bloodstain for each boiling regime was recognisable, where reduction rings appeared at natural convection boiling regime and an evaporation constant could be established. Further rings were tangible in the nucleate boiling regime and blood appeared cooked and flaky in the transition boiling regime. The ability to distinguish between regimes by sight alone means it would be possible to estimate a surface temperature from the appearance of the bloodstain.

The second part of this section was cleaning. Two studies were conducted, firstly, following the heated surface study the effectiveness of DNA extraction was analysed when both heat and cleaning were applied in conjunction with one another. Secondly, fabric cleaning was evaluated, where detergent types, washing techniques, drying techniques, repeated cycles and temperature were analysed.

The first study employed several methods of cleaning alongside the surface temperatures discussed in the boiling curve experiments. The effectiveness of cleaning in conjunction with heat was evaluated using presumptive testing, DNA extraction and DNA quantifying. TMB was found to be the best form of presumptive testing compared to luminol and Kastle-Meyer. Bleach was the most effective way of cleaning a surface when presumptive testing was used, giving the most negative results, indicating no trace of blood. Temperature did not affect the ability to extract DNA from bloodstains, however it did significantly decrease the amount of viable DNA available for extraction. All types of cleaning removed DNA, even water. It is important to note that cleaning is a difficult area to fully evaluate the effectiveness of since not everybody cleans the same, further studies using a range of different types of cleaners could be used to establish if it is the solvents themselves which dictate the absence of DNA or way it was cleaned *i.e.* rigorous.

The last study of this research was conducted on fabric cleaning. Fabric in itself is a difficult surface to analyse, where distortion of stains is often associated. A current method of stabilising fabrics was used [50] where fabrics no longer change significantly in structure after six repeated cycle washes, this was evaluated in terms of BPA. Detergents were found to significantly increase the size of bloodstains, this is associated with the surfactant layer, which is likely to be present on the surface of the fabric, therefore changing the surface tension of the fabric. Secondary rings were discovered on silk and polyester fabrics, further testing showed this to be the case for all polyester and silk fabrics, therefore a constant accounting for the reduction (secondary) ring was formulated. Fabrics stabilised after 6 repeated cycles, though

this was not the case for all fabrics. Using the washing machine and tumble dryer led to the most stain distortion, where fabric fibres shrunk. This comprehensive study highlighted the issues with fabric pre-treatment, since most literature focuses on the removal of stains and concealing of evidence this work has offered some novel insights, emphasizing the importance of surface condition and history.

Overall this work did give an insight into some important aspects previously unexplored within BPA, particularly PCV% and the effects of surface manipulation. Although standard equations which encompassed all variables could not be formulated, this work has highlighted where provisions need to be made when conducting analysis and that it is not as simple as measuring a bloodstain. This research offers a groundwork for further work to be conducted, introducing more surface types, which may offer greater insights and will hopefully lead to a more scientifically based discipline which can no longer be considered as subjective.

7. FUTURE WORK

The complex nature of blood and the insurmountable number of environments in which blood can be imparted, means there is still much research to be conducted before a full understanding is established.

This research has focused on some fundamental parameters of blood; changing the ratio of its components to manipulate the flow resistance. Future works could focus on red blood cells, where deformation due to disease (*i.e.* sickle cell anaemia) could be a factor. The drying study (section 3.4) showed that shape of the red blood cells (*i.e.* sphere to elongate) is important when considering the mechanism of drying liquids and thus changes could alter the way blood dries.

Further studies could also include the coagulation mechanism present in blood. The blood used throughout this work contained anticoagulant or had the fibrin removed to prevent coagulation.

The surface analysis conducted in this work only scraped the surface of the types and conditions of available surfaces. Other important surface interaction, which would be useful to explore, are carpet, leather, plastic, paper and hydrophobic or hydrophilic surfaces. It would also be beneficial to carry out further analysis regarding heat and other conditions which may alter the apparent age of a bloodstain.

8. PUBLICATIONS

Larkin, Bethany AJ, and Craig E. Banks. "Preliminary Study on the Effect of Heated Surfaces upon Bloodstain Pattern Analysis." *Journal of forensic sciences* 58, no. 5 (2013): 1289-1296.

Larkin, Bethany AJ, Meerna El-Sayed, Dale AC Brownson, and Craig E. Banks. "Crime scene investigation III: Exploring the effects of drugs of abuse and neurotransmitters on Bloodstain Pattern Analysis." *Analytical Methods* 4, no. 3 (2012): 721-729.

Larkin, Bethany AJ, and Craig E. Banks. "Bloodstain pattern analysis: looking at impacting blood from a different angle." *Australian Journal of Forensic Sciences* 45, no. 1 (2013): 85-102.

Larkin, Bethany AJ, and Craig E. Banks. "Exploring the implications of Packed Cell Volume upon Bloodstain Pattern Analysis." CSEye e-magazine. http://stage.cseye.fss.stage.ap16.com/content/2014/february/research/pc%20volume

Larkin, Bethany AJ, and Craig E. Banks, "Exploring the applicability of equine blood to bloodstain pattern analysis." *Med Sci Law*, doi: 10.1177/0025802414542456, In Press

9. REFERENCES

E. Locard, La police et les méthodes scientifiques, Editions Rieder, Paris, 1934.

Z. Erzinclioglu, Every Contact Leaves a Trace: Scientific Detection in the Twentieth Century, 1st ed., Carlton Books; London UK, 2001.

W. J. Tilstone, Forensic Science: An Encyclopedia of History, Methods, and Techniques, 1st ed. ABC-CLIO; USA, 2004.

S. H. James, P. E. Kish, and T. P. Sutton, Principles of Bloodstain Pattern Analysis: Theory and Practice, CRC Press, Taylor and Francis Group, USA, 2005.

M. A. Raymond, Australian J. Forensic Sci. 2000, 32, 41.

T. Raymond, Australian J. Forensic Sci. 1997, 29, 69

A. Y. Wonder, Bloodstain Pattern Evidence: Objective Approaches and Case Applications, 1st ed. Academic Press, 2007.

W. G. Eckert and S. H. James, Interpretation of Bloodstain Evidence at Crime Scenes, 2nd ed. CRC Press, 1998.

A. Y. Wonder, Blood Dynamics, 1st ed. Academic Press, USA, 2001

A. A. Lewis and H. L.MacDonell, The evidence never lies: the casebook of a modern Sherlock Holmes, 1st ed. Holt, Rinehart and Winston, New York, 1984.

H. L. MacDonell, Bloodstain pattern interpretation, 1st ed. Laboratory of Forensic Science Corning, N.Y. 1970.

M. Harvey, Pure Evil, 1st ed. John Blake Publishing Ltd, UK, 2008.

J. Glatt, One Deadly Night : A State Trooper, Triple Homicide, and a Search for Justice, 1st ed. St Martin's Press, USA, 2005.

J. Fraser and R. Williams, (Eds.) Handbook of forensic science. Routledge, 2013.

http://www.theguardian.com/uk/2008/dec/18/rachel-nickell-colin-stagg accessed January 2015

http://www.telegraph.co.uk/comment/5012733/Sean-Hodgson-victim-of-a-double-miscarriage-of-justice.html accessed January 2015.

C. Knock and M. Davison, J. Forensic Sci., 2007, 52, 1044.

L. Hulse-Smith, N. Z. Mehdizadeh and S. Chandra, J. Forensic Sci., 2005, 50, 54.

K. G. de Bruin, R. D. Stoel and J. C. M. Limborgh, J. Forensic Sci., 2011, 56, 1476.

H. L. MacDonell, Flight characteristics and stain patterns of human blood, National Institute of Law Enforcement and Criminal Justice, 1971.

Scientific Working Group on Bloodstain Pattern Analysis (SWGSTAIN), Recommended Terminology Forensic Science Communications, v.11(No.2) accessed at www.swgstain.org (January 2015).

L. Hulse-Smith, and M. Illes, J. Forensic Sci., 2007, 52, 65.

http://www.hoovedesigns.com/woods.html accessed January 2013

T. Bevel and R. M. Gardner, Bloodstain Pattern Analysis with an Introduction to Crime Scene Reconstruction, 3rd ed. CRC Press, 2008.

K. Rogers, Blood: Physiology and Circulation, 1st Ed. Britannica Educational Pub, 2011

R. E. Wells, and E. W. Merrill, J Clin Invest. 1962, 41, 1591.

D. A. C. Brownson and C. E. Banks, Anal. Methods, 2010, 2, 1885.

B. A. J. Larkin, M. El-Sayed, D. A. C. Brownson and C. E. Banks, Anal. Methods, 2012, 4, 721.

D. M. Eckmann, S. Bowers, M. Stecker & A. T. Cheung, Anesthesia & Analgesia, 2000, 91, 539.

W. Wu, T. L. Schifftner, W. G. Henderson, JAMA, 2007, 297, 2481.

W. Schmidt, B. Biermann,, P. Winchenbach, S. Lison & D. Boning, International journal of sports medicine, 2000, 21, 133.

P. Thirup, Haematocrit. Sports Medicine, 2003, 33, 231.

L. McNally, R. C. Shaler, M. Baird, I. Balazs, P. De Forest and L. Kobilinsky, J. of Forensic Sci, 1989, 34 1059.

http://www.npr.org/2011/08/17/139681851/scientists-crack-the-physics-of-coffee-rings accessed March 2012

R. D. Deegan, O. Bakajin, T. F. Dupont, G. Huber, S. R. Nagel and T. A. Witten, Nature 1997, 389, 827.

P. J. Yunker, T. Still, M. A. Lohr and A. G. Yodh, Nature, 2011, 476, 308.

D. Brutin, B. Sobac, B, Loquet and J. Sampol, J. Fluid Mech. 2011, 667, 85.

M. B. Amar, A. Goriely, M. M. Muller, New Trends in Physics and Mechanics in Biological Systems, Oxford Uni Press, UK, 2011.

H. C. Lee, R. E. Gaensslen and E. M. Pagliaro, IABPA News, 1986, 3, 47.

A. Grafit, A. Cohen and Y. Cohen, Journal of Forensic Identification, 2012, 62, 305.

H. F. Bartz, Estimating original bloodstain volume: the development of a new technique relating volume and surface area, 4th Year thesis, Laurentian University, USA, 2003.

https://www.bevelgardner.com/assets/files/Measuring%20Small%20Droplets%20MacDonnel%20Lige%201990.pdf

M. Rein, Fluid Dyn Res, 1993, 12, 61

M. Pasandideh-Fard, R. Bhola, S. Chandra, J. Mostaghimi, Phys Fluids, 1996, 8, 650.

N. Z. Mehdizadeh, S. Chandra, J. Mostaghimi, J Fluid Mechanics, 2004, 510, 353.

V. Balthazard, R. Piedelievre, H. Desoille, L. DeRobert, Ann Med Leg Criminol Police Sci Toxicol 1939, 19, 265.

P. L. Kirk and J. I. Thornton, Crime Investigation, 2nd ed. John Wiley & Sons Inc, 1974.

T. de Castro, T. Nickson, D. Carr and C. Knock, Int J Legal Med, 2013, 127, 251.

H. F. Miles, R. M. Morgan and J. E. Millington. Science & Justice, 2014, 4, 262.

J. A. Slemko, IABPA Newsletter, 2003, 19, 3.

B. White, Can Soc of Forensic Sci. J, 1986, 19, 3.

M. Holbrook, "Evaluation of blood deposition on fabric: distinguishing spatter and transfer stains." International Association of Bloodstain Pattern Analysts News 26, no. 1, 2010.

B. Karger B, S. P. Rand, B. Brinkmann Experimental bloodstain on fabric from contact and from droplets. Int J Legal Med, 1998, 111, 17.

E. Williams, E. Neumann, and M. Taylor. "2012 IABPA Officers 1 President's Message 2 Arterial Bloodstain Patterns on Clothing-An Interesting Case Linking the Accused to the Scene L. Allyn DiMeo and Jane Taupin, 3."

International Organization for Standardization, ISO 6330/A1:2009 textiles—domestic washing and drying procedures for textile testing. International Organization for Standardization, Switzerland, Geneva. 2009

http://www.thiscaringhome.org/products/low-temp-safety-burners.php   accessed January 2012.

K. L. Tontarski, K. A. Hoskins, T. G. Watkins, L. Brun-Conti, and A. L. Michaud, J Forensic Sci., 2009, 54, 37.

C. Luche, R. Jordan and T. Larkin, Canadian Society of Forensic Sci J. 2011, 44, 47

N. Zhang and W. J. Yang, Experiments in Fluids 1, 1980, 1, 101.

L. H. J. Watchers and N. A. J. Westerling, Chem. Eng. Sci. 1966, 21, 1047.

E. F. Crafton and W. Z. Black, International J Heat Mass Transfer, 2004, 47, 1187.

M. Thirumaleshwar, Fundamentals of Heat and Mass Transfer, 1st ed. Dorling Kindersley Pvt Ltd, 2006.

F. A. Farber and R. L. Scorah, Trans ASME, 1948, 79, 369.

G. Leak, IABPA Newsletter, 2006, 26 , 20

M. E. R. Walford, D. M. Hargreaves, S. Stuart-Smith, and M. V. Lowson, J. of Glaciology, 1991, 37, 47.

K. A. Harris, C.R. Thacker, D. Ballard and D. S. Court, International Congress Series, 2006, 1288, 589.

R. K. Farmen, P. Cortez and E. S. Frøyland, Forensic Sci. Int. Genetics Supplement Series, 2008, 1,418.

http://www.genewatch.org/sub-539478 accessed January 2015

J. M. Butler, Forensic DNA Typing: Biology, Technology, and Genetics of STR Markers, 2nd Revised ed., Academic Press Inc; London UK, 2005.

J. A. Bright, S. Cockerton, S. Harbison, A. Russell, O. Samson and K. Stevenson. (2011). The effect of cleaning agents on the ability to obtain DNA profiles using the Identifiler™ and PowerPlex® Y multiplex kits. *Journal of forensic sciences*, 2011, 56, 181.

J. A. Soares-Viera, D. R. Muñoz, E. S. Iwamura, L. de Almeida Cardoso and A. E. Billerbeck, A J FM P, 2001, 3, 308

C. Stein, S. H. Kyeck, C. J. Henssge, Forensic Sci. 1996, 6, 1012.

L. McNally, R. C. Shaler, M. Baird, I. Balazs, P. De Forest and L.Kobilinsky, J Forensic Sci., 1989, 34, 1059.

D. V. Christman, Virginia Dep. Forensic Sci., Bloodstain Pattern Analysts Training manual, Section 4.2.3.1, Oct.

B. E. Turvey, Forensic fraud: evaluating law enforcement and forensic science cultures in the context of examiner misconduct. Academic Press, 2013

W. Abbott, Searching for Justice: The Trials of David Camm, Tate Publishing, 2013.

http://wrongfulconvictionsblog.org/2012/04/30/blood-spatter-evidence/

E. W. Merrill, Rheology of blood. Physiol. Rev, 49, 4, 1969

E. O Ott, H. Lechner, and A. Aranibar, High blood viscosity syndrome in cerebral infarction. Stroke, 5, 3, 1974.

K. Lunkenheimer, and K. D. Wantke, Determination of the surface tension of surfactant solutions applying the method of Lecomte du Noüy (ring tensiometer). Colloid and Polymer Science, 259, 3, 1981.

D. Y. Kwok, and A. W. Neumann, Contact angle measurement and contact angle interpretation. Advances in colloid and interface science, 81, 3, 1999

L. M. Lander, L. M. Siewierski, W. J. Brittain, and E. A. Vogler, A systematic comparison of contact angle methods. Langmuir, 9, 8, 1993.

W. O. Randy, Light and Video Microscopy, Academic Press; 1 edition, 2008

B. H. Estridge and A. P. Reynolds, Basic Clinical Laboratory Techniques, Cengage Learning; 6 edition, 2011.

A. M. Gillespie Jr. Manual of Spectrofluorometric and Spectrophotometric Derivative Experiments, CRC Press, 1994.

R. A. Jukka, UV-Visible Reflection Spectroscopy of Liquids, Springer, 2010.

R. I. Handin, S. E. Lux, and T. P. Stossel, Blood: principles and practice of hematology, Lippincott Williams & Wilkins., Vol.1, 2003

E. Uthman, Understanding anemia. Univ. Press of Mississippi.2009

D. Twede, and S. E. Selke, Cartons, crates and corrugated board: handbook of paper and wood packaging technology. DEStech Publications, Inc. 2005

V. M. Huynh, and F. M. Luk, U.S. Patent No. 4,878,114. Washington, DC: U.S. Patent and Trademark Office. 1989.

M. Ezumi, and H. Todokoro, U.S. Patent No. 5,872,358. Washington, DC: U.S. Patent and Trademark Office. 1999

P. Echlin, Handbook of sample preparation for scanning electron microscopy and x-ray microanalysis. New York: Springer. 2009

B. Stuart, B, Infrared spectroscopy. John Wiley & Sons, Inc, 2005.

B. C. Smith, Fundamentals of Fourier transform infrared spectroscopy. CRC press, 2011

D. D. Chiras, Human biology. Jones & Bartlett Publishers, 2013.

G. Daniels, Human blood groups. John Wiley & Sons, 2013

C. D. Hillyer, Blood banking and transfusion medicine: basic principles & practice. Elsevier Health Sciences, 2007.

R. Biggs, and G. Macfarlane, Human blood coagulation and its disorders. Blackwell Scientific Publications, 1962.

http://www.aafp.org/afp/2001/0801/p419.html accessed June 2013

http://www.tcsbiosciences.co.uk/animal_blood_products.php accessed June 2012

http://www.pmlmicro.com/assets/TDS/133.pdf accessed June 1012

N. M. Palenske and D. K. Saunders, J. Thermal Bio, 2002, **27**, 479.

T. Hamazaki, H. Shishido, Thromb. Res., 1983, 30, 587.

C. Willis, A. K. Piranian, J. R. Donaggio, R. J. Barnett & W. F. Rowe, 'Errors in the estimation of the distance of fall and angles of impact blood drops,' Forensic Sci Int. 2001, 123, 1.

C. Carallo, C. Irace, M. S. De Franceschi, F. Coppoletta, R. Tiriolo, C. Scicchitano, F. Scavelli, and A. Gnasso. 'The effect of aging on blood and plasma viscosity. An 11.6 years follow-up study.' Clinical hemorheology and microcirculation, 2011, 47, 67.

S. Chien, et al. J Applied Phys, 1966, 21.1, 81

O. K. Baskurt and H. J. Meiselman, New York: Stratton Intercontinental Medical Book Corporation, 29, 5, c1974-, 2003

R. Cheeseman, J. Forensic Ident. 1999, 49, 261

A. R. Shen, G. J. Brostow, and R. Cipolla. Crime and Security, 2006. The Institution of Engineering and Technology Conference on. IET, 2006.

H. O. Stone, H. K. Thompson, and K. Schmidt-Nielsen, Am J. of Physiol, 1968, 214, 913.

G. Demir, and M. Paç, Am J of Hypertension, 1999, 12, 739.

Z. Erzinclioglu, Every Contact Leaves a Trace: Scientific Detection in the Twentieth Century, 1st ed., Carlton Books; London UK, 2001.

A. R.W. Jackson and J. M. Jackson, Forensic Science, 3 ed., Prentice Hall; London UK, 2011.

Kabaliuk, N., et al. "Blood drop size in passive dripping from weapons." Forensic science international 228.1 (2013): 75-82.

C. Corby, C. Hauke, B. Gestring and L. Quarino, Investigative Sci. J., 2012, 4, 18.

R. N. Walmsley, L. R. Watkinson and H. J. Cain, Cases in Chemical Pathology: A Diagnostic Approach, 4th ed., WSPC, USA, 1999.

J. M. Burkitt Creedon and H. Davis, (2012) Advanced Monitoring and Procedures for Small Animal Emergency and Critical Care, 1st ed., Wiley-Blackwell, USA,

J. D. Kirschmann, Nutrition Almanac, 6th ed. McGraw-Hill Contemporary, 2007.

Martin, C. (2005). The surface texture book: more than 800 colour and texture samples for every surface, furnishing and finish. Thames & Hudson.

H. Dagnall, (1980). Exploring surface texture, Leicester; England: Rank Taylor Hobson.

M. P. Groover, (2007). Fundamentals of modern manufacturing: materials processes, and systems. John Wiley & Sons.

American National Standards Institute, Surface texture: surface roughness, waviness and lay, American Society of Mechanical Engineers, 1986

J. Radkau, (2011). Wood: a history. Polity.

J. Fromm, (2013). Xylem development in trees: from cambial divisions to mature wood cells. In Cellular Aspects of Wood Formation, Springer Berlin Heidelberg.

Wilson, B. F. (1984). The growing tree. Univ of Massachusetts Press.

R. Shmulsky, and P. D. Jones, Forest products and wood science. John Wiley & Sons, 2011

M. Andersson, L. Persson, L and S. Svanberg, Spectroscopic studies of wood-drying processes. Optics express, 14, 8, 2006

A. Aghayere, and J. Vigil, Structural Wood Design: A Practice-Oriented Approach. John Wiley & Sons, 2007.

http://workshopcompanion.com/KnowHow/Wood/Hardwoods_&_Softwoods/3_Physical_Properties/3_Physical_Properties.htm#openclosedgrain accessed January 2013

A. J. Panshin, and C. D. Zeeuw, Textbook of wood technology. Volume I. Structure, identification, uses, and properties of the commercial woods of the United States and Canada. Textbook of wood technology. Volume I. Structure, identification, uses, and properties of the commercial woods of the United States and Canada. (3rd ed.), 1970.

M. Dresdner, The new wood finishing book. Taunton Press, 1999.

D. Bollinger, Hardwood Floors: Laying, Sanding and Finishing. Taunton Press, 1990.

S. Adanur, Handbook of weaving. CRC press. 2000

N. Gokarneshan, Fabric structure and design. New Age International, 2004

http://denisebrain.blogspot.co.uk/2012/11/fabric-term-of-week-basic-weaves.html accessed January 2013

C. Compton, and S. Whiting, The Knitting and Crochet Bible. David & Charles. 2008.

https://creatingruth.wordpress.com/category/tutorial/ accessed January 2013

http://www.en.neulakintaat.fi/12 accessed January 2013

http://freeknitstitches.com/knitlaceeyelets.php accessed January 2013

http://www.pinterest.com/alpacaknitster/knit-stitches/ accessed January 2013

http://www.craftelf.com/knitting-stitch-patterns/beaded-rib-knitting-stitch.html accessed January 2013

M. Schwartz, M, Innovations in materials manufacturing, fabrication, and environmental safety. CRC press. 2010

http://www.reinforcedplastics.com/view/31414/sigmatex-introduces-sigmast-spread-tow-fabric/ accessed January 2013

http://candostreet.com/blog-parents/2010/12/making-braid-cloth-wreaths-fun-for-man-me/ accessed January 2013

C. Dahl, Transforming Fabric: Creative Ways to Paint, Dye and Pattern Cloth. Krause Publications Craft. 2004

S. Sekhri, Textbook of Fabric Science: Fundamentals to Finishing. PHI Learning Pvt. Ltd, 2012.

http://www.laceforless.com/cgi-bin/fabricshop/gallery.cgi?Allover%20Lace%20Fabric#.VGYWpfmsVic accessed January 2013

W. Albrecht, H. Fuchs, and W. Kittelmann, (Eds.). Nonwoven fabrics: raw materials, manufacture, applications, characteristics, testing processes. John Wiley & Sons. 2006

http://www.supplierlist.com/product_view/kkingwang/150408/100919/non_woven_fabric.htm accessed January 2013

N. Belfer, Batik and tie dye techniques. Courier Dover Publications.1992.

http://dianebecka.com/ice-dyeing/ accessed January 2013

K. Lacasse, and W. Baumann, Textile Chemicals: Environmental data and facts. Springer, 2004.

http://electricstorm.blogspot.co.uk/2010/04/spiral-pattern.html accessed January 2013

I. Denamur, I and P. Ferbos, Moroccan: Textile Embroidery. Flammarion-Pere Castor. 2003

http://mbroider.net/indian-embroidered-fabric/ accessed January 2013

W. Endrei, The first hundred years of European textile-printing. Akadémiai Kiadó, 1998.

http://www.pinterest.com/katewhitehead/printing-block-woodblock-printing-is-a-technique-f/ accessed January 2013

W. S. Simpson, and G. Crawshaw, Wool: science and technology. Elsevier, 2002.

http://www.adopt-a-sheep.com/sheep/041.htm accessed January 2013

S. Eichhorn, J. W. S Hearle, M. Jaffe, and T. Kikutani, Handbook of textile fibre structure: Fundamentals and manufactured polymer fibres (Vol. 1). Elsevier, 2009.

S. Radhakrishnan, H. G. Alexander and M. K. Gandhi, Mahatma Gandhi-100 Years. Gandhi Peace Foundation, 1968.

http://www.rsc.org/chemistryworld/2012/07/silky-solution-storing-vaccines-and-drugs accessed January 2013

S. Yafa, Cotton: the biography of a revolutionary fiber. Penguin, 2006

http://blog.massagetoday.com/wibb/2011/04/21/raw-material-costs-on-the-rise/cotton-plant/ accessed January 2013

J. E. McIntyre, Synthetic fibres: nylon, polyester, acrylic, polyolefin. Elsevier, 2004

http://www.pslc.ws/macrog/nylon.htm accessed January 2013

http://phys.org/news177936316.html accessed January 2013

P. Baines, Flax and linen (No. 133). Osprey Publishing, 1985

http://fabrics.fibre2fashion.com/denim-fabric_buyers_p2065.html

I. Finlayson, Denim: an American legend. Parke Sutton, 1990

http://infohost.nmt.edu/~petro/faculty/Engler524/PET524-1b-porosity.pdf accessed January 2013.

P. T. Craddock, Mining and metal production through the ages. British Museum Pubns Ltd, 2003.

N. Wiberg, Holleman-Wiberg's inorganic chemistry. Academic Press, New York, 2001.

R. Lumley, Fundamentals of aluminium metallurgy: Production, processing and applications. Elsevier, 2010.

R. V. Singh, Aluminium Rolling: Processes, Principles & Applications, Tata McGraw-Hill Education Private Limited, 2011

A. Ghosh, and A. Chatterjee, Iron Making and Steelmaking: Theory and Practice. PHI Learning Pvt. Ltd..M, 2008.

M. J. King, K. C. Sole, and W. G. Davenport, Extractive metallurgy of copper. Elsevier, 2011.

L. Pugazhenthy, Zinc handbook: properties, processing, and use in design. CRC Press, 1991.

M. H. G. Kuijpers, Bronze Age metalworking in the Netherlands (c. 2000-800 BC): a research into the preservation of metallurgy related artefacts and the social position of the smith. Sidestone Press, 2008.

N. Hall, and J. Mazia, Metal Finishing Guidebook. Metals & Plastics, 1970.

M. Hryniuk, and F. Korvemaker. Legacy of Stone: Saskatchewan's Stone Buildings. Coteau Books, 2008.

M. R. Smith, Stone: Building stone, rock fill and armourstone in construction. Geological Society of London, 1999

P. Brinkman, Rock Types. Benchmark Education Company. 2006.

F. J. Pettijohn, Sand and sandstone. Springer. 1987.

G. V. Chilingar, H. J. Bissell, and R. W. Fairbridge, Carbonate rocks (Vol. 9). Elsevier, 2011.

D. R. Stille, Metamorphic Rocks: Recycled Rock. Capstone, 2008

J. Mattern, J. Igneous Rocks and the Rock Cycle. The Rosen Publishing Group, 2006.

C. B. Carter, and M. G. Norton, Ceramic materials. Springer Science+ Business Media, LLC, 2007.

D. J. Hall, and N. M. Giglio, Architectural Graphic Standards for Residential Construction (Vol. 13). John Wiley & Sons, 2010.

C. Binggeli, Interior Graphic Standards: Student Edition (Vol. 21). John Wiley & Sons, 2011.

M. F. Knott, Kitchen and Bath Design: A Guide to Planning Basics. John Wiley & Sons, 2010.

R. Bean, B. W. Olesen, and K. W. Kim, History of Radiant Heating 3 Cooling Systems. Ashrae Journal, 52, 1, 2010

D. E. Watkins, Heating services in buildings. John Wiley & Sons, 2011.

K. Moss, and K. J. Moss, Heating and water services design in buildings. Routledge, 2013.

P. Mitchell, Central Heating, Installation, Maintenance and Repair. WritersPrintShop, 2008.

R. Matthews, All about Selfbuild: A Comprehensive Guide to Building Your Own Unique Home. Blackberry Books, 2004.

E. Botonjic-Sehic, C. W. Brown, M. Lamontagne, and M. Tsaparikos, Forensic application of near-infrared spectroscopy: aging of bloodstains.Spectroscopy, 24, 2, 2009

R. H. Bremmer, G. Edelman, T. D. Vegter, T. Bijvoets, and M. C. Aalders, Remote Spectroscopic Identification of Bloodstains*. Journal of forensic sciences, 56, 6, , 2011.

G. Edelman, T. G. van Leeuwen, and M. C. Aalders, Hyperspectral imaging for the age estimation of blood stains at the crime scene. Forensic science international, 223, 1, 2012.

B. Atkinson, R. Lovegrove, and G. Gundry, Electrical installation designs. John Wiley & Sons. 2012.

M. Anson, J. M. Ko, and E. S. S. Lam, Advances in Building Technology. Elsevier, 2002.

P. Bright, Insider's Guide to Renovating for Profit. Brolga Publishing, 2011

N. Barton, Fireplace Decorating Ideas. Clinton Gilkie. 2012

W. E. Ranz and W. R. Marshall, Chemical Engineering Progress, 1952, **48**, 173.

H. J. Holterman, Kinetics and evaporation of water drops in air, Wageningen: IMAG, 2003.

http://www.proteinguru.com/protocols/NaOH%20and%20column%20cleaning.pdf accessed September 2012.

G. E Healthcare, Use of sodium hydroxide for cleaning and sanitising chromatography media and systems. Application note 18-1124-57 AE, 2006.

K. Sutthapodjanarux, N. Panvisavas, and N. Chaikum, The Effect of Temperature and pH on Forensic Examination of biological Evidence, Bangkok: Mahidol University; 2010.

http://chemistry.about.com/od/glowinthedarkprojects/a/luminolblood.htm Accessed May 2013

https://static.dna.gov/labmanual/Linked%20Documents/Protocols/pdi_lab_pro_2.19.pdf Accessed May 2013

https://static.dna.gov/labmanual/Linked%20Documents/Protocols/pdi_lab_pro_2.15.pdf Accessed May 2013

T. V. Aravindakshan, A. M. Nainar, K. Nachimuthu, Indian J Exp. Biol.,1997, 35, 903.

P. Bastien, G. W. Procop and U. Reischl, J Clin Microbiol, 2008, 46, 1897.

K. Biedermann, N. Dandachi, M. Trattner, G. Vogl, H. Doppelmayr, E. Moré, A. Staudach, O. Dietze, and C. Hauser-Kronberger. J of clinical microbiology, 2004, 42, 3758.

A. D. Kloosterman, B. Budowle, and P. Daselaar. Intl J of Legal Med. 1993, 105.5, 257.

M. V. Bloom, Human DNA fingerprinting by polymerase chain reaction, 1st ed.,C. A. Goldman; USA, 1994.

http://dna.uga.edu/docs/QIAamp_DNA_Mini_and_Blood_Mini_Handbook%20(Qiagen).pdf Accessed May 2013

H. H. Lee and O.Olsvik, Nucleic Acid Amplification Technologies: Application to Disease Diagnosis, 1st ed., BirkhauserVerlag AG; USA, 1997.

M. A. Innis, D. H. Gelfand and J. J. Sninsky, Pcr Strategies, 1st ed., Academic Press; London UK , 1995.

M. Roederer, Cytometry: New Developments, 4th ed., Academic Press; London UK, 2004.

http://www.marketingmagazine.co.uk/article/1142455/sector-insight-laundry-detergents-fabric-conditioners accessed January 2013

U. Zoller, Handbook of Detergents, Part E: Applications, CRC Press, 2008.

D. R. Berndt, and J. M. Griffiss. "Dry cleaning method and solvent/detergent mixture." U.S. Patent 6,063,135, issued May 16, 2000.

L. Higgins, S. C. Anand, M. E. Hall, and D. A. Holmes. "Factors during tumble drying that influence dimensional stability and distortion of cotton knitted fabrics." International Journal of Clothing Science and Technology 15, no. 2 (2003): 126-139.

Appendix 1- Categorising Bloodstains

Spatter Stains

Spatter stains are defined as bloodstains which are formed and dispersed through the air as a result of an application of an external force.

Morphological features of non-spatter stains can be: regular margins, spines, secondary spatter.

Impact

An impact pattern is a radiating pattern created by an external force exhibited on blood. Small individual stains are generated which can be used to define an area of impact, or, in some cases, where the attack originated.

Cast-offs

Blood projected onto a surface via a centripetal force, for example blood being flung off a weapon during an attack. The first blow of a weapon will cause bleeding, subsequent blows the blood adheres to the weapon creating a cast off pattern in line with the movement of the weapon.

Spurt

A spurt pattern is created when an artery or the heart is breached causing large streams of blood under extreme pressure to be ejected. This pattern consists of large elliptical stains, often in the pattern of a wave with possible flows in individual stains (indicating a large volume).

Drip Trail

Individual spatter stains which demonstrate movement from one point to another, these stains tend to large and circular in shape.

Drip

Again these stain types are individual spatter stains however in this case the stains offer no directional orientation. Drips can be exhibited from a stationary bloody weapon/or individual, for example a bloodied hand.

<u>Expiration Pattern</u>

Expiration or expectorate bloodstains are generated when blood is forced from the mouth, nose or respiratory system under pressure. Sometimes mistaken for an impact pattern expectorate bloodstains contain characteristics such as colour dilution or air vacuoles *etc.* which distinguishes them from other patterns.

<u>Mist Pattern</u>

A mist pattern consists of very small spatter, where a large number of the spatter will be sized just 0.1mm. Mist pattern is generated by a high impact event such as a gunshot.

Non-Spatter Stains

Non-spatter stains are defined as other stain orientation where the primary stain is neither elliptical nor circular in shape.

Morphological features of non-spatter stains can be: regular/ irregular margins, spines, secondary spatter and feathering.

<u>Gush/Splash</u>

This pattern is created when a large volume of blood is ejected onto a surface.

<u>Blood into Blood</u>

Blood into blood like its name suggests involves the dripping of blood into a liquid blood stain causing an accumulation of satellite spatter on the periphery of the stain.

<u>Smear</u>

A stain created by the transfer of blood from one source to another through contact with a lateral movement.

<u>Wipe</u>

A wipe pattern alters the appearance of the already existing pattern. It is created by the movement of an object or item through the wet bloodstain.

<u>Swipe</u>

Conversely a swipe pattern is created when a bloodied moving object comes into contact with a non-bloodied surface, transferring the stain.

Pattern Transfer

Transfer patterns are defined as the patterns created due to contact between two surfaces, where a minimum of one of them is bloodied. To be defined as a pattern transfer there needs to be a recognisable pattern or image within the bloodstain *i.e.* shape of a blade edge from a knife.

Pool Pattern

A pool pattern is an accumulation of blood in one place due to the blood source remaining stationary. Pool patterns can be used to determine blood loss and can hold clues to timing and sequence of events according to coagulation.

Saturation

This stain is generated when an accumulation of blood absorbs into a permeable surface.

Flow

A flow pattern is the movement of liquid blood as a mass under the effect of gravity. Flow patterns can indicate movement, direction change and large volume stains.

Appendix 2 - Ethics, COSHH and Risk Assessments

The MANCHESTER METROPOLITAN UNIVERSITY
Faculty of Science and Engineering
RISK ASSESSMENT COVER SHEET

REFERENCE NUMBER (XYZ/ddmmyy/LLn.nn): BAJL/HES / 150212 / T1.17

(XYZ = initials of the originator; ddmmyy = date; LLn.nn = room number)

SCHOOL: Chemistry and the Environment

TITLE OF WORK: Blood Spatter Experiments

LOCATION OF WORK (LLn.nn): T1.17 & T1.10

If off-site give contact details: N/A

INTENDED ACTIVITIES (attach methods sheets (e.g. standard operating practices) and work schedules to this form):

The whole blood will be drawn up into a disposable pipette approximately 1mL at time and slowly released in droplets from varying heights up to 2m onto various different surfaces. The spatter pattern will then be photographed and the drying pattern will also be visualised under a microscope over time, using a time lapse camera.

Blood will also be centrifuged in order to obtain plasma this will then be subjected to the same experiments as for whole blood above.

The work will involve screened human whole blood, supplied by The Blood Transfusion Service, Plymouth grove, Manchester.

PERSONS AT RISK (list names of all individuals (including status e.g. staff/student), and/or unit(s) / course(s) undertaking the activity. For students please indicate course and level, for staff give contact email / phone number):

Bethany Larkin, Technical Staff, and any persons in the vicinity.

HAZARDS (provide a summary of the hazards anticipated and attach detailed assessments with appropriate risk control methods to this form):

- Infection Risk – pathogenic organisms / viruses examples include MRSA, *Human Immunodeficiency Virus* (HIV) and *Human Hepatitis B Virus* (HBV) (note is not an exhaustive list)

- Routes of infection: Cuts, Abrasions, needle stick, mucosal membranes aerosols

- Working at heights

Are these hazards necessary in order to achieve the objectives of the activity? Yes – the experiment was first tested out using defibrinated horse blood – in order to reduce the risks further, however the defibrination process does not give reflective results in relation to the drying process as the most of the cells are lysed.

Hazard Rating (delete as appropriate): / **Medium** /

HAZARDOUS SUBSTANCES/MATERIALS USED AND HAZARD CLASSIFICATION

(appropriate COSHH data sheets / risk assessments must be attached to this form):

ALL CONTAINERS OF HAZARDOUS SUBSTANCES SHOULD BEAR CORRECT HAZARD WARNING LABELS.

NAME OF MATERIAL *Please provide also approximate quantity and concentration if applicable.*	HAZARD CLASS	HAZARD LABEL	DISPOSAL *Hazardous materials must not be removed from laboratories.* List disposal arrangements for all materials listed below *in the location where* the work will be carried out:
Whole Human Blood (Screened)	Biological	N/A	Follow clinical waste disposal procedure, AS3 (Attached) All surfaces will be disinfected with 2% Virkon solution, before and after experimentation.

RISK CONTROL METHODS (provide a summary of the hazards anticipated and attach detailed assessments with appropriate risk control methods to this form):

- Infection Risk – pathogenic organisms / viruses examples include MRSA, *Human Immunodeficiency Virus* (HIV) and *Human Hepatitis B Virus* (HBV) (note is not an exhaustive list)

- Routes of infection: Cuts, Abrasions, needle stick, mucosal membranes aerosols

- Working at heights

Screened Human whole blood (reduced risk)

All work involving human blood is regulated by the human tissue act and work with relevant material should be carried out only by competently trained personnel – see required training.

Centrifugation should be carried out in sealed centrifuge tubes – should a breakage occur the lid/seal should not be opened for at least one hour to allow all aerosol to settle (if possible transfer centrifuge to Class II biohazard cabinet)

All relevant material must be logged/recorded in the central HTA database, See relevant Designated

Persons or Designated Individual, Currently Michael Head and Bill Gilmore respectively.

All work involving relevant material should be carried out in a minimum Containment Level 2 laboratory.

Biohazard signs should be displayed on the entrance doors to the laboratory

Work involving relevant material must be confined to a designated area and clearly identifiable, the work station must be cleared of any unnecessary equipment before work commences, The bench surface and equipment should be disinfected immediately after completion of the work and at the end of every working day.

Personal protective equipment: Laboratory coat, Nitrile gloves and safety glasses (BS EN166).

Hands must always be washed immediately after potential contamination and again before leaving the laboratory, moving to another workstation or computer.

The use of sharps should be avoided whenever possible.

Hand contact with mucosal surfaces must be avoided, for examples do not rub your eyes or place fingers in your nose or mouth.

All waste should be disposed of in accordance with the faculty clinical waste procedure, AS3 (attached).

Open wounds, cuts abrasions or other lesions should be covered with a waterproof dressing.

Working at heights – ensure stepladders or kick stool has no defects and is safe to use, this assessment should be undertaken following relevant training, see below.

General Risk control measures:

There must be no eating, drinking, smoking, application of cosmetics or storage of food and mouth pipetting is strictly forbidden.

Unauthorized and casual visitors should be prohibited

Hazard Rating with Control Methods (delete as appropriate):   **Low**

Will any specific **training** *be required (if* YES *give details)?* Yes

1. Under take e-learning course http://www.rsclearn.mrc.ac.uk/
2. Training from technical team in relation to waste disposal and disinfection procedure.
3. Working at heights training – online course via HR e-learning or attend training session.

Are there any specific **first aid** *issues (if* YES *give details)?*   No

PROCEDURE FOR EMERGENCY SHUT-DOWN (if applicable): N/A

IF OFF-SITE INDICATE ANY OTHER ISSUES (e.g. associated with: individual's health and dietary requirements (obtain off-site health forms for all participating individuals and indicate where this information will be located); social activities, transportation, ID requirements; permissions for access and sampling).

N/A

	NAME	STAFF/STUDENT No.	DATE
Originator	Helen Sutton	01900254	15/02/12
	Bethany Larkin	0898316	15/02/12
Supervisor (*XYZ*)	Craig Banks		
Technical Manager	Alan Parkinson		
Divisional / School Health and Safety Coordinator (p.p. HoS)	Julia Dickinson		
	Mike Bennett	5301182L	17/2/12
DATE TO BE REVIEWED BY:		17/2 /13	

FACULTY Science and Engineering	SCHOOL OF CHEMISTRY and the Environment DIVISION: Chemistry

TITLE OF ACTIVITY

Blood spatter Experiments

REASONS FOR ACTIVITY

Research

STATUS OF PERSONS UNDERTAKING ACTIVITY
Student Name (if applicable) Bethany Alexandria Jane Larkin
Student Course and Level (if applicable): MPhil
Supervisor/Staff Name and Status: Dr Craig Banks
Specific location (Room Number) where work is to be carried out: T7.01

HAZARDOUS SUBSTANCES/MATERIALS USED AND HAZARD CLASSIFICATION

HAZARD NAME	HAZARD LABEL	R/S No. if available	RISK/SAFETY/HAZARD PHRASES
Equine Blood	Classification according to Directive 67/548/EEC or Directive 1999/45/EC This product contains no hazardous constituents.		
D-Amphetamine hemisulfate	Toxic	R25 S45	Toxic if swallowed. In case of accident or if you feel unwell, seek medical advice immediately (show the label where possible).
Acetone	Highly flammable Irritant	R11 R36 R66 R67 S9 S16 S26	Highly flammable. Irritating to eyes. Repeated exposure may cause skin dryness or cracking. Vapours may cause drowsiness and dizziness. Keep container in a well-ventilated place. Keep away from sources of ignition - No smoking. In case of contact with eyes, rinse immediately with plenty of water and seek medical advice.
Dopamine	Irritant Dangerous to the environment	R22. R50/53 S61	Harmful if swallowed Very toxic to aquatic organisms, may cause long-term adverse effects in the aquatic environment Avoid release to the environment. Refer to special instructions/ Safety data sheets

Serotonin creatinine sulfate monohydrate	Harmful	R63	Possible risk of harm to the unborn child.
		S36/37	Wear suitable protective clothing and gloves
Epinephrine	Toxic	R24 R36/37/38	Toxic in contact with skin. Irritating to eyes, respiratory system and skin.
		S26	In case of contact with eyes, rinse immediately with plenty of water and seek medical advice.
		S36/37	Wear suitable protective clothing and gloves
		S45	In case of accident or if you feel unwell, seek medical advice immediately (Show the label where possible).
Acetylcholine Bromide	Irritant	R36/37/38	Irritating to eyes, respiratory system and skin.
		S26	In case of contact with eyes, rinse immediately with plenty of water and seek medical advice.
		S36	Wear suitable protective clothing
Decon 90 Detergent	Irritant	R36/38 S24/25	Irritating to eyes and skin. Avoid contact with skin and eyes.
		S26	In case of contact with eyes, rinse immediately with plenty of water and seek medical advice.

ALL CONTAINERS OF HAZARDOUS SUBSTANCES SHOULD BEAR THE CORRECT HAZARD WARNING LABELS

COSHH RISK ASSESSMENT SUMMARY

All experiments shall be conducted according to the safety guidelines laid down in the safety datasheets attached. Personal protective equipment such as lab coat, gloves and safety goggles shall be worn at all times when handling all chemicals in this COSHH risk assessment. All chemicals shall be treated as potentially hazardous and guidelines relating to specific details of each chemical agent shall be followed at all times. General cleanliness of the laboratory bench/working area, good industrial hygiene and safety shall be observed at all times. Hand hygiene shall be observed before and after the laboratory session.

Due to the flammable nature or hazardous decomposition of products being formed, all chemicals will be kept away from heat, sparks or an open flame. All chemicals will be stored in a cool, dry

and well-ventilated area in tightly closed upright containers with acetonitrile also being stored and handled under inert gas.

DISPOSAL

Hazardous materials must not be removed from the laboratories. Disposal arrangements in the specified location where work is to be carried out for the materials listed above are:

Chemicals shall be disposed in appropriate containers. All chemicals, Vapours, Corrosive substances shall be discarded in special and appropriate containers and will be disposed of by special companies. Acidic waste shall be discarded in acidic waste containers. Contaminated and broken glass will be disposed in a broken glass bin.

19/10/12

DATE OF ASSESSMENT: 29/09/2011	DATE TO BE REVIEWED BY: ~~29/09/2013~~
SIGNATURES OF ASSESSORS Student:	**SIGNATURE OF HEAD OF DIVISION**
Supervisor/Staff:	**SIGNATURE OF HEAD OF SCHOOL**
Health & Safety Coordinator:	
BCHS SCHOOL REFERENCE NUMBER:	BAJL /240911 / T7·01

NB: This COSHH Risk Assessment is valid only if the individual COSHH summary sheets are attached for the substances/materials listed, the signatures of the Assessors have been obtained, and a BCHS School Reference Number has been allocated.

ETHICS CHECK FORM

Manchester
Metropolitan
University

This checklist must be completed for every project. It is used to identify whether there are any ethical issues associated with your project and if a full application for ethics approval is required. If a full application is required, you will need to complete the 'Application for Ethical Approval' form and submit it to the relevant Faculty Academic Ethics Committee, or, if your research falls within the NHS, you will need to obtain the required application form from the National Research Ethics Service available at www.nres.npsa.nhs.uk/ and submit it to a local NHS REC.

Before completing this form, please refer to the University's Academic Ethical Framework (www.rdu.mmu.ac.uk/ethics/mmuframework) and the University's Guidelines on Good Research Practice (www.rdu.mmu.ac.uk/rdegrees/goodpractice.doc).

Project and Applicant Details

Name of applicant (Principal Investigator):	BETH LARKIN
Telephone Number:	07914541828
Email address:	bethise live.co.uk
Status: (please circle as appropriate)	Undergraduate Student Postgraduate Student (Taught or Research) Staff
Department/School/Other Unit:	Chemistry
Programme of study (if applicable):	MPhL / DPh.C
Name of supervisor (if applicable):	DR CLAIR SANA
Project Title:	EXPANDING THE HORIZON OF EPA
Does the project require NHS Trust approval? If yes, has approval been granted by the Trust? Attach copy of letter of approval.	YES/NO

Ethics Checklist (Please answer each question by ticking the appropriate box)

		Yes	No	N/A
1.	Will the study involve recruitment of patients or staff through the NHS, or involve NHS resources? If yes, you may need full ethical approval from the NHS.			✓
2.	Does the study involve participants who are particularly vulnerable or unable to give informed consent (e.g. children, people with learning disabilities, your own students)?			✓
3.	Will the study require the co-operation of a gatekeeper for initial access to the groups or individuals to be recruited (e.g. students at school, members of self-help group, nursing home residents)?			✓
4.	Will the study involve the use of participants' images or sensitive data (e.g. participants personal details stored electronically, image capture techniques)?			✓
5.	Will the study involve discussion of sensitive topics (e.g. sexual activity, drug use)?			✓
6.	Could the study induce psychological stress or anxiety or cause harm or negative consequences beyond the risks encountered in normal life?			✓
7.	Will blood or tissue samples be obtained from participants?		✓	
8.	Are drugs, placebos or other substances (e.g. food substances, vitamins) to be administered to the study participants or will the study involve invasive, intrusive or potentially harmful procedures of any kind?			✓
9.	Is pain or more than mild discomfort likely to result from the study?			✓
10.	Will the study involve prolonged or repetitive testing?			✓

Ethics Matters

	Yes	No	N/A
11. Will it be necessary for participants to take part in the study without their knowledge and informed consent at the time (e.g. covert observation of people in non-public places)?			✓
12. Will financial inducements (other than reasonable expenses and compensation for time) be offered to participants?			✓
13. Is there any possible risk to the researcher (e.g. working alone with participants, interviewing in secluded or dangerous)?			✓
14. Has appropriate assessment of risk been undertaken in relation to this project?	✓		
15. Does any relationship exist between the researcher(s) and the participant(s), other than that required by the activities associated with the project (e.g., fellow students, staff, etc)?			✓
16. Faculty specific question, e.g., will the study sample group exceed the minimum effective size?			✓

If you have ticked 'no' or 'n/a' to all questions, attach the completed and signed form to your project approval form, or equivalent. Undergraduate and taught higher degree students should retain a copy of the form and submit it with their research report or dissertation (bound in at the end). MPhil/PhD, and other higher degree by research, students should submit a copy to the Faculty Research Degrees Sub-Committee with their application for registration (RD1) and forward a copy to their Faculty Academic Ethics Committee. Members of staff should send a copy to their Faculty Academic Ethics Committee before commencement of the project.

If you have ticked 'yes' to **any** of the questions, please describe the ethical issues raised on a separate page. You will need to submit your plans for addressing the ethical issues raised by your proposal using the 'Application for Ethical Approval' form which should be submitted to the relevant Faculty Academic Ethics Committee. This can be obtained from the University website (http://www.rdu.mmu.ac.uk/ethics/index.php).

If you answered 'yes' to question 1, you may also need to submit an application to the appropriate external health authority ethics committee, via the National Research Ethics Service (NRES), found at http://www.nres.npsa.nhs.uk/, and send a copy to the Faculty Academic Ethics Committee for their records.

Please note that it is your responsibility to follow the University's Guidelines on Good Research Practice and any relevant academic or professional guidelines in the conduct of your study. **This includes providing appropriate information sheets and consent forms, and ensuring confidentiality in the storage and use of data.** Any significant change in the question, design or conduct over the course of the research should be notified to the relevant committee (either Faculty Academic Ethics Committee of Local Research Ethics Committee if an NHS-related project) and may require a new application for ethics approval.

Approval for the above named proposal is granted

I confirm that there are no ethical issues requiring further consideration. *(Any subsequent changes to the nature of the project will require a review of the ethical consideration(s).)*   Signature of Supervisor (for students), or Manager (for staff): _____ Dr Craig Bru   Date: 30/2/2013

Approval for the above named proposal is not granted

I confirm that there are ethical issues requiring further consideration and will refer the project proposal to the Faculty Academic Ethics Committee.   Signature of Supervisor (for students), or Manager (for staff): _____   Date: _____

Ethics Matters

354

Separate page for ethical issues:-

Ethics Matters

The MANCHESTER METROPOLITAN UNIVERSITY
Faculty of Science and Engineering
RISK ASSESSMENT COVER SHEET

REFERENCE NUMBER (XYZ/ddmmyy/LLn.nn).   BAJL   /   290911   /   T7.01
(XYZ = initials of the originator; ddmmyy = date; LLn.nn = room number)

SCHOOL: Science and the Environment

TITLE OF WORK: Bloodspatter experiments

LOCATION OF WORK (*LLn.nn*): Labs T7.01

If off-site give contact details:

INTENDED ACTIVITIES (attach methods sheets (e.g. standard operating practices) and work schedules to this form):

Dropping of equine blood from various heights.

PERSONS AT RISK (list names of all individuals (including status e.g. staff/student), and/or unit(s) / course(s) undertaking the activity. For students please indicate course and level, for staff give contact email / phone number):

Bethany Larkin (student)

HAZARDS (provide a summary of the hazards anticipated and attach detailed assessments with appropriate risk control methods to this form):

Splashing of blood

Equine Blood (horse blood) - Stable liquid containing horse plasma and red blood cells.

Non Hazardous

TOXICOLOGICAL INFORMATION

No specific information.

Sensitisation: May cause allergic or hypersensitive reaction in individuals allergic

to blood serum.

Are these hazards necessary in order to achieve the objectives of the activity? Yes

	environment. Refer to special instructions/ Safety data sheets		
Serotonin creatinine sulfate monohydrate	**R63** Possible risk of harm to the unborn child. **S36/37-** Wear suitable protective clothing and gloves	**Harmful**	Hand to supervisor for disposal
Epinephrine	**R24-** Toxic in contact with skin **R36/37/38-** Irritating to eyes, respiratory system and skin. **S26-** In case of contact with eyes, rinse immediately with plenty of water and seek medical advice **S36/37-** Wear suitable protective clothing and gloves **S45-** In case of accident or if you feel unwell, seek medical advice immediately (Show the label where possible).	**Toxic**	Hand to supervisor for disposal

Hazard Rating (delete as appropriate):   **Low**

HAZARDOUS SUBSTANCES/MATERIALS USED AND HAZARD CLASSIFICATION (appropriate COSHH data sheets / risk assessments must be attached to this form):

ALL CONTAINERS OF HAZARDOUS SUBSTANCES SHOULD BEAR CORRECT HAZARD WARNING LABELS.

NAME OF MATERIAL *Please provide also approximate quantity and concentration if applicable.*	HAZARD CLASS	HAZARD LABEL	DISPOSAL *Hazardous materials must not be removed from laboratories. List disposal arrangements for all materials listed below in the location where the work will be carried out:*
Equine Blood	Classification according to Directive 67/548/EEC or Directive 1999/45/EC This product contains no hazardous constituents.		Autoclave Bag for sterilisation at 121°C for 15 mins
D-Amphetamine hemisulfate	**R25-** Toxic if swallowed. **S45-** In case of accident or if you feel unwell, seek medical advice immediately (show the label where possible).	**Toxic**	Hand to supervisor for disposal

357

| Acetone | R11 -Highly flammable.

R36 -Irritating to eyes.

R66 -Repeated exposure may cause skin dryness or cracking.

R67- Vapours may cause drowsiness and dizziness.

S9 -Keep container in a well-ventilated place.

S16- Keep away from sources of ignition - No smoking.

S26 -In case of contact with eyes, rinse immediately with plenty of water and seek medical advice. | Highly flammable

Irritant | Dispose of down the drain with large quantities of water |
| Dopamine | R22- Harmful if swallowed

R50/53- Very toxic to aquatic organisms, may cause long-term adverse effects in the aquatic environment

S61- Avoid release to the | Irritant

Dangerous to the environment | Hand to supervisor for disposal |

Acetylcholine Bromide	R36/37/38- Irritating to eyes, respiratory system and skin. S26- In case of contact with eyes, rinse immediately with plenty of water and seek medical advice. S36- Wear suitable protective clothing	Irritant	Hand to supervisor for disposal
Decon 90 Detergent	R36/38-Irritating to eyes and skin. S24/25- Avoid contact with skin and eyes. S26- In case of contact with eyes, rinse immediately with plenty of water and seek medical advice.	Irritant	Dispose of down the drain with large quantities of water

RISK CONTROL METHODS (provide a summary of the hazards anticipated and attach detailed assessments with appropriate risk control methods to this form):

<u>**HANDLING AND STORAGE**</u>

Handling precautions – No special measures required.

Storage precautions – Store at 2-8^{0}C

<u>**PROTECTION**</u>

Personal protection – Wear anti-splash eye protection and gloves. Wash hands

after use. Work in an enclosed space.

FIRST AID MEASURES

Skin contact – In the case of skin contact, rinse well with water.

In severe cases, *obtain medical attention.*

Eye contact – If the substance has entered the eyes, rinse thoroughly with

water/eyewash.

Ingestion – Be alert for early indications of allergic reactions or hypersensitivity/

Inhalation – Remove person to fresh air. Ingestion – Be alert for early indications of allergic reactions or hypersensitivity.

FIRE FIGHTING MEASURES

Special risks –None.

Extinguishing media – use those suitable for the surrounding environment.

ACCIDENTAL RELEASE MEASURES

Personal protection – Gloves should be used if contact is possible.

Spillages –Small spillages may be cleaned up using absorbent material.

Clean-up procedures – Prevent material from reaching sewage system, holes and cellars. However, the material will degrade in the environment without harm.

DISPOSAL CONSIDERATIONS
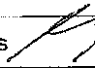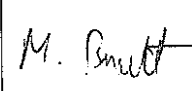
Waste disposal – All hazardous characteristics can be destroyed by typical refuse incineration methods.

Hazard Rating with Control Methods (delete as appropriate): Low

Will any specific **training** *be required (if* YES *give details)? No*

Are there any specific **first aid** *issues (if* YES *give details)?* No

PROCEDURE FOR EMERGENCY SHUT-DOWN (if applicable):

360

N/A

IF OFF-SITE INDICATE ANY OTHER ISSUES (e.g. associated with: individual's health and dietary requirements (obtain off-site health forms for all participating individuals and indicate where this information will be located); social activities, transportation, ID requirements; permissions for access and sampling).

	NAME	STAFF/STUDENT No.	DATE
Originator	Bethany Larkin	08987516	29/09/2011
Supervisor (*XYZ*)	Dr Craig Banks	5501190	3\10\11
Technical Manager	A. Parkinson	1990014	3/10/11
Divisional / School Health and Safety Coordinator (p.p. HoS)	M. Smith	950114?2	20/10/11
DATE TO BE REVIEWED BY: 20/10/12			

Application Number_____
Date Received_____

APPLICATION FOR ETHICAL APPROVAL

Manchester
Metropolitan
University

Introduction

All university activity must be reviewed for ethical approval. In particular, all undergraduate, postgraduate and staff research work, projects and taught programmes must obtain approval from the Academic Ethics committee.

Application Procedure

The form should be completed legibly (preferably typed) and, so far as possible, in a way which would enable a layperson to understand the aims and methods of the research. Every relevant section should be completed. Applicants should also include a copy of any proposed advert, information sheet, consent form and, if relevant, any questionnaire being used. The Principal Investigator should sign the application form. Supporting documents, together with one copy of the full protocol should be sent to the Faculty/Campus Research Group Officer.

Your application will require external ethical approval by an NHS Research Ethics Committee if your research involves staff, patients or premises of the NHS (see guidance notes)

Work with children and vulnerable adults

You will be required to have an Enhanced CRB Disclosure, if your work involves children or vulnerable adults.

The Academic Ethics Committee will respond as soon as possible, and where appropriate, will operate a process of expedited review.

Applications that require approval by an NHS Research Ethics Committee or a Criminal Disclosure will take longer.

1. Details of Applicants	
1.1. Name of applicant (Principal Investigator): Bethany Larkin	
Telephone Number: 07914541828	
Email address: beth15@live.co.uk	
Status: Postgraduate Research Student	Postgraduate Student (Taught or Research) Staff
Department/School/Other Unit: School of Science and Engineering	
Programme of study (if applicable): MPhil with possibility of transfer to PhD in Chemistry by Research	
Name of supervisor/Line manager: Dr Craig Banks	
1.2. Co-Workers and their role in the project: (e.g. students, external collaborators, etc) N/A	
Name:	Name:

Application Number_____
Date Received_____

Telephone Number:	Telephone Number:
Role:	Role:
Email Address:	Email Address:

2. Details of the Project

2.1. Title: Blood Spatter Experiments

2.2. Description of the Project: (please outline the background and the purpose of the research project, 250 words max)   See attached sheet)

2.3. Describe what type of study this is (e.g. qualitative or quantitative; also indicate how the data will be collected and analysed). Additional sheets may be attached.
See attached sheet)

2.4. Are you going to use a questionnaire?
YES (Please attach a copy)   N/A
NO

2.5. Start Date / Duration of project: February 2013 - 2014

2.6. Location of where the project and data collection will take place:
7th Floor Tower Block John Dalton Building

2.7. Nature/Source of funding   Self funded

2.8. Are there any regulatory requirements?
YES (Provide details, e.g. from professional bodies)
NO

3. Details of Participants

3.1. How many?   1 (me)

3.2. Age: 23

3.3. Sex: Female

3.4. How will they be recruited? (Attach a copy of any proposed advertisement) N/A

3.5. Status of participants: (e.g. students, public, colleagues, children, hospital patients, prisoners, including young offenders, participants with mental illness or learning difficulties.)   Postgraduate Researcher

3.6. Inclusion and exclusion from the project: (indicate the criteria to be applied).   N/A

3.7. Payment to volunteers: (indicate any sums to be paid to volunteers).   N/A

3.8. Study information:

Application Number_____
Date Received_____

Have you provided a study information sheet for the participants?
        YES (Please attach a copy)
        NO   N/A

3.9. Consent:
(A written consent form for the study participants MUST be provided in all cases, unless the research is a questionnaire.)
Have you produced a written consent form for the participants to sign for your records?
        YES (Please attach a copy)   N/A
        NO

4. Risks and Hazards

4.1. Are there any risks to the researcher and/or participants?
(Give details of the procedures and processes to be undertaken, e.g., if the researcher is a lone-worker.)   (see attached sheet)

4.2. State precautions to minimise the risks and possible adverse events:
        (see attached sheet)

4.3. What discomfort (physical or psychological) danger or interference with normal activities might be suffered by the researcher and/or participant(s)? State precautions which will be taken to minimise them: None

5. Ethical Issues

5.1. Please describe any ethical issues raised and how you intend to address these:
        (see attached sheet)

6. Safeguards/Procedural Compliance

6.1. Confidentiality:
    6.1.1. Indicate what steps will be taken to safeguard the confidentiality of participant records. If the data is to be computerised, it will be necessary to ensure compliance with the requirements of the Data Protection Act 1998.
    6.1.2. If you are intending to make any kind of audio or visual recordings of the participants, please answer the following questions:
        6.1.2.1. How long will the recordings be retained and how will they be stored?
        6.1.2.2. How will they be destroyed at the end of the project?
        6.1.2.3. What further use, if any, do you intend to make of the recordings?   N/A

6.2. The Human Tissue Act
The Human Tissue Act came into force in November 2004, and requires appropriate consent for, and regulates the removal, storage and use of all human tissue.

    6.2.1. Does your project involve taking tissue samples, e.g., blood, urine, hair etc., from human subjects?
        YES
        NO
    6.2.2. Will this be discarded when the project is terminated?
        YES
        NO

If NO – Explain how the samples will be placed into a tissue bank under the Human Tissue Act regulations:

6.3. Insurance

The University holds insurance policies in place to cover claims for negligence arising from the conduct of the University's normal business, which includes research carried out by staff and by undergraduate and postgraduate students as part of their course. This does not extend to clinical negligence.

In addition, the University has provision to award indemnity and/or compensation in the event of claims for non-negligent harm. This is on the condition that the project is accepted by the insurers prior to the commencement of the research project and approval has been granted for the project from a suitable ethics committee.

Research which is applicable to non-negligent harm cover involves humans and physical intervention which could give rise to a physical injury or illness which is outside the participants day to day activities. This includes strenuous exercise, ingestion of substances, injection of substances, topical application of any substances, insertion of instruments, blood/tissue sampling of participants and scanning of participants.

The following types of research are not covered automatically for non-negligent harm if they are classed as the activities above and they involve:

1) Anything that assists with and /or alters the process of contraception, or investigating or participating in methods of contraception
2) Anything involving genetic engineering other than research in which the medical purpose is treating or diagnosing disease
3) Where the substance under investigation has been designed and /or manufactured by MMU
4) Pregnant women
5) Drug trials
6) Research involving children under sixteen years of age
7) Professional sports persons and or elite athletes.
8) Overseas research

Will the proposed project result in you undertaking any research that includes any of the 8 points above or would not be considered as normal University business? If so, please detail below: N/A

6.4. Notification of Adverse Events (e.g., negative reaction, counsellor, etc):
(Indicate precautions taken to avoid adverse reactions.)

Please state the processes/procedures in place to respond to possible adverse reactions. N/A

In the case of clinical research, you will need to abide by specific guidance. This may include notification to GP and ethics committee. Please seek guidance for up to date advice, e.g., see the NRES website at http://www.nres.npsa.nhs.uk/

Page 4 of 5

Application Number_____
Date Received_____

SIGNATURE OF PRINCIPAL INVESTIGATOR:	Date	08/02/2013
SIGNATURE OF FACULTY'S HEAD OF ETHICS:	Date:	08/02/2013

Checklist of attachments needed:
1. Participant consent form
2. Participant information sheet
3. Full protocol
4. Advertising details
5. Insurance notification forms
6. NHS Approval Letter (where appropriate)
7. Other evidence of ethical approval (e.g., another University Ethics Committee approval)

366

Ethics Application

Project outline

This project investigates the influence of surface on bloodstains; bloodstains are used forensically in Bloodstain Pattern Analysis to determine sequence of events etc. The objective of this study is to evaluate the stains produced on these various surfaces and establish equations which can be directly applied at crime scenes.

Fresh human blood will be needed towards the end of the experiments to confirm consistency of these equations which will have been produced using equine and human blood bank blood.

Blood will be taken from the researcher by a trained professional where it will subsequently be frozen in 2 mL aliquots. Blood will be thawed when needed for experiments which involve the dropping of blood using pipettes from a maximum height of 2 metres. When the blood is fully dry it will be measured using a magnifying loupe to determine size of bloodstain.

Since these surfaces will be manipulated in various ways, i.e. heat, DNA extraction will also be utilized, where dried blood will be scrapped or swabbed for mitochondria DNA analysis, which will involve PCR and gel electrophoresis.

Throughout the experiments appropriate clothing (i.e. goggles, lab overalls, mask and gloves) will be worn

Type of Data

Both qualitative and quantitative data will be collected; bloodstains will be measured to construct equations, also visual descriptions of the bloodstains (after heat) will be completed as these investigations are novel and therefore need to be explored fully.

<u>Risks and Hazards</u>

There are no risks to the researcher; the blood used is from the researcher therefore removing the hazards associated with blood (HIV, Hepatitis etc.). All work is to be conducted on the 7th Floor Lab Tower and therefore no work will be carried out alone. As blood is merely dropped onto the surfaces it is not though necessary to use a separate room, however the experiment will be carried out at least a lab bench distance away from any other student as a precaution.

Throughout the experiments appropriate clothing (i.e. goggles, lab overalls, mask and gloves) will be worn.
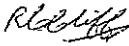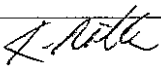
Blood will be extracted from the researcher by a qualified trained professional.

<u>Ethics</u>

Associated with the use of human blood, as blood is extracted from researcher ethical issues are minimized.

RISK ASSESSMENT

FACULTY/DEPARTMENT	BUILDING
Science and Engineering	John Dalton Tower

1) ACTIVITY
Use of Loaned Audio Visual Equipment items for Assignments and Projects

2) PERSONS AT RISK
Loanee and any Assistant(s)
Subjects being photographed, filmed or recorded, general public

3a) HAZARDS
Slips, Trips and Falls; general. Motor Traffic; cars, buses, motor cycles, Trams, Trains, Bicycles, Pedestrians. Rivers, Canals, Railway Station Platforms. Weight of items, e.g. large video camera, lighting rig. Cumbersome items. Dropping of items on limbs and/or appendages. Trips over tripod legs and subsequent falls. Lone Working. Potential for suffering theft or mugging. Battery Charging and Disposal of dry batteries. Activation of camera flash, Eyesight Damage. Lighting, temperature. Liquid and Food Contamination of AV Equipment. Chargers and Mains Plug-In items. Weather; protection of equipment from moisture. Cable runs. When working within University Buildings; Emergency Evacuations

3b) Hazard Rating Medium

4a) RISK CONTROL METHOD
Appropriate Training in all item(s) to be used
Careful selection of location for work; Weight of items considered and correct manual handling methods adopted; Avoidance of Lone Working to lessen the chance of equipment loss and possibility of mugging. In event of confrontation and possible robbery, equipment to be surrendered, as personal safety is paramount. Batteries which are charging must be checked every half hour to check for completion / overheating. Dry batteries must be disposed of in a safe and environmentally responsible manner. Warn subjects and where possible passers-by if flash lights are to be activated. Lighting should be allowed to cool prior to handling. No Bulbs or Fuses to be replaced by loanees. All mains electrical items are regularly PAT tested. Arrange any cable runs to minimise trip hazards. Always use rain covers if available and necessary. Do not eat or drink in close proximity to any AV equipment. If an emergency evacuation is activated whilst performing an activity within a university building; Evacuate the building by the nearest safe route. The equipment should only be brought out if by doing so evacuation is not delayed. In general leave the equipment and evacuate the building.

4b) Hazard Rating with control methods Low

5) FURTHER ACTION REQUIRED
None

NAME AND TITLE OF ASSESSOR	SIGNATURE	DATE
Robert Cliff, TTL Digital Technology	*R.Cliff*	03/03/2011
		REVIEW DATE 03/03/2012
SIGNATURE OF DEAN/H.O.D	*J. Rule*	DATE 7/3/11
		REVIEW DATE 7/3/12

Manchester
Metropolitan
University

RISK ASSESSMENT

FACULTY/DEPARTMENT	BUILDING
Science & Engineering/Molecular Sciences	John Dalton Tower

1) ACTIVITY

Clinical Waste Disposal. (AS3)

2) PERSONS AT RISK
3)
Technical Staff, other laboratory users and any persons in the vicinity

3A) HAZARDS

Main hazard: Risk of infection
Other hazards:
Punctures to the skin
Skin contamination
Spread of infection

3B) Hazard Rating   LOW ☐ MEDIUM **X** HIGH ☐

4A) RISK CONTROL METHODS

Laboratory users must use personal protective equipment (gloves, lab coats and safety glasses (BS EN 166).

Non sharp clinical waste: MUST be placed in yellow Clinical waste bags supported on the underside; normally in the form of a bin, labelled hazardous and clinical waste. Ensure significant amounts of liquid in contaminated containers are removed before disposal (refer to COSHH guidelines for specific details of liquids)

When a yellow clinical waste bag is 3/4 full, it is the laboratory user's responsibility to replace it with a new bag.

Securing the yellow clinical waste bags: tie either with a swan neck knot or plastic zip-tie, label the bag with the date and laboratory number. Place bag in the large

yellow waste clinical waste container located next to the goods lift, 1st floor JD tower. The key to the clinical waste bin is kept in the grey key box in the corridor outside the T1.10 Cell culture laboratory.

Sharp clinical waste: i.e. pipette tips, needles and syringes or any other item which may puncture the yellow clinical waste bags must be placed in clinical waste sharps bins. When these containers are full they must be labelled with the date and laboratory number and placed in the large yellow clinical waste container located next to the goods lift, 1st floor JD tower.

If the large clinical waste container or all sharps binsis full contact a Technical officer or Technical Team Leader.

Chemical waste should not be disposed of as clinical waste, it must be disposed of in accordance with COSHH guidelines.

Contaminated broken glass should be placed in a sharps bin.

Non-clinical waste should be disposed of or recycled in ordinary bins for domestic waste recyclable waste bins.

4B) Hazard Rating with control methods   LOW **X** MEDIUM ☐ HIGH ☐

5) FURTHER ACTION REQUIRED

NAME AND TITLE OF ASSESSOR Glenn Ferris (Technical Officer)	SIGNATURE	DATE 31/05/2011
	ID Number: **AS3**	
SIGNATURE Technical Service Manager or Technical Group Manager		DATE
		REVIEW DATE

AP
16|2|12

Manchester
Metropolitan
University

RISK ASSESSMENT

FACULTY/DEPARTMENT	BUILDING
Science & Engineering/Molecular Sciences	John Dalton Tower

1) ACTIVITY

Clinical Waste Disposal. (AS3)

2) PERSONS AT RISK
3)
Technical Staff, other laboratory users and any persons in the vicinity

3A) HAZARDS

Main hazard: Risk of infection
Other hazards:
Punctures to the skin
Skin contamination
Spread of infection

3B) Hazard Rating　　　　　　　　　LOW ☐　MEDIUM **X**　HIGH ☐

4A) RISK CONTROL METHODS

Laboratory users must use personal protective equipment (gloves, lab coats and safety glasses (BS EN 166).

Non sharp clinical waste: MUST be placed in yellow Clinical waste bags supported on the underside; normally in the form of a bin, labelled hazardous and clinical waste. Ensure significant amounts of liquid in contaminated containers are removed before disposal (refer to COSHH guidelines for specific details of liquids)

When a yellow clinical waste bag is 3/4 full, it is the laboratory user's responsibility to replace it with a new bag.

Securing the yellow clinical waste bags: tie either with a swan neck knot or plastic zip-tie, label the bag with the date and laboratory number. Place bag in the large

yellow waste clinical waste container located next to the goods lift, 1st floor JD tower. The key to the clinical waste bin is kept in the grey key box in the corridor outside the T1.10 Cell culture laboratory.

Sharp clinical waste: i.e. pipette tips, needles and syringes or any other item which may puncture the yellow clinical waste bags must be placed in clinical waste sharps bins. When these containers are full they must be labelled with the date and laboratory number and placed in the large yellow clinical waste container located next to the goods lift, 1st floor JD tower.

If the large clinical waste container or all sharps binsis full contact a Technical officer or Technical Team Leader.

Chemical waste should not be disposed of as clinical waste, it must be disposed of in accordance with COSHH guidelines.

Contaminated broken glass should be placed in a sharps bin.

Non-clinical waste should be disposed of or recycled in ordinary bins for domestic waste recyclable waste bins.

4B) Hazard Rating with control methods   LOW X   MEDIUM ☐   HIGH ☐

5) FURTHER ACTION REQUIRED

NAME AND TITLE OF ASSESSOR Glenn Ferris (Technical Officer)	SIGNATURE	DATE 31/05/2011
	ID Number: **AS3**	
SIGNATURE Technical Service Manager or Technical Group Manager		DATE
		REVIEW DATE

Manchester
Metropolitan
University

RISK ASSESSMENT

FACULTY/DEPARTMENT	BUILDING
Health Care Sciences	John Dalton Tower

1) ACTIVITY

Working with Human tissue and body fluids (relevant material) (AS14)

2) PERSONS AT RISK

Academic/ technical Staff, Students PG/UG and persons in the vacinity

3) HAZARDS

- Infection Risk – pathogenic organisms / viruses examples include MRSA, *Human Immunodeficiency Virus* (HIV) and *Human Hepatitis B Virus* (HBV) (note is not an exhaustive list)
- Routes of infection: Cuts, Abrasions, needle stick, mucosal membranes aerosols

3B) Hazard Rating   **MEDIUM**

4) RISK CONTROL METHODS

When working with unscreened blood/relevant material, all users should be made aware and vaccination against hepatitis B should is advised.

All work involving relevant material should be carried out only by competently trained personnel.

All relevant material must be logged/recorded in the central HTA database, See relevant Designated Persons or Designated Individual, Currently Michael Head and Bill Gilmore respectively.

All work involving relevant material should be carried out in a minimum Containment Level 2 laboratory.

Biohazard signs should be displayed on the entrance doors to the laboratory

Work involving relevant material must be confined to a designated area and clearly identifiable, the work station must be cleared of any unnecessary equipment before work commences, The bench

Page 1 of 2

374

surface and equipment should be disinfected immediately after completion of the work and at the end of every working day.

Personal protective equipment: Laboratory coat, Nitrile gloves and safety glasses (BS EN166).

Hands must always be washed immediately after potential contamination and again before leaving the laboratory, moving to another workstation or computer.

The use of sharps should be avoided whenever possible.

Centrifugation should be carried out in sealed centrifuge tubes – should a breakage occur the lid/seal should not be opened for at least one hour to allow all aerosol to settle (if possible transfer centrifuge to Class II biohazard cabinet)

Procedures such as blending, vortexing, sonication, a Class II Microbiological cabinet should be used.

Any equipment used with relevant material which could result in the production of aerosols should be fitted with an appropriate filter.

Hand contact with mucosal surfaces must be avoided, for examples do not rub your eyes or place fingers in your nose or mouth.

Open wounds, cuts abrasions or other lesions should be covered with a waterproof dressing.

There must be no eating, drinking, smoking, application of cosmetics or storage of food and mouth pipetling is strictly forbidden.

Unauthorized and casual visitors should be prohibited

4B) Hazard Rating with control methods   LOW

5) FURTHER ACTION REQUIRED

Regular Occupational Check up's in relation to titre levels for HBV

Under take e-learning course http://www.rsclearn.mrc.ac.uk/ and/or
http://www.hta.gov.uk/trainingandconferences/onlinetraining/trainingfordesignatedindividuals.cfm

NAME AND TITLE OF ASSESSOR Helen Sutton Technical Team Leader	SIGNATURE	DATE
	Number: **AS14**	REVIEW DATE
SIGNATURE Dean/ Head of School		DATE

Page 2 of 2

Appendix 3 - Three blood types impacting four surfaces

3.1 Alsever's Blood

Paper

Table A3.1: Bloodstain diameters exhibited using Alsever's blood 1mm pipette on paper.

1mm	Height 30.5cm						Average	S.D
	Spines N	22	18	19	18	18	19	1.732051
	Diameter (mm)	13	13	12	12	12	12.4	0.547723
	Height 60.9cm							
	Spines N	22	22	26	29	27	25.2	3.114482
	Diameter (mm)	15	15.5	15	15.5	14.5	15.1	0.41833
	Height 91.4cm							
	Spines N	32	34	36	37	28	33.4	3.577709
	Diameter (mm)	16.5	16	17	17	17	16.7	0.447214
	Height 121.9cm							
	Spines N	37	33	32	31	35	33.6	2.408319
	Diameter (mm)	17	17	16.5	17.5	17	17	0.353553

1.77mm	Height 30.5cm							
	Spines N	25	23	23	24	25	24	1
	Diameter (mm)	16	15.5	15.5	16	15.5	15.7	0.273861
	Height 60.9cm							
	Spines N	33	34	30	33	27	31.4	2.880972
	Diameter (mm)	19	18	18	18	18	18.2	0.447214
	Height 91.4cm							
	Spines N	38	36	38	37	35	36.8	1.30384
	Diameter (mm)	19	19.5	20	19	19.5	19.4	0.41833
	Height 121.9cm							
	Spines N	41	38	38	45	38	40	3.082207
	Diameter (mm)	20	20	19.5	19.5	19.5	19.7	0.273861

Table A3.12: Bloodstain diameters exhibited using Alsever's blood 1.77mm pipette on paper.

Steel

Table A3.13: Bloodstain diameters exhibited using Alsever's blood 1mm pipette on steel.

1mm	Height 30.5cm						Average	S.D
	Spines N	13	7	15	15	10	12	3.464102
	Diameter (mm)	13.5	13.5	14	14	14	13.8	0.273861
	Height 60.9cm							
	Spines N	21	22	25	19	22	21.8	2.167948
	Diameter (mm)	16	16	15.5	16.5	17	16.2	0.570088
	Height 91.4cm							
	Spines N	27	29	29	28	28	28.2	0.83666
	Diameter (mm)	18	18	17.5	18	18	17.9	0.223607
	Height 121.9cm							
	Spines N	29	25	33	29	32	29.6	3.130495
	Diameter (mm)	18.5	18.5	17.5	18	18	18.1	0.41833

1.77mm	Height 30.5cm						Average	S.D
	Spines N	7	9	15	4	5	8	4.358899
	Diameter (mm)	16.5	17	16.5	16	16.5	16.5	0.353553
	Height 60.9cm							
	Spines N	27	30	26	23	23	25.8	2.949576
	Diameter (mm)	19	18	18.5	19	18.5	18.6	0.41833
	Height 91.4cm							
	Spines N	30	31	31	34	33	31.8	1.643168
	Diameter (mm)	20	20	20	20	19.5	19.9	0.223607
	Height 121.9cm							
	Spines N	30	35	39	32		34	3.91578
	Diameter (mm)	20	23	21.5	20.5		21.25	1.322876

Table A3.14: Bloodstain diameters exhibited using Alsever's blood 1.77mm pipette on steel.

Plastic

Table A3.15: Bloodstain diameters exhibited using Alsever's blood 1mm pipette on plastic.

1mm	Height 30.5cm						Average	S.D
	Spines N	17	19	18	15	20	17.8	1.923538
	Diameter (mm)	13.5	13	13	13.5	13	13.2	0.273861
	Height 60.9cm							
	Spines N	24	29	24	27	32	27.2	3.420526
	Diameter (mm)	16	16	17	17	16	16.4	0.547723
	Height 91.4cm							
	Spines N	37	28	25	30	26	29.2	4.764452
	Diameter (mm)	17	17	17	17	16.5	16.9	0.223607
	Height 121.9cm							
	Spines N	32	32	34	32	33	32.6	0.894427
	Diameter (mm)	18	17	16.5	18	17.5	17.4	0.65192

1.77mm	Height 30.5cm						Average	S.D
	Spines N	21	21	23	23	27	23	2.44949
	Diameter (mm)	18	16.5	17.5	17	17	17.2	0.570088
	Height 60.9cm							
	Spines N	33	30	36	36	33	33.6	2.50998
	Diameter (mm)	20	19.5	19	19	19.5	19.4	0.41833
	Height 91.4cm							
	Spines N	41	43	40	41	44	41.8	1.643168
	Diameter (mm)	21	20.5	21	21	20	20.7	0.447214
	Height 121.9cm							
	Spines N	41	40	41	40	44	41.2	1.643168
	Diameter (mm)	22.5	21	21.5	21	21.5	21.5	0.612372

Table A3.16: Bloodstain diameters exhibited using Alsever's blood 1.77mm pipette on plastic.

Tile

Table A3.17: Bloodstain diameters exhibited using Alsever's blood 1mm pipette on tile.

1mm	Height 30.5cm						Average	S.D
	Spines N	23	22	20	22	17	20.8	2.387467
	Diameter (mm)	15	15	15	15	15	15	0
	Height 60.9cm							
	Spines N	24	24	20	21	22	22.2	1.788854
	Diameter (mm)	16.5	16.5	16.5	16	16	16.3	0.273861
	Height 91.4cm							
	Spines N	27	24	25	28	27	26.2	1.643168
	Diameter (mm)	17	17	17	17	17.5	17.1	0.223607
	Height 121.9cm							
	Spines N	32	23	32	29	28	28.8	3.701351
	Diameter (mm)	20	19	18	19	18	18.8	0.83666

1.77mm	Height 30.5cm						Average	S.D
	Spines N	21	19	23	20	20	20.6	1.516575
	Diameter (mm)	19	19	19	18.5	19	18.9	0.223607
	Height 60.9cm							
	Spines N	27	28	23	27	31	27.2	2.863564
	Diameter (mm)	22	21	22	21	21	21.4	0.547723
	Height 91.4cm							
	Spines N	27	24	27	32	24	26.8	3.271085
	Diameter (mm)	23.5	22.5	23	22.5	22.5	22.8	0.447214
	Height 121.9cm							
	Spines N	32	38	34	36	36	35.2	2.280351
	Diameter (mm)	23.5	23.5	23.5	22.5	22	23	0.707107

Table A3.18: Bloodstain diameters exhibited using Alsever's blood 1.77mm pipette on tile.

3.2 Human Blood

Paper

Table A3.21: Bloodstain diameters exhibited using human blood 1mm pipette on paper.

1mm	Height 30.5cm						Average	S.D
	Spines N	17	18	18	14	16	16.6	1.67332
	Diameter (mm)	11	11	12	11.5	11.5	11.4	0.41833
	Height 60.9cm							
	Spines N	23	26	23	25	23	24	1.414214
	Diameter (mm)	13	13	13.5	13.5	14	13.4	0.41833
	Height 91.4cm							
	Spines N	21	24	25	28	27	25	2.738613
	Diameter (mm)	14	14	14	13	14	13.8	0.447214
	Height 121.9cm							
	Spines N	32	30	30	34		31.5	1.914854
	Diameter (mm)	15	15	14.5	15		14.875	0.25

1.77mm	Height 30.5cm						Average	S.D
	Spines N	24	25	21	20	22	22.4	2.073644
	Diameter (mm)	15	15	14	14	14	14.4	0.547723
	Height 60.9cm							
	Spines N	33	27	27	26		28.25	3.201562
	Diameter (mm)	16.5	17	17	16.5	16.5	16.7	0.273861
	Height 91.4cm							
	Spines N	31	29	32	32	32	31.2	1.30384
	Diameter (mm)	17	16.5	17.5	17	18	17.2	0.570088
	Height 121.9cm							
	Spines N	39	33	35	31	33	34.2	3.03315
	Diameter (mm)	18.5	18	18	18	17.5	18	0.353553

Table A3.22: Bloodstain diameters exhibited using human blood 1.77mm pipette on paper.

Steel

Table A3.23: Bloodstain diameters exhibited using human blood 1mm pipette on steel.

1mm	Height 30.5cm						Average	S.D
	Spines N	2	7	3	0	0	2.4	2.880972
	Diameter (mm)	12	12	12	12.5	12	12.1	0.223607
	Height 60.9cm							
	Spines N	9	7	10	5	7	7.6	1.949359
	Diameter (mm)	14	14	14	13.5	14	13.9	0.223607
	Height 91.4cm							
	Spines N	17	19	16	19	16	17.4	1.516575
	Diameter (mm)	14.5	14.5	14.5	14.5	14.5	14.5	0
	Height 121.9cm							
	Spines N	17	20	17	20	20	18.8	1.643168
	Diameter (mm)	15.5	14.5	15.5	15.5	15.5	15.3	0.447214

1.77mm	Height 30.5cm						Average	S.D
	Spines N	3	3	2	3	3	2.8	0.447214
	Diameter (mm)	15	14.5	15	14.5	14.5	14.7	0.273861
	Height 60.9cm							
	Spines N	12	11	13	13	11	12	1
	Diameter (mm)	17	17	17.5	17.5	16.5	17.1	0.41833
	Height 91.4cm							
	Spines N	22	24	22	22	19	21.8	1.788854
	Diameter (mm)	18	18	17.5	18	17.5	17.8	0.273861
	Height 121.9cm							
	Spines N	25	21	22	25		23.25	2.061553
	Diameter (mm)	18.5	17.5	18	18.5		18.125	0.478714

Table A3.24: Bloodstain diameters exhibited using human blood 1.77mm pipette on steel.

Tile

Table A3.25: Bloodstain diameters exhibited using human blood 1mm pipette on tile.

1mm	Height 30.5cm						Average	S.D
	Spines N	0	0	2	2	2	1.2	1.095445
	Diameter (mm)	11	11	11	11.5	12	11.3	0.447214
	Height 60.9cm							
	Spines N	9	6	6	2	7	6	2.54951
	Diameter (mm)	14	14	13.5	14	14	13.9	0.223607
	Height 91.4cm							
	Spines N	9	11	6	5	10	8.2	2.588436
	Diameter (mm)	15	15	15	15	15	15	0
	Height 121.9cm							
	Spines N	15	17	15	18	10	15	3.082207
	Diameter (mm)	15	16	16	16.5	15.5	15.8	0.570088

1.77mm	Height 30.5cm						Average	S.D
	Spines N	7	7	8	6	7	7	0.707107
	Diameter (mm)	15	15	14.5	15.5	15.5	15.1	0.41833
	Height 60.9cm							
	Spines N	9	10	7	7	10	8.6	1.516575
	Diameter (mm)	17	16.5	17.5	17.5	17	17.1	0.41833
	Height 91.4cm							
	Spines N	17	16	16	21	19	17.8	2.167948
	Diameter (mm)	17.5	18.5	17.5	19	18.5	18.2	0.67082
	Height 121.9cm							
	Spines N	24	19	17	21	19	20	2.645751
	Diameter (mm)	19.5	19.5	19.5	18.5	19	19.2	0.447214

Table A3.26: Bloodstain diameters exhibited using human blood 1.77mm pipette on tile.

Plastic

Table A3.27: Bloodstain diameters exhibited using human blood 1mm pipette on plastic.

1mm	Height 30.5cm						Average	S.D
	Spines N	12	12	17	16	5	12.4	4.722288
	Diameter (mm)	11.5	11	11	11.5	11.5	11.3	0.273861
	Height 60.9cm							
	Spines N	18	17	21	18	15	17.8	2.167948
	Diameter (mm)	13.5	13.5	14	13.5	13	13.5	0.353553
	Height 91.4cm							
	Spines N	26	22	19	20	27	22.8	3.563706
	Diameter (mm)	14	14.5	14	14	14	14.1	0.223607
	Height 121.9cm							
	Spines N	24	24	19	23	26	23.2	2.588436
	Diameter (mm)	14.5	14.5	14.5	14.5	15	14.6	0.223607

1.77mm	Height 30.5cm						Average	S.D
	Spines N	19	15	19	18	14	17	2.345208
	Diameter (mm)	15	15	14	15	15.5	14.9	0.547723
	Height 60.9cm							
	Spines N	22	25	23	24	21	23	1.581139
	Diameter (mm)	18	17	17	18	18	17.6	0.547723
	Height 91.4cm							
	Spines N	28	27	23	30	31	27.8	3.114482
	Diameter (mm)	18.5	18	18.5	18	18	18.2	0.273861
	Height 121.9cm							
	Spines N	20	33	26	24	20	24.6	5.366563
	Diameter (mm)	19.5	18.5	19	19.5	19.5	19.2	0.447214

Table A3.28: Bloodstain diameters exhibited using human blood 1.77mm pipette on plastic.

3.3 Defibrinated Blood

Paper

Table A3.31: Bloodstain diameters exhibited using defibrinated horse blood 1mm pipette on paper.

1mm	Height 30.5cm						Average	S.D
	Spines N	14	19	20	14	18	17	2.828427
	Diameter (mm)	12	12	12	12.5	12.5	12.2	0.273861
	Height 60.9cm							
	Spines N	24	29	26	25	25	25.8	1.923538
	Diameter (mm)	14	13.5	14	13	13	13.5	0.5
	Height 91.4cm							
	Spines N	30	29	25	27	29	28	2
	Diameter (mm)	14	14	14	14	14	14	0
	Height 121.9cm							
	Spines N	35	30	34	35	29	32.6	2.880972
	Diameter (mm)	15	15	14	14.5	14	14.5	0.5

1.77mm	Height 30.5cm						Average	S.D
	Spines N	23	22	24	22	22	22.6	0.894427
	Diameter (mm)	15	15	15	15	15	15	0
	Height 60.9cm							
	Spines N	29	31	32	27	28	29.4	2.073644
	Diameter (mm)	17	17	17.5	17	17.5	17.2	0.273861
	Height 91.4cm							
	Spines N	27	33	32	36	32	32	3.24037
	Diameter (mm)	17	17	17	18	18	17.4	0.547723
	Height 121.9cm							
	Spines N	37	33	35	34	38	35.4	2.073644
	Diameter (mm)	18	18	17.5	17.5	17	17.6	0.41833

Table A3.32: Bloodstain diameters exhibited using defibrinated horse blood 1.77mm pipette on paper.

Steel

1mm	Height 30.5cm						Average	S.D
	Spines N	4	2	3	1	0	2	1.581139
	Diameter (mm)	12.5	12	12	12	12	12.1	0.223607
	Height 60.9cm							
	Spines N	8	9	12	12	12	10.6	1.949359
	Diameter (mm)	13.5	14	13.5	13.5	13.5	13.6	0.223607
	Height 91.4cm							
	Spines N	8	11	11	9	9	9.6	1.341641
	Diameter (mm)	13.5	14	14	13.5	14	13.8	0.273861
	Height 121.9cm							
	Spines N	2	4	5	2	2	3	1.414214
	Diameter (mm)	14	14.5	14.5	14.5	14.5	14.4	0.223607

1.77mm	Height 30.5cm						Average	S.D
	Spines N	5	9	3	3	6	5.2	2.48998
	Diameter (mm)	15	14.5	14.5	14.5	14.5	14.6	0.223607
	Height 60.9cm							
	Spines N	12	9	16	8	13	11.6	3.209361
	Diameter (mm)	16.5	16.5	16.5	16	16.5	16.4	0.223607
	Height 91.4cm							
	Spines N	21	28	23	26	23	24.2	2.774887
	Diameter (mm)	19.5	18	18	19	19.5	18.8	0.758288
	Height 121.9cm							
	Spines N	25	26	23	30	20	24.8	3.701351
	Diameter (mm)	19	19	20	19.5	18.5	19.2	0.570088

Table A3.34: Bloodstain diameters exhibited using defibrinated horse blood 1.77mm pipette on steel.

Plastic

1mm

Height 30.5cm						Average	S.D
Spines N	5	6	8	7	5	6.2	1.30384
Diameter (mm)	12	12	12	12.5	12.5	12.2	0.273861
Height 60.9cm							
Spines N	17	15	16	18	18	16.8	1.30384
Diameter (mm)	14	14	14	14	14.5	14.1	0.223607
Height 91.4cm							
Spines N	26	21	23	17	18	21	3.674235
Diameter (mm)	14.5	14.5	15	14.5	15	14.7	0.273861
Height 121.9cm							
Spines N	31	23	28	27	31	28	3.316625
Diameter (mm)	15	15.5	16	15	15	15.3	0.447214

1.77mm

Height 30.5cm						Average	S.D
Spines N	21	12	12	17	16	15.6	3.781534
Diameter (mm)	15	15.5	15.5	16	15.5	15.5	0.353553
Height 60.9cm							
Spines N	28	29	29	27	27	28	1
Diameter (mm)	18	18	18	18	18.5	18.1	0.223607
Height 91.4cm							
Spines N	31	30	27	25	31	28.8	2.683282
Diameter (mm)	18.5	18.5	18	19	19	18.6	0.41833
Height 121.9cm							
Spines N	35	37	37	39	35	36.6	1.67332
Diameter (mm)	19	19	20	20	19	19.4	0.547723

Table A3.36: Bloodstain diameters exhibited using defibrinated horse blood 1.77mm pipette on plastic.

Tile

1mm

Height 30.5cm						Average	SD
Spines N	10	12	10	11	12	11	1
Diameter (mm)	13	13.5	13.5	13.5	12.5	13.2	0.447214
Height 60.9cm							
Spines N	13	12	15	11	17	13.6	2.408319
Diameter (mm)	14.5	14.5	14	14	14	14.2	0.273861
Height 91.4cm							
Spines N	21	20	19	25	16	20.2	3.271085
Diameter (mm)	15	15	15.5	15.5	15	15.2	0.273861
Height 121.9cm							
Spines N	19	22	16	20	24	20.2	3.03315
Diameter (mm)	16	16	15.5	15	15.5	15.6	0.41833

1.77mm

Height 30.5cm						Average	SD
Spines N	12	9	16	10		11.75	3.095696
Diameter (mm)	16	16	17	17	17	16.6	0.547723
Height 60.9cm							
Spines N	9	11	1	9	12	8.4	4.335897
Diameter (mm)	19	19	19	19	18.5	18.9	0.223607
Height 91.4cm							
Spines N	23	20	27	20		22.5	3.316625
Diameter (mm)	19.5	19.5	19	19		19.25	0.288675
Height 121.9cm							
Spines N	14	14	14	18	15	15	1.732051
Diameter (mm)	19	20	20.5	20	19.5	19.8	0.570088

Table A3.38: Bloodstain diameters exhibited using defibrinated horse blood 1.77mm pipette on tile.

Appendix 4 – Blood Impacting Angled Surfaces

4.1 Plastic (1.77 mm)

									Average	Standard Dev.
90	50	width	14.5	15	15	15.5	15		15	0.353553
		length								
		spines	19	17	20	16	19		18.2	1.643168
	100	width	18	18	17	17	17.5		17.5	0.5
		length								
		spines	33	31	23	27	25		27.8	4.147288
	150	width	19	18	18.5	18.5	18		18.4	0.41833
		length								
		spines	34	37	31	37	34		34.6	2.50998
	200	width	19	18.5	18.5	18	18		18.4	0.41833
		length								
		spines	37	33	36	35	34		35	1.581139

Table A4.1.1: Bloodstain diameters exhibited using 1.77mm pipette on angled plastic

									Average	Standard Dev.
78.8	50	width	16	17	16	17	16.5		16.5	0.5
		length	16.5	17.5	17	17	17		17	0.353553
		spines	5	12	8	12	8		9	3
	100	width	17	17.5	18	18	17.5		17.6	0.41833
		length	18	18	18.5	18	18		18.1	0.223607
		spines	20	18	17	20	21		19.2	1.643168
	150	width	19.5	19	19.5	19	19		19.2	0.273861
		length	20	20	20	20	20		20	0
		spines	14	19	16	16	14		15.8	2.04939
	200	width	19.5	19	19.5	18.5	18		18.9	0.65192
		length	20	19.5	20	19	19		19.5	0.5
		spines	31	17	24	27	31		26	5.830952

Table A4.1.2: Bloodstain diameters exhibited using 1.77mm pipette on angled plastic.

								Average	Standard Dev.
56.3	50	width	16	15.5	15.5	15.5	15.5	15.6	0.223607
		length	18	17.5	17.5	17.5	17.5	17.6	0.223607
		spines	12	9	9	12	12	10.8	1.643168
	100	width	17	17.5	18.5	17	17.5	17.5	0.612372
		length	19.5	20	20.5	19.5	19.5	19.8	0.447214
		spines	19	20	13	17	17	17.2	2.683282
	150	width	19	18.5	18.5	18.5	18	18.5	0.353553
		length	21.5	21	21	21	21	21.1	0.223607
		spines	23	24	18	30	24	23.8	4.266146
	200	width	19	19	19	18.5	19	18.9	0.223607
		length	22	21.5	22	21.5	21	21.6	0.41833
		spines	29	29	38	31	34	32.2	3.834058

Table A4.1.3: Bloodstain diameters exhibited using 1.77mm pipette on angled plastic.

								Average	Standard Dev.
61.6	50	width	15	15	15	15	15	15	0
		length	17	17	16.5	16.5	16.5	16.7	0.273861
		spines	12	10	11	7	13	10.6	2.302173
	100	width	17	16	17.5	16	17	16.7	0.67082
		length	19	18	18.5	17.5	18.5	18.3	0.570088
		spines	15	19	14	16	17	16.2	1.923538
	150	width	17.5	17	17	17.5	18	17.4	0.41833
		length	19	19	19.5	19.5	19.5	19.3	0.273861
		spines	24	22	28	30	28	26.4	3.286335
	200	width	18.5	19	17.5	18	18	18.2	0.570088
		length	20	20	19	19.5	19.5	19.6	0.41833
		spines	32	28	28	29	30	29.4	1.67332

Table A4.1.4: Bloodstain diameters exhibited using 1.77mm pipette on angled plastic

								Average	Standard Dev.
43.3	50	width	13.5	14	13	13.5	13	13.4	0.41833
		length	20	20	19	19	19	19.4	0.547723
		spines	4	3	2	3	5	3.4	1.140175
	100	width	16.5	16.5	16.5	16.5	16.5	16.5	0
		length	22.5	22.5	21	22	21.5	21.9	0.65192
		spines	3	8	5	6	9	6.2	2.387467
	150	width	17	16.5	16.5	16.5	16.5	16.6	0.223607
		length	23.5	24.5	23	23.5	24	23.7	0.570088
		spines	25	27	19	19	17	21.4	4.335897
	200	width	17.5	17	17.5	17.5	17	17.3	0.273861
		length	25	23.5	23.5	23	22.5	23.5	0.935414
		spines	16	15	20	15	16	16.4	2.073644

Table A4.1.5: Bloodstain diameters exhibited using 1.77mm pipette on angled plastic

								Average	Standard Dev.
22.7	50	width	10	10.5	10	10	10.5	10.2	0.273861
		length	27	28	28	26.5	28.5	27.6	0.821584
		spines	0	0	0	0	0	0	0
	100	width	11.5	12	12.5	12	12.5	12.1	0.41833
		length	29	29	31	28	30	29.4	1.140175
		spines	2	0	0	1	0	0.6	0.894427
	150	width	12	11	11.5	12.5	12	11.8	0.570088
		length	31	31	31	30.5	30.5	30.8	0.273861
		spines	3	1	2	1	0	1.4	1.140175
	200	width	12.5	12.5	12.5	12.5	12.5	12.5	0
		length	33.5	33.5	33.5	33.5	30.5	32.9	1.341641
		spines	1	2	4	1	2	2	1.224745

Table A4.1.6: Bloodstain diameters exhibited using 1.77mm pipette on angled plastic

Plastic (1 mm)

								Average	Standard Dev.
90	50	width	13	13.5	13.5	13	13	13.2	0.273861
		length							
		spines	5	2	5	4		4	1.414214
	100	width	14	14.5	15	14.5	14.5	14.5	0.353553
		length							
		spines	2	4	2	2	3	2.6	0.894427
	150	width	15	15.5	15.5	15	15	15.2	0.273861
		length							
		spines	2	3	5	4	0	2.8	1.923538
	200	width	15.5	16	16	16	15.5	15.8	0.273861
		length							
		spines	5	6	6	5		5.5	0.57735

Table A4.1.7: Bloodstain diameters exhibited using 1mm pipette on angled plastic

								Average	Standard Dev.
78.8	50	width	13	13	13	13	12	12.8	0.447214
		length	13.5	13.5	13.5	13.5	12.5	13.3	0.447214
		spines	10	10	14	15	17	13.2	3.114482
	100	width	14	13.5	13	13	13	13.3	0.447214
		length	14.5	14	13.5	13.5	13.5	13.8	0.447214
		spines	9	6	3	10	7	7	2.738613
	150	width	14.5	15	15	15	14.5	14.8	0.273861
		length	15	15.5	15.5	15.5	15	15.3	0.273861
		spines	18	16	21	27	19	20.2	4.207137
	200	width	15	15	15	15	15	15	0
		length	16	16	16	16	15.5	15.9	0.223607
		spines	26	30	25	23	34	27.6	4.393177

Table A4.1.8: Bloodstain diameters exhibited using 1mm pipette on angled plastic

61.6	50							Average	Standard Dev.
	50	width	12	12	11	12	12	11.8	0.447214
		length	13	13	12	13	13	12.8	0.447214
		spines	13	10	11	9	10	10.6	1.516575
	100	width	13.5	13.5	13	13.5	14	13.5	0.353553
		length	15	15	14.5	14.5	15	14.8	0.273861
		spines	14	13	14	14	14	13.8	0.447214
	150	width	14.5	14.5	15	15	14	14.6	0.41833
		length	16	16	16	16	15	15.8	0.447214
		spines	24	21	26	17	21	21.8	3.420526
	200	width	15	15	15.5	15.5	15	15.2	0.273861
		length	17	17	17.5	17	17	17.1	0.223607
		spines	24	29	33	30	32	29.6	3.507136

Table A4.1.9: Bloodstain diameters exhibited using 1mm pipette on angled plastic

56.3	50							Average	Standard Dev.
	50	width	11.5	11	11	12	11	11.3	0.447214
		length	13	13	13.5	14	13	13.3	0.447214
		spines	2	2	4	5	6	3.8	1.788854
	100	width	13	13.5	13	13.5	13.5	13.3	0.273861
		length	15.5	16	15	15.5	16	15.6	0.41833
		spines	8	9	7	10	10	8.8	1.30384
	150	width	14.5	14.5	15	14.5	15	14.7	0.273861
		length	18.5	18.5	18.5	18	18.5	18.4	0.223607
		spines	8	10	10	7	13	9.6	2.302173
	200	width	14.5	15	14.5	14.5	14.5	14.6	0.223607
		length	18	19	19	18.5	18.5	18.6	0.41833
		spines	15	14	14	14	13	14	0.707107

Table A4.1.10: Bloodstain diameters exhibited using 1mm pipette on angled plastic

43.3								Average	Standard Dev.
	50	width	10.5	11	11	10	10.5	10.6	0.41833
		length	16	16.5	16.5	16	16	16.2	0.273861
		spines	4	5	5	3	7	4.8	1.48324
	100	width	12	12.5	12.5	12.5	12.5	12.4	0.223607
		length	17	18	18	18	18	17.8	0.447214
		spines	6	6	2	11	8	6.6	3.286335
	150	width	13.5	12.5	13	13.5	13.5	13.2	0.447214
		length	18	18	18.5	17.5	18	18	0.353553
		spines	8	6	9	8	12	8.6	2.19089
	200	width	13.5	13.5	13.5	13	13.5	13.4	0.223607
		length	19	19	18.5	18	19	18.7	0.447214
		spines	6	5	13	16	4	8.8	5.357238

Table A4.1.11: Bloodstain diameters exhibited using 1mm pipette on angled plastic.

22.7								Average	Standard Dev.
	50	width	7.5	7.5	7.5	7	7.5	7.4	0.223607
		length	25.5	25	24.5	23.5	24	24.5	0.790569
		spines	0	0	0	0	0	0	0
	100	width	7.5	8.5	7.5	9	9	8.3	0.758288
		length	26.5	24	25.5	27	26.5	25.9	1.193734
		spines	0	0	0	0	0	0	0
	150	width	9.5	10	10	10	10	9.9	0.223607
		length	24	25	26	24.5	25	24.9	0.74162
		spines	6	5	3	5	3	4.4	1.341641
	200	width	9.5	10	10.5	10	10	10	0.353553
		length	25.5	25.5	27	27.5	27.5	26.6	1.024695
		spines	5	5	1	4	4	3.8	1.643168

Table A4.1.12: Bloodstain diameters exhibited using 1mm pipette on angled plastic

4.2 Steel (1.77mm)

90								Average	Standard Dev.
	50	width	16.5	16.5	16.5	16.5	16	16.4	0.223607
		length							
		spines	0	0	0	0	0	0	0
	100	width	17.5	18.5	18.5	18.5	18	18.2	0.447214
		length							
		spines	5	5	8	10	11	7.8	2.774887
	150	width	19	19	18.5	18	19	18.7	0.447214
		length							
		spines	18	10	12	10	12	12.4	3.286335
	200	width	19.5	19	20	20	19.5	19.6	0.41833
		length							
		spines	5	19	30	24	24	20.4	9.449868

Table A4.2.1: Bloodstain diameters exhibited using 1.77mm pipette on angled steel.

78.8								Average	Standard Dev.
	50	width	16	16	15.5	15.5	16	15.8	0.273861
		length	16.5	16.5	16.5	16	16.5	16.4	0.223607
		spines	3	4	3	5	5	4	1
	100	width	17.5	18.5	18	19		18.25	0.645497
		length	18	19	18.5	19		18.625	0.478714
		spines	9	12	10	14		11.25	2.217356
	150	width	17	18	18	18	18	17.8	0.447214
		length	17.5	18	18.5	19	19	18.4	0.65192
		spines	29	31	36	35	30	32.2	3.114482
	200	width	18	18	18.5	18.5		18.25	0.288675
		length	19	19	19	19		19	0
		spines	31	36	35	32	28	32.4	3.209361

Table A4.2.2: Bloodstain diameters exhibited using 1.77mm pipette on angled steel.

								Average	Standard Dev.
61.6	50	width	14	14.5	14.5	14	14.5	14.3	0.273861
		length	17	17	17.5	17	17.5	17.2	0.273861
		spines	1	3	6	5	6	4.2	2.167948
	100	width	16	16	15.5	16.5	17	16.2	0.570088
		length	19.5	19.5	18.5	19.5	19.5	19.3	0.447214
		spines	17	9	14	15	10	13	3.391165
	150	width	17	17.5	17.5	17.5	17.5	17.4	0.223607
		length	20	20	20	20	21	20.2	0.447214
		spines	17	13	24	17	19	18	4
	200	width	18	18	17	18	17	17.6	0.547723
		length	20	20.5	20	20.5	20	20.2	0.273861
		spines	19	8	8	20	19	14.8	6.220932

Table A4.2.3: Bloodstain diameters exhibited using 1.77mm pipette on angled steel.

								Average	Standard Dev.
56.3	50	width	15	14.5	14.5	14	15	14.6	0.41833
		length	19.5	19.5	19	19	19	19.2	0.273861
		spines	3	3	0	1	2	1.8	1.30384
	100	width	16	16.5	16	16.5	16.5	16.3	0.273861
		length	21	21.5	21	21.5	21.5	21.3	0.273861
		spines	8	7	8	7	6	7.2	0.83666
	150	width	17	17.5	17.5	17	17	17.2	0.273861
		length	22	22	22.5	22.5	22	22.2	0.273861
		spines	14	14	15	14	12	13.8	1.095445
	200	width	17.5	18	17.5	17	17.5	17.5	0.353553
		length	22.5	22	22	22	22.5	22.2	0.273861
		spines	12	20	21	14	18	17	3.872983

Table A4.2.4: Bloodstain diameters exhibited using 1.77mm pipette on angled steel.

								Average	Standard Dev.
43.3	50	width	14	13.5	13	12.5	13	13.2	0.570088
		length	23.5	23.5	22	22.5	22.5	22.8	0.67082
		spines	2	2	0	0	0	0.8	1.095445
	100	width	15	15.5	15.5	14.5	14.5	15	0.5
		length	24	25	25	24	24	24.4	0.547723
		spines	7	7	9	4	6	6.6	1.81659
	150	width	16	15	15	16.5	15.5	15.6	0.65192
		length	29	27.5	26	28	28.5	27.8	1.151086
		spines	8	6	8	6	9	7.4	1.341641
	200	width	16.5	15.5	16	16	15.5	15.9	0.41833
		length	29	27	27.5	27.5	27	27.6	0.821584
		spines	6	6	9	10		7.75	2.061553

Table A4.2.5: Bloodstain diameters exhibited using 1.77mm pipette on angled steel.

								Average	Standard Dev.
22.7	50	width	10.5	11	10.5	10.5	10	10.5	0.353553
		length	29.5	30.5	30.5	31	30.5	30.4	0.547723
		spines	0	0	0	0	0	0	0
	100	width	12	12.5	12	12	12	12.1	0.223607
		length	32	30.5	32	32	32	31.7	0.67082
		spines	0	0	0	0	0	0	0
	150	width	12	12.5	12.5	12.5	12	12.3	0.273861
		length	35	33.5	34	34	34	34.1	0.547723
		spines	0	0	0	0	0	0	0
	200	width	13.5	13.5	13.5	13.5	13.5	13.5	0
		length	36.5	34.5	36	36	36	35.8	0.758288
		spines	0	0	0	0	0	0	0

Table A4.2.6: Bloodstain diameters exhibited using 1.77mm pipette on angled steel.

Steel (1mm)

									Average	Standard Dev.
90	50	width	12.5	12.5	12.5	12.5	12.5		12.5	0
		length								
		spines	5	2	2	4	4		3.4	1.341641
	100	width	14.5	14.5	13.5	14.5	14.5		14.3	0.447214
		length								
		spines	6	8	6	6	7		6.6	0.894427
	150	width	15	15	15	15.5	15.5		15.2	0.273861
		length								
		spines	13	14	11	9	12		11.8	1.923538
	200	width	16	16	16	15.5	16		15.9	0.223607
		length								
		spines	8	5	8	9	5		7	1.870829

Table A4.2.7: Bloodstain diameters exhibited using 1mm pipette on angled steel.

									Average	Standard Dev.
78.8	50	width	12	12.5	12.5	12.5	12.5		12.4	0.223607
		length	12.5	13	13	13	13		12.9	0.223607
		spines	3	1	0	0	0		0.8	1.30384
	100	width	13	14	14	14	13.5		13.7	0.447214
		length	13.5	14.5	14.5	14.5	14		14.2	0.447214
		spines	3	0	8	6	2		3.8	3.193744
	150	width	14	14.5	14.5	14.5	14.5		14.4	0.223607
		length	14.5	15	15	15	15		14.9	0.223607
		spines	6	10	5	7	3		6.2	2.588436
	200	width	15	15	15.5	15			15.125	0.25
		length	15.5	15.5	16	15.5			15.625	0.25
		spines	5	5	6	3	3		4.4	1.341641

Table A4.2.8: Bloodstain diameters exhibited using 1mm pipette on angled steel.

								Average	Standard Dev.
61.6	50	width	12	12	12.5	12	12	12.1	0.223607
		length	14.5	14.5	14.5	14.5	13.5	14.3	0.447214
		spines	0	5	2	0	5	2.4	2.50998
	100	width	13	13	13.5	13	13	13.1	0.223607
		length	15	15	15.5	15	15	15.1	0.223607
		spines	7	6	7	7	8	7	0.707107
	150	width	14	14	13.5	14.5	14	14	0.353553
		length	16.5	16	16	16.5	16	16.2	0.273861
		spines	10	12	14	11	11	11.6	1.516575
	200	width	15	14.5	14.5	14.5	14	14.5	0.353553
		length	17.5	17	17	17	16.5	17	0.353553
		spines	15	15	17	19	16	16.4	1.67332

Table A4.2.9: Bloodstain diameters exhibited using 1mm pipette on angled steel

								Average	Standard Dev.
56.3	50	width	11.5	11.5	12	11.5	10.5	11.4	0.547723
		length	15	15.5	16	15.5	14.5	15.3	0.570088
		spines	0	0	0	0	2	0.4	0.894427
	100	width	14.5	14	13.5	13.5	14	13.9	0.41833
		length	18	17.5	17.5	17.5	17.5	17.6	0.223607
		spines	3	3	7	3	6	4.4	1.949359
	150	width	13.5	13.5	14	14	14	13.8	0.273861
		length	15.5	16	16	16	16	15.9	0.223607
		spines	18	18	18	24	20	19.6	2.607681
	200	width	14	14.5	14.5	15	14	14.4	0.41833
		length	16	16	17	18	17	16.8	0.83666
		spines	20	24	21	22	32	23.8	4.816638

Table A4.2.10: Bloodstain diameters exhibited using 1mm pipette on angled steel

								Average	Standard Dev.
43.3	50	width	11	11	11	10.5	10.5	10.8	0.273861
		length	18.5	18.5	18	18	18	18.2	0.273861
		spines	2	0	1	3	1	1.4	1.140175
	100	width	12	12.5	12	12	11.5	12	0.353553
		length	19	19.5	18.5	19	18	18.8	0.570088
		spines	2	2	4	5	5	3.6	1.516575
	150	width	12.5	12.5	12.5	13.5	12.5	12.7	0.447214
		length	19	19	19.5	20.5	18.5	19.3	0.758288
		spines	3	6	2	4	5	4	1.581139
	200	width	13.5	13.5	13.5	13.5	13	13.4	0.223607
		length	21	20	20.5	21	20.5	20.6	0.41833
		spines	3	8	5	7	7	6	2

Table A4.2.11: Bloodstain diameters exhibited using 1mm pipette on angled steel

								Average	Standard Dev.
22.7	50	width	7.5	7	7.5	8	7.5	7.5	0.353553
		length	26	26	26	26	26	26	0
		spines	0	0	0	0	0	0	0
	100	width	9	8.5	8.5	8.5	8.5	8.6	0.223607
		length	28	27	27.5	27	27.5	27.4	0.41833
		spines	0	0	0	0	0	0	0
	150	width	10.5	10.5	10	10.5	10	10.3	0.273861
		length	30	30	28	29	29	29.2	0.83666
		spines	0	0	0	0	0	0	0
	200	width	10	10.5	10.5	10	10	10.2	0.273861
		length	29	29	29	30	29	29.2	0.447214
		spines	0	0	0	0	0	0	0

Table A4.2.12: Bloodstain diameters exhibited using 1mm pipette on angled steel

4.3 Paper (1.77mm)

								Average	Standard Dev
90	50	width	15	15	15	15	15.5	15.1	0.223607
		length							
		spines	23	25	26	25	24	24.6	1.140175
	100	width	16	16.5	17	16	16	16.3	0.447214
		length							
		spines	33	30	31	33		31.75	1.5
	150	width	16.5	16	15.5	17.5	16.5	16.4	0.74162
		length							
		spines	33	30	35	34	34	33.2	1.923538
	200	width	18	18	17.5	18.5	18	18	0.353553
		length							
		spines	40	37	36	39		38	1.825742

Table A4.3.1: Bloodstain diameters exhibited using 1.77mm pipette on angled paper

								Average	Standard Dev
78.8	50	width	16	16	16	16	16	16	0
		length	17.5	17	17	17	17	17.1	0.223607
		spines	13	14	14	15	14	14	0.707107
	100	width	17.5	17.5	17.5	17		17.375	0.25
		length	18.5	18.5	18.5	18		18.375	0.25
		spines	30	30	29	27	28	28.8	1.30384
	150	width	17.5	17.5	18	18	18	17.8	0.273861
		length	19	19	19	19	19	19	0
		spines	38	38	36	37	36	37	1
	200	width	18.5	19	19	19		18.875	0.25
		length	20	20	20.5	20		20.125	0.25
		spines	39	37	37	35	37	37	1.414214

Table A4.3.2: Bloodstain diameters exhibited using 1.77mm pipette on angled paper.

								Average	Standard Dev
61.6	50	width	14.5	14	15	14.5	14.5	14.5	0.353553
		length	17	16.5	16.5	16.5	16.5	16.6	0.223607
		spines	14	20	19	22	19	18.8	2.949576
	100	width	16.5	16.5	16.5	16.5	16.5	16.5	0
		length	19	19.5	19.5	19	19	19.2	0.273861
		spines	27	30	23	28	29	27.4	2.701851
	150	width	17	16	16.5	16.5	16.5	16.5	0.353553
		length	19.5	19.5	19.5	19	20	19.5	0.353553
		spines	34	31	31	33	29	31.6	1.949359
	200	width	17	17	16.5	17.5	18	17.2	0.570088
		length	19.5	20	20	21	20.5	20.2	0.570088
		spines	33	35	33	34	38	34.6	2.073644

Table A4.3.3: Bloodstain diameters exhibited using 1.77mm pipette on angled paper

								Average	Standard Dev
56.3	50	width	14.5	14	15	15	14.5	14.6	0.41833
		length	17.5	18	17	17.5	18.5	17.7	0.570088
		spines	19	18	24	15		19	3.741657
	100	width	16	15.5	15.5	16	15	15.6	0.41833
		length	19.5	19.5	19.5	19.5	19	19.4	0.223607
		spines	22	26	29	23	29	25.8	3.271085
	150	width	17	17	16.5	16.5	16.5	16.7	0.273861
		length	20	20.5	20.5	20.5	20.5	20.4	0.223607
		spines	33	35	33	30	32	32.6	1.81659
	200	width	16.5	17	17	17	17.5	17	0.353553
		length	21	21	21	20.5	20.5	20.8	0.273861
		spines	32	33	35	35	28	32.6	2.880972

Table A4.3.4: Bloodstain diameters exhibited using 1.77mm pipette on angled paper

								Average	Standard Dev
43.3	50	width	13	13.5	13.5	13	13	13.2	0.273861
		length	20	20	20.5	20.5	21	20.4	0.41833
		spines	10	13	15	11	11	12	2
	100	width	15	15	15	15	15	15	0
		length	22	22	22	22.5	22	22.1	0.223607
		spines	20	21	25	20	21	21.4	2.073644
	150	width	15	15	15	15	14.5	14.9	0.223607
		length	22.5	22.5	23.5	22	22.5	22.6	0.547723
		spines	19	21	25	20		21.25	2.629956
	200	width	16.5	15.5	16	16	16	16	0.353553
		length	24	25	24	23.5	25	24.3	0.67082
		spines	23	22	25	27	22	23.8	2.167948

Table A4.3.5: Bloodstain diameters exhibited using 1.77mm pipette on angled paper

								Average	Standard Dev
22.7	50	width	10	9.5	10	10	10	9.9	0.223607
		length	29.5	30	30.5	30.5	30.5	30.2	0.447214
		spines	0	0	0	0	0	0	0
	100	width	11	11	11	11	10.5	10.9	0.223607
		length	29	31	32.5	31.5	32.5	31.3	1.440486
		spines	4	3	3	2	1	2.6	1.140175
	150	width	11.5	11.5	11.5	11.5	12	11.6	0.223607
		length	33	33	33.5	34	35	33.7	0.83666
		spines	4	5	4	7	3	4.6	1.516575
	200	width	13	13	12	12	12.5	12.5	0.5
		length	34.5	34.5	34.5	35	33.5	34.4	0.547723
		spines	4	5	4	2	4	3.8	1.095445

Table A4.3.6: Bloodstain diameters exhibited using 1.77mm pipette on angled paper

Paper (1.77mm)

								Average	Standard Dev
90	50	width	12.5	12.5	12.5	12.5	12.5	12.5	0
		length							
		spines	22	22	22	22	23	22.2	0.447214
	100	width	13	13	13	13	13	13	0
		length							
		spines	28	27	26	27	26	26.8	0.83666
	150	width	14.5	14.5	14.5	13.5	14	14.2	0.447214
		length							
		spines	36	35	33	32	30	33.2	2.387467
	200	width	15	15	15	14.5	15.5	15	0.353553
		length							
		spines	35	35	34	36	34	34.8	0.83666

Table A4.3.7: Bloodstain diameters exhibited using 1mm pipette on angled paper

								Average	Standard Dev
78.8	50	width	12.5	13	13	13	12	12.7	0.447214
		length	13	13.5	13.5	13.5	12.5	13.2	0.447214
		spines	23	24	21	22	22	22.4	1.140175
	100	width	13.5	13.5	12.5	13	13.5	13.2	0.447214
		length	14	14	13	13.5	14	13.7	0.447214
		spines	25	26	26	25	28	26	1.224745
	150	width	14.5	14	14	14	14.5	14.2	0.273861
		length	15	14.5	14.5	14.5	15	14.7	0.273861
		spines	31	31	32	36	32	32.4	2.073644
	200	width	14.5	15	14.5	14.5	15	14.7	0.273861
		length	15	15.5	15	15	15.5	15.2	0.273861
		spines	36	37	38	30	36	35.4	3.130495

Table A4.3.8: Bloodstain diameters exhibited using 1mm pipette on angled paper

								Average	Standard Dev
61.6	50	width	12	12..5	12.5	12	11.5	12	0.408248
		length	13.5	14.5	14	14.5	14	14.1	0.41833
		spines	16	19	17	15	15	16.4	1.67332
	100	width	13	13.5	13	12.5	13	13	0.353553
		length	15.5	15.5	15.5	15	15	15.3	0.273861
		spines	21	22	23	19	27	22.4	2.966479
	150	width	14	14.5	14.5	14	14	14.2	0.273861
		length	16	16	17	16	16.5	16.3	0.447214
		spines	29	30	29	28	26	28.4	1.516575
	200	width	15	15	14.5	14.5	14	14.6	0.41833
		length	17	16.5	16.5	17	17	16.8	0.273861
		spines	27	36	35	35	34	33.4	3.646917

Table A4.3.9: Bloodstain diameters exhibited using 1mm pipette on angled paper

								Average	Standard Dev
56.3	50	width	12.5	11.5	11.5	11.5	12	11.8	0.447214
		length	14.5	14	14	13.5	14	14	0.353553
		spines	10	15	15	18	16	14.8	2.949576
	100	width	12.5	13	13.5	13	13	13	0.353553
		length	16	15.5	15.5	15	15.5	15.5	0.353553
		spines	23	26	22	24	22	23.4	1.67332
	150	width	13	13	14	13	13.5	13.3	0.447214
		length	15.5	16	16	16	15.5	15.8	0.273861
		spines	25	23	25	26	28	25.4	1.81659
	200	width	14	14.5	14	14.5	14	14.2	0.273861
		length	17.5	17	17	17	17.5	17.2	0.273861
		spines	34	32	31	24	32	30.6	3.847077

Table A4.3.10: Bloodstain diameters exhibited using 1mm pipette on angled paper

								Average	Standard Dev
43.3	50	width	10.5	10	10.5	10.5	10.5	10.4	0.223607
		length	16.5	16.5	16.5	16.5	15.5	16.3	0.447214
		spines	6	7	10	7	10	8	1.870829
	100	width	11	12	12	12	12.5	11.9	0.547723
		length	19	18.5	17	18.5	18.5	18.3	0.758288
		spines	10	11	10	12	14	11.4	1.67332
	150	width	12	12.5	12	12.5	12.5	12.3	0.273861
		length	20	19.5	19	20	18	19.3	0.83666
		spines	16	15	16	14	17	15.6	1.140175
	200	width	13	13	13	13.5	13.5	13.2	0.273861
		length	20.5	20	20	20	20	20.1	0.223607
		spines	22	23	21	12	18	19.2	4.438468

Table A4.3.11: Bloodstain diameters exhibited using 1mm pipette on angled paper

								Average	Standard Dev
22.7	50	width	8	8	8	7.5	7.5	7.8	0.273861
		length	26.5	26	26	27	25	26.1	0.74162
		spines	0	0	0	0	0	0	0
	100	width	8.5	8.5	8.5	8.5	8.5	8.5	0
		length	28.5	28.5	28.5	27.5	28	28.2	0.447214
		spines	0	0	0	0	0	0	0
	150	width	9.5	10	9	9.5	9.5	9.5	0.353553
		length	29	31.5	28.5	31	29	29.8	1.350926
		spines	4	4	3	3	3	3.4	0.547723
	200	width	9.5	9.5	9.5	9.5	9.5	9.5	0
		length	29.5	30	28.5	29	29.5	29.3	0.570088
		spines	1	3	3	3	3	2.6	0.894427

Table A4.3.12: Bloodstain diameters exhibited using 1mm pipette on angled paper

Appendix 5 – Bloodstains on Wood Surfaces

Wood Surface (1mm)

European Maple Oak

	Diameter (mm)	Diameter (mm)	Diameter (mm)	Diameter (mm)	Diameter (mm)	Average	Standard Dev.
Height 50cm	13	13	13	13	14	13.2	0.447214
Height 100cm	14	14	14	14	14	14	0
Height 150cm	16	16	16	16	16	16	0
Height 200cm	16	16	16	17	17	16.4	0.547723

Table A5.1: 1mm pipette drop results on European Maple Oak

Clear Oil Oak

	Diameter (mm)	Diameter (mm)	Diameter (mm)	Diameter (mm)	Diameter (mm)	Average	Standard Dev.
Height 50cm	13	13	13	13	13	13	0
Height 100cm	14	14	14	14	15	14.2	0.447214
Height 150cm	15	15	15	16	16	15.4	0.547723
Height 200cm	16	17	17	17	17	16.8	0.447214

Table A5.2: 1mm pipette drop results on Clear Oil Oak.

Oak Natural Siera Matt Lacquered

	Diameter (mm)	Diameter (mm)	Diameter (mm)	Diameter (mm)	Diameter (mm)	Average	Standard Dev.
Height 50cm	13	13	13	13	14	13.2	0.447214
Height 100cm	15	15	15	15	15	15	0
Height 150cm	15	16	16	16	16	15.8	0.447214
Height 200cm	17	17	17	17	18	17.2	0.447214

Table A5.3: 1mm pipette drop results on Oak Natural Siera Matt Lacquered.

Maple Silk Matt Lacquered

	Diameter (mm)	Diameter (mm)	Diameter (mm)	Diameter (mm)	Diameter (mm)	Average	Standard Dev.
Height 50cm	13	13	13	13	14	13.2	0.447214
Height 100cm	15	15	15	15	15	15	0
Height 150cm	15	16	16	16	16	15.8	0.447214
Height 200cm	18	18	18	18	18	18	0

Table A5.4: 1mm pipette drop results on Maple Silk Matt Lacquered

Natura American Black Walnut Rosshill

	Diameter (mm)	Diameter (mm)	Diameter (mm)	Diameter (mm)	Diameter (mm)	Average	Standard Dev.
Height 50cm	13	13	13	14	14	13.4	0.547723
Height 100cm	14	14	14	14	14	14	0
Height 150cm	16	16	16	16	16	16	0
Height 200cm	17	17	17	17	17	17	0

Table A5.5: 1mm pipette drop results on Natura American Black Walnut Rosshill

Natura Walnut Ironbank Mississippi

	Diameter (mm)	Diameter (mm)	Diameter (mm)	Diameter (mm)	Diameter (mm)	Average	Standard Dev.
Height 50cm	13	13	13	13	13	13	0
Height 100cm	14	15	15	15	15	14.8	0.447214
Height 150cm	16	16	16	14	16	15.6	0.894427
Height 200cm	16	16	17	17	17	16.6	0.547723

Table A5.6: 1mm pipette drop results on Natura Walnut Ironbank Mississippi

Quickstep Villa Walnut Satin Lacquer

	Diameter (mm)	Diameter (mm)	Diameter (mm)	Diameter (mm)	Diameter (mm)	Average	Standard Dev.
Height 50cm	14	14	14	14	13	13.8	0.447214
Height 100cm	14	14	14	15	15	14.4	0.547723
Height 150cm	16	16	16	16	16	16	0
Height 200cm	16	17	17	17	18	17	0.707107

Table A5.7: 1mm pipette drop results on Quickstep Villa Walnut Satin Lacquer

Kahrs Maple Toronto Satin Lacquer

	Diameter (mm)	Diameter (mm)	Diameter (mm)	Diameter (mm)	Diameter (mm)	Average	Standard Dev.
Height 50cm	13	13	12	12	12	12.4	0.547723
Height 100cm	14	14	14	14	14	14	0
Height 150cm	15	15	16	16	16	15.6	0.547723
Height 200cm	16	16	17	17	17	16.6	0.547723

Table A5.8: 1mm pipette drop results on Kahrs Maple Toronto Satin Lacquer

Kahrs Walnut Rustic Nature Oil

	Diameter (mm)	Diameter (mm)	Diameter (mm)	Diameter (mm)	Diameter (mm)	Average	Standard Dev.
Height 50cm	13	13	12	12	12	12.4	0.547723
Height 100cm	14	14	14	14	14	14	0
Height 150cm	16	16	16	15	15	15.6	0.547723
Height 200cm	16	16	17	17	17	16.6	0.547723

Table A5.9: 1mm pipette drop results on Kahrs Walnut Rustic Nature Oil

Maple Ultra Matt Lacquered

	Diameter (mm)	Diameter (mm)	Diameter (mm)	Diameter (mm)	Diameter (mm)	Average	Standard Dev.
Height 50cm	13	13	13	14	14	13.4	0.547723
Height 100cm	15	15	15	15	15	15	0
Height 150cm	16	16	16	16	16	16	0
Height 200cm	16	17	17	17	17	16.8	0.447214

Table A5.10: 1mm pipette drop results on Maple Ultra Matt Lacquered

Oak Silk Matt

	Diameter (mm)	Diameter (mm)	Diameter (mm)	Diameter (mm)	Diameter (mm)	Average	Standard Dev.
Height 50cm	14	14	14	14	14	14	0
Height 100cm	15	15	15	15	15	15	0
Height 150cm	16	16	15	17	16	16	0.707107
Height 200cm	17	17	17	17	17	17	0

Table A5.11: 1mm pipette drop results on Oak Silk Matt

Kahrs Maple Bevelled Edge Rustic

	Diameter (mm)	Diameter (mm)	Diameter (mm)	Diameter (mm)	Diameter (mm)	Average	Standard Dev.
Height 50cm	14	14	14	14	14	14	0
Height 100cm	15	15	15	15	15	15	0
Height 150cm	16	16	16	16	16	16	0
Height 200cm	17	17	17	17	17	17	0

Table A5.12: 1mm pipette drop results on Kahrs Maple Bevelled Edge Rustic.

Kahrs Maple Natural Satin Lacquer

	Diameter (mm)	Diameter (mm)	Diameter (mm)	Diameter (mm)	Diameter (mm)	Average	Standard Dev.
Height 50cm	13	13	13	14	14	13.4	0.547723
Height 100cm	15	15	15	15	15	15	0
Height 150cm	15	15	16	16	16	15.6	0.547723
Height 200cm	16	17	17	17	17	16.8	0.447214

Table A5.13: 1mm pipette drop results on Kahrs Maple Natural Satin Lacquer.

Kahrs Linnea Walnut Bloom Prime Satin Lacquer

	Diameter (mm)	Diameter (mm)	Diameter (mm)	Diameter (mm)	Diameter (mm)	Average	Standard Dev.
Height 50cm	13	13	14	14	14	13.6	0.547723
Height 100cm	15	15	15	16	16	15.4	0.547723
Height 150cm	16	16	17	17	17	16.6	0.547723
Height 200cm	17	17	17	17	17	17	0

Table A5.14: 1mm pipette drop results on Kahrs Linnea Walnut Bloom Prime Satin Lacquer.

Kahrs Linnea Walnut Microbevelled Edge Prime Matt Lacquer

	Diameter (mm)	Diameter (mm)	Diameter (mm)	Diameter (mm)	Diameter (mm)	Average	Standard Dev.
Height 50cm	13	13	13	14	14	13.4	0.547723
Height 100cm	15	15	15	15	15	15	0
Height 150cm	15	15	16	16	16	15.6	0.547723
Height 200cm	17	17	17	17	18	17.2	0.447214

Table A5.15: 1mm pipette drop results on Kahrs Linnea Walnut Microbevelled Edge Prime Matt Lacquer.

Natura Walnut Lacquered Satin Lacquer

	Diameter (mm)	Diameter (mm)	Diameter (mm)	Diameter (mm)	Diameter (mm)	Average	Standard Dev.
Height 50cm	13	13	13	13	13	13	0
Height 100cm	15	15	15	15	15	15	0
Height 150cm	15	16	16	16	16	15.8	0.447214
Height 200cm	17	17	17	17	17	17	0

Table A5.16: 1mm pipette drop results on Natura Walnut Lacquered Satin Lacquer

Kahrs Oak Sienna Natural

	Diameter (mm)	Diameter (mm)	Diameter (mm)	Diameter (mm)	Diameter (mm)	Average	Standard Dev.
Height 50cm	13	13	13	13	14	13.2	0.447214
Height 100cm	15	15	15	16	16	15.4	0.547723
Height 150cm	16	16	16	16	16	16	0
Height 200cm	17	17	17	17	18	17.2	0.447214

Table A5.17: 1mm pipette drop results on Kahrs Oak Sienna Natural.

Natura Oak Prime Parquet

	Diameter (mm)	Diameter (mm)	Diameter (mm)	Diameter (mm)	Diameter (mm)	Average	Standard Dev.
Height 50cm	10	10	11	11	12	10.8	0.83666
Height 100cm	12	13	13	13	14	13	0.707107
Height 150cm	13	13	14	13	14	13.4	0.547723
Height 200cm	13	14	14	14	14	13.8	0.447214

Table A5.18: 1mm pipette drop results on Natura Oak Prime Parquet.

Kahrs Oak Siena Engineered Natural

	Diameter (mm)	Diameter (mm)	Diameter (mm)	Diameter (mm)	Diameter (mm)	Average	Standard Dev.
Height 50cm	12	13	13	13	13	12.8	0.447214
Height 100cm	13	13	13	13	13	13	0
Height 150cm	13	13	13	13	14	13.2	0.447214
Height 200cm	14	14	14	14	14	14	0

Table A5.19: 1mm pipette drop results on Kahrs Oak Siena Engineered Natural.

Oak Solid Plank Untreated

	Diameter (mm)	Diameter (mm)	Diameter (mm)	Diameter (mm)	Diameter (mm)	Average	Standard Dev.
Height 50cm	9	9	9	10	10	9.4	0.547723
Height 100cm	13	13	13	13	14	13.2	0.447214
Height 150cm	14	14	14	14	14	14	0
Height 200cm	14	14	14	14	14	14	0

Table A5.20: 1mm pipette drop results on Oak Solid Plank Untreated.

Wood (1.77mm)

European Maple Oak

	Diameter (mm)	Diameter (mm)	Diameter (mm)	Diameter (mm)	Diameter (mm)	Average	Standard Dev.
Height 50cm	16	16	16	16	16	16	0
Height 100cm	17	17	17	17	18	17.2	0.447214
Height 150cm	18	18	19	19	20	18.8	0.83666
Height 200cm	19	19	19	19	20	19.2	0.447214

Table A5.21: 1.77mm pipette drop results on European Maple Oak.

Clear Oil Oak

	Diameter (mm)	Diameter (mm)	Diameter (mm)	Diameter (mm)	Diameter (mm)	Average	Standard Dev.
Height 50cm	15	15	15	15	16	15.2	0.447214
Height 100cm	16	16	16	16	17	16.2	0.447214
Height 150cm	17	17	18	18	18	17.6	0.547723
Height 200cm	18	18	18	18	19	18.2	0.447214

Table A5.22: 1.77mm pipette drop results on Clear Oil Oak.

Oak Natural Siera Matt Lacquered

	Diameter (mm)	Diameter (mm)	Diameter (mm)	Diameter (mm)	Diameter (mm)	Average	Standard Dev.
Height 50cm	16	16	16	15	15	15.6	0.547723
Height 100cm	18	18	17	17	17	17.4	0.547723
Height 150cm	19	19	19	18	18	18.6	0.547723

	Diameter (mm)	Diameter (mm)	Diameter (mm)	Diameter (mm)	Diameter (mm)	Average	Standard Dev.
Height 200cm	20	19	19	19	19	19.2	0.447214

Table A5.23: 1.77mm pipette drop results on Oak Natural Siera Matt Lacquered.

Maple Silk Matt Lacquered

	Diameter (mm)	Diameter (mm)	Diameter (mm)	Diameter (mm)	Diameter (mm)	Average	Standard Dev.
Height 50cm	16	16	16	16	15	15.8	0.447214
Height 100cm	17	17	17	17	18	17.2	0.447214
Height 150cm	19	19	19	19	19	19	0
Height 200cm	19	20	19	19	19	19.2	0.447214

Table A5.24: 1.77mm pipette drop results on Maple Silk Matt Lacquered.

Natura American Black Walnut Rosshill

	Diameter (mm)	Diameter (mm)	Diameter (mm)	Diameter (mm)	Diameter (mm)	Average	Standard Dev.
Height 50cm	17	17	17	17	16	16.8	0.447214
Height 100cm	17	17	17	18	18	17.4	0.547723
Height 150cm	18	18	18	18	19	18.2	0.447214
Height 200cm	19	19	19	19	20	19.2	0.447214

Table A5.25: 1.77mm pipette drop results on Natura American Black Walnut Rosshill.

Natura Walnut Ironbank Mississippi

	Diameter (mm)	Diameter (mm)	Diameter (mm)	Diameter (mm)	Diameter (mm)	Average	Standard Dev.
Height 50cm	15	15	15	16	16	15.4	0.547723
Height 100cm	17	17	17	17	18	17.2	0.447214
Height 150cm	19	19	19	19	18	18.8	0.447214
Height 200cm	19	19	19	20	20	19.4	0.547723

Table A5.26: 1.77mm pipette drop results on Natura Walnut Ironbank Mississippi.

Quickstep Villa Walnut Satin Lacquer

	Diameter (mm)	Diameter (mm)	Diameter (mm)	Diameter (mm)	Diameter (mm)	Average	Standard Dev.
Height 50cm	17	17	16	16	16	16.4	0.547723
Height 100cm	18	18	18	17	17	17.6	0.547723

	Diameter (mm)	Diameter (mm)	Diameter (mm)	Diameter (mm)	Diameter (mm)	Average	Standard Dev.
Height 150cm	18	19	19	19	19	18.8	0.447214
Height 200cm	19	19	19	19	20	19.2	0.447214

Table A5.27: 1.77mm pipette drop results on Quickstep Villa Walnut Satin Lacquer.

Kahrs Maple Toronto Satin Lacquer

	Diameter (mm)	Diameter (mm)	Diameter (mm)	Diameter (mm)	Diameter (mm)	Average	Standard Dev.
Height 50cm	16	16	16	16	16	16	0
Height 100cm	17	17	17	18	18	17.4	0.547723
Height 150cm	18	18	18	19	19	18.4	0.547723
Height 200cm	19	19	19	20	20	19.4	0.547723

Table A5.28: 1.77mm pipette drop results on Kahrs Maple Toronto Satin Lacquer.

Kahrs Walnut Rustic Nature Oil

	Diameter (mm)	Diameter (mm)	Diameter (mm)	Diameter (mm)	Diameter (mm)	Average	Standard Dev.
Height 50cm	15	15	15	16	16	15.4	0.547723
Height 100cm	17	17	17	18	18	17.4	0.547723
Height 150cm	19	19	18	18	18	18.4	0.547723
Height 200cm	19	20	20	20	21	20	0.707107

Table A5.29: 1.77mm pipette drop results on Kahrs Walnut Rustic Nature Oil.

Maple Ultra Matt Lacquered

	Diameter (mm)	Diameter (mm)	Diameter (mm)	Diameter (mm)	Diameter (mm)	Average	Standard Dev.
Height 50cm	15	15	15	15	15	15	0
Height 100cm	17	17	17	17	17	17	0
Height 150cm	18	19	19	19	19	18.8	0.447214
Height 200cm	19	19	20	20	20	19.6	0.547723

Table A5.30: 1.77mm pipette drop results on Maple Ultra Matt Lacquered.

Oak Silk Matt

	Diameter (mm)	Diameter (mm)	Diameter (mm)	Diameter (mm)	Diameter (mm)	Average	Standard Dev.
Height 50cm	16	16	16	16	17	16.2	0.447214

	Diameter (mm)	Diameter (mm)	Diameter (mm)	Diameter (mm)	Diameter (mm)	Average	Standard Dev.
Height 100cm	18	18	18	17	17	17.6	0.547723
Height 150cm	19	19	19	19	20	19.2	0.447214
Height 200cm	19	19	19	20	20	19.4	0.547723

Table A5.31: 1.77mm pipette drop results on Oak Silk Matt.

Kahrs Maple Bevelled Edge Rustic

	Diameter (mm)	Diameter (mm)	Diameter (mm)	Diameter (mm)	Diameter (mm)	Average	Standard Dev.
Height 50cm	16	16	16	16	17	16.2	0.447214
Height 100cm	19	19	18	18	17	18.2	0.83666
Height 150cm	19	19	19	19	19	19	0
Height 200cm	20	20	20	19	19	19.6	0.547723

Table A5.32: 1.77mm pipette drop results on Kahrs Maple Bevelled Edge Rustic.

Kahrs Maple Natural Satin Lacquer

	Diameter (mm)	Diameter (mm)	Diameter (mm)	Diameter (mm)	Diameter (mm)	Average	Standard Dev.
Height 50cm	16	16	16	16	16	16	0
Height 100cm	17	17	18	18	18	17.6	0.547723
Height 150cm	18	19	19	19	20	19	0.707107
Height 200cm	18	19	19	20	20	19.2	0.83666

Table A5.33: 1.77mm pipette drop results on Kahrs Maple Natural Satin Lacquer.

Kahrs Linnea Walnut Bloom Prime Satin Lacquer

	Diameter (mm)	Diameter (mm)	Diameter (mm)	Diameter (mm)	Diameter (mm)	Average	Standard Dev.
Height 50cm	15	15	16	16	16	15.6	0.547723
Height 100cm	17	17	17	17	17	17	0
Height 150cm	18	19	19	19	20	19	0.707107
Height 200cm	19	19	19	20	20	19.4	0.547723

Table A5.34: 1.77mm pipette drop results on Kahrs Linnea Walnut Bloom Prime Satin Lacquer.

Kahrs Linnea Walnut Microbevelled Edge Prime Matt Lacquer

	Diameter (mm)	Diameter (mm)	Diameter (mm)	Diameter (mm)	Diameter (mm)	Average	Standard Dev.
Height 50cm	15	15	15	15	15	15	0
Height 100cm	17	17	18	18	18	17.6	0.547723
Height 150cm	18	18	18	18	19	18.2	0.447214
Height 200cm	18	19	19	19	19	18.8	0.447214

Table A5.35: 1.77mm pipette drop results on Kahrs Linnea Walnut Microbevelled Edge Prime Matt Lacquer.

Natura Walnut Lacquered Satin Lacquer

	Diameter (mm)	Diameter (mm)	Diameter (mm)	Diameter (mm)	Diameter (mm)	Average	Standard Dev.
Height 50cm	15	16	16	16	16	15.8	0.447214
Height 100cm	18	18	18	18	18	18	0
Height 150cm	18	18	19	19	19	18.6	0.547723
Height 200cm	19	19	19	19	20	19.2	0.447214

Table A5.36: 1.77mm pipette drop results on Natura Walnut Lacquered Satin Lacquer.

Kahrs Oak Sienna Natural

	Diameter (mm)	Diameter (mm)	Diameter (mm)	Diameter (mm)	Diameter (mm)	Average	Standard Dev.
Height 50cm	15	15	15	15	15	15	0
Height 100cm	17	17	17	18	18	17.4	0.547723
Height 150cm	18	18	19	19	19	18.6	0.547723
Height 200cm	19	19	19	19	20	19.2	0.447214

Table A5.37: 1.77mm pipette drop results on Kahrs Oak Sienna Natural.

Natura Oak Prime Parquet

	Diameter (mm)	Diameter (mm)	Diameter (mm)	Diameter (mm)	Diameter (mm)	Average	Standard Dev.
Height 50cm	15	15	15	14	14	14.6	0.547723
Height 100cm	15	16	16	16	16	15.8	0.447214
Height 150cm	17	16	17	16	17	16.6	0.547723
Height 200cm	17	17	17	17	17	17	0

Table A5.38: 1.77mm pipette drop results on Natura Oak Prime Parquet.

Kahrs Oak Siena Engineered Natural

	Diameter (mm)	Diameter (mm)	Diameter (mm)	Diameter (mm)	Diameter (mm)	Average	Standard Dev.
Height 50cm	14	14	14	14	14	14	0
Height 100cm	16	16	16	16	17	16.2	0.447214
Height 150cm	17	17	17	17	16	16.8	0.447214
Height 200cm	17	17	17	17	17	17	0

Table A5.39: 1.77mm pipette drop results on Kahrs Oak Siena Engineered Natural.

Oak Solid Plank Untreated

	Diameter (mm)	Diameter (mm)	Diameter (mm)	Diameter (mm)	Diameter (mm)	Average	Standard Dev.
Height 50cm	14	14	14	15	15	14.4	0.547723
Height 100cm	15	15	16	16	16	15.6	0.547723
Height 150cm	15	16	16	16	17	16	0.707107
Height 200cm	18	19	19	19	19	18.8	0.447214

Table A5.40: 1.77mm pipette drop results on Oak Solid Plank Untreated.

Wood Angled

European Maple Oak

					Average	Calculated Angle
80	16	16	16	16	16	72.78945
	16.5	16.5	17	17	16.75	
60	16	16	16	16	16	58.57609
	18.5	19	19	18.5	18.75	
40	14	14	14	13.5	13.875	35.5316
	23.5	24	24	24	23.875	
20	10.5	10.5	10	10	10.25	16.66129
	35	36	36	36	35.75	

Table A5.41: angle drop results on European Maple Oak.

Clear Oil
Oak

					Average	Calculated Angle
80	17	16.5	16.5	16.5	16.625	76.12063
	17.5	17	17	17	17.125	
60	15.5	15	15	15	15.125	53.25677
	18.5	19	19	19	18.875	
40	14	14	13.5	13.5	13.75	34.74661

	25	24	24	23.5	24.125	
20	10	10	10	9.5	9.875	16.5094
	34	35	35	35	34.75	

Table A5.42: angle drop results on Clear Oil Oak.

Oak Natural Siera Matt Lacquered

					Average	Calculated Angle
80	17	17	17.5	17.5	17.25	78.15973
	17.5	17.5	17.5	18	17.625	
60	16	16	16.5	16.5	16.25	60.07357
	19	19	18.5	18.5	18.75	
40	14.5	14.5	14.5	14	14.375	38.19061
	24	23.5	23	22.5	23.25	
20	9	9.5	9.5	9.5	9.375	15.25752
	35	35	36.5	36	35.625	

Table A5.43: angle drop results on Oak Natural Siera Matt Lacquered.

Maple Silk Matt Lacquered

					Average	Calculated Angle
80	17	17	16.5	16.5	16.75	73.16502
	17.5	17.5	17.5	17.5	17.5	
60	16	16	16	16	16	57.3631
	19	19	19	19	19	
40	14	14	14.5	14.5	14.25	36.8699
	24	24	23.5	23.5	23.75	
20	10	10	10	10.5	10.125	15.50525
	38	38	38	37.5	37.875	

Table A5.44: angle drop results on Maple Silk Matt Lacquered.

Natura American Black Walnut Rosshill

					Average	Calculated Angle
80	17	17	17	17.5	17.125	76.31987
	18	17.5	17.5	17.5	17.625	
60	16.5	15.5	16	16	16	53.61329
	20	20.5	19.5	19.5	19.875	
40	14	14	14	13.5	13.875	35.5316
	24	24	24	23.5	23.875	
20	9	9	9.5	10	9.375	14.18763
	39	38	38	38	38.25	

Table A5.45: angle drop results on Natura American Black Walnut Rosshill.

Natura Walnut Ironbank Mississippi

					Average	Calculated Angle
80	17	17	17.5	17.5	17.25	74.80404
	18	18	18	17.5	17.875	
60	16	16	16	16	16	54.1083
	19.5	19.5	20	20	19.75	
40	14	14	13.5	13	13.625	34.18423
	23.5	24.5	24	25	24.25	
20	10	10	10	9.5	9.875	14.8621
	38	38	38	40	38.5	

Table A5.46: angle drop results on Natura Walnut Ironbank Mississippi.

Quickstep Villa Walnut Satin Lacquer

					Average	Calculated Angle
80	16.5	17	17	17.5	17	76.27087
	17	17.5	17.5	18	17.5	
60	15.5	15.5	16	16.5	15.875	58.46809
	19	18	18.5	19	18.625	
40	14	14	14	13.5	13.875	35.31877
	24	24	24	24	24	
20	10	10	10.5	10.5	10.25	15.54373
	38	38	38	39	38.25	

Table A5.47: angle drop results on Quickstep Villa Walnut Satin Lacquer

Kahrs Maple Toronto Satin Lacquer

					Average	Calculated Angle
80	17	17	16.5	16.5	16.75	76.17126
	17	17	17.5	17.5	17.25	
60	16	16	16	16	16	57.3631
	19	19	19	19	19	
40	13.5	13.5	14	14	13.75	35.81051
	23	23	24	24	23.5	
20	10	10	10	10	10	15.9008
	37	37	36	36	36.5	

Table A5.48: angle drop results on Kahrs Maple Toronto Satin Lacquer.

Kahrs Walnut Rustic Nature Oil

					Average	Calculated Angle
80	16	16	16.5	17	16.375	74.4155
	17	17	17.5	16.5	17	
60	16.5	16.5	16.5	15.5	16.25	58.78882
	19	19	19	19	19	
40	14	14	14	14	14	34.25063
	25	25	25	24.5	24.875	
20	10	10	9.5	9.5	9.75	16.05713
	35	35	35	36	35.25	

Table A5.49: angle drop results on Kahrs Walnut Rustic Nature Oil.

Maple Ultra Matt
Lacquered

					Average	Calculated Angle
80	17	17	17	17	17	76.27087
	17.5	17.5	17.5	17.5	17.5	
60	16	15.5	15.5	15.5	15.625	55.87489
	18.5	19	19	19	18.875	
40	14	14	14	14	14	36.3412
	24	24	23.5	23	23.625	
20	9	9	9.5	9.5	9.25	14.7838
	35	35	37.5	37.5	36.25	

Table A5.50: angle drop results on Maple Ultra Matt Lacquered.

Oak Silk Matt

					Average	Calculated Angle
80	17	17	17.5	18	17.375	76.41633
	17.5	17.5	18	18.5	17.875	
60	16	16	16	16	16	57.3631
	19	19	19	19	19	
40	14	14	14	14	14	35.90107
	24	24	24	23.5	23.875	
20	10.5	10.5	10.5	10.5	10.5	15.98644
	38	38	38	38.5	38.125	

Table A5.51: 1mm pipette angle drop results on Oak Silk Matt.

Kahrs Maple Edge Rustic

					Average	Calculated Angle
80	17	17	17	17	17	74.696
	17.5	17.5	17.5	18	17.625	
60	15.5	15.5	16	16.5	15.875	58.46809
	19	18.5	18.5	18.5	18.625	
40	14	14	14	14	14	35.68533
	24	24	24	24	24	
20	10	10	10	9.5	9.875	16.15096
	35	35	36	36	35.5	

Table A5.52: angle drop results on Kahrs Maple Edge Rustic.

Kahrs Linnea Walnut Bloom Prime Satin Lacquer

					Average	Calculated Angle
80	16	16.5	16.5	17	16.5	74.47284
	17	17	17	17.5	17.125	
60	16.5	15.5	15.5	16	15.875	56.67068
	19	19	19	19	19	
40	13.5	13	13.5	14	13.5	34.4332
	24	24	24	23.5	23.875	
20	10	9.5	9.5	9.5	9.625	15.73133
	35	35	35	37	35.5	

Table A5.53: angle drop results on Kahrs Linnea Walnut Bloom Prime Satin Lacquer.

Kahrs Linnea Walnut Microbevelled Edge Prime Matt Lacquer

					Average	Calculated Angle
80	17	17	16.5	16.5	16.75	74.58563
	17	17	17.5	18	17.375	
60	16	16	16	16.5	16.125	58.06884
	19	19	18.5	19.5	19	
40	14	14	14	14	14	35.68533
	24	24	24	24	24	
20	10	10	10	9.5	9.875	15.4794
	38	36.5	36.5	37	37	

Table A5.54: angle drop results on Kahrs Linnea Walnut Microbevelled Edge Prime Matt Lacquer.

Natura Walnut Lacquered Satin
Lacquer

					Average	Calculated Angle
80	17	17.5	17	17	17.125	76.31987
	17.5	17.5	17.5	18	17.625	
60	16.5	17	16	15	16.125	61.34834
	18	18	19	18.5	18.375	
40	14.5	14.5	14.5	14	14.375	37.71268
	24	23	23.5	23.5	23.5	
20	10	10	9.5	9.5	9.75	15.22595
	37.5	37.5	37	36.5	37.125	

Table A5.55: angle drop results on Natura Walnut Lacquered Satin Lacquer.

Kahrs Oak Sienna Natural

					Average	Calculated Angle
80	16.5	16.5	17	17	16.75	76.17126
	17	17	17.5	17.5	17.25	
60	16	16	16.5	16.5	16.25	56.44269
	19.5	19.5	19	20	19.5	
40	13.5	13.5	13.5	13	13.375	34.07028
	24	24.5	23.5	23.5	23.875	
20	10	10	10	10	10	15.8451
	36.5	36	37	37	36.625	

Table A5.56: angle drop results on Kahrs Oak Sienna Natural.

Natural Oak Prime Parquet

					Average	Calculated Angle
80	14	14	13.5	13.5	13.75	74.77724
	14.5	14.5	14	14	14.25	
60	15	15	14.5	14.5	14.75	58.76774
	17.5	17.5	17	17	17.25	
40	13	13	13.5	13.5	13.25	40.86818
	21	20	20	20	20.25	
20	9	9	8.5	8.5	8.75	14.74665
	35	33.5	35	34	34.375	

Table A5.57: angle drop results on Natural Oak Prime Parquet.

Kahrs Oak Siena Engineered Natural

					Average	Calculated Angle
80	16.5	16.5	16.5	16	16.375	76.01769
	17	17	17	16.5	16.875	
60	16	16	16	15.5	15.875	57.85095
	18	19	19	19	18.75	
40	13.5	13.5	13.5	14	13.625	36.79124
	23	23	22.5	22.5	22.75	
20	9.5	10	10	10	9.875	16.6325
	33	35	35	35	34.5	

Table A5.58: angle drop results on Kahrs Oak Siena Engineered Natural.

Oak Solid Plank
Untreated

					Average	Calculated Angle
80	15	15	15	15	15	75.40745
	15.5	15.5	15.5	15.5	15.5	
60	14	13.5	13.5	14.5	13.875	57.23624
	16.5	16.5	17	16	16.5	
40	13.5	13.5	13.5	14	13.625	39.8796
	22	22	21	20	21.25	
20	9	9	9	8.5	8.875	14.9622
	35	35	33.5	34	34.375	

Table A5.59: angle drop results on Oak Solid Plank Untreated.

Appendix 6 – Bloodstains on Fabric Surfaces

Nylon

1mm

	Diameter (mm)	Diameter (mm)	Diameter (mm)	Diameter (mm)	Diameter (mm)	Average	S.D
Height 50 cm	4	3	4	4	4	3.8	0.45
Height 100 cm	4	4	4	4	4	4	0.00
Height 150 cm	5	5	5	5	5	5	0.00
Height 200 cm	5	4	4	4	4	4.2	0.45

Table A6.1: Bloodstain diameters exhibited using a 1mm pipette on Nylon.

Angle (º)							Average	S.D	Calculated Angle (º)
20º	Length (mm)	2	1	2	2	1	1.6	0.55	38.68
	Diameter (mm)	1	1	1	1	1	1	0.00	
40º	Length (mm)	3	4	4	4	4	3.8	0.45	43.17
	Diameter (mm)	2	3	3	2	3	2.6	0.55	
60º	Length (mm)	6	5	5	5	5	5.2	0.45	43.81
	Diameter (mm)	4	3	3	4	4	3.6	0.45	
80º	Length (mm)	4	4	4	4	4	4	0.00	64.16
	Diameter (mm)	4	4	4	3	3	3.6	0.45	

Table A6.2: Bloodstain diameters exhibited using a 1mm pipette on angled Nylon.

1.77mm

	Diameter (mm)	Diameter (mm)	Diameter (mm)	Diameter (mm)	Diameter (mm)	Average	S.D
Height 50 cm	4	5	5	5	5	4.8	0.45
Height 100 cm	5	5	5	5	5	5	0.00
Height 150 cm	5	5	6	5	5	5.2	0.45
Height 200 cm	5	5	5	6	6	5.4	0.55

Table A6.3: Bloodstain diameters exhibited using a 1.77mm pipette on Nylon

Angle (°)							Average	S.D	Calculated Angle (°)
20°	Length (mm)	2	2	3	3	4	2.8	0.84	20.92
	Diameter (mm)	1	1	1	1	1	1	0.00	
40°	Length (mm)	3	3	4	4	4	3.6	0.55	30
	Diameter (mm)	2	2	1	2	2	1.8	0.45	
60°	Length (mm)	7	7	7	7	7	7	0.00	32.88
	Diameter (mm)	4	4	4	4	3	3.8	0.45	
80°	Length (mm)	7	6	6	6	6	6.2	0.45	64.59
	Diameter (mm)	6	5	6	5	6	5.6	0.55	

Table A6.4: Bloodstain diameters exhibited using a 1.77mm pipette on angled Nylon.

Poly/linen/rayon Pandora Devore
1mm

	Diameter (mm)	Diameter (mm)	Diameter (mm)	Diameter (mm)	Diameter (mm)	Average	S.D
Height 50 cm	8	9	9	9	9	8.8	0.45
Height 100 cm	9	9	9	9	8	8.8	0.45
Height 150 cm	10	10	10	10	10	10	0.00
Height 200 cm	10	10	11	10	11	10.4	0.55

Table A6.5: Bloodstain diameters exhibited using a 1mm pipette on Poly/linen/rayon.

Angle (°)							Average	S.D	Calculated Angle (°)
20°	Length (mm)	17	20	24	24	24	22	3.19	14.21
	Diameter (mm)	5	5	5	6	6	5.4	0.55	
40°	Length (mm)	18	16	15	16	16	16.2	1.10	24.82
	Diameter (mm)	6	8	7	6	7	6.8	0.84	
60°	Length (mm)	11	12	11	11	12	11.4	0.55	47.46
	Diameter (mm)	7	8	9	9	9	8.4	0.89	
80°	Length (mm)	10	10	11	11	10	10.4	0.55	62.20
	Diameter (mm)	9	9	9	10	9	9.2	0.45	

Table A6.6: Bloodstain diameters exhibited using a 1mm pipette on angled Poly/linen/rayon.

.

1.77mm

	Diameter (mm)	Diameter (mm)	Diameter (mm)	Diameter (mm)	Diameter (mm)	Average	S.D
Height 50 cm	12	12	11	13	12	12	0.71
Height 100 cm	11	12	12	13	13	12.2	0.84
Height 150 cm	13	14	13	14	12	13.2	0.84
Height 200 cm	13	14	14	14	13	13.6	0.55

Table A6.7: Bloodstain diameters exhibited using a 1.77mm pipette on Poly/linen/rayon.

Angle (°)							Average	S.D	Calculated Angle (°)
20°	Length (mm)	16	27	21	21	23	21.6	3.97	19.47
	Diameter (mm)	7	7	7	8	7	7.2	0.45	
40°	Length (mm)	14	14	15	15	16	14.8	0.84	40.44
	Diameter (mm)	9	9	10	10	10	9.6	0.55	
60°	Length (mm)	11	13	12	13	12	12.2	0.84	64.37
	Diameter (mm)	10	11	12	11	11	11	0.71	
80°	Length (mm)	11	11	11	11	12	11.6	0.00	71.49
	Diameter (mm)	11	12	11	12	11	11	0.55	

Table A6.8: Bloodstain diameters exhibited using a 1.77mm pipette on angled Poly/linen/rayon.

Wool Delaine

1mm

	Diameter (mm)	Diameter (mm)	Diameter (mm)	Diameter (mm)	Diameter (mm)	Average	S.D
Height 50 cm	5	5	6	5	5	5.2	0.45
Height 100 cm	7	7	7	7	7	7	0.00
Height 150 cm	8	7	8	8	7	7.6	0.55
Height 200 cm	8	8	9	8	9	8.4	0.55

Table A6.9: Bloodstain diameters exhibited using a 1mm pipette on Wood Delaine

Angle (º)							Average	S.D	Calculated Angle (º)
20º	Length (mm)	18	19	17	21	22	19.4	2.07	10.69
	Diameter (mm)	4	3	4	3	4	3.6	0.55	
40º	Length (mm)	7	8	9	9	9	8.4	0.89	34.85
	Diameter (mm)	5	5	5	4	5	4.8	0.45	
60º	Length (mm)	8	7	6	7	7	7	0.71	47.98
	Diameter (mm)	5	5	6	5	5	5.2	0.45	
80º	Length (mm)	7	6	7	6	6	6.4	0.55	64.99
	Diameter (mm)	6	6	6	6	5	5.8	0.45	

Table A6.10: Bloodstain diameters exhibited using a 1mm pipette on angled Wood Delaine

1.77mm

	Diameter (mm)	Diameter (mm)	Diameter (mm)	Diameter (mm)	Diameter (mm)	Average	S.D
Height 50 cm	4	4	3	4	4	3.8	0.45
Height 100 cm	4	4	4	4	5	4.2	0.45
Height 150 cm	5	4	4	5	4	4.4	0.55
Height 200 cm	5	5	4	5	5	4.8	0.45

Table A6.11: Bloodstain diameters exhibited using a 1.77mm pipette on Wood Delaine

Angle (º)							Average	S.D	Calculated Angle (º)
20º	Length (mm)	20	25	20	19	21	21	2.35	11.54
	Diameter (mm)	4	4	4	4	5	4.2	0.45	
40º	Length (mm)	13	14	13	14	12	13.2	0.84	27.04
	Diameter (mm)	6	5	6	6	7	6	0.71	
60º	Length (mm)	8	10	10	10	10	9.6	0.89	56.44
	Diameter (mm)	8	8	8	8	8	8	0.00	
80º	Length (mm)	7	8	8	9	7	7.8	0.84	90
	Diameter (mm)	7	7	8	9	8	7.8	0.84	

Table A6.12: Bloodstain diameters exhibited using a 1.77mm pipette on angled Wood Delaine

Raised Natural Cotton

1mm

	Diameter (mm)	Diameter (mm)	Diameter (mm)	Diameter (mm)	Diameter (mm)	Average	S.D
Height 50 cm	7	7	7	7	8	7.2	0.45
Height 100 cm	10	9	10	9	9	9.4	0.55
Height 150 cm	9	10	9	10	10	9.6	0.55
Height 200 cm	9	11	11	11	10	10.4	0.89

Table A6.13: Bloodstain diameters exhibited using a 1mm pipette on Raised Natural Cotton

Angle (º)							Average	S.D	Calculated Angle (º)
20º	Length (mm)	8	10	9	9	9	9	0.71	12.84
	Diameter (mm)	2	2	2	2	2	2	0.00	
40º	Length (mm)	7	6	8	5	6	6.4	1.14	25.94
	Diameter (mm)	3	3	2	3	3	2.8	0.45	
60º	Length (mm)	5	5	5	4	5	4.8	0.45	48.59
	Diameter (mm)	4	3	4	3	4	3.6	0.55	
80º	Length (mm)	5	5	4	5	5	4.8	0.45	52.34
	Diameter (mm)	4	4	3	4	4	3.8	0.45	

Table A6.14: Bloodstain diameters exhibited using a 1mm pipette on angled Raised Natural Cotton

1.77mm

	Diameter (mm)	*Diameter (mm)*	*Diameter (mm)*	*Diameter (mm)*	*Diameter (mm)*	*Average*	*S.D*
Height 50 cm	*5*	*5*	*5*	*5*	*5*	*5*	*0.00*
Height 100 cm	*5*	*6*	*6*	*5*	*6*	*5.6*	*0.55*
Height 150 cm	*6*	*6*	*6*	*6*	*5*	*5.8*	*0.45*
Height 200 cm	*6*	*6*	*6*	*6*	*6*	*6*	*0 .00*

Table A6.15: Bloodstain diameters exhibited using a 1.77mm pipette on Raised Natural Cotton

Angle (º)							Average	S.D	Calculated Angle (º)
20º	Length (mm)	14	12	14	11	13	12.8	1.30	11.72
	Diameter (mm)	2	3	3	2	3	2.6	0.55	
40º	Length (mm)	9	10	8	8	9	8.8	0.84	22.73
	Diameter (mm)	4	4	3	3	3	3.4	0.55	
60º	Length (mm)	6	5	5	6	6	5.6	0.55	45.58
	Diameter (mm)	4	4	4	4	4	4	0.00	
80º	Length (mm)	5	5	5	5	5	5	0.00	53.13
	Diameter (mm)	4	4	4	4	4	4	0.00	

Table A6.16: Bloodstain diameters exhibited using a 1mm pipette on angled Raised Natural Cotton

Heavyweight Cotton

1mm

	Diameter (mm)	Diameter (mm)	Diameter (mm)	Diameter (mm)	Diameter (mm)	Average	S.D
Height 50 cm	10	10	10	10	10	10	0.00
Height 100 cm	10	11	11	11	10	10.6	0.55
Height 150 cm	10	10	11	12	11	10.8	0.84
Height 200 cm	11	11	11	11	11	11	0.00

Table A6.17: Bloodstain diameters exhibited using a 1mm pipette on Heavyweight Cotton

Angle (º)							Average	S.D	Calculated Angle (º)
20º	Length (mm)	35	31	29	30	32	31.4	2.30	9.16
	Diameter (mm)	5	5	5	5	5	5	0.00	
40º	Length (mm)	18	19	19	24	19	19.8	2.39	21.95
	Diameter (mm)	7	8	8	7	7	7.4	0.55	
60º	Length (mm)	12	11	11	10	11	11	0.71	46.66
	Diameter (mm)	8	8	8	8	8	8	0.00	
80º	Length (mm)	9	10	10	10	10	9.8	0.45	66.69
	Diameter (mm)	9	9	9	9	9	9	0.00	

Table A6.18: Bloodstain diameters exhibited using a 1mm pipette on angled Heavyweight Cotton

1.77mm

	Diameter (mm)	Diameter (mm)	Diameter (mm)	Diameter (mm)	Diameter (mm)	Average	S.D
Height 50 cm	4	4	4	4	4	4	0.00
Height 100 cm	5	5	5	5	5	5	0.00
Height 150 cm	6	5	6	5	6	5.6	0.55
Height 200 cm	7	6	6	6	6	6.2	0.45

Table A6.19: Bloodstain diameters exhibited using a 1.77mm pipette on Heavyweight Cotton

Angle (º)							Average	S.D	Calculated Angle (º)
20º	Length (mm)	35	34	37	33	36	35	1.58	8.54
	Diameter (mm)	5	5	5	6	5	5.2	0.45	
40º	Length (mm)	21	20	20	21	20	20.4	0.55	23.70
	Diameter (mm)	7	8	9	9	8	8.2	0.84	
60º	Length (mm)	13	12	14	14	14	13.4	0.89	47
	Diameter (mm)	10	9	10	10	10	9.8	0.45	
80º	Length (mm)	12	12	12	12	11	11.8	0.45	68.78
	Diameter (mm)	11	11	11	11	11	11	0.00	

Table A6.20: Bloodstain diameters exhibited using a 1.77mm pipette on angled Heavyweight Cotton.

Peasant Cotton

1mm

	Diameter (mm)	Diameter (mm)	Diameter (mm)	Diameter (mm)	Diameter (mm)	Average	S.D
Height 50 cm	12	12	12	12	12	12	0.00
Height 100 cm	12	12	12	13	13	12.4	0.55
Height 150 cm	12	12	13	13	13	12.6	0.55
Height 200 cm	13	12	13	13	13	12.8	0.45

Table A6.21: Bloodstain diameters exhibited using a 1mm pipette on Peasant Cotton.

Angle (°)							Average	S.D	Calculated Angle (°)
20°	Length (mm)	7	9	9	10	9	8.8	1.10	21.32
	Diameter (mm)	4	3	3	3	3	3.2	0.45	
40°	Length (mm)	8	8	7	6	7	7.2	0.84	31.86
	Diameter (mm)	4	4	3	4	4	3.8	0.45	
60°	Length (mm)	5	5	6	6	6	5.6	0.55	51.79
	Diameter (mm)	5	4	5	4	4	4.4	0.55	
80°	Length (mm)	5	5	5	5	5	5	0.00	66.93
	Diameter (mm)	5	5	4	5	4	4.6	0.45	

Table A6.22: Bloodstain diameters exhibited using a 1mm pipette on angled Peasant Cotton.

1.77mm

Table A6.23: Bloodstain diameters exhibited using a 1.77mm pipette on Peasant Cotton.

	Diameter (mm)	*Diameter (mm)*	*Diameter (mm)*	*Diameter (mm)*	*Diameter (mm)*	*Average*	*S.D*
Height 50 cm	*6*	*6*	*6*	*6*	*5*	*5.8*	*0.45*
Height 100 cm	*6*	*6*	*7*	*7*	*7*	*6.6*	*0.55*
Height 150 cm	*6*	*6*	*7*	*7*	*7*	*6.6*	*0.55*
Height 200 cm	*7*	*8*	*7*	*6*	*7*	*7*	*0.71*

Angle (°)							Average	S.D	Calculated Angle (°)
20°	Length (mm)	18	17	17	19	18	17.8	0.84	11.01
	Diameter (mm)	3	3	4	4	3	3.4	0.55	
40°	Length (mm)	8	8	8	8	8	8	0.00	30
	Diameter (mm)	4	4	4	4	4	4	0.00	
60°	Length (mm)	6	6	7	7	6	6.4	0.55	43.43
	Diameter (mm)	4	5	5	4	4	4.4	0.55	
80°	Length (mm)	6	7	6	6	6	6.2	0.45	53.75
	Diameter (mm)	5	5	5	5	5	5	0.00	

Table A6.24: Bloodstain diameters exhibited using a 1.77mm pipette on angled Peasant Cotton.

Cotton Poplin

1mm

Table A6.25: Bloodstain diameters exhibited using a 1mm pipette on Cotton Poplin

	Diameter (mm)	Diameter (mm)	Diameter (mm)	Diameter (mm)	Diameter (mm)	Average	S.D
Height 50 cm	11	11	10	11	9	10.4	0.89
Height 100 cm	13	13	11	11	11	11.8	1.10
Height 150 cm	11	11	11	11	10	10.8	0.45
Height 200 cm	9	9	9	10	9	9.2	0.45

Angle (°)							Average	S.D	Calculated Angle (°)
20°	Length (mm)	29	33	34	25	30	30.2	3.56	7.61
	Diameter (mm)	3	4	4	5	4	4	0.71	
40°	Length (mm)	25	23	20	17	21	21.2	3.03	17.57
	Diameter (mm)	7	6	6	7	6	6.4	0.55	
60°	Length (mm)	15	13	12	12	13	13	1.22	48.92
	Diameter (mm)	10	10	10	9	10	9.8	0.45	
80°	Length (mm)	13	11	11	11	11	11.4	0.89	74.78
	Diameter (mm)	11	11	11	11	11	11	0.00	

Table A6.26: Bloodstain diameters exhibited using a 1mm pipette on angled Cotton Poplin

1.77mm

	Diameter (mm)	Diameter (mm)	Diameter (mm)	Diameter (mm)	Diameter (mm)	Average	S.D
Height 50 cm	15	15	15	17	15	15.4	0.89
Height 100 cm	15	16	15	15	16	15.4	0.55
Height 150 cm	15	15	12	14	15	14.2	1.30
Height 200 cm	12	12	15	14	13	13.2	1.30

Table A6.27: Bloodstain diameters exhibited using a 1.77mm pipette on Cotton Poplin

Angle (º)							Average	S.D	Calculated Angle (º)
20º	Length (mm)	35	47	44	50	46	44.4	5.68	5.69
	Diameter (mm)	4	5	5	4	4	4.4	0.55	
40º	Length (mm)	37	29	28	45	35	34.8	6.87	9.93
	Diameter (mm)	6	6	7	5	6	6	0.71	
60º	Length (mm)	17	19	18	20	18	18.4	1.14	46.74
	Diameter (mm)	14	13	12	14	14	13.4	0.89	
80º	Length (mm)	17	17	17	17	17	17	0.00	63.40
	Diameter (mm)	15	16	15	15	15	15.2	0.45	

Table A6.28: Bloodstain diameters exhibited using a 1.77mm pipette on angled Cotton Poplin

Resida Bump Cotton

1mm

	Diameter (mm)	Diameter (mm)	Diameter (mm)	Diameter (mm)	Diameter (mm)	Average	S.D
Height 50 cm	3	4	3	3	3	3.2	0.45
Height 100 cm	4	3	4	4	3	3.6	0.55
Height 150 cm	4	3	4	3	4	3.6	0.55
Height 200 cm	4	4	4	3	3	3.6	0.55

Table A6.29: Bloodstain diameters exhibited using a 1mm pipette on Resida Bump Cotton

Angle (º)							Average	S.D	Calculated Angle (º)
20º	Length (mm)	8	7	7	8	7	7.4	0.55	23.92
	Diameter (mm)	3	3	3	3	3	3	0.00	
40º	Length (mm)	7	6	6	7	7	6.6	0.55	25.10
	Diameter (mm)	3	3	3	3	2	2.8	0.45	
60º	Length (mm)	5	5	5	5	5	5	0.00	39.79
	Diameter (mm)	4	3	3	3	3	3.2	0.45	
80º	Length (mm)	4	5	4	5	4	4.4	0.55	46.66
	Diameter (mm)	3	3	4	3	3	3.2	0.45	

Table A6.30: Bloodstain diameters exhibited using a 1mm pipette on angled Resida Bump Cotton

1.77mm

	Diameter (mm)	Diameter (mm)	Diameter (mm)	Diameter (mm)	Diameter (mm)	Average	S.D
Height 50 cm	5	4	4	4	5	4.4	0.55
Height 100 cm	4	4	5	4	5	4.4	0.55
Height 150 cm	4	5	5	5	5	4.8	0.45
Height 200 cm	5	5	5	5	5	5	0.00

Table A6.31: Bloodstain diameters exhibited using a 1.77mm pipette on Resida Bump Cotton

Angle (º)							Average	S.D	Calculated Angle (º)
20º	Length (mm)	12	15	15	14	14	14	1.22	14.06
	Diameter (mm)	4	4	3	3	3	3.4	0.55	
40º	Length (mm)	9	9	9	9	9	9	0.00	26.39
	Diameter (mm)	4	4	5	3	4	4	0.71	
60º	Length (mm)	7	7	7	7	7	7	0.00	34.85
	Diameter (mm)	4	4	4	4	4	4	0.00	
80º	Length (mm)	5	5	5	5	5	5	0.00	53.13
	Diameter (mm)	4	4	4	4	4	4	0.00	

Table A6.32: Bloodstain diameters exhibited using a 1.77mm pipette on angled Resida Bump Cotton

Fuji Silk

1mm

	Diameter (mm)	Diameter (mm)	Diameter (mm)	Diameter (mm)	Diameter (mm)	Average	S.D
Height 50 cm	13	14	14	14	16	14.2	1.09
Height 100 cm	15	15	14	14	14	14.4	0.55
Height 150 cm	12	14	14	14	13	13.4	0.89
Height 200 cm	14	15	15	15	15	14.8	0.45

Table A6.33: Bloodstain diameters exhibited using a 1mm pipette on Fuji Silk

Angle (°)							Average	S.D	Calculated Angle (°)
20°	Length (mm)	31	23	33	32	32	30.2	4.09	20.55
	Diameter (mm)	10	11	11	11	10	10.6	0.55	
40°	Length (mm)	25	25	24	24	25	24.6	0.55	31.90
	Diameter (mm)	12	12	14	14	13	13	1	
60°	Length (mm)	20	20	21	20	20	20.2	0.45	53.32
	Diameter (mm)	17	16	16	16	16	16.2	0.45	
80°	Length (mm)	16	18	18	18	16	17.2	1.10	66.72
	Diameter (mm)	14	16	17	17	15	15.8	1.30	

Table A6.34: Bloodstain diameters exhibited using a 1mm pipette on angld Fuji Silk

1.77mm

	Diameter (mm)	Diameter (mm)	Diameter (mm)	Diameter (mm)	Diameter (mm)	Average	S.D
Height 50 cm	17	17	17	16	16	16.6	0.55
Height 100 cm	19	18	17	17	18	17.8	0.84
Height 150 cm	17	18	17	18	18	17.6	0.55
Height 200 cm	18	20	19	17	19	18.6	1.14

Table A6.35: Bloodstain diameters exhibited using a 1.77mm pipette on angled Fuji Silk

Angle (°)							Average	S.D	Calculated Angle (°)
20°	Length (mm)	54	42	40	46	52	46.8	6.10	13.85
	Diameter (mm)	11	12	12	11	10	11.2	0.84	
40°	Length (mm)	26	29	32	34	31	30.4	3.05	31.76
	Diameter (mm)	16	16	16	16	16	16	0.00	
60°	Length (mm)	21	25	26	22	24	23.6	2.07	53.62
	Diameter (mm)	19	19	19	19	19	19	0.00	
80°	Length (mm)	20	22	22	22	22	21.6	0.89	66.44
	Diameter (mm)	19	21	19	20	20	19.8	0.84	

Table A6.36: Bloodstain diameters exhibited using a 1.77mm pipette on Fuji Silk

Medium Habotai Silk

1mm

	Diameter (mm)	Diameter (mm)	Diameter (mm)	Diameter (mm)	Diameter (mm)	Average	S.D
Height 50 cm	10	10	10	10	10	10	0.00
Height 100 cm	9	9	9	9	10	9.2	0.45
Height 150 cm	10	10	10	10	10	10	0.00
Height 200 cm	10	11	11	11	11	10.8	0.45

Table A6.37: Bloodstain diameters exhibited using a 1mm pipette on Medium Habotai Silk

Angle (°)							Average	S.D	Calculated Angle (°)
20°	Length (mm)	44	49	45	50	46	46.8	2.59	17.15
	Diameter (mm)	10	9	16	19	15	13.8	4.21	
40°	Length (mm)	38	32	36	32	31	84.5	3.03	14.81
	Diameter (mm)	19	21	21	24	23	21.6	1.95	
60°	Length (mm)	27	28	27	27	29	27.6	0.89	58.77
	Diameter (mm)	22	25	23	25	23	23.6	1.34	
80°	Length (mm)	28	25	25	29	25	26.4	1.95	61.50
	Diameter (mm)	21	24	25	24	25	23.2	1.64	

Table A6.38: Bloodstain diameters exhibited using a 1mm pipette on angled Medium Habotai Silk

1.77mm

	Diameter (mm)	Diameter (mm)	Diameter (mm)	Diameter (mm)	Diameter (mm)	Average	S.D
Height 50 cm	18	18	18	17	18	17.8	0.45
Height 100 cm	17	17	16	17	18	17	0.71
Height 150 cm	17	18	18	18	18	17.8	0.45
Height 200 cm	19	19	19	19	18	18.8	0.45

Table A6.39: Bloodstain diameters exhibited using a 1.77mm pipette on Medium Habotai Silk

Angle (º)							Average	S.D	Calculated Angle (º)
20º	Length (mm)	48	45	45	43	51	46.4	3.13	25.26
	Diameter (mm)	20	21	21	16	21	19.8	2.17	
40º	Length (mm)	45	38	39	38	40	40	2.91	39.42
	Diameter (mm)	21	28	26	26	26	25.4	2.61	
60º	Length (mm)	30	32	32	32	33	31.8	1.10	58.11
	Diameter (mm)	26	29	26	27	27	27	2.05	
80º	Length (mm)	29	29	30	29	31	29.6	0.89	67.77
	Diameter (mm)	26	28	29	27	27	27.4	1.14	

Table A6.40: Bloodstain diameters exhibited using a 1.77mm pipette on angled Medium Habotai Silk.

Denim

1mm

	Diameter (mm)	Diameter (mm)	Diameter (mm)	Diameter (mm)	Diameter (mm)	Average	S.D
Height 50 cm	6	6	6	6	5	5.8	0.45
Height 100 cm	6	6	6	6	7	6.2	0.45
Height 150 cm	7	7	7	7	7	7	0.00
Height 200 cm	8	8	7	8	8	7.8	0.45

Table A6.41: Bloodstain diameters exhibited using a 1mm pipette on Denim

Angle (º)							Average	S.D	Calculated Angle (º)
20º	Length (mm)	22	19	25	25	26	23.4	2.88	8.35
	Diameter (mm)	3	4	4	3	3	3.4	0.55	
40º	Length (mm)	7	9	10	9	14	9.8	2.59	30.68
	Diameter (mm)	5	5	5	5	5	5	0.00	
60º	Length (mm)	10	9	10	9	10	9.6	0.55	37.17
	Diameter (mm)	6	6	5	6	6	5.8	0.45	
80º	Length (mm)	7	6	7	6	7	6.6	0.55	69.95
	Diameter (mm)	7	6	6	6	6	6.2	0.45	

Table A6.41: Bloodstain diameters exhibited using a 1mm pipette on angled Denim

1.77mm

	Diameter (mm)	Diameter (mm)	Diameter (mm)	Diameter (mm)	Diameter (mm)	Average	S.D
Height 50 cm	13	13	14	14	14	13.6	0.55
Height 100 cm	14	15	15	14	15	14.6	0.55
Height 150 cm	15	16	15	16	15	15.4	0.55
Height 200 cm	15	15	16	16	15	15.4	0.55

Table A6.42: Bloodstain diameters exhibited using a 1.77mm pipette on Denim

Angle (º)							Average	S.D	Calculated Angle (º)
20º	Length (mm)	25	31	31	32	29	29.6	2.79	8.16
	Diameter (mm)	4	5	4	4	4	4.2	0.45	
40º	Length (mm)	12	14	15	15	15	14.2	1.30	27.70
	Diameter (mm)	6	6	7	7	7	6.6	0.55	
60º	Length (mm)	9	11	12	11	11	10.8	1.10	39.02
	Diameter (mm)	6	7	6	8	7	6.8	0.84	
80º	Length (mm)	9	9	10	10	10	9.6	0.55	54.34
	Diameter (mm)	8	8	8	8	7	7.8	0.45	

Table A6.43: Bloodstain diameters exhibited using a 1.77mm pipette on angled Denim

M&S T-Shirt Jersey

1mm

Table A6.44: Bloodstain diameters exhibited using a 1mm pipette on M & S Jersey

	Diameter (mm)	Diameter (mm)	Diameter (mm)	Diameter (mm)	Diameter (mm)	Average	S.D
Height 50 cm	8	8	9	9	8	8.4	0.55
Height 100 cm	9	9	10	10	9	9.4	0.55
Height 150 cm	10	9	10	11	11	10.2	0.84
Height 200 cm	11	12	11	11	10	11	0.71

Angle (°)							Average	S.D	Calculated Angle (°)
20°	Length (mm)	25	30	30	31	24	28	3.25	14.06
	Diameter (mm)	7	7	6	7	7	6.8	0.45	
40°	Length (mm)	15	14	14	15	16	14.8	0.84	37.45
	Diameter (mm)	9	9	9	9	9	9	0.00	
60°	Length (mm)	12	12	12	13	13	12.4	0.55	52.22
	Diameter (mm)	10	9	10	10	10	9.8	0.45	
80°	Length (mm)	11	12	12	12	12	11.8	0.45	66.24
	Diameter (mm)	10	10	12	11	11	10.8	0.84	

Table A6.45: Bloodstain diameters exhibited using a 1mm pipette on angled M & S Jersey

1.77mm

	Diameter (mm)	Diameter (mm)	Diameter (mm)	Diameter (mm)	Diameter (mm)	Average	S.D
Height 50 cm	13	13	14	14	13	13.4	0.55
Height 100 cm	14	16	14	14	15	14.6	0.89
Height 150 cm	15	15	16	16	16	15.6	0.55
Height 200 cm	14	14	14	15	15	14.4	0.55

Table A6.46: Bloodstain diameters exhibited using a 1.77mm pipette on M & S Jersey

Angle (°)							Average	S.D	Calculated Angle (°)
20°	Length (mm)	27	27	30	24	32	28	3.08	15.75
	Diameter (mm)	8	8	7	8	7	7.6	0.55	
40°	Length (mm)	21	23	18	20	17	19.8	2.39	31.01
	Diameter (mm)	10	10	10	10	11	10.2	0.45	
60°	Length (mm)	15	17	17	15	17	16.2	1.10	48.86
	Diameter (mm)	12	13	12	12	12	12.2	0.45	
80°	Length (mm)	13	14	14	15	16	14.4	1.14	66.44
	Diameter (mm)	12	13	13	13	15	13.2	1.10	

Table A6.47: Bloodstain diameters exhibited using a 1.77mm pipette on angled M & S Jersey.

Light Grey Polyester Twill

1mm

	Diameter (mm)	Diameter (mm)	Diameter (mm)	Diameter (mm)	Diameter (mm)	Average	S.D
Height 50 cm	28	28	28	28	28	28	0.00
Height 100 cm	26	27	27	27	27	26.8	0.45
Height 150 cm	27	28	28	28	29	28	0.71
Height 200 cm	27	27	28	28	27	27.4	0.55

Table A6.48: Bloodstain diameters exhibited using a 1mm pipette on Light Polyester Twill.

Angle (º)							Average	S.D	Calculated Angle (º)
20º	Length (mm)	39	40	40	39	38	39.2	0.84	21.55
	Diameter (mm)	15	14	14	15	14	14.4	0.55	
40º	Length (mm)	31	30	30	31	31	30.6	0.55	34.65
	Diameter (mm)	18	17	18	17	17	17.4	0.55	
60º	Length (mm)	29	29	29	30	29	29.2	0.45	39.57
	Diameter (mm)	19	19	18	19	18	18.6	0.55	
80º	Length (mm)	20	21	20	20	21	20.4	0.55	N/A
	Diameter (mm)	25	29	28	27	27	27.2	1.48	

Table A6.49: Bloodstain diameters exhibited using a 1mm pipette on angled Light Polyester Twill.

1.77mm

	Diameter (mm)	Diameter (mm)	Diameter (mm)	Diameter (mm)	Diameter (mm)	Average	S.D
Height 50 cm	25	26	25	25	26	25.4	0.55
Height 100 cm	25	25	25	26	26	25.4	0.55
Height 150 cm	26	25	25	25	25	25.2	0.45
Height 200 cm	27	22	24	24	24	24.2	1.79

Table A6.50: Bloodstain diameters exhibited using a 1.77mm pipette on Light Polyester Twill.

Angle (°)							Average	S.D	Calculated Angle (°)
20°	Length (mm)	39	42	41	41	40	40.6	1.14	31.15
	Diameter (mm)	21	22	21	21	20	21	0.71	
40°	Length (mm)	26	28	28	29	27	27.6	1.14	N/A
	Diameter (mm)	31	33	33	32	30	31.8	1.30	
60°	Length (mm)	24	24	24	25	25	24.4	0.55	N/A
	Diameter (mm)	33	33	34	34	33	33.4	0.55	
80°	Length (mm)	22	23	25	22	23	23	1.22	N/A
	Diameter (mm)	34	34	36	34	34	34.4	0.89	

Table A6.51: Bloodstain diameters exhibited using a 1.77mm pipette on angled Light Polyester Twill.

Jupiter Linen

1mm

	Diameter (mm)	Diameter (mm)	Diameter (mm)	Diameter (mm)	Diameter (mm)	Average	S.D
Height 50 cm	9	9	8	8	8	8.4	0.55
Height 100 cm	10	10	10	10	10	10	0.00
Height 150 cm	9	9	10	9	9	9.2	0.45
Height 200 cm	11	11	11	10	11	10.8	0.45

Table A6.52: Bloodstain diameters exhibited using a 1mm pipette on Jupiter Linen.

Angle (°)							Average	S.D	Calculated Angle (°)
20°	Length (mm)	20	22	19	24	24	21.8	2.28	12.18
	Diameter (mm)	4	5	5	5	4	4.6	0.55	
40°	Length (mm)	15	16	14	14	15	14.8	0.84	29.11
	Diameter (mm)	7	7	8	7	7	7.2	0.45	
60°	Length (mm)	12	11	11	11	11	11.2	0.45	47.07
	Diameter (mm)	8	8	9	8	8	8.2	0.45	
80°	Length (mm)	9	9	8	9	10	9	0.71	65.66
	Diameter (mm)	8	8	8	8	9	8.2	0.45	

Table A6.53: Bloodstain diameters exhibited using a 1mm pipette on angled Jupiter Linen.

1.77mm

	Diameter (mm)	Diameter (mm)	Diameter (mm)	Diameter (mm)	Diameter (mm)	Average	S.D
Height 50 cm	12	12	12	12	12	12	0.00
Height 100 cm	12	12	12	12	12	12	0.00
Height 150 cm	11	11	11	11	11	11	0.00
Height 200 cm	11	11	12	12	11	11.4	0.55

Table A6.54: Bloodstain diameters exhibited using a 1.77mm pipette on Jupiter Linen.

Angle (º)							Average	S.D	Calculated Angle (º)
20º	Length (mm)	34	33	24	32	34	31.4	4.22	11.02
	Diameter (mm)	5	5	8	6	6	6	1.22	
40º	Length (mm)	18	19	18	16	19	18	1.22	30
	Diameter (mm)	8	9	9	9	10	9	0.71	
60º	Length (mm)	13	15	12	13	14	13.4	1.14	50.91
	Diameter (mm)	10	10	11	11	10	10.4	0.55	
80º	Length (mm)	12	12	11	12	14	12.2	1.10	71.96
	Diameter (mm)	10	10	13	11	14	11.6	1.82	

Table A6.55: Bloodstain diameters exhibited using a 1.77mm pipette on angled Jupiter Linen.

Cotton Duck

1mm

	Diameter (mm)	Diameter (mm)	Diameter (mm)	Diameter (mm)	Diameter (mm)	Average	S.D
Height 50 cm	10	10	11	12	12	11	1.00
Height 100 cm	14	13	14	13	13	13.4	0.55
Height 150 cm	14	13	14	14	13	13.6	0.55
Height 200 cm	13	14	16	13	14	14	1.22

Table A6.56: Bloodstain diameters exhibited using a 1mm pipette on Cotton Duck.

Angle (º)							Average	S.D	Calculated Angle (º)
20º	Length (mm)	29	35	35	31	31	32.2	2.68	10.38
	Diameter (mm)	6	6	6	5	6	5.8	0.45	
40º	Length (mm)	12	14	15	13	14	13.8	1.14	34.42
	Diameter (mm)	7	8	8	8	8	7.8	0.45	
60º	Length (mm)	11	11	12	11	11	11.2	0.45	57.06
	Diameter (mm)	9	10	9	10	9	9.4	0.55	
80º	Length (mm)	10	11	11	11	11	10.8	0.45	74.36
	Diameter (mm)	10	11	10	11	10	10.4	0.55	

Table A6.57: Bloodstain diameters exhibited using a 1mm pipette on angled Cotton Duck.

1.77mm

	Diameter (mm)	Diameter (mm)	Diameter (mm)	Diameter (mm)	Diameter (mm)	Average	S.D
Height 50 cm	15	16	16	15	16	15.6	0.55
Height 100 cm	15	15	16	15	15	15.2	0.45
Height 150 cm	15	15	15	16	15	15.2	0.45
Height 200 cm	15	15	16	15	15	15.2	0.45

Table A6.58: Bloodstain diameters exhibited using a 1.77mm pipette on Cotton Duck.

Angle (º)							Average	S.D	Calculated Angle (º)
20º	Length (mm)	40	42	50	32	27	38.2	8.95	11.78
	Diameter (mm)	7	8	7	9	8	7.8	0.84	
40º	Length (mm)	20	22	20	21	18	20.2	1.48	32.32
	Diameter (mm)	10	11	11	11	11	10.8	0.45	
60º	Length (mm)	16	17	16	15	16	16	0.71	53.13
	Diameter (mm)	11	13	14	13	13	12.8	1.10	
80º	Length (mm)	15	14	14	14	14	14.2	0.45	N/A
	Diameter (mm)	14	15	15	14	15	14.6	0.55	

Table A6.59: Bloodstain diameters exhibited using a 1.77mm pipette on angled Cotton Duck.

Polysatin Heavy

1mm

	Diameter (mm)	Diameter (mm)	Diameter (mm)	Diameter (mm)	Diameter (mm)	Average	S.D
Height 50 cm	10	10	10	11	12	10.6	0.89
Height 100 cm	10	10	12	11	11	10.8	0.84
Height 150 cm	11	11	10	10	11	10.6	0.55
Height 200 cm	12	12	10	10	10	10.8	1.10

Table A6.60: Bloodstain diameters exhibited using a 1mm pipette on Polysatin Heavy.

Angle (º)							Average	S.D	Calculated Angle (º)
20º	Length (mm)	28	36	17	26	16	24.6	8.29	18.00
	Diameter (mm)	5	9	9	8	7	7.6	1.67	
40º	Length (mm)	16	14	14	13	12	13.8	1.48	42.93
	Diameter (mm)	8	10	10	10	9	9.4	0.89	
60º	Length (mm)	9	9	11	10	9	9.6	0.89	N/A
	Diameter (mm)	9	11	11	12	11	10.8	1.10	
80º	Length (mm)	9	10	8	9	8	8.8	0.84	N/A
	Diameter (mm)	11	14	12	13	13	12.6	1.14	

Table A6.61: Bloodstain diameters exhibited using a 1mm pipette on angled Polysatin Heavy.

1.77mm

	Diameter (mm)	Diameter (mm)	Diameter (mm)	Diameter (mm)	Diameter (mm)	Average	S.D
Height 50 cm	14	14	14	14	13	13.8	0.45
Height 100 cm	17	16	16	16	16	16.2	0.45
Height 150 cm	14	14	15	16	16	15	1.00
Height 200 cm	15	16	15	16	15	15.4	0.55

Table A6.62: Bloodstain diameters exhibited using a 1.77mm pipette on Polysatin Heavy.

Angle (°)							Average	S.D	Calculated Angle (°)
20°	Length (mm)	25	31	25	24	28	26.6	2.88	13.92
	Diameter (mm)	6	8	6	6	6	6.4	0.89	
40°	Length (mm)	26	22	24	24	24	24	1.41	22.54
	Diameter (mm)	9	10	9	9	9	9.2	0.45	
60°	Length (mm)	20	20	18	17	19	18.8	1.30	37.33
	Diameter (mm)	12	12	11	11	11	11.4	0.55	
80°	Length (mm)	17	17	14	15	16	15.8	1.30	54.11
	Diameter (mm)	12	12	13	13	14	12.8	0.84	

Table A6.63: Bloodstain diameters exhibited using a 1.77mm pipette on angled Polysatin Heavy.

Cotton Jersey Ecru

1mm

	Diameter (mm)	Diameter (mm)	Diameter (mm)	Diameter (mm)	Diameter (mm)	Average	S.D
Height 50 cm	4	3	4	3	4	3.6	0.55
Height 100 cm	3	4	3	4	3	3.4	0.55
Height 150 cm	4	4	4	4	4	4	0.00
Height 200 cm	4	4	4	5	4	4.2	0.45

Table A6.64: Bloodstain diameters exhibited using a 1mm pipette on Cotton Jersey Ecru

Angle (°)							Average	S.D	Calculated Angle (°)
20°	Length (mm)	24	22	22	15	14	19.4	4.56	8.90
	Diameter (mm)	3	3	3	3	3	3	0.00	
40°	Length (mm)	7	7	5	6	6	6.2	0.84	35.50
	Diameter (mm)	3	4	4	4	3	3.6	0.55	
60°	Length (mm)	5	5	5	4	5	4.8	0.45	56.44
	Diameter (mm)	4	4	4	4	4	4	0.00	
80°	Length (mm)	4	4	4	4	4	4	0.00	90
	Diameter (mm)	4	4	4	4	4	4	0.00	

Table A6.65: Bloodstain diameters exhibited using a 1mm pipette on angled Cotton Jersey Ecru

1.77mm

	Diameter (mm)	Diameter (mm)	Diameter (mm)	Diameter (mm)	Diameter (mm)	Average	S.D
Height 50 cm	5	5	5	5	5	5	0.00
Height 100 cm	5	5	6	6	6	5.6	0.55
Height 150 cm	5	6	5	6	5	5.4	0.55
Height 200 cm	6	6	6	6	6	6	0.00

Table A6.66: Bloodstain diameters exhibited using a 1.77mm pipette on Cotton Jersey Ecru.

Angle (º)							Average	S.D	Calculated Angle (º)
20º	Length (mm)	15	16	22	23	18	18.8	3.56	10.42
	Diameter (mm)	3	3	3	3	5	3.4	0.89	
40º	Length (mm)	6	7	7	7	7	6.8	0.45	36.03
	Diameter (mm)	4	4	4	4	4	4	0.00	
60º	Length (mm)	5	6	5	6	6	5.6	0.55	51.79
	Diameter (mm)	4	4	5	5	4	4.4	0.55	
80º	Length (mm)	5	5	5	5	5	5	0.00	N/A
	Diameter (mm)	6	5	5	6	5	5.4	0.55	

Table A6.67: Bloodstain diameters exhibited using a 1.77mm pipette on angled Cotton Jersey Ecru

Wool Mix Suiting

1mm

	Diameter (mm)	Diameter (mm)	Diameter (mm)	Diameter (mm)	Diameter (mm)	Average	S.D
Height 50 cm	7	7	7	7	7	7	0.00
Height 100 cm	9	9	9	9	9	9	0.00
Height 150 cm	10	10	10	10	10	10	0.00
Height 200 cm	10	10	10	11	11	10.4	0.55

Table A6.68: Bloodstain diameters exhibited using a 1mm pipette on Wool Mix Suiting

Angle (°)							Average	S.D	Calculated Angle (°)
20°	Length (mm)	23	25	25	25	25	24.6	0.89	12.20
	Diameter (mm)	5	5	6	5	5	5.2	0.45	
40°	Length (mm)	13	15	14	13	13	13.6	0.89	33.97
	Diameter (mm)	7	7	8	8	8	7.6	0.55	
60°	Length (mm)	8	9	8	11	10	9.2	1.30	49.54
	Diameter (mm)	7	7	7	7	7	7	0.00	
80°	Length (mm)	7	7	7	8	8	7.4	0.55	90
	Diameter (mm)	7	7	7	8	8	7.4	0.55	

Table A6.69: Bloodstain diameters exhibited using a 1mm pipette on angled Wool Mix Suiting

1.77mm

	Diameter (mm)	Diameter (mm)	Diameter (mm)	Diameter (mm)	Diameter (mm)	Average	S.D
Height 50 cm	10	10	10	10	10	10	0.00
Height 100 cm	11	11	11	11	11	11	0.00
Height 150 cm	11	11	11	11	12	11.2	0.45
Height 200 cm	12	12	12	12	12	12	0.00

Table A6.70: Bloodstain diameters exhibited using a 1.77mm pipette on Wool Mix Suiting

Angle (°)							Average	S.D	Calculated Angle (°)
20°	Length (mm)	27	26	28	31	30	28.4	2.07	10.55
	Diameter (mm)	4	5	6	5	6	5.2	0.84	
40°	Length (mm)	17	19	19	19	14	17.6	2.19	29.25
	Diameter (mm)	8	9	8	9	9	8.6	0.55	
60°	Length (mm)	13	13	13	14	12	13	0.71	57.80
	Diameter (mm)	11	12	11	10	11	11	0.71	
80°	Length (mm)	10	11	11	11	11	10.8	0.45	90
	Diameter (mm)	10	11	11	11	11	10.8	0.45	

Table A6.71: Bloodstain diameters exhibited using a 1.77mm pipette on angled Wool Mix Suiting

Silk Chiffon

1mm

	Diameter (mm)	Diameter (mm)	Diameter (mm)	Diameter (mm)	Diameter (mm)	Average	S.D
Height 50 cm	10	10	10	10	10	10	0.00
Height 100 cm	12	12	12	12	11	11.8	0.45
Height 150 cm	13	13	13	12	12	12.6	0.55
Height 200 cm	13	13	13	15	15	13.8	1.10

Table A6.72: Bloodstain diameters exhibited using a 1mm pipette on Silk Chiffon

Angle (º)							Average	S.D	Calculated Angle (º)
20º	Length (mm)	40	27	30	35	37	33.8	5.26	13.34
	Diameter (mm)	8	8	7	8	8	7.8	0.45	
40º	Length (mm)	20	31	22	22	22	23.4	4.34	24.76
	Diameter (mm)	10	9	10	10	10	9.8	0.45	
60º	Length (mm)	18	20	20	15	20	18.6	2.19	46.99
	Diameter (mm)	15	15	12	12	14	13.6	1.52	
80º	Length (mm)	15	12	20	16	18	16.2	3.03	64.32
	Diameter (mm)	16	14	13	16	14	14.6	1.34	

Table A6.73: Bloodstain diameters exhibited using a 1mm pipette on angled Silk Chiffon

1.77mm

	Diameter (mm)	Diameter (mm)	Diameter (mm)	Diameter (mm)	Diameter (mm)	Average	S.D
Height 50 cm	12	13	12	12	12	12.2	0.45
Height 100 cm	12	11	13	11	13	12	1.00
Height 150 cm	12	14	14	14	14	13.6	0.89
Height 200 cm	14	14	14	13	13	13.6	0.55

Table A6.74: Bloodstain diameters exhibited using a 1.77mm pipette on Silk Chiffon

Angle (°)							Average	S.D	Calculated Angle (°)
20°	Length (mm)	53	38	50	46	37	44.8	7.12	15.27
	Diameter (mm)	11	11	10	13	14	11.8	1.64	
40°	Length (mm)	29	31	30	31	39	32	4	40.07
	Diameter (mm)	20	24	24	19	16	20.6	3.44	
60°	Length (mm)	19	19	29	20	23	22	4.24	51.43
	Diameter (mm)	17	18	18	17	16	17.2	0.84	
80°	Length (mm)	17	17	21	19	21	19	2	N/A
	Diameter (mm)	17	19	20	21	19	19.2	1.48	

Table A6.75: Bloodstain diameters exhibited using a 1.77mm pipette on angled Silk Chiffon

Silk Dupion

1mm

	Diameter (mm)	Diameter (mm)	Diameter (mm)	Diameter (mm)	Diameter (mm)	Average	S.D
Height 50 cm	9	10	9	8	9	9	0.71
Height 100 cm	9	9	11	11	9	9.8	1.10
Height 150 cm	10	10	10	9	10	9.8	0.45
Height 200 cm	11	10	9	10	10	10	0.71

Table A6.76: Bloodstain diameters exhibited using a 1mm pipette on Silk Dupion.

Angle (°)							Average	S.D	Calculated Angle (°)
20°	Length (mm)	12	27	24	17	29	21.8	7.12	11.64
	Diameter (mm)	5	5	4	4	4	4.4	0.55	
40°	Length (mm)	11	10	11	10	13	11	1.22	33.06
	Diameter (mm)	5	6	7	6	6	6	0.71	
60°	Length (mm)	11	12	10	11	12	11.2	0.84	38.68
	Diameter (mm)	7	7	8	7	6	7	0.71	
80°	Length (mm)	9	10	9	9	8	9	0.71	43.55
	Diameter (mm)	6	6	7	6	6	6.2	0.45	

Table A6.77: Bloodstain diameters exhibited using a 1mm pipette on angled Silk Dupion.

1.77mm

	Diameter (mm)	Diameter (mm)	Diameter (mm)	Diameter (mm)	Diameter (mm)	Average	S.D
Height 50 cm	10	10	8	10	9	9.4	0.89
Height 100 cm	10	12	11	10	11	10.8	0.84
Height 150 cm	11	13	13	11	13	12.2	1.10
Height 200 cm	13	12	14	12	13	12.8	0.84

Table A6.78: Bloodstain diameters exhibited using a 1.77mm pipette on Silk Dupion.

Angle (º)							Average	S.D	Calculated Angle (º)
20º	Length (mm)	30	32	26	29	28	29	2.24	9.13
	Diameter (mm)	5	5	5	4	4	4.6	0.55	
40º	Length (mm)	14	12	15	19	18	15.4	2.88	24.56
	Diameter (mm)	7	7	7	6	5	6.4	0.89	
60º	Length (mm)	10	10	13	10	11	10.8	1.30	51.06
	Diameter (mm)	8	8	11	7	8	8.4	1.52	
80º	Length (mm)	10	10	10	12	10	10.4	0.89	55.78
	Diameter (mm)	9	7	9	10	8	8.6	1.14	

Table A6.79: Bloodstain diameters exhibited using a 1.77mm pipette on angled Silk Dupion.

Appendix 7- Bloodstains on Metal Surfaces

Aluminium Satin Anodised – Horizontal and Angled Data

FLAT   Table A7.1

						Mean	SD
1.7	50	13	14	13.5	13	13.5	13.4	0.418
	100	15	15	15	15	15	15	0
	150	16	16	16	16	15.5	15.9	0.224
	200	16.5	17	16.5	16	17	16.6	0.418

Table A7.2

						Mean	SD
1	50	12.5	12.5	12.5	12.5	12.5	12.5	0
	100	13.5	14	13.5	13.5	13.5	13.6	0.224
	150	13.5	14.5	14	14	14	14	0.354
	200	14.5	14.5	14.5	15	15	14.7	0.274

ANGLED

80   Table A7.3

					Mean	SD	Angle (calc)
50	13	13	13	13	13	13	0	74.357
L	13.5	13.5	13.5	13.5	13.5	13.5	0	
100	13.5	13.5	13.5	14	14	13.7	0.274	74.750
L	14	14	14	14.5	14.5	14.2	0.274	
150	14.5	14.5	14.5	15	14.5	14.6	0.224	75.214
L	15	15	15	15.5	15	15.1	0.224	
200	15.5	15.5	15.5	15.5	15.5	15.5	0	75.638
L	16	16	16	16	16	16	0	

60   Table A7.4

					Mean	SD	Angle (calc)
50	12.5	12.5	12.5	12.5	12.5	12.5	0	58.249
L	14.5	14.5	14.5	15	15	14.7	0.274	
100	13.5	13.5	13	13.5	13.5	13.4	0.224	63.295
L	15	15	15	15	15	15	0	
150	13.5	14	14	14	14	13.9	0.224	59.096
L	16.5	16	16.5	16	16	16.2	0.274	
200	14	14	14	14	14	14	0	58.047
L	16.5	16.5	16.5	16.5	16.5	16.5	0	

40 Table A7.5

						Mean	SD	Angle (calc)
50	10.5	10.5	10.5	10.5	10.5	10.5	0	35.234
L	18	18	18	18.5	18.5	18.2	0.274	
100	11.5	11.5	12	11.5	12	11.7	0.274	37.775
L	19	19	19	19.5	19	19.1	0.224	
150	12.5	12.5	12.5	12.5	12.5	12.5	0	36.530
L	21	21	21	21	21	21	0	
200	12.5	12.5	12.5	13	13	12.7	0.27	36.207
L	21	21	21	22.5	22	21.5	0.707	

20 Table A7.6

						Mean	SD	Angle (calc)
50	7.5	7.5	7.5	7.5	7.5	7.5	0	16.967
L	25	25.5	26	26	26	25.7	0.447	
100	8.5	8.5	8.5	8.5	8.5	8.5	0	17.672
L	28	28	28	28	28	28	0	
150	9	9	9.5	9.5	9	9.2	0.274	18.500
L	29	29	29	29	29	29	0	
200	9.5	9.5	9.5	9.5	9.5	9.5	0	18.852
L	28	29	30	30	30	29.4	0.894	

Brushed Satin Aluminium   – Horizontal and Angled Data

FLAT   Table A7.7

						Mean	SD
1.7	50	13	13	13	12	12.5	12.7	0.447

							Mean	SD
1.7	50	13	13	13	12	12.5	12.7	0.447
	100	13.5	13.5	13.5	14	13.5	13.6	0.224
	150	15.5	14.5	14	14.5	14	14.5	0.612
	200	14.5	15	14.5	15	15	14.8	0.274

Table A7.8

							Mean	SD
1	50	11	11	10.5	11.5	10.5	10.9	0.418
	100	12.5	13.5	13.5	13	13	13.1	0.418
	150	13.5	13.5	13.5	14	14.5	13.8	0.447
	200	14	14.5	14.5	14.5	14.5	14.4	0.224

320

ANGLED

80   Table A7.9

1	50	12.5	12.5	12.5	12.5	12.5
	L	12	12	12	11.5	12
	100	12.5	12.5	13	13	13
	L	13	13	12.5	12.5	12.5
	150	13.5	13.5	13.5	13.5	13.5
	L	14	14	14	13.5	13.5
	200	13.5	13.5	13.5	13.5	13.5
	L	14	14	14	14	14

60   Table A7.10

1	50	11.5	11.5	11.5	12	11.5
	L	13	13	13.5	13.5	13
	100	13	12.5	12.5	12.5	13
	L	14.5	14.5	15	15	15
	150	13	13	13	13.5	13.5
	L	15	15	15.5	15.5	15.5
	200	14.5	14.5	14.5	13.5	14
	L	16	16	16.5	16.5	16

40   Table A7.11

1	50	10	10	10	10	10
	L	16	16	16	16	16
	100	11	11	11	11	11
	L	18	18	18.5	18	18.5
	150	11.5	11.5	11.5	12	11.5
	L	18.5	18.5	19	18.5	19
	200	12	12	12	12	12
	L	20	20	19.5	19.5	19.5

20   Table A7.12

1	50	7.5	7.5	7.5	7.5	7.5
	L	26	26	28	26	27
	100	8.5	8.5	8	8.5	8
	L	31	31	32	31	32
	150	9	9	9.5	9	9.5
	L	35	35	34	33	35
	200	9.5	9.5	10	9.5	10
	L	36	36	37	36	37

Stucco Aluminium – Horizontal and Angled Data

FLAT

Table A7.13

1.7

						Mean	SD
50	13.5	13.5	12.5	13.5	12	13	0.707
100	15	15	14	15	15	14.8	0.447
150	14.5	15.5	15	15	15	15	0.354
200	16.5	16.5	16.5	16	16	16.3	0.274

Table A7.14

1

						Mean	SD
50	12	12	11.5	12	12	11.9	0.224
100	13	12.5	12.5	12.5	13	12.7	0.274
150	13	13.5	13.5	13	13	13.2	0.274
200	14.5	14	14.5	14.5	14	14.3	0.274

ANGLED

80 Table A7.15

1

50	12	12.5	12	13	12.5
L	13	13	13	13.5	13.5
100	14	14	14	14	14
L	14.5	14.5	14.5	14.5	14.5
150	14.5	14.5	15	15	15
L	15	15	15.5	15.5	15.5
200	15	15.5	15	15.5	14.5
L	15.5	16	15.5	16	15

60 Table A7.16

1

50	11	11.5	11	11	11
L	13	13.5	13	14	13.5
100	13.5	13	13.5	13	13
L	15.5	15.5	15.5	15.5	15
150	14	13	13.5	13.5	13
L	16.5	16	15.5	15.5	15
200	14	14	13.5	14	14
L	16	16.5	16	16.5	16

40 Table A7.17

1	50	10	10.5	10.5	10	10.5
	L	18	18	18	18	18
	100	11.5	12	11.5	12	12
	L	24	24	24	24	23
	150	12	12	12	12	12
	L	25	25	24	24.5	25.5
	200	13	12.5	12.5	12.5	13
	L	26	26	25	25.5	24

20 Table A7.18

1	50	7.5	7.5	7.5	7.5	7.5
	L	27	27	27	27	27
	100	8.5	8.5	8.5	8.5	8
	L	28	30	29	30	29
	150	9	9	9	9	9
	L	33	31	31	31	33
	200	8.5	9	9	9.5	9.5
	L	28	30	29	30	33

Natural Semi Bright Aluminium – Horizontal and Angled Data

FLAT Table A7.19

							Mean	SD
1.7	50	14.5	14.5	14.5	14.5	15	14.6	0.224
	100	16.5	17	16.5	16.5	16	16.5	0.354
	150	16.5	16.5	17	17	17	16.8	0.274
	200	17.5	17.5	17.5	17	17	17.3	0.274

Table A7.20

							Mean	SD
1	50	12.5	12.5	13	13	13	12.8	0.274
	100	14.5	14.5	14.5	14.5	14.5	14.5	0
	150	14.5	15	15	15	15	14.9	0.224
	200	15.5	15.5	15.5	16	16	15.7	0.274

ANGLED

80   Table A7.21

50	12.5	13	13	13.5	13
L	13	13.5	13.5	13.5	13.5
100	14.5	14	14	14	14
L	14.5	14.5	14.5	14.5	14.5
150	15	15	14.5	14.5	14.5
L	15.5	15.5	15	15	15
200	15	15.5	15.5	15.5	15
L	15.5	16	16	16	15.5

(row label: 1)

60   Table A7.22

50	12	12	12	12	12
L	14	14	14	14	14
100	13.5	13	13	13	13.5
L	16	16	16	15.5	15.5
150	13.5	13.5	14	14	14
L	16	16.5	16	16.5	16
200	14.5	14.5	14.5	14.5	14
L	17	17	17.5	17	17

(row label: 1)

40   Table A7.23

50	10.5	11	11.5	10.5	10.5
L	18.5	18	18	19	18.5
100	11.5	12	11.5	11.5	11.5
L	19	19	19	19	19
150	13	12.5	12.5	12.5	12.5
L	19.5	19.5	20	19.5	20
200	13	12.5	12.5	13	13
L	20	20	20	20	20

(row label: 1)

20   Table A7.24

50	7.5	7.5	7.5	8	8
L	25	25	26	26	26
100	8.5	8.5	8.5	8.5	8.5
L	27.5	27	27.5	27	27.5
150	9	9	9	9	9
L	28	28	28	28	28
200	9.5	9.5	9	9	9
L	29.5	29	28	28	28

(row label: 1)

324

Bright Polished Aluminium– Horizontal and Angled Data

ANGLED

FLAT   Table A7.25

						Mean	SD
1.7	50	14.5	14.5	14.5	14	15	14.5	0.354
	100	15	15	16	16	15.5	15.5	0.5
	150	16.5	16.5	16.5	17.5	16.5	16.7	0.447
	200	17.5	16.5	17.5	18	17	17.3	0570

Table A7.26

						Mean	SD
1	50	13.5	13	13.5	13.5	13.5	13.4	0.224
	100	13.5	14	14	14.5	14	14	0.354
	150	14	14.5	14.5	14.5	14.5	14.4	0.224
	200	14.5	14.5	15.5	15	14.5	14.8	0.447

80   Table A7.27

1	50	13	13	13	13	13
	L	13.5	13.5	13.5	13.5	13.5
	100	14	14	14	14	14
	L	14.5	14.5	14.5	14.5	14.5
	150	14.5	14.5	14.5	14.5	14.5
	L	15	15	15	15	15
	200	15	15.5	15.5	15	15
	L	15.5	16	16	15.5	15.5

60   Table A7.28

1	50	11	11	11	11	11
	L	13	13	13	13	13
	100	12.5	12.5	12.5	12.5	12.5
	L	14.5	14.5	14	14.5	14.5
	150	13	13	12.5	12.5	12.5
	L	15	15.5	15	14.5	14.5
	200	13	13	13	13	13
	L	14.5	15	15	15.5	15

Copper Mirror Polish – Horizontal and Angled Data

40 Table A7.29

1	50	11	10.5	11	10.5	10.5
	L	18	18	18.5	18.5	18
	100	12	12	12	12	12
	L	20	19.5	20	20	20
	150	13	13	13	12.5	12.5
	L	20.5	20.5	20	20	20
	200	13	13	13	13	13
	L	20.5	20.5	20.5	20	21

20 Table A7.30

1	50	7.5	7.5	7.5	7.5	7.5
	L	26.5	27	27	28	28.5
	100	8.5	8.5	8.5	8.5	9
	L	29	29	29	29	29
	150	9	9	9	9	9
	L	30	29	29	29.5	30
	200	9.5	9.5	9.5	10	10
	L	30	30	30	30	30

FLAT Table A7.31

							Mean	SD
1.7	50	14.5	14.5	14.5	14.5	14.5	14.5	0
	100	16.5	16.5	16.5	16.5	17	16.6	0.224
	150	17	17	17	17	16.5	16.9	0.224
	200	17	17	17	17	18	17.2	0.447

Table A7.32

							Mean	SD
1	50	12	12	12.5	12	12	12.1	0.224
	100	14	14	13.5	13.5	13.5	13.7	0.274
	150	14.5	14.5	14.5	14.5	14.5	14.5	0
	200	14.5	15	15.5	15	15	15	0.354

ANGLED

80   Table A7.33

50	13	13	13	13	13.5
L	13.5	13.5	13.5	13.5	13.5
100	14	14	14	14	14
L	14.5	14.5	14.5	14.5	14.5
150	14.5	14.5	14.5	15	14.5
L	15	15.5	15	15.5	15
200	15.5	15.5	15.5	15.5	15.5
L	16	16	16	16	16

60   Table A7.34

50	11.5	11.5	12	12	12
L	14.5	14.5	14	14.5	14
100	13.5	13.5	14	13.5	13.5
L	16	16	16	15.5	15.5
150	14	14	14	14	14
L	16	16	15.5	16.5	16
200	14.5	14.5	15	15	14.5
L	17.5	17.5	17	17.5	17

40   Table A7.35

50	11	11	11	10.5	11
L	19.5	19.5	19	19.5	20
100	11.5	11.5	12	12	11.5
L	19.5	20.5	20	20	20
150	12	12	12.5	12.5	12
L	20.5	20.5	20.5	20	20
200	13	13	13	12.5	12.5
L	21	21	21.5	21.5	21

20   Table A7.36

50	7.5	7.5	7.5	7.5	7.5
L	28	27.5	28	28	27.5
100	8.5	8.5	8.5	9	9
L	30	30	30	30	30
150	9.5	9.5	9.5	9.5	9.5
L	34	34	34	34	34
200	9.5	9.5	9.5	10	10
L	35	35	35	36	36

ANGLED

FLAT 80 Table A7.39

Table A7.37

1.7

50	17	17.5	17	16.5	17
100	17.5	18	18.5	18	18
150	18.5	19	19	18.5	18.5
200	20	20	19.5	19.5	19.5

Table A7.38

1

50	12.5	12.5	12.5	12.5	12.5
100	14	14	14	14	14
150	14	14.5	14.5	14.5	14.5
200	14.5	15	15	15	15.5

Table A7.39

1

50	12.5	12.5	12.5	12.5	12.5
L	13	13	13	13	13
100	14	14	13.5	13.5	13.5
L	14.5	14.5	14	14	14
150	14.5	14.5	14.5	14.5	14.5
L	15	15	15	15	15
200	14.5	14.5	15	15	15
L	15	15	15.5	15.5	15.5

60 Table A7.40

1

50	12.5	12.5	12.5	12.5	12.5
L	15	15	15	15	15
100	13.5	14	14	14	14
L	16	16	16	16	16
150	14.5	14.5	14.5	14.5	14.5
L	16.5	16.5	16.5	17	17
200	15	15	15	15	15
L	17.5	17.5	17.5	17.5	17.5

40   Table A7.41

1					
50	11	10.5	10.5	10.5	10.5
L	18.5	18.5	18.5	18.5	18.5
100	12	12	12	12	12
L	19.5	19	20	19.5	19
150	13	13	12.5	12.5	12.5
L	20.5	20.5	20.5	20	20
200	13	13.5	13.5	13.5	13
L	21	21	21	21.5	20.5

20   Table A7.42

1					
50	7.5	7.5	7.5	7.5	7.5
L	27	27	27	27	27
100	8.5	8.5	8.5	8.5	8.5
L	28	28	29	28.5	28
150	9.5	9.5	9	9	9
L	36	36	36	34	32
200	9.5	9.5	9.5	9.5	9.5
L	38	38	38	40	40

Galvanised Mild Steel – Horizontal and Angled Data

FLAT   Table A7.43

1.7					
50	13.5	14	14	14	14.5
100	15	16	15.5	15.5	16
150	16.5	16.5	16.5	16.5	16.5
200	16.5	16.5	16.5	17	17

Table A7.44

1					
50	12.5	12.5	12.5	12.5	12.5
100	14	14	14.5	14.5	14
150	15	14.5	14.5	14.5	14.5
200	15	15.5	15.5	15.5	15.5

ANGLED

Table A7.45

1	50	13.5	12.5	12.5	13	12.5
	L	13.5	13.5	13.5	13.5	13.5
	100	14.5	14.5	14	14	14.5
	L	15	15	14.5	14.5	15
	150	15.5	15.5	15	16	15
	L	16	16	15.5	16.5	15.5
	200	16	15.5	15.5	15.5	16
	L	16.5	16	16	16	16.5

Table A7.46

1	50	12	12	12	12	12
	L	14	14	14	14	14
	100	14	14	14	14	14
	L	16	16	16	16	16
	150	14.5	14.5	14.5	14.5	14.5
	L	16.5	16.5	16.5	16.5	16.5
	200	15.5	15.5	16	16	15.5
	L	18	18	18	18	18

Table A7.47

1	50	10.5	10.5	10	10	10
	L	17	17.5	17.5	17.5	17.5
	100	12	12	12	12	12
	L	19.5	20	20	20	19.5
	150	12.5	12.5	13	13	12.5
	L	20	21	20	21	21
	200	13.5	13.5	13.5	13.5	13.5
	L	21	22	21	22	21.5

Table A7.48

1	50	8	7.5	8	7.5	7.5
	L	26	26.5	27	26.5	27
	100	9	9	8.5	8.5	8.5
	L	28.5	28.5	28	28.5	28
	150	9	9	9	9	9
	L	28	28	27.5	28	28
	200	9	9.5	9.5	9.5	9
	L	30	30	30	29	29

Zintec Sheet – Horizontal and Angled Data

ANGLED

FLAT Table A7.49

<table>
<tr><td rowspan="4">1.7</td><td>50</td><td>12.5</td><td>12.5</td><td>13</td><td>13</td><td>12.5</td></tr>
<tr><td>100</td><td>13.5</td><td>13</td><td>14</td><td>13</td><td>14</td></tr>
<tr><td>150</td><td>14.5</td><td>14</td><td>14</td><td>14</td><td>14</td></tr>
<tr><td>200</td><td>14.5</td><td>14.5</td><td>15</td><td>14.5</td><td>15.5</td></tr>
</table>

Table A7.50

<table>
<tr><td rowspan="4">1</td><td>50</td><td>12.5</td><td>12.5</td><td>12.5</td><td>12.5</td><td>12.5</td></tr>
<tr><td>100</td><td>13</td><td>13</td><td>13</td><td>13</td><td>13</td></tr>
<tr><td>150</td><td>13.5</td><td>13.5</td><td>13.5</td><td>13.5</td><td>14</td></tr>
<tr><td>200</td><td>14</td><td>13.5</td><td>13.5</td><td>13.5</td><td>13.5</td></tr>
</table>

80 Table A7.51

<table>
<tr><td rowspan="10">1</td><td>50</td><td>11.5</td><td>11.5</td><td>11.5</td><td>11.5</td><td>11</td></tr>
<tr><td>L</td><td>12</td><td>12</td><td>12.5</td><td>12.5</td><td>12</td></tr>
<tr><td>100</td><td>12.5</td><td>13</td><td>13</td><td>13</td><td>13</td></tr>
<tr><td>L</td><td>13</td><td>13.5</td><td>13.5</td><td>13.5</td><td>13.5</td></tr>
<tr><td>150</td><td>14</td><td>14</td><td>13.5</td><td>13.5</td><td>14</td></tr>
<tr><td>L</td><td>14.5</td><td>14.5</td><td>14</td><td>14</td><td>14.5</td></tr>
<tr><td>200</td><td>14</td><td>14</td><td>14</td><td>14</td><td>13.5</td></tr>
<tr><td>L</td><td>14.5</td><td>14.5</td><td>14.5</td><td>14.5</td><td>14</td></tr>
</table>

60 Table A7.52

<table>
<tr><td rowspan="10">1</td><td>50</td><td>11</td><td>11</td><td>11</td><td>11</td><td>11.5</td></tr>
<tr><td>L</td><td>13.5</td><td>13.5</td><td>13.5</td><td>13.5</td><td>14</td></tr>
<tr><td>100</td><td>12.5</td><td>12.5</td><td>12.5</td><td>12.5</td><td>12.5</td></tr>
<tr><td>L</td><td>15</td><td>15</td><td>15.5</td><td>15.5</td><td>15.5</td></tr>
<tr><td>150</td><td>13</td><td>13</td><td>13</td><td>13</td><td>13</td></tr>
<tr><td>L</td><td>15.5</td><td>15.5</td><td>15.5</td><td>16</td><td>16</td></tr>
<tr><td>200</td><td>14</td><td>14</td><td>14</td><td>14.5</td><td>14</td></tr>
<tr><td>L</td><td>17</td><td>17</td><td>17</td><td>17.5</td><td>17</td></tr>
</table>

40   Table A7.53

1					
50	9.5	9.5	9.5	9.5	10
L	15	15	15	15	15
100	11	10.5	10.5	10.5	10.5
L	16.5	16	17	17	16.5
150	11.5	11.5	11.5	11.5	11
L	18	18	18	18	17.5
200	12	12	12	12	12
L	19	19	18.5	18.5	19

20   Table A7.54

1					
50	7	7	7	6.5	6.5
L	27	26	27	26	26.5
100	7.5	7.5	7.5	8	8
L					
150	8.5	8.5	8.5	8.5	8.5
L					
200	9	9	9	9	9
L					

Stainless Steel Brushed– Horizontal and Angled Data

FLAT   Table A7.55

1.7					
50	14.5	14.5	14.5	15	14.5
100	16	16	15.5	15	16
150	16.5	17	16.5	16.5	16.5
200	16.5	17	17.5	17	16.5

Table A7.56

1					
50	11.5	12	11.5	12.5	12.5
100	14	14	14.5	14.5	14
150	14.5	14.5	14.5	14.5	14
200	15	15	15	15	15

ANGLED

80 Table A7.57

1					
50	12.5	12.5	12.5	13	13
L	12	12	12.5	12.5	12.5
100	13.5	13.5	13.5	13.5	13
L	13	13	13	13	12.5
150	14.5	14	14.5	14	14.5
L	14	13.5	14	13.5	14
200	14	14	14	14	14.5
L	14	14	14.5	14	14.5

60 Table A7.58

1					
50	13	13	13	13	13
L	14	14	14	14	14
100	13.5	13.5	13.5	14	14
L	15	15	15	14.5	14.5
150	14.5	14.5	14.5	14.5	14.5
L	15.5	16	15.5	16	16
200	15	15	14.5	14.5	15
L	16	16	16	16	15.5

40 Table A7.59

1					
50	10.5	10.5	10.5	10.5	10.5
L	16	16	16.5	16.5	16.5
100	11.5	12	12	11.5	11.5
L	17.5	17.5	17.5	17.5	17
150	12	12	12	12	12
L	18.5	18.5	18.5	18	18
200	12	12	12.5	12.5	12.5
L	19	19	18.5	18.5	18.5

20 Table A7.60

1					
50	7.5	7.5	7.5	7.5	7.5
L	24	23.5	26	24.5	24.5
100	9	8.5	8.5	8.5	8.5
L	28	28	28	28	28
150	9	9	9	9	9
L	30	30	30	30	30
200	9.5	9.5	9	9	9.5
L	34	34	33	34	33

316 Stainless Sheet– Horizontal and Angled Data

FLAT   Table A7.61

1.7

50	13	13	14	14	14
100	15	15	14.5	14.5	15.5
150	15.5	15.5	16	16.5	17
200	18	18	18	18.5	17.5

Table A7.62

1

50	12	12	12.5	12	12
100	13.5	13.5	13.5	13.5	14
150	14	14	13.5	14.5	14.5
200	15	15	14.5	14	15

ANGLED

80   Table A7.63

1

50	13	13	13	13	13
L	13.5	13.5	13.5	13.5	13.5
100	14	14	14	14	14
L	14.5	14.5	14.5	14.5	14.5
150	15	15	14.5	14.5	14.5
L	15.5	15.5	15	15	15
200	14.5	15	15	15.5	15
L	15	15.5	15.5	16	15.5

60   Table A7.64

1

50	12	12	12	12	12
L	14	14	14.5	14.5	14
100	13	13.5	13.5	13.5	13.5
L	15	15.5	15.5	15.5	15.5
150	14	14	14	14	14
L	16.5	16.5	16.5	16.5	16.5
200	15	14.5	14.5	14.5	14.5
L	17	17	17	17	17

40 Table A7.65

1	50	10.5	10.5	10.5	10.5	10.5
	L	18	18	18	18	18
	100	11	11	11.5	11.5	11
	L	18.5	18.5	18.5	19	19
	150	12	12	12	11.5	11.5
	L	22	22	20	22	20
	200	12	12.5	12.5	12.5	12.5
	L	24	24	23	22	23

20 Table A7.66

1	50	7.5	7.5	7.5	7.5	7.5
	L	25	25.5	26	26	25
	100	7.5	7.5	8	8	8
	L	27	27	27	28	30
	150	8.5	8.5	8.5	8.5	8.5
	L	28	28	29	30	29
	200	8.5	8.5	9	9	9
	L	34	32	33	32	34

430 bright steel– Horizontal and Angled Data

FLAT Table A7.67

1.7	50	15	15.5	16	16	15
	100	17	16.5	16.5	17.5	16.5
	150	17.5	17.5	18	17.5	16.5
	200	18	18	18.5	18.5	18

Table A7.68

1	50	11.5	11.5	11	11	11.5
	100	13.5	13.5	13.5	13.5	13.5
	150	14.5	14.5	14.5	14.5	14.5
	200	15	15	15	15.5	14.5

ANGLED

80

Table A7.69

1					
50	13.5	13.5	13	14	13
L	14	14	13.5	14.5	13.5
100	14.5	14.5	14.5	14.5	14.5
L	15	15	15	15	15
150	15	15.5	15.5	15.5	15.5
L	15.5	16	16	16	16
200	17	16.5	16.5	16.5	16
L	17.5	17	17	17	16.5

60

Table A7.70

1					
50	12.5	13	13	12.5	13
L	15.5	15	15	15.5	15
100	14.5	14	14	14.5	14
L	16.5	17	17	16.5	17
150	14.5	14.5	14.5	14.5	14.5
L	17.5	17	17	17	17
200	15	15	15	15	15.5
L	18	18	18	18	18.5

40

Table A7.71

1					
50	10	10	10	10	10
L	18	18	17.5	18	17.5
100	12	12	12	12	12
L	21	21	21	21	21
150	12.5	12.5	12.5	12.5	12.5
L	21.5	21.5	21.5	21.5	21.5
200	12.5	13	13	13	12.5
L	22	22	21.5	21.5	22

20

Table A7.72

1					
50	8	8	7.5	7.5	7.5
L	28	28	28	28	28
100	8.5	8.5	9	9	8.5
L	30.5	30.5	31	31	30.5
150	9.5	9.5	9.5	9.5	9
L	31	31	31	31	32
200	10	10	10	10	9.5
L	31.5	32	32	32	32

430 Brush Stainless Steel – Horizontal and Angled Data

ANGLED

Table A7.75

FLAT Table A7.73

1	50	13	13	13	13	13
	L	12	12.5	12.5	12.5	12
	100	13.5	13.5	14	14	13.5
	L	13.5	13.5	13.5	14	13
	150	15	15	14.5	14.5	14.5
	L	14.5	14.5	14	14	14
	200	15	15	15.5	15.5	15
	L	14.5	14.5	15	15	14.5

1.7	50	14.5	14.5	14.5	14.5	14
	100	14.5	14.5	15.5	16	16
	150	16	16	15.5	16	15.5
	200	17	16	16	17	16.5

Table A7.74

60   Table A7.76

1	50	12.5	12.5	13	12.5	12.5
	100	14	14	14	14	14
	150	14.5	14.5	14.5	14.5	14.5
	200	15	14.5	14.5	14.5	14.5

1	50	12	12	12	12	12
	L	13.5	13.5	13.5	13.5	13.5
	100	13.5	13.5	13.5	13.5	13.5
	L	15	15	15	15.5	15
	150	13.5	13.5	14	14	13.5
	L	16.5	15.5	16	16	16.5
	200	14	14	14	14	14
	L	16.5	16	16.5	16.5	16

40 Table A7.77

1	50	10	10	10.5	10	10.5
	L	17	17	16.5	17	16.5
	100	11	11.5	11	11.5	11
	L	17.5	17.5	17	17	17.5
	150	12	12	12	12	12
	L	20	21	20	21	20
	200	12	12	12	12.5	12
	L	22	20	22	20	20

20 Table A7.78

1	50	7.5	7.5	7.5	7.5	7.5
	L	26	25.5	26	26	25.5
	100	8	8	8	8	8
	L	28	28	28	29	28
	150	8.5	8.5	8.5	8.5	8.5
	L	30	30	30	29	30
	200	9	9	9	9	9
	L	31	31	31	31	31

430 Circles Stainless Steel – Horizontal and Angled Data

FLAT Table A7.79

1.7	50	14	14	14	15	14.5
	100	16.5	16.5	16.5	16	16.5
	150	17	17	16.5	17.5	17.5
	200	17.5	17.5	17.5	17.5	18

Table A7.80

1	50	13	13	12.5	13	13
	100	13.5	13.5	13.5	14	14
	150	15	15.5	15	15	15.5
	200	15.5	15.5	15.5	16	16

ANGLED

80   Table A7.81

50	13	13	13	13.5	13
L	13.5	13.5	13.5	13	13.5
100	14.5	14.5	14.5	14.5	14.5
L	15	15	15	15	15
150	15.5	15.5	15.5	15.5	15.5
L	16	16	16	16	16
200	16	16	16	16.5	16
L	16.5	16.5	16.5	16.5	17

60   Table A7.82

50	12	12	12	12	12.5
L	14.5	14.5	14.5	14.5	14.5
100	14	14	13.5	13.5	13.5
L	16	16	16	16	16.5
150	14.5	14.5	14.5	14.5	14.5
L	16.5	16.5	17	17	16.5
200	15	15	15	15	14.5
L	17	17	17	17	17

40   Table A7.83

50	11	11	11	11	11
L	18	18	18	18	18
100	11.5	12	12	12	12
L	18.5	20	20	20	19
150	13	12.5	12.5	12.5	12.5
L	20.5	20.5	20	20	20
200	13.5	13.5	13.5	13.5	13.5
L	21.5	21.5	22	21.5	21.5

20   Table A7.84

50	8	8	8	7.5	7.5
L	26	26	26	26	26.5
100	9	8.5	8.5	8.5	8.5
L	27	27.5	28	28	28
150	9	9	9.5	9.5	9.5
L	29	29	30	31	31
200	10	10	10	10	10
L	30	30	30	31	31

Stainless Sheet Super Mirror – Horizontal and Angled Data

FLAT   Table A7.85

1.7					
50	14.5	13.5	13.5	14	14.5
100	16	16.5	17.5	17	16.5
150	17	17	17.5	17.5	17
200	17.5	17.5	17.5	17	18

Table A7.86

1					
50	13	12.5	12.5	13	12.5
100	14.5	14.5	13.5	13.5	13.5
150	14.5	15	15	15	14.5
200	15	15.5	15.5	14.5	15.5

ANGLED

80   Table A7.87

50	13	13	12.5	12.5	13.5
L	13.5	13.5	13	13	13.5
100	14	13.5	14.5	14.5	14
L	14.5	14	14.5	14.5	15
150	15	14.5	14.5	14.5	14.5
L	15.5	15	15	15	15
200	15	15.5	15.5	15.5	15.5
L	15.5	16	16	15.5	16

60

1					
50	12	12	12	12	11.5
L	14	14.5	14	14.5	14.5
100	14	13.5	13	13	13
L	16	16.5	15.5	16.5	16.5
150	14	14.5	14.5	14.5	14.5
L	17	17	17	17	17
200	14.5	14.5	15	15	15
L	17.5	17.5	17	17	17

Table A7.88

40 Table A7.89

1 50	10	10	10.5	10.5	10
L	19	19	18	18	18
100	11.5	11.5	12	12	12
L	20	20	19.5	21	20
150	12	12	12	12	12
L	20	20.5	20.5	20	20
200	13	12.5	12.5	12	13
L	21	21	21	21	21

20 Table A7.90

1 50	7.5	7.5	7.5	7.5	7.5
L	28	28	28	28	28
100	8.5	8.5	8.5	8.5	8.5
L	30	30	30	29.5	30
150	9	9	9	9	9
L	30	30.5	31.5	31.5	31
200	9.5	9.5	9.5	9.5	9.5
L	32	32	32	32	32

Sheet Metal, Zinc– Horizontal and Angled Data

FLAT Table A7.91

1.7 50	14	14.5	14.5	14.5	14.5
100	16.5	16.5	16.5	16.5	16.5
150	16.5	16.5	17	16.5	17
200	17	17	16.5	16.5	17

Table A7.92

1 50	12.5	12.5	12.5	12.5	12.5
100	13.5	13	14.5	14	14
150	14.5	14	14	14	14
200	15.5	15	15	15	15

ANGLED

80 Table A7.93

50	13.5	13.5	14	13	13
L	14	14	14.5	14.5	13.5
100	14	14	14	14	14
L	14.5	14.5	14.5	14.5	14.5
150	14	14	14.5	14.5	14.5
L	14.5	14.5	15	15	15
200	15	15.5	15.5	15.5	15
L	16	16	16	16	15.5

1 (row label)

60 Table A7.94

50	12	12	12.5	12.5	12.5
L	14.5	14.5	14.5	14	14
100	14	14	14	14	14
L	16	16	16	16	16.5
150	14.5	14.5	14.5	14.5	14.5
L	16.5	17.5	17.5	16.5	16.5
200	16.5	16.5	16	16	16
L	17.5	17.5	18.5	17.5	18.5

1 (row label)

40 Table A7.95

50	10.5	10.5	10.5	10.5	10.5
L	17.5	17.5	17.5	17	17
100	12	12	12	11	11
L	19.5	19.5	19	19	19
150	12.5	12.5	12.5	13	13.5
L	20.5	20.5	20	19.5	20
200	13	13	13	13	13.5
L	21	21	20.5	19.5	20.5

1 (row label)

20 Table A7.96

50	7.5	7.5	7.5	7.5	7.5
L	27	27	27	27	27
100	8.5	8.5	8.5	8.5	8.5
L	30	30	30	29	29
150	9	9	9	9	9
L	36	36	36	36	36
200	9	9.5	9.5	9.5	9
L	36	37	38	37	37

1 (row label)

sheet-metal-quartz-zinc – Horizontal and Angled Data

ANGLED

FLAT

Table A7.97

1.7	50	13	13	13	12.5	13
	100	14.5	14.5	14.5	14.5	14.5
	150	15.5	15.5	15.5	15	15
	200	16.5	16.5	16.5	16.5	16

Table A7.98

1	50	11	11.5	11.5	11.5	11.5
	100	13	13	13.5	13	13
	150	13.5	14	14	14	14
	200	14.5	14.5	14	14	14.5

80   Table A7.99

1	50	11.5	11.5	11.5	11.5	11.5
	L	12	12	12	12	12
	100	12	12	12	11.5	11.5
	L	12.5	12.5	12.5	12	12.5
	150	14	13.5	13.5	13.5	13.5
	L	14	14	14	14	14
	200	14	14	14	13.5	13.5
	L	14	14.5	14.5	14	14

60   Table A7.100

1	50	12	12	12	12	12
	L	13.5	13.5	13.5	13.5	13.5
	100	13	12.5	12.5	13	12.5
	L	14.5	14.5	14.5	14.5	14.5
	150	13.5	13.5	13.5	13.5	13.5
	L	15.5	15.5	15.5	15.5	15.5
	200	14.5	14.5	14.5	14.5	14.5
	L	16	16	16.5	16.5	16.5

40 Table A7.101

1					
50	10	10	10	10	10
L	16	16	16.5	16.5	16
100	10	10.5	10.5	10.5	10.5
L	16	16	17	17	17
150	11	11	11	11	11
L	16	17	17	17	17
200	11	11.5	11.5	11.5	11.5
L	18	18	18.5	18	18.5

20 Table A7.102

1					
50	6.5	7	7	7	7
L	26	25	26	26	25
100	7.5	7.5	7.5	7.5	7
L	30	30	30	30	30
150	8	8	8	8	8
L	32	32	31	32	32
200	8.5	8.5	8.5	8.5	8
L	34	34	35	34	34

Brass Mirror Polish – Horizontal and Angled Data

FLAT Table A7.103

1.7					
50	13.5	13.5	14	14	14
100	15.5	16	16	15.5	15.5
150	17	16	16	16.5	16.5
200	17.5	17.5	17.5	17.5	17.5

Table A7.104

1					
50	12.5	12.5	12.5	13	12.5
100	14	14	14	13.5	13.5
150	14.5	14.5	14.5	14.5	14.5
200	14.5	15	15	15	15

ANGLED

80

Table A7.105

50	12.5	12.5	12.5	12.5	12.5
L	13	13	13	13	13
100	13	13	14	14	14
L	13.5	13.5	14.5	14.5	14
150	14	14	14.5	14.5	14
L	14.5	14.5	14.5	15	15
200	15	15	14.5	14.5	15
L	15.5	15.5	15	15	15.5

Table A7.107

50	11	11	11	11	10.5
L	19	19	19	19	19
100	11.5	11.5	11.5	11.5	11.5
L	19.5	19.5	19.5	20	20
150	12	12	12	12.5	12
L	20	20.5	20.5	20.5	20
200	12.5	12.5	12.5	12	12.5
L	21	21	20.5	20.5	20.5

60

20

Table A7.106

Table A7.108

50	12.5	12	12	12	12.5
L	14.5	14.5	14	14	14
100	13.5	13.5	13.5	13.5	13
L	15.5	15.5	15	15.5	16
150	14	14	14.5	14	14.5
L	15.5	16	16	16.5	16
200	15	15	15	15	14.5
L	17.5	17.5	17.5	17.5	17

50	8	7.5	7.5	8	7.5
L	25	27	27	28	27
100	8.5	8.5	8.5	8.5	8.5
L	29	29	29	29	30
150	9	9	9.5	9.5	9
L	32	32	32	31	32
200	9	9.5	9.5	9.4	9.5
L	34	34	34	34	34

Sheet Metal, Copper – Horizontal and Angled Data

FLAT   Table A7.109

1.7

50	13.5	13.5	14	14	14
100	15.5	15.5	16	16	16
150	16	16.5	16.5	16.5	16.5
200	17	17	17	16.5	16

Table
A7.110

1

50	13	13	13	13	13
100	14	14	14	13.5	14.5
150	14.5	14.5	14.5	14.5	15
200	14.5	15	15	15	15

ANGLED

80   Table A7.111

1

50	12.5	13	13	13	12.5
L	13	13	13	13	13.5
100	14	14	14	14	13.5
L	14.5	14.5	14.5	14.5	14
150	15	15	14.5	14.5	14.5
L	15.5	15.5	15	15	15
200	15	15.5	15.5	15	15.5
L	15.5	16	16	15.5	16

60   Table A7.112

1

50	12	12	12.5	12.5	12
L	14.5	14.5	14.5	15	15
100	13	13	13.5	13.5	13.5
L	15.5	16	16	15.5	16
150	14.5	14.5	14.5	14	14
L	16	16	16.5	16.5	16..5
200	15	15	15	14.5	15
L	16.5	17	17	17	17.5

40   Table A7.113

1

50	10.5	10.5	11	11	11
L	18	18	18	18.5	18.5
100	12	12	12	12	12
L	19.5	19.5	19.5	19.5	19.5
150	12.5	12.5	12.5	12.5	12.5
L	20	20	20	20	20.5
200	13	13	13.5	13.5	13.5
L	21	21	21	21.5	21.5

20   Table A7.114

1

50	8	8	8	8	8
L	27	29	27	27	27
100	9	9	9	9	9
L	29	29	29	30	29
150	10	10	10	10	10
L	32	32	32	31	31
200	10	10.5	10	10.5	10.5
L	36	36	36	35	35

Natural Semi Bright Aluminium - rough

– Horizontal and Angled Data

FLAT   Table A7.115

1.7

50	12.5	12.5	12.5	12.5	12
100	13	13	13.5	13	13
150	14.5	15	14.5	14	14
200	16	15.5	15.5	15	16

Table A7.116

1

50	11.5	12	12	11.5	11.5
100	13.5	13	12	13	13
150	13.5	13.5	13.5	13.5	13.5
200	13.5	14	14	14	14

ANGLED

80   Table A7.117

50	12	12.5	12.5	12	12
L	12.5	12.5	12.5	12.5	12.5
100	12.5	12.5	12.5	12.5	13
L	13	13	13	13	13.5
150	14	14	14	14	13.5
L	14.5	14.5	14	14.5	14
200	14.5	14.5	14	14.5	14
L	15	15	15	14.5	14.5

(row label: 1)

60   Table A7.118

50	11	11	11	11	11
L	13	13	13	13	13
100	12.5	12.5	13	13	13
L	14.5	14.5	14.5	15	15
150	12.5	12.5	13.5	13	13.5
L	15	15	16	16	15
200	13	13	13	13	13
L	16	15.5	16	15.5	16

(row label: 1)

40   Table A7.119

50	10	10	10	10	10
L	18	18	19	19	19
100	11	11	11	11	11
L	21	21	20	20	21
150	12	12	12	11.5	11.5
L	22	21	22	21	21
200	12	12.5	12	12	12
L	22	22	23	23	23

(row label: 1)

20   Table A7.120

50	7	7	7	7	7
L	26	26	26	26	26
100	8.5	8.5	8	8	8
L	32	32	28	28	28
150	8.5	8.5	9	9	9
L	30	30	32	32	32
200	9	9	9.5	9.5	9.5
L	34	34	34	33	32

(row label: 1)

Mild Steel – Rough

 – Horizontal and Angled Data

FLAT   Table A7.121

1.7	50	13	12.5	13	13	13.5
	100	15	15	14.5	15.5	15
	150	15.5	15.5	15.5	15.5	15.5
	200	16	15	16	16.5	16

Table
A7.122

1	50	11.5	11.5	11	12	11.5
	100	13	13	13.5	13	13
	150	13	13.5	14.5	13.5	13.5
	200	14.5	14.5	14	14.5	14.5

ANGLED

80   Table A7.123

1	50	12	12	12	12	12
	L	12.5	12.5	12.5	12.5	12.5
	100	13	13	13	13	13
	L	13.5	13.5	13.5	13.5	13.5
	150	13.5	13.5	13.5	14	14
	L	14	14	14	14.5	14.5
	200	15	14.5	14.5	14.5	15
	L	15.5	15	15	15	15.5

60   Table A7.124

1	50	12	12	12	11.5	11.5
	L	14	14	14	15	15
	100	12	12	12	12.5	12.5
	L	14.5	14.5	14.5	14	14.5
	150	14	13.5	13.5	13.5	14
	L	15	15.5	15.5	15	15
	200	14	14	14.5	14.5	14
	L	16	16	16.5	16	16

40   Table A7.125

1	50	10	10	10	10.5	10.5
	L	18	18	18	18	18.5
	100	11	11	11	11	11.5
	L	18	19	20	18	19
	150	12	12	11.5	11.5	11.5
	L	19.5	18.5	18.5	20	18.5
	200	12.5	12.5	12.5	12.5	12.5
	L	20	20	19.5	19.5	20

20   Table A7.126

1	50	7	7	7	7	7
	L	27	27	28	28	27
	100	8	8	8	8	8
	L	35	35	35	34	34
	150	8.5	8.5	8.5	8	8
	L					
	200	8.5	8.5	8.5	9	9
	L					

316 Stainless Sheet - Rough

– Horizontal and Angled Data

FLAT   Table A7.127

1.7	50	14	14	14.5	14.5	14.5
	100	15.5	16	17	16.5	16.5
	150	16.5	16.5	16.5	17	16.5
	200	17	17	17.5	17	17

Table A7.128

1	50	12	12	12	12	12
	100	12.5	13	12.5	12.5	12.5
	150	13.5	13	13	13	13
	200	13.5	14	14	13.5	13.5

ANGLED

80   Table A7.129

1	50	11	11	11	11.5	11.5
	L	11.5	11.5	11.5	12	12
	100	13	12.5	13	12.5	12.5
	L	13.5	13	13.5	13	13
	150	13	13.5	13	13	13.5
	L	13.5	14	13.5	13.5	14
	200	13.5	13.5	13.5	13.5	13.5
	L	14	14	13.5	13.5	14

60   Table A7.130

1	50	12	12	12	12	12
	L	14	14	14	14	14
	100	12.5	12.5	13	13.5	13
	L	14.5	15	15	15.5	15
	150	13.5	13.5	13.5	13.5	13.5
	L	15.5	15.5	15.5	15.5	15.5
	200	13.5	14	14	14	14
	L	15	15	16	15.5	15.5

40   Table A7.131

1	50	10	10	10	10	10
	L	17	17.5	17	17.5	18
	100	11.5	11.5	11.5	11.5	11
	L	19	19	19	18.5	19
	150	11.5	11.5	12	12	11.5
	L	19	19.5	19.5	19	19.5
	200	12	12	12	12.5	12.5
	L	20	20	20	21	21

20   Table A7.132

1	50	11.5	11.5	11.5	11.5	11.5
	L	28	28	28	27	27
	100	8.5	8.5	8	8	8.5
	L	28	30	30	30	28
	150	8.5	9	9	9	8.5
	L	35	35	35	34	34
	200	9	9	9.5	9.5	9
	L	36	36	37	37	37

430 Bright Stainless Steel - **Rough**

– Horizontal and Angled Data

FLAT Table A7.133

1.7

50	13.5	13.5	14	13.5	13.5
100	14.5	14.5	14.5	15	15.5
150	15.5	15	15	15	14.5
200	16.5	16	15	15.5	15.5

Table A7.134

1

50	11.5	11.5	11.5	12	11.5
100	13	13	12.5	12.5	13
150	13.5	13.5	13.5	13.5	13.5
200	14	14	14	14.5	14.5

ANGLED

80 Table A7.135

1

50	12	12	12	12.5	12
L	12.5	12.5	12.5	12.5	12.5
100	13	13	13	13	13
L	13.5	13.5	13.5	13.5	13.5
150	13.5	13.5	13.5	13.5	13.5
L	14	14	14	14	14
200	13.5	13.5	14	14	13.5
L	14	14	14	14.5	14.5

60 Table A7.136

1

50	11.5	11.5	11.5	11.5	12
L	14	14	14	14	13.5
100	12.5	12.5	12.5	12.5	12
L	14.5	14.5	14.5	14.5	15
150	13.5	13.5	13.5	13.5	13.5
L	16	16	16	16	16.5
200	14	14	14	14	14
L	17	17	16.5	17	16.5

40   Table A7.137

1	50	10	10	10	10	9.5
	L	17	17	17	16.5	17
	100	11	11	11	10.5	11
	L	17	17	17	17.5	17
	150	12	12	12	11.5	11.5
	L	19	19	19	18.5	19
	200	12.5	12.5	12.5	12.5	12.5
	L	19.5	19.5	19	19.5	20

20   Table A7.138

1	50	11.5	11.5	11	11.5	11					
	L	28	28	26.5	27	27					
	100	8.5	8.5	8	8	8.5					
	L	28	31	30	30	29					
	150	8.5	9	9	9	8.5					
	L	36	35	36	34	34					
	200	9	9	9.5	9.5	9					
	L	36	36	37	37	37					

Appendix 8- Bloodstains on Stones Surfaces

Stones (1mm)

Rusty Slate Paving

	Diameter (mm)	Diameter (mm)	Diameter (mm)	Diameter (mm)	Diameter (mm)	Average	SD
Height 50cm	13	13	13	13	13	13	0
Height 100cm	14	14	14	14	14	14	0
Height 150cm	15	15	15	15	15	15	0
Height 200cm	15	15	15	15	16	15.2	0.447214

Table A8.1: 1mm pipette drop results on Rusty Slate Paving.

Beige Marble Polished

	Diameter (mm)	Diameter (mm)	Diameter (mm)	Diameter (mm)	Diameter (mm)	Average	SD
Height 50cm	14	14	13	14	14	13.8	0.447214
Height 100cm	14	14	14	14	14	14	0
Height 150cm	15	15	15	15	14	14.8	0.447214
Height 200cm	16	16	16	16	16	16	0

Table A8.2: 1mm pipette drop results on Beige Marble Polished.

Classic Chipped Edge Filled and Honed

	Diameter (mm)	Diameter (mm)	Diameter (mm)	Diameter (mm)	Diameter (mm)	Average	SD
Height 50cm	12	13	13	13	13	12.8	0.447214
Height 100cm	14	14	15	14	15	14.4	0.547723
Height 150cm	15	14	14	14	15	14.4	0.547723
Height 200cm	15	15	15	15	15	15	0

Table A8.3: 1mm pipette drop results on Classic Chipped Edge Filled and Honed

Classic Travertine Filled and Honed

	Diameter (mm)	Diameter (mm)	Diameter (mm)	Diameter (mm)	Diameter (mm)	Average	SD
Height 50cm	13	13	13	13	13	13	0
Height 100cm	14	14	14	14	14	14	0
Height 150cm	15	15	15	15	15	15	0
Height 200cm	15	15	15	16	16	15.4	0.547723

Table A8.4: 1mm pipette drop results on Classic Travertine Filled and Honed.

Classic Tumbled Unfilled Travertine

	Diameter (mm)	Diameter (mm)	Diameter (mm)	Diameter (mm)	Diameter (mm)	Average	SD
Height 50cm	13	13	13	13	13	13	0
Height 100cm	14	13	13	14	13	13.4	0.547723
Height 150cm	13	13	14	14	14	13.6	0.547723
Height 200cm	15	15	15	15	14	14.8	0.447214

Table A8.5: 1mm pipette drop results on Classic Tumbled Unfilled Travertine

Indian Sandstone Paving Raj Blend Tumbled

	Diameter (mm)	Diameter (mm)	Diameter (mm)	Diameter (mm)	Diameter (mm)	Average	SD
Height 50cm	12	12	13	13		12.5	0.57735
Height 100cm	13	14	13	13	13	13.2	0.447214
Height 150cm	14	14	14	14	14	14	0
Height 200cm	15	15	14	14	14	14.4	0.547723

Table A8.6: 1mm pipette drop results on Indian Sandstone Paving Raj Blend Tumbled.

Indian Sandstone Paving Raj Blend Economy

	Diameter (mm)	Diameter (mm)	Diameter (mm)	Diameter (mm)	Diameter (mm)	Average	SD
Height 50cm	11	11	11	11	11	11	0
Height 100cm	13	13	13	13	13	13	0
Height 150cm	14	13	13	13	13	13.2	0.447214
Height 200cm	14	14	14	15	14	14.2	0.447214

Table A8.7: 1mm pipette drop results on Indian Sandstone Paving Raj Blend Economy

Indian Sandstone Paving Sahara Yellow

	Diameter (mm)	Diameter (mm)	Diameter (mm)	Diameter (mm)	Diameter (mm)	Average	SD
Height 50cm	11	11	11	11	12	11.2	0.447214
Height 100cm	14	13	14	13	14	13.6	0.547723
Height 150cm	13	14	14	13	14	13.6	0.547723
Height 200cm	14	14	14	15	14	14.2	0.447214

Table A8.8: 1mm pipette drop results on Indian Sandstone Paving Sahara Yellow.

Indian Sandstone Paving Rippon Buff

	Diameter (mm)	Diameter (mm)	Diameter (mm)	Diameter (mm)	Diameter (mm)	Average	SD
Height 50cm	11	12	12	11	12	11.6	0.547723
Height 100cm	11	11	12	12	11	11.4	0.547723
Height 150cm	13	14	14	14	13	13.6	0.547723
Height 200cm	14	15	15	15	15	14.8	0.447214

Table A8.9: 1mm pipette drop results on Indian Sandstone Paving Rippon Buff

Indian Sandstone Paving Modak

	Diameter (mm)	Diameter (mm)	Diameter (mm)	Diameter (mm)	Diameter (mm)	Average	SD
Height 50cm	13	13	13	13	13	13	0
Height 100cm	14	14	15	15	15	14.6	0.547723
Height 150cm	14	15	14	15	15	14.6	0.547723
Height 200cm	15	15	15	15	15	15	0

Table A8.10: 1mm pipette drop results on Indian Sandstone Paving Modak.

Classic Honed Travertine Paving

	Diameter (mm)	Diameter (mm)	Diameter (mm)	Diameter (mm)	Diameter (mm)	Average	SD
Height 50cm	13	13	13	13		13	0
Height 100cm	14	14	14	13	13	13.6	0.547723
Height 150cm	14	14	15	14	14	14.2	0.447214
Height 200cm	15	15	15	15	15	15	0

Table A8.11: 1mm pipette drop results on Classic Honed Travertine Paving.

Silver Latte Tumbled Travertine Paving

	Diameter (mm)	Diameter (mm)	Diameter (mm)	Diameter (mm)	Diameter (mm)	Average	SD
Height 50cm	13	13	13	13	13	13	0
Height 100cm	14	13	13	13	14	13.4	0.547723
Height 150cm	14	15	14	14	14	14.2	0.447214
Height 200cm	15	15	15	15	15	15	0

Table A8.12: 1mm pipette drop results on Silver Latte Tumbled Travertine Paving.

Yellow Limestone Paving

	Diameter (mm)	Diameter (mm)	Diameter (mm)	Diameter (mm)	Diameter (mm)	Average	SD
Height 50cm	10	11	11	11	11	10.8	0.447214
Height 100cm	12	12	12	12	13	12.2	0.447214
Height 150cm	13	13	13	13	13	13	0
Height 200cm	14	14	14	14	15	14.2	0.447214

Table A8.13: 1mm pipette drop results on Yellow Limestone Paving.

Brazilian Black Slate Paving

	Diameter (mm)	Diameter (mm)	Diameter (mm)	Diameter (mm)	Diameter (mm)	Average	SD
Height 50cm	13	13	13	13	13	13	0
Height 100cm	13	13	13	14	14	13.4	0.547723
Height 150cm	14	14	14	14	14	14	0
Height 200cm	15	15	15	15	15	15	0

Table A8.14: 1mm pipette drop results on Brazilian Black Slate Paving.

Seal Grey Flamed

	Diameter (mm)	Diameter (mm)	Diameter (mm)	Diameter (mm)	Diameter (mm)	Average	SD
Height 50cm	13	13	14	14	14	13.6	0.547723
Height 100cm	15	14	14	15	14	14.4	0.547723
Height 150cm	15	16	16	16	16	15.8	0.447214
Height 200cm	16	16	16	16	16	16	0

Table A8.15: 1mm pipette drop results on Seal Grey Flamed.

Artic Grey Sawn and Tumbled Cobble

	Diameter (mm)	Diameter (mm)	Diameter (mm)	Diameter (mm)	Diameter (mm)	Average	SD
Height 50cm	13	14	14	13	13	13.4	0.547723
Height 100cm	14	14	14	15	15	14.4	0.547723
Height 150cm	15	15	15	15	14	14.8	0.447214
Height 200cm	15	16	16	16	16	15.8	0.447214

Table A8.16: 1mm pipette angle drop results on Artic Grey Sawn and Tumbled Cobble.

Artic Grey Flamed and Brushed

	Diameter (mm)	Diameter (mm)	Diameter (mm)	Diameter (mm)	Diameter (mm)	Average	SD
Height 50cm	13	13	13	13	13	13	0
Height 100cm	14	14	14	14	14	14	0
Height 150cm	14	14	15	15	15	14.6	0.547723
Height 200cm	15	15	15	15	16	15.2	0.447214

Table A8.17: 1mm pipette drop results on Artic Grey Flamed and Brushed.

Artic Grey Flamed Polished

	Diameter (mm)	Diameter (mm)	Diameter (mm)	Diameter (mm)	Diameter (mm)	Average	SD
Height 50cm	13	13	13	13	14	13.2	0.447214
Height 100cm	15	15	15	15	15	15	0
Height 150cm	17	17	17	17	17	17	0
Height 200cm	17	17	17	17	17	17	0

Table A8.18: 1mm pipette drop results on Artic Grey Flamed Polished.

Blood Drop Impact Measurement on Stones (1.77mm)

Rusty Slate Paving

	Diameter (mm)	Diameter (mm)	Diameter (mm)	Diameter (mm)	Diameter (mm)	Average	SD
Height 50cm	15	15	15	15	15	15	0
Height 100cm	16	17	17	17	17	16.8	0.447214
Height 150cm	20	20	19	20	19	19.6	0.547723
Height 200cm	20	20	20	20		20	0

Table A8.19: 1.77mm pipette drop results on Rusty Slate Paving.

Beige Marble Polished

	Diameter (mm)	Diameter (mm)	Diameter (mm)	Diameter (mm)	Diameter (mm)	Average	SD
Height 50cm	16	16	16	16	16	16	0
Height 100cm	17	18	18	18	18	17.8	0.447214
Height 150cm	22	21	22	21	21	21.4	0.547723
Height 200cm	22	22	22	22	22	22	0

Table A8.20: 1.77mm pipette drop results on Beige Marble Polished.

Classic Chipped Edge Filled and Honed

	Diameter (mm)	Diameter (mm)	Diameter (mm)	Diameter (mm)	Diameter (mm)	Average	SD
Height 50cm	15	15	15	15	15	15	0
Height 100cm	17	17	17	17	17	17	0
Height 150cm	20	20	21	21	20	20.4	0.547723
Height 200cm	21	21	21	22	21	21.2	0.447214

Table A8.21: 1.77mm pipette drop results on Classic Chipped Edge Filled and Honed.

Classic Travertine Filled and Honed

	Diameter (mm)	Diameter (mm)	Diameter (mm)	Diameter (mm)	Diameter (mm)	Average	SD
Height 50cm	15	15	15	15	15	15	0

	Diameter (mm)	Diameter (mm)	Diameter (mm)	Diameter (mm)	Diameter (mm)	Average	SD
Height 100cm	17	17	17	18	17	17.2	0.447214
Height 150cm	22	22	22	21	21	21.6	0.547723
Height 200cm	22	22	22	22	22	22	0

Table A8.22: 1.77mm pipette drop results on Classic Travertine Filled and Honed.

Classic Tumbled Unfilled Travertine

	Diameter (mm)	Diameter (mm)	Diameter (mm)	Diameter (mm)	Diameter (mm)	Average	SD
Height 50cm	15	14	15	15	14	14.6	0.547723
Height 100cm	16	16	16	16	16	16	0
Height 150cm	19	19	19	20	19	19.2	0.447214
Height 200cm	21	21	21	21	21	21	0

Table A8.23: 1.77mm pipette drop results on Classic Tumbled Unfilled Travertine.

Indian Sandstone Paving Raj Blend Tumbled

	Diameter (mm)	Diameter (mm)	Diameter (mm)	Diameter (mm)	Diameter (mm)	Average	SD
Height 50cm	15	15	15	16	15	15.2	0.447214
Height 100cm	16	16	16	16	16	16	0
Height 150cm	20	20	19	19	19	19.4	0.547723
Height 200cm	19	20	20	20	20	19.8	0.447214

Table A8.24: 1.77mm pipette drop results on Indian Sandstone Paving Raj Blend Tumbled.

Indian Sandstone Paving Raj Blend Economy

	Diameter (mm)	Diameter (mm)	Diameter (mm)	Diameter (mm)	Diameter (mm)	Average	SD
Height 50cm	14	14	14	14	14	14	0
Height 100cm	15	15	15	15	15	15	0
Height 150cm	19	20	19	20	19	19.4	0.547723
Height 200cm	21	20	20	21	20	20.4	0.547723

Table A8.25: 1.77mm pipette drop results on Indian Sandstone Paving Raj Blend Economy.

Indian Sandstone Paving Sahara Yellow

	Diameter (mm)	Diameter (mm)	Diameter (mm)	Diameter (mm)	Diameter (mm)	Average	SD
Height 50cm	14	14	15	15	15	14.6	0.547723
Height 100cm	16	16	16	16	16	16	0

	Diameter (mm)	Diameter (mm)	Diameter (mm)	Diameter (mm)	Diameter (mm)	Average	SD
Height 150cm	20	21	20	20	20	20.2	0.447214
Height 200cm	21	21	20	20	21	20.6	0.547723

Table A8.26: 1.77mm pipette drop results on Indian Sandstone Paving Sahara Yellow.

Indian Sandstone Paving Rippon Buff

	Diameter (mm)	Diameter (mm)	Diameter (mm)	Diameter (mm)	Diameter (mm)	Average	SD
Height 50cm	14	14	14	14	14	14	0
Height 100cm	15	15	15	15	15	15	0
Height 150cm	15	15	15	16	16	15.4	0.547723
Height 200cm	17	18	18	18	19	18	0.707107

Table A8.27: 1.77mm pipette drop results on Indian Sandstone Paving Rippon Buff.

Indian Sandstone Paving Modak

	Diameter (mm)	Diameter (mm)	Diameter (mm)	Diameter (mm)	Diameter (mm)	Average	SD
Height 50cm	14	15	15	15	15	14.8	0.447214
Height 100cm	17	17	17	18	17	17.2	0.447214
Height 150cm	19	19	19	19	20	19.2	0.447214
Height 200cm	21	21	22	22	21	21.4	0.547723

Table A8.28: 1.77mm pipette drop results on Indian Sandstone Paving Modak.

Classic Honed Travertine Paving

	Diameter (mm)	Diameter (mm)	Diameter (mm)	Diameter (mm)	Diameter (mm)	Average	SD
Height 50cm	15	15	15	15	15	15	0
Height 100cm	16	16	16	16	17	16.2	0.447214
Height 150cm	19	20	20	20	19	19.6	0.547723
Height 200cm	20	22	22	22	22	21.6	0.894427

Table A8.29: 1.77mm pipette drop results on Classic Honed Travertine Paving.

Silver Latte Tumbled Travertine Paving

	Diameter (mm)	Diameter (mm)	Diameter (mm)	Diameter (mm)	Diameter (mm)	Average	SD
Height 50cm	15	15	15	15	15	15	0
Height 100cm	16	16	16	16	16	16	0

Height 150cm	20	21	21	21	21	20.8	0.447214
Height 200cm	20	21	21	21	21	20.8	0.447214

Table A8.30: 1.77mm pipette drop results on Silver Latte Tumbled Travertine Paving.

Yellow Limestone Paving

	Diameter (mm)	Diameter (mm)	Diameter (mm)	Diameter (mm)	Diameter (mm)	Average	SD
Height 50cm	15	15	15	15	15	15	0
Height 100cm	15	16	15	15	16	15.4	0.547723
Height 150cm	16	16	16	17	16	16.2	0.447214
Height 200cm	17	18	17	18	18	17.6	0.547723

Table A8.31: 1.77mm pipette drop results on Yellow Limestone Paving.

Brazilian Black Slate Paving

	Diameter (mm)	Diameter (mm)	Diameter (mm)	Diameter (mm)	Diameter (mm)	Average	SD
Height 50cm	15	15	15	15	15	15	0
Height 100cm	16	16	16	16	16	16	0
Height 150cm	20	20	20	20	20	20	0
Height 200cm	20	20	20	21	21	20.4	0.547723

Table A8.32: 1.77mm pipette drop results on Brazilian Black Slate Paving.

Classic Travertine Filled and Honed

	Diameter (mm)	Diameter (mm)	Diameter (mm)	Diameter (mm)	Diameter (mm)	Average	SD
Height 50cm	15	15	15	15	13	14.6	0.894427
Height 100cm	17	17	16	17	16	16.6	0.547723
Height 150cm	22	22	22	21	21	21.6	0.547723
Height 200cm	21	22	22	22	22	21.8	0.447214

Table A8.33: 1.77mm pipette drop results on Classic Travertine Filled and Honed.

Seal Grey Flamed

	Diameter (mm)	Diameter (mm)	Diameter (mm)	Diameter (mm)	Diameter (mm)	Average	SD
Height 50cm	15	15	15	15	16	15.2	0.447214

Height 100cm	15	15	16	16	16	15.6	0.547723
Height 150cm	16	16	16	15	15	15.6	0.547723
Height 200cm	16	16	16	16	16	16	0

Table A8.34: 1.77mm pipette drop results on Seal Grey Flamed.

Artic Grey Sawn and Tumbled Cobble

	Diameter (mm)	Diameter (mm)	Diameter (mm)	Diameter (mm)	Diameter (mm)	Average	SD
Height 50cm	14	15	15	15	15	14.8	0.447214
Height 100cm	15	16	16	16	16	15.8	0.447214
Height 150cm	16	16	16	16	16	16	0
Height 200cm	17	17	16	17	17	16.8	0.447214

Table A8.35: 1.77mm pipette drop results on Artic Grey Sawn and Tumbled Cobble.

Artic Grey Flamed and Brushed

	Diameter (mm)	Diameter (mm)	Diameter (mm)	Diameter (mm)	Diameter (mm)	Average	SD
Height 50cm	15	15	15	15	14	14.8	0.447214
Height 100cm	16	16	16	16	16	16	0
Height 150cm	16	17	16	16	17	16.4	0.547723
Height 200cm	18	18	18	17	17	17.6	0.547723

Table A8.36: 1.77mm pipette drop results on Artic Grey Flamed and Brushed.

Artic Grey Flamed Polished

	Diameter (mm)	Diameter (mm)	Diameter (mm)	Diameter (mm)	Diameter (mm)	Average	SD
Height 50cm	17	17	17	17	17	17	0
Height 100cm	18	18	18	18	18	18	0
Height 150cm	18	18	18	18	18	18	0

Height 200cm	20	20	20	19	19	19.6	0.547723

Table A8.37: 1.77mm pipette drop results on Artic Grey Flamed Polished.

Appendix 9 - Bloodstains on a Heated Surfaces

Stone Surfaces

Rusty Slate Paving

	Diameter (mm)	Diameter (mm)	Diameter (mm)	Diameter (mm)	Diameter (mm)	Average	SD
25	12	12	12	12	12	12	0
30	12	12	12	12	12	12	0

40	12	12	12	12	12	12	0

Table 9.1: Bloodstain diameters exhibited using a 1mm pipette on Rusty Slate Paving

Beige Marble Polished

	Diameter (mm)	Diameter (mm)	Diameter (mm)	Diameter (mm)	Diameter (mm)	Average	SD
25	13	13	13	13	13	13	0
30	13	13	13	13	13	13	0
40	13	13	13	13	13	13	0

Table 9.2: Bloodstain diameters exhibited using a 1mm pipette on Beige Marble Polished

Classic Chipped Edge Filled and Honed

	Diameter (mm)	Diameter (mm)	Diameter (mm)	Diameter (mm)	Diameter (mm)	Average	SD
25	12	13	12	13	12	12.4	0.547723
30	12	12	12	12	12	12	0
40	12	12	12	12	12	12	0

Table 9.3: Bloodstain diameters exhibited using a 1mm pipette on Classic Chipped Edge Filled and Honed

Classic Travertine Filled and Honed

	Diameter (mm)	Diameter (mm)	Diameter (mm)	Diameter (mm)	Diameter (mm)	Average	SD
25	13	13	13	13	13	13	0
30	12	13	13	13	13	12.8	0.447214
40	12	12	12	12	12	12	0

Table 9.4: Bloodstain diameters exhibited using a 1mm pipette on Classic Travertine Filled and Honed

Indian Sandstone Paving Raj Blend Tumbled

	Diameter (mm)	Diameter (mm)	Diameter (mm)	Diameter (mm)	Diameter (mm)	Average	SD
25	11.5	11.5	12	12	12	11.8	0.273861
30	11	12	12	12	12	11.8	0.447214
40	12	12	13	13	12	12.4	0.547723

Table 9.5: Bloodstain diameters exhibited using a 1mm pipette on Indian Sandstone Paving Raj Blend Tumbled

Indian Sandstone Paving Raj Blend Economy

	Diameter (mm)	Diameter (mm)	Diameter (mm)	Diameter (mm)	Diameter (mm)	Average	SD
25	11	11	12	12	12	11.6	0.547723

	Diameter (mm)	Diameter (mm)	Diameter (mm)	Diameter (mm)	Diameter (mm)	Average	SD
30	13	13	12	12	12	12.4	0.547723
40	12	12	12	12	12	12	0

Table 9.6: Bloodstain diameters exhibited using a 1mm pipette on Indian Sandstone Paving Raj Blend Economy

Indian Sandstone Paving Sahara Yellow

	Diameter (mm)	Diameter (mm)	Diameter (mm)	Diameter (mm)	Diameter (mm)	Average	SD
25	12	12	12	12	12	12	0
30	12	12	12	12	12	12	0
40	12	11	11.5	12	12	11.7	0.447214

Table 9.7: Bloodstain diameters exhibited using a 1mm pipette on Indian Sandstone Paving Sahara Yellow

Indian Sandstone Paving Rippon Buff

	Diameter (mm)	Diameter (mm)	Diameter (mm)	Diameter (mm)	Diameter (mm)	Average	SD
25	11.5	11	11	11.5	11.5	11.3	0.273861
30	12	12	12	12	12	12	0
40	13	12	12	12	12	12.2	0.447214

Table 9.8: Bloodstain diameters exhibited using a 1mm pipette on Indian Sandstone Paving Rippon Buff

Indian Sandstone Paving Modak

	Diameter (mm)	Diameter (mm)	Diameter (mm)	Diameter (mm)	Diameter (mm)	Average	SD
25	12	12	12	12	12	12	0
30	12	12	12	12	12	12	0
40	13	13	12	12	12	12.4	0.547723

Table 9.9: Bloodstain diameters exhibited using a 1mm pipette on Indian Sandstone Paving Modak

Classic Honed Travertine Paving

	Diameter (mm)	Diameter (mm)	Diameter (mm)	Diameter (mm)	Diameter (mm)	Average	SD
25	12	12	12	12	12	12	0
30	13	12	12	12	12	12.2	0.447214
40	13	12	12	12	12	12.2	0.447214

Table 9.10: Bloodstain diameters exhibited using a 1mm pipette on Classic Honed Travertine Paving

Silver Latte Tumbled Travertine Paving

	Diameter (mm)	Diameter (mm)	Diameter (mm)	Diameter (mm)	Diameter (mm)	Average	SD
25	12	12	12	12	12	12	0
30	12.5	12.5	12	12	12	12.2	0.273861
40	12	11	11	12	12	11.6	0.547723

Table 9.11: Bloodstain diameters exhibited using a 1mm pipette on Silver Latte Tumbled Travertine Paving

Yellow Limestone Paving

	Diameter (mm)	Diameter (mm)	Diameter (mm)	Diameter (mm)	Diameter (mm)	Average	SD
25	12	11	11	11	11	11.2	0.447214
30	11	12	11	11	11	11.2	0.447214
40	11	12	11	11	11	11.2	0.447214

Table 9.12: Bloodstain diameters exhibited using a 1mm pipette on Yellow Limestone Paving

Brazilian Black Slate Paving

	Diameter (mm)	Diameter (mm)	Diameter (mm)	Diameter (mm)	Diameter (mm)	Average	SD
25	12	12	13	13	12	12.4	0.547723
30	12	12	12	12	12	12	0
40	12	12	12	12	12	12	0

Table 9.13: Bloodstain diameters exhibited using a 1mm pipette on Brazilian Black Slate Paving

Beige Marble Polished

	Diameter (mm)	Diameter (mm)	Diameter (mm)	Diameter (mm)	Diameter (mm)	Average	SD
25	13	13	13	13	13	13	0
30	13	13	13	13	13	13	0
40	13	13	13	13	13	13	0

Table 9.14: Bloodstain diameters exhibited using a 1mm pipette on Beige Marble Polished

Blood on a Heated Tile Surface (1 mm pipette)

Sandstone Rivon

	Diameter (mm)	Diameter (mm)	Diameter (mm)	Diameter (mm)	Diameter (mm)	Average	SD
25	14	14	14	13.5	13.5	13.8	0.273861
30	14.5	14.5	14.5	14.5	14.5	14.5	0
40	14	14	14.5	13.5	14	14	0.353553

Table 9.15: Bloodstain diameters exhibited using a 1mm pipette on Sandstone Rivon

Super White Matt

	Diameter (mm)	Diameter (mm)	Diameter (mm)	Diameter (mm)	Diameter (mm)	Average	SD
25	12	13	12.5	13	13	12.7	0.447214
30	13	13	13	13	13	13	0
40	13.5	13.5	13.5	13.5	13.5	13.5	0

Table 9.16: Bloodstain diameters exhibited using a 1mm pipette on Super White Matt

Ceramic Matt

	Diameter (mm)	Diameter (mm)	Diameter (mm)	Diameter (mm)	Diameter (mm)	Average	SD
25	14	14.5	14	14	15	14.3	0.447214
30	15	15	15.5	15	15	15.1	0.223607
40	15.5	15	16	16	15.5	15.6	0.41833

Table 9.17: Bloodstain diameters exhibited using a 1mm pipette on Ceramic Matt

Ceramic Polished

	Diameter (mm)	Diameter (mm)	Diameter (mm)	Diameter (mm)	Diameter (mm)	Average	SD
25	14	14	14	14	14	14	0
30	13.5	13.5	13.5	13.5	13.5	13.5	0
40	13	13	13	13	13	13	0

Table 9.18: Bloodstain diameters exhibited using a 1mm pipette on Ceramic Polished

Blood on a Wood Surface (1mm pipette)

Oak

European Maple Oak

	1mm Mean	1mm SD	1.7mm Mean	1.7mm SD
50 cm	13.2	0.447214	16	0
100 cm	14	0	17.2	0.447214
150 cm	16	0	18.8	0.83666
200 cm	16.4	0.547723	19.2	0.447214

Table 9.19: Bloodstain diameters exhibited using a 1mm pipette on European Maple Oak

Clear Oil Oak

	1mm Mean	1mm SD	1.7mm Mean	1.7mm SD
50 cm	13	0	15.2	0.447214
100 cm	14.2	0.447214	16.2	0.447214
150 cm	15.4	0.547723	17.6	0.547723
200 cm	16.8	0.447214	18.2	0.447214

Table 9.20: Bloodstain diameters exhibited using a 1mm pipette on Clear Oil Oak

Oak Natural Siera Matt Lacquered

	1mm Mean	1mm SD	1.7mm Mean	1.7mm SD
50 cm	13	0.447214	15.6	0.489898

	1mm Mean	1mm SD	1.7mm Mean	1.7mm SD
100 cm	14.2	0	17.4	0.489898
150 cm	15.4	0.447214	18.6	0.489898
200 cm	16.8	0.447214	19.2	0.4

Table 9.21: Bloodstain diameters exhibited using a 1mm pipette on Oak Natural Siera Matt Lacquered

Oak Silk Matt

	1mm Mean	1mm SD	1.7mm Mean	1.7mm SD
50 cm	14	0	16.2	0.447214
100 cm	15	0	17.6	0.547723
150 cm	16	0.707107	19.2	0.447214
200 cm	17	0	19.4	0.547723

Table 9.22: Bloodstain diameters exhibited using a 1mm pipette on Oak Silk Matt

Kahrs Oak Sienna Natural

	1mm Mean	1mm SD	1.7mm Mean	1.7mm SD
50 cm	13.2	0.447214	15	0
100 cm	15.4	0.547723	17.4	0.547723
150 cm	16	0	18.6	0.547723
200 cm	17.2	0.447214	19.2	0.447214

Table 9.23: Bloodstain diameters exhibited using a 1mm pipette on Kahrs Oak Sienna Natural

Natura Oak Prime Parquet

	1mm Mean	1mm SD	1.7mm Mean	1.7mm SD
50 cm	10.8	0.447214	14.6	0.547723
100 cm	13	0.547723	15.8	0.447214
150 cm	13.4	0	16.6	0.547723
200 cm	13.8	0.447214	17	0

Table 9.24: Bloodstain diameters exhibited using a 1mm pipette on Natura Oak Prime Parquet

Kahrs Oak Siena Engineered Natural

	1mm Mean	1mm SD	1.7mm Mean	1.7mm SD
50 cm	12.8	0.447214	14	0
100 cm	13	0	16.2	0.447214
150 cm	13.2	0.447214	16.8	0.447214
200 cm	14	0	17	0

Table 9.25: Bloodstain diameters exhibited using a 1mm pipette on Kahrs Oak Siena Engineered Natural

Oak Solid Plank Untreated

	1mm Mean	1mm SD	1.7mm Mean	1.7mm SD
50 cm	9.4	0.547723	14.4	0.547723
100 cm	13.2	0.447214	15.6	0.547723

150 cm	14	0	16	0.707107
200 cm	14	0	18.8	0.447214

Table 9.26: Bloodstain diameters exhibited using a 1mm pipette on Oak Solid Plank Untreated

Maple

Maple Silk Matt Lacquered

	1mm Mean	**1mm SD**	**1.7mm Mean**	**1.7mm SD**
50 cm	13.2	0.447214	15.8	0.447214
100 cm	15	0	17.2	0.447214
150 cm	15.8	0.447214	19	0
200 cm	18	0	19.2	0.447214

Table 9.27: Bloodstain diameters exhibited using a 1mm pipette on Maple Silk Matt Lacquered

Kahrs Maple Toronto Satin Lacquer

	1mm Mean	**1mm SD**	**1.7mm Mean**	**1.7mm SD**
50 cm	12.4	0.547723	16	0
100 cm	14	53.66563	17.4	0.547723
150 cm	15.6	0.547723	18.4	0.547723
200 cm	16.6	0.547723	19.4	0.547723

Table 9.28: Bloodstain diameters exhibited using a 1mm pipette on Kahrs Maple Toronto Satin Lacquer

Maple Ultra Matt Lacquered

	1mm Mean	**1mm SD**	**1.7mm Mean**	**1.7mm SD**
50 cm	13.4	0.547723	15	0
100 cm	15	0	17	0
150 cm	16	0	18.8	0.447214
200 cm	16.8	0.447214		0.547723

Table 9.29: Bloodstain diameters exhibited using a 1mm pipette on Maple Ultra Matt Lacquered

Kahrs Maple Bevelled Edge Rustic

	1mm Mean	**1mm SD**	**1.7mm Mean**	**1.7mm SD**
50 cm	14	0	16.2	0.447214
100 cm	15	0	18.2	0.83666
150 cm	16	0	19	0
200 cm	17	0	19.6	0.547723

Table 9.30: Bloodstain diameters exhibited using a 1mm pipette on Kahrs Maple Bevelled Edge Rustic

Kahrs Maple Natural Satin Lacquer

	1mm Mean	**1mm SD**	**1.7mm Mean**	**1.7mm SD**
50 cm	13.4	0.547723	16	0
100 cm	15	0	17.6	0.547723
150 cm	15.6	0.547723	19	0.707107
200 cm	16.8	0.447214	19.2	0.83666

Table 9.31: Bloodstain diameters exhibited using a 1mm pipette on Kahrs Maple Natural Satin Lacquer

Walnut

Natura American Black Walnut Rosshill

	1mm Mean	1mm SD	1.7mm Mean	1.7mm SD
50 cm	13.4	0.547723	16.8	0.447214
100 cm	14	0	17.4	0.547723
150 cm	16	0	18.2	0.447214
200 cm	17	0	19.2	0.447214

Table 9.32: Bloodstain diameters exhibited using a 1mm pipette on Natura American Black Walnut Rosshill

Natura Walnut Ironbank Mississippi

	1mm Mean	1mm SD	1.7mm Mean	1.7mm SD
50 cm	13	0	15.4	0.547723
100 cm	14.8	0.447214	17.2	0.447214
150 cm	15.6	0.894427	18.8	0.447214
200 cm	16.6	0.547723	19.4	0.547723

Table 9.33: Bloodstain diameters exhibited using a 1mm pipette on Natura Walnut Ironbank Mississippi

Quickstep Villa Walnut Satin Lacquer

	1mm Mean	1mm SD	1.7mm Mean	1.7mm SD
50 cm	13.8	0.447214	16.4	0.547723
100 cm	14.4	0.547723	17.6	0.547723
150 cm	16	0	18.8	0.447214
200 cm	17	0.707107	19.2	0.447214

Table 9.34: Bloodstain diameters exhibited using a 1mm pipette on Quickstep Villa Walnut Satin Lacquer

Kahrs Walnut Rustic Nature Oil

	1mm Mean	1mm SD	1.7mm Mean	1.7mm SD
50 cm	12.4	0.547723	15.4	0.547723
100 cm	14	0	17.4	0.547723
150 cm	15.6	0.547723	18.4	0.547723
200 cm	16.6	0.547723	20	0.707107

Table 9.35: Bloodstain diameters exhibited using a 1mm pipette on Kahrs Walnut Rustic Nature Oil

Kahrs Linnea Walnut Bloom Prime Satin Lacquer

	1mm Mean	1mm SD	1.7mm Mean	1.7mm SD
50 cm	13.6	0.547723	15.6	0.547723
100 cm	15.4	0.547723	17	0
150 cm	16.6	0.547723	19	0.707107
200 cm	17	0	19.4	0.547723

Table 9.36: Bloodstain diameters exhibited using a 1mm pipette on Kahrs Linnea Walnut Bloom Prime Satin Lacquer

Kahrs Linnea Walnut Microbevelled Edge Prime Matt Lacquer

	1mm Mean	1mm SD	1.7mm Mean	1.7mm SD
50 cm	13.4	0.547723	15	0
100 cm	15	0	17.6	0.547723
150 cm	15.6	0.547723	18.2	0.447214
200 cm	17.2	0.447214	18.8	0.447214

Table 9.37: Bloodstain diameters exhibited using a 1mm pipette on Kahrs Linnea Walnut Microbevelled Edge Prime Matt Lacquer

Natura Walnut Lacquered Satin Lacquer

	1mm Mean	1mm SD	1.7mm Mean	1.7mm SD
50 cm	13	0	15.8	0.447214
100 cm	15	0	18	0
150 cm	15.8	0.447214	18.6	0.547723
200 cm	17	0	19.2	0.447214

Table 9.38: Bloodstain diameters exhibited using a 1mm pipette on Natura Walnut Lacquered Satin Lacquer

Appendix 10 – DNA Profiles for Cleaned Surfaces

Beth

GeneMapper ID v3.2

Sample Name	Panel	SQ
N	NGMSElect_panel_v2	

D10S1248 vWA D16S539 D2S1338

D8S1179 D21S11 D18S51

D22S... D19S... TH01 FGA

D2S... D3S1358 D1S1656 D12S391 SE33

60.0 100.0 140.0 180.0 220.0 280.0 340.0 400.0 460.0 514.0
80.0 120.0 160.0 200.0 250.0 300.0 360.0 414.0 480.0
114.0 214.0 260.0 314.0 380.0 440.0 500.0
240.0 320.0 420.0 520.0
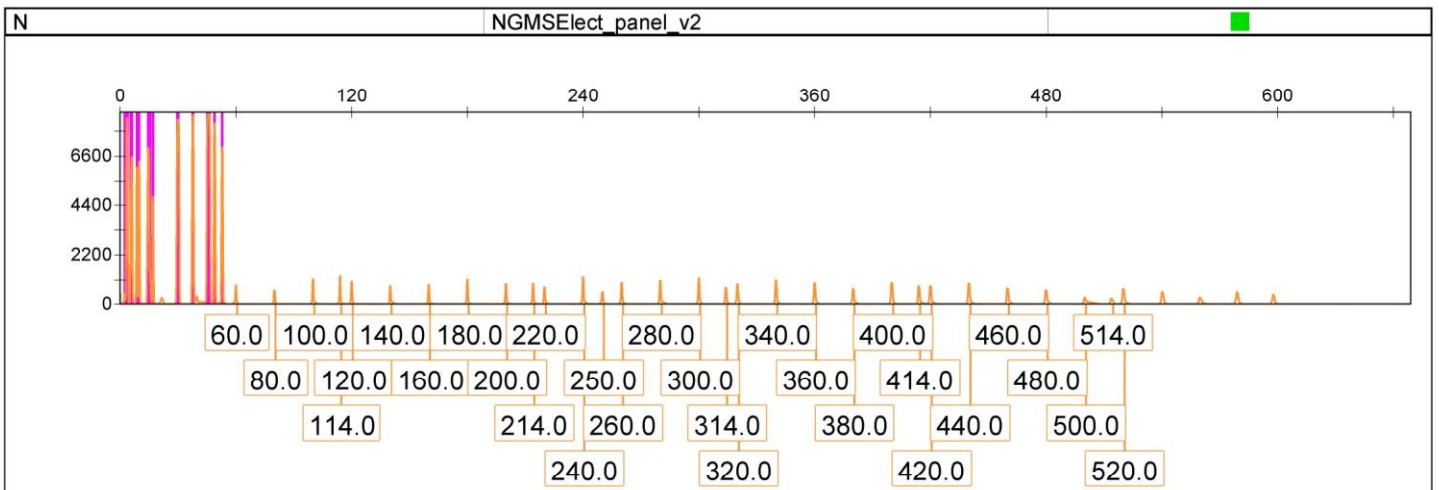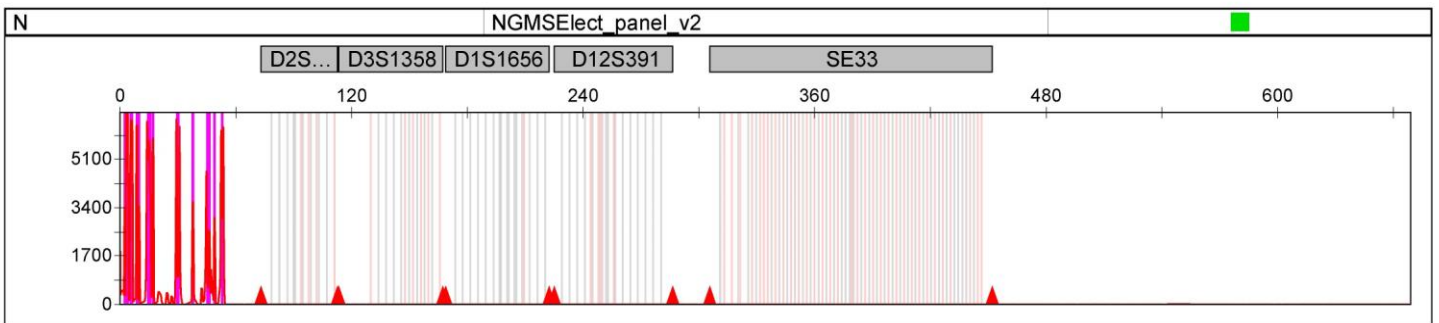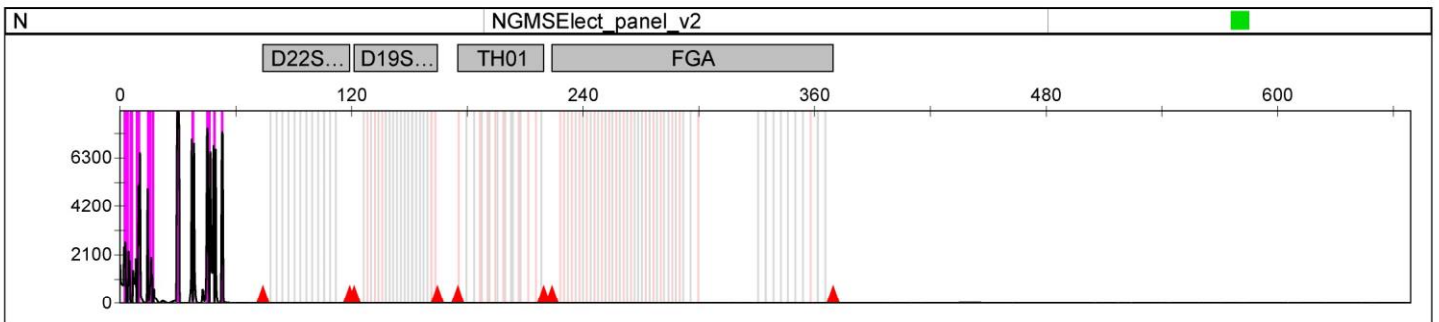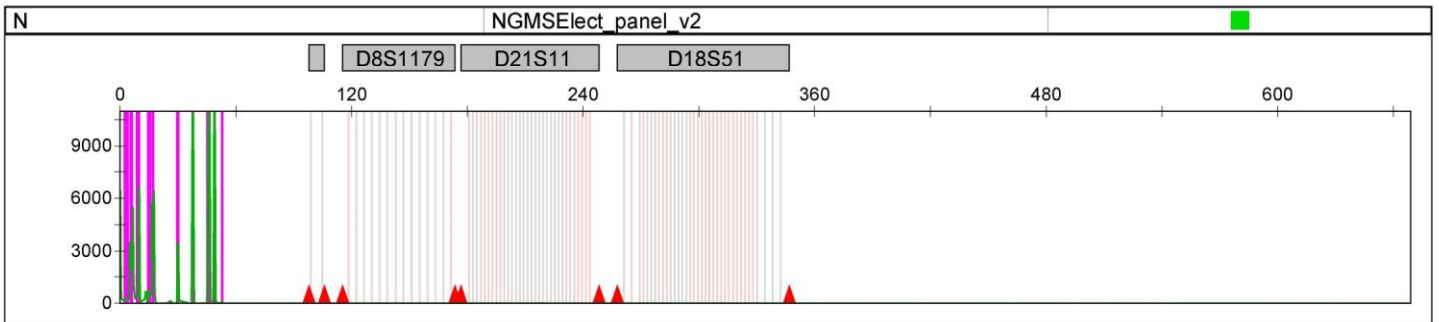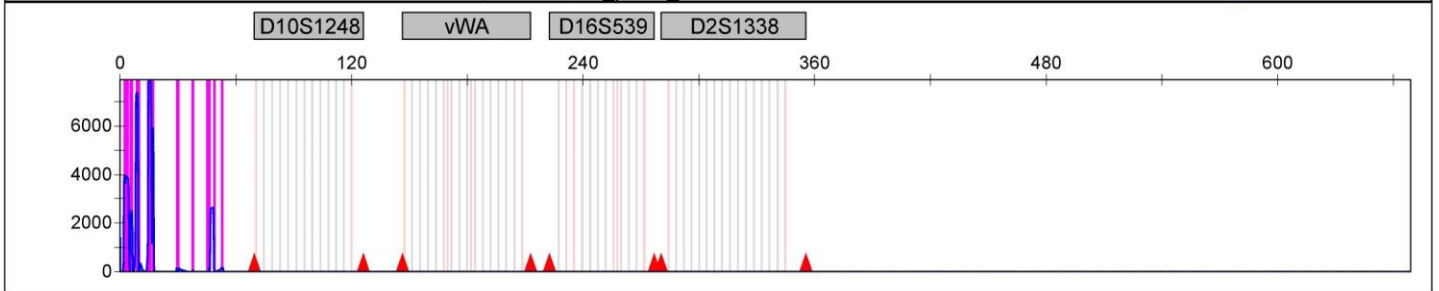
		Dye/Sample Peak	Sample File Name	Marker	Allele	Size	Height	Area	Data Point
1	■	B,1	A11_N.fsa				98	1255	1107
2	■	B,2	A11_N.fsa				88	1129	1143
3	■	B,3	A11_N.fsa				71	686	1174
4	■	B,4	A11_N.fsa				82	856	1211
5	■	B,5	A11_N.fsa				104	875	1295
6	■	B,6	A11_N.fsa				258	3408	1319
7	■	B,7	A11_N.fsa				160	2258	1350
8	■	B,8	A11_N.fsa				71	588	1366
9	■	B,9	A11_N.fsa				291	3567	1418
10	■	B,10	A11_N.fsa				197	1961	1434
11	■	B,11	A11_N.fsa				153	1249	1453
12	■	B,12	A11_N.fsa				253	2989	1464
13	■	B,13	A11_N.fsa				189	1662	1482
14	■	B,14	A11_N.fsa				111	747	1513
15	■	B,15	A11_N.fsa				4547	54399	1550
16	■	B,16	A11_N.fsa			2.48	4053	52633	1586
17	■	B,17	A11_N.fsa			5.97	2529	36334	1631
18	■	B,18	A11_N.fsa			10.47	443	4662	1689
19	■	B,19	A11_N.fsa			14.96	7905	101489	1747
20	■	B,20	A11_N.fsa			15.89	7935	100051	1759
21	■	B,21	A11_N.fsa			17.05	5957	58181	1774
22	■	B,22	A11_N.fsa			29.3	213	807	1932
23	■	B,23	A11_N.fsa			30.7	227	840	1950
24	■	B,24	A11_N.fsa			32.4	55	1482	1972
25	■	B,25	A11_N.fsa			37.75	148	539	2041
26	■	B,26	A11_N.fsa			44.88	111	452	2133
27	■	B,27	A11_N.fsa			47.75	2670	34250	2170
28	■	B,28	A11_N.fsa			52.64	231	1350	2233
29	■	B,29	A11_N.fsa			53.33	237	1212	2242
30	■	G,1	A11_N.fsa				63	954	1113
31	■	G,2	A11_N.fsa				50	1465	1163
32	■	G,3	A11_N.fsa				202	2238	1212
33	■	G,4	A11_N.fsa				167	1675	1307
34	■	G,5	A11_N.fsa				159	1928	1323
35	■	G,6	A11_N.fsa				555	6097	1380
36	■	G,7	A11_N.fsa				167	3987	1421
37	■	G,8	A11_N.fsa				55	607	1458
38	■	G,9	A11_N.fsa				2174	23489	1492
39	■	G,10	A11_N.fsa				5083	41370	1546
40	■	G,11	A11_N.fsa			0.08	6442	55046	1555

41	🟩	G,12	A11_N.fsa			1.16	356	3647	1569
42	🟩	G,13	A11_N.fsa			2.02	148	830	1580
43	🟩	G,14	A11_N.fsa			2.71	354	2445	1589
44	🟩	G,15	A11_N.fsa			5.19	3559	41940	1621
45	🟩	G,16	A11_N.fsa			6.67	5521	49817	1640
46	🟩	G,17	A11_N.fsa			8.45	380	3540	1663
47	🟩	G,18	A11_N.fsa			9.92	6652	53266	1682

		Dye/Sample Peak	Sample File Name	Marker	Allele	Size	Height	Area	Data Point
48	🟩	G,19	A11_N.fsa			13.33	790	11611	1726
49	🟩	G,20	A11_N.fsa			14.65	728	4086	1743
50	🟩	G,21	A11_N.fsa			15.27	373	3960	1751
51	🟩	G,22	A11_N.fsa			16.59	5749	40718	1768
52	🟩	G,23	A11_N.fsa			17.52	6451	49552	1780
53	🟩	G,24	A11_N.fsa			26.36	260	3361	1894
54	🟩	G,25	A11_N.fsa			30.0	3502	32569	1941
55	🟩	G,26	A11_N.fsa			31.01	58	465	1954
56	🟩	G,27	A11_N.fsa			37.67	10853	129119	2040
57	🟩	G,28	A11_N.fsa			46.05	10960	160811	2148
58	🟩	G,29	A11_N.fsa			47.44	84	1046	2166
59	🟩	G,30	A11_N.fsa			48.91	10965	115684	2185
60	🟩	G,31	A11_N.fsa			50.16	141	1553	2201
61	🟩	G,32	A11_N.fsa			52.95	268	1125	2237
62	🟨	Y,1	A11_N.fsa				88	973	1493
63	🟨	Y,2	A11_N.fsa				1048	3362	1544
64	🟨	Y,3	A11_N.fsa			0.16	1692	11548	1556
65	🟨	Y,4	A11_N.fsa			2.02	2452	18856	1580
66	🟨	Y,5	A11_N.fsa			2.79	2647	20353	1590
67	🟨	Y,6	A11_N.fsa			4.42	2269	12528	1611
68	🟨	Y,7	A11_N.fsa			5.04	1845	9311	1619
69	🟨	Y,8	A11_N.fsa			6.74	1441	10493	1641
70	🟨	Y,9	A11_N.fsa			8.14	1954	11765	1659
71	🟨	Y,10	A11_N.fsa			9.46	5116	36483	1676
72	🟨	Y,11	A11_N.fsa			10.31	6549	45428	1687
73	🟨	Y,12	A11_N.fsa			14.26	5001	32043	1738
74	🟨	Y,13	A11_N.fsa			16.05	2020	21480	1761
75	🟨	Y,14	A11_N.fsa			17.6	655	3336	1781
76	🟨	Y,15	A11_N.fsa			18.45	209	3551	1792
77	🟨	Y,16	A11_N.fsa			22.4	166	1790	1843
78	🟨	Y,17	A11_N.fsa			26.67	55	679	1898
79	🟨	Y,18	A11_N.fsa			27.75	102	845	1912
80	🟨	Y,19	A11_N.fsa			28.6	171	1515	1923
81	🟨	Y,20	A11_N.fsa			29.69	8291	89317	1937
82	🟨	Y,21	A11_N.fsa			30.31	8318	83579	1945
83	🟨	Y,22	A11_N.fsa			37.13	7133	45431	2033
84	🟨	Y,23	A11_N.fsa			38.29	6947	45053	2048
85	🟨	Y,24	A11_N.fsa			42.87	692	6609	2107
86	🟨	Y,25	A11_N.fsa			45.27	7582	95821	2138
87	🟨	Y,26	A11_N.fsa			46.82	6589	51036	2158

88	🟨	Y,27	A11_N.fsa			48.37	6857	45836	2178
89	🟨	Y,28	A11_N.fsa			49.46	6690	41717	2192
90	🟨	Y,29	A11_N.fsa			52.95	7452	86360	2237
91	🟨	Y,30	A11_N.fsa			54.26	91	1261	2254
92	🟥	R,1	A11_N.fsa				5553	45775	1550
93	🟥	R,2	A11_N.fsa			2.33	3429	21618	1584
94	🟥	R,3	A11_N.fsa			3.33	6756	62829	1597

		Dye/Sample Peak	Sample File Name	Marker	Allele	Size	Height	Area	Data Point
95	■	R,4	A11_N.fsa			3.88	6749	63436	1604
96	■	R,5	A11_N.fsa			6.12	6554	66356	1633
97	■	R,6	A11_N.fsa			8.68	6379	70533	1666
98	■	R,7	A11_N.fsa			9.84	3460	28651	1681
99	■	R,8	A11_N.fsa			14.03	6465	71190	1735
100	■	R,9	A11_N.fsa			14.73	5787	100739	1744
101	■	R,10	A11_N.fsa			17.05	5893	57096	1774
102	■	R,11	A11_N.fsa			20.16	506	10956	1814
103	■	R,12	A11_N.fsa			24.42	448	5759	1869
104	■	R,13	A11_N.fsa			26.82	369	3414	1900
105	■	R,14	A11_N.fsa			29.15	6544	58606	1930
106	■	R,15	A11_N.fsa			30.85	6287	51875	1952
107	■	R,16	A11_N.fsa			35.97	77	781	2018
108	■	R,17	A11_N.fsa			37.75	3657	41834	2041
109	■	R,18	A11_N.fsa			42.33	647	6205	2100
110	■	R,19	A11_N.fsa			44.73	4703	48107	2131
111	■	R,20	A11_N.fsa			46.2	2648	30577	2150
112	■	R,21	A11_N.fsa			47.13	1230	12411	2162
113	■	R,22	A11_N.fsa			48.91	3067	30280	2185
114	■	R,23	A11_N.fsa			52.4	6149	65004	2230
115	■	R,24	A11_N.fsa			53.49	6275	55437	2244
116	■	R,25	A11_N.fsa			57.83	68	600	2300
117	■	O,1	A11_N.fsa				1596	11331	1550
118	■	O,2	A11_N.fsa			2.33	499	3301	1584
119	■	O,3	A11_N.fsa			3.64	8378	104010	1601
120	■	O,4	A11_N.fsa			5.97	6567	74135	1631
121	■	O,5	A11_N.fsa			8.68	6132	45910	1666
122	■	O,6	A11_N.fsa			9.92	6415	48016	1682
123	■	O,7	A11_N.fsa			14.73	7052	106985	1744
124	■	O,8	A11_N.fsa			17.05	4808	34142	1774
125	■	O,9	A11_N.fsa			21.78	357	4955	1835
126	■	O,10	A11_N.fsa			37.75	8460	102076	2041
127	■	O,11	A11_N.fsa			39.84	449	4553	2068
128	■	O,12	A11_N.fsa			46.12	8541	201002	2149
129	■	O,13	A11_N.fsa			48.91	8073	91652	2185
130	■	O,14	A11_N.fsa			52.95	7056	77390	2237
131	■	O,15 *	A11_N.fsa			60.0	883	7800	2328
132	■	O,16 *	A11_N.fsa			80.0	707	5994	2586
133	■	O,17 *	A11_N.fsa			100.0	1189	9889	2840
134	■	O,18 *	A11_N.fsa			114.0	1331	10995	3014

135	🟧	O,19	*	A11_N.fsa			120.0	1104	9158	3091
136	🟧	O,20	*	A11_N.fsa			140.0	869	7149	3342
137	🟧	O,21	*	A11_N.fsa			160.0	939	7878	3583
138	🟧	O,22	*	A11_N.fsa			180.0	1184	9958	3825
139	🟧	O,23	*	A11_N.fsa			200.0	992	8513	4063
140	🟧	O,24	*	A11_N.fsa			214.0	998	8605	4232
141	🟧	O,25	*	A11_N.fsa			220.0	834	7379	4303

		Dye/Sample Peak	Sample File Name	Marker	Allele	Size	Height	Area	Data Point
142		O,26 *	A11_N.fsa			240.0	1287	11600	4541
143		O,27 *	A11_N.fsa			250.0	608	5651	4657
144		O,28 *	A11_N.fsa			260.0	1031	9523	4778
145		O,29 *	A11_N.fsa			280.0	1155	10958	5015
146		O,30 *	A11_N.fsa			300.0	1233	11898	5254
147		O,31 *	A11_N.fsa			314.0	852	8416	5421
148		O,32 *	A11_N.fsa			320.0	943	9489	5488
149		O,33 *	A11_N.fsa			340.0	1175	12231	5722
150		O,34 *	A11_N.fsa			360.0	1025	10870	5954
151		O,35 *	A11_N.fsa			380.0	709	7729	6187
152		O,36 *	A11_N.fsa			400.0	1063	11915	6416
153		O,37 *	A11_N.fsa			414.0	907	10322	6578
154		O,38 *	A11_N.fsa			420.0	900	10451	6645
155		O,39 *	A11_N.fsa			440.0	989	11879	6873
156		O,40 *	A11_N.fsa			460.0	814	9873	7094
157		O,41 *	A11_N.fsa			480.0	744	9293	7317
158		O,42 *	A11_N.fsa			500.0	330	4184	7532
159		O,43 *	A11_N.fsa			514.0	370	4757	7682
160		O,44 *	A11_N.fsa			520.0	766	9955	7746
161		O,45	A11_N.fsa			540.25	599	8044	7962
162		O,46	A11_N.fsa			559.84	411	5696	8171
163		O,47	A11_N.fsa			578.97	596	8344	8375
164		O,48	A11_N.fsa			597.81	445	6353	8576

Applied Biosystems

19.04.13BethsBloodStudy
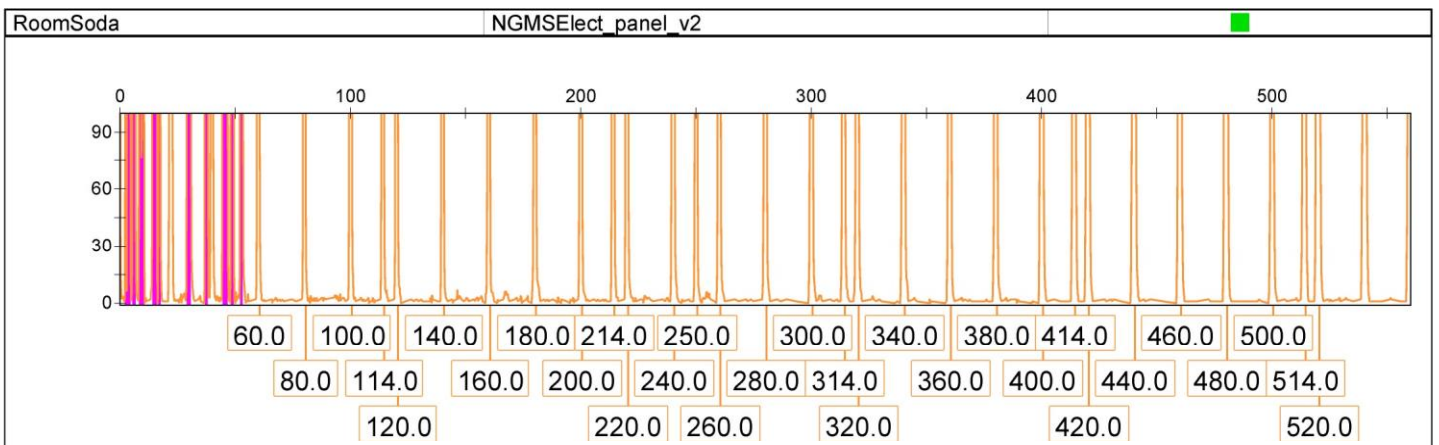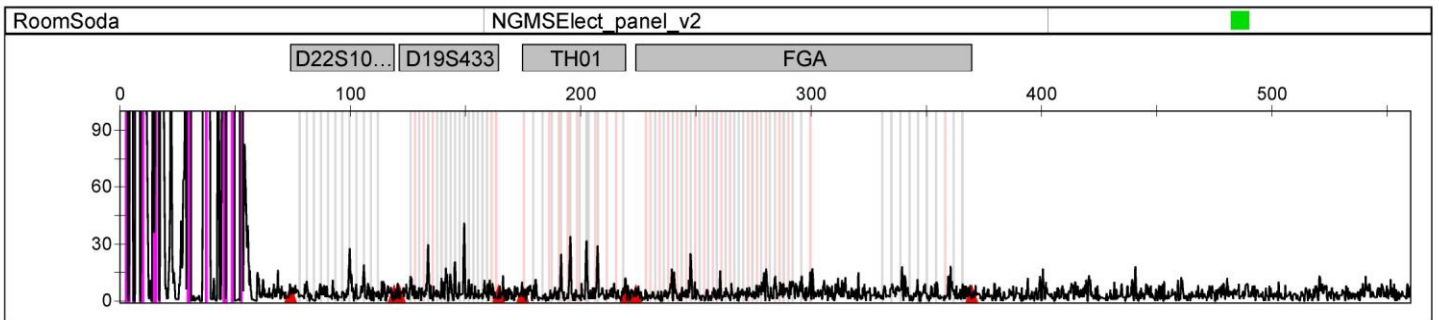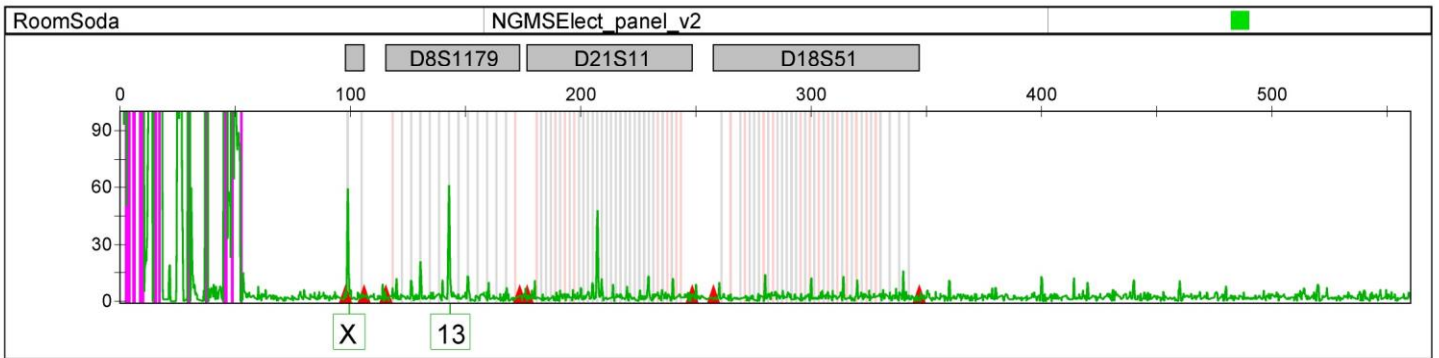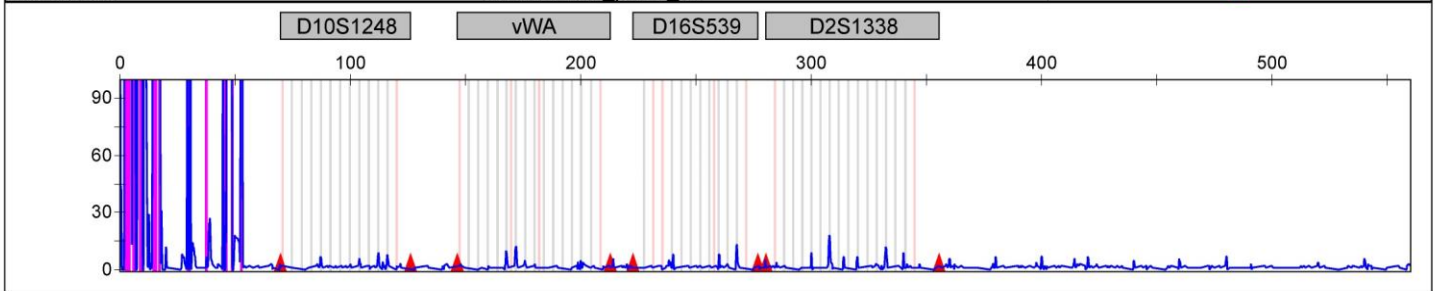
		Dye/Sample Peak	Sample File Name	Marker	Allele	Size	Height	Area	Data Point
1		B,1	E11_RoomSoda.fsa				75	1102	1359
2		B,2	E11_RoomSoda.fsa				56	856	1394
3		B,3	E11_RoomSoda.fsa				59	635	1431
4		B,4	E11_RoomSoda.fsa				68	722	1472
5		B,5	E11_RoomSoda.fsa				78	953	1563
6		B,6	E11_RoomSoda.fsa				133	1686	1590
7		B,7	E11_RoomSoda.fsa				115	1670	1628
8		B,8	E11_RoomSoda.fsa				142	1534	1701
9		B,9	E11_RoomSoda.fsa				127	1427	1716
10		B,10	E11_RoomSoda.fsa				94	788	1738
11		B,11	E11_RoomSoda.fsa				179	1934	1750
12		B,12	E11_RoomSoda.fsa				152	1344	1771
13		B,13	E11_RoomSoda.fsa				3972	42397	1841
14		B,14	E11_RoomSoda.fsa			2.39	5365	68547	1880
15		B,15	E11_RoomSoda.fsa			4.01	5243	67525	1903
16		B,16	E11_RoomSoda.fsa			6.06	3433	49475	1932
17		B,17	E11_RoomSoda.fsa			8.38	7785	80578	1965
18		B,18	E11_RoomSoda.fsa			10.49	346	4019	1995
19		B,19	E11_RoomSoda.fsa			14.93	8021	103097	2058
20		B,20	E11_RoomSoda.fsa			15.77	8101	110008	2070
21		B,21	E11_RoomSoda.fsa			17.04	5698	50650	2088
22		B,22	E11_RoomSoda.fsa			29.23	235	969	2261
23		B,23	E11_RoomSoda.fsa			30.49	257	1019	2279
24		B,24	E11_RoomSoda.fsa			44.65	144	600	2480
25		B,25	E11_RoomSoda.fsa			47.11	2835	47814	2515
26		B,26	E11_RoomSoda.fsa			47.68	2833	34151	2523
27		B,27	E11_RoomSoda.fsa			52.96	277	3552	2598
28		G,1	E11_RoomSoda.fsa				149	1657	1471
29		G,2	E11_RoomSoda.fsa				55	533	1578
30		G,3	E11_RoomSoda.fsa				123	1834	1595
31		G,4	E11_RoomSoda.fsa				409	5016	1656
32		G,5	E11_RoomSoda.fsa				85	889	1687
33		G,6	E11_RoomSoda.fsa				130	2634	1703
34		G,7	E11_RoomSoda.fsa				1480	18475	1778
35		G,8	E11_RoomSoda.fsa				5922	47502	1837
36		G,9	E11_RoomSoda.fsa				6878	62675	1846
37		G,10	E11_RoomSoda.fsa			1.13	215	2735	1862
38		G,11	E11_RoomSoda.fsa			2.68	430	4363	1884
39		G,12	E11_RoomSoda.fsa			3.31	338	3565	1893
40		G,13	E11_RoomSoda.fsa			4.23	331	3506	1906
41		G,14	E11_RoomSoda.fsa			5.35	4623	52793	1922
42		G,15	E11_RoomSoda.fsa			6.69	6030	56004	1941
43		G,16	E11_RoomSoda.fsa			8.52	611	5928	1967
44		G,17	E11_RoomSoda.fsa			8.94	607	4310	1973
45		G,18	E11_RoomSoda.fsa			9.93	5492	42066	1987

46		G,19	E11_RoomSoda.fsa			13.31	509	8132	2035
47		G,20	E11_RoomSoda.fsa			14.72	614	3573	2055

		Dye/Sample Peak	Sample File Name	Marker	Allele	Size	Height	Area	Data Point
48		G,21	E11_RoomSoda.fsa			15.21	343	3884	2062
49		G,22	E11_RoomSoda.fsa			16.62	6128	47062	2082
50		G,23	E11_RoomSoda.fsa			17.46	6881	61590	2094
51		G,24	E11_RoomSoda.fsa			25.0	176	2005	2201
52		G,25	E11_RoomSoda.fsa			26.27	457	5018	2219
53		G,26	E11_RoomSoda.fsa			29.86	2598	23436	2270
54		G,27	E11_RoomSoda.fsa			30.85	60	530	2284
55		G,28	E11_RoomSoda.fsa			37.46	11048	126866	2378
56		G,29	E11_RoomSoda.fsa			45.92	11059	151852	2498
57		G,30	E11_RoomSoda.fsa			46.97	58	544	2513
58		G,31	E11_RoomSoda.fsa			47.54	57	488	2521
59		G,32	E11_RoomSoda.fsa			48.66	10169	105928	2537
60		G,33	E11_RoomSoda.fsa			49.93	163	2602	2555
61		G,34	E11_RoomSoda.fsa			51.34	89	928	2575
62		G,35	E11_RoomSoda.fsa	AMEL	X	98.85	59	568	3246
63		G,36	E11_RoomSoda.fsa	D8S1179	13	142.73	61	650	3860
64		Y,1	E11_RoomSoda.fsa				1036	3414	1836
65		Y,2	E11_RoomSoda.fsa			0.07	1752	11391	1847
66		Y,3	E11_RoomSoda.fsa			1.55	762	6030	1868
67		Y,4	E11_RoomSoda.fsa			2.18	2597	22259	1877
68		Y,5	E11_RoomSoda.fsa			2.96	2746	26474	1888
69		Y,6	E11_RoomSoda.fsa			4.51	2280	13537	1910
70		Y,7	E11_RoomSoda.fsa			5.28	1832	10041	1921
71		Y,8	E11_RoomSoda.fsa			6.76	1550	17342	1942
72		Y,9	E11_RoomSoda.fsa			8.24	2103	12411	1963
73		Y,10	E11_RoomSoda.fsa			9.58	6332	50487	1982
74		Y,11	E11_RoomSoda.fsa			10.28	7235	61589	1992
75		Y,12	E11_RoomSoda.fsa			14.37	3553	19358	2050
76		Y,13	E11_RoomSoda.fsa			15.99	2255	25811	2073
77		Y,14	E11_RoomSoda.fsa			17.46	797	6939	2094
78		Y,15	E11_RoomSoda.fsa			22.11	136	1711	2160
79		Y,16	E11_RoomSoda.fsa			28.31	125	1876	2248
80		Y,17	E11_RoomSoda.fsa			29.86	8698	166248	2270
81		Y,18	E11_RoomSoda.fsa			36.9	7653	55535	2370
82		Y,19	E11_RoomSoda.fsa			38.03	7534	55614	2386
83		Y,20	E11_RoomSoda.fsa			42.54	325	2686	2450
84		Y,21	E11_RoomSoda.fsa			45.07	7345	93205	2486
85		Y,22	E11_RoomSoda.fsa			46.48	6398	44891	2506
86		Y,23	E11_RoomSoda.fsa			48.17	6769	47117	2530
87		Y,24	E11_RoomSoda.fsa			49.23	6640	44181	2545
88		Y,25	E11_RoomSoda.fsa			52.68	7382	79057	2594
89		Y,26	E11_RoomSoda.fsa			54.01	83	1359	2613
90		R,1	E11_RoomSoda.fsa				4797	35115	1841
91		R,2	E11_RoomSoda.fsa			1.2	477	8304	1863
92		R,3	E11_RoomSoda.fsa			1.83	497	4394	1872

93		R,4	E11_RoomSoda.fsa			2.39	1465	8232	1880
94		R,5	E11_RoomSoda.fsa			3.45	6779	67570	1895

		Dye/Sample Peak	Sample File Name	Marker	Allele	Size	Height	Area	Data Point
95		R,6	E11_RoomSoda.fsa			4.01	6778	62767	1903
96		R,7	E11_RoomSoda.fsa			6.06	6533	104444	1932
97		R,8	E11_RoomSoda.fsa			8.73	6542	71326	1970
98		R,9	E11_RoomSoda.fsa			9.93	2994	25122	1987
99		R,10	E11_RoomSoda.fsa			14.15	6830	88110	2047
100		R,11	E11_RoomSoda.fsa			17.04	5831	54155	2088
101		R,12	E11_RoomSoda.fsa			20.28	327	8211	2134
102		R,13	E11_RoomSoda.fsa			24.23	323	4514	2190
103		R,14	E11_RoomSoda.fsa			26.62	203	1979	2224
104		R,15	E11_RoomSoda.fsa			29.08	6989	68745	2259
105		R,16	E11_RoomSoda.fsa			30.63	6717	62432	2281
106		R,17	E11_RoomSoda.fsa			37.46	3632	40932	2378
107		R,18	E11_RoomSoda.fsa			42.04	434	4456	2443
108		R,19	E11_RoomSoda.fsa			44.51	5462	58990	2478
109		R,20	E11_RoomSoda.fsa			45.92	2646	30189	2498
110		R,21	E11_RoomSoda.fsa			46.76	1162	11732	2510
111		R,22	E11_RoomSoda.fsa			48.66	2796	28724	2537
112		R,23	E11_RoomSoda.fsa			52.25	6858	78935	2588
113		R,24	E11_RoomSoda.fsa			53.17	6856	69937	2601
114		R,25	E11_RoomSoda.fsa			57.82	55	753	2667
115		O,1	E11_RoomSoda.fsa				1007	7289	1841
116		O,2	E11_RoomSoda.fsa			2.39	256	1581	1880
117		O,3	E11_RoomSoda.fsa			3.73	8091	102991	1899
118		O,4	E11_RoomSoda.fsa			6.06	4892	53987	1932
119		O,5	E11_RoomSoda.fsa			8.73	4285	32921	1970
120		O,6	E11_RoomSoda.fsa			9.93	4575	34790	1987
121		O,7	E11_RoomSoda.fsa			14.79	6557	88808	2056
122		O,8	E11_RoomSoda.fsa			17.04	3023	22527	2088
123		O,9	E11_RoomSoda.fsa			22.18	463	6906	2161
124		O,10	E11_RoomSoda.fsa			29.86	8240	149913	2270
125		O,11	E11_RoomSoda.fsa			37.46	8009	98739	2378
126		O,12	E11_RoomSoda.fsa			39.86	586	6576	2412
127		O,13	E11_RoomSoda.fsa			45.77	8535	202251	2496
128		O,14	E11_RoomSoda.fsa			48.66	7664	86578	2537
129		O,15	E11_RoomSoda.fsa			52.68	6434	66165	2594
130		O,16 *	E11_RoomSoda.fsa			60.0	1139	11147	2698
131		O,17 *	E11_RoomSoda.fsa			80.0	913	8674	2982
132		O,18 *	E11_RoomSoda.fsa			100.0	1511	14119	3262
133		O,19 *	E11_RoomSoda.fsa			114.0	1687	15519	3456
134		O,20 *	E11_RoomSoda.fsa			120.0	1394	13034	3542
135		O,21 *	E11_RoomSoda.fsa			140.0	1092	10121	3823
136		O,22 *	E11_RoomSoda.fsa			160.0	1168	11121	4092
137		O,23 *	E11_RoomSoda.fsa			180.0	1432	13911	4364
138		O,24 *	E11_RoomSoda.fsa			200.0	1196	11847	4633
139		O,25 *	E11_RoomSoda.fsa			214.0	1204	12053	4825

140		O,26	*	E11_RoomSoda.fsa			220.0	1016	10342	4905
141		O,27	*	E11_RoomSoda.fsa			240.0	1570	16287	5176

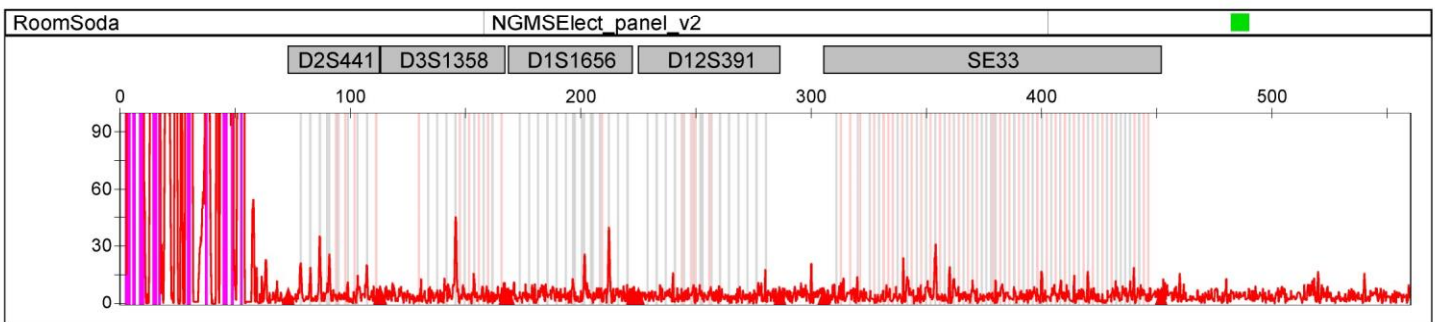|		Dye/Sample Peak	Sample File Name	Marker	Allele	Size	Height	Area	Data Point
142		O,28 *	E11_RoomSoda.fsa			250.0	740	7785	5308
143		O,29 *	E11_RoomSoda.fsa			260.0	1273	13606	5446
144		O,30 *	E11_RoomSoda.fsa			280.0	1417	15494	5716
145		O,31 *	E11_RoomSoda.fsa			300.0	1524	16997	5989
146		O,32 *	E11_RoomSoda.fsa			314.0	1060	12063	6180
147		O,33 *	E11_RoomSoda.fsa			320.0	1138	13289	6257
148		O,34 *	E11_RoomSoda.fsa			340.0	1446	17425	6523
149		O,35 *	E11_RoomSoda.fsa			360.0	1233	15177	6788
150		O,36 *	E11_RoomSoda.fsa			380.0	854	10822	7053
151		O,37 *	E11_RoomSoda.fsa			400.0	1280	16721	7315
152		O,38 *	E11_RoomSoda.fsa			414.0	1076	14396	7500
153		O,39 *	E11_RoomSoda.fsa			420.0	1089	14699	7577
154		O,40 *	E11_RoomSoda.fsa			440.0	1202	16791	7837
155		O,41 *	E11_RoomSoda.fsa			460.0	966	13689	8091
156		O,42 *	E11_RoomSoda.fsa			480.0	901	13077	8345
157		O,43 *	E11_RoomSoda.fsa			500.0	393	5922	8592
158		O,44 *	E11_RoomSoda.fsa			514.0	450	6848	8765
159		O,45 *	E11_RoomSoda.fsa			520.0	924	14278	8839
160		O,46	E11_RoomSoda.fsa			540.11	710	11185	9087

									5

Sample Name	Panel	SQ
RoomNothing	NGMSElect_panel_v2	

D10S1248   vWA   D16S539   D2S1338

RoomNothing — NGMSElect_panel_v2

D8S1179   D21S11   D18S51

Sample Name	Panel	SQ
RoomNothing	NGMSElect_panel_v2	🟩
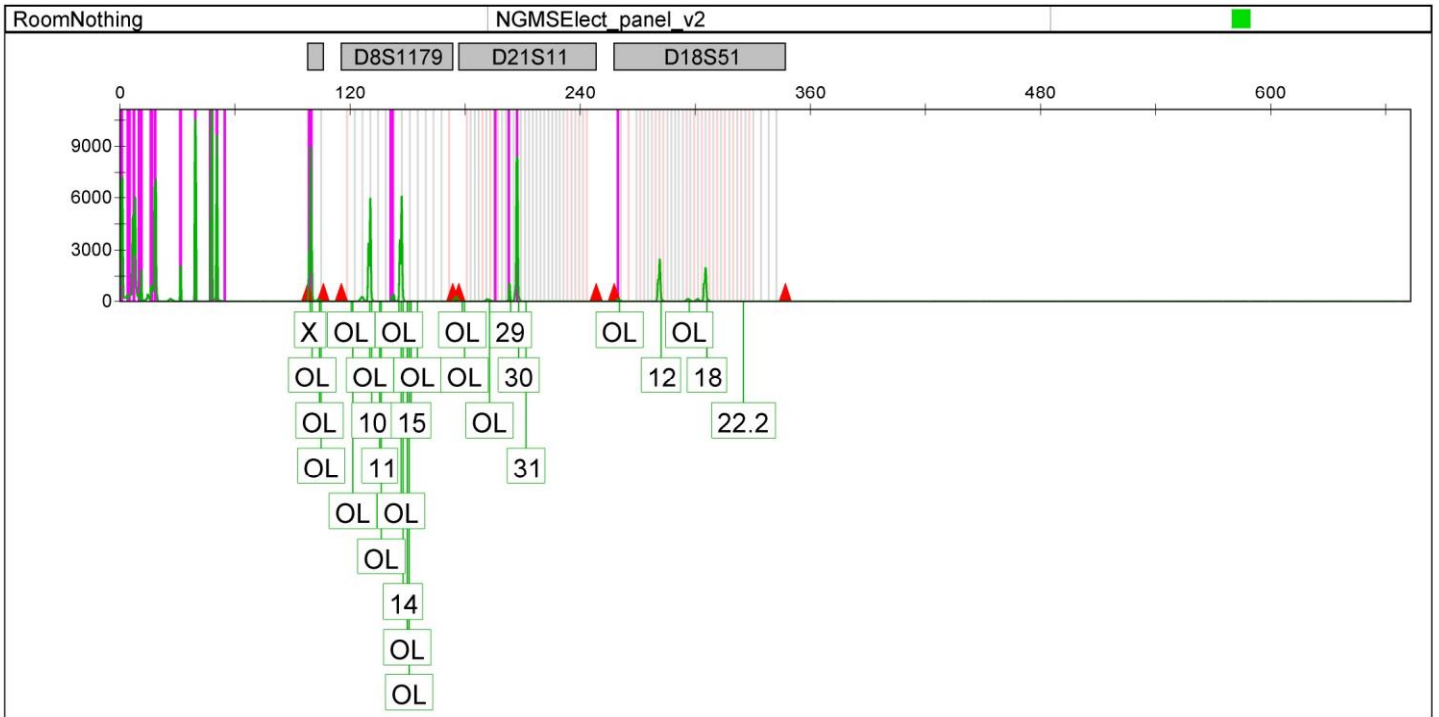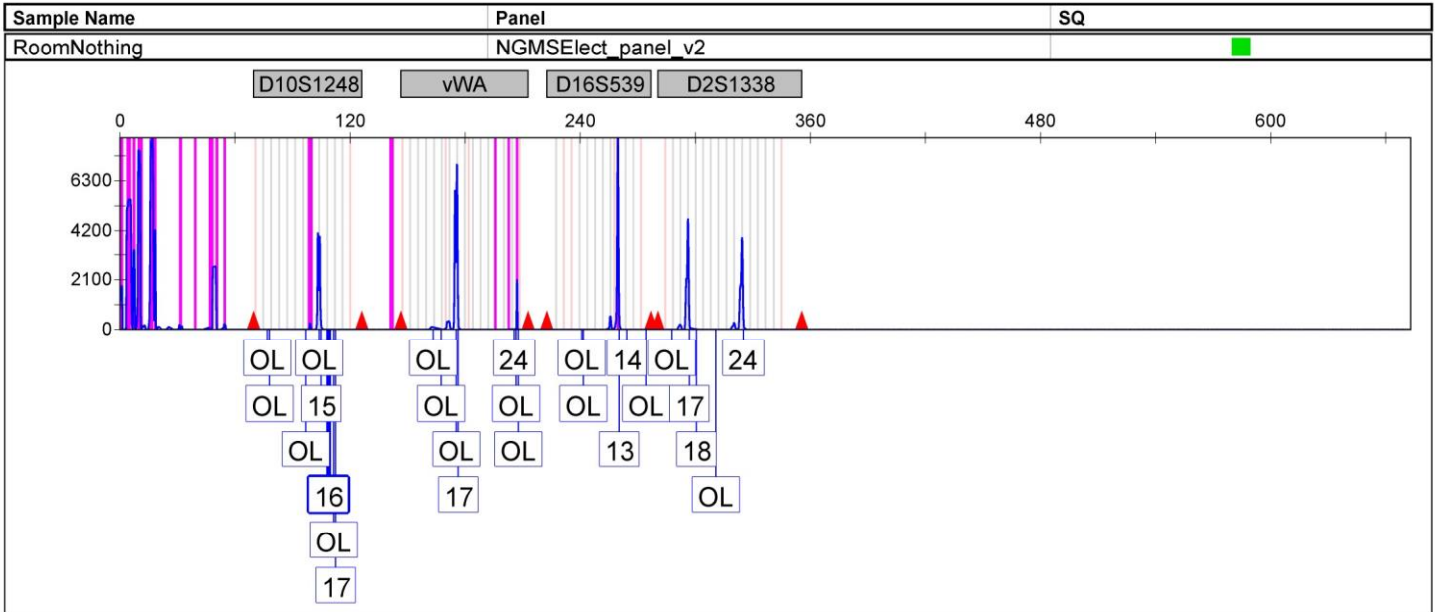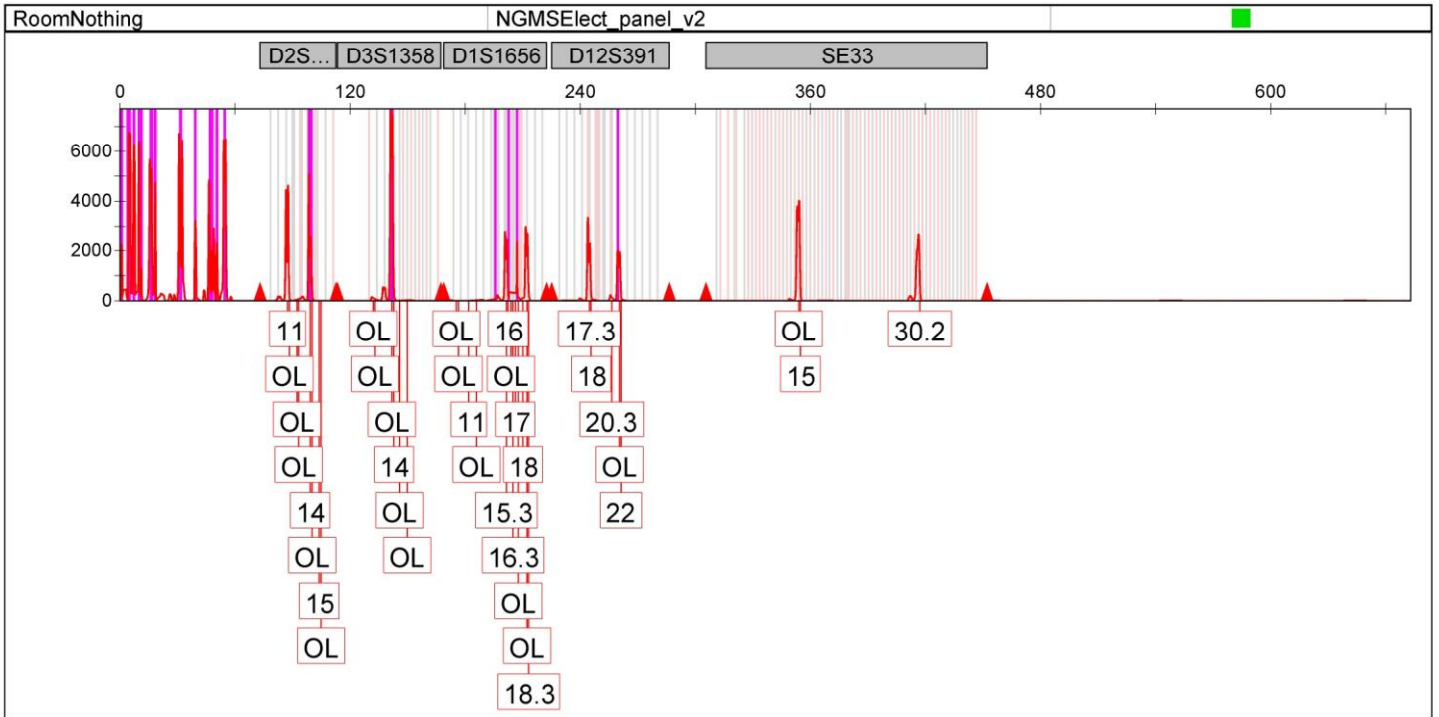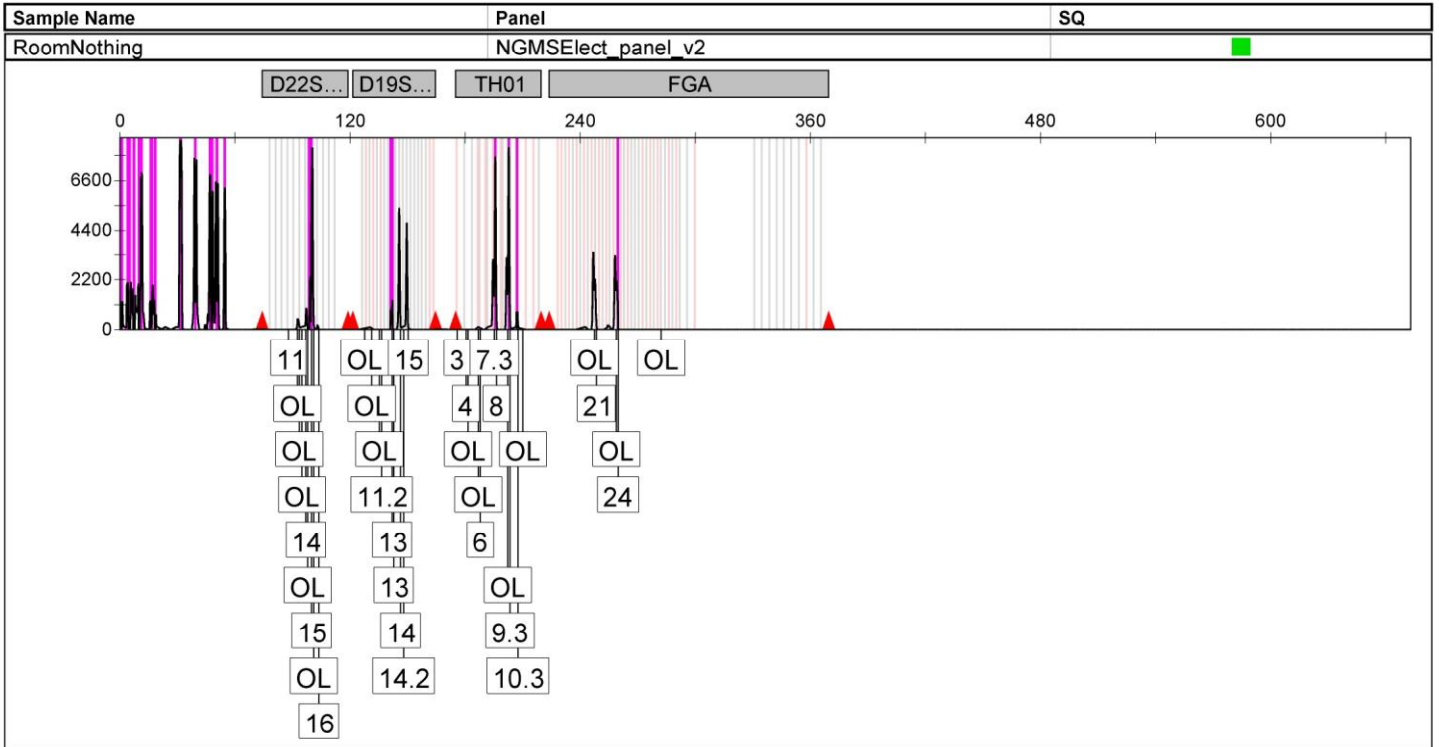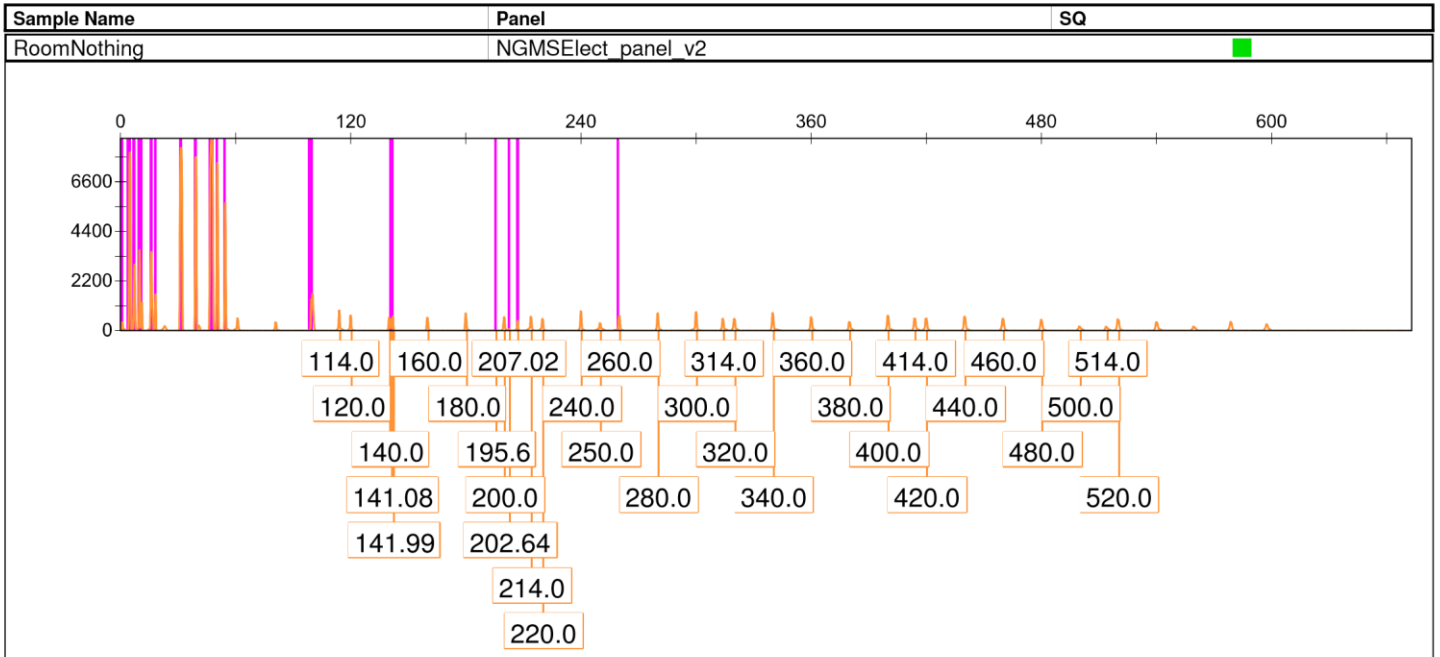
		Dye/Sample Peak	Sample File Name	Marker	Allele	Size	Height	Area	Data Point
1	🟦	B,1	E10_RoomNothing.fsa				76	1024	1102
2	🟦	B,2	E10_RoomNothing.fsa				69	917	1139
3	🟦	B,3	E10_RoomNothing.fsa				53	481	1169
4	🟦	B,4	E10_RoomNothing.fsa				61	662	1206
5	🟦	B,5	E10_RoomNothing.fsa				79	646	1293
6	🟦	B,6	E10_RoomNothing.fsa				158	2520	1317
7	🟦	B,7	E10_RoomNothing.fsa				173	1899	1347
8	🟦	B,8	E10_RoomNothing.fsa				51	438	1364
9	🟦	B,9	E10_RoomNothing.fsa				175	1804	1414
10	🟦	B,10	E10_RoomNothing.fsa				138	1373	1425
11	🟦	B,11	E10_RoomNothing.fsa				87	692	1446
12	🟦	B,12	E10_RoomNothing.fsa				185	1612	1459
13	🟦	B,13	E10_RoomNothing.fsa				143	1117	1478
14	🟦	B,14	E10_RoomNothing.fsa			0.31	1777	15047	1535
15	🟦	B,15	E10_RoomNothing.fsa			0.94	1859	13813	1543
16	🟦	B,16	E10_RoomNothing.fsa			3.66	5250	47590	1578
17	🟦	B,17	E10_RoomNothing.fsa			5.14	5554	79519	1597
18	🟦	B,18	E10_RoomNothing.fsa			7.25	3420	38475	1624
19	🟦	B,19	E10_RoomNothing.fsa			9.58	7618	71972	1654
20	🟦	B,20	E10_RoomNothing.fsa			11.45	259	1351	1678
21	🟦	B,21	E10_RoomNothing.fsa			12.94	206	1360	1697
22	🟦	B,22	E10_RoomNothing.fsa			16.21	8056	100514	1739
23	🟦	B,23	E10_RoomNothing.fsa			16.91	8121	92307	1748
24	🟦	B,24	E10_RoomNothing.fsa			18.23	4238	29599	1765
25	🟦	B,25	E10_RoomNothing.fsa			20.42	147	1900	1793
26	🟦	B,26	E10_RoomNothing.fsa			25.64	121	2593	1860
27	🟦	B,27	E10_RoomNothing.fsa			30.94	260	1185	1928
28	🟦	B,28	E10_RoomNothing.fsa			32.18	221	818	1944
29	🟦	B,29	E10_RoomNothing.fsa			36.08	56	710	1994
30	🟦	B,30	E10_RoomNothing.fsa			42.16	63	594	2072

		Dye/Sample Peak	Sample File Name	Marker	Allele	Size	Height	Area	Data Point
31	■	B,31	E10_RoomNothing.fsa			46.52	144	720	2128
32	■	B,32	E10_RoomNothing.fsa			49.64	2703	40285	2168
33	■	B,33	E10_RoomNothing.fsa			54.78	276	3094	2234
34	■	B,34	E10_RoomNothing.fsa	D10S1248	OL	76.13	53	382	2508
35	■	B,35	E10_RoomNothing.fsa	D10S1248	OL	77.22	92	645	2522
36	■	B,36	E10_RoomNothing.fsa	D10S1248	OL	96.08	94	1644	2764
37	■	B,37	E10_RoomNothing.fsa			99.12	287	1914	2803
38	■	B,38	E10_RoomNothing.fsa			100.44	93	415	2820
39	■	B,39	E10_RoomNothing.fsa	D10S1248	OL	103.17	4137	35330	2855
40	■	B,40	E10_RoomNothing.fsa	D10S1248	15	104.1	3987	35092	2867
41	■	B,41	E10_RoomNothing.fsa	D10S1248	16	107.92	59	502	2916
42	■	B,42	E10_RoomNothing.fsa	D10S1248	OL	110.73	51	543	2952
43	■	B,43	E10_RoomNothing.fsa	D10S1248	17	111.74	73	753	2965
44	■	B,44	E10_RoomNothing.fsa			141.08	62	415	3333
45	■	B,45	E10_RoomNothing.fsa			141.99	75	373	3344
46	■	B,46	E10_RoomNothing.fsa	vWA	OL	162.57	119	2395	3590
47	■	B,47	E10_RoomNothing.fsa	vWA	OL	166.71	51	409	3640
48	■	B,48	E10_RoomNothing.fsa			170.69	419	3675	3688
49	■	B,49	E10_RoomNothing.fsa			171.6	465	4211	3699
50	■	B,50	E10_RoomNothing.fsa	vWA	OL	174.68	5908	50150	3736
51	■	B,51	E10_RoomNothing.fsa	vWA	17	175.67	7006	64199	3748
52	■	B,52	E10_RoomNothing.fsa	vWA	24	204.86	51	1005	4095
53	■	B,53	E10_RoomNothing.fsa	vWA	OL	205.86	75	938	4107
54	■	B,54	E10_RoomNothing.fsa	vWA	OL	207.02	2126	10550	4121
55	■	B,55	E10_RoomNothing.fsa	D16S539	OL	240.09	75	744	4513
56	■	B,56	E10_RoomNothing.fsa	D16S539	OL	240.88	83	1187	4522
57	■	B,57	E10_RoomNothing.fsa			255.72	626	5875	4696
58	■	B,58	E10_RoomNothing.fsa	D16S539	13	259.59	8147	82484	4743
59	■	B,59	E10_RoomNothing.fsa	D16S539	14	263.54	52	395	4790
60	■	B,60	E10_RoomNothing.fsa	D16S539	OL	273.62	82	1377	4909
61	■	B,61	E10_RoomNothing.fsa	D2S1338	OL	286.99	69	1269	5067
62	■	B,62	E10_RoomNothing.fsa			292.2	283	4036	5129
63	■	B,63	E10_RoomNothing.fsa	D2S1338	17	296.14	4710	65511	5176
64	■	B,64	E10_RoomNothing.fsa	D2S1338	18	299.83	55	932	5220
65	■	B,65	E10_RoomNothing.fsa	D2S1338	OL	310.08	57	1000	5343
66	■	B,66	E10_RoomNothing.fsa			320.26	349	4957	5459
67	■	B,67	E10_RoomNothing.fsa	D2S1338	24	324.36	3934	56814	5506
68	■	G,1	E10_RoomNothing.fsa				149	1655	1206
69	■	G,2	E10_RoomNothing.fsa				124	1179	1303
70	■	G,3	E10_RoomNothing.fsa				131	1518	1317
71	■	G,4	E10_RoomNothing.fsa				436	4618	1376
72	■	G,5	E10_RoomNothing.fsa				82	745	1402
73	■	G,6	E10_RoomNothing.fsa				133	2517	1417
74	■	G,7	E10_RoomNothing.fsa				1672	18234	1485
75	■	G,8	E10_RoomNothing.fsa			1.17	7239	99109	1546
76	■	G,9	E10_RoomNothing.fsa			2.49	173	1751	1563
77	■	G,10	E10_RoomNothing.fsa			3.82	451	4008	1580

		Dye/Sample Peak	Sample File Name	Marker	Allele	Size	Height	Area	Data Point
78		G,11	E10_RoomNothing.fsa			4.44	321	3142	1588
79		G,12	E10_RoomNothing.fsa			5.61	324	3138	1603
80		G,13	E10_RoomNothing.fsa			6.62	5003	49648	1616
81		G,14	E10_RoomNothing.fsa			7.87	6075	64158	1632
82		G,15	E10_RoomNothing.fsa			9.74	430	5797	1656
83		G,16	E10_RoomNothing.fsa			11.14	1895	9549	1674
84		G,17	E10_RoomNothing.fsa			12.47	111	804	1691
85		G,18	E10_RoomNothing.fsa			14.49	498	5894	1717
86		G,19	E10_RoomNothing.fsa			15.97	950	6126	1736
87		G,20	E10_RoomNothing.fsa			16.6	961	9218	1744
88		G,21	E10_RoomNothing.fsa			17.92	6711	54588	1761
89		G,22	E10_RoomNothing.fsa			18.62	7174	56164	1770
90		G,23	E10_RoomNothing.fsa			25.25	60	478	1855
91		G,24	E10_RoomNothing.fsa			26.42	191	2312	1870
92		G,25	E10_RoomNothing.fsa			27.51	221	2536	1884
93		G,26	E10_RoomNothing.fsa			31.56	2167	16927	1936
94		G,27	E10_RoomNothing.fsa			39.27	10548	106154	2035
95		G,28	E10_RoomNothing.fsa			47.69	11112	132144	2143
96		G,29	E10_RoomNothing.fsa			50.49	9655	91360	2179
97		G,30	E10_RoomNothing.fsa			51.74	146	1799	2195
98		G,31	E10_RoomNothing.fsa			52.83	104	1526	2209
99		G,32	E10_RoomNothing.fsa			53.77	84	627	2221
100		G,33	E10_RoomNothing.fsa			84.94	71	592	2621
101		G,34	E10_RoomNothing.fsa			90.62	65	494	2694
102		G,35	E10_RoomNothing.fsa			91.48	134	1285	2705
103		G,36	E10_RoomNothing.fsa	AMEL	X	98.49	2921	23063	2795
104		G,37	E10_RoomNothing.fsa	AMEL	OL	99.43	8996	92131	2807
105		G,38	E10_RoomNothing.fsa	AMEL	OL	103.25	175	1601	2856
106		G,39	E10_RoomNothing.fsa	AMEL	OL	104.1	183	1853	2867
107		G,40	E10_RoomNothing.fsa	D8S1179	OL	119.84	58	378	3069
108		G,41	E10_RoomNothing.fsa	D8S1179	OL	120.63	117	1317	3079
109		G,42	E10_RoomNothing.fsa			125.53	194	1570	3141
110		G,43	E10_RoomNothing.fsa			126.41	334	3997	3152
111		G,44	E10_RoomNothing.fsa	D8S1179	OL	129.61	3431	26943	3192
112		G,45	E10_RoomNothing.fsa	D8S1179	10	130.49	5973	56260	3203
113		G,46	E10_RoomNothing.fsa	D8S1179	11	134.69	84	752	3255
114		G,47	E10_RoomNothing.fsa	D8S1179	OL	135.51	104	1220	3265
115		G,48	E10_RoomNothing.fsa			141.66	351	2075	3340
116		G,49	E10_RoomNothing.fsa			142.74	539	4420	3353
117		G,50	E10_RoomNothing.fsa	D8S1179	OL	144.74	62	392	3377
118		G,51	E10_RoomNothing.fsa	D8S1179	OL	145.91	3610	28822	3391
119		G,52	E10_RoomNothing.fsa	D8S1179	14	146.83	6087	56828	3402
120		G,53	E10_RoomNothing.fsa	D8S1179	OL	149.08	85	453	3429
121		G,54	E10_RoomNothing.fsa	D8S1179	OL	150.09	93	664	3441

122		G,55	E10_RoomNothing.fsa	D8S1179	15	151.01	85	671	3452
123		G,56	E10_RoomNothing.fsa	D8S1179	OL	154.36	83	612	3492
124		G,57	E10_RoomNothing.fsa			174.68	246	2204	3736

Printed by: gmid

Beth

		Dye/Sample Peak	Sample File Name	Marker	Allele	Size	Height	Area	Data Point
125		G,58	E10_RoomNothing.fsa			175.67	312	3267	3748
126		G,59	E10_RoomNothing.fsa	D21S11	OL	177.84	53	343	3774
127		G,60	E10_RoomNothing.fsa	D21S11	OL	178.92	53	442	3787
128		G,61	E10_RoomNothing.fsa	D21S11	OL	191.96	219	3122	3941
129		G,62	E10_RoomNothing.fsa			199.07	50	654	4025
130		G,63	E10_RoomNothing.fsa	D21S11	29	203.05	1094	8860	4073
131		G,64	E10_RoomNothing.fsa	D21S11	30	207.18	8400	103654	4123
132		G,65	E10_RoomNothing.fsa	D21S11	31	211.0	105	858	4169
133		G,66	E10_RoomNothing.fsa	D18S51	OL	259.84	227	2636	4746
134		G,67	E10_RoomNothing.fsa			277.36	130	1756	4953
135		G,68	E10_RoomNothing.fsa	D18S51	12	281.43	2523	36010	5001
136		G,69	E10_RoomNothing.fsa	D18S51	OL	296.14	169	2885	5176
137		G,70	E10_RoomNothing.fsa			301.4	177	2648	5239
138		G,71	E10_RoomNothing.fsa	D18S51	18	305.37	2083	30264	5287
139		G,72	E10_RoomNothing.fsa	D18S51	22.2	324.45	136	2272	5507
140		Y,1	E10_RoomNothing.fsa				51	734	1488
141		Y,2	E10_RoomNothing.fsa			0.7	1257	4645	1540
142		Y,3	E10_RoomNothing.fsa			1.25	1258	5895	1547
143		Y,4	E10_RoomNothing.fsa			2.49	125	1206	1563
144		Y,5	E10_RoomNothing.fsa			3.9	2090	24940	1581
145		Y,6	E10_RoomNothing.fsa			5.61	2104	11920	1603
146		Y,7	E10_RoomNothing.fsa			6.55	1821	9814	1615
147		Y,8	E10_RoomNothing.fsa			7.87	1526	9569	1632
148		Y,9	E10_RoomNothing.fsa			9.43	2040	11898	1652
149		Y,10	E10_RoomNothing.fsa			11.38	6958	90374	1677
150		Y,11	E10_RoomNothing.fsa			13.56	66	433	1705
151		Y,12	E10_RoomNothing.fsa			14.73	144	880	1720
152		Y,13	E10_RoomNothing.fsa			15.66	1289	4864	1732
153		Y,14	E10_RoomNothing.fsa			17.06	1955	17548	1750
154		Y,15	E10_RoomNothing.fsa			17.84	1309	6636	1760
155		Y,16	E10_RoomNothing.fsa			18.7	689	2993	1771
156		Y,17	E10_RoomNothing.fsa			19.87	119	1714	1786
157		Y,18	E10_RoomNothing.fsa			20.88	96	1055	1799
158		Y,19	E10_RoomNothing.fsa			23.84	153	1905	1837
159		Y,20	E10_RoomNothing.fsa			27.58	67	729	1885
160		Y,21	E10_RoomNothing.fsa			29.3	121	2006	1907
161		Y,22	E10_RoomNothing.fsa			30.08	123	1129	1917
162		Y,23	E10_RoomNothing.fsa			38.73	7602	55854	2028
163		Y,24	E10_RoomNothing.fsa			39.82	7540	57314	2042
164		Y,25	E10_RoomNothing.fsa			44.34	255	1638	2100
165		Y,26	E10_RoomNothing.fsa			45.74	759	5083	2118
166		Y,27	E10_RoomNothing.fsa			46.91	6904	79811	2133
167		Y,28	E10_RoomNothing.fsa			48.31	6152	46679	2151
168		Y,29	E10_RoomNothing.fsa			49.95	6560	44476	2172

169		Y,30	E10_RoomNothing.fsa			50.96	6483	46851	2185
170		Y,31	E10_RoomNothing.fsa			54.62	6292	60580	2232
171		Y,32	E10_RoomNothing.fsa	D22S1045	11	87.04	71	434	2648

6

Printed by: gmid

Beth

		Dye/Sample Peak	Sample File Name	Marker	Allele	Size	Height	Area	Data Point
172		Y,33	E10_RoomNothing.fsa	D22S1045	OL	91.79	60	392	2709
173		Y,34	E10_RoomNothing.fsa	D22S1045	OL	92.73	571	6619	2721
174		Y,35	E10_RoomNothing.fsa	D22S1045	OL	94.21	127	1533	2740
175		Y,36	E10_RoomNothing.fsa	D22S1045	14	96.16	160	1188	2765
176		Y,37	E10_RoomNothing.fsa	D22S1045	OL	97.09	1026	8929	2777
177		Y,38	E10_RoomNothing.fsa	D22S1045	15	99.12	2335	13156	2803
178		Y,39	E10_RoomNothing.fsa	D22S1045	OL	100.29	8106	85417	2818
179		Y,40	E10_RoomNothing.fsa	D22S1045	16	103.01	310	2059	2853
180		Y,41	E10_RoomNothing.fsa	D19S433	OL	126.89	67	761	3158
181		Y,42	E10_RoomNothing.fsa	D19S433	OL	130.57	141	1703	3204
182		Y,43	E10_RoomNothing.fsa	D19S433	OL	134.53	58	698	3253
183		Y,44	E10_RoomNothing.fsa	D19S433	11.2	135.67	52	473	3267
184		Y,45	E10_RoomNothing.fsa			138.61	70	1431	3303
185		Y,46	E10_RoomNothing.fsa	D19S433	13	141.16	864	4338	3334
186		Y,47	E10_RoomNothing.fsa	D19S433	13	141.99	1306	7130	3344
187		Y,48	E10_RoomNothing.fsa	D19S433	14	145.57	5403	45990	3387
188		Y,49	E10_RoomNothing.fsa	D19S433	14.2	147.16	61	580	3406
189		Y,50	E10_RoomNothing.fsa	D19S433	15	149.5	4755	40399	3434
190		Y,51	E10_RoomNothing.fsa	TH01	3	175.09	60	372	3741
191		Y,52	E10_RoomNothing.fsa	TH01	4	179.75	55	474	3797
192		Y,53	E10_RoomNothing.fsa	TH01	OL	180.76	117	1436	3809
193		Y,54	E10_RoomNothing.fsa	TH01	OL	186.11	94	713	3872
194		Y,55	E10_RoomNothing.fsa	TH01	6	187.21	221	3029	3885
195		Y,56	E10_RoomNothing.fsa			191.62	127	916	3937
196		Y,57	E10_RoomNothing.fsa	TH01	7.3	194.5	3108	27467	3971
197		Y,58	E10_RoomNothing.fsa	TH01	8	195.6	7667	68010	3984
198		Y,59	E10_RoomNothing.fsa			198.73	81	603	4021
199		Y,60	E10_RoomNothing.fsa	TH01	OL	201.56	3187	27326	4055
200		Y,61	E10_RoomNothing.fsa	TH01	9.3	202.64	8120	72121	4068
201		Y,62	E10_RoomNothing.fsa	TH01	10.3	206.77	805	3810	4118
202		Y,63	E10_RoomNothing.fsa	TH01	OL	209.42	66	956	4150
203		Y,64	E10_RoomNothing.fsa			242.89	208	2266	4545
204		Y,65	E10_RoomNothing.fsa	FGA	OL	246.8	3427	33145	4590
205		Y,66	E10_RoomNothing.fsa	FGA	21	247.67	2213	19960	4600
206		Y,67	E10_RoomNothing.fsa			254.4	249	2535	4680
207		Y,68	E10_RoomNothing.fsa			255.31	147	1123	4691
208		Y,69	E10_RoomNothing.fsa	FGA	OL	258.11	3281	33653	4725
209		Y,70	E10_RoomNothing.fsa	FGA	24	259.02	2185	21781	4736
210		Y,71	E10_RoomNothing.fsa	FGA	OL	281.43	51	899	5001
211		R,1	E10_RoomNothing.fsa			1.01	2257	11942	1544
212		R,2	E10_RoomNothing.fsa			3.12	510	12877	1571
213		R,3	E10_RoomNothing.fsa			4.68	6744	54645	1591
214		R,4	E10_RoomNothing.fsa			5.14	6744	61785	1597
215		R,5	E10_RoomNothing.fsa			7.32	6340	81334	1625

216		R,6	E10_RoomNothing.fsa			8.26	350	2720	1637
217		R,7	E10_RoomNothing.fsa			9.9	6457	62681	1658
218		R,8	E10_RoomNothing.fsa			11.14	1277	6012	1674

Beth

		Dye/Sample Peak	Sample File Name	Marker	Allele	Size	Height	Area	Data Point
219		R,9	E10_RoomNothing.fsa			15.51	5699	61612	1730
220		R,10	E10_RoomNothing.fsa			16.13	5330	58217	1738
221		R,11	E10_RoomNothing.fsa			17.38	620	3458	1754
222		R,12	E10_RoomNothing.fsa			18.23	4734	33074	1765
223		R,13	E10_RoomNothing.fsa			20.18	201	2623	1790
224		R,14	E10_RoomNothing.fsa			21.66	403	9529	1809
225		R,15	E10_RoomNothing.fsa			26.1	323	4170	1866
226		R,16	E10_RoomNothing.fsa			28.29	298	2836	1894
227		R,17	E10_RoomNothing.fsa			30.78	6737	62847	1926
228		R,18	E10_RoomNothing.fsa			32.34	6462	60179	1946
229		R,19	E10_RoomNothing.fsa			39.27	3305	32369	2035
230		R,20	E10_RoomNothing.fsa			43.87	500	4936	2094
231		R,21	E10_RoomNothing.fsa			46.36	4860	43656	2126
232		R,22	E10_RoomNothing.fsa			47.69	2026	17158	2143
233		R,23	E10_RoomNothing.fsa			48.78	2938	27157	2157
234		R,24	E10_RoomNothing.fsa			50.49	2309	21881	2179
235		R,25	E10_RoomNothing.fsa			54.16	6483	68349	2226
236		R,26	E10_RoomNothing.fsa			55.01	6510	63774	2237
237		R,27	E10_RoomNothing.fsa			57.82	253	1903	2273
238		R,28	E10_RoomNothing.fsa			82.44	202	1605	2589
239		R,29	E10_RoomNothing.fsa			83.53	218	1911	2603
240		R,30	E10_RoomNothing.fsa	D2S441	11	86.57	4457	40911	2642
241		R,31	E10_RoomNothing.fsa	D2S441	OL	87.58	4653	42016	2655
242		R,32	E10_RoomNothing.fsa	D2S441	OL	91.56	101	1088	2706
243		R,33	E10_RoomNothing.fsa	D2S441	OL	92.49	64	649	2718
244		R,34	E10_RoomNothing.fsa			94.44	172	1445	2743
245		R,35	E10_RoomNothing.fsa			95.38	221	2278	2755
246		R,36	E10_RoomNothing.fsa	D2S441	14	98.42	5091	47498	2794
247		R,37	E10_RoomNothing.fsa	D2S441	OL	99.43	2601	25329	2807
248		R,38	E10_RoomNothing.fsa	D2S441	15	103.17	95	804	2855
249		R,39	E10_RoomNothing.fsa	D2S441	OL	104.1	59	596	2867
250		R,40	E10_RoomNothing.fsa	D3S1358	OL	131.38	237	2479	3214
251		R,41	E10_RoomNothing.fsa	D3S1358	OL	132.18	199	2235	3224
252		R,42	E10_RoomNothing.fsa			137.22	612	5947	3286
253		R,43	E10_RoomNothing.fsa			138.12	589	5837	3297
254		R,44	E10_RoomNothing.fsa	D3S1358	OL	141.08	7713	82141	3333
255		R,45	E10_RoomNothing.fsa	D3S1358	14	142.08	7561	87945	3345
256		R,46	E10_RoomNothing.fsa	D3S1358	OL	144.99	60	467	3380
257		R,47	E10_RoomNothing.fsa	D3S1358	OL	149.0	69	634	3428
258		R,48	E10_RoomNothing.fsa	D1S1656	OL	174.68	97	807	3736
259		R,49	E10_RoomNothing.fsa	D1S1656	OL	175.76	90	907	3749
260		R,50	E10_RoomNothing.fsa	D1S1656	11	181.1	60	667	3813
261		R,51	E10_RoomNothing.fsa	D1S1656	OL	185.09	64	870	3860
262		R,52	E10_RoomNothing.fsa			196.87	267	2548	3999

263		R,53	E10_RoomNothing.fsa			197.71	214	1809	4009
264		R,54	E10_RoomNothing.fsa	D1S1656	15.3	200.82	2802	26675	4046
265		R,55	E10_RoomNothing.fsa	D1S1656	16	201.65	2505	23894	4056

Beth

		Dye/Sample Peak	Sample File Name	Marker	Allele	Size	Height	Area	Data Point
266		R,56	E10_RoomNothing.fsa	D1S1656	OL	203.21	406	4625	4075
267		R,57	E10_RoomNothing.fsa	D1S1656	16.3	204.2	403	7140	4087
268		R,58	E10_RoomNothing.fsa	D1S1656	17	205.44	422	7728	4102
269		R,59	E10_RoomNothing.fsa	D1S1656	OL	207.02	2434	12197	4121
270		R,60	E10_RoomNothing.fsa			208.43	189	1726	4138
271		R,61	E10_RoomNothing.fsa	D1S1656	18	209.42	59	434	4150
272		R,62	E10_RoomNothing.fsa	D1S1656	OL	211.5	3010	28156	4175
273		R,63	E10_RoomNothing.fsa	D1S1656	18.3	212.42	2717	27193	4186
274		R,64	E10_RoomNothing.fsa			239.92	201	1805	4511
275		R,65	E10_RoomNothing.fsa			240.96	117	1080	4523
276		R,66	E10_RoomNothing.fsa	D12S391	17.3	244.02	3347	32946	4558
277		R,67	E10_RoomNothing.fsa	D12S391	18	244.98	2298	22465	4569
278		R,68	E10_RoomNothing.fsa	D12S391	20.3	255.72	300	3048	4696
279		R,69	E10_RoomNothing.fsa			256.71	187	1841	4708
280		R,70	E10_RoomNothing.fsa	D12S391	OL	259.75	2027	24085	4745
281		R,71	E10_RoomNothing.fsa	D12S391	22	260.59	1982	19920	4755
282		R,72	E10_RoomNothing.fsa			349.05	159	1247	5793
283		R,73	E10_RoomNothing.fsa			350.0	159	1376	5804
284		R,74	E10_RoomNothing.fsa	SE33	OL	353.19	3867	41577	5841
285		R,75	E10_RoomNothing.fsa	SE33	15	354.05	4100	46363	5851
286		R,76	E10_RoomNothing.fsa			412.35	251	4029	6522
287		R,77	E10_RoomNothing.fsa	SE33	30.2	416.41	2724	50614	6568
288		O,1	E10_RoomNothing.fsa			1.01	445	3042	1544
289		O,2	E10_RoomNothing.fsa			3.66	100	414	1578
290		O,3	E10_RoomNothing.fsa			4.91	7974	89439	1594
291		O,4	E10_RoomNothing.fsa			7.32	2955	27705	1625
292		O,5	E10_RoomNothing.fsa			9.9	3601	25020	1658
293		O,6	E10_RoomNothing.fsa			11.14	1333	8185	1674
294		O,7	E10_RoomNothing.fsa			16.13	3518	39594	1738
295		O,8	E10_RoomNothing.fsa			18.23	1617	10921	1765
296		O,9	E10_RoomNothing.fsa			23.22	250	3512	1829
297		O,10	E10_RoomNothing.fsa			31.56	8189	130984	1936
298		O,11	E10_RoomNothing.fsa			39.27	7766	84322	2035
299		O,12	E10_RoomNothing.fsa			40.99	313	3218	2057
300		O,13	E10_RoomNothing.fsa			47.61	8526	180608	2142
301		O,14	E10_RoomNothing.fsa			50.49	7490	76382	2179
302		O,15	E10_RoomNothing.fsa			54.55	5683	49446	2231
303		O,16	E10_RoomNothing.fsa			61.01	627	5606	2314
304		O,17	E10_RoomNothing.fsa			80.88	498	4326	2569
305		O,18	E10_RoomNothing.fsa			98.49	61	325	2795
306		O,19	E10_RoomNothing.fsa			99.43	1464	10343	2807
307		O,20	E10_RoomNothing.fsa			100.13	1645	18240	2816
308		O,21 *	E10_RoomNothing.fsa			114.0	942	7970	2994
309		O,22 *	E10_RoomNothing.fsa			120.0	780	6731	3071

310		O,23	*	E10_RoomNothing.fsa			140.0	629	5155	3320
311		O,24		E10_RoomNothing.fsa			141.08	540	2792	3333
312		O,25		E10_RoomNothing.fsa			141.99	701	3831	3344

Beth

		Dye/Sample Peak	Sample File Name	Marker	Allele	Size	Height	Area	Data Point
313		O,26 *	E10_RoomNothing.fsa			160.0	677	5810	3559
314		O,27 *	E10_RoomNothing.fsa			180.0	842	7336	3800
315		O,28	E10_RoomNothing.fsa			195.6	81	359	3984
316		O,29 *	E10_RoomNothing.fsa			200.0	712	6266	4036
317		O,30	E10_RoomNothing.fsa			202.64	201	804	4068
318		O,31	E10_RoomNothing.fsa			207.02	512	3163	4121
319		O,32 *	E10_RoomNothing.fsa			214.0	702	6272	4205
320		O,33 *	E10_RoomNothing.fsa			220.0	598	5522	4275
321		O,34 *	E10_RoomNothing.fsa			240.0	926	8618	4512
322		O,35 *	E10_RoomNothing.fsa			250.0	435	4185	4627
323		O,36 *	E10_RoomNothing.fsa			260.0	736	8069	4748
324		O,37 *	E10_RoomNothing.fsa			280.0	833	8329	4984
325		O,38 *	E10_RoomNothing.fsa			300.0	881	8804	5222
326		O,39 *	E10_RoomNothing.fsa			314.0	615	6293	5389
327		O,40 *	E10_RoomNothing.fsa			320.0	659	7010	5456
328		O,41 *	E10_RoomNothing.fsa			340.0	853	9044	5688
329		O,42 *	E10_RoomNothing.fsa			360.0	723	7961	5920
330		O,43 *	E10_RoomNothing.fsa			380.0	513	5708	6152
331		O,44 *	E10_RoomNothing.fsa			400.0	770	8857	6379
332		O,45 *	E10_RoomNothing.fsa			414.0	662	7617	6541
333		O,46 *	E10_RoomNothing.fsa			420.0	643	7661	6608
334		O,47 *	E10_RoomNothing.fsa			440.0	730	8890	6833
335		O,48 *	E10_RoomNothing.fsa			460.0	578	7317	7054
336		O,49 *	E10_RoomNothing.fsa			480.0	542	7003	7275
337		O,50 *	E10_RoomNothing.fsa			500.0	236	3096	7489
338		O,51 *	E10_RoomNothing.fsa			514.0	262	3531	7638
339		O,52 *	E10_RoomNothing.fsa			520.0	557	7534	7702
340		O,53	E10_RoomNothing.fsa			540.16	433	5945	7917
341		O,54	E10_RoomNothing.fsa			559.66	302	4251	8125
342		O,55	E10_RoomNothing.fsa			578.69	427	6153	8328
343		O,56	E10_RoomNothing.fsa			597.53	318	4663	8529

19.04.13BethsBloodStudy

Sample Name	Panel	SQ

RoomNaCl — NGMSElect_panel_v2

D10S1248 | vWA | D16S539 | D2S1338

RoomNaCl — NGMSElect_panel_v2

... | D8S1179 | D21S11 | D18S51

X | 10 | 13

RoomNaCl — NGMSElect_panel_v2

D22S1045 | D19S433 | TH01 | FGA

15 | 13 | 8

RoomNaCl — NGMSElect_panel_v2

D2S441 | D3S1358 | D1S1656 | D12S391 | SE33

RoomNaCl — NGMSElect_panel_v2

80.0 | 114.0 | 140.0 | 180.0 | 214.0 | 240.0 | 280.0 | 314.0 | 340.0 | 380.0 | 414.0 | 440.0

100.0 | 160.0 | 200.0 | 250.0 | 300.0 | 360.0 | 400.0

120.0 | 220.0 | 260.0 | 320.0 | 420.0
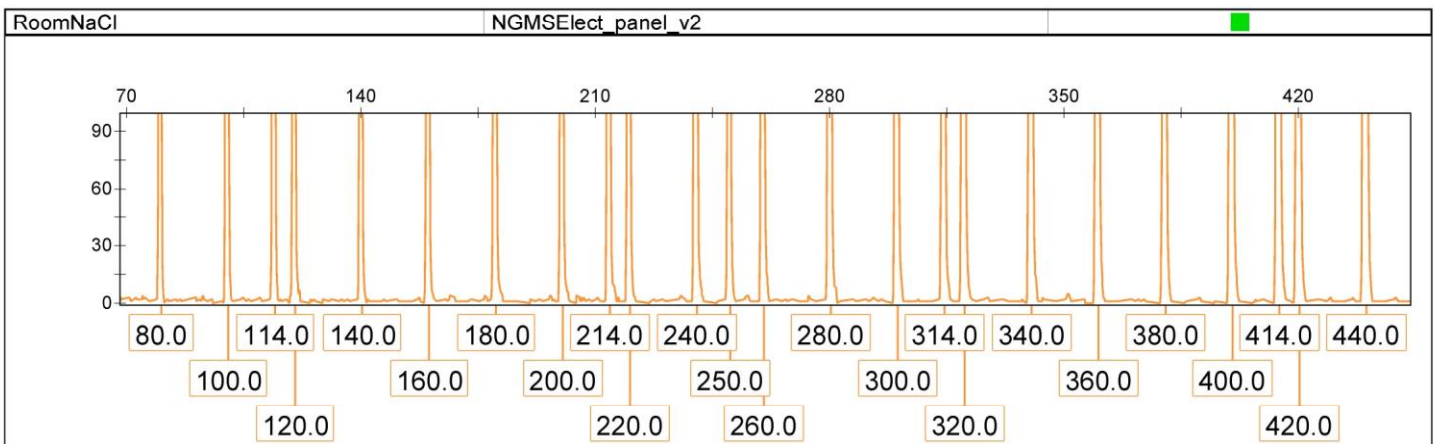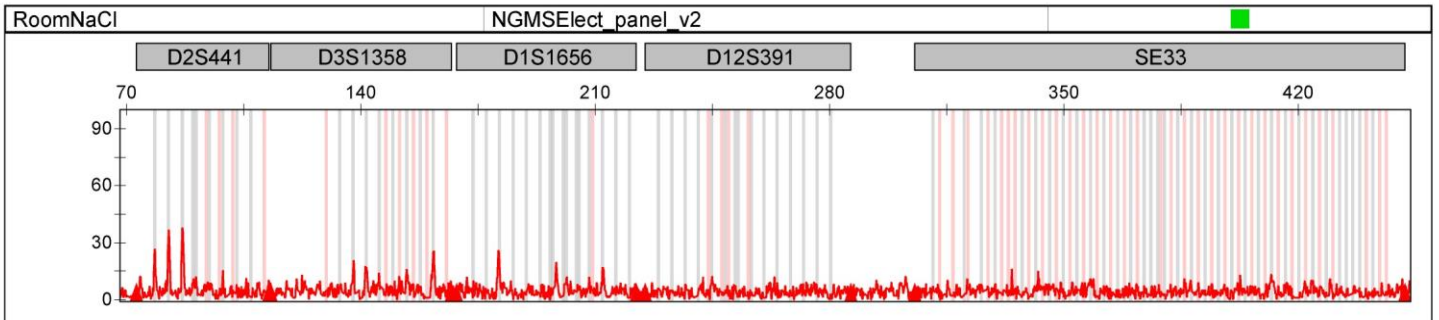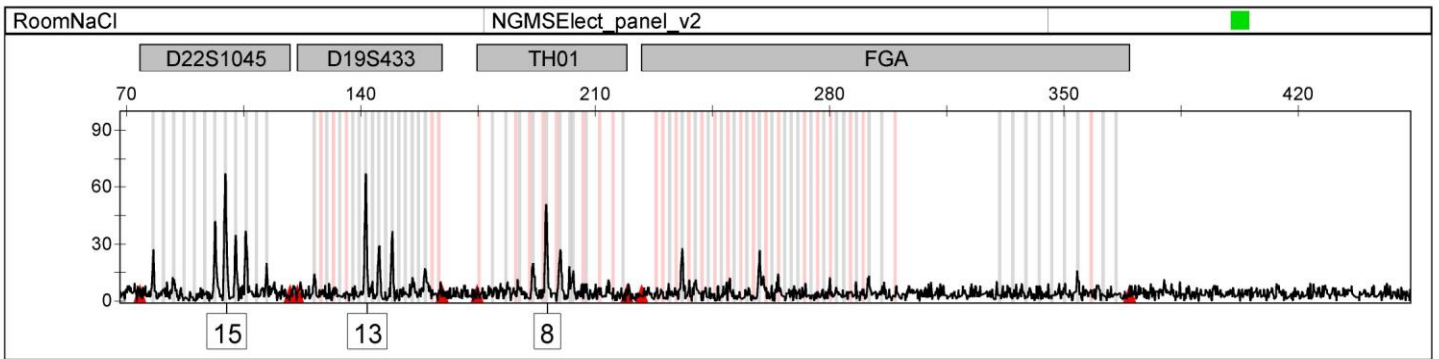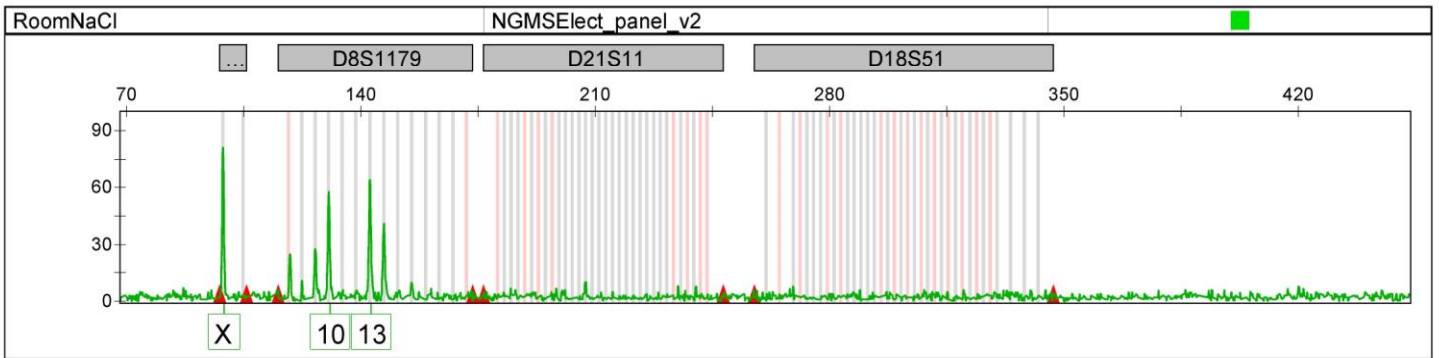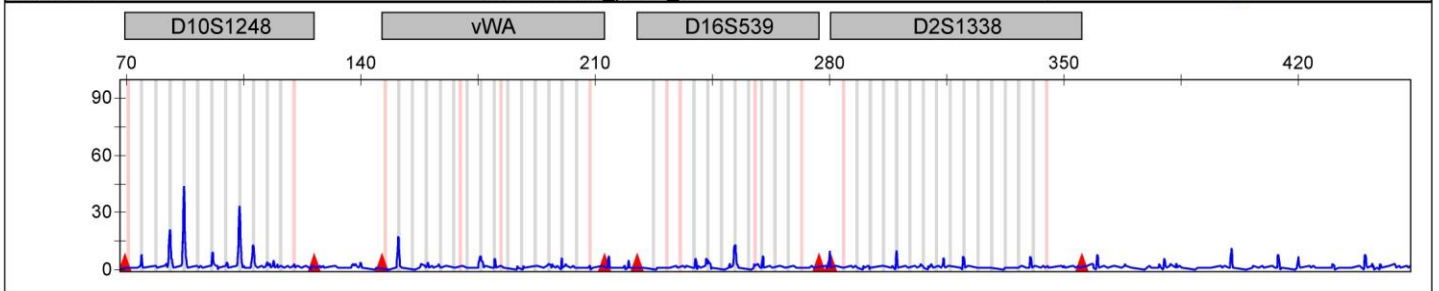
		Dye/Sample Peak	Sample File Name	Marker	Allele	Size	Height	Area	Data Point
1		B,1	H11_RoomNaCl.fsa				82	1168	1369
2		B,2	H11_RoomNaCl.fsa				59	878	1400
3		B,3	H11_RoomNaCl.fsa				61	623	1442
4		B,4	H11_RoomNaCl.fsa				69	800	1483
5		B,5	H11_RoomNaCl.fsa				72	917	1575
6		B,6	H11_RoomNaCl.fsa				130	1686	1602
7		B,7	H11_RoomNaCl.fsa				117	1686	1640
8		B,8	H11_RoomNaCl.fsa				140	1523	1713
9		B,9	H11_RoomNaCl.fsa				119	1322	1728
10		B,10	H11_RoomNaCl.fsa				95	825	1749
11		B,11	H11_RoomNaCl.fsa				170	1745	1762
12		B,12	H11_RoomNaCl.fsa				156	1417	1783
13		B,13	H11_RoomNaCl.fsa				3978	43746	1854
14		B,14	H11_RoomNaCl.fsa			2.39	5111	65544	1893
15		B,15	H11_RoomNaCl.fsa			4.0	5006	63361	1916
16		B,16	H11_RoomNaCl.fsa			6.04	3312	48451	1945
17		B,17	H11_RoomNaCl.fsa			10.46	388	4509	2008
18		B,18	H11_RoomNaCl.fsa			14.95	7835	99432	2072
19		B,19	H11_RoomNaCl.fsa			15.72	7884	109969	2083
20		B,20	H11_RoomNaCl.fsa			16.98	5681	50292	2101
21		B,21	H11_RoomNaCl.fsa			29.26	252	1069	2276
22		B,22	H11_RoomNaCl.fsa			30.53	276	1098	2294
23		B,23	H11_RoomNaCl.fsa			44.7	142	618	2496
24		B,24	H11_RoomNaCl.fsa			47.09	2881	36610	2530
25		B,25	H11_RoomNaCl.fsa			47.65	2883	46795	2538
26		B,26	H11_RoomNaCl.fsa			52.49	277	1951	2607
27		B,27	H11_RoomNaCl.fsa			53.05	292	2258	2615
28		G,1	H11_RoomNaCl.fsa				152	1608	1482
29		G,2	H11_RoomNaCl.fsa				58	606	1592
30		G,3	H11_RoomNaCl.fsa				123	1787	1607
31		G,4	H11_RoomNaCl.fsa				407	4963	1669
32		G,5	H11_RoomNaCl.fsa				91	972	1700
33		G,6	H11_RoomNaCl.fsa				125	2603	1714
34		G,7	H11_RoomNaCl.fsa				1476	18269	1791
35		G,8	H11_RoomNaCl.fsa				5940	48329	1850
36		G,9	H11_RoomNaCl.fsa				6857	62270	1859
37		G,10	H11_RoomNaCl.fsa			1.12	219	2707	1875
38		G,11	H11_RoomNaCl.fsa			2.18	419	2423	1890
39		G,12	H11_RoomNaCl.fsa			2.67	450	2707	1897
40		G,13	H11_RoomNaCl.fsa			3.23	326	3104	1905
41		G,14	H11_RoomNaCl.fsa			4.21	331	4150	1919
42		G,15	H11_RoomNaCl.fsa			5.33	4403	49122	1935
43		G,16	H11_RoomNaCl.fsa			6.67	5766	55913	1954
44		G,17	H11_RoomNaCl.fsa			8.49	448	4008	1980
45		G,18	H11_RoomNaCl.fsa			8.91	464	3816	1986

46		G,19	H11_RoomNaCl.fsa			9.89	5539	43064	2000
47		G,20	H11_RoomNaCl.fsa			13.26	514	7851	2048

		Dye/Sample Peak	Sample File Name	Marker	Allele	Size	Height	Area	Data Point
48		G,21	H11_RoomNaCl.fsa			14.67	762	4314	2068
49		G,22	H11_RoomNaCl.fsa			16.56	6075	48535	2095
50		G,23	H11_RoomNaCl.fsa			17.4	6720	60575	2107
51		G,24	H11_RoomNaCl.fsa			24.98	146	1521	2215
52		G,25	H11_RoomNaCl.fsa			26.25	366	3933	2233
53		G,26	H11_RoomNaCl.fsa			29.89	2655	23915	2285
54		G,27	H11_RoomNaCl.fsa			30.88	51	571	2299
55		G,28	H11_RoomNaCl.fsa			37.54	11104	129495	2394
56		G,29	H11_RoomNaCl.fsa			45.96	11230	157591	2514
57		G,30	H11_RoomNaCl.fsa			47.37	97	1474	2534
58		G,31	H11_RoomNaCl.fsa			48.77	10316	109954	2554
59		G,32	H11_RoomNaCl.fsa			49.89	120	1608	2570
60		G,33	H11_RoomNaCl.fsa			51.65	54	913	2595
61		G,34	H11_RoomNaCl.fsa	AMEL	X	98.79	81	812	3265
62		G,35	H11_RoomNaCl.fsa	D8S1179	10	130.42	58	660	3713
63		G,36	H11_RoomNaCl.fsa	D8S1179	13	142.7	64	726	3885
64		Y,1	H11_RoomNaCl.fsa				917	3012	1849
65		Y,2	H11_RoomNaCl.fsa			0.07	1874	12874	1860
66		Y,3	H11_RoomNaCl.fsa			2.18	2564	22061	1890
67		Y,4	H11_RoomNaCl.fsa			2.88	2947	28255	1900
68		Y,5	H11_RoomNaCl.fsa			4.49	2352	14875	1923
69		Y,6	H11_RoomNaCl.fsa			5.26	1965	11783	1934
70		Y,7	H11_RoomNaCl.fsa			6.74	1739	11839	1955
71		Y,8	H11_RoomNaCl.fsa			8.21	2202	13992	1976
72		Y,9	H11_RoomNaCl.fsa			9.54	6135	51057	1995
73		Y,10	H11_RoomNaCl.fsa			10.32	6899	54365	2006
74		Y,11	H11_RoomNaCl.fsa			14.32	3075	15685	2063
75		Y,12	H11_RoomNaCl.fsa			15.93	2194	26736	2086
76		Y,13	H11_RoomNaCl.fsa			17.47	791	3691	2108
77		Y,14	H11_RoomNaCl.fsa			22.11	133	1552	2174
78		Y,15	H11_RoomNaCl.fsa			28.42	109	1736	2264
79		Y,16	H11_RoomNaCl.fsa			29.89	8458	101542	2285
80		Y,17	H11_RoomNaCl.fsa			36.91	7285	51747	2385
81		Y,18	H11_RoomNaCl.fsa			38.11	7227	50927	2402
82		Y,19	H11_RoomNaCl.fsa			42.6	309	2597	2466
83		Y,20	H11_RoomNaCl.fsa			45.12	7504	100498	2502
84		Y,21	H11_RoomNaCl.fsa			46.53	6159	42364	2522
85		Y,22	H11_RoomNaCl.fsa			48.21	6559	43516	2546
86		Y,23	H11_RoomNaCl.fsa			49.26	6436	40106	2561
87		Y,24	H11_RoomNaCl.fsa			52.77	7412	80894	2611
88		Y,25	H11_RoomNaCl.fsa			53.96	101	1620	2628
89		Y,26	H11_RoomNaCl.fsa	D22S1045	15	99.57	67	788	3276
90		Y,27	H11_RoomNaCl.fsa	D19S433	13	141.53	67	701	3869
91		Y,28	H11_RoomNaCl.fsa	TH01	8	195.35	51	607	4606
92		R,1	H11_RoomNaCl.fsa				4814	35403	1854

93		R,2	H11_RoomNaCl.fsa			1.05	461	7465	1874
94		R,3	H11_RoomNaCl.fsa			2.39	1729	10382	1893

		Dye/Sample Peak	Sample File Name	Marker	Allele	Size	Height	Area	Data Point
95		R,4	H11_RoomNaCl.fsa			3.44	6973	65049	1908
96		R,5	H11_RoomNaCl.fsa			4.0	6973	71091	1916
97		R,6	H11_RoomNaCl.fsa			6.11	6805	112049	1946
98		R,7	H11_RoomNaCl.fsa			8.7	6641	74172	1983
99		R,8	H11_RoomNaCl.fsa			9.89	3154	26192	2000
100		R,9	H11_RoomNaCl.fsa			14.18	6578	82288	2061
101		R,10	H11_RoomNaCl.fsa			16.98	6054	58019	2101
102		R,11	H11_RoomNaCl.fsa			20.42	326	7797	2150
103		R,12	H11_RoomNaCl.fsa			24.35	309	4375	2206
104		R,13	H11_RoomNaCl.fsa			26.6	214	2115	2238
105		R,14	H11_RoomNaCl.fsa			29.12	6804	69636	2274
106		R,15	H11_RoomNaCl.fsa			30.67	6612	59371	2296
107		R,16	H11_RoomNaCl.fsa			36.28	104	1706	2376
108		R,17	H11_RoomNaCl.fsa			37.54	4068	48287	2394
109		R,18	H11_RoomNaCl.fsa			42.11	435	4426	2459
110		R,19	H11_RoomNaCl.fsa			44.56	5152	58611	2494
111		R,20	H11_RoomNaCl.fsa			45.96	2796	32436	2514
112		R,21	H11_RoomNaCl.fsa			46.81	1135	13314	2526
113		R,22	H11_RoomNaCl.fsa			48.77	2945	30638	2554
114		R,23	H11_RoomNaCl.fsa			52.28	6613	77631	2604
115		R,24	H11_RoomNaCl.fsa			53.26	6632	66595	2618
116		O,1	H11_RoomNaCl.fsa				944	6801	1854
117		O,2	H11_RoomNaCl.fsa			2.39	275	1828	1893
118		O,3	H11_RoomNaCl.fsa			3.72	8075	103584	1912
119		O,4	H11_RoomNaCl.fsa			6.11	4955	54558	1946
120		O,5	H11_RoomNaCl.fsa			8.7	4294	33396	1983
121		O,6	H11_RoomNaCl.fsa			9.96	4452	34235	2001
122		O,7	H11_RoomNaCl.fsa			14.81	6605	89901	2070
123		O,8	H11_RoomNaCl.fsa			16.98	3051	22908	2101
124		O,9	H11_RoomNaCl.fsa			22.11	394	6042	2174
125		O,10	H11_RoomNaCl.fsa			29.89	8260	150933	2285
126		O,11	H11_RoomNaCl.fsa			37.54	7971	99258	2394
127		O,12	H11_RoomNaCl.fsa			39.86	494	5568	2427
128		O,13	H11_RoomNaCl.fsa			45.82	8521	204276	2512
129		O,14	H11_RoomNaCl.fsa			48.77	7659	87931	2554
130		O,15	H11_RoomNaCl.fsa			52.77	6504	68189	2611
131		O,16 *	H11_RoomNaCl.fsa			60.0	956	9499	2714
132		O,17 *	H11_RoomNaCl.fsa			80.0	751	7222	2999
133		O,18 *	H11_RoomNaCl.fsa			100.0	1248	11956	3282
134		O,19 *	H11_RoomNaCl.fsa			114.0	1347	13088	3478
135		O,20 *	H11_RoomNaCl.fsa			120.0	1141	11175	3564
136		O,21 *	H11_RoomNaCl.fsa			140.0	890	8632	3848
137		O,22 *	H11_RoomNaCl.fsa			160.0	949	9375	4120
138		O,23 *	H11_RoomNaCl.fsa			180.0	1153	11758	4396
139		O,24 *	H11_RoomNaCl.fsa			200.0	977	10163	4670

140		O,25	*	H11_RoomNaCl.fsa			214.0	969	10340	4867
141		O,26	*	H11_RoomNaCl.fsa			220.0	823	8957	4950

		Dye/Sample Peak	Sample File Name	Marker	Allele	Size	Height	Area	Data Point
142		O,27 *	H11_RoomNaCl.fsa			240.0	1252	13972	5231
143		O,28 *	H11_RoomNaCl.fsa			250.0	596	6780	5368
144		O,29 *	H11_RoomNaCl.fsa			260.0	1016	11628	5512
145		O,30 *	H11_RoomNaCl.fsa			280.0	1117	13166	5791
146		O,31 *	H11_RoomNaCl.fsa			300.0	1191	14234	6073
147		O,32 *	H11_RoomNaCl.fsa			314.0	825	10124	6270
148		O,33 *	H11_RoomNaCl.fsa			320.0	902	11217	6348
149		O,34 *	H11_RoomNaCl.fsa			340.0	1135	14538	6621
150		O,35 *	H11_RoomNaCl.fsa			360.0	977	12598	6894
151		O,36 *	H11_RoomNaCl.fsa			380.0	664	8873	7165
152		O,37 *	H11_RoomNaCl.fsa			400.0	1024	13891	7431
153		O,38 *	H11_RoomNaCl.fsa			414.0	854	11891	7619
154		O,39 *	H11_RoomNaCl.fsa			420.0	860	12037	7697
155		O,40 *	H11_RoomNaCl.fsa			440.0	957	13797	7960
156		O,41 *	H11_RoomNaCl.fsa			460.0	756	11186	8216
157		O,42 *	H11_RoomNaCl.fsa			480.0	718	10749	8474
158		O,43 *	H11_RoomNaCl.fsa			500.0	305	4704	8723
159		O,44 *	H11_RoomNaCl.fsa			514.0	354	5548	8896
160		O,45 *	H11_RoomNaCl.fsa			520.0	722	11493	8971
161		O,46	H11_RoomNaCl.fsa			539.92	558	8928	9220

Sample Name	Panel	SQ
RoomCold	NGMSElect_panel_v2	■

D10S1248 | vWA | D16S539 | D2S1338

11

RoomCold	NGMSElect_panel_v2	■

... | D8S1179 | D21S11 | D18S51

X

RoomCold	NGMSElect_panel_v2	■

D22S1045 | D19S433 | TH01 | FGA

8

RoomCold	NGMSElect_panel_v2	■

D2S441 | D3S1358 | D1S1656 | D12S391 | SE33

11 14   14

Sample Name		Panel	SQ
RoomCold		NGMSElect_panel_v2	🟩
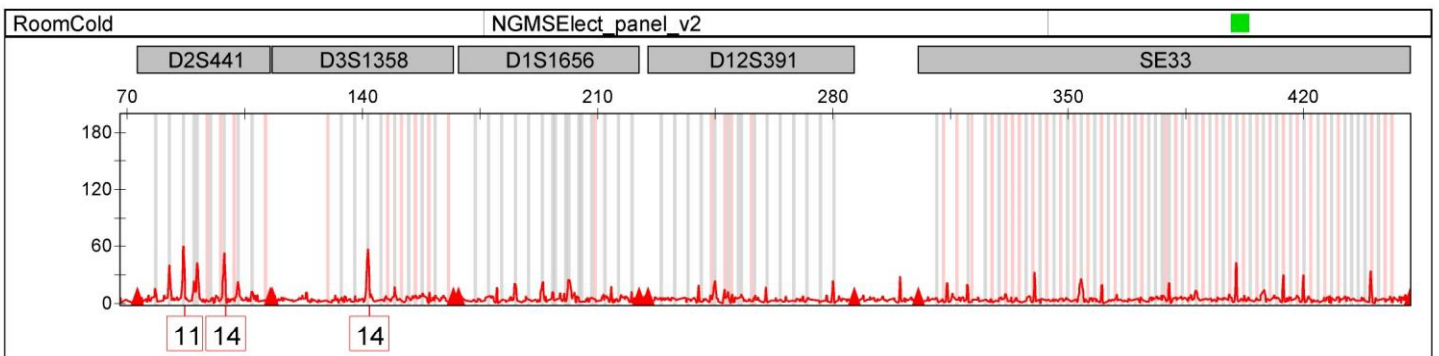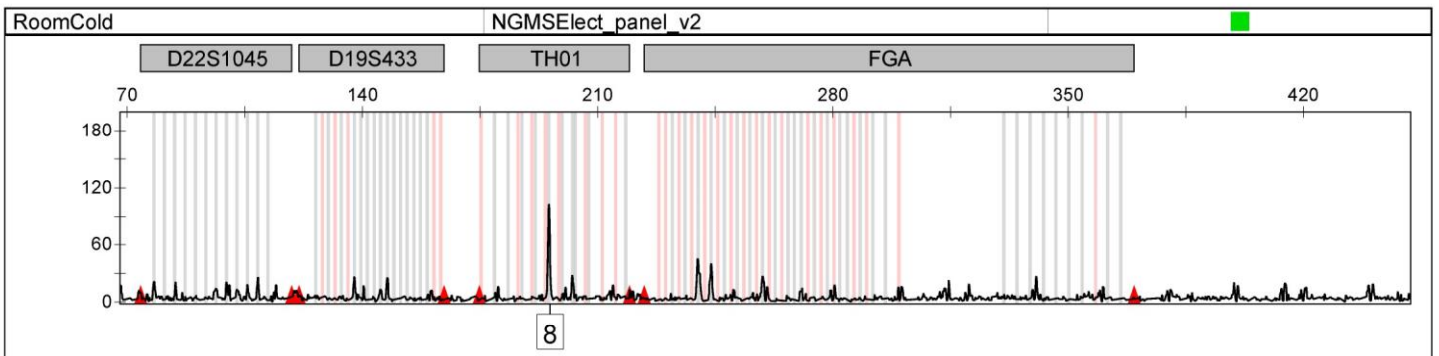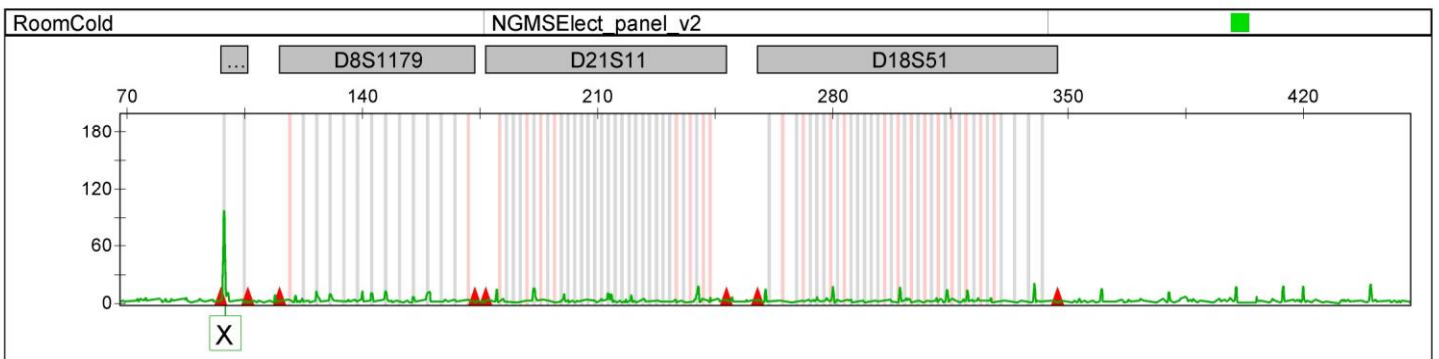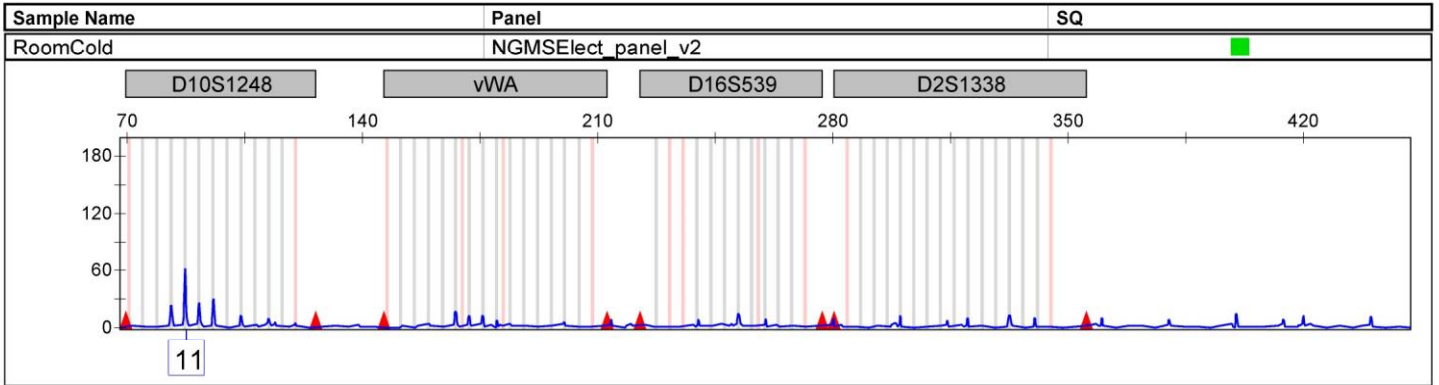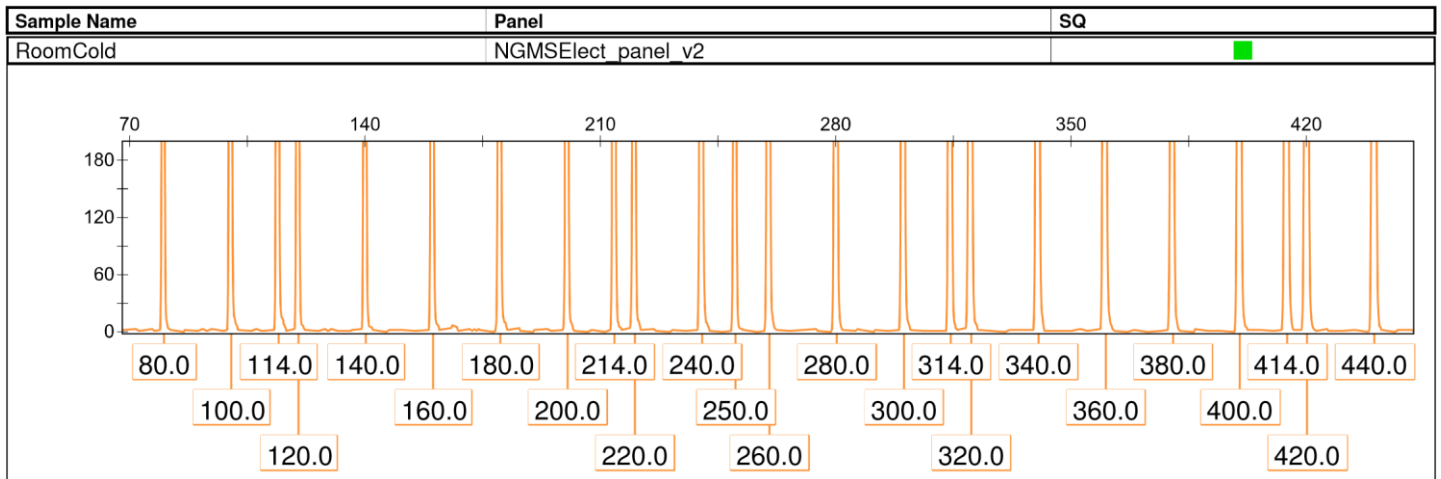
		Dye/Sample Peak	Sample File Name	Marker	Allele	Size	Height	Area	Data Point
1		B,1	A12_RoomCold.fsa				84	1185	1299
2		B,2	A12_RoomCold.fsa				64	924	1333
3		B,3	A12_RoomCold.fsa				66	698	1370
4		B,4	A12_RoomCold.fsa				69	730	1410
5		B,5	A12_RoomCold.fsa				84	1001	1499
6		B,6	A12_RoomCold.fsa				151	1814	1526
7		B,7	A12_RoomCold.fsa				105	1658	1564
8		B,8	A12_RoomCold.fsa				50	474	1577
9		B,9	A12_RoomCold.fsa				165	2202	1634
10		B,10	A12_RoomCold.fsa				163	1667	1651
11		B,11	A12_RoomCold.fsa				115	993	1672
12		B,12	A12_RoomCold.fsa				192	2325	1682
13		B,13	A12_RoomCold.fsa				158	1411	1703
14		B,14	A12_RoomCold.fsa				4291	47346	1772
15		B,15	A12_RoomCold.fsa			2.44	4640	58856	1812
16		B,16	A12_RoomCold.fsa			4.01	4530	57013	1834
17		B,17	A12_RoomCold.fsa			6.02	2886	43305	1862
18		B,18	A12_RoomCold.fsa			8.32	7502	78123	1894
19		B,19	A12_RoomCold.fsa			10.47	462	5790	1924
20		B,20	A12_RoomCold.fsa			12.47	51	440	1952
21		B,21	A12_RoomCold.fsa			14.91	7908	96995	1986
22		B,22	A12_RoomCold.fsa			15.84	7976	113569	1999

		Dye/Sample Peak	Sample File Name	Marker	Allele	Size	Height	Area	Data Point
23		B,23	A12_RoomCold.fsa			16.99	5786	55089	2015
24		B,24	A12_RoomCold.fsa			29.03	245	986	2183
25		B,25	A12_RoomCold.fsa			30.32	233	929	2201
26		B,26	A12_RoomCold.fsa			37.35	53	167	2299
27		B,27	A12_RoomCold.fsa			44.52	149	613	2399
28		B,28	A12_RoomCold.fsa			46.88	2781	40736	2432
29		B,29	A12_RoomCold.fsa			52.19	250	1768	2506
30		B,30	A12_RoomCold.fsa			52.83	259	1770	2515
31		B,31	A12_RoomCold.fsa	D10S1248	11	87.23	62	553	2994
32		G,1	A12_RoomCold.fsa				50	671	1301
33		G,2	A12_RoomCold.fsa				156	1667	1409
34		G,3	A12_RoomCold.fsa				72	740	1513

		Dye/Sample Peak	Sample File Name	Marker	Allele	Size	Height	Area	Data Point
35		G,4	A12_RoomCold.fsa				146	2085	1530
36		G,5	A12_RoomCold.fsa				435	5167	1590
37		G,6	A12_RoomCold.fsa				104	1103	1623
38		G,7	A12_RoomCold.fsa				144	2734	1636
39		G,8	A12_RoomCold.fsa				51	452	1672
40		G,9	A12_RoomCold.fsa				1644	19347	1711
41		G,10	A12_RoomCold.fsa				5372	41646	1768
42		G,11	A12_RoomCold.fsa				6780	62801	1778
43		G,12	A12_RoomCold.fsa			1.15	273	3339	1794
44		G,13	A12_RoomCold.fsa			2.15	379	2850	1808
45		G,14	A12_RoomCold.fsa			2.65	384	2420	1815
46		G,15	A12_RoomCold.fsa			3.23	338	3655	1823
47		G,16	A12_RoomCold.fsa			4.23	333	3733	1837
48		G,17	A12_RoomCold.fsa			5.3	3974	46932	1852
49		G,18	A12_RoomCold.fsa			6.67	5563	54411	1871
50		G,19	A12_RoomCold.fsa			8.53	384	3557	1897
51		G,20	A12_RoomCold.fsa			8.96	391	2531	1903
52		G,21	A12_RoomCold.fsa			9.89	5896	47274	1916
53		G,22	A12_RoomCold.fsa			13.26	554	7367	1963
54		G,23	A12_RoomCold.fsa			14.7	616	3650	1983
55		G,24	A12_RoomCold.fsa			16.56	5821	45242	2009
56		G,25	A12_RoomCold.fsa			17.42	6515	58052	2021
57		G,26	A12_RoomCold.fsa			25.3	114	1146	2131
58		G,27	A12_RoomCold.fsa			26.31	414	4688	2145
59		G,28	A12_RoomCold.fsa			29.68	2923	27247	2192
60		G,29	A12_RoomCold.fsa			30.68	67	557	2206
61		G,30	A12_RoomCold.fsa			37.35	10968	129540	2299
62		G,31	A12_RoomCold.fsa			45.73	11044	159469	2416
63		G,32	A12_RoomCold.fsa			46.81	61	471	2431
64		G,33	A12_RoomCold.fsa			47.46	65	611	2440
65		G,34	A12_RoomCold.fsa			48.53	10754	113594	2455
66		G,35	A12_RoomCold.fsa			49.75	150	2183	2472

67		G,36	A12_RoomCold.fsa			51.04	71	679	2490
68		G,37	A12_RoomCold.fsa			51.68	74	662	2499
69		G,38	A12_RoomCold.fsa			52.54	57	185	2511
70		G,39	A12_RoomCold.fsa	AMEL	X	98.83	98	903	3153
71		Y,1	A12_RoomCold.fsa				69	943	1712
72		Y,2	A12_RoomCold.fsa				1074	3424	1767
73		Y,3	A12_RoomCold.fsa				1635	11480	1778
74		Y,4	A12_RoomCold.fsa			2.15	2488	20043	1808
75		Y,5	A12_RoomCold.fsa			2.87	2761	27853	1818
76		Y,6	A12_RoomCold.fsa			4.44	2326	13213	1840
77		Y,7	A12_RoomCold.fsa			5.23	1820	10034	1851
78		Y,8	A12_RoomCold.fsa			6.74	1652	17249	1872
79		Y,9	A12_RoomCold.fsa			8.24	2090	12237	1893
80		Y,10	A12_RoomCold.fsa			9.53	5537	41204	1911
81		Y,11	A12_RoomCold.fsa			10.32	6665	55635	1922

		Dye/Sample Peak	Sample File Name	Marker	Allele	Size	Height	Area	Data Point
82		Y,12	A12_RoomCold.fsa			14.34	4393	27670	1978
83		Y,13	A12_RoomCold.fsa			16.06	2217	25911	2002
84		Y,14	A12_RoomCold.fsa			17.49	984	7480	2022
85		Y,15	A12_RoomCold.fsa			22.01	147	1736	2085
86		Y,16	A12_RoomCold.fsa			26.24	73	684	2144
87		Y,17	A12_RoomCold.fsa			28.17	173	2587	2171
88		Y,18	A12_RoomCold.fsa			29.53	8580	93105	2190
89		Y,19	A12_RoomCold.fsa			29.89	8592	89910	2195
90		Y,20	A12_RoomCold.fsa			36.77	7345	49629	2291
91		Y,21	A12_RoomCold.fsa			37.92	7229	51490	2307
92		Y,22	A12_RoomCold.fsa			42.37	484	4793	2369
93		Y,23	A12_RoomCold.fsa			44.95	7479	97398	2405
94		Y,24	A12_RoomCold.fsa			46.38	6487	49631	2425
95		Y,25	A12_RoomCold.fsa			48.03	6681	46121	2448
96		Y,26	A12_RoomCold.fsa			49.1	6623	42902	2463
97		Y,27	A12_RoomCold.fsa			52.54	7550	85023	2511
98		Y,28	A12_RoomCold.fsa			53.84	80	1605	2529
99		Y,29	A12_RoomCold.fsa	TH01	8	195.47	103	987	4444
100		R,1	A12_RoomCold.fsa				5212	39964	1773
101		R,2	A12_RoomCold.fsa			2.37	1965	11793	1811
102		R,3	A12_RoomCold.fsa			3.44	6784	61533	1826
103		R,4	A12_RoomCold.fsa			4.01	6779	68541	1834
104		R,5	A12_RoomCold.fsa			6.09	6659	112879	1863
105		R,6	A12_RoomCold.fsa			8.75	6516	73558	1900
106		R,7	A12_RoomCold.fsa			9.89	3333	28769	1916
107		R,8	A12_RoomCold.fsa			14.12	6724	84393	1975
108		R,9	A12_RoomCold.fsa			14.7	5827	92330	1983
109		R,10	A12_RoomCold.fsa			16.99	6011	58104	2015
110		R,11	A12_RoomCold.fsa			20.22	352	8177	2060
111		R,12	A12_RoomCold.fsa			24.01	353	4888	2113
112		R,13	A12_RoomCold.fsa			26.45	268	2544	2147
113		R,14	A12_RoomCold.fsa			28.89	6667	61029	2181
114		R,15	A12_RoomCold.fsa			30.47	6581	56825	2203
115		R,16	A12_RoomCold.fsa			37.35	3716	43388	2299
116		R,17	A12_RoomCold.fsa			41.86	508	5022	2362
117		R,18	A12_RoomCold.fsa			44.37	5202	54625	2397
118		R,19	A12_RoomCold.fsa			45.81	2585	30122	2417
119		R,20	A12_RoomCold.fsa			46.67	1289	13600	2429
120		R,21	A12_RoomCold.fsa			48.53	3027	31212	2455
121		R,22	A12_RoomCold.fsa			52.04	6457	70170	2504
122		R,23	A12_RoomCold.fsa			52.97	6418	63966	2517
123		R,24	A12_RoomCold.fsa	D2S441	11	86.72	60	613	2987
124		R,25	A12_RoomCold.fsa	D2S441	14	98.9	53	542	3154
125		R,26	A12_RoomCold.fsa	D3S1358	14	141.67	57	648	3738
126		O,1	A12_RoomCold.fsa				1249	8911	1773

127		O,2	A12_RoomCold.fsa			2.37	314	1966	1811
128		O,3	A12_RoomCold.fsa			3.73	8268	105050	1830

		Dye/Sample Peak	Sample File Name	Marker	Allele	Size	Height	Area	Data Point
129		O,4	A12_RoomCold.fsa			6.09	5448	62269	1863
130		O,5	A12_RoomCold.fsa			8.75	4940	38216	1900
131		O,6	A12_RoomCold.fsa			9.89	5339	41370	1916
132		O,7	A12_RoomCold.fsa			14.77	6670	96406	1984
133		O,8	A12_RoomCold.fsa			16.99	3685	27366	2015
134		O,9	A12_RoomCold.fsa			22.15	615	9078	2087
135		O,10	A12_RoomCold.fsa			29.68	8256	151376	2192
136		O,11	A12_RoomCold.fsa			37.35	8203	102069	2299
137		O,12	A12_RoomCold.fsa			39.86	761	8314	2334
138		O,13	A12_RoomCold.fsa			45.66	8536	207216	2415
139		O,14	A12_RoomCold.fsa			48.53	7862	91250	2455
140		O,15	A12_RoomCold.fsa			52.47	6812	73816	2510
141		O,16 *	A12_RoomCold.fsa			60.0	1504	14253	2615
142		O,17 *	A12_RoomCold.fsa			80.0	1189	11017	2894
143		O,18 *	A12_RoomCold.fsa			100.0	1993	18086	3169
144		O,19 *	A12_RoomCold.fsa			114.0	2231	19931	3358
145		O,20 *	A12_RoomCold.fsa			120.0	1831	16525	3442
146		O,21 *	A12_RoomCold.fsa			140.0	1437	12982	3716
147		O,22 *	A12_RoomCold.fsa			160.0	1541	14160	3978
148		O,23 *	A12_RoomCold.fsa			180.0	1925	17706	4243
149		O,24 *	A12_RoomCold.fsa			200.0	1617	15171	4503
150		O,25 *	A12_RoomCold.fsa			214.0	1608	15480	4689
151		O,26 *	A12_RoomCold.fsa			220.0	1398	13515	4767
152		O,27 *	A12_RoomCold.fsa			240.0	2104	20939	5029
153		O,28 *	A12_RoomCold.fsa			250.0	993	9938	5157
154		O,29 *	A12_RoomCold.fsa			260.0	1692	17361	5291
155		O,30 *	A12_RoomCold.fsa			280.0	1878	19766	5552
156		O,31 *	A12_RoomCold.fsa			300.0	2023	21923	5817
157		O,32 *	A12_RoomCold.fsa			314.0	1422	15395	6003
158		O,33 *	A12_RoomCold.fsa			320.0	1545	17243	6077
159		O,34 *	A12_RoomCold.fsa			340.0	1979	22536	6337
160		O,35 *	A12_RoomCold.fsa			360.0	1707	19960	6596
161		O,36 *	A12_RoomCold.fsa			380.0	1181	14130	6856
162		O,37 *	A12_RoomCold.fsa			400.0	1803	22140	7115
163		O,38 *	A12_RoomCold.fsa			414.0	1529	19301	7299
164		O,39 *	A12_RoomCold.fsa			420.0	1531	19455	7376
165		O,40 *	A12_RoomCold.fsa			440.0	1706	22230	7635
166		O,41 *	A12_RoomCold.fsa			460.0	1359	18029	7887
167		O,42 *	A12_RoomCold.fsa			480.0	1281	17486	8142
168		O,43 *	A12_RoomCold.fsa			500.0	560	7885	8387
169		O,44 *	A12_RoomCold.fsa			514.0	631	8922	8558
170		O,45 *	A12_RoomCold.fsa			520.0	1307	18638	8632
171		O,46	A12_RoomCold.fsa			539.95	1008	14645	8878
172		O,47	A12_RoomCold.fsa			559.24	702	10540	9116
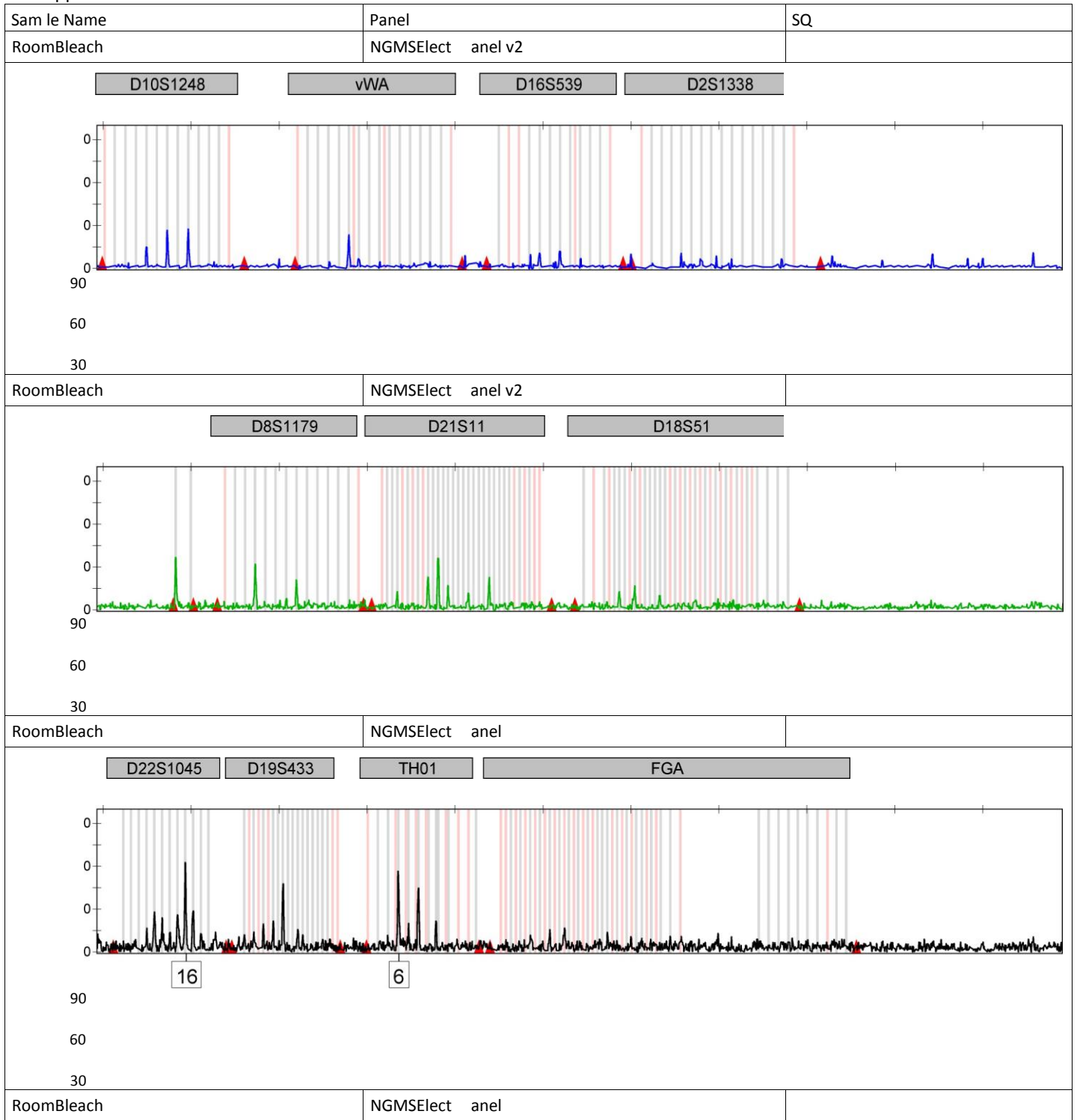
Sam le Name	Panel	SQ
RoomBleach	NGMSElect anel v2	

D10S1248   vWA   D16S539   D2S1338

90

60

30

RoomBleach	NGMSElect anel v2	

D8S1179   D21S11   D18S51

90

60

30

RoomBleach	NGMSElect anel	

D22S1045   D19S433   TH01   FGA

16   6

90

60

30

RoomBleach	NGMSElect anel	

| D2S441 | D3S1358 | D1S1656 | D12S391 | SE33 |

0
0
0
90

60

30

| 11 | 15 |

RoomBleach | NGMSElect   anel v2 |

70   140   210   280   350   420

90
60
30
0

| 80.0 | 114.0 | 140.0 | 180.0 | 214.0 | 240.0 | 280.0 | 314.0 | 340.0 | 380.0 | 414.0 | 440.0 |

| 100.0 | 160.0 | 200.0 | 250.0 | 300.0 | 360.0 | 400.0 |

| 120.0 | 220.0 | 260.0 | 320.0 | 420.0 |

Applied Biosystems
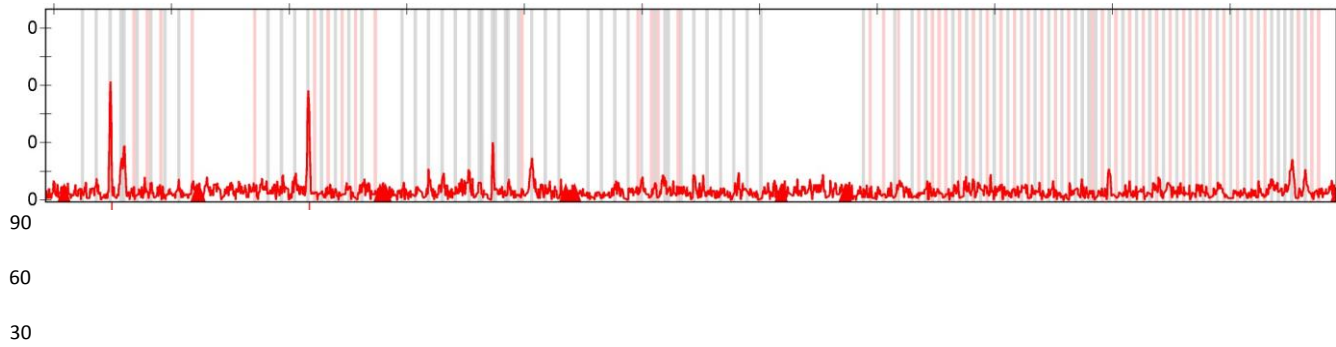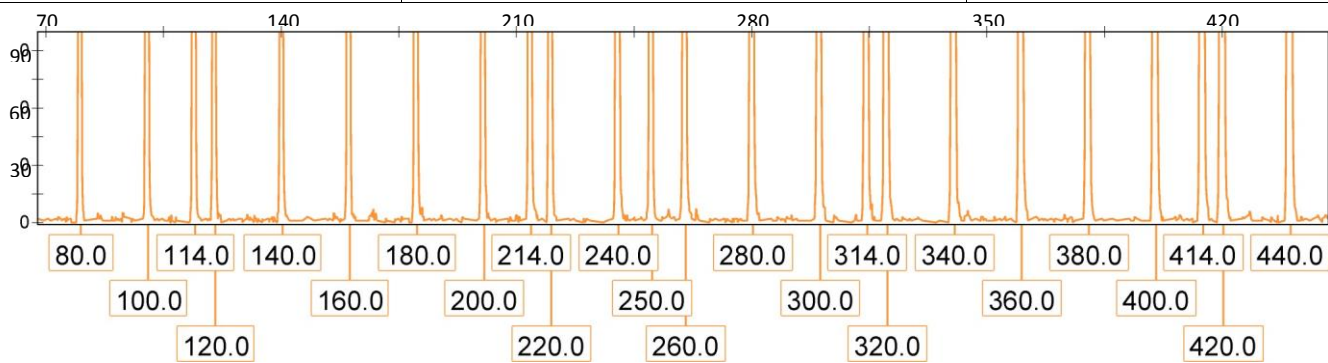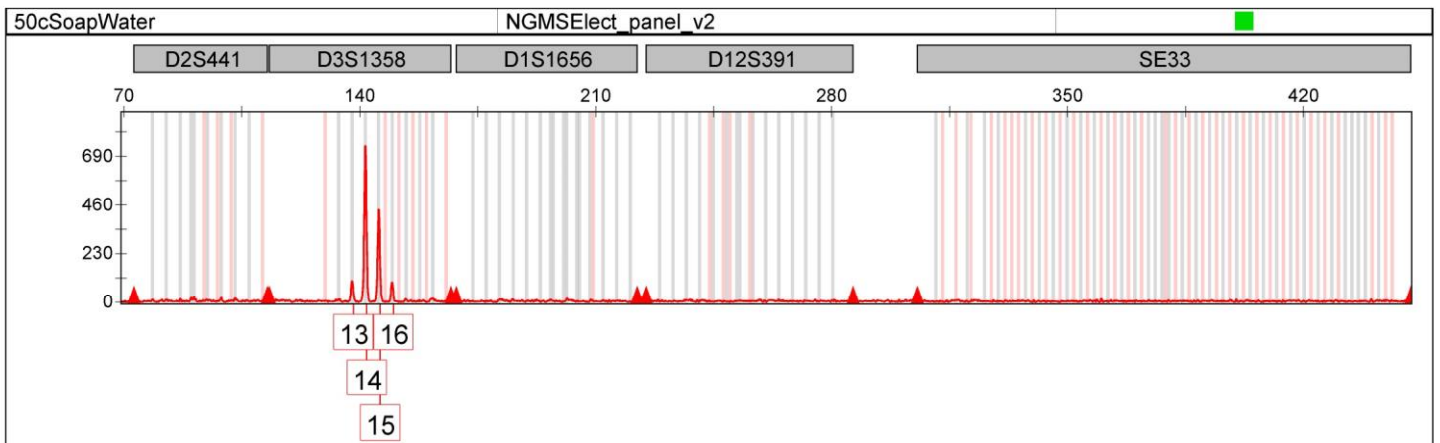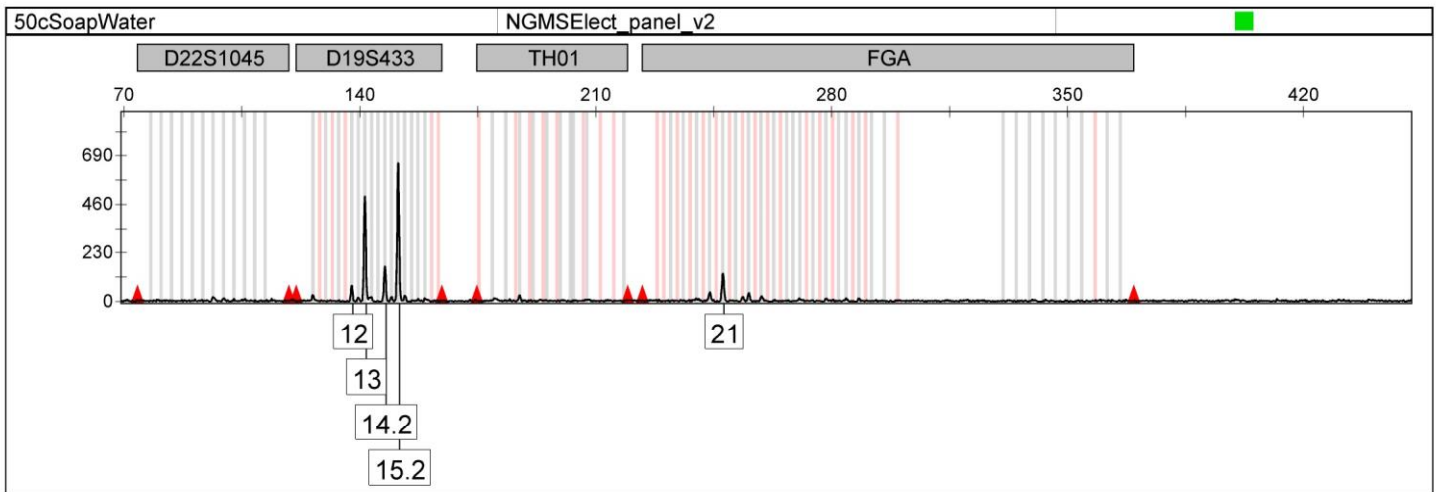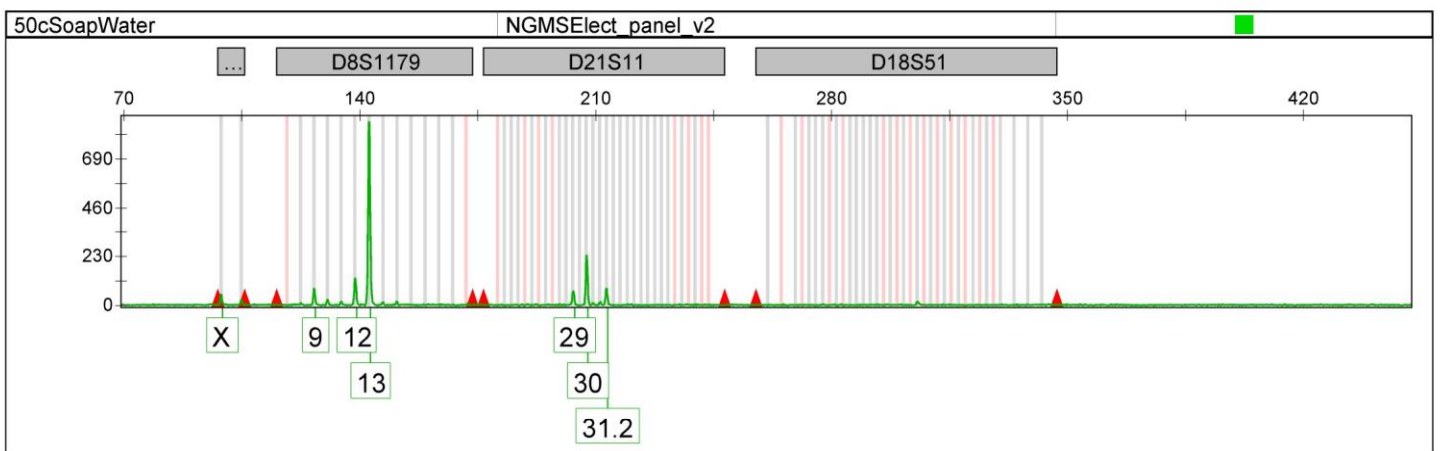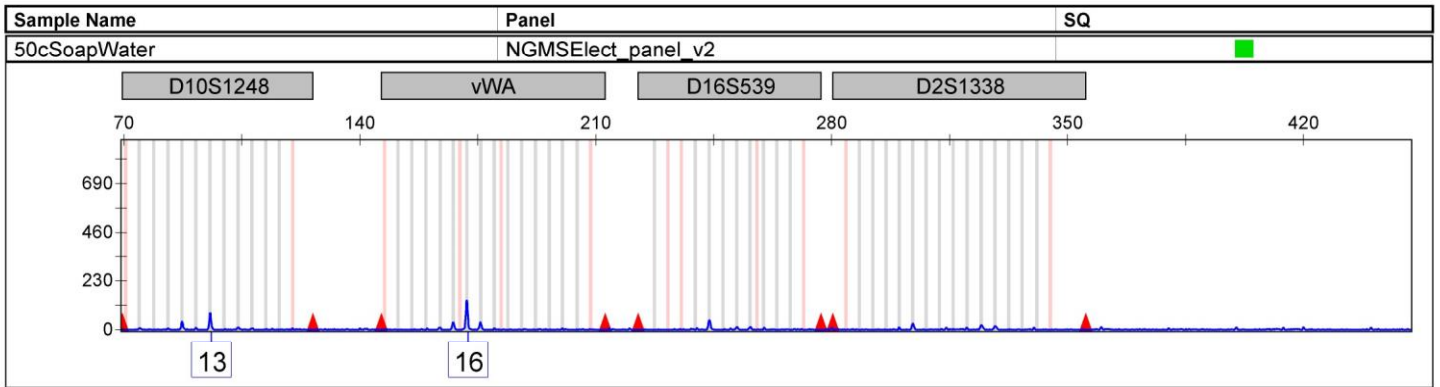
Sample Name	Panel	SQ
50cSoapWater	NGMSElect_panel_v2	🟩